

TG

THIRTEENTH TRANSDUCER WORKSHOP

4-6 JUNE 1985

MONTEREY, CALIFORNIA

TELEMETRY GROUP

RANGE COMMANDERS COUNCIL

WHITE SANDS MISSILE RANGE
KWAJALEIN MISSILE RANGE
YUMA PROVING GROUND

PACIFIC MISSILE TEST CENTER
NAVAL WEAPONS CENTER
ATLANTIC FLEET WEAPONS TRAINING FACILITY
NAVAL AIR TEST CENTER

EASTERN SPACE AND MISSILE CENTER
ARMAMENT DIVISION
WESTERN SPACE AND MISSILE CENTER
AIR FORCE SATELLITE CONTROL FACILITY
AIR FORCE FLIGHT TEST CENTER
AIR FORCE TACTICAL FIGHTER WEAPONS CENTER

DISTRIBUTION STATEMENT A: APPROVED FOR PUBLIC RELEASE;
DISTRIBUTION UNLIMITED.

SECRETARIAT

RANGE COMMANDERS COUNCIL

WSMR-KMR-YPG-PMTC-AFWTF-WWC-NATC-AFSCF-AFTFWC-AD-ESMC-WSMC-AFFTC

9 July 1986

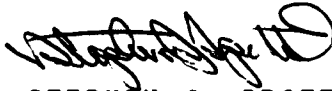
RCC Secretariat, STEWS-SA-R
White Sands Missile Range, NM 88002

REPLY TO
ATTN TO:

SUBJECT: 13th Transducer Workshop

TO: Holders of 13th Transducer Workshop Proceedings

The enclosed paper by Dennis Page of White Sands Missile Range was presented during Session 1 of the 13th Transducer Workshop. Unfortunately, the paper was inadvertently omitted from the workshop document you recently received. The Vehicular Instrumentation/Transducer Committee of the Range Commanders Council Telemetry Group regrets this oversight.



STEPHEN J. SPOTTS
Executive Secretary
Range Commanders Council

Enclosure

A 10,000 FT-LB
TORQUE CALIBRATION SYSTEM

Dennis W. Page
Mechanical Engineer
US Army TMDE Support Center
White Sands Missile Range, New Mexico 88002

ABSTRACT

As the state of torque technology has advanced, higher range and accuracy torque measuring instruments have become available.

Within the last few years a significant number of static torque measuring instruments have been received for calibration with ranges as high as 4,000 foot-pounds (ft-lb) and with stated accuracies of 0.1% full scale (F.S.).

To calibrate these instruments a high torque calibration system (HTCS) with the following characteristics was required:

- (1) Ability to generate a known torque from a few 100 ft-lb to 10,000 ft-lb with an accuracy on the order of 0.05% of reading.
- (2) Compatibility with a wide variety of high torque measuring instruments.
- (3) Ease of use.

Described here is a HTCS that incorporates these characteristics.

INTRODUCTION

Until recently, the local requirement for calibrating torque measuring instruments above 1,000 ft-lb was rarely encountered. The stated accuracy of the instruments to be calibrated was usually no better than 1% at best with 2% to 3% accuracy the norm. These instruments were calibrated on commercially available torque calibration standards. They consist of a beam anchored in a box. The torque is applied to one end of the beam through a bearing restraint that permits only a pure moment to be applied. The applied torque produces a deflection in the beam which is measured by a dial indicator. The deflection is proportional to the torque applied. The instruments are available up to 1,000 ft-lb with an accuracy of 0.5%. The torque is applied to the test instrument by hand and compared with the reading of the calibration standard. This procedure is satisfactory up to about 1,000 ft-lb, after which manual application of torque becomes difficult.

Within the last few years a wide variety of torque measuring instruments with capacities as large as 4,000 ft-lb and stated accuracies of 0.1% F.S. have been received for calibration. To support this continuing high torque workload a HTCS was required.

Performance Requirements

The quality and quantity of instruments to be calibrated determined the performance requirements and the resulting system design. Three basic performance requirements were developed.

Requirement #1 - Range and Accuracy

A 10,000 ft-lb maximum was selected to accommodate any future requirements above the existing 4,000 ft-lb range. Since this was an initial design, extending the range to anticipate future needs was considered cost effective. The accuracy requirement of .05% of reading was selected to give a minimum standard-to-test-instrument accuracy ratio of 2 to 1 for the most accurate instrument to be calibrated, i.e., 0.1% F.S. torque transducers.

Requirement #2 - Versatility

Due to the large variety of high torque instruments calibrated the system had to be very versatile. The instruments that arrived for calibration were typically:

Torque Transducers (0 - 4,000 ft-lb)
Torque Wrenches (0 - 2,000 ft-lb)
Torque Multipliers (0 - 2,500 ft-lb)
Torque Analyzers (0 - 1,000 ft-lb)

Requirement #3 - Ease of Use

The system had to be easy to use, i.e., one person could operate it without performing a great number of complex operations or a large expenditure of labor. The system must produce and measure clockwise (CW) and counterclockwise (CCW) torque.

A product review revealed the existing commercial systems to be deficient by one or more of the

three performance requirements outlined above. Accordingly, the system was designed and fabricated locally.

Design Considerations

Since the Test Measurement and Diagnostic Equipment (TMDE) Support Center at White Sands Missile Range (WSMR), New Mexico maintains accurate force and dimensional standards, the basic approach was to use the principle of: torque = force x length. If a known force is applied to a known lever arm (length), then the resulting torque is known. Once the basic approach was chosen, certain considerations were essential to assure compliance with the three performance requirements:

Requirement #1 - To assure the desired accuracy and range it was necessary to consider the following:

- The applied force and lever arm must remain at 90 to each other.
- The accuracy of the produced torque was dependent on the accuracy of: 1) the applied force and 2) the length of the lever arm.
- A pure moment without side loading must be applied - some instruments are sensitive to side loads.
- Friction must be reduced to insignificant levels or quantified for correction purposes.
- The center line (ϕ) of the torque arm must be coincident with the ϕ of the output shaft so the measured lever arm length is equal to the effective lever arm.

Due to the forces and accuracies encountered, the following areas required consideration:

- Sufficient torque arm rigidity to assure a constant effective lever length and orientation with respect to (w.r.t.) the applied forces.
- Selection of size and material of the output shaft and test instrument coupling systems to maintain safe stresses at full load.

Requirement #2 - To assure interfacing with the variety of instruments encountered, the calibration system must provide a method by which:

- The test instrument could be coupled to the output shaft of the calibration system.
- The test instrument could be attached and/or made to react against.

Requirement #3 - The following were considerations relating to ease of system operation:

- No hand loading or unloading of deadweights necessary.

- One man required to apply torque and read test instrument simultaneously.
- Minimal or no calculations required to determine the applied torque.
- System calibration easily convertible to CW and CCW torque application.

The design, incorporating the above considerations, was an iterative process with the completed design a combination of trade-offs to accommodate the three performance requirements. A description of the HTCS follows.

Length

A torque arm was used with a segment of a circle at each end and a flexible tension member to connect the applied force to each end of the torque arm (Figure 1). The torque arm and the flexible tension member combination would allow rotation of the torque arm and still maintain perpendicularity between the torque arm and the applied force. It would also maintain a constant lever arm length during rotation. Rotation of the torque arm was necessary due to:

- Compliance of the test instruments.
- The different positions of the torque arm required for set-up of the various instruments calibrated.

To prevent side loading, two equal and opposite diametrically opposed forces were used on the torque arm (F_1 & F_2 , Figure 1). If

$$F_1 = F_2 \text{ and } r_1 = r_2 \text{ and } F_1 \parallel F_2$$

then a pure moment is applied to the torque arm equal to

$$(F_1 \cdot r_1 + F_2 \cdot r_2).$$

To produce large torque, a large force and a small lever arm or a large lever arm and a small force, or a compromise of the two was required. If the lever arm was too large, the size of the completed system would be too large for the space available. If too small a lever arm was used the forces would be large and the hardware used to connect the applied forces to the torque arm would be large and bulky. As a compromise a 2-foot radius was used, i.e., a 4-foot diameter torque arm. Wire rope was used as the tension member. Investigation⁽¹⁾ indicated the ϕ of a force applied to a wire rope over a groove in a pulley acts through the ϕ of the wire rope. This is significant since a wire rope diameter of .375 inch was used. If the effective ϕ of the force was not coincident with the geometric ϕ of the wire rope, lever arm length errors as large as 1.5% could be made. This was clearly unacceptable with an accuracy goal of .05%. A groove was machined in the circumference of the sector of the circle to support and guide the wire rope. The groove was machined at a diameter such that the distance from center line of the torque arm to center line of the wire rope was 2

feet. After fabrication, the torque arm lengths from the center of torque arm to the bottom of the sector groove were measured with an uncertainty of ± 0.002 inch @ 68° F. The diameter of the wire rope was also measured and the effective lever arm lengths were:

$(r_1 + \frac{1}{2} \text{ wire rope diameter})$

$(r_2 + \frac{1}{2} \text{ wire rope diameter})$

The torque arm was fabricated in sections from aluminum and steel. The two end sections were made of steel to provide resistance to abrasion by the wire rope as the torque arm rotated. The main portion of the torque arm was made of 1 inch thick aluminum plate to reduce the weight of the torque arm. An internally splined, 24-tooth companion flange was bolted to the torque arm. The companion flange coupled the torque arm to the output torque shaft. The output torque shaft had an external spline that mated with the internal spline of the companion flange. All splines were of involute profile for strength and to provide self centering⁽²⁾ of the torque arm on the torque shaft once torque was applied. The 24-tooth spline permitted orientation of the output shaft w.r.t. the torque arm in 15° increments. The torque arm could rotate through 30° ($\pm 15^\circ$ from longitudinal ϕ of torque arm). With this combination, any orientation (0 through 360°) of the test instrument w.r.t. the torque arm was possible.

The required torque shaft diameter and material was determined^(2,3) and several torque shafts were fabricated with different configurations on the output end to permit attachment of the various type of torque instruments received for calibration. The torque shafts were fabricated from 4130 steel and had a diameter of 3.1485 inches. The splined components were held together axially by a nut that tightened on a threaded stud of the torque shaft extending through a hole in the ϕ of the torque arm (See Figure 2). To assure the concentricity of the torque arm w.r.t. the output shaft the torque arm grooves were machined with the torque arm mounted on its ϕ hole.

The output torque shaft rotated in two 3.1495 inch bore radial bearings. The bearings required a torque of 0.162 in-lb to start rotation under zero radial load. The bearings were mounted in a bearing housing that was bolted to the back of the main frame. To allow for future requirements of numerous holes to mount torque instruments on, a 14" square section was removed from the center of the main frame. A step was machined around the inside of the square hole to accept a plate machined with a similar step which could be exchanged once it was full of instrument mounting holes (See Figure 2). The output shaft either extended through or was flush with the surface of the removable torque plate, depending on the torque shaft selected. (See Figure 2)

A 1-inch thick 8-foot wide x 4-foot tall cold rolled steel plate mounted vertically was used as the main frame (See Figure 3).

The torque arm was statically balanced after it was installed on the torque shaft, to assure that no extraneous torque was applied by a torque arm imbalance.

Force

The forces F_1 and F_2 (Figure 1) needed to be known to fairly close tolerances to attain the system accuracy goal of 0.05% of reading. Performance requirement #3 prevented the use of deadweight so an alternative method of easily applying two known forces was required. The method selected to generate the required forces was hydraulic cylinders in conjunction with a two-speed hydraulic hand pump. Since CW and CCW torque was to be produced, provision to attach hydraulic cylinders on either side of the torque arm was necessary. This was accomplished by flexible tension member attachments that permitted bolting to either side of the torque arm as required by the torque direction. The hand pump was connected to a directional control valve (DCV) which permitted selection of the CW or CCW set of hydraulic cylinders (Figure 3). A flex hose was used for the line connecting the hand pump to the DCV to allow placement of the hand pump where it was needed. Initially, consideration was given to calculating the forces produced by the hydraulic cylinders from the measured pressure and inside diameters of the cylinders. However, the accuracy of this method was inadequate, so calibrated load cells were used. The load cells were connected in-line between the hydraulic cylinder shaft and the flexible tension member. This also permitted the load cells to be used in tension to help prevent side load errors associated with compression use. Tension flexures were used to reduce possible side load errors caused by any slight mis-alignment of the load cell with the tension member or torque arm. The load cells were calibrated on a deadweight machine that produced force values with an uncertainty of less than 40 parts per million. The load cell calibration included a report containing a ~~prediction equation based on calibration data.~~ An uncertainty estimate equation for the forces was also available from the report⁽⁴⁾. Using the force prediction equation and the load cell outputs the forces generated by the hydraulic cylinders were calculated. Further, using the uncertainty equation, an estimate was made of the accuracy of the two force measurements.

The completed HTCS functioned as follows. The hydraulic cylinder/load cell combinations produced and measured the forces. The wire rope coupled the generated force to the torque arm and permitted rotation of the arm while the applied forces remained perpendicular. The torque arm converted the forces (equal, opposite, and diametrically opposed) to a moment. The produced torque was applied to the test instrument by the splined interchangeable output torque shaft.

Instrumentation

The output of the two load cells was detected by two digital voltmeters (DVM). Both DVM outputs

were read by a computer which used the load cell prediction equations to calculate the forces and uncertainty based on five independent load cell readings. The total uncertainty of the produced torque was also calculated and printed out each time the a program was executed. The printed results could then be compared to the indication of the test instrument.

To account for zero drift of the load cell, a no-load-reading of each load cell was taken at the beginning and end of each run. These values were used by the computer to correct for any change in zero that might have occurred during the run. To obtain a repeatable no-load-zero-reading, all force applied by the hydraulic cylinders had to be removed from the load cells. By releasing the pressure in the hydraulic cylinders and rotating the torque arm a slight amount by hand, the wire rope was disengaged from positive end contact with the torque arm and repeatable no-load-zero readings were obtained. This was made possible by wire rope end attachments that permitted slipping of the wire rope during compression.

RESULTS

The torque system was assembled and used to calibrate instruments with ranges as high as 4,000 ft-lb, with good results. During operation of the system it was noticed that under load the wire rope would "unwind", imparting a torque on the load cell. The torque was of an unknown magnitude but equal to the resistance of the seals in the hydraulic cylinders. Tests revealed an axial torque sensitivity as large as 0.45% F.S./ft-lb for the load cells used. Through tests it was also discovered that the wire rope appeared to "flatten out" under increasing load. The wire rope diameter was changing at a rate of approximately .001 inch/1,000 ft-lb.

Further investigation revealed behavior of wire rope on a sheave that contributed to the errors of the system.

Close observation of a cable which is passing over a sheave will reveal a small standing wave at each sheave tangent point⁽⁵⁾.....

This is due to a complicated relationship between the individual wire strands that make up the wire rope . The internal friction between the individual wire strands causes the wire rope to pull away at the point where it enters the sheave and cling to the sheave as it exits (See Figure 4). The result leads to an error in the effective radius of the sheave and thus the lever arm length. The magnitude of this effect was undetermined but is proportional to the ratio d/D ; where d = the diameter of the wire rope and D = the diameter of the sheave⁽⁶⁾.

The same internal friction produces losses in the transmitted forces as the wire rope bends around the sheave⁽⁶⁾. The magnitude of this error was also undetermined.

To correct these problems the wire rope was replaced with a thin high strength strap, .055 inch thick and 2 inches wide. The groove on the end of the circular segment was replaced by a smooth 2-inch wide circular segment surface. The distance from the ϕ of the torque arm to the ϕ of the strap was 2 feet.

To obtain the most stable load cell readings a short wait was required after the applied torque was changed. This was due to the heating or cooling induced by the pressure increase or decrease in the closed hydraulic system. The wait permitted the hydraulic system temperatures and thus the produced forces, to stabilize.

The DVM was set at the fastest sample rate (24 samples/sec) to reduce the effect of temperature drift and permit a required wait time of about 30 seconds for all but the most accurate calibrations.

The resulting torque calibration system was analyzed to determine system accuracy. The results follow:

UNCERTAINTY ANALYSIS

Torque = Force x Distance

Systematic Error:

Force

Load cell calibration

Maximum error for either load cell = .02%
(from calibration report)

Bearing Friction

0.16 in-lb at 0 lb radial load

0.16 in-lb x (2 bearings) = 0.32 in-lb
(negligible)

Measurement of the bearing friction @ side load of 125 lbs (100 lb torque arm weight + 25 lb unequal loading) = 0.1 ft-lb
(negligible)

Distance

Uncertainty of measured radius arm = $\pm .002$ in

$$\frac{.002 \text{ in}}{24 \text{ in}} = \pm .0083\%$$

Random Errors:

Force - Random error calculated from five DVM readings as follows:

Using prediction equation calculate force

Calculate standard deviation (σ) of five force values.

Calculate limit of random error of force from:

$$\frac{3\sigma}{5}$$

(variable but typical results) $\pm .03\%$
Distance

Error in torque arm due to thermal expansion:

$$\Delta t = \pm 5^\circ\text{F} \text{ (temp controlled to } \pm 5^\circ\text{F)}$$

Length of aluminum portion = 20.4 in

$$13. \mu\text{ in/in}^\circ\text{F} \times 5^\circ\text{F} \times 20.4 \text{ in} = .0013 \text{ in}$$

Length of steel portion = 3.4 in

$$6.7 \mu\text{ in/in}^\circ\text{F} \times 5^\circ\text{F} \times 3.6 \text{ in} = .0001 \text{ in}$$

Total error due to thermal expansion = .0014 in

$$\text{@ } \Delta t \text{ of } 5^\circ\text{F} \frac{.0014 \text{ in}}{24 \text{ in}} = \pm .006\%$$

Estimate of total uncertainty:

Systematic

Force: $\pm .02\%$

Distance: $\pm .0083\%$

Random

Force: $\pm .03\%$

Distance: (due to temp changes) $\pm .006\%$

Total Typical Results = $\pm .064\%$

CONCLUSION

Comparison of the completed system with the three performance requirements indicates substantial compliance with the original goals. Although no 10,000 ft-lb instruments have been calibrated, the design of the system and performance at lower torque values indicate satisfactory full scale performance. Where an accurately known high static torque is desired, this method could be applied.

ACKNOWLEDGEMENT

I would like to express my appreciation to J.A. Harmon, Chief of the TMDE Support Center-White Sands, for his support during development of the system, the WSMR Precision Machine Section for its contribution to the quality of the completed hardware, and C.E. Holstein for his assistance during testing of the system.

REFERENCES

1. Wheeler, R., 1984. Wire Rope Corporation of America, Inc. St. Joseph, Missouri. Personal communication.
2. Dudley, D.W., 1957. How to Design Involute Splines. Product Engineering - October 28, 1957.
3. Dudley, D.W., 1957. When Splines Need Stress Control. Product Engineering - December 23, 1957.
4. Downs, R., 1979. Estimated Standard Deviations for Values Established from Calibration Curves. TE-OE, White Sands Missile Range, New Mexico.
5. Gibson, P.T., 1984. Operational Characteristics of Electromechanical Cables, Proc. of American Society of Mechanical Engineers 3rd International Offshore Mechanics and Arctic Engineering Symposium, New Orleans, Louisiana, February 12-17, 1984.
6. Gibson, P.T., 1985. Tension Member Technology, Huntington Beach, California. Personal communication.

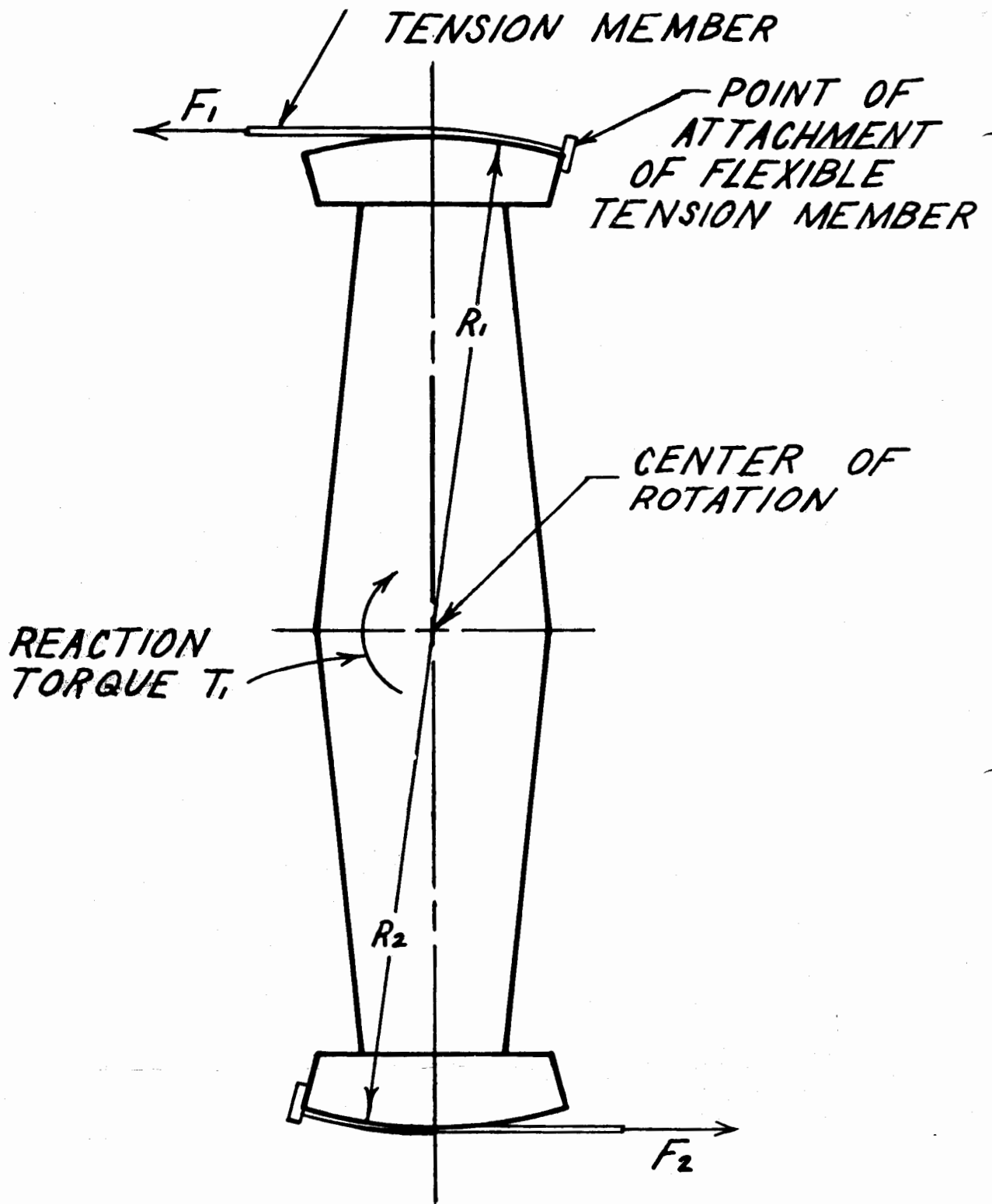


Figure 1. Torque system freebody diagram

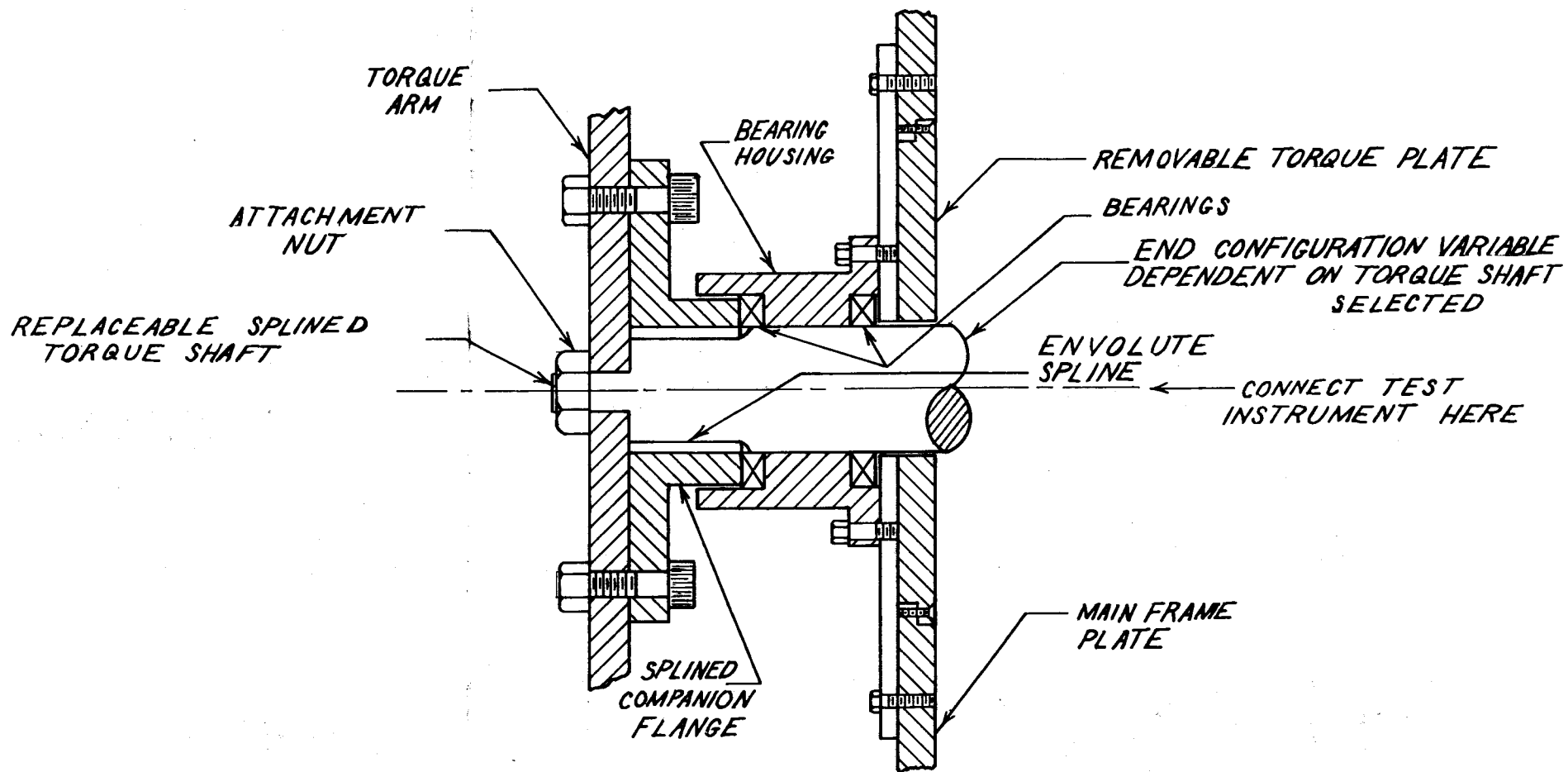


Figure 2. Torque shaft assembly

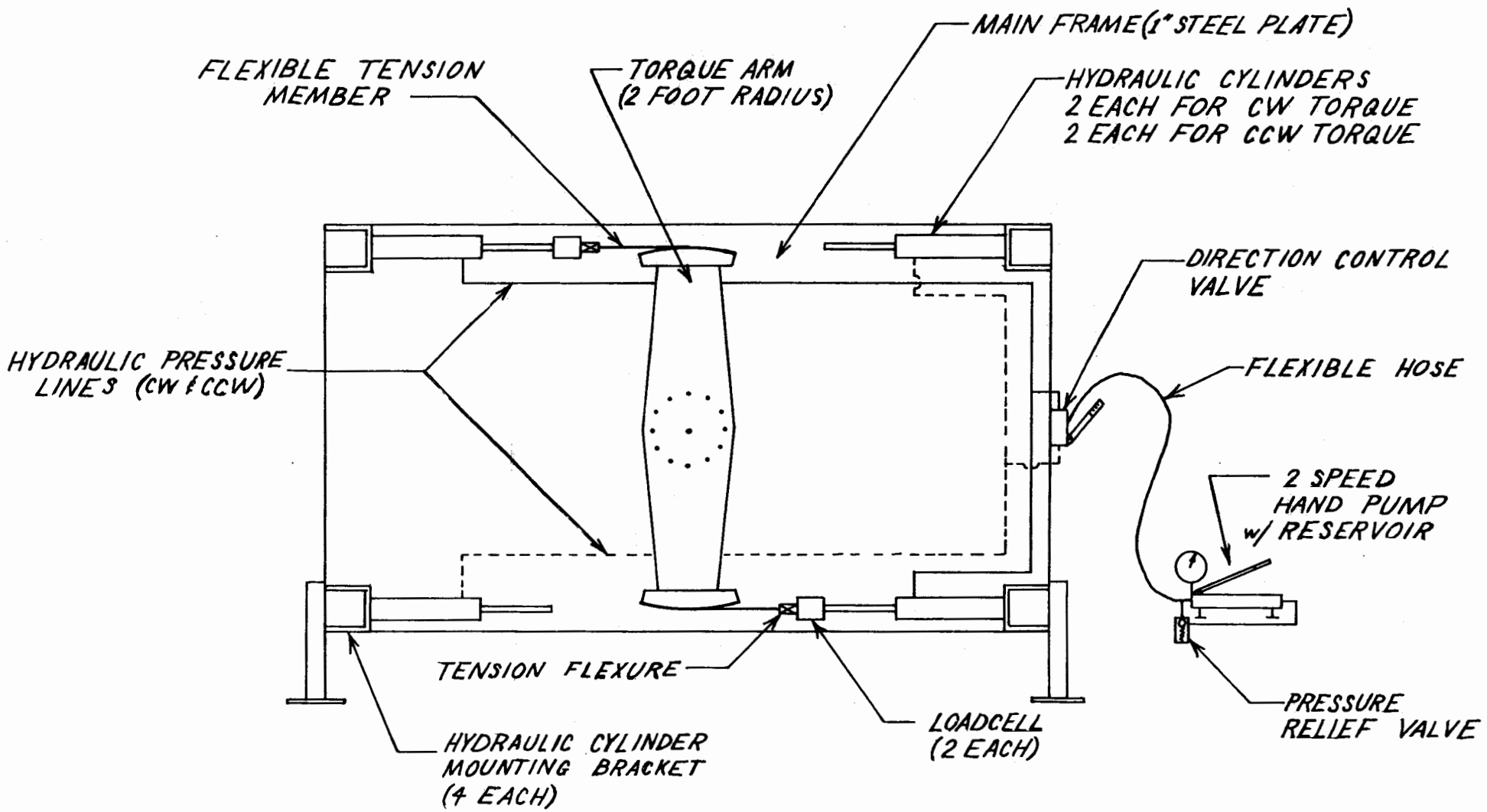


Figure 3. Torque calibration system - rear view

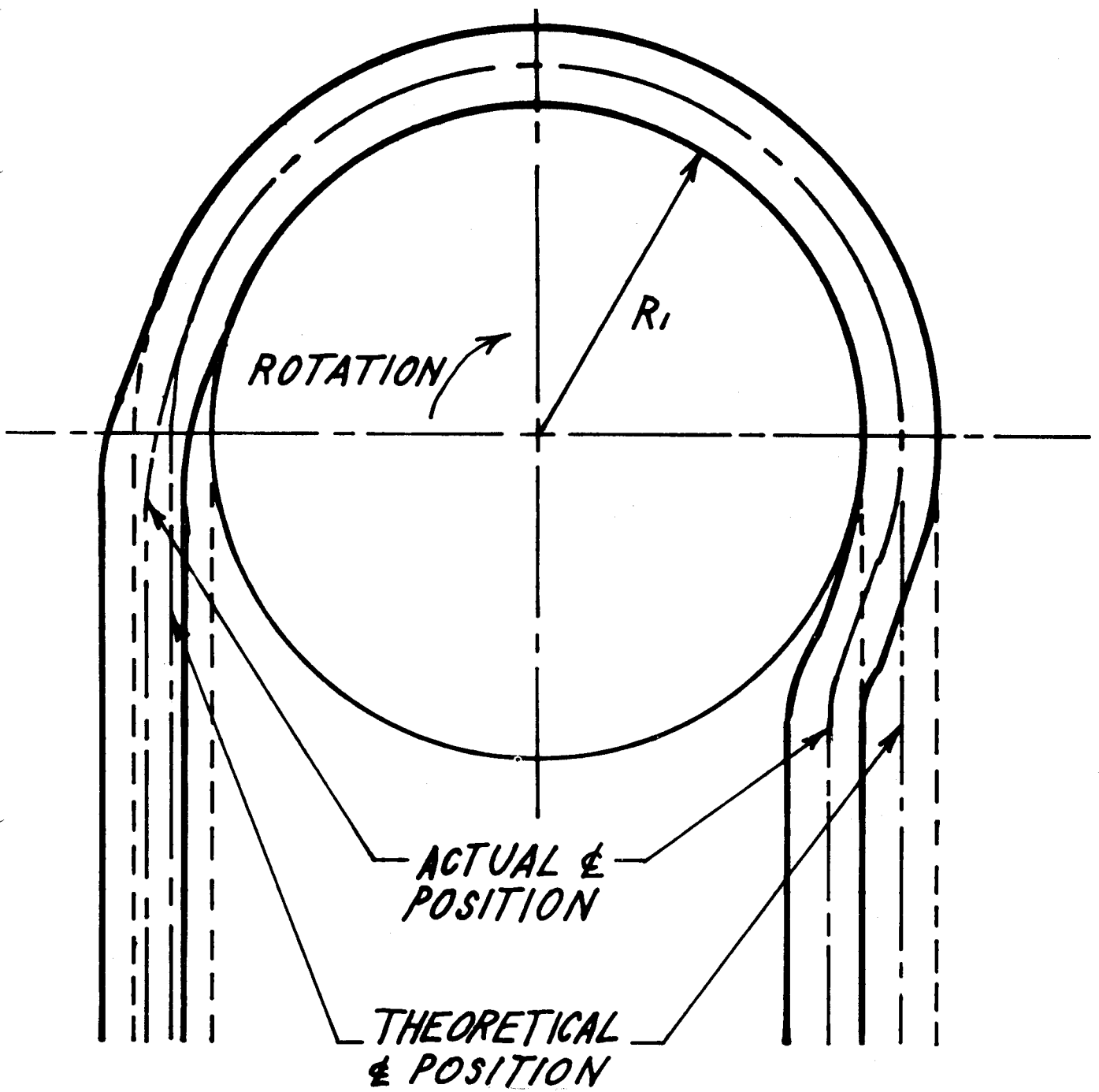
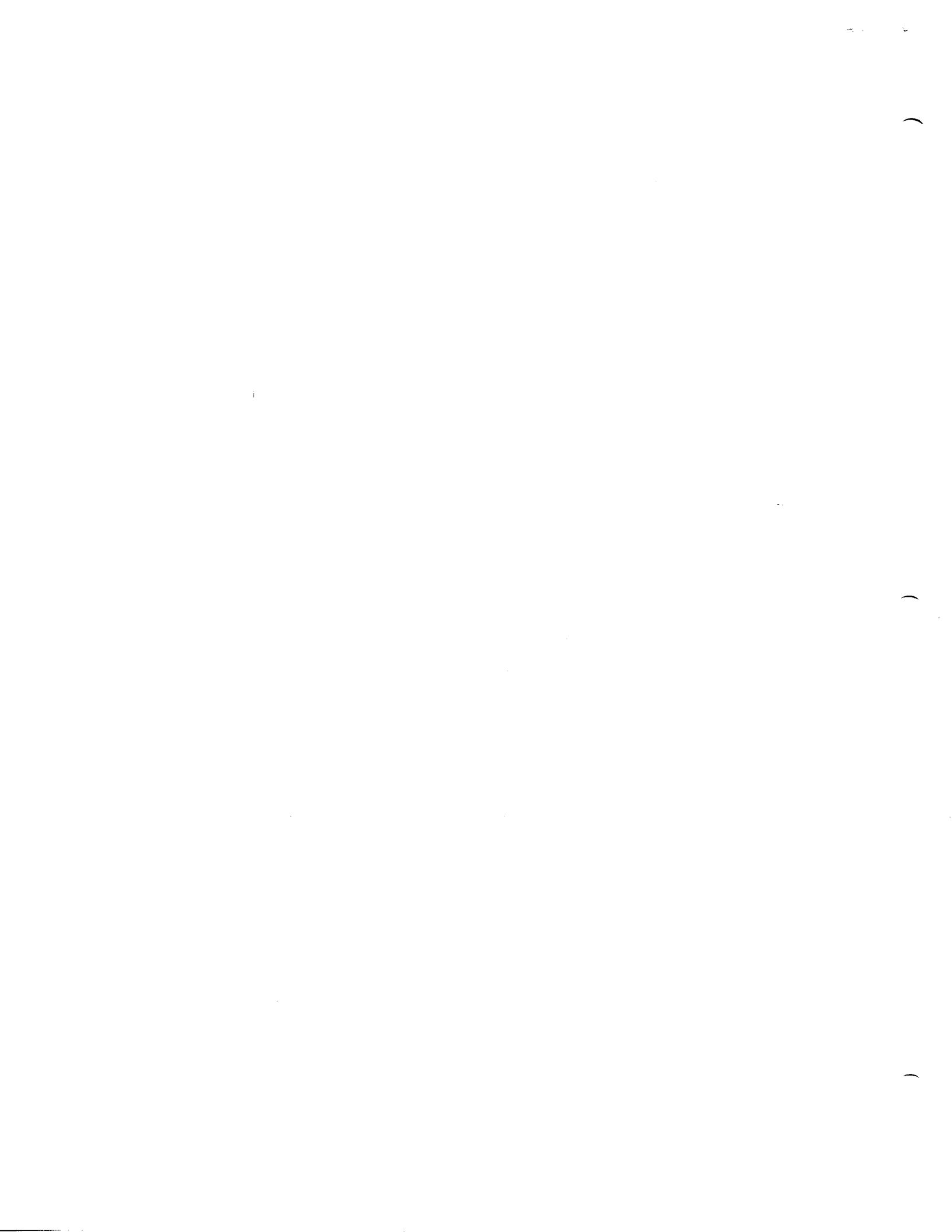


Figure 4. Wire rope in tension on sheave (exaggerated)



**THIRTEENTH
TRANSDUCER
WORKSHOP**

4-6 JUNE 1985

MONTEREY, CALIFORNIA

**TRANSDUCER COMMITTEE
TELEMETRY GROUP
RANGE COMMANDERS COUNCIL**

Published and Distributed by

**Secretariat
Range Commanders Council
White Sands Missile Range,
New Mexico 88002**

100

100

100

100

100

100

DISCLAIMER

This document has been published for information purposes only. The material contained herein does not necessarily represent the position or conclusions of the Range Commanders Council (RCC).

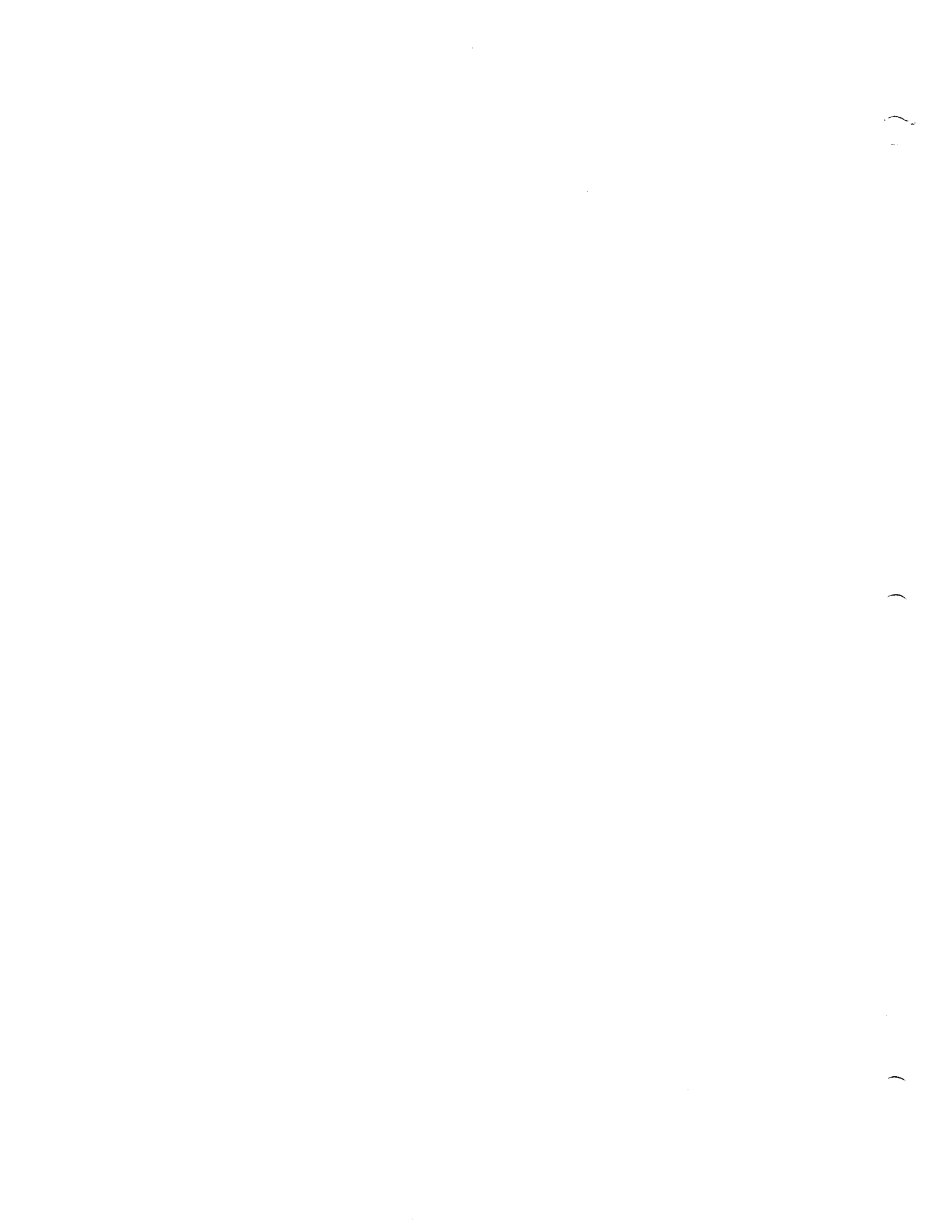


TABLE OF CONTENTS

	<u>PAGE</u>
INTRODUCTION - WELCOMING ADDRESS.....	vii
TELEMETRY GROUP COMMITTEES.....	xiii
TRANSDUCER COMMITTEE OBJECTIVES.....	xv
TRANSDUCER WORKSHOP SUMMARY.....	xvii
AGENDA - DEFINITION OF THE TRANSDUCER WORKSHOP.....	xix
LIST OF ATTENDEES.....	xxiii
SESSION 1	1
"A Minicomputer-Based Sensor Calibration System" - Martha Pierce Willis, Rockwell International.....	2
"Automating Accelerometer Calibrations for Users" - David Banaszak, Air Force Wright Aeronautical Labs.....	10
"Quantifying Automotive Test Course Profiles" - W. H. Connon, S. F. Harley, J. Schimminger, T. Shrader, Material Testing Directorate, Aberdeen Proving Ground...	23
Discussion Summary.....	39
SESSION 2	49
"Rms Response of an Accelerometer to a Random Vibration Environment" - Dr. G. A. Articolo, Schaevitz Engineering	50
"An Intelligent Amplifier" - Richard D. Talmadge, Air Force Wright Aeronautical Labs.....	81
"An Improved Particle-Velocity Transducer for Equation- of-State Experiments - Sam J. Spataro, Lawrence Livermore National Laboratory.....	92
"Instrumenting and Interpreting the Time-Varying Response of Structural Systems" - P. L. Walter, Sandia National Laboratories.....	115
Discussion Summary.....	137

	<u>PAGE</u>
SESSION 3.....	147
"A 150,000 Pounds Per Square Inch Dynamic Pressure Calibrator" - A. A. Juhasz, D. H. Newhall, C. D. Bullock, J. O. Pilcher II, M. B. Krummerich, U.S. Army Ballistic Research Laboratory.....	148
"Evaluation of a New High Pressure Transducer" - J. R. Miller III, Lori Edmondson, Greg Rigney, D. E. Woodliff, Physical Standards & Development Laboratory.....	162
"'Aronson' Shockless Pressure-Step Generator" - J. F. Lally, PCB Piezotronics, Inc.....	204
"Ceramic Diaphragm Thick Film Strain Gage Pressure Transducer" - Jean-Pierre Pugnare, DJ International, Inc.....	214
"Sensors for Shock Pressure Measurements in Confined Explosives" - James G. Faller, J. David Dykstra, U.S. Army Combat Systems Test Activity, Aberdeen Proving Ground.....	220
"Underwater Blast Measurements" - Larry L. Brown, Denver Research Institute.....	245
Discussion Summary.....	261
SESSION 4.....	273
Manufacturers' Panel - Peter K. Stein, Chairman.....	274
SESSION 5.....	275
"Recent Stress Gage Developments" - J. Kalinowski, T. Stubbs, L. Davies, EG&G Energy Measurements, Inc.; B. Hudson, Lawrence Livermore National Laboratories.....	276
"Practical Application of Magnetostriction to a High-Speed Torquemeter" - Francis E. Scoppe, Kenneth S. Collinge, AVCO Lycoming Division.....	287
"Multiplexing Instrumentation Cables Downhole" - D. B. Longinotti, EG&G Energy Measurements, Inc.....	300
"High Accuracy Rotary and Linear INDUCTOSYN [®] Position Transducers" - George Quinn, Farrand Industries, Inc....	309
Discussion Summary.....	326

ROBERT H. SCHUMAKER
Rear Admiral, USN
Superintendent
U.S. Naval Post Graduate School

INTRODUCTION - WELCOMING ADDRESS

We know that the introductions may be longer than the address. I heard a story the other day about a fellow who was in Washington for many years and his wife asked him to accompany her to her hometown in Oklahoma to talk, among other things, to the Rotary Club. And in sharp contrast to the introduction I just got here, the president of the Rotary Club got up and said, "Now we're going to hear the dope from Washington." He wasn't real sure whether that was contrived or accidental. Well, this really isn't much of an address. It's more of a welcome to sunny Monterey. Hang in there folks, it's going to turn sunny; I see some blue off in the sky there.

Transducers. I'll tell you about all I know about transducers in about the next 30 seconds. My understanding is it's a device for changing energy of one form to another form. Generally, low power applications, mostly involving signals of communication.

I'll tell you a story about communication. I really believe in communication. In fact, I was going to bring a transducer in to show you today. It looks very similar to a metal cup. You see when we were in Vietnam, the Vietnamese philosophy was to separate prisoners from each other. The theory is a prisoner will be more pliable and susceptible to propaganda. So they had a guard to prisoner ratio of 1 1/2 to 1. It was so high in order to keep prisoner A from talking to prisoner B. Well, we thwarted them through a communication system. We were living in separate cells with walls made of concrete about a foot thick. We could tap very lightly on one wall and it would be received on the other. But if we were caught they'd hammer us pretty hard. So we took this transducer; now this is energy, mechanical tapping energy that got transduced into or reconfigured into acoustic energy. Very, very softly we'd take this cup, turn it upside down, put it against the wall, and be able to hear just very, very soft tapping. If you're curious, the tapping code was a kind of simple one. Most of us aviators knew Morse Code, but when you tap you don't have those two binary dots and dashes. You just have little pecking things. So what we did was to take the alphabet and arrange it into a matrix of five rows and five letters. We had to leave off one letter, of course, and that was the letter K. The first row would read A, B, C, D, and E. We called it the AFLQV code because that's the first column. If you wanted to send the letter D for example, it would be one for first row and the fourth column. You could get going pretty fast with this code which sounded like a bunch of soft woodpeckers in there with the aid of that transducer cup.

I'll tell you a story about communication too. A woman experiencing marital problems that might end in a divorce approached a marriage counselor. The counselor, in exploring the problem, asked her if she had any grounds. She thought for a minute and said, "Well,

yes. We have about five acres around the house." He said, "No, what I meant was do you have a grudge?" And she said, "No, we don't, but we have a carport." Almost in exasperation, the counselor said, "Well, does he beat you up?" "Not really, she said, I get up about 15 minutes before he does, but I think we have a communication problem."

I'd like to tell you before I forget that I did use transducers a lot. One of the missiles that I got involved with as a major project manager was the HARM missile, which stands for High Speed Anti-Radiation Missile. When fired from an airplane, it would go zinging on out some distance and blow up the enemies radar sets. We went through quite a number of years of testing that very sophisticated missile. Usually you think of a radar missile as having a little antenna that swings back and forth. This missile doesn't have any moving parts except the wings. I'm not sure I ever figured out how it works, but it does. Anyway, we had a lot of transducers there to control its flight profile, and we had some difficulties at times. Some of the transducers wouldn't pick up the right signals and that put us on a different profile than we wanted. So that's the challenge I'm throwing to you is to improve those transducers.

I would like to tell you a little bit about the school that's operated just down the road here. This is my flight lieutenant, Lieutenant Williams. This school has been around for about 76 years but not always here in Monterey. It was in Annapolis starting in 1909, and then in 1952 in what may have been the latest, or the best land grab since Seward's Folly, the Navy bought these six hundred acres in all. There was an old hotel there that had been constructed in 1870. It was called the Del Monte Hotel and it was in the center of the Monterey Peninsula which we're showing right here - the social center of it, that is. I hate to tell you what we paid for it; 2.5 million bucks and that would probably buy my house that's located in there now. We built a number of academic buildings. Here's the main campus, and in this location we have a number of houses for our students. We have about 1600 students; however, we can only accommodate about 60% of them. The rest are scattered around town in rental places. There's another school in town run by the Army that's sometimes confused with ours. It's the Defense Language Institute with about 3000 students, and it's located right at what we call the Presidio of Monterey. This whole area is a hill. There's a road and from here to here is only about four miles, but there are a lot of bends in the road. The road turns out to be about 17 miles as you roam around there. It costs you about four dollars to get in the gate. This is the highest point of the peninsula. And there's a gate there, one over in Carmel, and two in Pacific Grove. If you do have time and haven't done that before I think you'd enjoy that ride, particularly this area down in here along Pebble Beach. Golfing is the big thing and there are four golf courses. The town of Carmel is really called Carmel-by-the-Sea. What doesn't show on the map is a valley that goes out in this direction about 12 miles called Carmel Valley.

The mission of the school is the advanced education of commissioned officers; primarily men who wear my color of uniform. We have quite a number of people there. I'll show you the composition of

the school in a moment. Basically, the school offers a master's degree program with most of the 1600 students working on that degree and about 25 students working on a professional engineering degree. We provide other services as asked, and we do quite a bit of research at this place - about 15 million dollars worth. The theory behind the research is that our professors are sharper as a result of keeping their skills honed. Every officer in the Navy has a primary skill, and Lieutenant William's primary skill is keeping me happy, I guess. But, most important is that he's a surface officer and I'm an aviator and those are primary warfare skills. About 11 percent of our 70 thousand officers have subspecialties; however, we're trying to increase that to about 20 percent. A subspecialty would be acquired through a master's degree either at the school down the road or somewhere else. For example, my subspecialty is electrical engineering, where normally I would be flying airplanes on one tour and then come ashore to a job called a billet in the Navy, that would use those skills as an electrical engineer. I don't want to dwell on the coding system here. Let's go ahead with the next viewgraph which, I think, shows it a little bit better.

This time line shows how you can become an admiral in 25 years, that's from ensign to admiral. What we're showing up here is about a year into a person's commissioning. We have a group at the school down the road that reviews their college transcripts and their exposure to math and physics. Then we do a screen and about 93 percent of them are acceptable for one of the 41 curricula we teach. After about four or five years, we have a screening board in Washington that judges not only their academic performance but how well they performed as an officer and their potential for leadership. The one in three that passed the screen can volunteer for the school. They are not ordered to the school because the two years they spend at the school obligates them to four years of additional service. But if that person does volunteer (and by the way they aren't all males, we have about eight percent females in that school), they're in school for a two-year period. From then on until they make admiral, they're cycling back and forth between sea duty and a warfare tour. Then they'd go into whatever is their subspecialty: aeronautical engineering, transducers, or financial management. We like to get about 750 naval officers a year into post-graduate education; however, they don't all come to Monterey. About 80 percent of them come to Monterey, and about 20 percent are sent to MIT or other schools that teach curricula we're not involved in. We bring students in every three months and graduate them every three months. The input isn't always the same as the output, so we fluctuate a bit through the year. This particular one we're a little lower than we expect to be in about three months. But this blue line, naturally, is the Navy and within the Navy we have communities. Here's the aviation community and the general line community. About 62 percent of those students are U.S. Naval officers and the red guys are the Army, Air Force, Marines, and others. I showed this viewgraph at a space conference we had about ten days ago. I'm surprised you people didn't put the bite on me for an auditorium. We have an auditorium with about 1000 seats down there, so it gets a lot of action. There was a marine general there and he saw that I'd stuck him between - he claimed - the Greeks and Turks. He got a

little mad about the whole thing, so I'm redoing the viewgraph. In fact, I listed him as an other. They'll probably put me back to ensign here pretty shortly.

This as you can see is a computer printout. What we're showing here are numbers of people. Here, the electrical engineering and communication engineering people have about 250 to 250 students and the code on the other side shows that these are the Navy and those are from other services including the Marines. Those are the international guys up there. About 75 percent of these curricula, about 30 of them, are from engineering and scientific fields, the rest of them are from intelligence, political science, and other such fields.

If you read the paper, the thin little paper we put out here, The Monterey Peninsula, this morning, you know that the Navy has been taking some licks. Even before you make it into the office in the morning, you'll see that they captured a fourth spy. They're nipping on the heels of Rickover trying to close down General Dynamics. There was an editorial about the Star Wars program here, and something about ashtrays that caused a friend of mine to get fired. We are working our way through these problems, and one of the reasons we're discovering some of these problems is we have this very aggressive Secretary of the Navy, John Lehman. He's really jumping in and doing a fine job of helping us clean house. Unfortunately, when you start sweeping things, there are some things that get kicked up in the air, so let me tell you what we're trying to do to correct situations like the ashtrays, for example. Ashtrays are nothing compared to F18s, but the philosophy is that we want to be good stewards of the public trust and we want to squeeze that dollar for every value it's capable of giving. And so when something like that happens, I think Lehman is doing just the right thing, making sure people are indeed accountable for their decisions.

Some of you are familiar with a Navy procurement system or materiel world. For years we operated with a materiel command in Washington. There was a four-star admiral who ran the systems commands. The Naval Air Systems Command was the one I worked for. Well, we abolished that Navy Materiel Command several months ago and the four-star admiral is now retired. Actually, in my judgement, we should have done that about ten years ago to get rid of the layering. We are putting a lot of emphasis in the Navy on the procurement of materiel and trying to do it in an efficient manner. And notwithstanding are a few of these bizarre cases that come out like hammers, ashtrays, diodes, and things that the newspapers have picked up. Incidentally, most of these situations, the \$400 hammer, come about as a result of our own internal auditing. One of the sad things, and this sounds like a defensive statement I suppose, is that the newspapers pick up on our own internal audits and it comes out in the presses that the newspaper has picked up all this stuff. We are really trying to clean up our own shop.

One of the things that I'm excited about is a thing called the materiel professional. And if you'll look back over the last hundred years of the Navy, we've tried this concept a couple of times. It's called the wet/dry concept where a Naval officer is either an operator

running ships around or flying airplanes, or he's a dry sailor and doesn't go to sea very often because he's involved in materiel acquisition. That hasn't really worked out too well in the last two or three times we've tried it. The reason it hasn't worked out too well is because the dry sailors forget that the whole reason we're in business is because of the wet side. They lose the communication skills. What we're trying now is this concept of the materiel professional, where we are going to have about one third of our flag officers in the Navy, we have about 250 flag officers, but one third of these fellows are going to be dry sailors or materiel professionals. They're going to become experts in acquisition and contracting and just hard-nosed business men. I think this time it's going to work because we're not going to transition those people until a later time in their career. In fact, I mentioned the admirals, but really starting at the rank of commander we're going to allow officers who have the skills to transition into this materiel professional. By the time they're commanders they've had about 20 years of service and they've enough blue water in their veins so they don't forget the wet side. Then they become skilled professional people in the acquisition world.

Well, I think that's about all I wanted to chat with you about unless you have some questions. I think you will enjoy your tour down there at the school tomorrow afternoon. Be sure to see the museum down in the basement. I think we have the best view in town from the top of the tower and the public affairs officer will run you through there. The school burned down twice. It was built in 1870 and burned down seven years later, they rebuilt it but had a hell of a time with the Public Works Department because they rebuilt it in a year's time. Just to show you the callousness of some of the people that came to the hotel. They were rather wealthy people. It burned down again in 1925 during a ball. The ballroom caught on fire late at night, so the orchestra just moved out on the lawn and started playing "There'll Be A Hot Time In The Old Town Tonight." At any rate, they rebuilt it in 1925, fortunately. I'd appreciate no smoking because I don't want that place burned down on my watch. Enjoy the tour. There are other exciting things to do in town. We recently built an aquarium and if you get a chance, I think you'd enjoy that. It's a 50 million dollar aquarium located down on Cannery Row. Are there any questions you'd like to address to me? I hope you have a good stay here and enjoy yourselves. Thank you.

)

)

)

TELEMETRY GROUP COMMITTEES

Chairman, Don K. Manoa (WSMC)
Vice Chairman, Phillip D. Sharp (WSMR)

Data Multiplex
RF Systems
Recorder/Reproducer
Vehicular Instrumentation/Transducer

MEMBERS OF THE VEHICULAR INSTRUMENTATION/TRANSDUCER COMMITTEE

LeRoy Bates
NSWSES - Code 4250
Port Hueneme, CA 93043

Larry Rollingson
NWC - Code 6421
China Lake, CA 93555-6001

Richard Hasbrouck
Lawrence Livermore National Laboratories
P.O. Box 808, L154
Livermore, CA 94550

Steve Kuehn
Sandia National Laboratories
P.O. Box 5800, Div. 7545
Albuquerque, NM 87185

Walter Lipe
6520 TESTG/ENID, Stop 239
Edwards AFB, CA 93523-5000

John Ach
AFWAL/FIBGA
Wright-Patterson AFB, OH 45433

Pat Curran
NWC - Code 6213
China Lake, CA 93555-6001

Dennis Henry
Physical Science Laboratory
New Mexico State University
P.O. Box 3548
Las Cruces, NM 88003

Raymond Faulstich
NATC
Range Directorate (RD42)
Patuxent River, MD 20670-5304

Richard Krizan
ESMC/RSL
Patrick AFB, FL 32925-5532

)

)

)

TRANSDUCER COMMITTEE OBJECTIVES

This committee informs the Telemetry Group (TG) of significant progress in the field of telemetry transducers; maintains any necessary liaison between the TG and the National Bureau of Standards and their transducers' program or any other related telemetry transducer efforts; coordinates TG activities with other professional technical groups; collects and passes on information on techniques of measurement, evaluation, reliability, calibration, reporting and manufacturing; and recommends uniform practices for calibration, testing and evaluation of telemetry transducers.



TRANSDUCER WORKSHOP SUMMARY

<u>Workshop Number</u>	<u>Date</u>	<u>Host</u>	<u>General Chairman</u>	<u>Number Attendees</u>	<u>RCC TG Transducer Chairman</u>
1	March 1960	Albuquerque, NM			
2	25-26 July 1961	Holloman AFB Alamogordo, NM	W. M. Sanders Holloman AFB, NM	46	Paul Polishuk Wright-Patterson Dayton, OH
3	21-23 June 1962	NBS Washington, D.C.	Arnold Wexler NBS Washington, D.C.	106	Paul Polishuk Wright-Patterson Dayton, OH
4	18-19 June 1964	Wright-Patterson Dayton, OH	Jack Lynch NATC Patuxent River, MD	53	Jack Lynch NATC Patuxent River, MD
5	3-4 October 1967	NBS Gaithersburg, MD	Loyt L. Lathrop Sandia Labs Albuquerque, NM	106	Loyt L. Lathrop Sandia Labs Albuquerque, NM
6	22-24 October 1969	Langley Research Ctr. NASA Hampton, VA	Paul Lederer NBS Washington, D.C.	49	Loyt L. Lathrop Sandia Labs Albuquerque, NM
7	4-6 April 1972	Sandia Labs Albuquerque, NM	W. G. James AEFDL Wright-Patterson Dayton, OH	111	Pat Walter Sandia Labs First Manufacturers' Panel Boo-Boos
8	22-24 April 1975	Wright-Patterson Dayton, OH	Pierre F. Fuselier Lawrence Livermore Labs Livermore, CA	74	Pat Walter Sandia Labs

XVII

<u>Workshop Number</u>	<u>Date</u>	<u>Host</u>	<u>General Chairman</u>	<u>Number Attendees</u>	<u>RCC TG Transducer Chairman</u>
9	26-28 April 1977	Fort Walton Beach Eglin AFB, FL	Kenny Cox NWC China Lake, CA	100	William Anderson Patuxent River, MD
10	12-14 June 1979	Colorado Springs Colorado North American Air Defense Command	Richard Hasbrouck Lawrence Livermore Labs Livermore, CA	106	William Anderson Patuxent River, MD
11	2-4 June 1981	Seattle, WA, Air Force Plant Repre- sentative Office, Det. 9	LeRoy Bates NSWSES Port Hueneme, CA	95	William Anderson Patuxent River, MD
12	7-9 June 1983	Melbourne, FL Patrick AFB, FL	Kenneth D. Cox NWC China Lake, CA		William Anderson Patuxent River, MD
13	4-6 June 1985	Monterey, CA	Richard Krizan Patrick AFB, FL		LeRoy Bates NSWSES Port Hueneme, CA

THIRTEENTH TRANSDUCER WORKSHOP

DEFINITION OF THE TRANSDUCER WORKSHOP

History:

The Workshop is sponsored by the Vehicular Instrumentation/Transducer Committee, Telemetry Group, of the Range Commanders Council. This committee is tasked to provide IRIG Standards for transducer applications. The twelve previous workshops, beginning in 1960, were held at two year intervals at, or near, various U. S. Government installations around the country.

Attendees:

Attendees are working-level people who must solve real-life hardware problems and are strongly oriented to the practical approach. Their field is making measurements of physical parameters using transducers. Test and project people who attend will benefit from exposure to the true complexity of transducer evaluation, selection, and application.

Subjects:

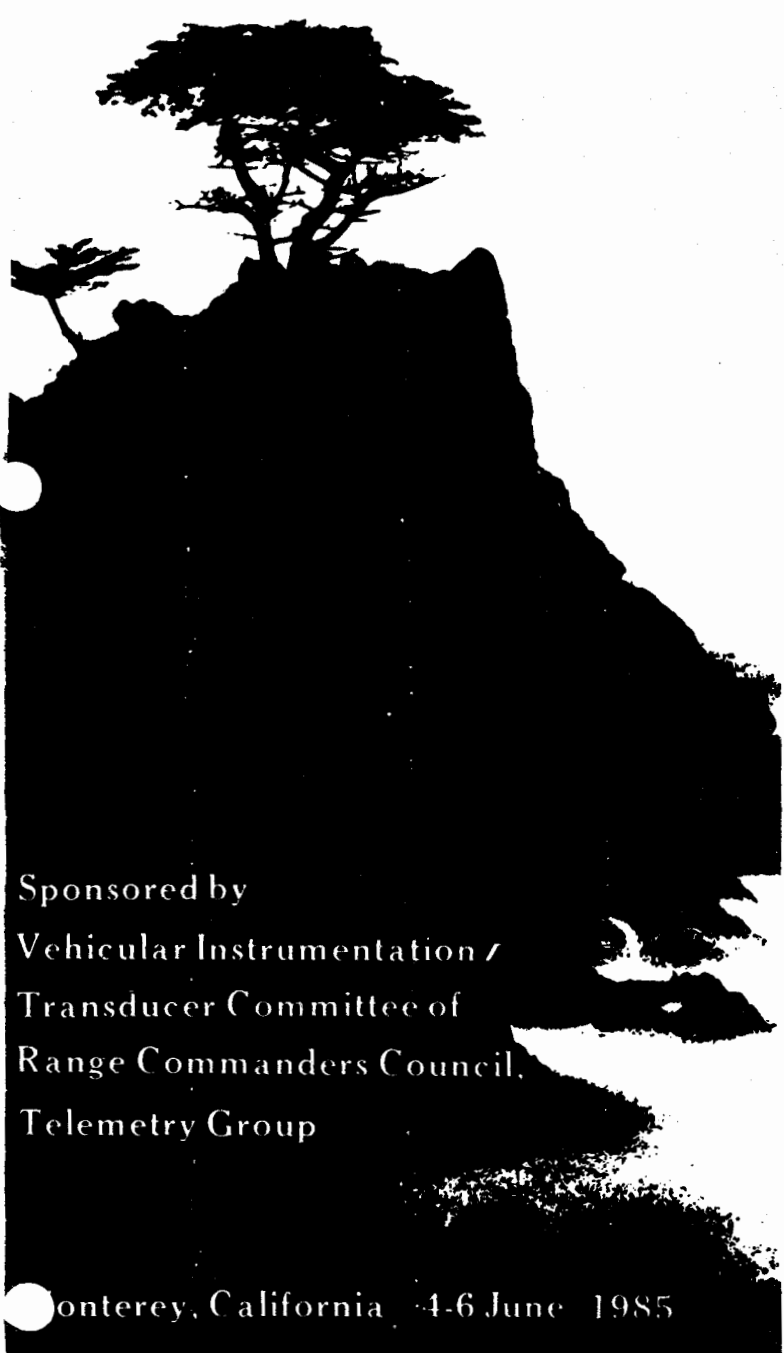
Practical problems involving transducers, signal conditioners, and readout devices will be considered separately and in systems. Engineering tests, laboratory calibrations, transducer developments and evaluations represent potential applications of the ideas presented. Measurands include force, pressure, flow, acceleration, velocity, displacement, temperature and others.

Emphasis:

1. A practical approach to the solution of measurement problems.
2. Strong focus on transducers and related instrumentation used in measurements engineering.
3. The ratio of discussion to presentation of papers is high.
4. Open discussion and problem solving through the sharing of knowledge and experience. Session chairmen will present the speakers as a panel to stimulate discussions with and within the audience.

Goals:

To bring together those people who use transducers; to identify problems and hopefully suggest some solutions; to identify areas of common interest; and to provide a



Sponsored by
Vehicular Instrumentation /
Transducer Committee of
Range Commanders Council,
Telemetry Group

Monterey, California 4-6 June 1985

communication channel within the community of transducer users. Some examples are:

1. Improve the coordination of information regarding transducer standards, test techniques, evaluations, and application practices among the national test ranges, range users, range contractors, other transducer users, and transducer manufacturers.

2. Encourage the establishment of special sessions so that attendees with measurement problems in specific areas can form subgroups and remain to discuss these problems after the workshop concludes.

3. Solicit suggestions and comments on past, present and future Vehicular Instrumentation/Transducer Committee efforts.

General Chairman

RICHARD KRIZAN

ESMC/RSL

Patrick AFB, Florida 32925

(305) 494-5107 Autovon 854-5107

PROGRAM

MONDAY, 3 JUNE 1985

2000 Social Hour, at the Holiday Inn, courtesy of the Vehicular Instrumentation/Transducer Committee
All attendees welcome.

TUESDAY, 4 JUNE 1985

0730 Registration
0800 Welcome: ROBERT H. SCHUMAKER, Commodore USN, Superintendent U. S. Naval Post Graduate School
Introductions: LEROY BATES, Chairman Vehicular Instrumentation/Transducer Committee, RCC/TG
RICHARD KRIZAN, General Chairman
Thirteenth Transducer Workshop

0900 Session 1:
Chairman: WILLIAM D. ANDERSON, Naval Air Test Center
Paper Presentations (15- 20 minutes each):

* "Large Torque Calibration System"
Dennis Page,
Calibration Lab, White Sands Missile Range

* "A Microprocessor Based Sensor Calibration System"
M. P. Willis,
Rocketdyne

1015

1030

1130

1200

1330

* "Automating Accelerometer Calibrations For Users"
David Banaszak,
U. S. Air Force AFWAL

* "The Aberdeen Proving Ground Test Course Profilometer"
W. H. Connon III,
U. S. Army Combat System Test Activity

BREAK

Session 1 open discussion, with speakers sitting as a panel
"Telemetry Group Function and Goals," LEROY BATES, Chairman, Vehicular Instrumentation/Transducer Committee

LUNCH

Session 2:

Chairman: STEVE KUEHN, Sandia Laboratories
Paper Presentations (15- 20 minutes each):

* "Correction Of Abberant Signals In High G Shock Accelerometry"
Donald Baker Moore,
Explosives Tecnology

* "RMS Response Of An Accelerometer To A Random Vibration Environment"
G. A. Articulo Ph. D.,
Schaevitz Engineering

* "Automatic Gain Ranging Amplifer"
Richard Talmadge,
Air Force Wright Aeronautical Laboratories

* "An Improved Particle Velocity Transducer For Equation Of State Experiments"
Sam Spataro,
Lawrence Livermore National Laboratory

* "Instrumenting And Interpreting The Time-Varying Response Of Structural Systems"
Dr. Patrick Walter,
Sandia Laboratories

1500

BREAK

1515

Session 2 open discussion, with speakers sitting as a panel

WEDNESDAY, 5 JUNE 1985

0830

Session 3:
Chairman: LARRY SIRES,
Naval Weapons Center
Paper Presentations
(15- 20 minutes each):

- * "Dynamic Step Calibration Of Ballistic Pressure Transducers"
Arpad A. Juhasz & Charles D. Bullock,
U. S. Army DARCOM/Ballistics Research Laboratory
- * "Evaluation Of A New High Pressure Transducer"
J. R. Miller III,
U. S. Army TMDE Support Group
- * "Shockless Pressure Step Generator"
J. F. Lally,
PCB Piezotronics Inc.
- * "Ceramic Diaphragm Thick Film Strain Gage Pressure Transducers"
John Pugnaire & Fred Smith,
DJ Instruments Inc.
- * "Shock Pressure Measurements In Confined Explosive Charges"
J. G. Faller & J. D. Dykstra,
U. S. Army Combat Systems Test Activity
- * "Underwater Blast Pressure Measurements"
Larry L. Brown,
Denver Research Institute

1030

BREAK

1045

Session 3 open discussion, with speakers sitting as panel

1145

LUNCH

1300

Tour of Del Monte Hotel and Seventeen Mile Drive

1730

No-host social hour at hotel

1830

Banquet at hotel

2000

Session 4: Manufacturers' Panel
Chairman: PETER K. STEIN,
Stein Engineering Services, Inc.

0830

Panel Members:
PRECISE SENSORS
HOTTINGER BALDWIN MEASUREMENTS, INC.
EATON CORPORATION
HY-CAL ENGINEERING
TELEDYNE TATOR
GULTON INDUSTRIES, INC.

THURSDAY, 6 JUNE 1985

Session 5:
Chairman: JOHN ACH,
Air Force Wright Aeronautical Laboratories
Paper Presentations
(15- 20 minutes each)

- * "Recent Stress Gage Development At Lawrence Livermore Laboratories"
J. Kalinowski, L. Davies,
B. Hudson, and T. Stubbs
EG & G Inc.
- * "Multiplexing Ground Motion Instrumentation Cables Downhole"
David B. Longinotti,
EG & G Inc.
- * "Practical Application Of Magnetostriction To A High Speed Torquemeter"
F. E. Scoppe & K. S. Collinge,
Avco Lycoming Division
- * "High Accuracy Rotary And Linear Position Transducers"
George A. Quinn,
Farrand Controls

BREAK

Session 5 open discussion, with speakers sitting as a panel

LUNCH

Session 6: Informal Wrap-up
Chairman: LEROY BATES, Naval Ships Weapon System Engineering Station

This session is provided to encourage small group discussions between transducer users and vendors with regard to instrumentation problems and future needs.

BREAK

Closing Remarks - Vehicular Instrumentation/Transducer Committee

WORKSHOP CONCLUDES

1000
1015

1130
1300

1410
1420

1500

GENERAL INFORMATION

This Thirteenth Transducer Workshop will be held 4-6 June 1985 at the Holiday Inn on the Del Monte Beach in Monterey, California. The hosting agency is the Naval Post-Graduate School.

Registration

The registration consists of two parts: a written "Murphyism" of one page or less, and a fee of \$60.00.

A "Murphyism" can describe any measurement attempt that went astray, with the objective of learning from our errors and keeping our feet on the ground. It should be something generic rather than common human oversight--something from which we can learn. The tone should be relaxed, with a sense of humor. The "Murphyism" should be anonymous and must not embarrass any person, organization, or company. While this is not a mandatory requirement, the "Murphyism" submissions are strongly encouraged; and the best will be included in the program.

Advance registration is desirable. Please use the enclosed registration form, include a check or money order for \$60.00 payable to the Thirteenth Transducer Workshop, and mail to the Workshop Treasurer by 17 May 1985. (Note: Purchase orders are not acceptable.)

The registration fee covers coffee, tea, soft drinks, and doughnuts, the Wednesday evening fixed-menu dinner at the hotel, Del Monte Tour, and a copy of the proceedings of the workshop. Late registration will be provided for at the Workshop registration desk in the hotel.

Hotel Accommodations

The official hotel for the Workshop is the Holiday Inn, 2600 San Dunes Drive, Monterey, California 93940. A block of rooms has been reserved at the special rates indicated on the enclosed registration card. Hotel registrations must be received by 10 May 1985.

No formal program will be provided for spouses or guests. However, they will be most welcome at the Social Hour on Monday and the dinner on Wednesday (\$20.00 additional per guest for the dinner). Note: Final count for the banquet must be known by 11 am, 4 June.

Tour - Wednesday Afternoon

A 3-1/2 hour tour of the Del Monte Hotel, Carmel Mission, and Seventeen Mile Drive is planned for Wednesday, June 5, 1985. Please indicate on the registration form if you will be accompanied by guests so that adequate transportation may be provided. Cost per guest is \$13 regardless of age and may be included with the advanced registration fee.

Format and Background

The traditional discussion format will be observed. Workshops are just what the name implies: everyone should come prepared to contribute something from his knowledge and experience. In a workshop the attendees become the program in the sense that the extent and enthusiasm of their participation determines the success of the workshop.

Participants will have the opportunity to hear what their colleagues have been doing and how it went; to explore areas of common interest and common problems; to offer ideas and suggestions about what's needed in transducers, techniques, and applications. A few manufacturers, selected to represent a fair sampling of transduction methods and measurands, have been invited to the Thirteenth Transducer Workshop. Consider the questions, comments, and topics you want to present to the manufacturers. Include them with your mail, in registration form, or they may be left at the registration desk on Tuesday morning.

Additional Information

May be obtained from the General Chairman or, Proceedings Chairman and Treasurer

LEROY BATES
NSWSES Code W250
Port Hueneme, CA 93043
(805) 982-4569
(Autovon) 360-4569

Facilities and Local Support Chairman

PAT CURRAN
Naval Weapons Center, Code 6213
China Lake, CA 93555
(619) 939-7427
(Autovon) 437-7427

Papers Chairman

LARRY ROLLINGSON
Naval Weapons Center, Code 6421
China Lake, CA 93555
(619) 939-3761
(Autovon) 437-3761

LIST OF ATTENDEES

ACH, John T.
Air Force Wright Aeronautical Labs.
FIBGA
Wright-Patterson AFB, OH 45433

ANDERSON, William D.
Naval Air Test Center
Range Directorate
Patuxent River, MD 20670-5304

ARTICOLO, George (Dr)
Schaevitz Engineering
P.O. Box 505
Camden, NJ 08101

BANASZAK, David
AFWAL/FIBGB
Wright-Patterson AFB, OH 45433

BARTHELOW, Patrick J.
Performance Data Systems
810 Airport Road
Monterey, CA 93940

BATEMAN, Vesta I.
Sandia National Labs.
Division 7545
P.O. Box 5800
Albuquerque, NM 87185

BATES, LeRoy
NSWSES
Code 4250
Port Hueneme, CA 93043-5007

BELENSKY, Charles R.
Grumman Aerospace Corp.
M/S T01-05
Bethpage, NY 11714

BENEDICT, Frank L.
Endevco
1717 So. State College Blvd.
Suite 180
Anaheim, CA 92806

BOHLE, Robert J.
Gould/Statham
27051 Encinas
Mission Viejo, CA 92692

BOREMANN, D.
Monsanto Research Corp.
Miamisburg, OH 45342

BRODERICK, N. E.
EG&G/SRO ENG
2801 Old Crow Canyon Road
San Ramon, CA 94583

BROWN, Larry L.
Denver Research Institute
LAM Division
University of Denver
P.O. Box 10127
Denver, CO 80210

BROWN, Vondalee
Denver Research Institute
LAM Division
University of Denver
P. O. Box 10127
Denver, CO 80210

BULLOCK, Charles D.
Ballistic Research Laboratory
DRDAR-BLT
Aberdeen Proving Ground, MD
21005-5066

CAYERE, Paul
Physics International Co.
2700 Meeced St.
San Leandro, CA 94577

CLARK, Robert F.
Endevco
1717 So. State College Blvd
Suite 180
Anaheim, CA 92806

CLARKE, Harry
Naval Air Test Center
Range Directorate (TS-70)
Patuxent River, MD 20670-5304

CLARKE, Helen M.
Naval Air Test Center
Systems Engrg. Test Directorate
(S4JO)
Patuxent River, MD 20670-5304

CLARKE, Richard N.
Celeco Transducer Products, Inc.
7800 Deering Drive
Canoga Park, CA 91304-5005

CLAYTON, Wilson A.
HY-CAL Engineering
9650 Telstar Avenue
El Monte, CA 91731

COLEE, Andrew
3246 Test Wing/TFED-2
(Airborne Instrumentation) Bldg 961
Eglin AFB, FL 32542

CONNON, W. H., III
U.S. Army Combat System Test Activity
Aberdeen Proving Ground, MD 21005

CURRAN, Pat
Naval Weapons Center
Code 6213
China Lake, CA 93555-6001

DAVIES, Lee
EG&G, Energy Measurements Group, Inc.
P.O. Box 1912, M/S N-28
Las Vegas, NV 89125

DIERCKS, Allen
Endevco
30700 Rancho Viejo Road
San Juan Capistrano, CA 92675

DORSEY, Jim
Measurements Group, Inc.
P.O. Box 27777
Raleigh, NC 27611

DUBLER, John M.
Kistler Instrument Corp.
75 John Glenn Drive
Amherst, NY 14120

DYKSTRA, J. David
U.S. Army Combat Systems Test Activity
STECs-E-BM (Dykstra), Bldg 363
Aberdeen Proving Ground, MD 21005-5066

ENGLUND, Mike
Garrett Turbine Engine Company
402-T S. 36th Street
Phoenix, AZ 85034

ERICKSON, LeRoy M.
Lawrence Livermore National Lab.
P.O. Box 808, L-368
Livermore, CA 94500

ESCUE, Tom
Gulton Servonic
P.O. Box 305
Tanner, AL 35671

FAULSTICH, Raymond J.
Naval Air Test Center
Range Directorate (RD-42)
Patuxent River, MD 20670-5304

FINNEY, Jefferson
EG&G, Energy Measurements Group, Inc.
P.O. Box 1912, M/S S-05
Las Vegas, NV 89125

FORBES, Chuck
Naval Weapons Center
Code 3354
China Lake, CA 93555-6001

FREYNIK, Henry S., Jr.
Lawrence Livermore National Lab.
P.O. Box 808, L-145
Livermore, CA 94550

GARTNER, Jeff
Travis Corporation
3636 Hwy 49 So.
Mariposa, CA 95338

GILMORE, Hal
General Dynamics
Box 85357, MZ 23-6624
San Diego, CA 92138

GRABENSTEIN, Charles
C. Grabenstein Industries, Inc.
50 Maple St., P.O. Box 603
Branford, CT 06405

GRANATH, Ben
PCB Piezotronics, Inc.
3425 Walden Ave.
Depew, NY 14043

GREEN, Louis F.
EG&G, Energy Measurements Group, Inc.
P.O. Box 1912, M/S S-05
Las Vegas, NV 89125

GREGORY, Lloyd
Canadian Forces
Box 1886
Grand Centre, Alberta, Canada Toaito

HALL, Gary C.
Computer Sciences Corp.
P.O. Box 715
Rosamound, CA 93560

HALL, John
Micro Engineering
14 N. Benson Ave.
Upland, CA 91786

HAM, Ben
Endevco
9004 Menaul, NE, #20
Albuquerque, NM 87112

HASBROUCK, Richard T.
Lawrence Livermore National Lab.
P.O. Box 808, L-154
Livermore, CA 94550

HATCH, Melton A., Jr.
EG&G/SRO Eng.
2801 Old Crow Road
San Ramon, CA 94583-9983

HATTAWAY, Clyde J.
AFATZ/DLMR
Eglin AFB, FL 32542

HAZELTON, Elmer
Gulton, Industries, Inc.
1644 Whittier Ave.
Costa Mesa, CA 92627

HENRY, Dennis G.
PSL/NMSU
P.O. Box 3548
Las Cruces, NM 88003

HOLSTEIN, Charles E.
TMDE Support Center
AMX-TM-CW-WS
White Sands Missile Range, NM 88002

HORNER, Jerry
EG&G, Energy Measurements Group, Inc.
P.O. Box 1912, M/S L-01
Las Vegas, NV 89125

JORGENSON, Eric D.
EG&G, Energy Measurements Group, Inc.
P.O. Box 1912, M/S L-01
Las Vegas, NV 89125

JUHASZ, Arpad A.
U.S. Army Ballistic Research Lab.
DRDAR-BLT
Aberdeen Proving Ground, MD 21005

KALINOWSKI, John A.
EG&G, Energy Measurements Group, Inc.
2801 Old Crow Canyon Road
San Ramon, CA 94583-9983

KITCHEN, Walter R.
EG&G, Energy Measurements Group, Inc.
P.O. Box 1912, M/S D-05
Las Vegas, NV 98125

KRUMMERICH, Melinda B.
Ballistic Research Laboratory
AMXBR-IBD
Aberdeen Proving Ground, MD 21005-5066

KRIZAN, Richard W.
ESMC/RSL
Patrick AFB, FL 32925-5532

KUEHN, Stephen F.
Sandia National Laboratories
P.O. Box 5800, Division 7545
Albuquerque, NM 87185

LALLY, Jim
PCB Piezotronics, Inc.
3425 Walden Ave.
Depew, NY 14043

LARA, J.
Lockheed Missile & Space Co., Inc.
P.O. Box 3504
Sunnyvale, CA 94088-3504

LEISHER, William B.
Sandia National Laboratories
P.O. Box 5800, Division 7545
Albuquerque, NM 87185

LICHT, Torbin
Bruel & Kjaer Instruments, Inc.
185 Forest Street
Marlborough, MA 01752

LONGINOTTI, David B.
EG&G, Energy Measurements Group, Inc.
2801 Old Crow Canyon Road
P.O. Box 204
San Ramon, CA 94583-9983

MACALUSO, Tom
MRT Corp.
320 Hillen Road
Towson, MD 21204

MAGDZIAK, John
Schaevitz Engineering
P.O. Box 505
Camden, NJ 08101

MAIER, Len
Endevco
30700 Rancho Viejo Road
San Juan Capistrano, CA 92675

McGEE, Jim
General Dynamics/Pomona
P.O. Box 2507
Mail Zone 4-53
Pomona, CA 91769

McLEOD, Donald
Naval Air Test Center
Technical Support Directorate
Patuxent River, MD 20670-5304

McMAHON, Daniel
Endevco
30700 Rancho Viejo Road
San Juan Capistrano, CA 92675

MILLER, Jim R., III
U.S. Army TMBE Support Group
AMXTM-SP, Bldg 5435
Redstone Arsenal, AL 35809

MILLER, Thomas B.
Lawrence Livermore National Lab.
P.O. Box 808, L-145
Livermore, CA 94550

MULHALL, J. Patrick
EG&G, Energy Measurements Group, Inc.
P.O. Box 1912, M/S L-01
Las Vegas, NV 89125

NOYES, Roger P.
EG&G, Energy Measurements Group, Inc.
P.O. Box 1912 M/S N-28
Las Vegas, NV 89125

ORTIZ, Monico
EG&G, Energy Measurements Group, Inc.
P.O. Box 1912, M/S N-28
Las Vegas, NV 89125

PAGE, Dennis
TMDE Support Center WSMR
AMX-TM-CW-WS
WSMR, NM 88002

PATTERSON, Gary R.
Precise Sensors
235 West Chestnut Street
Monrovia, CA 91016

POUNDS, Thomas S.
EG&G, Energy Measurements Group, Inc.
P.O. Box 1912, M/S S-05
Las Vegas, NV 89125

PUGNAIRE, Jean-Pierre
DJ Instruments, Inc.
18-T Republic Road
North Billerica, MA 01862

QUINN, George A.
Farrand Controls
99 Wall Street
Valhalla, NY 10595

RAMBO, John T.
Lawrence Livermore National Lab.
P.O. Box 808
Livermore, CA 94550

RECTOR, Norman
Lawrence Livermore National Lab.
P.O. Box 808, L-154
Livermore, CA 94550

REED, Ray
Sandia National Laboratories
Division 7116
Albuquerque, NM 87185

REMPERT, Lawrence A.
Allison Gas Turbine, Div. of GM
Box 420, S-6
Indianapolis, IN 46206

RENDLA, Gary M.
Endevco
30700 Rancho Viejo Road
San Juan Capistrano, CA 92675

ROLLINGSON, Larry
Naval Weapons Center
Code 6421
China Lake, CA 93555-6001

SCHELBY, Frederick
Sandia National Laboratories
Division 7545
Albuquerque, NM 87185

SCHONTHAL, Ernst
Bruel & Kjaer Instruments, Inc.
185 Forest Street
Marlborough, MA 01752

SCOPPE, Francis E.
Avco Lycoming Division
550 South Main Street
Stratford, CT 06469

SHAY, William M.
Lawrence Livermore National Lab.
P.O. Box 808, L-145
Livermore, CA 94550

SIEGEL, S. A.
Volumetrics
3025 Buena Vista Road
Paso Robles, CA 93446

SILL, Robert D.
Endevco
30700 Rancho Viejo Road
San Juan Capistrano, CA 92675

SIRES, Lawrence M.
Naval Weapons Center
Code 6213
China Lake, CA 93555-6001

SISEMORE, Clyde
Lawrence Livermore National Lab.
P.O. Box 808
Livermore, CA 94550

SMITH, Fred
D. J. Instruments, Inc.
18-T Republic Road
North Billerica, MA 01862

SMITH, Lawrence A., Jr.
Pacific Missile Test Center
Code 1032
Point Mugu, CA 93042

SPATARO, S. J.
Lawrence Livermore National Lab.
P.O. Box 808, L-201
Livermore, CA 94550

STEIN, Peter
Stein Engineering Services, Inc.
5602 E. Monte Rosa
Phoenix, AZ 85018

STONELAKE, Harry
Gulton Industries
Servonics Division
P.O. Box 1356
Ventura, CA 93002

STRINGHAM, Walt
Garrett Pneumatic Systems Division
P.O. Box 22200
Tempe, AZ 85282

STRY, Henry
Teledyne Tabor
455 Bryant Street
N. Tonawanda, NY 14120

STUBBS, T.
EG&G, Energy Measurements Group, Inc.
P.O. Box 1912
Las Vegas, NV 89125

STUEBNER, Gwen
Naval Weapons Center
Code 3354
China Lake, CA 93555-6001

TALMADGE, Richard D.
AFWAL/FIBGA
Wright-Patterson AFB, OH 45433

TAVIS, John A.
Tavis Corporation
3636 Hwy 49 So.
Mariposa, CA 95338

TAYLOR, Donald R.
U.S. Army Airborne Special
Operations Test Board
255 Ramona Drive
Fayetteville, NC 28303

THORSTENSEN-WOLL, Knut
Control Data, Canada
M.S. 3-11 H,
P.O. Box 8508
Ottawa, Canada

WILLIS, Martha
Rockwell International
Rocketdyne Division
6633 Canoga Ave., M/S 5311
Canoga Park, CA 91304

TUSSING, Ronald B.
Naval Surface Weapons Center
White Oak (R-15)
Silver Spring, MD 20910

WILT, Malcolm (Mack)
Lawrence Livermore National Lab.
P.O. Box 808, L-135
Livermore, CA 94550

ULRICH, Charles
Endevco
1717 So. State College Blvd.
Suite 180
Anaheim, CA 92806

WNUK, Steve
Hitec Corporation
65 Power Road
Westford, MA 01886

URTIEW, Paul A.
Lawrence Livermore National Lab.
P.O. Box 808, L-368
Livermore, CA 94550

YORGIADIS, Alexander
Strainsert Company
West Coast Office
1404 Garza Street
Anaheim, CA 92804

VOLLMER, Don
Lawrence Livermore National Lab.
P.O. Box 808, L-54
Livermore, CA 94550

WALTER, Patrick L.
Sandia National Laboratories
Division 7545
P.O. Box 5800
Albuquerque, NM 87185

WEISS, Harvey
Grumman Aerospace Corp.
Flight Test Dept., M/S F05-07
Calverton, NY 11933

WENDELL, Lowell
Lawrence Livermore National Lab.
P.O. Box 808, M/S L-134
Livermore, CA 94550

WHITTIER, Robert M.
Endevco Corp.
30700 Rancho Viejo Road
San Juan Capistrano, CA 92675

NOTE: Complete addresses are not available for the following attendees:

DEXTER, Jim

RAKLROV, Fredrick

YULROSLR, Albert

SESSION 1

A MINICOMPUTER-BASED SENSOR CALIBRATION SYSTEM

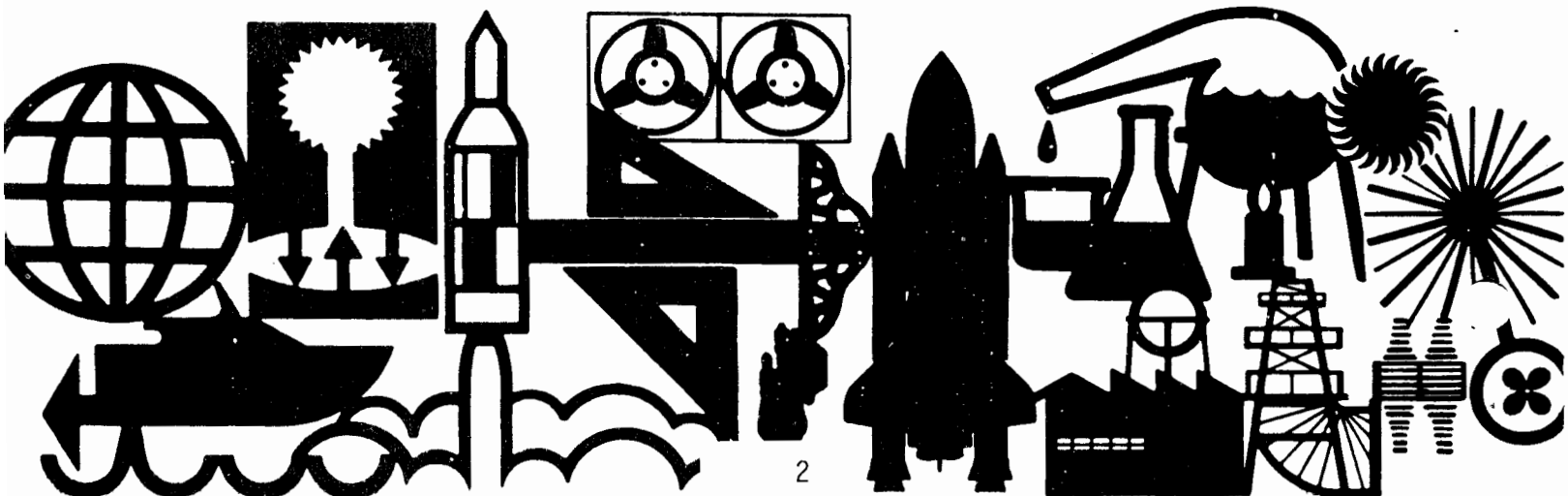
by Martha Pierce Willis

presented at the 13th Transducer Workshop, Monterey, California; 4-5 June 1985



Rockwell International

Rocketdyne Division



A MINICOMPUTER-BASED SENSOR CALIBRATION SYSTEM

Martha Pierce Willis

Rockwell International/Rocketdyne Division
Canoga Park, California

Abstract

A minicomputer-based sensor calibration system has been developed to support rocket engine and laser test programs. Previous methods used for managing sensor data employed manual acquisition, with offsite processing and storage. These methods increased total sensor calibration time and introduced the possibility of error. To improve quality and reduce the time needed for sensor calibration, a minicomputer-based calibration system has been employed. This paper discusses the hardware and software used in this system and future expansion aimed at achieving minicomputer control of all calibration functions.

Introduction

The Santa Susana Field Laboratory is a rocket engine and laser test facility. The instrumentation laboratory at this facility calibrates and services pressure, temperature, force, flow, vibration, and position sensors. Electronic signal conditioning equipment such as power supplies, amplifiers, and counters are also maintained at the laboratory.

Previous methods used to calibrate sensors were inefficient and utilized obsolete equipment. Data were acquired manually or with a panel meter system interfaced with a mechanical teletype. It was then processed and stored off-site. Processed data were analyzed for performance and sensors were dispositioned accordingly. Data failures were typically due to equipment malfunction and human data manipulation error. Sensor calibration turnaround time averaged 1 week.

To improve productivity and to expand and upgrade the laboratory's calibration capabilities, a minicomputer-based calibration system was proposed. Such a system had to be capable of acquiring, analyzing, and storing calibration data and controlling the calibration process.

System Description

Figure 1 is a functional block diagram of the data acquisition and management system. Hardware consists of the following: two low-speed analog subsystems, a central processing unit, a disk subsystem, a magnetic tape subsystem, a printer, four video display terminals, and a video graphic terminal. The low-speed analog systems each contain a multiplexer/control unit and a high-accuracy digital multimeter. Each of these are mounted in the desk cabinet of a remote console. Four video display terminals with detached keyboards and a multiplexer interface were procured. Two of these are used with the two remote control consoles. Figure 2 is a photograph of the remote control setup. One video display terminal is used as the master control console. The central processing unit has 32 bit instruction word length and addressing

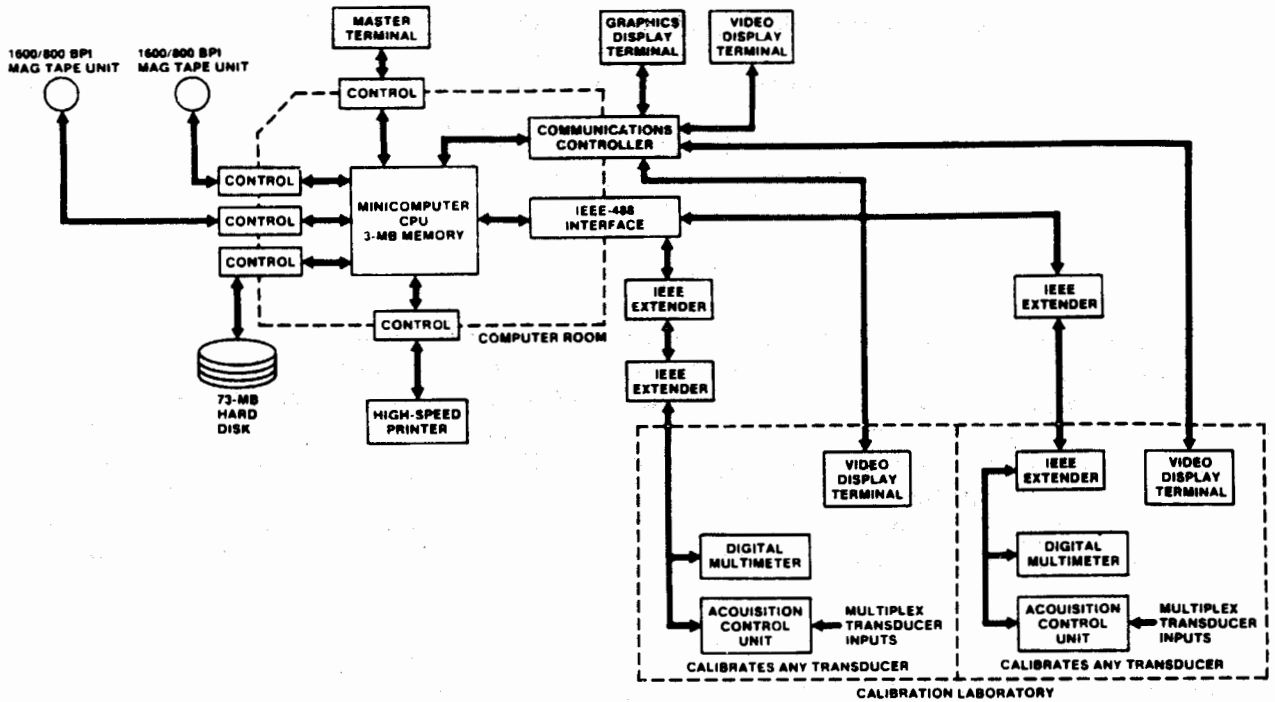


Fig. 1. Calibration Laboratory Computer System



Fig. 2. Remote Control Console

and 3 megabytes of random access memory. The disk storage subsystem is used for program and data file storage and consists of a 73-megabyte disk. The magnetic tape subsystem is used for system data backup. Hard copies of data are obtained using a laser printer. Figure 3 is a photograph of the system.

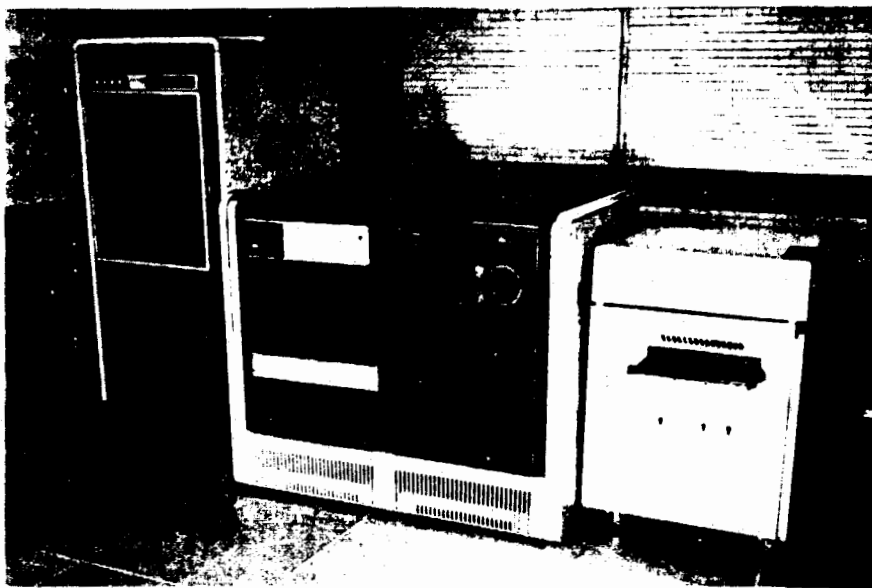


Fig. 3. Laboratory Calibration Data System

The data acquisition software consists of operating system and application software. Operating system software was supplied by the equipment manufacturer. It included the operating system, all input/output drivers, a disk editing program, and data-base management software. This software is written in Fortran 77, basic and assembly language. The Fortran programs have the capability of intermixing assembly language subroutines. The system is capable of supporting up to eight users simultaneously.

The application software is being prepared by Rocketdyne instrumentation laboratory personnel. All programs are written in Fortran 77. Data acquisition and processing software has been completed for static pressure sensors and platinum resistance temperature sensors. Data processing programs also exist for turbine type flowmeter calibrations.

System Operation

The pressure transducer program was written to acquire and process data for all pressure-related transducers. The test transducers are calibrated against a working standard transducer on a pneumatic calibration console. The medium is gaseous nitrogen. Operating ranges are 15 to 15,000 psi. Both absolute and gauge-referenced sensors are calibrated.

In calibrating pressure transducers, a key number is calculated that is the pressure equivalent of the electrical simulation of the transducer. An average key number is calculated for up to the 10 most recent data runs. Linearity is determined by using this average key number to calculate the indicated pressure at each point of the most recent data run. These calculated pressures are compared to the actual pressure indicated by the standard. The standard error of the mean is calculated for all key numbers included in the average. The uncertainty of the standard is included in the final uncertainty statement for the transducer. In calibrating pressure gauges, linearity and accuracy are verified by direct comparison to the pressure standard.

All sensors are described in a data based. They are filed by a control number and serial number. This combination of numbers is unique to each sensor. Approximately 40 pressure transducers are calibrated per week. These sensors are generally processed in batches of similar models and ranges. Up to seven transducers can be calibrated at once on the pneumatic console.

The general operation of the pressure program is as follows. The operator executes the program and is given a menu of calibration options from which to choose. The operator then inputs the control numbers and serial numbers of the sensors being calibrated. Based on historical information, the program instructs the operator on the number of runs of data required for each sensor. New or repaired transducers require a minimum of four data runs to establish a history file. Sensors that already have historical information stored require only one data run. The operator groups the sensors accordingly and mounts the sensors to the pneumatic console. The operator then inputs the control/serial numbers of the units installed. The program verifies that similar processes need to be performed on these units. It then instructs the operator on preliminary operations such as cable installation, leak and proof pressure checks, and diaphragm reseating. It performs insulation resistance checks and zero and shunt resistor calibration output checks. The operator is notified when sensor performance does not meet specification. The program then instructs the operator as to pressure set points. As points are set, the standard and test data are acquired. Upon operator request, the program then processes the data and prints out either a calibration sheet or a rejection summary sheet. Figures 4 and 5 are examples of these forms. The rejection summary sheet lists all current and historical information for a particular sensor. It serves as an engineering aid in determining the final disposition for the sensor.

Platinum resistance thermometers are calibrated by measuring their resistance values at three known temperatures. These values are the melting point of ice, the boiling point of liquid nitrogen, and the boiling point of liquid helium. A working standard resistance thermometer is used to measure the temperature of the boiling liquid nitrogen. The melting point of ice and the boiling point of liquid helium are known to a degree acceptable to the calibration. The average resistance at each calibration point is calculated for up to the 10 most recent data runs. The standard error of the mean is calculated for each of these points. Final uncertainty is expressed in ohms and includes the uncertainty of the standards used. A table of temperature versus resistance is then determined using the average resistance values and a scaling method similar to that outlined in Ref. 1.* The operating range of the transducers calibrated is -452 to +500 F. The resistance thermometer program acquires and processes the data for these sensors. There are approximately six resistance thermometers calibrated per week. Each of the sensors is described and filed in the data base. These sensors are also batch processed. A maximum of 10 sensors can be calibrated simultaneously.

*Corruccini, R. J., "Calibration of Platinum Resistance Thermometers," NBS Laboratory Note, File Number 57-25, Project Number 8131, December 11, 1957.

CONSTANT VOLTAGE
PRESSURE TRANSDUCER REDUCTION
LOW RANGE ABS. TRANSDUCERS

S/N: 881380 C/N: S584288
Model: 254
RANGE 15 PSI CAL DATE: 4/18/85

*****SUMMARY*****

AVERAGE KEY NUMBER = -10.538
NUMBER OF SAMPLES = 5
UNCERTAINTY = .361 % F.S.

LOW RANGE ABS. PRESSURE REDUCED DATA DUMP 4/19/85

Cn=S584288 Cal Type=CALIBRATION

Run	Slope	KeyNum	ZeroBal	UnBal	Sens	Hys
1	.13285E-02	-1.0522E+02	.17477E-04	-.45085E-05	.21332E-02	.73089E-03
2	.13248E-02	-1.0532E+02	.28908E-04	-.05951E-05	.21401E-02	.88273E-03
3	.13241E-02	-1.0538E+02	.28414E-04	-.74182E-05	.21389E-02	.27687E-03
4	.13242E-02	-1.0538E+02	.28312E-04	-.73699E-05	.21391E-02	.73023E-04
5	.13252E-02	-1.0524E+02	.28588E-04	-.49052E-05	.21407E-02	.12550E-02

Non Linearity

Run	3%	5%	7%	9%	5%	10%
1	-.95398E-04	-.75307E-03	-.11298E-05	.84459E-03	-.14298E-02	.00000E+00
2	-.47588E-03	-.89128E-03	-.43837E-03	.87938E-03	-.17253E-02	.00000E+00
3	-.32958E-03	-.14744E-02	-.42437E-03	.73031E-03	-.16992E-02	.00000E+00
4	-.89374E-03	-.13877E-02	-.23488E-03	.78842E-03	-.14413E-02	.00000E+00
5	-.14421E-03	-.62844E-03	.55282E-03	.83547E-03	-.17838E-02	.00000E+00

AvgKeyNum | Total Unc | MaxNonLin
|-1.0538E+02 | .36858E+00 | -.14298E-02

PRESSURE CALIBRATION DATA DUMP 4/18/85

TEST DATA:

S/N: 881389 Mfg: TABER Range: 151 Proof Press: 15
C/N: S584288 Mod: 254 ISpec: 524031 ReSeat Press: 15

	Run 1	Run 2	Run 3	Run 4	
Point	Pressure	Test Out	Pressure	Test Out	
3%	-9.43	5.7689	.00	.0000	
5%	-8.33	9.8783	.00	.0000	
7%	-3.37	13.7894	.00	.0000	
9%	-.37	17.7186	.00	.0000	
8%	-1.88	15.7889	.00	.0000	
5%	-6.37	9.8329	.00	.0000	
1%	-12.39	1.8844	.00	.0000	
0%	.00	18.1868	.00	.0000	
RCal= 4.2918		RCal= .0000		RCal= .0000	

STD DATA:

	Run 1	Run 2	Run 3	Run 4
Zero	.55424000E-02	.00000000E+00	.00000000E+00	.00000000E+00
RCal	.19462700E-01	.00000000E+00	.00000000E+00	.00000000E+00
3%	.17793000E-02	.00000000E+00	.00000000E+00	.00000000E+00
5%	.38162000E-02	.00000000E+00	.00000000E+00	.00000000E+00
7%	.41965000E-02	.00000000E+00	.00000000E+00	.00000000E+00
9%	.53919000E-02	.00000000E+00	.00000000E+00	.00000000E+00
8%	.47993000E-02	.00000000E+00	.00000000E+00	.00000000E+00
5%	.38829000E-02	.00000000E+00	.00000000E+00	.00000000E+00
1%	.55498000E-03	.00000000E+00	.00000000E+00	.00000000E+00
Zero	.55414000E-02	.00000000E+00	.00000000E+00	.00000000E+00
RCal	.19462300E-01	.00000000E+00	.00000000E+00	.00000000E+00

	DMM Std Coef	Pres Std Coef
C/N: N571853	C/N: S526872	
Range: .1880E+00	Range: .5880E+02	
Uncert: .1248E-01	Uncert: .8380E-01	
Coef0	.00000000E+00	.53182840E-02
Coef1	.10000000E+01	.34873887E+02
Coef2	.00000000E+00	-.49235487E+00
Coef3	.00000000E+00	.18587416E+01
Coef4	.00000000E+00	.39754860E+01
Coef5	.00000000E+00	-.28858859E+02
Coef6	.00000000E+00	.25589886E+02
Coef7	.00000000E+00	-.99852437E+01
Coef8	.00000000E+00	.00000000E+00
Coef9	.00000000E+00	.00000000E+00

PRESSURE SPECIFICATION CHECK 4/18/85

	Acceptance Data	PosZerBal	NegZerBal	UnBal	NonLin	Hys	KeyNumDev	Sens	Maximum Unc		
0	Control	No	Status	.15000E-03	-.15000E-03	.00000E+00	.50000E-02	.50000E-02	.10000E-01	.21000E-02	.20000E+01
1	S584288	PASS		.02000E+00	.00000E+00	.00000E+00	.00000E+00	.00000E+00	.00000E+00	.00000E+00	.00000E+00

Fig. 4. Calibration Sheet for Pressure Transducers

INSTRUMENTATION LABORATORY

DATE: 4/30/85

ITEM: PRESSURE TRANSDUCER

MODEL: 288

RANGE: 1000 PSI

S/N: 825881

C/N: 5581856

REASON:

Zero balance is less than allowed.

VALUE = -.95835E-03

Unbalance is out of limits.

VALUE = .11792E-01

Nonlinearity is greater than allowed

VALUE = -.28822E+08

Key number deviation out of bounds.

VALUE = .10900E+01

Sensitivity is not within limits.

VALUE = .33462E-02

Uncertainty is greater than allowed.

VALUE = .13264E+03

DID THIS FAIL DURING ACCEPTANCE TESTING?

YES

NO

RESPONSIBLE ENGINEER: *D. Powell*

TECHNICIAN: *D. Powell*

GAGE PRESSURE REDUCED DATA DUMP 4/30/85

Cn=5581856 Cat Type=CALIBRATION

Run	Slope	KeyNum	ZeroBal	UnBal	Sens	Mys
1	.37212E-01	28180E+01	.95835E-03	.11792E-01	.33462E-02	.31378E-03
2	.10831E-01	70880E+03	.11582E-04	.24387E-02	.24432E-02	.52358E-04
3	.10852E-01	70883E+03	.11331E-04	.24388E-02	.24433E-02	.24831E-03
4	.10830E-01	70836E+03	.11482E-04	.24388E-02	.24417E-02	.21501E-04
5	.10845E-01	70813E+03	.11105E-04	.24388E-02	.24424E-02	.37542E-04

Non Linearity

Run	1%	3%	5%	7%	9%	50%
1	-.28822E+08	-.14322E+08	-.84988E-01	-.28486E-01	-.28018E-01	-.86382E-01
2	-.22888E-02	-.26872E-02	-.15872E-02	-.24548E-03	-.68584E-03	-.12886E-02
3	-.22877E-02	-.17587E-02	-.18729E-02	-.31185E-03	-.82295E-03	-.83861E-03
4	-.21434E-02	-.20129E-02	-.13212E-02	-.37019E-03	-.31873E-03	-.13882E-02
5	-.21816E-02	-.16278E-02	-.87588E-03	-.28186E-03	-.68834E-03	-.98254E-03

AvgKeyNum | Total Unc | MaxNonLin
 | 12828E+04 | 13284E+03 | -.28822E+08

PRESSURE CALIBRATION DATA DUMP 4/30/85

TEST DATA:

S/N: 825881 M/S: TABER Range: 1000Psi Cool Press: 1500
 C/N: 5581856 Mod: 288 Ropc: 22482 RoSeal Press: 3100

	Run 1	Run 2	Run 3	Run 4
10%	.98155	1.84121	.88001	.88001
30%	499.85	9.78351	.88001	.88001
50%	788.83	13.48851	.88001	.88001
70%	899.43	17.48851	.88001	.88001
80%	888.25	15.58821	.88001	.88001
90%	499.53	9.72761	.88001	.88001
5%	.881	-.6.21831	.88001	.88001

RCal= 78.4383 | RCat= .8888 | RCat1= .8888 | RCat2= .8888

STD DATA:

	Run 1	Run 2	Run 3	Run 4
IZero	-.12328080E-03	.0000000E+00	.0000000E+00	.0000000E+00
IRCal	.15324380E-01	.0000000E+00	.0000000E+00	.0000000E+00
10%	.84230000E-03	.0000000E+00	.0000000E+00	.0000000E+00
30%	.27694000E-02	.0000000E+00	.0000000E+00	.0000000E+00
50%	.48131000E-02	.0000000E+00	.0000000E+00	.0000000E+00
70%	.84294000E-02	.0000000E+00	.0000000E+00	.0000000E+00
80%	.73762000E-02	.0000000E+00	.0000000E+00	.0000000E+00
90%	.46862000E-02	.0000000E+00	.0000000E+00	.0000000E+00
IZero	-.12500000E-03	.0000000E+00	.0000000E+00	.0000000E+00
IRCal	.15308180E-01	.0000000E+00	.0000000E+00	.0000000E+00

DMM Std Cost | Pres Std Cost

IC/N: M571653 | C/N: 5581148
 Range: 1000E+00 | Range: 2000E+04
 Uncert: 1240E-01 | Uncert: 1140E+01

Coef01	.0000000E+00	.1839382E+01
Coef11	.0000000E+00	.10666753E+04
Coef21	.0000000E+00	.0000000E+00
Coef31	.0000000E+00	.0000000E+00
Coef41	.0000000E+00	.0000000E+00
Coef51	.0000000E+00	.0000000E+00
Coef61	.0000000E+00	.0000000E+00
Coef71	.0000000E+00	.0000000E+00
Coef81	.0000000E+00	.0000000E+00

Fig. 5. Rejection Summary Sheet for Pressure Transducer

In general, the resistance thermometer program operates as follows. The operator executes the resistance thermometer program and is given a menu of options. He inputs the control numbers and serial numbers of the sensors being calibrated. The program verifies validity and informs the operator of the type of points and the number of data runs needed for each sensor. This information is maintained in a status file for a particular batch. The status file is updated by the computer and may be accessed by the operator at any time. The program instructs the operator on the performance of preliminary operations such as insulation and pin-to-pin resistance checks, and pressure tests. It monitors the sensors during these tests and evaluates sensor performance. When the operator is prepared to take temperature calibration data, he selects that option. The program monitors calibration bath temperatures and test output signals for stabilization. When these parameters are within prescribed tolerance, the data are acquired for each test sensor. The only manual operation is the placement of the test transducers in the proper bath. Test data points are compared to historical data at the time they are acquired. If a sensor is not in tolerance, the operator is immediately notified and all current and historical information on that particular sensor is printed. This aids in determining the failure mode and the sensors' disposition. After all points are taken, the data are processed and a calibration sheet is printed for each sensor.

Future Expansion

Planned system expansion includes both software additions and hardware procurement. To acquire and process data, software needs to be written for each type of sensor used at the facility. Currently in work are programs for low range absolute pressure sensors, thermocouples, accelerometers, and load cells. As those are completed, programs will be written for high frequency pressure and displacement sensors. Automation of all calibration functions is planned.

As the data base grows, additional disk storage space will be needed to support laboratory calibrations. Anticipating this requirement, two disk controllers and two 515 megabyte disks will be added to the disk subsystem in 1985. To support daily laboratory calibration functions, an additional remote console with an analog subsystem and a video display terminal will be required. Spares for the system were not included in the original microprocessor system and will be procured to ensure the system is not compromised by the failure of a single component. Plans for the future also include the development of graphics capability to aid in the analysis of calibration data.

Acknowledgement

The author wishes to acknowledge the contributions of J. P. Shonafelt for his technical background on the laboratory data system.

AUTOMATING ACCELEROMETER CALIBRATIONS FOR USERS

David Banaszak
Aeronautical Systems Division
Air Force Wright Aeronautical Laboratories
AFWAL/FIBG, Wright Patterson AFB, OH 45433

ABSTRACT

Advances in test and measurement equipment impact the end user's conventional techniques used to calibrate accelerometers. Conventional techniques involve a person applying various levels of known accelerations for excitation and manually writing the known engineering input and the corresponding voltage output. Normally, values are read from analog or digital voltmeters. The data collected are then plotted on graph paper; with output voltage on the y-axis and acceleration input on the x-axis. A best fit straight line is then found and the slope (sensitivity in volts/g) and y-intercept (zero output) are calculated. If time permits, transducer specifications such as linearity, repeatability and hysteresis are determined. The microcomputer provides accelerometer users the ability to quickly and accurately check accelerometer specifications at a reasonable cost and without the need for pencil and paper. This paper will discuss some traditional techniques used for statically and dynamically calibrating accelerometers. Excitation and measurement techniques will be reviewed and modern instruments which can automate accelerometer calibrations will be discussed. In particular, use of a smart dual channel digital oscilloscope for automatic accelerometer calibration will be detailed.

BACKGROUND

The ideas described in this paper are from an in-house project titled "Instrumentation, Facilities and Techniques for Collecting Dynamics and Loads Data on Air Force Weapon Systems". One of the efforts is to study new accelerometer calibration techniques.

In the calibration of accelerometers a precise and carefully documented procedure should be maintained. Every experimenter should take an active role in the process. For any experiment requiring the measurement of physical phenomenon, calibration of the transducer can be the most mundane and boring task. However, the test results rely heavily on the basic assumption that the transducer calibrations are accurate and correct for all environmental conditions. Calibration can be a repetitious, tedious, thankless, dull and unsatisfying task that one wants to finish quickly. In many reports the transducer and its calibration are briefly mentioned, when the main emphasis is the testing of an exotic, expensive weapon system or an imaginative piece of high tech machinery. Calibration and resulting tedious bookkeeping required are tailor made for automated procedures by transducer users. For example our organization has several hundred accelerometers of various sizes, types and shapes which need constant calibration checks and evaluation because of their high rate of usage on a variety of Air Force experiments.

STATIC CALIBRATIONS

Transducer calibration is a determination of electrical output versus physical input as shown in the diagram in Figure 1. Since most accelerometers are linear devices, much time is spent in determining the slope and intercept of the straight line which results when the output voltage is plotted versus the input acceleration(g).

In the slide rule days, calibration of aircraft accelerometers for a flight loads data program were performed on an one foot radius turn table(Figure 2). The sensors were calibrated from -3g to +9g. A variety of mounting brackets were required to ensure that the sensitive axis of the accelerometer was parallel to the centrifugal force of the turn table. Figure 3 shows the steps involved. The distance from the accelerometer's c.g. to the table's center was measured to determine the radius. Then the value of g's for the current table speed and the table radius was located in a long computer printout. Table I shows an abbreviated version of this printout. Today, the same data in the printout are easily generated using a portable computer. A typical calibration sheet and plot for two accelerometer axes is shown in Figure 4. These steady state calibrations were time consuming, required handwritten records and were very boring. There had to be ways to automate the calibration process.

When programmable calculators arrived, the handwritten observations were typed into the computer to obtain a statistical least square best fit straight line(BFSL) as shown in Figure 5. This eliminated interpolation in estimating slope and intercept from a hand prepared plot. A digital plotter with the calculator system was used to plot the data. This saved time trying to determine how many g's per square to use on the x-axis and how many volts per square to use on the y-axis. It also meant that now one could read legible tables off a computer printout rather than interpreting someone's handwriting. Titles such as transducer serial number, date and axis labels could be included on the plot to help document the test.

DYNAMIC CALIBRATIONS

Accelerometers used primarily to measure vibration of structures require different methods of calibration. Instead of using accelerometers which had high DC voltage outputs compatible with computer requirements; piezoelectric accelerometers with low voltage sensitivities, no DC response, and high output impedance are used.

A risky dynamic calibration at one frequency uses a 1g peak shaker. Sometimes a sensitivity is specified with units of mvrms/1g peak. These units are probably used because the shaker vibrates an accelerometer at precisely 1g peak and then a root mean square(rms) millivoltage(mv) is read on a voltmeter. This is equivalent to a DC sensitivity with mixed units. Since this is a sine wave calibration, one may apply the square root of 2 correction properly to get the numerator and denominator to be the same units. The 1g peak shaker technique relies on one amplitude and one frequency and assumes linearity. It does not test transducer operation over the entire amplitude and frequency spectrum as shown in Figure 6.

Another technique is an insert calibration. This technique consists of inserting an electrical signal equivalent to a known

output from the basic sensor. The insert calibration is often used in the field with piezoelectric accelerometers. One may get a good indication from an insert calibration but later find that the accelerometer was not functioning mechanically. An insert calibration should only be used as a last resort. An end to end calibration of a measurement system including the transducer in operation is the best technique. Wherever possible the transducer should be stimulated by a known value of the physical parameter being sensed and its output recorded by the final measurement device. This may be a digitally encoded signal recorded on tape, nonvolatile memory or other storage media. Laboratory calibration techniques described in this paper evaluate the sensor independent of signal conditioning.

Techniques for defining transducer frequency response include frequency sweep, random noise and impact techniques. With the frequency sweep method, one excites a shaker with a swept sine and might plot the transducer's output on a strip chart recorder as a function of frequency. This technique is still used, but is time consuming and may use old and costly equipment. Another technique uses random noise for shaker excitation and then uses a spectrum analyzer to look at inputs, outputs and transfer functions in the frequency domain. A two channel analyzer is preferable to obtain simultaneous input and output relationships. Two channel systems are also required to obtain transfer functions. One can also excite a transducer across a broadband of frequencies with impact techniques to determine if an accelerometer's frequency response is flat. Determining sensitivities with impact techniques is described in Reference 7. Sometimes impact techniques require trial and error to setup test equipment properly to obtain valid results. Recent efforts involve using time domain techniques for automating low frequency and static calibrations.

AUTOMATING STATIC CALIBRATIONS

A transient recording system captures a signal and saves it in memory for later analysis. A typical impact calibration system shown in Figure 7 uses a desktop microcomputer as a controller. It accepts two inputs, which means that it can replace the technique of manually recording g's in and volts out by acquiring the transducer output and input automatically. Once the data are stored, the computer then transfers the data from the transient recorder to its memory. A Basic program can manipulate the data, automatically compute slopes and intercepts and produce a plot on the printer. Since the software provided with the system was developed for transient time recording, Basic programs must be written to adapt the system for low frequency accelerometer calibrations. The transient recording system operates like a programmable dual channel digital oscilloscope with appropriate software. This oscilloscope can replace the transient recording system and automate checks for sensitivity, zero output, linearity, hysteresis, repeatability, resolution, creep and other evaluation factors as outlined in Reference 2.

A static calibration requires that the operator adjust and stop to read an output and do this for several different points. A digital scope reads and records input and output versus time and remembers the acquired readings. A smart digital scope can be programmed to rapidly and accurately evaluate the sensitivity calibrations for low frequency

response transducers. Five possible techniques using a digital scope to aid in near static evaluation of accelerometers will be described below. Other potential techniques are left to the reader's ingenuity. In addition, References 1, 3, 4, 5 and 6 have techniques which can be adapted to a digital scope. The digital scope used for this paper was manufactured by the Norland Corporation and contains built in data analysis capability. It is one of the new breed of intelligent test instruments which can accomplish these functions.

COMPARISON CALIBRATION USING TURNTABLE

The first example is a modern way of using the turntable as illustrated in Figure 8. A sensor detecting table rotation speed is measured by a channel of the digital oscilloscope. The scope is preprogrammed to compute g's from the sensor signal and the measured table radius. The accelerometer output is measured and recorded by the second channel of the scope. The turntable speed is increased to maximum and decreased while data are being acquired by the scope and stored in its memory. No stops or adjustments need to be made at intermediate points. When the speed of rotation is reduced back to zero, the scope displays the accelerometer's output and via a built in statistics routine can display sensitivity and $0g$ output. The final results are plotted on a digital plotter or can be recorded on video tape for future reference. Inexpensive, video cassette recorders(VCR) are commercially available and can be connected to a video hard copy device.

EXCITATION USING A SHAKER

The $1g$ shaker can be used with the digital scope to evaluate transducer performance as illustrated in Figure 9. The shaker is adjusted for $1g$ peak acceleration at a specified frequency. The scope computes the voltage($\max-\min/2$) to determine the sensitivity. When the shaker has a velocity output, the digital scope does the record keeping and number crunching to determine the g's in as the shaker amplitude or frequency is being varied.

3 POINT CAL(MANUAL)

In the field, a 3 point dump calibration is often used for DC responding accelerometers. This technique becomes more powerful with a digital scope as shown in Figure 10. The sensing direction of the accelerometer is established to give $+1g$, $0g$ and $-1g$. The scope records the output and computes sensitivity and intercept which can be produced as shown in the figure. The process could be further improved using a "robot" to position the accelerometer in all 3 earth reference g points.

HANDWAVE COMPARISON CALIBRATION VERSUS REFERENCE

This technique requires a reference accelerometer for comparison. The technique may appear to be crude, but it can be a very cheap and quick method for determining accelerometer sensitivities. The calibration is accomplished by first firmly grasping in one hand a reference and unknown accelerometer simultaneously. The hand or arm

is then waved while the scope measures the results as shown in Figure 11. The scope displays sensitivity and can do linearity computations automatically. This technique may be very useful in the field for checking accelerometers at the low frequencies. This is an additional technique which could use a "robot" to automate and improve the evaluations.

SENSITIVITY AS A FUNCTION OF PARAMETERS

Often many items on a specification sheet are inadequately evaluated by users due to the time involved. This is especially true in checking a transducer's sensitivity versus varying voltage excitation and thermal conditions. There are several accelerometers on the market whose sensitivity is a function of voltage excitation and thermal environment. The variation in sensitivity can be checked using a dual channel digital scope in a manner similar to procedures for a 3 point calibration. Measure the accelerometer output on one channel and the voltage excitation on the other. Continuously vary the excitation for each of the dump calibration points as shown in Figure 12. The scope records the output and excitation and computes and displays volt/g/volt of excitation assuming a linear relationship between sensitivity and excitation voltage. By measuring temperature with one channel and accelerometer output with the other channel, a quick measure of thermal zero and sensitivity shifts can be easily accomplished. Usually there is little time to check a sensor's thermal properties due to the extra time required for a proper evaluation of this critical performance parameter.

ROBOTIC CALIBRATIONS-THE FUTURE

From the above discussions, it is apparent that "robots" may eventually help in the calibration of static and low frequency transducers. The "robot" could provide rotation in a manner similar to the turn table or the hand 3 point calibration. A "robot" can swing up and down to simulate a mechanical input. Some day "robots" may be clever enough to count the transducers and make the electrical connections.

SUMMARY AND CONCLUSIONS

By using automated methods with a digital scope, an accelerometer user gains many advantages over earlier techniques. These include less time per unit, better accuracy, less human errors, improved record keeping, better repeatability and a more complete operational evaluation of the transducer and its specification than was previously available. In the turntable example, the many steps required to be done manually can be automated and accomplished in a couple of hours rather than several days. Accelerometer calibration can now be less tedious and more fun. The use of a digital scope can find analogous application in calibration of other sensors such as pressure transducers and strain gages with an integral thermocouple. The goal is to automate the tedious, repetitious parts of the calibration process so that man can utilize his intelligence to design, setup and implement experiments to meet future Air Force requirements.

REFERENCES

1. Oliver, Frank J., Practical Instrumentation Transducers, Hayden Book Company, Inc., N.Y., 1971.
2. Lederer, Paul S., "Sensor Performance Evaluation", *Measurements and Control*, pp202-209, September 1984.
3. Norton, Harry N., Handbook of Transducers for Electronic Measuring Systems, Prentice-Hall, N.J., 1969.
4. Doebelin, Ernest O., Measurement Systems: Application and Design, McGraw-Hill, 1975.
5. Broch, Jens Trampe, The Application of the Bruel and Kjaer Measuring Systems to Mechanical Vibration and Shock Measurements, Bruel and Kjaer, Denmark, Reprint June 1983.
6. Bouche, Raymond R., Calibration of Shock and Vibration Measuring Transducers, The Shock and Vibration Information Center, Naval Research Laboratory, Washington, D.C., 1979.
7. Lily, Robert W., "Gravimetric Calibration of Accelerometers", *TEST*, Oct/Nov 1978.

15 INCH RADIUS		9 INCH RADIUS	
Deg/Sec	"g"	Deg/SEC	"G"
100	.1182	375	1.0
200	.473	460	1.5
300	1.064	530	2.0
400	1.891	593	2.5
500	2.956	650	3.0
600	4.256	702	3.5
700	5.793	750	4.0
800	7.567	796	4.5
900	9.577	839	5.0
1000	11.823	880	5.5
		920	6.0
		957	6.5
		993	7.0
		1027	7.5
		1061	8.0
		1094	8.5
		1126	9.0
		1156	9.5
		1186	10.0

TABLE I Short Conversion Tables from Speed to G Given Radius

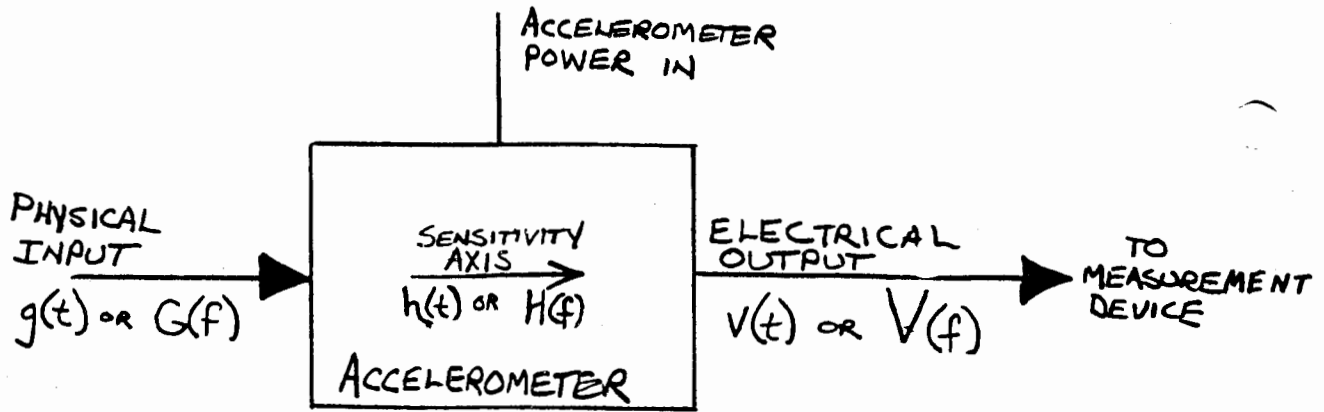
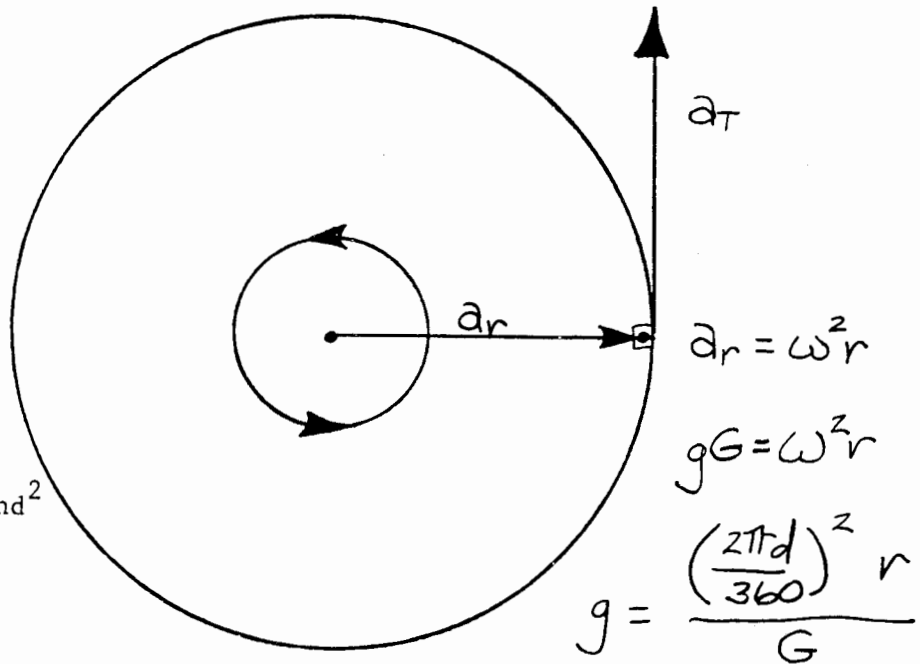


FIGURE 1: SIMPLE CALIBRATION SYSTEM



Where

$G = 386.089 \text{ inches/second}^2$

$r = \text{inches}$

$d = \text{degrees/second}$

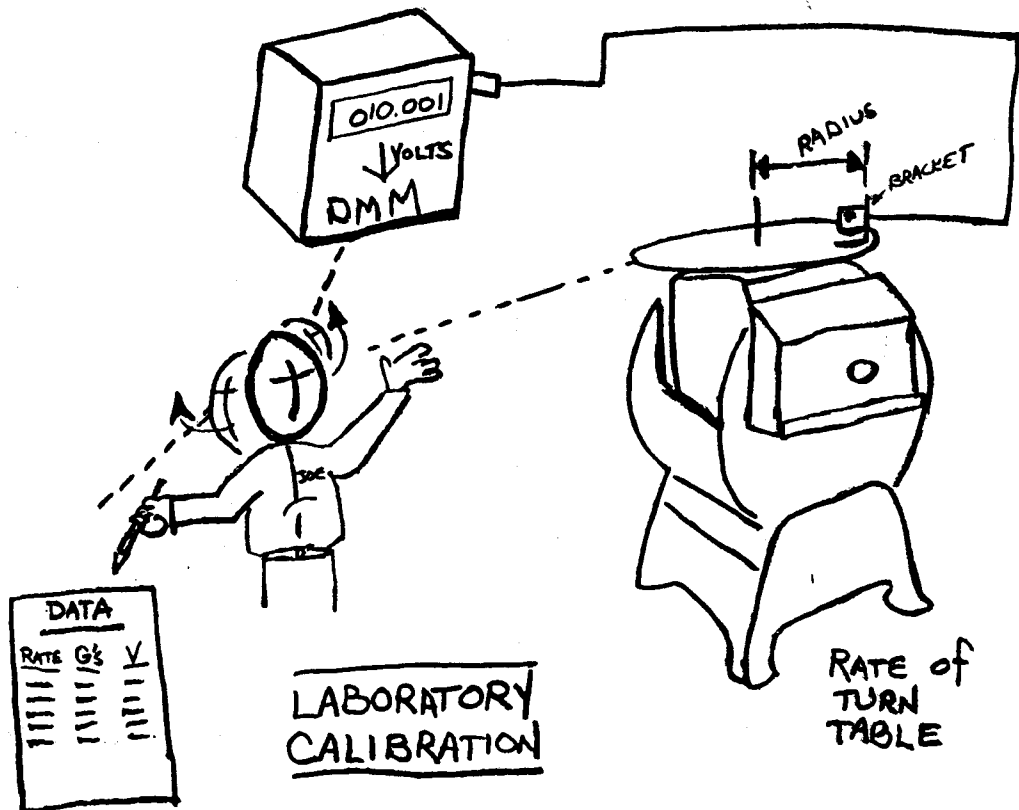
$w = \text{radians/second}$

$g = \text{number of gs}$

For a Computer use:

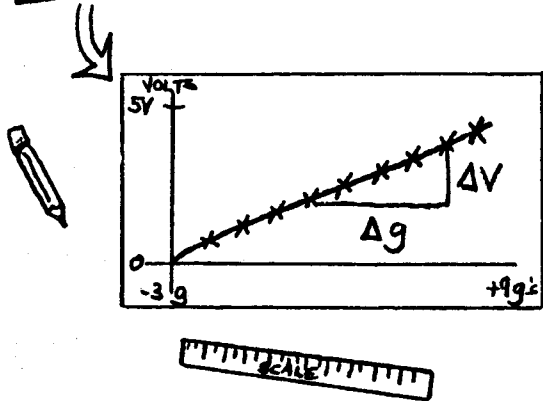
$g = ((d*2*\pi)/360)**2*r/G$

FIGURE 2: CONSTANT SPEED TURN TABLE



LABORATORY CALIBRATION

- MOUNT BRACKET
- MOUNT ACCELEROMETER
- MEASURE RADIUS TO C.G.
- CONNECT ELECTRONICS
- APPLY INPUT (ADJUST RATE)
- READ RATE (RECORD DATA)
- READ OUTPUT VOLTAGE (RECORD)
- CALCULATE g's-IN
- REPEAT (UNTIL DONE)
- PLOT DATA
- FIT LINE
- HAND WRITE LABELS
 - DATE
 - ID NUMBERS
 - MODEL
 - SERIAL NUMBERS
 - ETC
- COMPUTE $\Delta V / \Delta g$



⇒ THEN
BEFORE
AND
AFTER
TEST

THREE POINT FIELD CALIBRATION



FIGURE 3: CALIBRATION TECHNIQUE OF SLIDE RULE DAYS

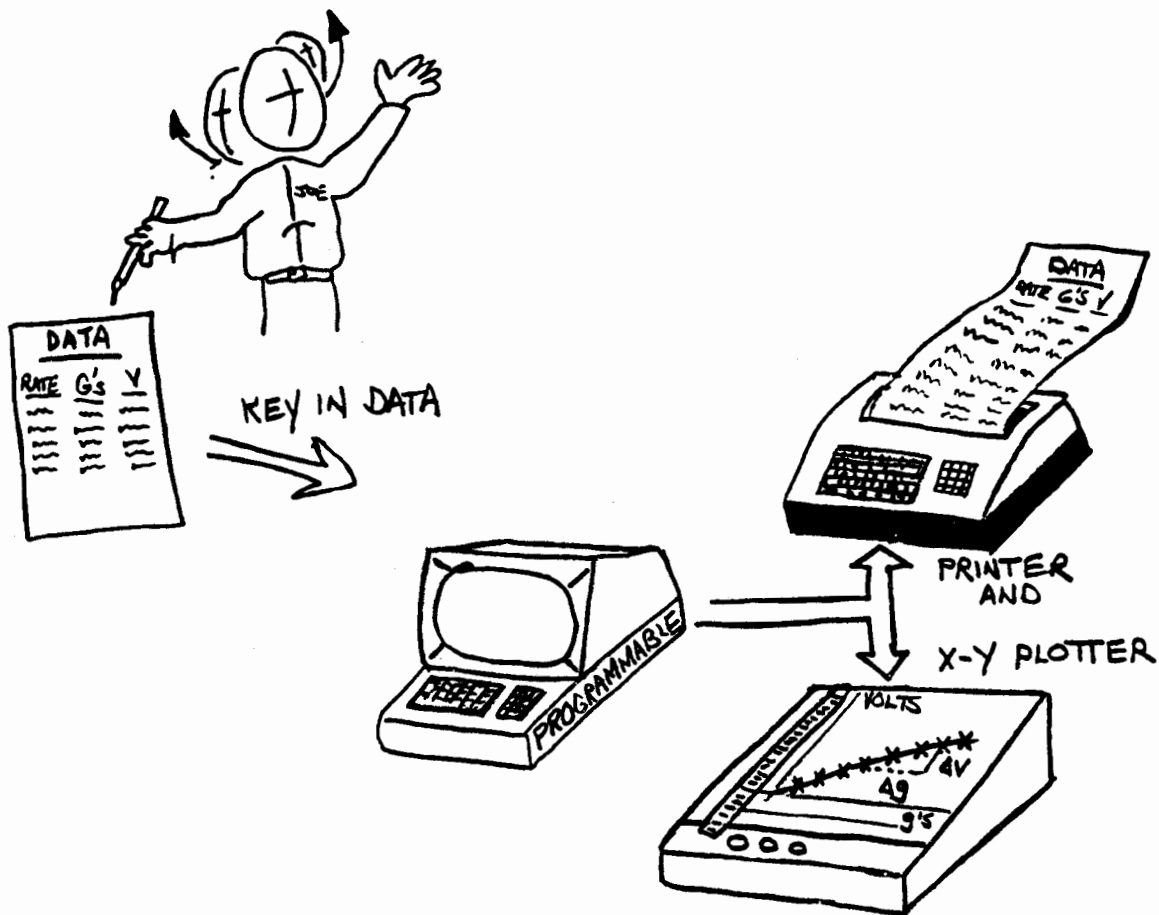
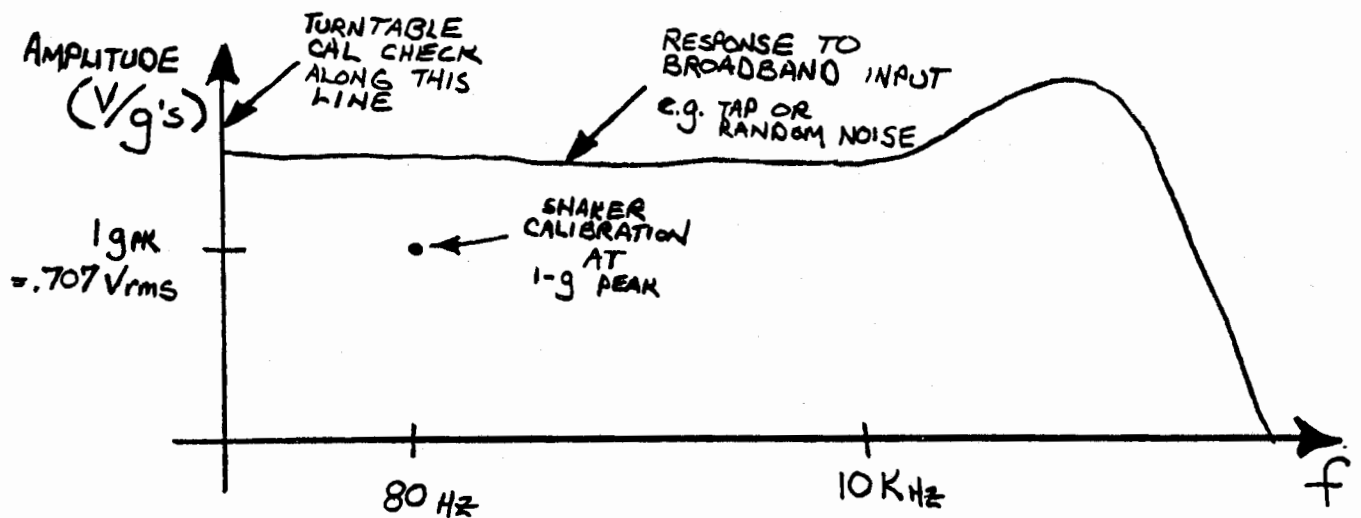


FIGURE 5: CALCULATOR TECHNIQUE



IDEAL EVALUATION COVERS ALL AMPLITUDES AND FREQUENCIES OF CONCERN

FIGURE 6: FREQUENCY DOMAIN

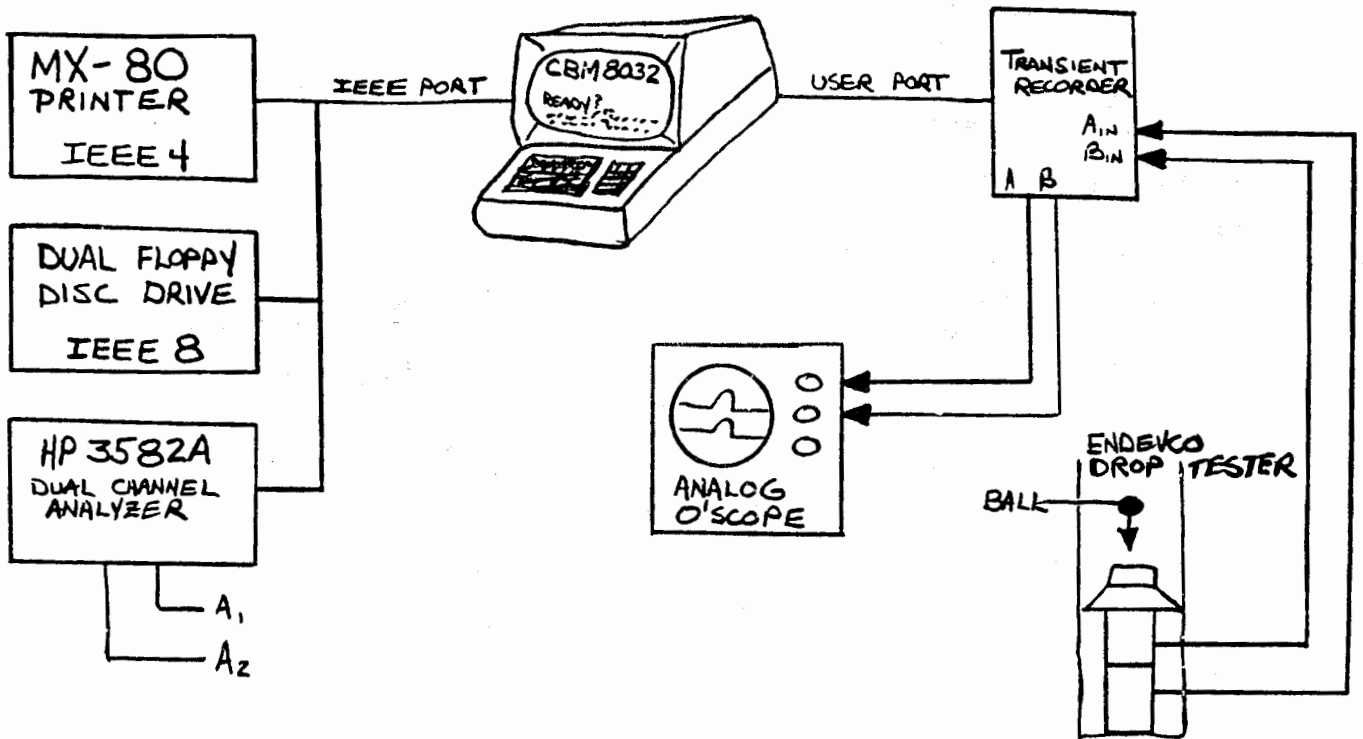


FIGURE 7: TRIAD SYSTEM TECHNIQUE (GHI, INC)

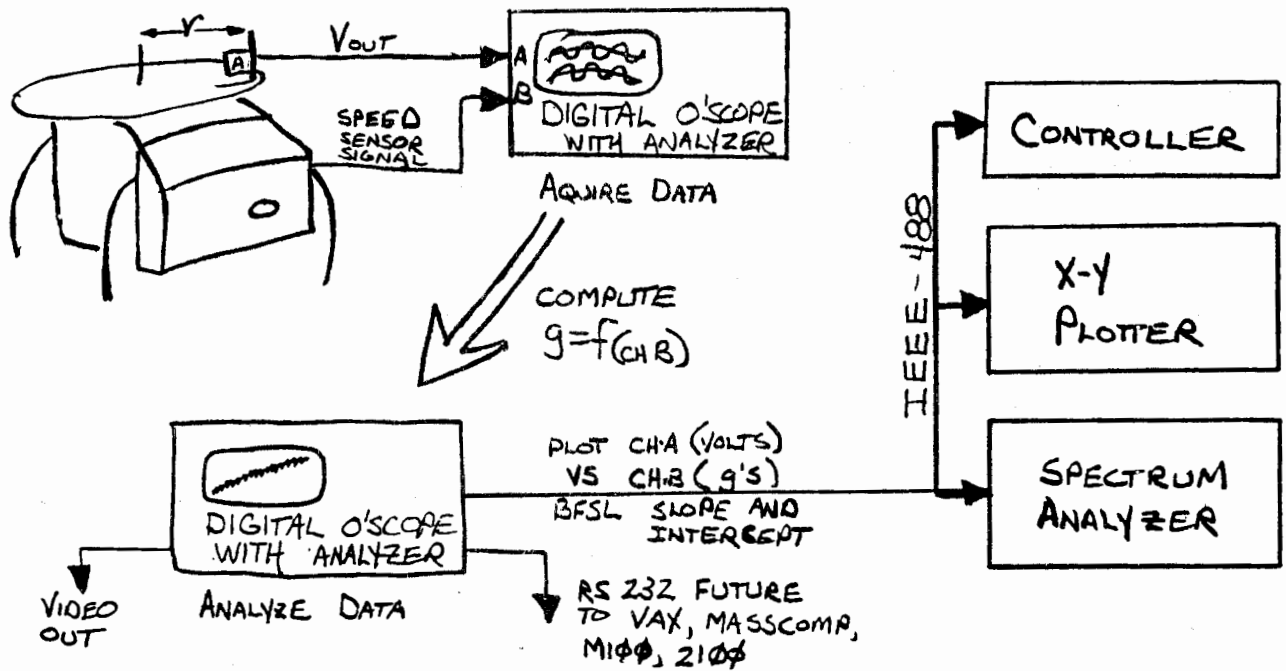


FIGURE 8: COMPARISON CALIBRATION W/ DIGITAL O'SCOPE

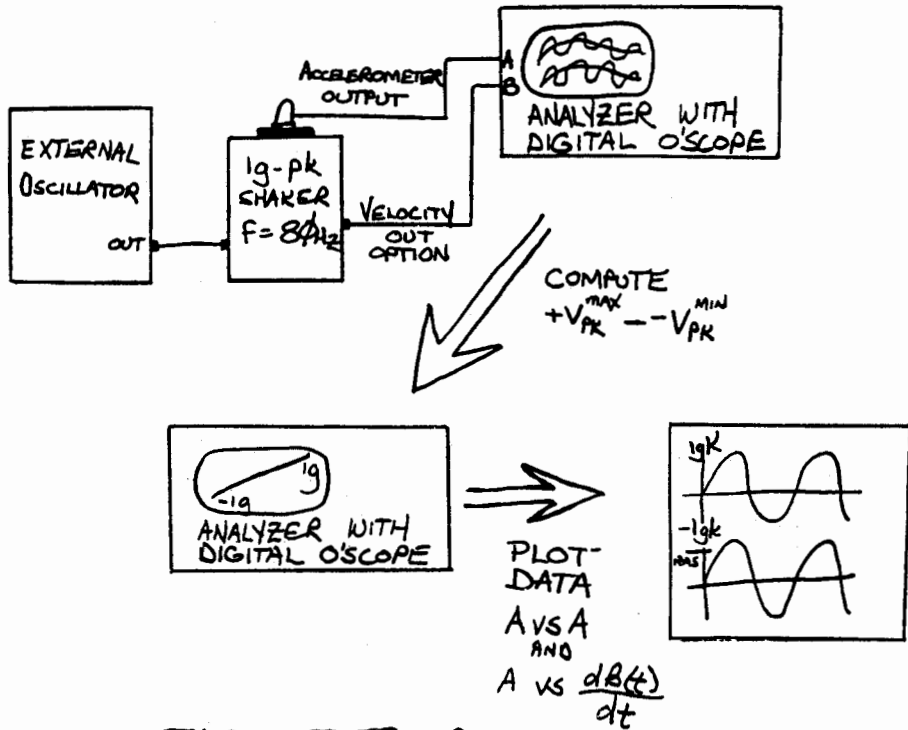


FIGURE 9: 1-G SHAKER AND VELOCITY OUT OPTION

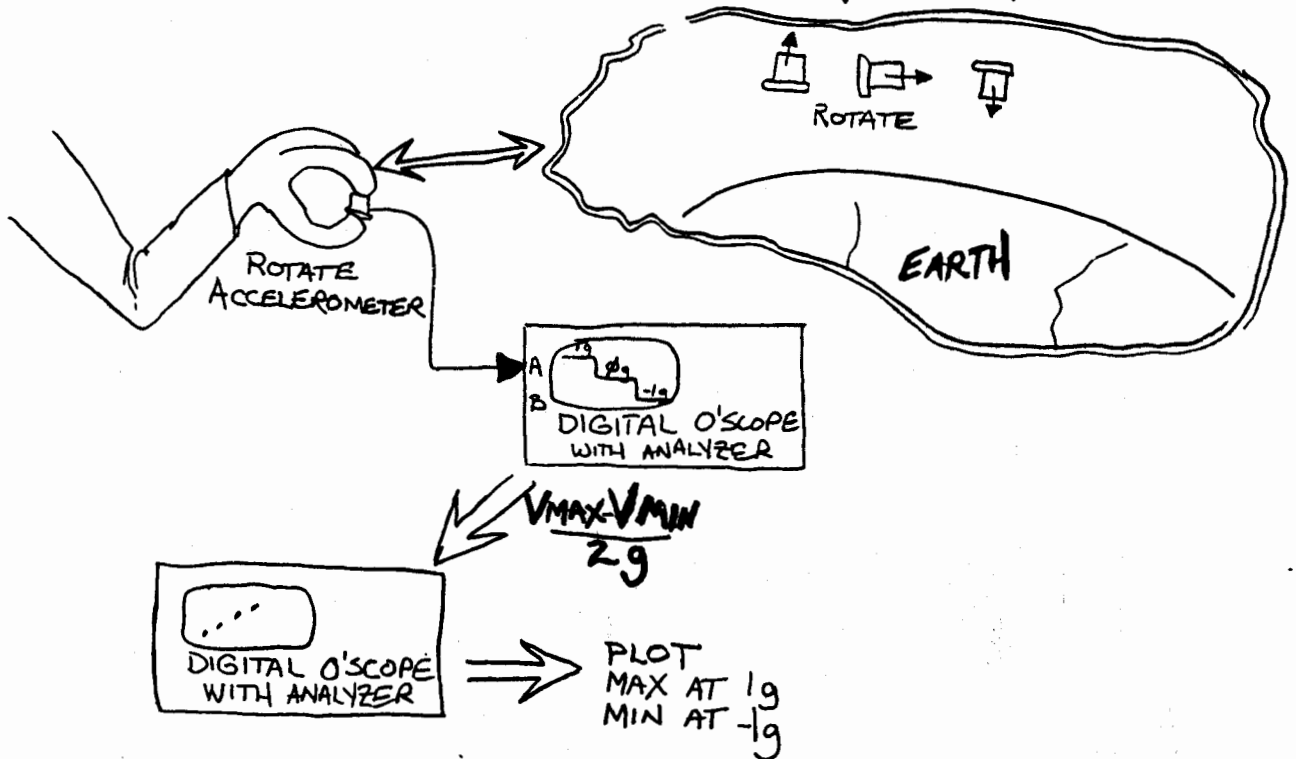


FIGURE 10: 3 POINT CAL

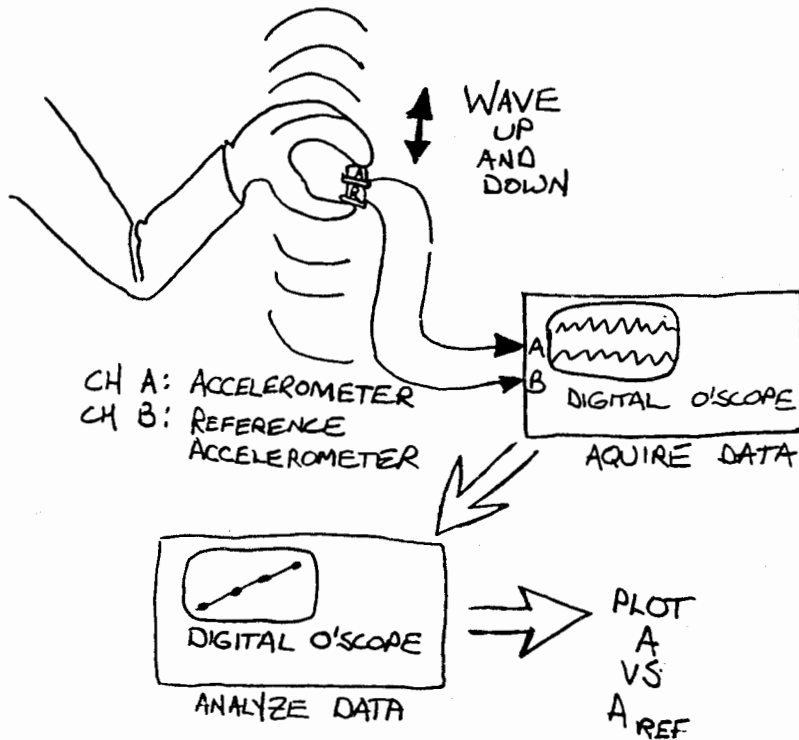


FIGURE 11: HANDWAVE CAL

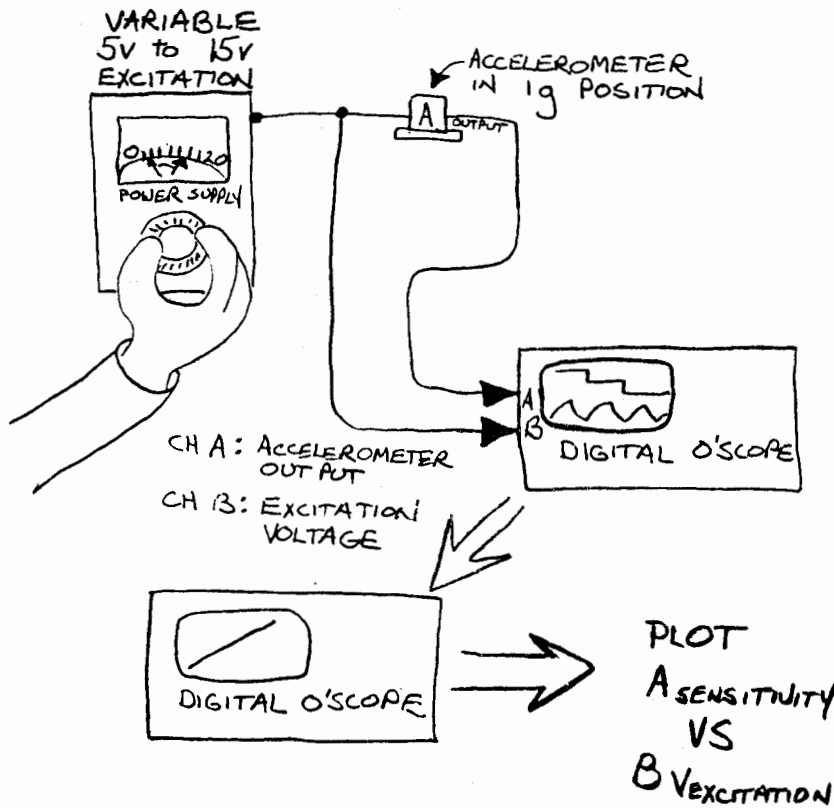


FIGURE 12: SENSITIVITY VARIATION

QUANTIFYING AUTOMOTIVE TEST COURSE PROFILES
by W. H. Connon; S. P. Harley; J. Schimminger; T. Shrader
Materiel Testing Directorate, Aberdeen Proving Ground, MD

William Connon is currently employed as a Mechanical Engineer, Dr. Samuel Harley as a Physicist, Joseph Schimminger as a Electronic Engineer and Timothy Shrader as a senior Electronics Technician at the Measurements and Analysis Division, Materiel Testing Directorate, Aberdeen Proving Ground, Maryland.

I. INTRODUCTION

The measurement of the severity of the test environment is a topic that has been studied at various times over the past several years (1,2,3). To fully quantify this environment requires measurements of the course profile, hardness, surface strength, dust and possibly other characteristics. This presentation is limited to automotive test course profiles.

US Army Aberdeen Proving Ground (APG) first used a profilometer in 1970 (1) and made subsequent mechanical improvements in 1974 (2) and data acquisition and processing improvements in 1983 (3). Much of APG's work is based upon earlier work by several groups and individuals as reported by Bekker (4). The thrust of the latest APG effort is to field a profilometer which can be used on an everyday basis to monitor the automotive test environment.

The profilometer system consists of a tow arm, data acquisition subsystem, and a minicomputer-based data analysis system. The tow arm follows the test course surface and generates signals related to the instantaneous slope of the course. The microprocessor-based data acquisition subsystem conditions and digitizes these signals, transforms them to angle data, and stores the result in non-volatile memory. The data analysis system retrieves and stores the data and performs a variety of data-processing functions.

II. PROFILOMETER TOW ARM

Figures 1 and 2 show the tow arm mounted on a jeep. Mounting is accomplished using clamps and existing openings and threaded holes. Modified pressurized shock absorbers are used to hold the wheels in contact with the surface. The shock absorbers are inflated to give the profilometer tires approximately the same bearing pressure as the jeep tires.

Figure 3 shows a schematic diagram of the tow arm. The gyroscope indicates the pitch angle θ of the tow arm. The angle of the wheel

frame relative to the tow arm ϕ is indicated by the relative angle potentiometer (RAP). These two angles added together form the instantaneous slope of the road surface. Four magnets mounted in the rear wheel and a pick up coil mounted on the wheel combine to generate a pulse each 6.614 inches of travel.

III. DATA ACQUISITION SUB-SYSTEM

The data acquisition subsystem is shown in figure 4. A block diagram is shown in figure 5.

Within the data acquisition subsystem the signal conditioning (figure 6) provides the necessary elements (e.g., excitation, amplification, and filtering) to present to the microprocessor section (figure 7) two analog signals representing the gyro and RAP angles and a pulse indicating equal increments of travel. At each of these equal travel pulses, the analog signals are sampled (digitized) and from these is calculated the inclination angle of the terrain test course at that instant. This angle, expressed as a floating point number, is saved in the 256-kbyte bubble memory (figure 8). Included as a part of the microprocessor section are 6 kbytes of PROM, 2 kbytes of RAM, and a hardware multiplier. Although at the present time no data processing other than scaling is performed, future enhancements include the addition of Fast Fourier Transform and histogram algorithms and a vector graphics display.

The operator interface to the data acquisition subsystem is through a micro-terminal, shown in figure 9. The operator uses this terminal to start and stop data collection, to calibrate the system, to read the directory of data stored, and to read the gyro or RAP inputs.

IV. DATA ANALYSIS

Profilometer data handling and data analysis is dependent upon the mini computer system shown in figure 10. Resident in this system is a task management package which provides for various functions, to include the following:

- a. Data retrieval (by a parallel data link in 256 word blocks)
- b. Data file and directory management
- c. Data plotting
- d. Spectral density analysis
- e. Histogram analysis

A list of the commands available in the task management program is presented in table 1.

TABLE 1. VALID TASK MANAGEMENT COMMANDS

Command	Definition
CL	Clear the directory
CK, code	Mag tape control
DL, list	Directory list
EX	Exit profilometer monitor
IN, run	Inspect the data
LC	List commands
PL, lu, run	Plot data
PR, lu, run	Process data (power spectral density)
AD, lu, run	Amplitude distribution of data
FU, run	Purge run from the directory
RE, nspe	Restore data from tape to disc
FU, prog	Run program
TP	Write data to tape
TR	Transfer data
EN	Find end of tape

Data retrieved from the data acquisition subsystem consists of a sequence of angles measured every 6.614 inches. The corresponding profile can be obtained through the integration process

$$y_i = \sum_{k=0}^i \sin \theta_k \Delta S \quad x_i = \sum_{k=0}^i \cos \theta_k \Delta S$$

where:

x = horizontal distance

y = vertical distance

θ_k = instantaneous angle

ΔS = sampling increment

This profile data is then converted to a sequence of height values corresponding to equal intervals of horizontal travel by

$$y_n = y_j + (x_n - x_j) \tan \theta_j$$

where the j subscripts refer to the members of the original sequence closest to but less than the converted point. This interval normalization process is required by the standard signal processing algorithms to be employed.

Any drift or initial zero offset in the angle measurements appears, after integration, as a continual or slowly varying slope which is not of great interest (even if it accurately represents the profile). In addition, the spectral analysis techniques assume stationarity, i.e., the mean and autocorrelation functions are invariant over the set of data being used. For these reasons, the profile data are high-pass filtered or 'de-trended'. This is accomplished by converting the interval-normalized data to

$$y_n = y_n - \left[\sum_{k=0}^n (y_{k+1} + y_{k-1}) e^{-\frac{k \Delta S}{\lambda}} \right] / \left(2 \sum_{k=0}^n e^{-\frac{k \Delta S}{\lambda}} \right)$$

This filter essentially subtracts from each point the average of the points in its neighborhood, but uses an exponentially weighted average to prevent points far from the datum being adjusted from exerting undue leverage on the averaging process. The parameters used in the averaging process are

$$N = 36 \\ \lambda = 30$$

With these parameters this process represents a filter with a 3 dB point of 0.0105/ft (wavelength 95 ft), and which passes 90% of values at frequencies greater than 0.0167/ft (wavelength less than 60 ft).

As an aid to data verification, a program is available to plot the terrain height, y, as a function of the horizontal distance, x. The operator can specify the plotting device (either a CRT or a digital plotter), the data run number and the length of the course to be plotted (up to 76 m (250 feet)). The program then reads in 736 words of the appropriate data (approximately 122 m (400 feet)), converts the data to normalized, detrended x, y coordinate data and plots the requested length of data. This process can be automatically repeated so that the entire course may be plotted. The operator can also specify a certain section of the course to be plotted (rather than start at the beginning). Because detrending alters the appearance of the data from the real world appearance and because plotting more than a short section of the course is impractical from a standpoint of visual resolution, use of this program is limited to data verification. Examples are presented in figures 11 and 13.

The final processing of profilometer data consists of power spectral density (PSD) and probability distribution analyses. As documented in references 1, 2 and 4, the spatial power spectral density (PSD) of the terrain (a spatial frequency domain representation of the squared terrain heights) is related to the energy absorbed by any vehicle traversing the terrain. To compute the PSD, 768 data points are read from disc storage, converted to interval normalized height data, and then filtered or de-trended. Then 512 points are extracted from this sequence, windowed with a Hanning function to reduce spectral leakage, and then subjected to a Fast Fourier Transform (FFT) process to convert the data to the spatial frequency domain. The PSD for each data block is formed by summing the squares of the real and imaginary components and applying the appropriate scaling. This process is repeated over the entire data set, with the results being accumulated into an average spectrum. Non-overlap processing is employed.

Figures 11 and 12 show the profile and PSD, respectively, of one of APJ's fixed test courses; a 6-inch concrete sine wave course. Figures 13 and 14 show similar data for a cross-country test course. Printed on figures 12 and 14 are data extracted from reference 4 depicting typical

gravel and rough roads. Also included is the RMS roughness as computed by integrating the PSD. The other major data processing algorithm employed is the calculation of the terrain height probability distribution. To perform these calculations detrended data are assigned to bins corresponding to the data values. This histogramming process uses 400 bins covering a range of +127 cm, with each bin corresponding to a height interval of 0.64 cm. The percentage of the total number is calculated after all data has been assigned to the appropriate bin and the results are plotted as a function of terrain height.

Figures 15 and 16 show the probability distribution functions for the courses in figures 11 and 13, respectively. Superimposed on these plots are the normal probability distribution curves with means identical to the actual data sets and with standard deviations equal to the RMS roughness of the course as calculated by

$$RMS = \left[\frac{1}{N} \sum y_i^2 \right]$$

where N is the number of data points involved and y represents the height values.

V. CONCLUSION

The profilometer described here provides a partial measure of the automotive test environment which is largely independent of vehicle effects and the speed of the measurement vehicle. Use of the on-board microprocessor-based data acquisition system and the flexibility of the data analysis task

management package enable raw data to be analyzed in any or all of the available formats discussed within minutes after the completion of a data run. As more improvements are installed, this system is becoming easier to use on a daily basis, and eventually it could be used as a constant monitor of test course severity. Areas which still require attention are parameters other than terrain profile which contribute to course severity.

VI. REFERENCES

1. Faules, P. and Harley, S., Special Study of Technique and Study of Automotive Test Course Index, Phase I and Phase II, TECOM Project No. 9-CO-011-COO-019, US Army Aberdeen Proving Ground, Report No. APG-MT-3635, August 1970.
2. Walton, W. Scott, Special Study of Technique and Study of Automotive Test Course Index, Phase III, TECOM Project No. 9-CO-091-COO-007, US Army Aberdeen Proving Ground, Report No. APG-MT-4533, October 1974.
3. Shrader, T., and Cannon, W., Profiling the Yuma Proving Ground Mid-East Desert Analog Test Course, TECOM Project No. 7-CO-RD3-API-012, US Army Aberdeen Proving Ground, Report No. APG-MT-5882, September 1983.
4. Bekker, M. G., Introduction to Terrain Vehicle Systems, The University of Michigan Press, 1969.
5. Fix, G. A., TARADCOM Signal Analysis Program, September 1978.

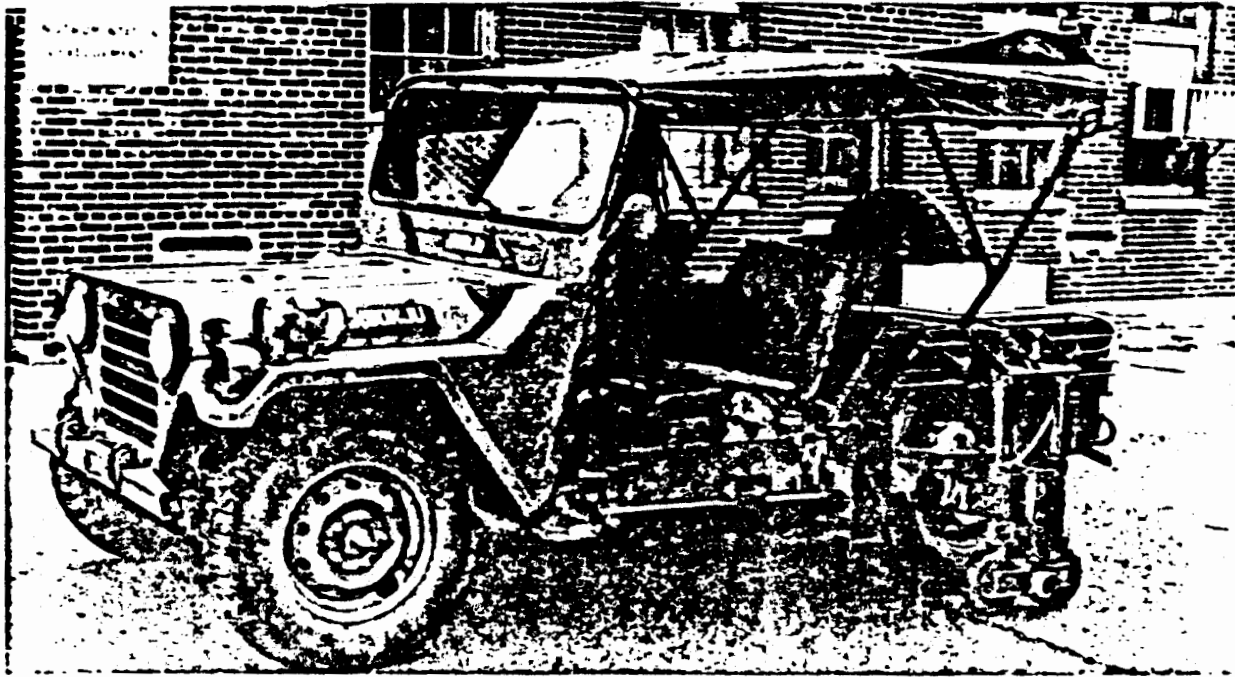


Figure 1. Profilometer Tow Arm

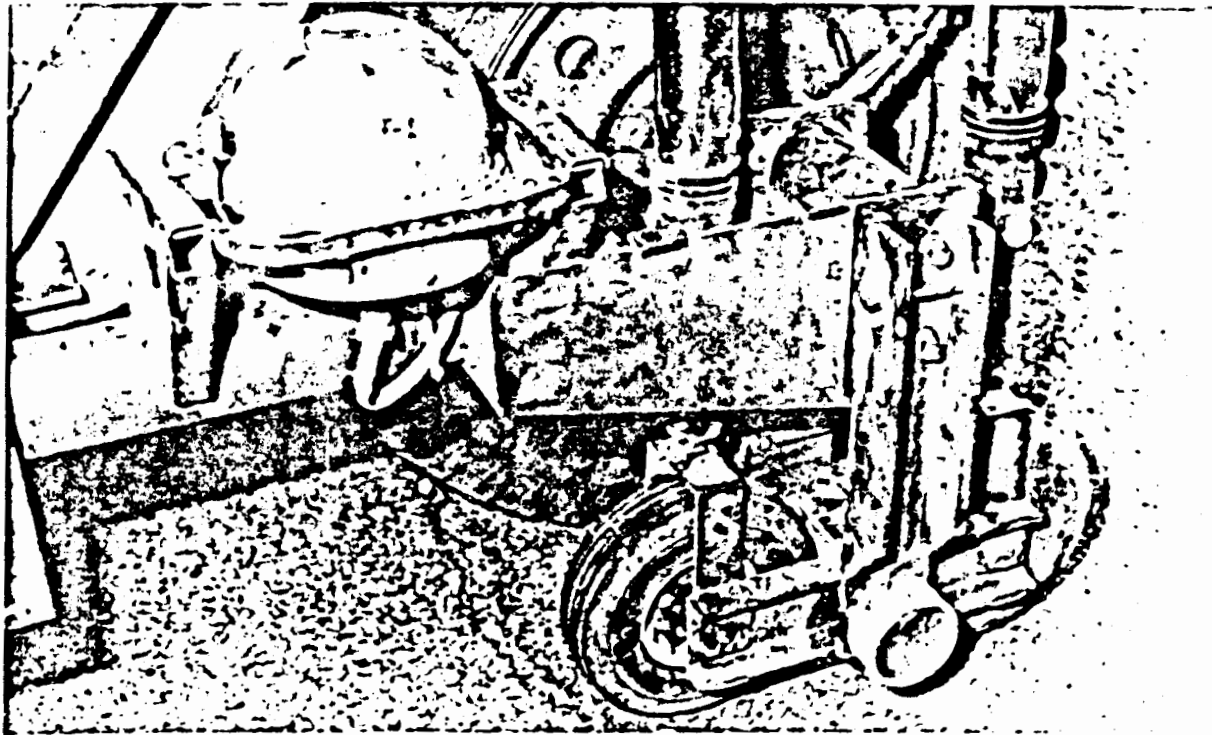
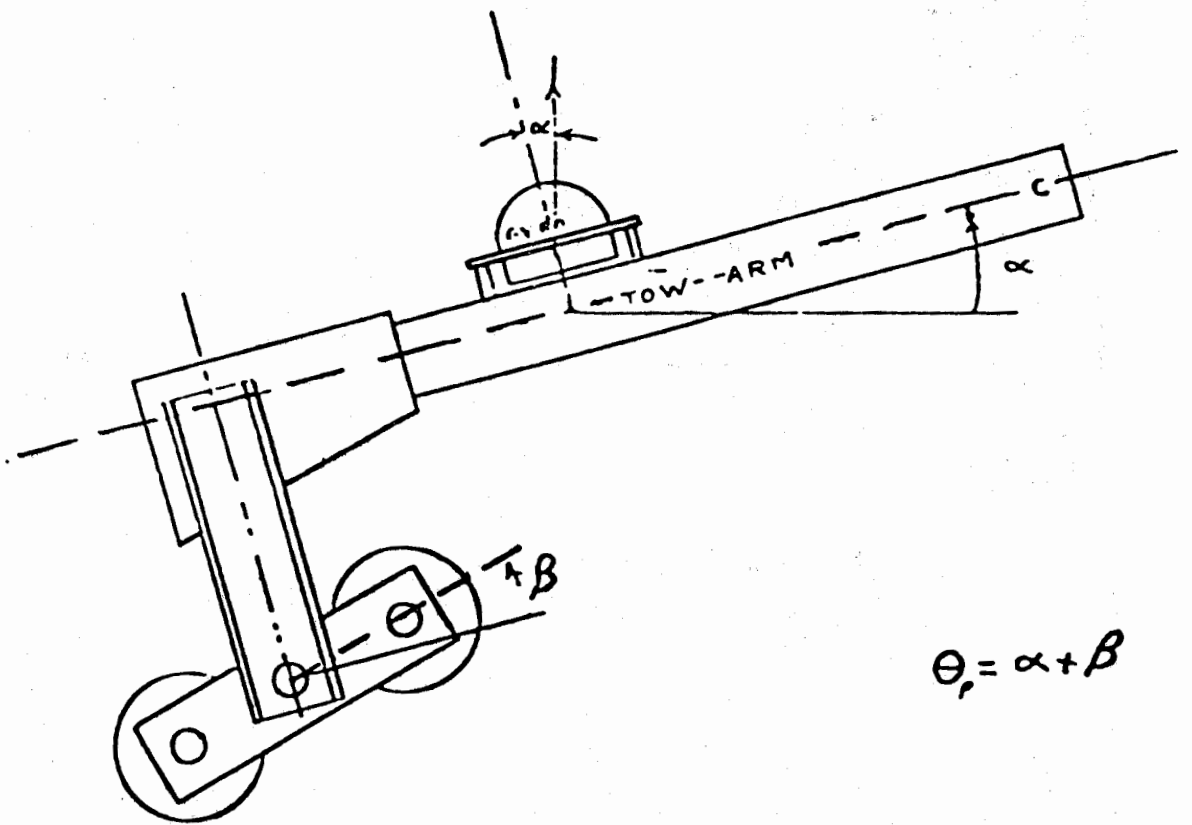


Figure 2. Profilometer Tow Arm



$$\theta_p = \alpha + \beta$$

Figure 3. Tow Arm Schematic

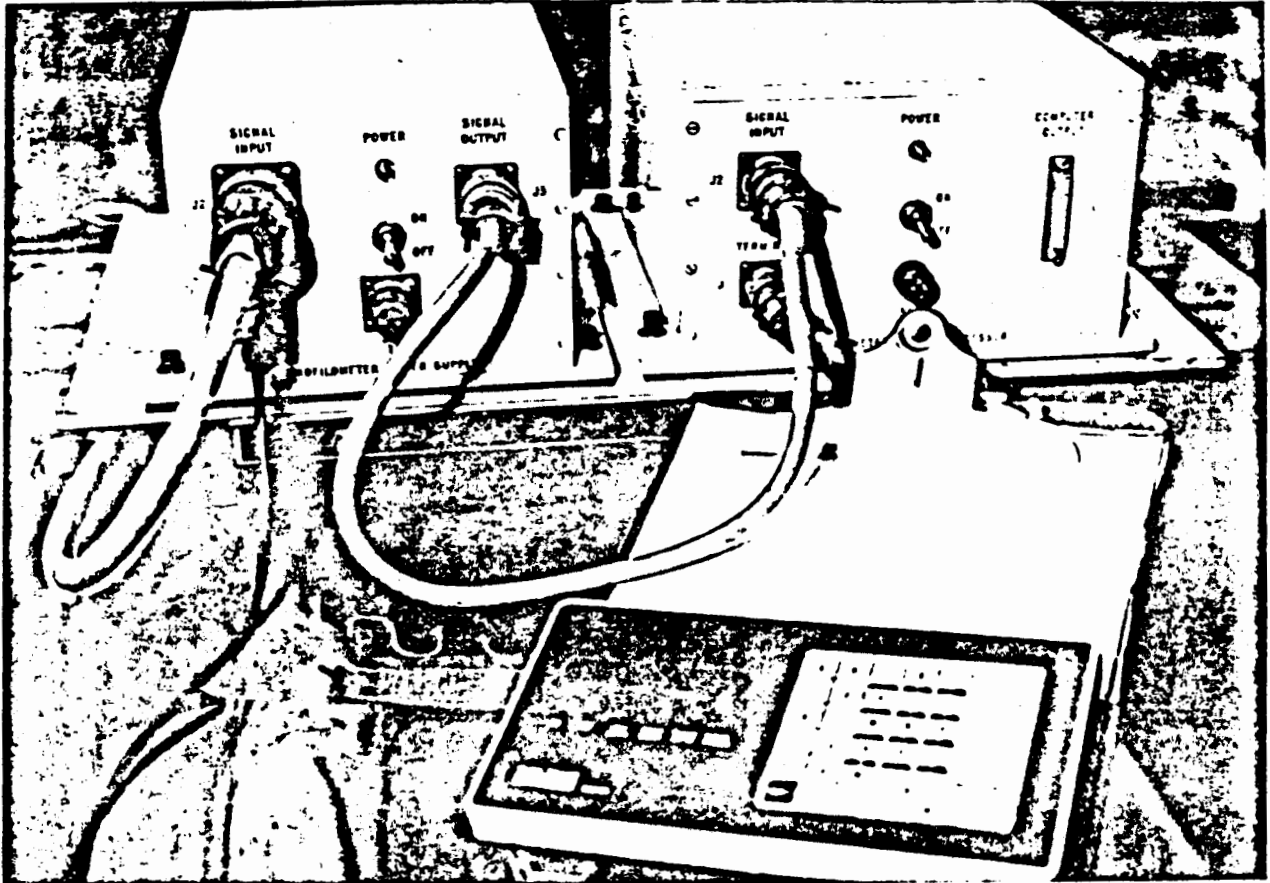


Figure 4. Profilometer Data Acquisition Subsystem

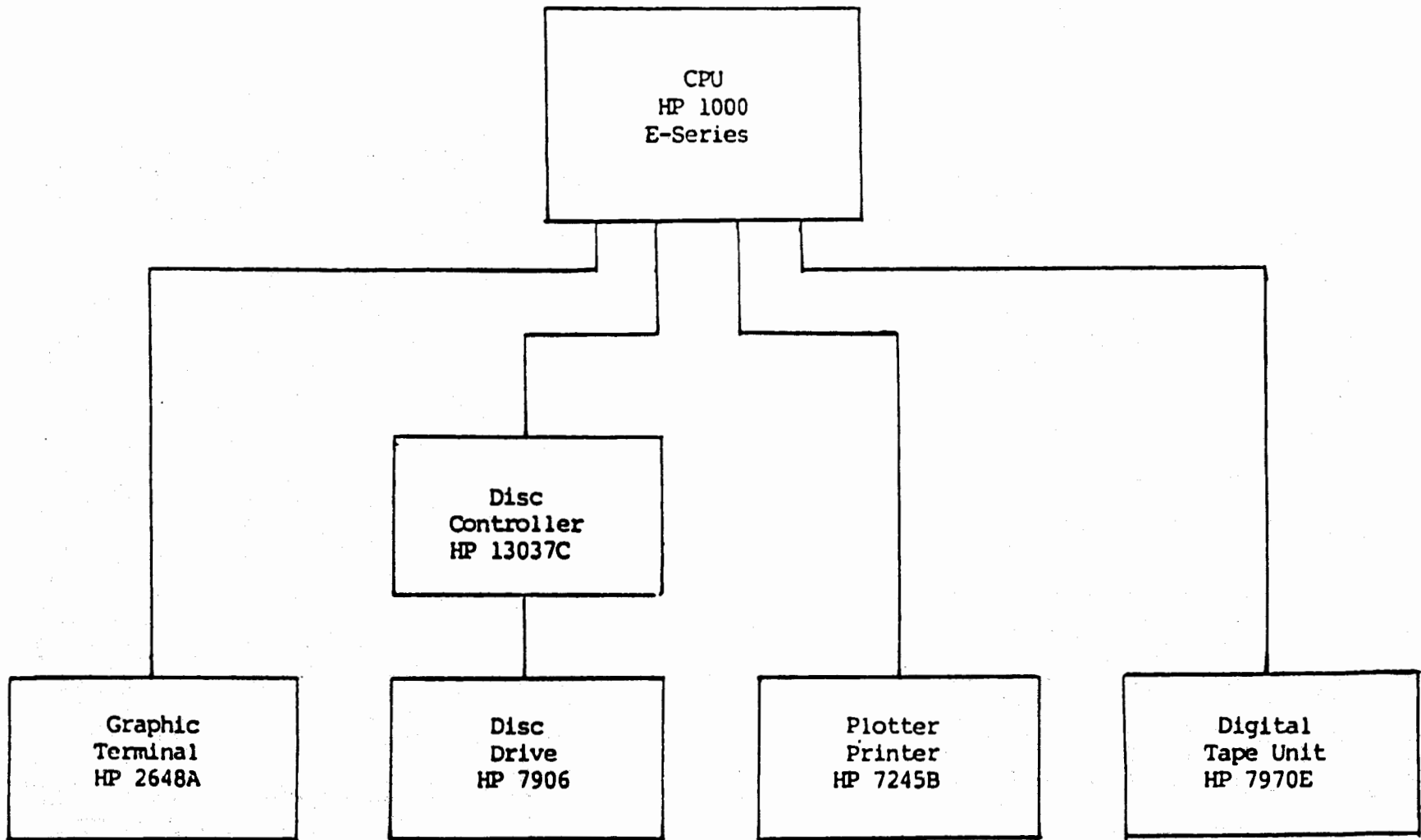


Figure 5. Profilometer data analysis system.

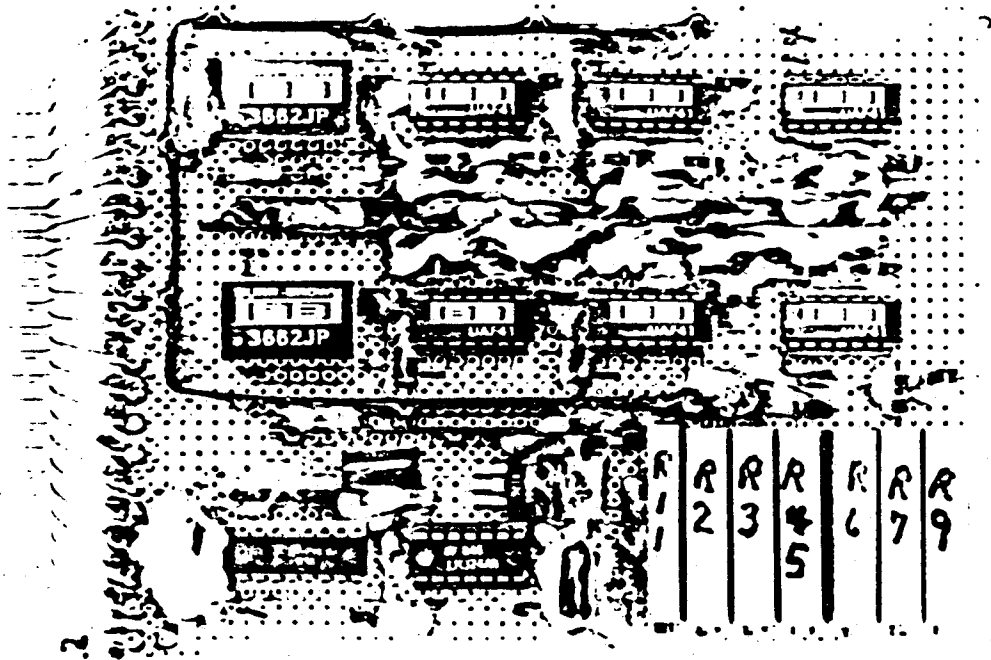


Figure 6. Signal Conditioning

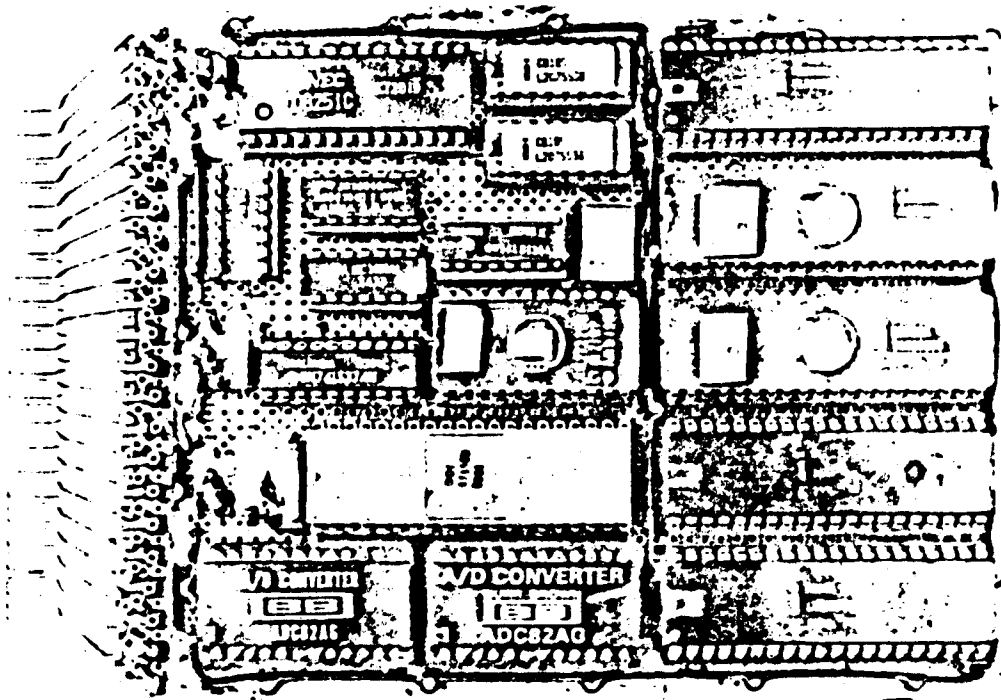


Figure 7. Microprocessor Section

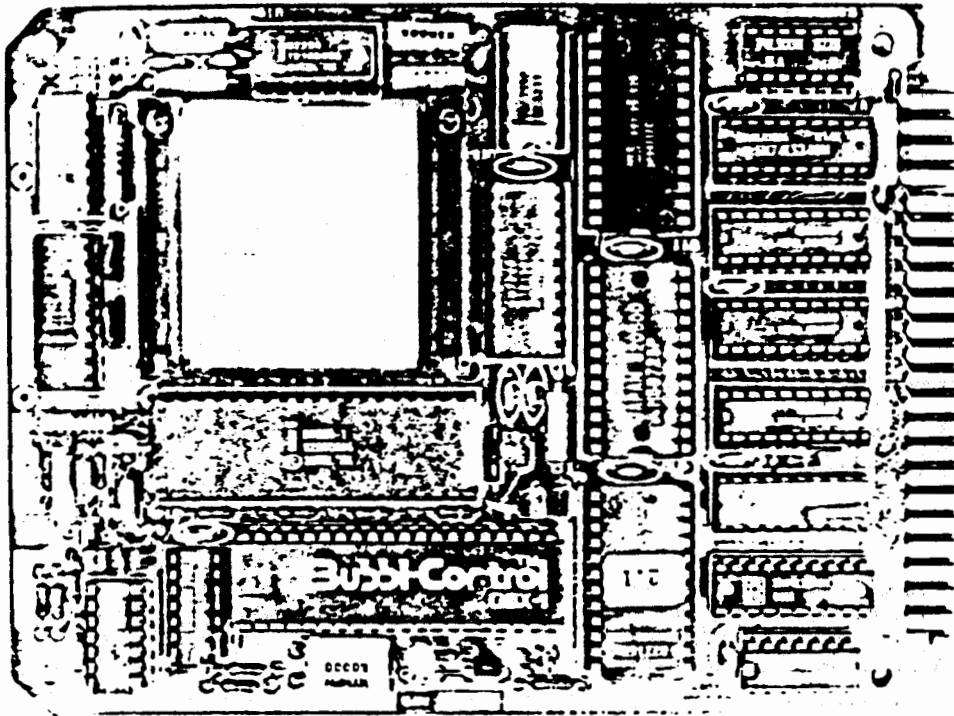


Figure 8. Bubble Memory

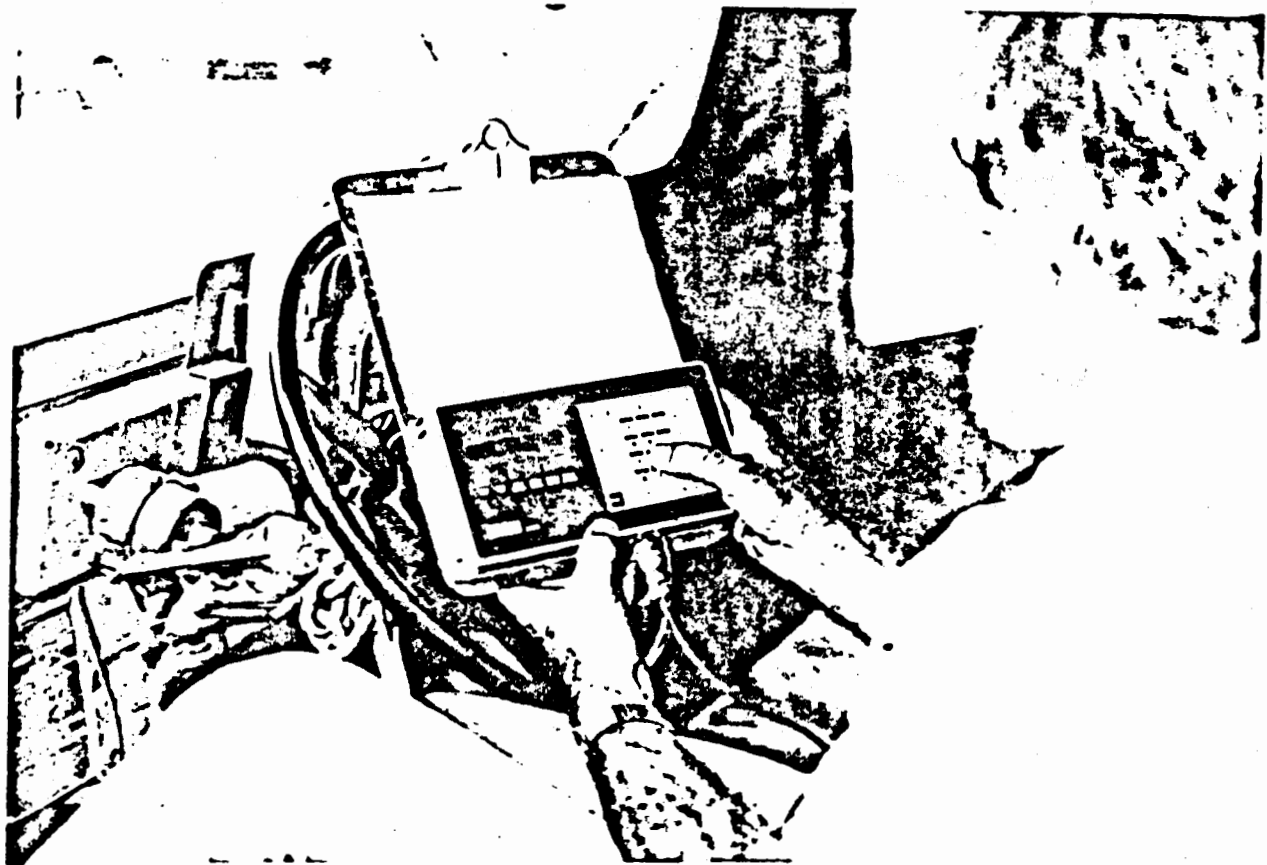


Figure 9. Micro Terminal

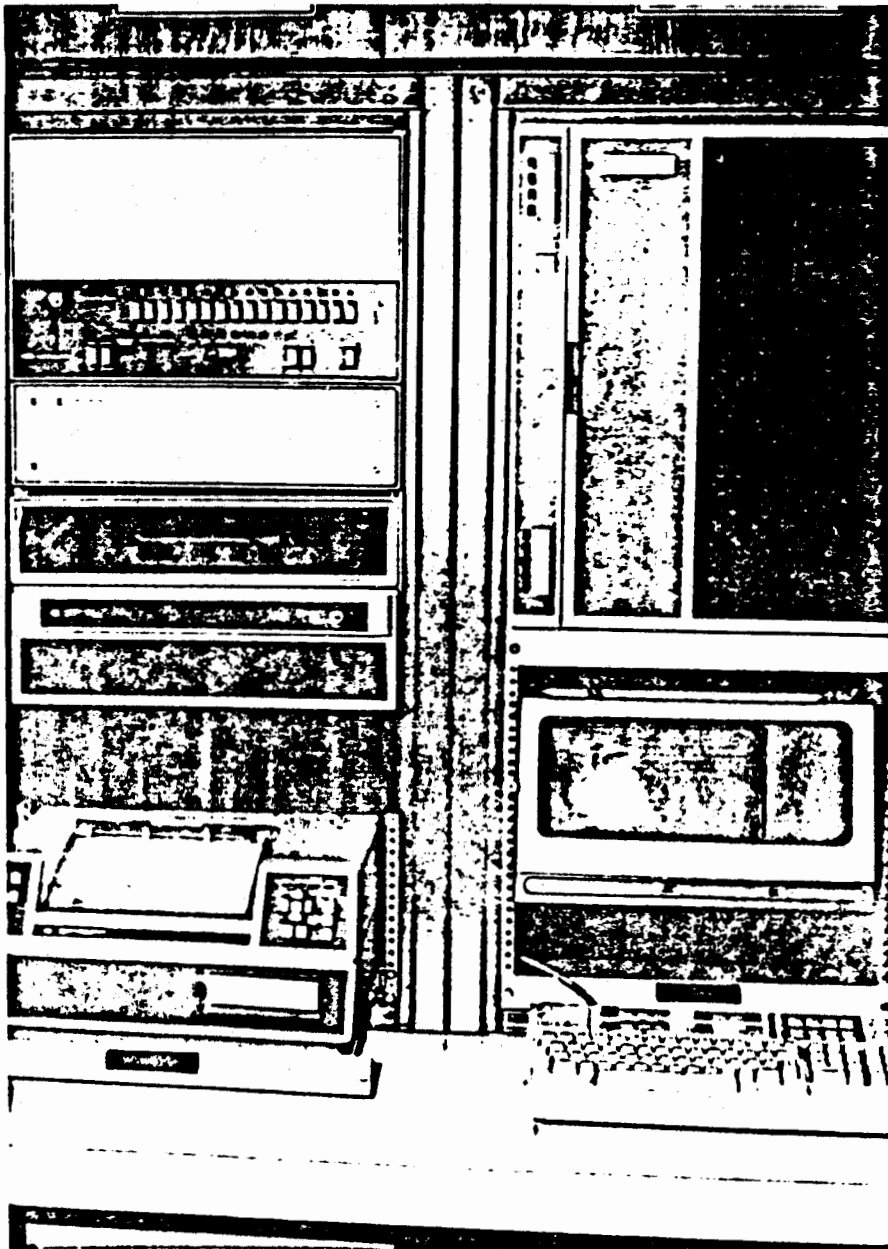


Figure 10. Data Analysis System

RUN 1 6" WASHBOARD 4/8/83

33

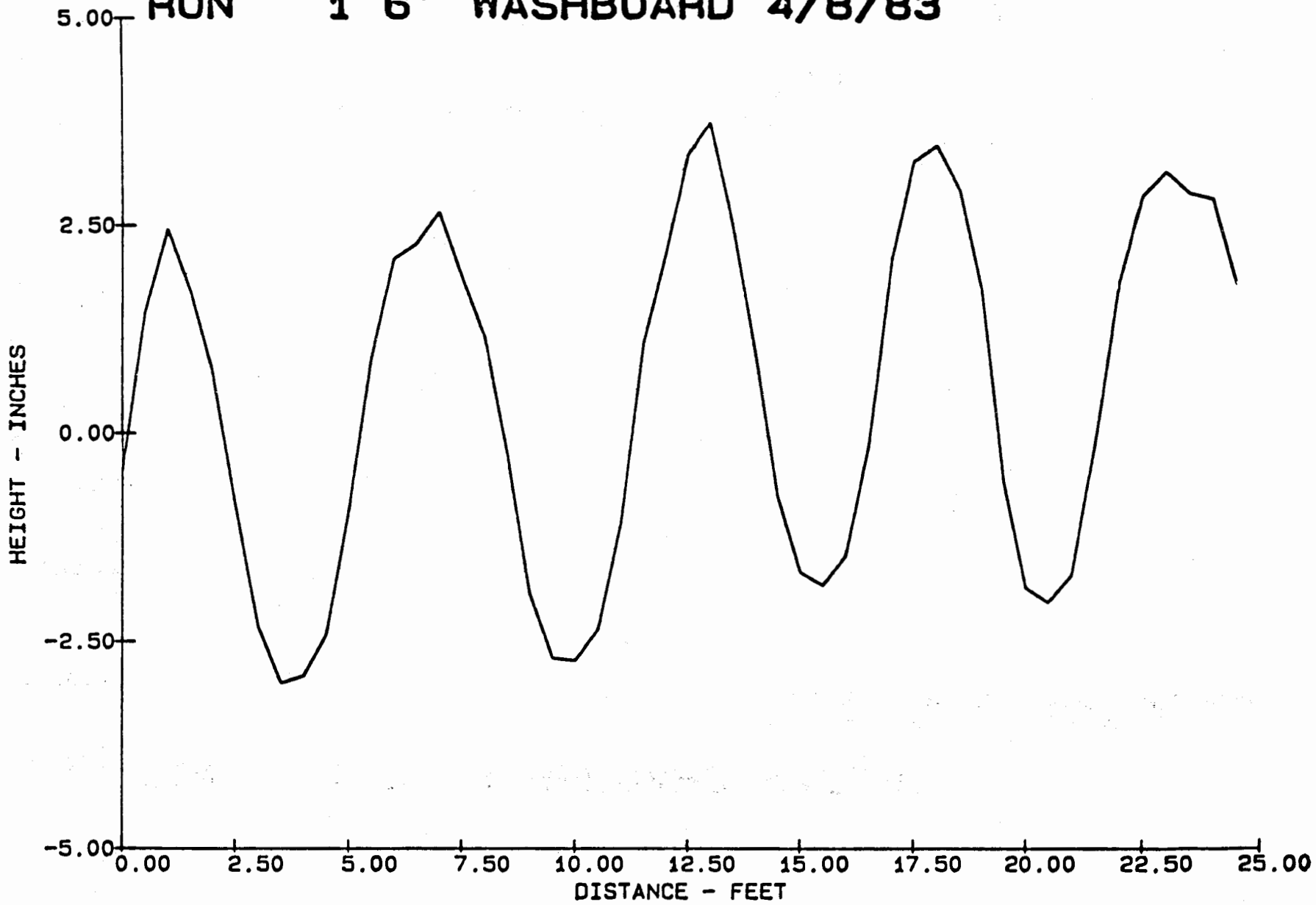


Figure 11

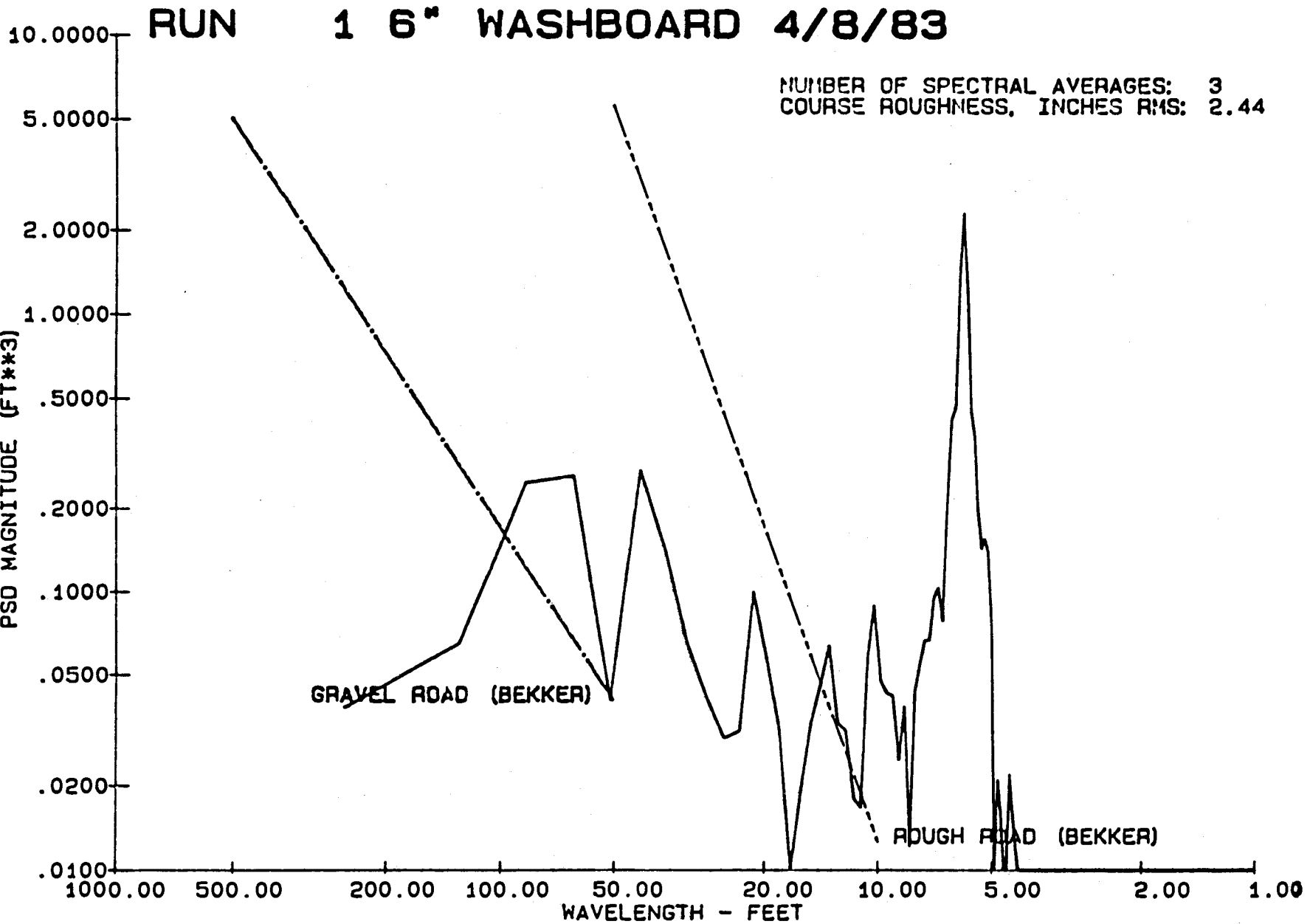


Fig 12

RUN 18 TANK HILL COURSE B 15/06/83

35

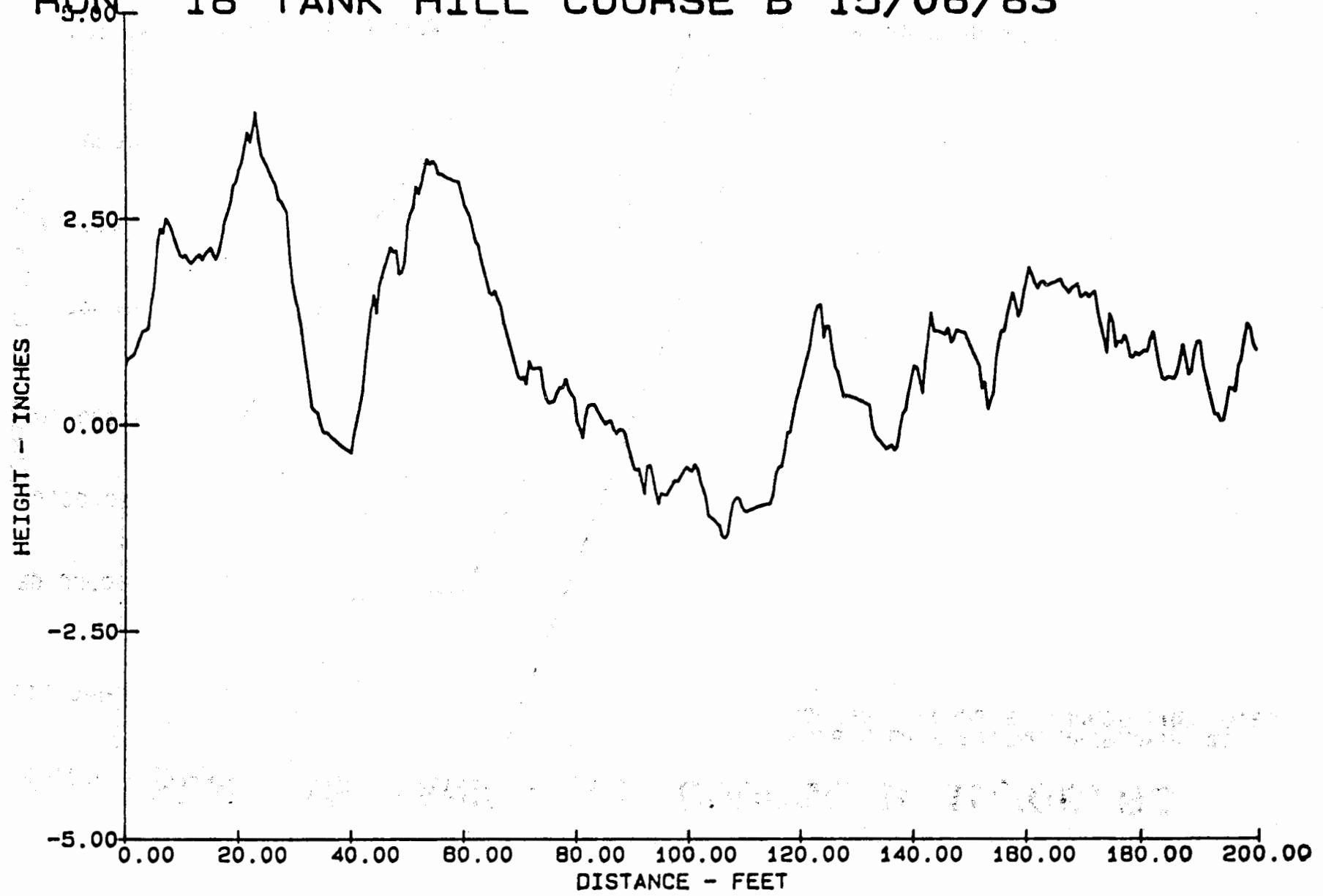


Figure 13

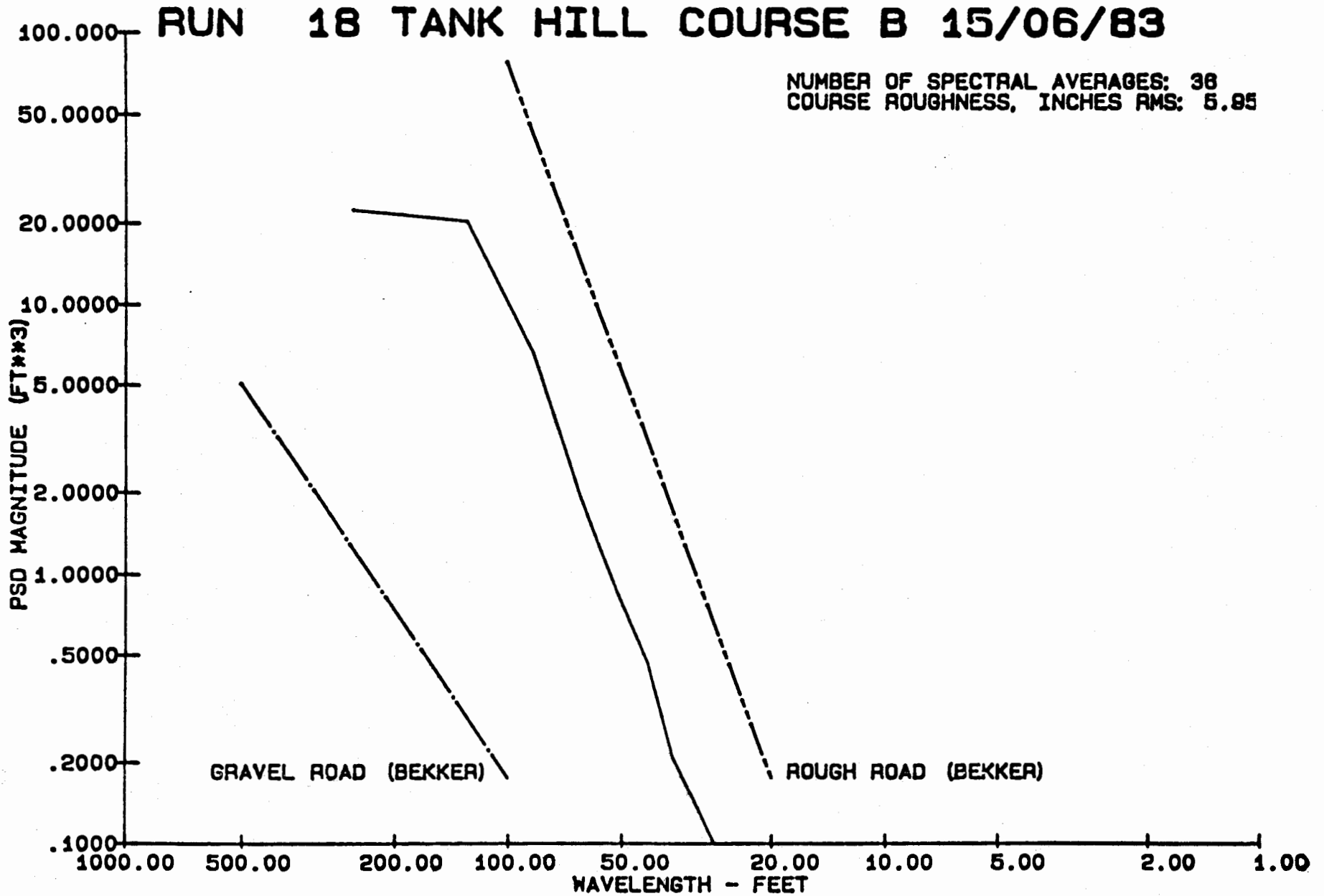


Figure 14.

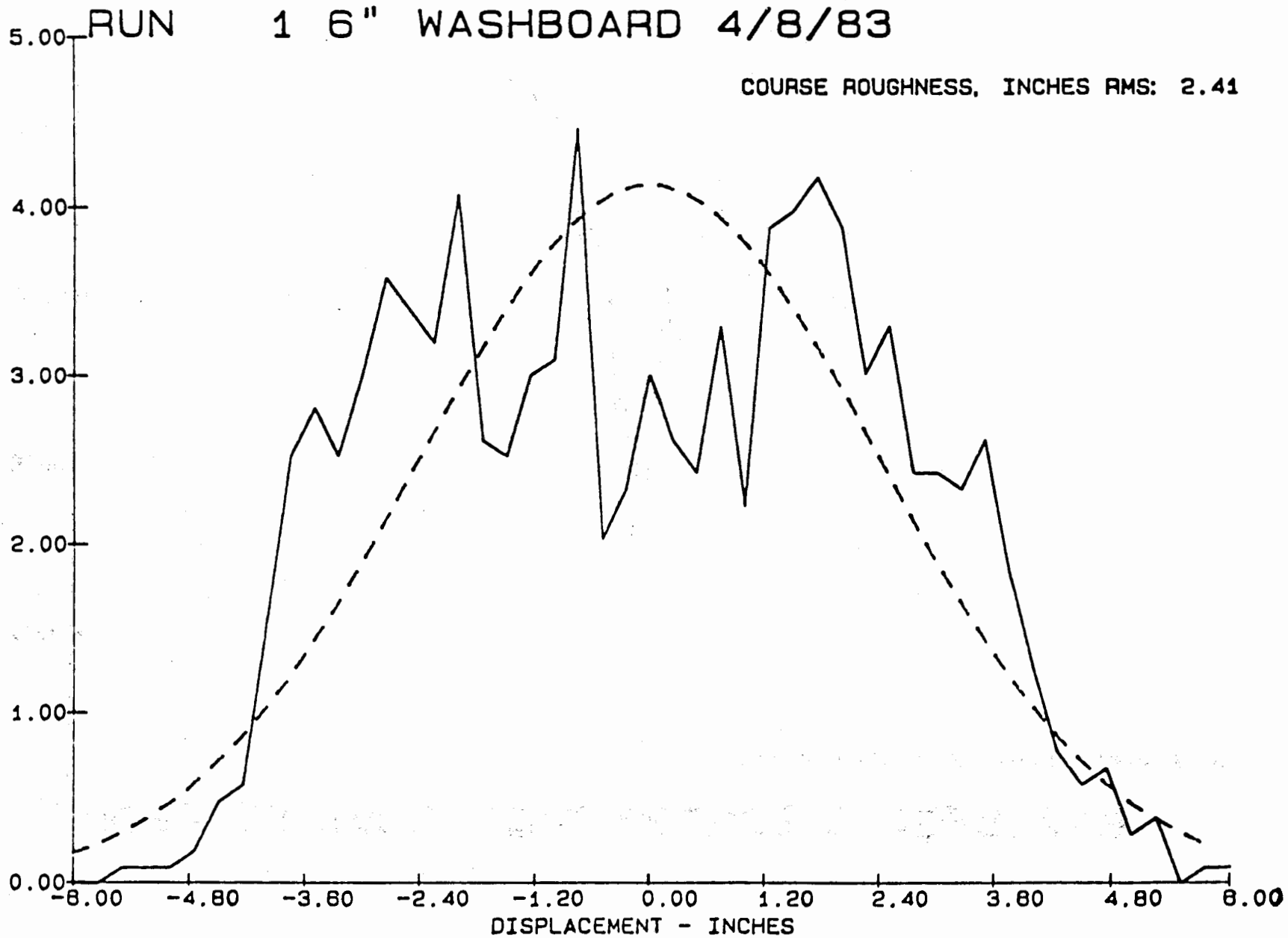


Figure 15

RUN 18 TANK HILL COURSE B 15/00/83

COURSE ROUGHNESS, INCHES RMS: 5.23

38

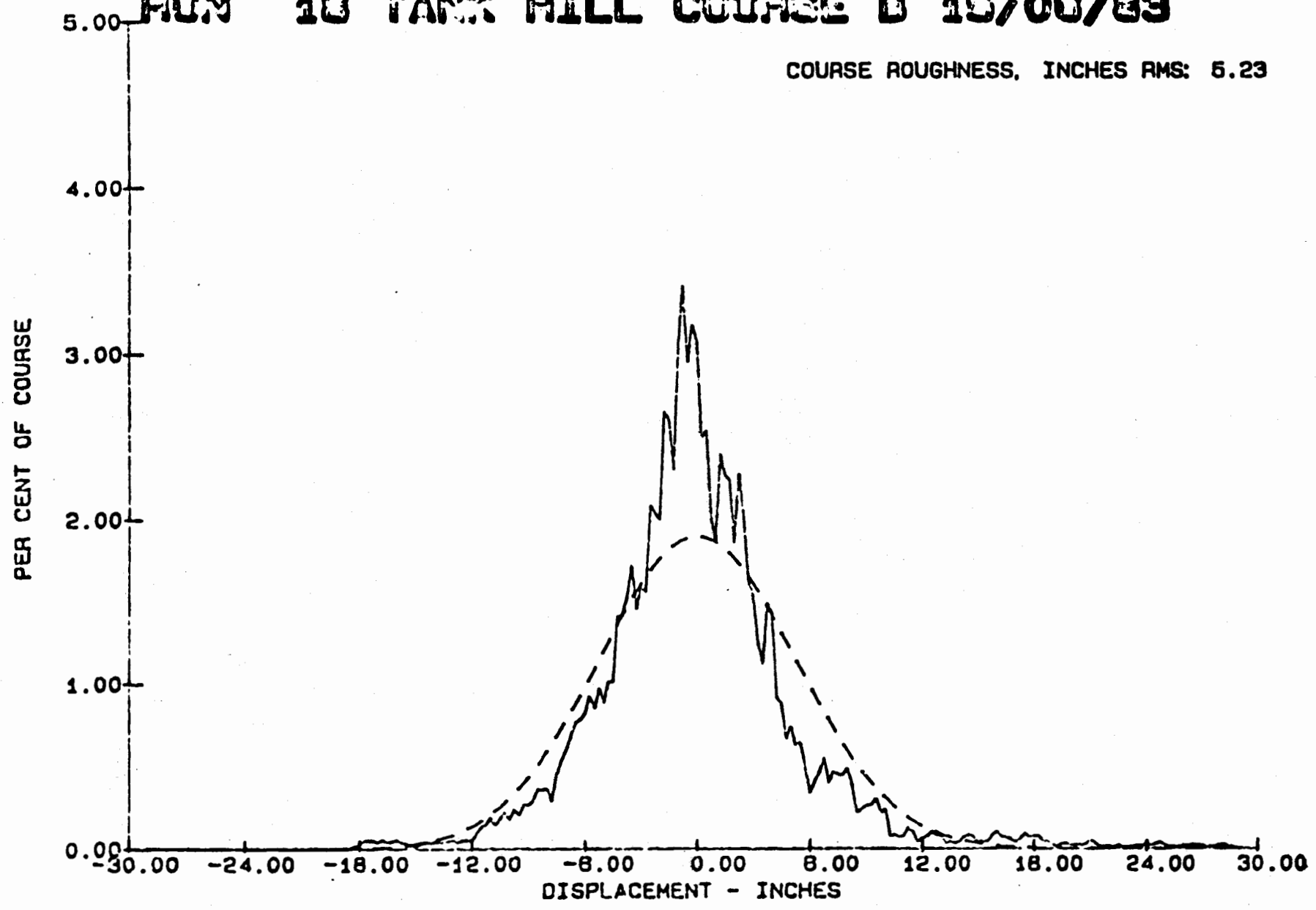


Figure 16.

SESSION 1

Q: BILL ANDERSON, NAVAL AIR TEST CENTER, PATUXENT RIVER, MD

The way we will run this is there are two microphones that will be passed to anyone who has a question, and we'd like the person who has the question to first state his name and his activity. This is because we make the question and answer session or the discussion session a part of the minutes and they are being recorded by a tape recorder over there. So make sure you state your name and activity. We'll pass this microphone back and forth. You can ask a question to a specific person. That's the way we'll work it. I'll start off.

Dennis, when you talked about producing this large torque calibration system, did you do an analysis of the length of time it took to manufacture and produce that and how much it cost the activity?

A: DENNIS PAGE, WSMR, NM

No, we didn't. The requirement existed and a substantial number of instruments were present. One of our primary goals is to be able to support these instruments that were received, so we just went ahead and built it. In answer to your questions, I can probably come up with a figure pretty easily since I know basically the amount of machine time required and design time on my part and debugging. I don't have it with me but I'll be glad to find that out for you.

BILL ANDERSON, NATC

Okay, any other questions anyone wants to ask? We're open. Yes, let's go.

Q: TOM MILLER, LAWRENCE LIVERMORE LABS., LIVERMORE, CA

I have a question on the step pressure calibrator. You talked about 150K upper end, what's the lower end? Have you explored that and what time constant is on the rise time there?

A: ARPAD A. JUHASZ, U.S. ARMY DARCOM/BALLISTICS RESEARCH LABORATORY, ABERDEEN PROVING GROUND, MD

Yes. Basically the series of tests we've been working on have been between 25 thousand and 150 thousand psi. There wasn't any substantial reduction in the time step in going to 25 thousand psi. Things are a little bit faster at 100 to 150 but it hasn't slowed down like two milliseconds or three or something like that. So the action time is really not quite really constant but within under one millisecond even down at 25K. The idea would be to try and get calibration values say at 25, 50, 75, 100, and that sort of thing. Then you have a number of different points.

Q: LARRY SIRES, NAVAL WEAPONS CENTER, CHINA LAKE, CA

Having a fair amount of experience trying to build dynamic pressure calibrators over the years, the pressure oscillation that is noted in your traces has also plagued all of my efforts. It creates a number of problems for me especially with the advent of digital acquisition systems used in calibration labs these days because you've got to figure out some way of getting past those oscillations, so you're getting the data beyond that and not of the oscillation itself. You'd have some kind of a peak - if you're trying to get the pressure out of, obviously if you're looking at the peak that's going to be different. Did you do anything to try to get rid of those oscillations? Have you done anything to try to minimize them? What was your experience in that area?

A: ARPAD A. JUHASZ, U.S. ARMY DARCOM/BALLISTICS RESEARCH LABORATORY

The answer to that is actually no. Experimentally, we just let the thing be the way it was. The next step would have been to do some fast fourier analysis of the signal and then clean things up. I've done that sort of thing with Close bomb data. If you have a Close bomb with reasonably long cavity length, of course you are plagued by an addition of this wave pattern onto essentially a pressure step which is quite similar to what we had in this device. So, I know we can get rid of this stuff provided there is a reasonably high frequency to the oscillations so that the step function and the frequency aren't too close together. But we experimentally didn't try to get rid of the thing yet nor have we really analyzed the data to do that. I always feel much more comfortable taking a straight edge and sort of passing a line through the center of the oscillations than going through this marvelous piece of electronics and not being sure just exactly what comes out. But I think that's a good question and something that needs to be addressed before we finally refine the tool.

Q: RONALD TUSSING, NAVAL ORDNANCE SERVICE WEAPONS CENTER, SILVER SPRING, MD

I again wanted to ask Arpad what size are those chambers of the gauges themselves? How do you get the leaves out? And would this be applicable to, say, underwater pressure gauges?

A: ARPAD A. JUHASZ, U.S. ARMY DARCOM/BALLISTICS RESEARCH LABORATORY

I don't know anything about underwater pressure gauges. As far as the gauge cavities are concerned, basically they will accept either the Kissler 607 or the PCB. I'm not sure if it's the 118 or the PCB analog to that. We also have imported some of the minihat gauges which BRL has been playing around with. The cavity that would lead to a Kissler type gauge or a PCB type gauge would have a cavity length of 90 thousandths and the diameter of the cavity would be just a hair smaller than that. And then it will come out to a cavity diameter of .25 inch and maybe ten thousandths in length. So it would come out like this before you hit the diaphragm. The test chamber volume excluding the wall that's in the test chamber and the piston that supports it, is about 1 cc, so we try purposely to keep that fairly

small. But we didn't want to flush mount the gauges in case the ball rattled around in there it could do a lot of damage to the gauges as we're testing. Probably some modification of this kind of design could be used. Again, this is not a shock wave type of a thing. These ballistic events, we think of them as a bang, but it's not at all like a shock wave. It's slower in terms of milliseconds.

RONALD TUSSING, NSWC

Thank you. I appreciate that.

Q: TOM MILLER, LAWRENCE LIVERMORE LAB

I just have two questions. One is the approximate cost for this item and the other is do you ever think you'll get a telephone system in the near future that you can be accessed with?

A: ARPAD A. JUHASZ, U.S. ARMY DARCOM/BALLISTICS RESEARCH LABORATORY

The answer to the second question is probably not. A few years ago they modernized our phone system and gave it this nice computerized thing you could forward calls and do everything. What they didn't do is change the number of trunk lines coming into the station and so it's hell trying to get in or out. And I suggest, if you do want to get a hold of me by phone, check the weather report in Maryland because when it's raining, the phone system goes completely haywire. Okay, on the approximate cost, I think when we started, Hardwood Engineering was the outfit that did the detail design and the building of this from the concepts we formulated. The initial contract with them was 23K and then we ran into a lot of problems with the linkages breaking and the toggle mechanism was really the hang-up on the whole thing. I think there was another 10 or 15K that was spent while we worked out that particular part of the problem. I think Hardwood lost some of their own money while they were working on this thing, but now things have evened out. Probably somewhere in the 20 to 30K range you could probably have one built.

Q: LARRY SIRES, NAVAL WEAPONS CENTER

Is that the reason for the buffer on the tripper mechanism because of the breakage? I was kind of curious about that.

A: ARPAD A. JUHASZ, U.S. ARMY DARCOM/BALLISTIC RESEARCH LABORATORY

The answer is yes. We went through a lot of different buffer configurations and the toggles themselves had to be beefed up and the materials of construction for them changed too.

Q: JOHN ACH, AIR FORCE WRIGHT AERONAUTICAL LABORATORY, OH

Yes, Bill, I have a question concerning the profilograph. I had some experience working with the Air Force on a device we call a profilograph which was very similar. We measured profiles and runways. We were always concerned with measuring in a straight line. We didn't

want to deviate more than a foot or so off course. Is there any provision for any guidance on your jeep or are you concerned about that?

A: W. H. CONNON

No, remember we measure one track and that's one of the limitations. Our courses are fairly wide; they're probably three jeeps wide, essentially. During a test a driver can run anywhere on the course. So the idea is to make several passes and to get some good average value.

Q: NOT IDENTIFIED

It must be mental telepathy because I had a question on the profilometer. Are there were any plans of putting another access; in other words, does it make any difference for your purposes as to whether the course pitches or rolls or whatever?

A: W. H. CONNON

Yes, it does. That's a good question. We're thinking of a towing type device that would get phase difference between two tracks because they do pitch from side to side. It's not a linear type motion. That's correct, you'd get the angle between them.

Q: DON BOREMANN, MOUND FACILITY, MIMESBERG, OH

I'd like to address my question to Mr. Arpad concerning your high pressure dynamic tester built by Hardwood. We have a requirement to calibrate several of the 607 Kisslers, like five or six hundred. This is for a production activity that we have and we calibrate maybe 50 of them a month. What I'd like to know is, would that equipment lend itself to multiple tests? What is the maximum number you could test at a time with that?

A: ARPAD J. JUHASZ

The answer to that is yes. Right now, the way the head is configured, you could put four gauges in there. One of the things that Mr. Bullock has been working with is an adapter so that you have sort of a universal adapter and you don't even have to take the gauge head out. But you put whatever gauge you want into this plug that screws into place. That makes the turnaround time a lot easier. So you could at least test four at a time. Danny how many runs have you done in a day with that machine? Quite a few; forty, he says. Now that the thing is working and the parts aren't breaking, it is really no trick at all to do a lot of them.

Q: DON BOREMANN

What about data collection? How do you handle that?

A: ARPAD A. JUHASZ

Okay, here we're going to give a plug to Nicolet Corporation. I really believe in their product. The digital oscilloscope, I think it's Explorer Three, that 20-94 series, whatever it is by Nicolet. I like it because it has an automatic triggering option. So there's a cursor triggering. It has a wraparound memory feature, and when you pass a given voltage then it remembers this pre-trigger time event and then it takes the rest of the data. So you're always assured of catching your event. And this thing can be put on a magnetic disk - a floppy - and then from there we simply dump it on a minicomputer and play with it. So, the Nicolets really do a good job. Now I think they've come out with a much better oscilloscope, a more expensive one with 16K of memory instead of four and I think it has four channels. That type of device I think would be quite reasonable.

Q: DON BOREMANN

Okay, one final question. Your transfer standard that you use, that you calibrate against your dead weight tester for traceability, is that a strain gauge type of instrument?

A: ARPAD A. JUHASZ

Yes.

Q: DON BOREMANN

What would you consider typical uncertainty on that then?

A: ARPAD A. JUHASZ

There is a lot of talking in the background without a mike so I'm not sure what else was said. I think I'm going to pass that on to Danny because that part of it I don't really know.

BILL ANDERSON

Okay, other questions?

Q: BILL ANDERSON, NATC

I'll ask a question then. I want to ask David Banaszak a question about his accelerometer techniques. I guess what I am trying to figure out is are you advocating the use of some of these infield techniques to replace laboratory type calibrations, and if so, have you done analysis on the accuracy that you're getting or, you know, what are you really giving up to do that?

A: DAVID BANASZAK, AIR FORCE AERONAUTICAL LAB, OH

I guess the question is about my advocating some field techniques to replace lab cal, like the 3 point cal technique. I think that could do that in many cases because there were references there that the main thing was keeping the accelerometer level with respect to earth.

I ran an experiment last week doing that and used one g technique, but the problem I always have is comparing sensitivities in accelerometers. If I run five different percentages, including using the manufacturer's one as a basis, I don't know which one's right. Maybe it will be 10.2 millivolts per g and they range from 9.8 to 10.6. I'll measure and maybe the manufactured one's in there too, and my biggest problem is when I compare them. I don't know which one's the right one. Last week I ran one and it was within, I think it was supposed to be 10.4 millivolts, and it was 10.2 using a one g technique. So, that's within a couple of percents.

Q: PETER STEIN, STEIN ENGINEERING, PHOENIX, AZ

I have a question for a number of the speakers. Mr. Page, you went to great trouble to try to keep extraneous movements and forces out of your calibration. By the same token you now would have a very nicely controllable method for applying extraneous torques and extraneous bending movements and things like that. Do you think your apparatus could be modified to evaluate transducers as to their sensitivity to extraneous torques and forces and things of that type, bending movements?

A: DENNIS PAGE

Let's see if I understand your question. In other words, be able to apply a known movement to various, for example, load cells or whatever?

Q: PETER STEIN

To evaluate torque meters in terms of their sensitivity to bending movements and axial forces and things of that type.

A: DENNIS PAGE

Well, I don't think it could be used without quite a bit of modification because it's set up to apply a pure movement and to apply axial and bending movements would require additional fixtures, instrumentation and methods by which we could apply this.

PETER STEIN

It just seems that with all those pistons and cylinders you have, you should be able to move things around and to buy almost anything you wanted. That's really why I asked.

A: DENNIS PAGE

Well, the big problem is that it's conceivable, and we could apply an axial load by moving the bearing. It was not restrained in that direction. However, bending would be a problem because it is restrained by two bearing systems. I guess, it's possible that that could be applied, however, we don't see a demand for that kind of testing. If we did, we might pursue that.

Q: PETER STEIN

I have a question for Mr. Banaszak. You showed a slide where you had different supply voltages that you were applying to the semiconductor, strain gauge type of accelerometer and you had different 0 shifts in calibration. There may be a manufacturer in the group who could lend some support to the question. I think the compensation of one of these accelerometers is only good at a particular supply voltage, the temperature compensation and other compensations. Did you see any evidence of that in your tests?

A: DAVID BANASZAK

I did evaluate temperature compensation as a varied supply voltage in that particular case. That would be a possibility by adding a couple more channels and maybe having a thermocouple on there at the same time. I forgot to mention in the presentation that this is not a strain gauge type device. This was a capacitive type of device and in this particular test it had the advantage of being single ended, common signal, common signal/common excitation so I could use the particular oscilloscope I used which had two single ended inputs. One of the tradeoffs in searching for a digital oscilloscope was that fact and that was kind of alluded to in the murphyism earlier. I liked the Nicolet oscilloscope I was looking at because it had differential inputs but the computational capability wasn't quite as strong. It's a world of tradeoffs all the time. You get one thing you like then you have to give up something else. That particular accelerometer, and I think I'm kind of running on here a little, but I know what you mean because when I was doing these kuliite pressure transducers, I had that question too. I asked them that. Okay I have an excitation of 10 volts on this, these were strain gauge type, if you go to five volts is it the same holding system? Well, not necessarily the same. So, I learned that, too, from experience and I appreciate you bringing that up.

BILL ANDERSON

Okay, any other questions?

Q: BILL HEDGE, EG&E

I guess it was David Banaszak. You mentioned in one of your slides that you had a digital scope with analyzer, is that correct? Is it built in?

A: DAVID BANASZAK

Yes, yes. This isn't the Norlan Corporation but their digital scope has computational capabilities. It's sort of like a baby computer; push a few buttons and you can manipulate the array of data that you collect and do various functions with those arrays of data. That's what I meant by analyze. Once the data was acquired, I took either a derivative of the array or plotted array A versus array B, similar to what you could do before on an XY plotter. You put channel A in the X axis and channel B in the Y axis, so that scope will have the ability

to display data that way. It has the ability to actually find the best fit straight line between two channels. It would give you a slope and intercept.

BILL ANDERSON

Another question over here.

Q: JOHN KALINOWSKI, EG&G, SAN RAMON, CA

I have a question for Mr. Connon. I believe you said that you were not interested in the surface of the road but in the vehicle surface where it makes contact. How can you relate a jeep surface to a tank surface in the profile?

A: W. H. CONNON

That's a good question. We can alter the pressure in the shock absorbers to get any type of ground pressure we want. Basically, this device is used for maintaining the courses. Our courses, unlike the state roads in Maryland, are maintained on a monthly basis, so we had to pick something to go with and we had it hooked to a jeep. We figured that was a reasonable thing to do. But if we needed to do something specifically for an M1 tank, for example, we could match the ground pressure to that.

BILL ANDERSON

Any other questions? Okay, then I'd like to...oh, is there one more?

Q: PETER STEIN

I have a question for Dr. Juhasz. At the last transducer workshop there was a paper presented by Scott Walton, I believe it was, who had a similar, very fast step pressure transducer calibrator. Are you at all connected with him or can you somehow compare the two apparatuses?

A: ARPAD A. JUHASZ

Actually, no. We're connected. We both work for the Army. He's up at Dover, New Jersey. I'm down at Maryland. As with many installations, somehow communication doesn't come off as well as it should. So, actually I, personally, wasn't even aware that he had a machine like that.

A: DAVE DYKSTRA, U.S. ARMY COMBAT SYSTEMS TEST ACTIVITY, ABERDEEN, MD

Could I address that? Actually, he's not at Dover, he's right across the fence. Scott Walton works in the Instrument Development Branch at CSDS.

ARPAD A. JOHASZ

My apologies.

DAVE DYKSTRA

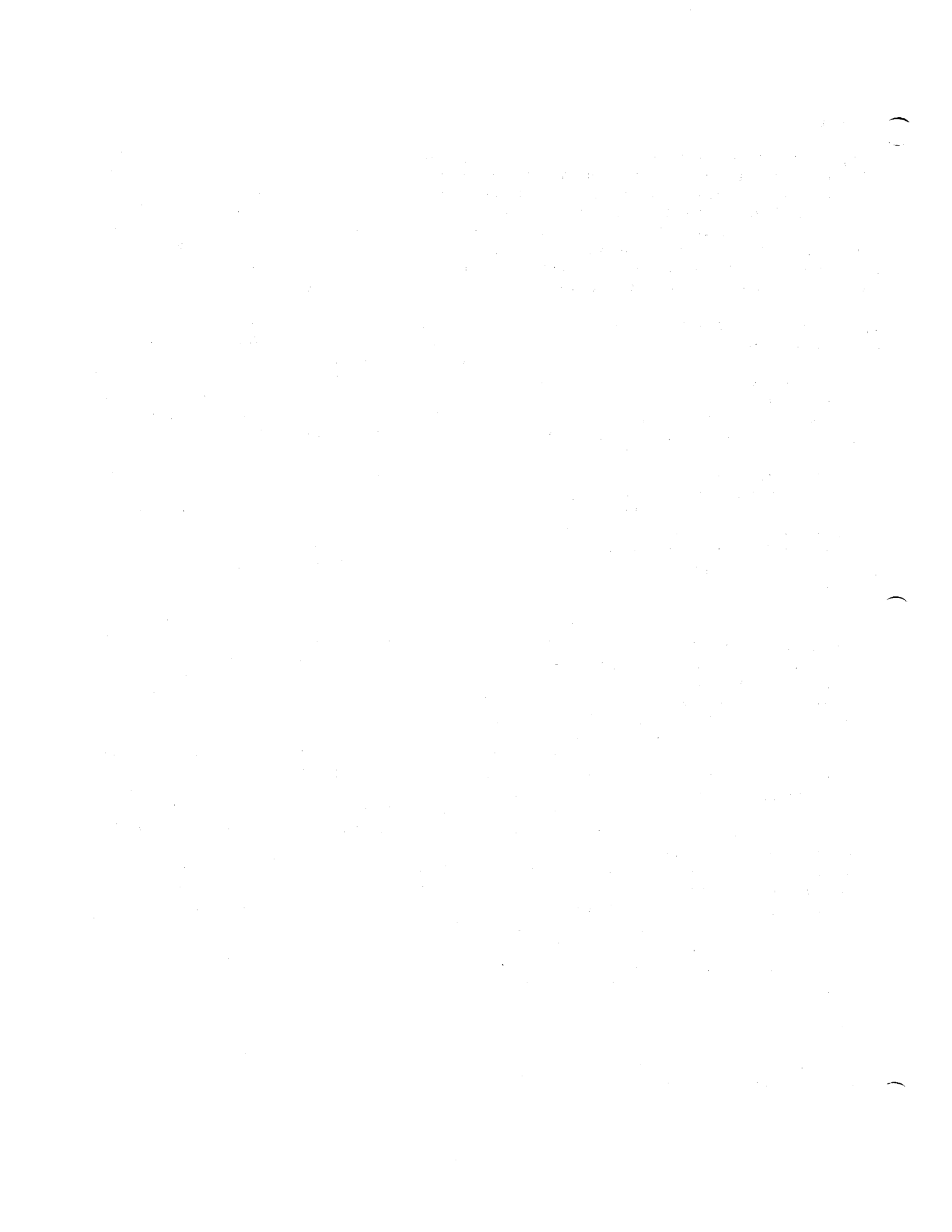
And, I believe I'm correct in stating that the device he reported was not a step generator or pulse generator. It was, essentially, a free piston compressor driven by gas pressure into a helium filled cylinder at sufficiently high velocities that it compressed the final volume to somewhere around 100 thousand psi with the duration of, I think it's something less than one millisecond. It's a way of generating a very fast transient test signal with which you can compare gauges. But it does not provide the absolute value that the step generator does.

As long as I'm on my feet, if I can say a couple more words to Mr. Banaszak and for the record, I guess. The idea of taking a continuous record of the output of a transducer of an accelerometer as you rotate it in the earth's field was actually mechanized by Paul Lederer at NBS quite a few years ago. I don't know if you have access to the NBS papers on their transducer program or not but he actually put the accelerometer on a precision angle table and took points at various rotations. The only limitations on that being, of course, that you have to know the cross action sensitivity. But for low accelerations, that turns out to be a very good way of getting precise values for low accelerations. The other thing you need to keep track of, of course, is the fact that the earth's gravity varies by something in excess of a tenth of a percent across the United States depending on the altitude and latitude. So if you want high precision, you have to chase after that a little bit.

One more comment on the step generator. I was involved in the early work with the Johnson and cross design step generator, and we saw those oscillation problems way back then. There seem to be at least three sources for that. If you're going to be working in that area, it ought to be kept in mind though we really can't quantify them or even assert that all three exist. The dominant things are the acoustic frequencies of the reservoir which is typically a few hundred hertz to a few kilohertz. The acoustic residence of the gauge cavity which is typically in the 10 to 20, 30 kilohertz territory. And the third thing which is sometimes overlooked is the possibility of mechanical, mechanically induced pressure, local pressure oscillations due to the motion of the valve. That ball may not drop neatly and then sit there. It probably does rattle around some and in the process will generate local frequency excursions. There's a third, or another deviation, a fourth deviation which will sometimes get buried in the other stuff. The fact is that both your valve design and the one that we were using result in a net change in the total volume of the system. There is a small ramp effect also sometimes hidden in the oscillation, but if you try to theorize what the wave form should look like, it can be taken into account.

BILL ANDERSON

Okay, other questions? Okay, I'd like to have everyone give a big hand to the speakers, then. (Applause)



SESSION 2

RMS RESPONSE OF AN ACCELEROMETER
TO A
RANDOM VIBRATION ENVIRONMENT

BY

G. A. ARTICOLO, Ph.D.
STAFF MATHEMATICAL PHYSICIST
SCHAEVITZ ENGINEERING

1985

PAPER PRESENTED AT THE THIRTEENTH TRANSDUCER
WORKSHOP, NAVAL POST-GRADUATE SCHOOL,
MONTEREY, CALIFORNIA, 1985

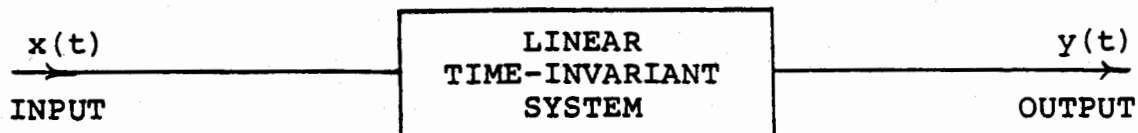
RMS RESPONSE OF AN ACCELEROMETER
TO A RANDOM VIBRATION ENVIRONMENT

In many engineering systems, it is of utmost interest to evaluate the effects on the system when it is subjected to an environment which has significant vibration noise. Often, the system contains sensitive instrumentation and transducers and it becomes an important consideration as to whether the noise vibration environment could possibly force the instrumentation into a saturation condition. Here, we show how the simple monitoring of the output of an accelerometer can be a useful means of measuring the vibration noise environment. In this analysis, we first investigate the response of linear transducers to vibration noise inputs which are assumed to be stationary and which can be characterized by some spectral density function whose profile can be partitioned into discrete frequency intervals. A generalized mathematical development is presented for evaluating the subsequent rms (root-mean-square) response in addition to familiar expression for the mean output power response of the system given by $P = \int_0^{\infty} |H(\omega)|^2 G(\omega) d\omega$. $H(\omega)$ is the linear system transfer function and $G(\omega)$ is the known input vibration power spectral density function. Since $G(\omega)$ is assumed to be partitioned into discrete frequency intervals, then it is shown that the above integral must be partitioned likewise. The outcome of this analysis is the development of a computer program which evaluates the above integral. Since accelerometers are often used to monitor the vibration noise environment, we consider the special case whereby the system transfer function $H(\omega)$ is characterized by a damped second-order function which is typical of accelerometers. A worked out illustrative example is provided. From the known transfer function of the transducer and the given input vibration power spectral density function, the developed computer program provides a convenient and useful means for evaluating and monitoring the effects of the noise vibration environment upon the engineering system.

I. INTRODUCTORY REVIEW

We begin by considering those simple electro-mechanical systems which can be characterized as being "linear time-invariant systems." A system is labeled such if its defining equations take on the form of "linear" differential equations with "time-invariant" coefficients.

A simple system can be schematically represented below:



Here, $x(t)$ is the time dependent input and $y(t)$ is the corresponding time dependent output of the system.

In operator form, the input-output relation of the above system can be expressed as

$$Ly(t) = x(t) \quad (1.1)$$

where L is a linear-differential operator with time-invariant (constant) coefficients.

Differential equations of the form above are generally solved using transform methods. We define the Fourier transform of $f(t)$ as $F(\omega)$ where:

$$F(\omega) = \int_{-\infty}^{+\infty} f(t) e^{-i\omega t} dt \quad (1.2)$$

and its corresponding inverse transform as:

$$f(t) = \frac{1}{2\pi} \int_{-\infty}^{+\infty} F(\omega) e^{i\omega t} d\omega \quad (1.3)$$

We assume, of course, that $f(t)$ satisfies restricted conditions so that the improper integral of equation (1.2) exists. Equations (1.2) and (1.3) form a "Fourier transform pair."

If we perform a Fourier transform operation on the differential equation (1.1), then it can be shown [1] that the corresponding transformed equation can be written as:

$$Y(\omega) = H(\omega) X(\omega) \quad (1.4)$$

In the above, $X(\omega)$ is the Fourier transform of the input $x(t)$, $Y(\omega)$ is the corresponding Fourier transform of the output $y(t)$ and $H(\omega)$ is called "the system transfer function" or the "system frequency response function."

From the inverse relation equation (1.3), we can evaluate the output solution of the system to be:

$$y(t) = \frac{1}{2\pi} \int_{-\infty}^{+\infty} Y(\omega) e^{i\omega t} d\omega = \frac{1}{2\pi} \int_{-\infty}^{+\infty} H(\omega) X(\omega) e^{i\omega t} d\omega. \quad (1.5)$$

In addition, from the "convolution theorem" [2], we can also express the solution as

$$y(t) = \int_{-\infty}^{+\infty} h(\tau) x(t-\tau) d\tau \quad (1.6)$$

where $h(t)$ is the corresponding inverse transform of $H(\omega)$; i.e.

$$h(t) = \frac{1}{2\pi} \int_{-\infty}^{+\infty} H(\omega) e^{i\omega t} d\omega \quad (1.7)$$

The physical significance of both $h(t)$ and $H(\omega)$ can be easily illustrated. For example, if the input to the system is a "unit impulse" at time $t = 0$, we can set

$$x(t) = \delta(t) \quad (1.8)$$

where $\delta(t)$ is the familiar "Dirac Delta" function. From equation (1.2) and the integral properties of the delta function [3], have

$$X(\omega) = \int_{-\infty}^{+\infty} \delta(t) e^{-i\omega t} dt = 1 \quad (1.9)$$

and from equations (1.5) and (1.7), the output solution corresponding to the unit impulse is given as

$$y(t) = \frac{1}{2\pi} \int_{-\infty}^{+\infty} H(\omega) e^{i\omega t} d\omega = h(t) \quad (1.10)$$

In a similar manner, from the convolution equation (1.6), we also get

$$y(t) = \int_{-\infty}^{+\infty} h(\tau) \delta(t-\tau) d\tau = h(t) \quad (1.11)$$

which is identical to the solution of (1.10). Thus, the significance of $h(t)$ is apparent from equations (1.10) and (1.11) and we see that $h(t)$ is simply the corresponding "unit impulse response" of the system.

As another example, if the input to the system is a pure sinusoidal wave at frequency ω_0 , then we can set

$$x(t) = e^{i\omega_0 t} \quad (1.12)$$

and its corresponding inverse from equation (1.2) becomes

$$X(\omega) = \int_{-\infty}^{+\infty} e^{i(\omega_0 - \omega)t} dt = 2\pi \delta(\omega - \omega_0). \quad (1.13)$$

The result of equation (1.13) takes advantage of the integral representation [3] of the Dirac delta function. From equation (1.5), the corresponding output response of the system becomes

$$y(t) = \frac{1}{2\pi} \int_{-\infty}^{+\infty} H(\omega) 2\pi \delta(\omega - \omega_0) e^{i\omega t} d\omega = H(\omega_0) e^{i\omega_0 t} \quad (1.14)$$

Thus, from equation (1.14), the physical significance of $H(\omega)$ becomes apparent in that $H(\omega)$ is the "frequency dependent amplitude response" of the system to a pure sinusoidal input. For this reason, the transfer function $H(\omega)$ is also referred to as the "system frequency response function".

II. ROOT-MEAN-SQUARE RESPONSE OF SYSTEM

First, we will be concerned with the "mean-output power" response of a linear time-invariant system to inputs which can be characterized as being "stationary random processes". Many noise-vibration environments can be labeled as such. It can be said [4] that if the input is a stationary random process, then for linear time-invariant systems, the corresponding output will also be a stationary random process.

Aside from these general consideration, we now proceed to the evaluation of the "mean output power" of a system. If the time-dependent output response of a system is denoted as $y(t)$, then the mean output power \bar{P} is defined as

$$\bar{P} = \lim_{T \rightarrow \infty} \frac{1}{2T} \int_{-T}^{+T} y^2(t) dt \quad (2.1)$$

where we assume that $y(t)$ is "real" as is the case for most physical systems.

We begin the evaluation of equation (2.1) by first defining the truncated Fourier transform [5] of $y(t)$ as

$$Y_T(\omega) = \frac{1}{2\pi} \int_{-T}^{+T} y(t) e^{i\omega t} dt \quad (2.2)$$

The ordinary transform $Y(\omega)$ is related to the truncated transform $Y_T(\omega)$ as

$$Y(\omega) = \lim_{T \rightarrow \infty} Y_T(\omega) . \quad (2.3)$$

From Parseval's theorem [2], we have a significant relation between the area under the graph of $y^2(t)$ in time space to the area under the graph of the transform magnitude squared $|Y(\omega)|^2$ in frequency space. This relation reads

$$\int_{-\infty}^{+\infty} y^2(t) dt = \frac{1}{2\pi} \int_{-\infty}^{+\infty} |Y(\omega)|^2 d\omega \quad (2.4)$$

where we have assumed $y(t)$ to be real.

In terms of the truncated Fourier transform $Y_T(\omega)$ defined above, we can express Parseval's equation as

$$\lim_{T \rightarrow \infty} \int_{-T}^{+T} y^2(t) dt = \lim_{T \rightarrow \infty} \left\{ \frac{1}{2\pi} \int_{-\infty}^{+\infty} |Y_T(\omega)|^2 d\omega \right\} \quad (2.5)$$

whereby we assume the continuity of all integrands so as to ensure the interchange ability of the limit and integration operation.

From the definition of the mean output power \bar{P} in equation (2.1), we can express this in terms of the truncated Fourier transform as

$$\bar{P} = \lim_{T \rightarrow \infty} \frac{1}{2T} \int_{-\infty}^{+\infty} \frac{|Y_T(\omega)|^2}{2\pi} d\omega . \quad (2.6)$$

Since it can be shown [2] that $Y_T(\omega)$ is generally an even function of ω for $y(t)$ real, then equation (2.6) can be rewritten as

$$\bar{P} = \int_0^{\infty} \left\{ \lim_{T \rightarrow \infty} \frac{|Y_T(\omega)|^2}{2\pi T} \right\} d\omega \quad (2.7)$$

If we define $G_y(\omega)$ to be the "output power spectral density function", whereby

$$G_y(\omega) = \lim_{T \rightarrow \infty} \frac{|Y_T(\omega)|^2}{2\pi T} \quad (2.8)$$

then the mean output power of the system for equation (2.1) can be written as

$$\bar{P} = \int_0^{\infty} G_y(\omega) d\omega \quad (2.9)$$

Thus, the mean output power of the system can be equivalently expressed as the area under the power spectral density function $G_y(\omega)$ in frequency space. This equivalence, of course, being afforded by the Parseval relation in equation (2.4).

Since, from equation (1.4) the relation between the input and output Fourier transform is given as

$$Y(\omega) = H(\omega)X(\omega) \quad (2.10)$$

then it follows that the relation between the corresponding truncated Fourier transforms is given as

$$Y_T(\omega) = H_T(\omega) X_T(\omega) \quad (2.11)$$

Thus, from equations (2.8) and (2.11) we have

$$G_y(\omega) = \lim_{T \rightarrow \infty} \frac{|Y_T(\omega)|^2}{2\pi T} = |H(\omega)|^2 \lim_{T \rightarrow \infty} \frac{|X_T(\omega)|^2}{2\pi T} \quad (2.12)$$

If we similarly define the "input power spectral density function" $G_x(\omega)$ as

$$G_x(\omega) = \lim_{T \rightarrow \infty} \frac{|X_T(\omega)|^2}{2\pi T} \quad (2.13)$$

then the relation between the input and output power spectral densities is simply

$$G_y(\omega) = |H(\omega)|^2 G_x(\omega) \quad (2.14)$$

Here, $H(\omega)$ is the system transfer function and equation (2.14) is the familiar expression which relates the output to the input power spectral density function by way of the square of the absolute value of the transfer function.

From equations (2.9) and (2.14) we can evaluate the mean output power of the system in terms of the input power spectral density function to be

$$\bar{P} = \int_0^{\infty} |H(\omega)|^2 G_x(\omega) d\omega \quad (2.15)$$

This expression has a geometric interpretation as being the area under the graph of the product $|H(\omega)|^2 G_x(\omega)$ in frequency - space. It is obvious that the larger the geometric overlap between the transfer function and the input spectral density function, the larger will be the output power of the system.

Finally, since the root-mean-square response of a system is defined to be the square root of the mean output power, we have

$$Y_{\text{RMS}} = \sqrt{\lim_{T \rightarrow \infty} \frac{1}{2T} \int_{-T}^{+T} y^2(t) dt} \quad (2.16)$$

Thus, from equations (2.15) and (2.16), we can evaluate the RMS response of the system in terms of the system transfer function $H(\omega)$ and the input power spectral density function $G_x(\omega)$ to be

$$y_{\text{RMS}} = \sqrt{\int_0^{\infty} |H(\omega)|^2 G_x(\omega) d\omega} \quad . \quad (2.17)$$

Equations (2.16) and (2.17) are interesting in that they demonstrate the equivalence between two integrals, one evaluated in time-space and the other in frequency-space.

III. A SECOND-ORDER SYSTEM EXAMPLE

A force-balance servo-accelerometer serves as a good example of a classic second order system. A simple model of such a system with a single degree of freedom is shown below:

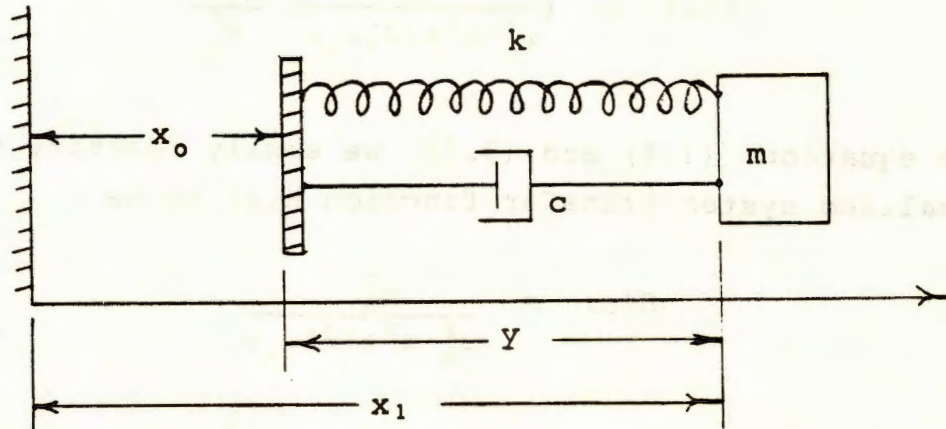


FIGURE 1

We define

Input $\ddot{x}_0 = a(t) \equiv$ Input acceleration of the base

and

Output $y = -(x_1 - x_0) \equiv$ Relative displacement of base and mass m . The differential equation describing the motion of the mass m is given as

$$m\ddot{y} + c\dot{y} + ky = ma(t) \quad . \quad (3.1)$$

In the above, c is the viscous damping coefficient and k is the effective spring constant of the servo-accelerometer. Equation (3.1) is of the form of a linear-differential equation with constant coefficients as described in equation (1.1).

We introduce the new variables $\omega_n^2 = k/m$ and $2\xi\omega_n = c/m$ (3.2)

where

$\omega_n \equiv$ natural resonance angular frequency

and

$\xi \equiv$ normalized damping coefficient.

Taking the Fourier transform of equation (3.1) and solving for the output transform $Y(\omega)$, in terms of the input transform $A(\omega)$, we get

$$Y(\omega) = \left(\frac{\omega_n^2}{\omega_n^2 - \omega^2 + i2\xi\omega_n\omega} \right) \frac{A(\omega)}{\omega_n^2} \quad (3.3)$$

From equations (1.4) and (3.3), we easily identify the normalized system transfer function $H(\omega)$ to be

$$H(\omega) = \frac{\omega_n^2}{\omega_n^2 - \omega^2 + i2\xi\omega_n\omega} \quad (3.4)$$

The above $H(\omega)$ is a standard second-order transfer function which is characteristic of force-balance servo-accelerometer systems. As demonstrated earlier in equation (1.14), $H(\omega)$ gives the normalized amplitude frequency response of the system to a pure sinusoidal input.

IV. COMPUTER EVALUATION FOR A SECOND-ORDER SYSTEM

We now consider the RMS response of a second-order system to an input which is characterized by a typical acceleration power spectral density function envelope shown below

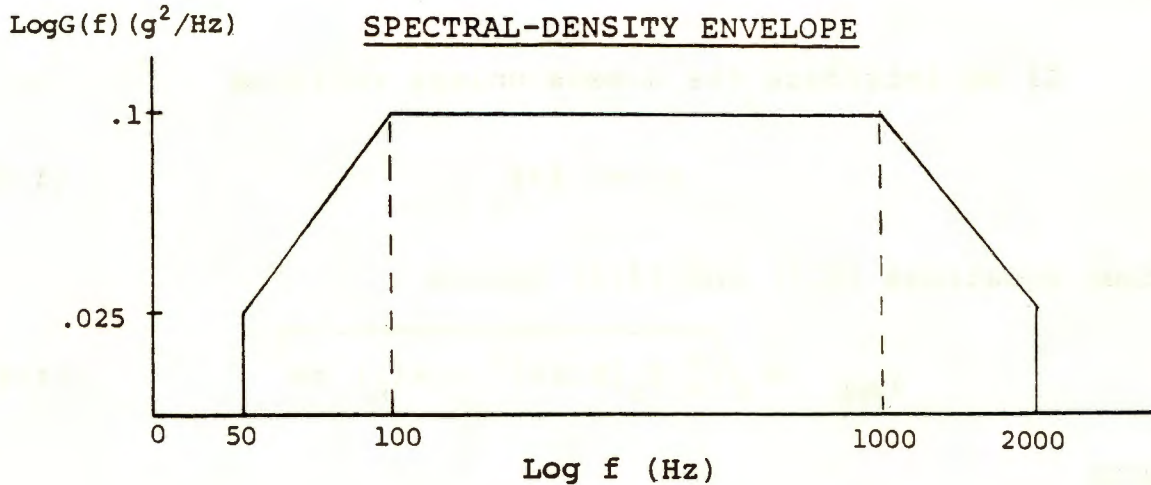


FIGURE 2

Note that the above graph is a display of the $\text{Log } G(f)$ versus $\text{Log } f$ where the dimensions of $G(f)$ are typically given as g^2/Hz and f has dimensions of Hz .

If we utilize the conversion $\omega = 2\pi f$ then in terms of the frequency variable f , equations (2.17) and (3.4) become, respectively,

$$Y_{\text{RMS}} = \sqrt{\int_0^{\infty} |H(f)|^2 G(f) df} \quad (4.1)$$

where, for the second-order, force balance servo-accelerometer system above,

$$H(f) = \frac{f_n}{f_n^2 - f^2 + i2\xi f_n f} \quad (4.2)$$

With $G(f)$ having dimensions g^2/Hz , y_{RMS} will have dimensions of g (gravity units). In the above, ξ continues to be the normalized viscous damping coefficient and f_n is the natural resonance frequency of the second order system with dimensions of Hz.

If we introduce the dimensionless variable

$$x = f/f_n \quad (4.3)$$

then equations (4.1) and (4.2) become

$$Y_{RMS} = \sqrt{\int_0^\infty f_n |H(x)|^2 G(xf_n) dx} \quad (4.4)$$

with

$$H(x) = \frac{1}{1-x^2+i2\xi x} \quad (4.5)$$

We now proceed to evaluate equation (4.4) using a linear integration procedure. Generally, the spectral function $G(f)$ is segmented into n partitions with dimensions of g^2/Hz along a $\log f$ axis. A typical partition is shown below.

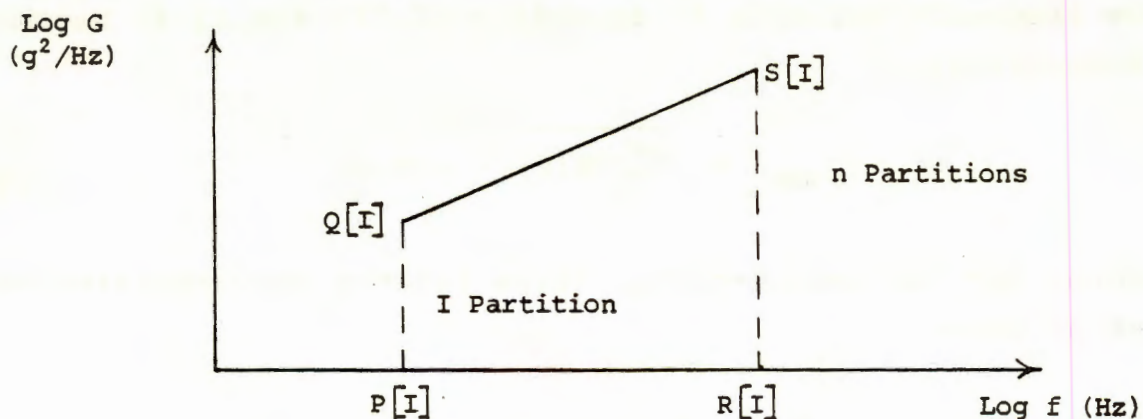


FIGURE 3

We note that $G(f)$ is generally expressed in terms of frequency (Hz) and we must use the conversion in equation (4.3) to obtain $G(xf_n)$.

Since the input power spectral density function display in the above figure is logarithmic, then in the I partition, we can express $G_I(xf_n)$ as

$$G_I(xf_n) = B[I] * (xf_n)^{M[I]} \quad (4.6)$$

where
$$B[I] = \frac{Q[I]}{P[I]^{M[I]}} \quad (4.7)$$

and
$$M[I] = \frac{\ln(S[I]/Q[I])}{\ln(R[I]/P[I])} \quad (4.8)$$

In the above, points $P[I]$ and $R[I]$ are the respective initial and final frequency points of the I partition and points $Q[I]$ and $S[I]$ are the corresponding magnitude points as illustrated in Figure 3 above. Within the I partition, the limits on x are given as

$$\frac{P[I]}{f_n} \leq x \leq \frac{R[I]}{f_n} \quad (4.9)$$

To perform the numerical integration of equation (4.4), we segment the I partition into K subintervals whereby the value of x at the J subinterval within the I partition is given as

$$x[I,J] = \frac{P[I]}{f_n} + (J-1)*D[I] \quad (4.10)$$

for

$$I = 1 \text{ to } N, J = 1 \text{ to } K + 1$$

and

$$D[I] = \frac{R[I] - P[I]}{f_n * K} \quad (4.11)$$

Within the J subinterval of the I partition, we set

$$V[I,J] = f_n * H[X[I,J]]^2 \quad (4.12)$$

and

$$G[I,J] = \frac{Q[I]}{P[I] + M[M]} * (f_n X[I,J]) + M[I] \quad (4.13)$$

In the numerical evaluation of equation (4.4), we use the simple, familiar trapezoidal rule [1]. Setting

$$Y[I,J] = V[I,J] * G[I,J] \quad (4.14)$$

then the numerical integration evaluation of y_{RMS} in equation (4.4) becomes

$$Y_{RMS} = \sqrt{\sum_{I=1}^N \left[\frac{Y[I,1]}{2} + \sum_{J=2}^K Y[I,J] + \frac{Y[I,K+1]}{2} \right] * D[I]} \quad (4.15)$$

The attached computer program GSPECT, done in simple BASIC, gives the evaluation of y_{RMS} (in units of g), for various cases of spectral density profiles, damping coefficients, and system resonance frequencies. We see this exercise as being a very useful means of evaluating an accurate RMS response of second-order systems, such as force-balance accelerometers, to known input noise spectral density functions.

REFERENCES

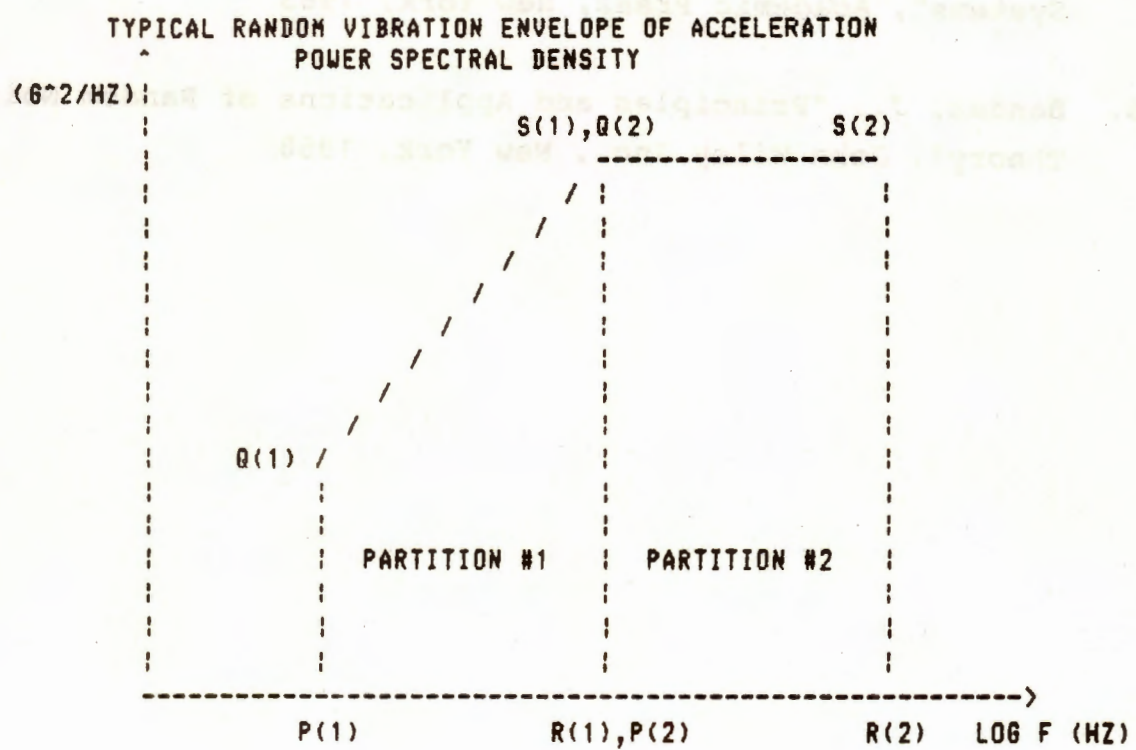
1. Wylie, C. Ray, "Advanced Engineering Mathematics", McGraw-Hill Book Company, New York, 1982
2. Papoulis, A., "The Fourier Integral and Its Applications", McGraw-Hill Book Company, New York, 1962
3. Butkov, E., "Mathematical Physics", Addison-Wesley Publishing Co., Reading, Mass., 1968
4. Crandall, S. and Mark, W., "Random Vibration in Mechanical Systems", Academic Press, New York, 1963
5. Bendat, J., "Principles and Applications of Random Noise Theory", John Wiley Inc., New York, 1958

PROGRAM GSPECT

RUN

PROGRAM GSPECT

THIS PROGRAM EVALUATES THE RMS RESPONSE OF AN ACCELEROMETER
(CHARACTERIZED BY A KNOWN NATURAL RESONANCE FREQUENCY AND
NORMALIZED DAMPING COEFFICIENT) TO A GIVEN NOISE SPECTRAL
DENSITY INPUT



RUN
 HOW MANY PARTITIONS ARE IN THE SPECTRAL DENSITY ENVELOPE ?3

FROM THE ABOVE DISPLAY, EACH PARTITION HAS AN INITIAL
 POINT P(I),Q(I) AND A FINAL POINT R(I),S(I)

INPUT POINTS P(1),Q(1) AND R(1),S(1)
 ? 50,.025,100,.1

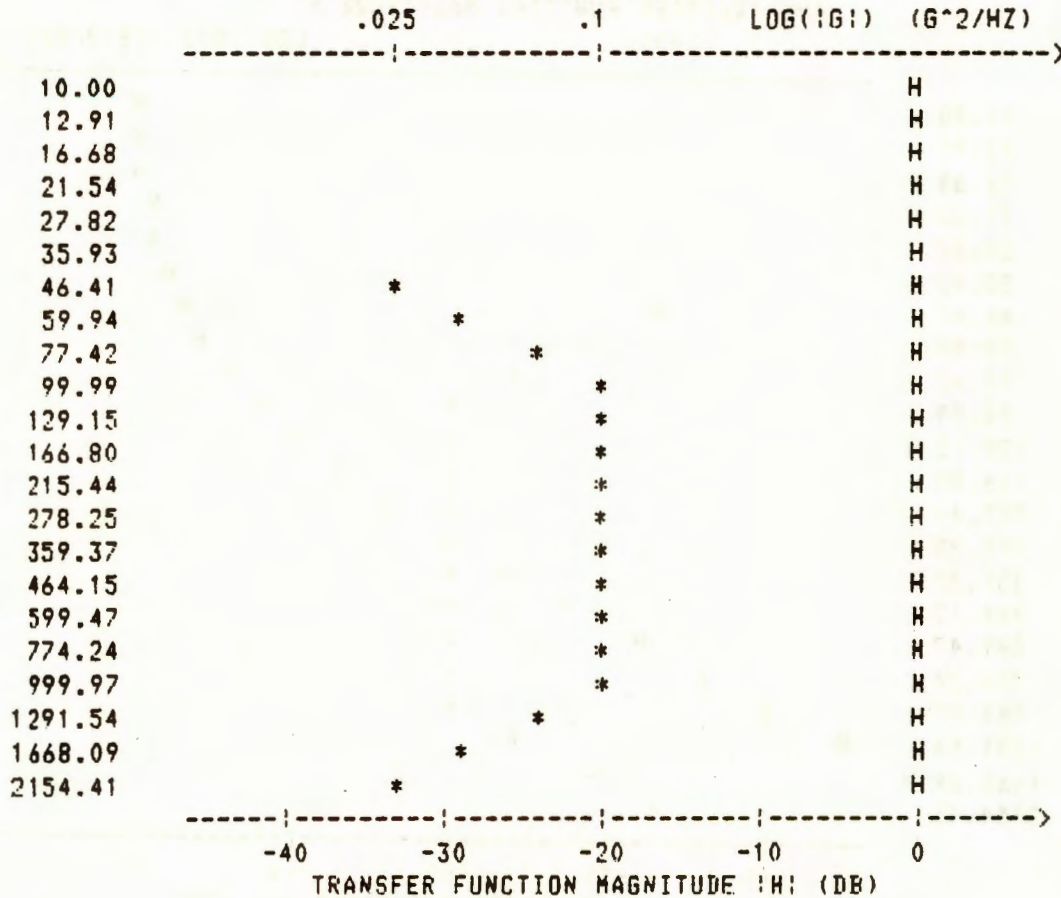
INPUT POINTS P(2),Q(2) AND R(2),S(2)
 ? 100,.1,1000,.1

INPUT POINTS P(3),Q(3) AND R(3),S(3)
 ? 1000,.1,2000,.025

NATURAL RESONANCE FREQUENCY (HZ) OF ACCELEROMETER =?10000

NORMALIZED DAMPING COEFFICIENT =?.7

SUPERIMPOSED PLOT OF SPECTRAL DENSITY FUNCTION G
 AND TRANSFER FUNCTION MAGNITUDE H



RMS OUTPUT VALUE IN G UNITS = 11.95

RUN
 HOW MANY PARTITIONS ARE IN THE SPECTRAL DENSITY ENVELOPE ?3

FROM THE ABOVE DISPLAY, EACH PARTITION HAS AN INITIAL
 POINT P(I),Q(I) AND A FINAL POINT R(I),S(I)

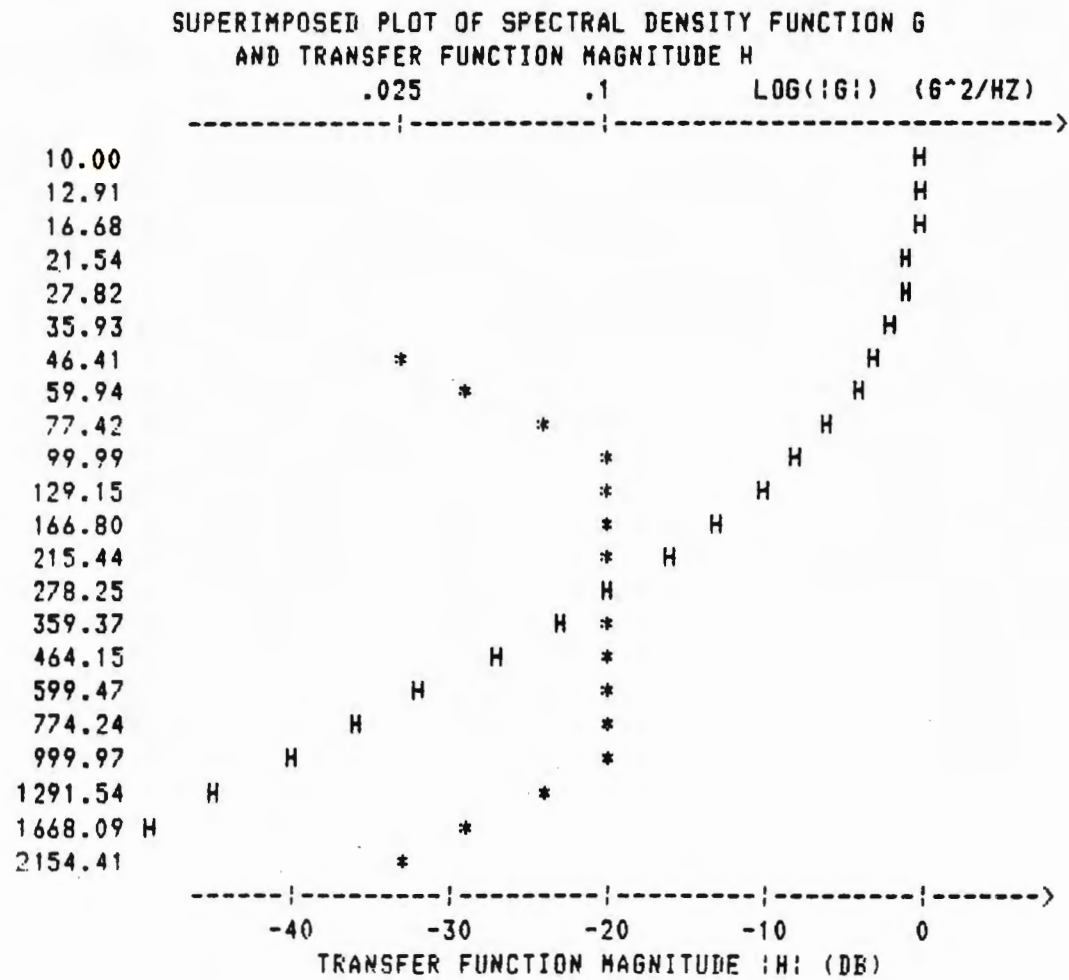
INPUT POINTS P(1),Q(1) AND R(1),S(1)
 ? 50,.025,100,.1

INPUT POINTS P(2),Q(2) AND R(2),S(2)
 ? 100,.1,1000,.1

INPUT POINTS P(3),Q(3) AND R(3),S(3)
 ? 1000,.1,2000,.025

NATURAL RESONANCE FREQUENCY (HZ) OF ACCELEROMETER =?100

NORMALIZED DAMPING COEFFICIENT =?1.2



RMS OUTPUT VALUE IN G UNITS = 1.36

RUN
 HOW MANY PARTITIONS ARE IN THE SPECTRAL DENSITY ENVELOPE ?3

FROM THE ABOVE DISPLAY, EACH PARTITION HAS AN INITIAL
 POINT P(I),Q(I) AND A FINAL POINT R(I),S(I)

INPUT POINTS P(1),Q(1) AND R(1),S(1)
 ? 50,.025,100,.1

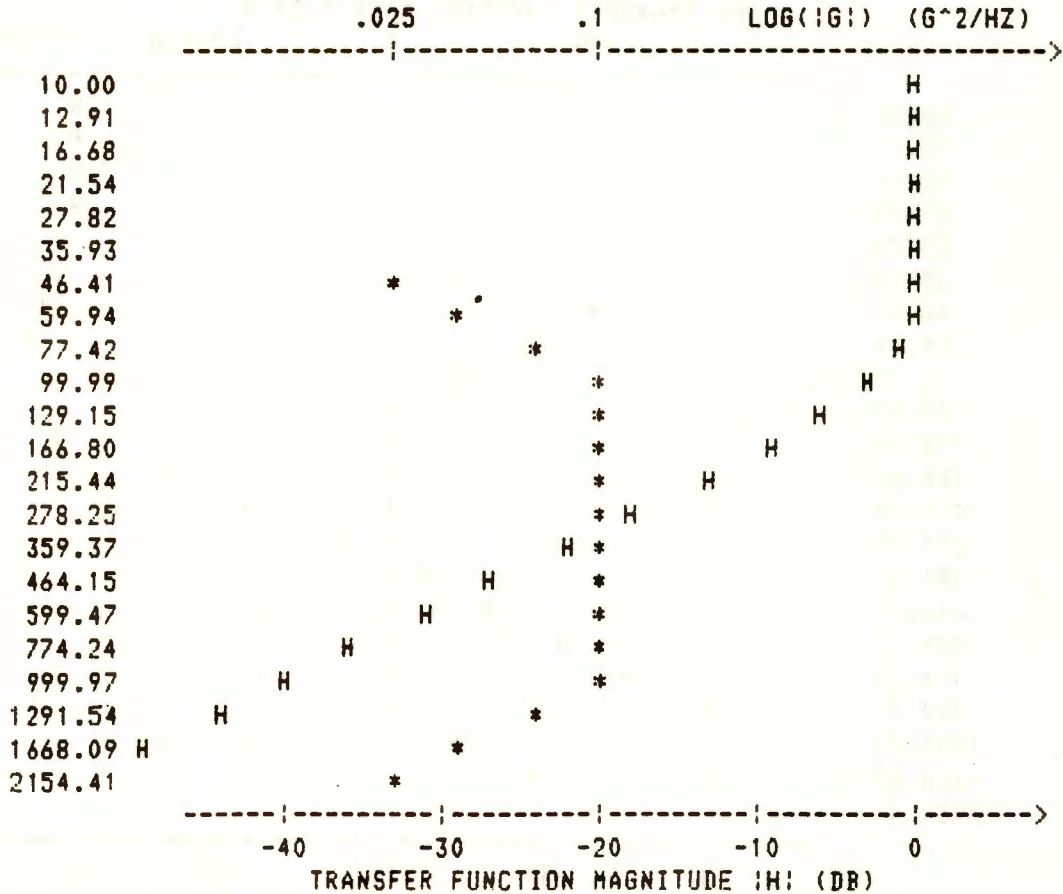
INPUT POINTS P(2),Q(2) AND R(2),S(2)
 ? 100,.1,1000,.1

INPUT POINTS P(3),Q(3) AND R(3),S(3)
 ? 1000,.1,2000,.025

NATURAL RESONANCE FREQUENCY (HZ) OF ACCELEROMETER =?100

NORMALIZED DAMPING COEFFICIENT =?.7

SUPERIMPOSED PLOT OF SPECTRAL DENSITY FUNCTION G
 AND TRANSFER FUNCTION MAGNITUDE H



RMS OUTPUT VALUE IN G UNITS = 2.12

RUN
 HOW MANY PARTITIONS ARE IN THE SPECTRAL DENSITY ENVELOPE ?3

FROM THE ABOVE DISPLAY, EACH PARTITION HAS AN INITIAL
 POINT P(I),Q(I) AND A FINAL POINT R(I),S(I)

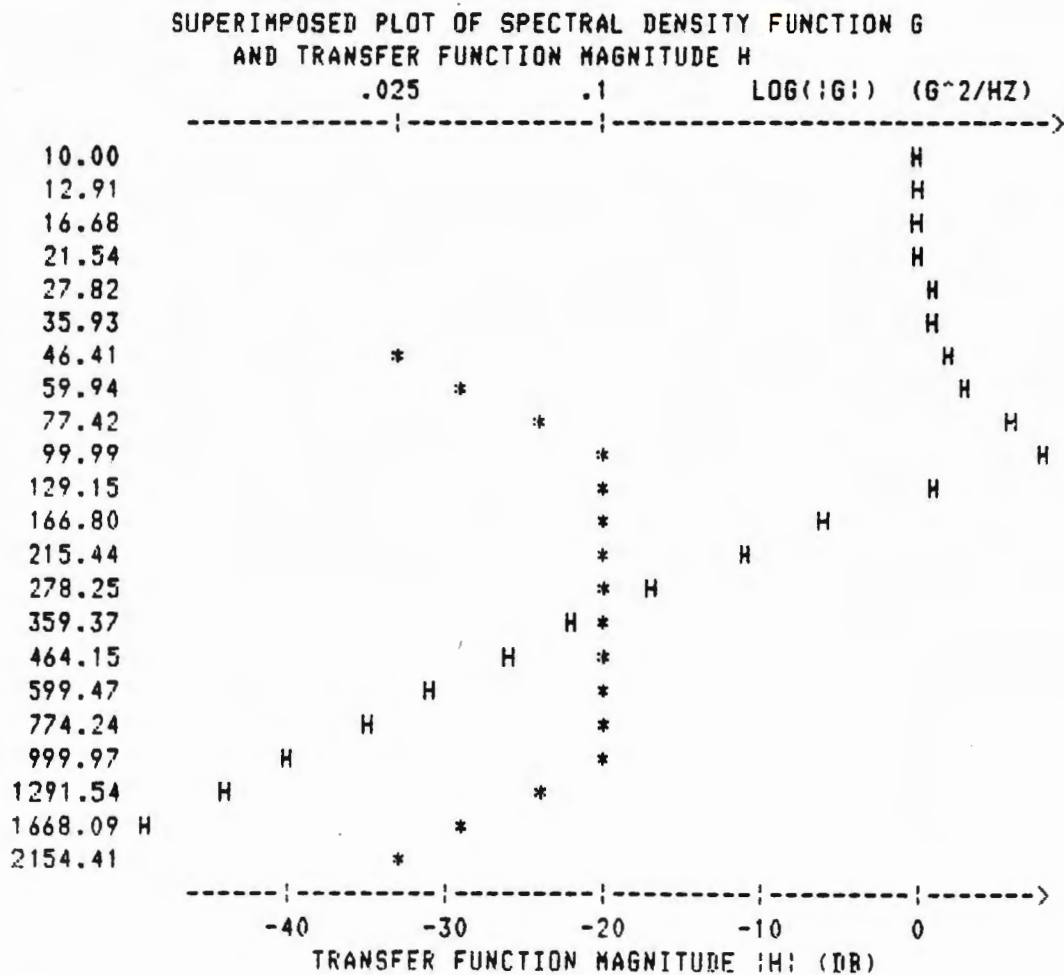
INPUT POINTS P(1),Q(1) AND R(1),S(1)
 ? 50,.025,100,.1

INPUT POINTS P(2),Q(2) AND R(2),S(2)
 ? 100,.1,1000,.1

INPUT POINTS P(3),Q(3) AND R(3),S(3)
 ? 1000,.1,2000,.025

NATURAL RESONANCE FREQUENCY (HZ) OF ACCELEROMETER =?100

NORMALIZED DAMPING COEFFICIENT =?.2



RMS OUTPUT VALUE IN G UNITS = 5.18

RUN
 HOW MANY PARTITIONS ARE IN THE SPECTRAL DENSITY ENVELOPE ?3

FROM THE ABOVE DISPLAY, EACH PARTITION HAS AN INITIAL
 POINT P(I),Q(I) AND A FINAL POINT R(I),S(I)

INPUT POINTS P(1),Q(1) AND R(1),S(1)
 ? 50,.025,100,.1

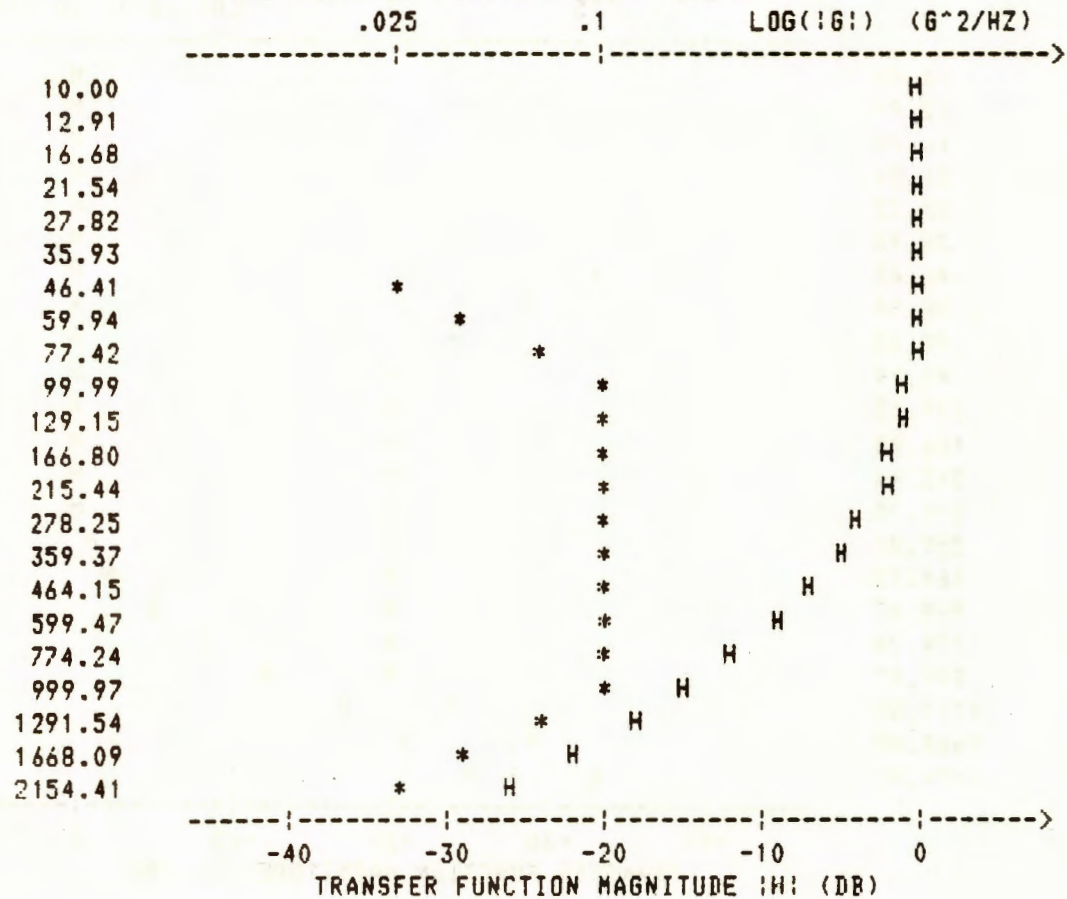
INPUT POINTS P(2),Q(2) AND R(2),S(2)
 ? 100,.1,1000,.1

INPUT POINTS P(3),Q(3) AND R(3),S(3)
 ? 1000,.1,2000,.025

NATURAL RESONANCE FREQUENCY (HZ) OF ACCELEROMETER =?500

NORMALIZED DAMPING COEFFICIENT =?1.2

SUPERIMPOSED PLOT OF SPECTRAL DENSITY FUNCTION G
 AND TRANSFER FUNCTION MAGNITUDE H



RMS OUTPUT VALUE IN G UNITS = 5.01

RUN
 HOW MANY PARTITIONS ARE IN THE SPECTRAL DENSITY ENVELOPE ?3

FROM THE ABOVE DISPLAY, EACH PARTITION HAS AN INITIAL
 POINT P(I),Q(I) AND A FINAL POINT R(I),S(I)

INPUT POINTS P(1),Q(1) AND R(1),S(1)
 ? 50,-.025,100,.1

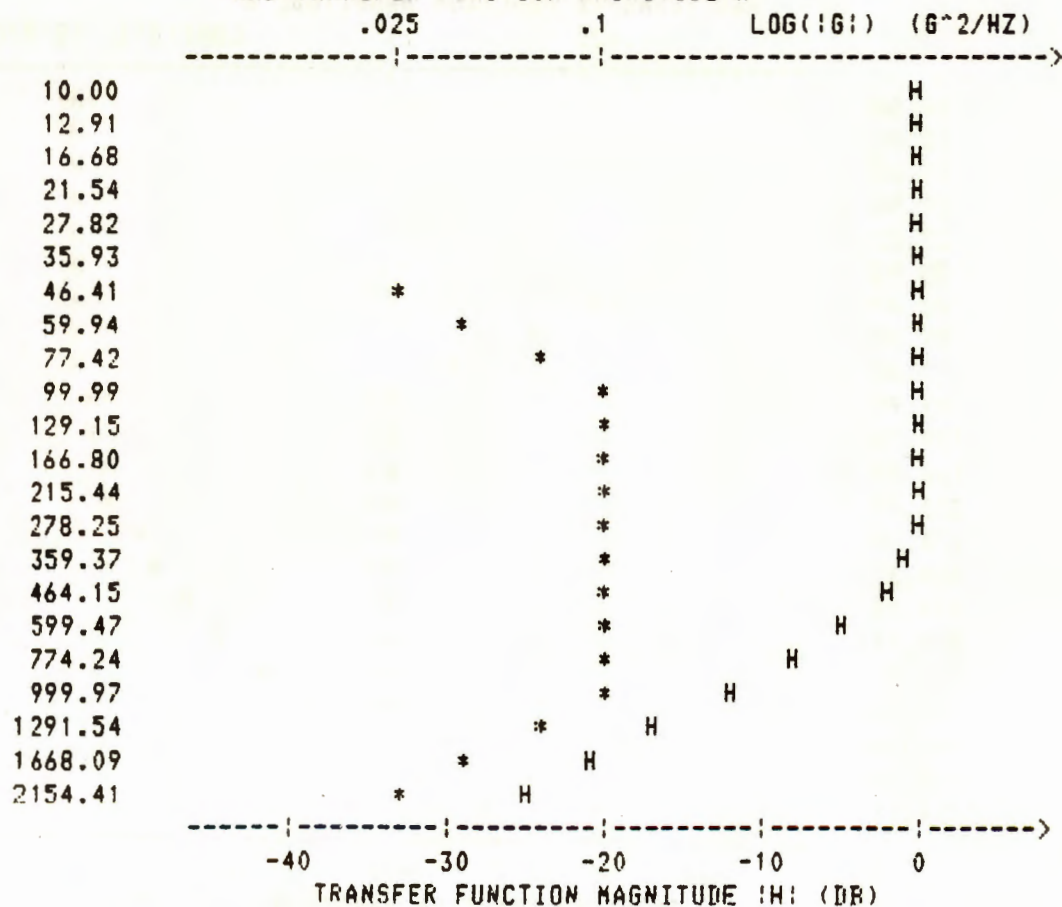
INPUT POINTS P(2),Q(2) AND R(2),S(2)
 ? 100,-.1,1000,.1

INPUT POINTS P(3),Q(3) AND R(3),S(3)
 ? 1000,-.1,2000,.025

NATURAL RESONANCE FREQUENCY (HZ) OF ACCELEROMETER =?500

NORMALIZED DAMPING COEFFICIENT =?.7

SUPERIMPOSED PLOT OF SPECTRAL DENSITY FUNCTION G
 AND TRANSFER FUNCTION MAGNITUDE H



RMS OUTPUT VALUE IN G UNITS = 6.93

RUN
 HOW MANY PARTITIONS ARE IN THE SPECTRAL DENSITY ENVELOPE ?3

FROM THE ABOVE DISPLAY, EACH PARTITION HAS AN INITIAL
 POINT P(I),Q(I) AND A FINAL POINT R(I),S(I)

INPUT POINTS P(1),Q(1) AND R(1),S(1)
 ? 50,-.025,100,.1

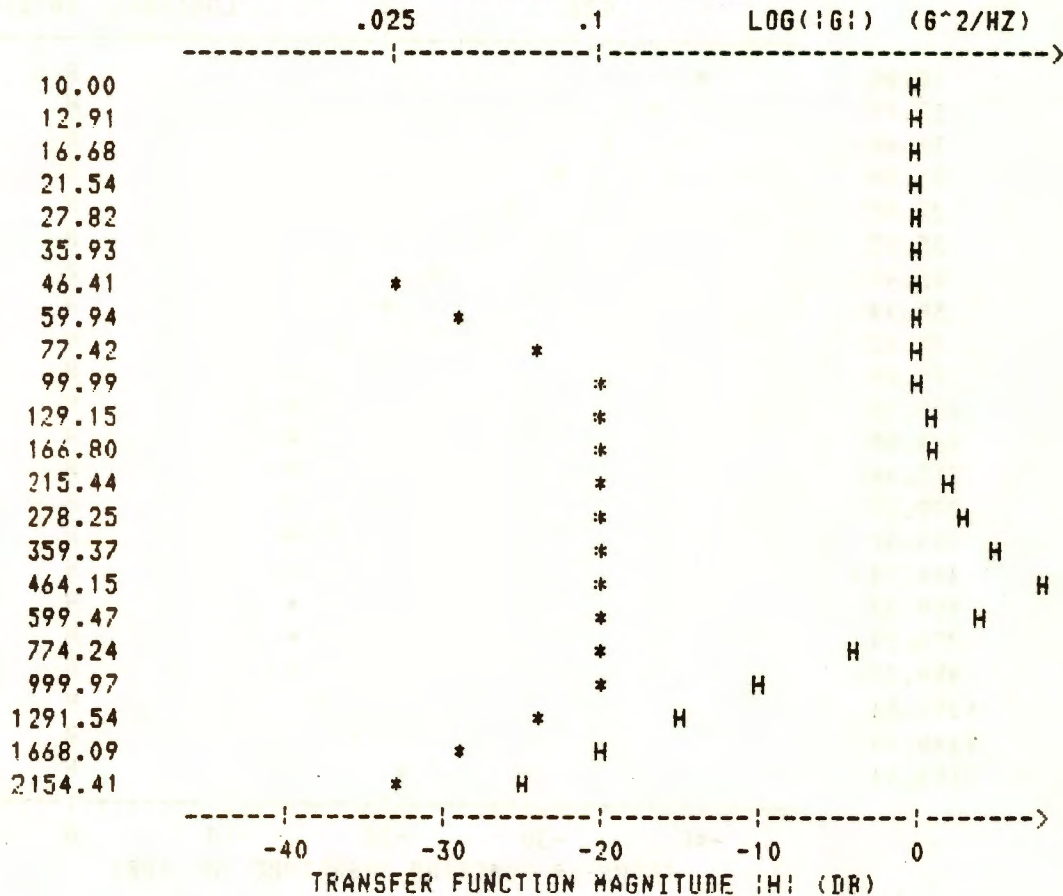
INPUT POINTS P(2),Q(2) AND R(2),S(2)
 ? 100,-.1,1000,.1

INPUT POINTS P(3),Q(3) AND R(3),S(3)
 ? 1000,-.1,2000,.025

NATURAL RESONANCE FREQUENCY (HZ) OF ACCELEROMETER =?500

NORMALIZED DAMPING COEFFICIENT =?.2

SUPERIMPOSED PLOT OF SPECTRAL DENSITY FUNCTION G
 AND TRANSFER FUNCTION MAGNITUDE H



RMS OUTPUT VALUE IN G UNITS = 13.67

RUN
 HOW MANY PARTITIONS ARE IN THE SPECTRAL DENSITY ENVELOPE ?3

FROM THE ABOVE DISPLAY, EACH PARTITION HAS AN INITIAL
 POINT P(I),Q(I) AND A FINAL POINT R(I),S(I)

INPUT POINTS P(1),Q(1) AND R(1),S(1)
 ? 10,.01,100,.2

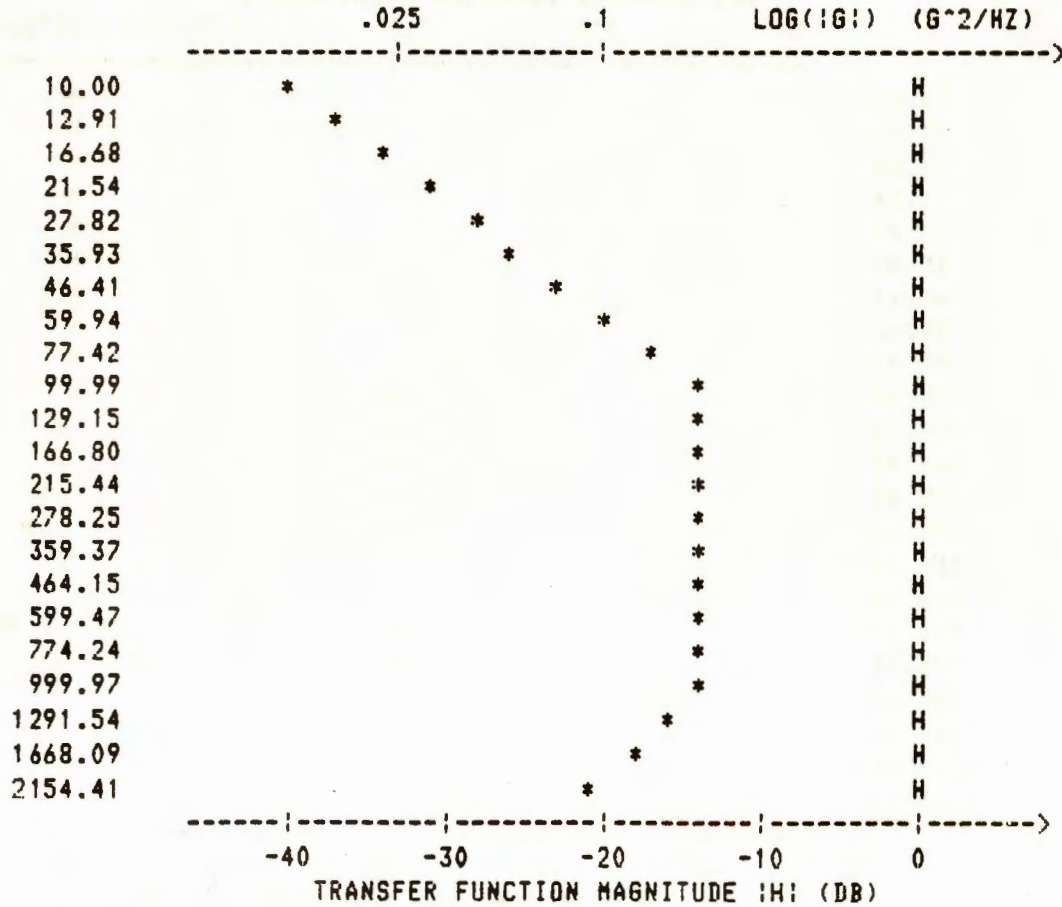
INPUT POINTS P(2),Q(2) AND R(2),S(2)
 ? 100,.2,1000,.2

INPUT POINTS P(3),Q(3) AND R(3),S(3)
 ? 1000,.2,2000,.1

NATURAL RESONANCE FREQUENCY (HZ) OF ACCELEROMETER =?10000

NORMALIZED DAMPING COEFFICIENT =?.7

SUPERIMPOSED PLOT OF SPECTRAL DENSITY FUNCTION G
 AND TRANSFER FUNCTION MAGNITUDE H



RMS OUTPUT VALUE IN G UNITS = 18.09

RUN
 HOW MANY PARTITIONS ARE IN THE SPECTRAL DENSITY ENVELOPE ?3

FROM THE ABOVE DISPLAY, EACH PARTITION HAS AN INITIAL
 POINT P(I),Q(I) AND A FINAL POINT R(I),S(I)

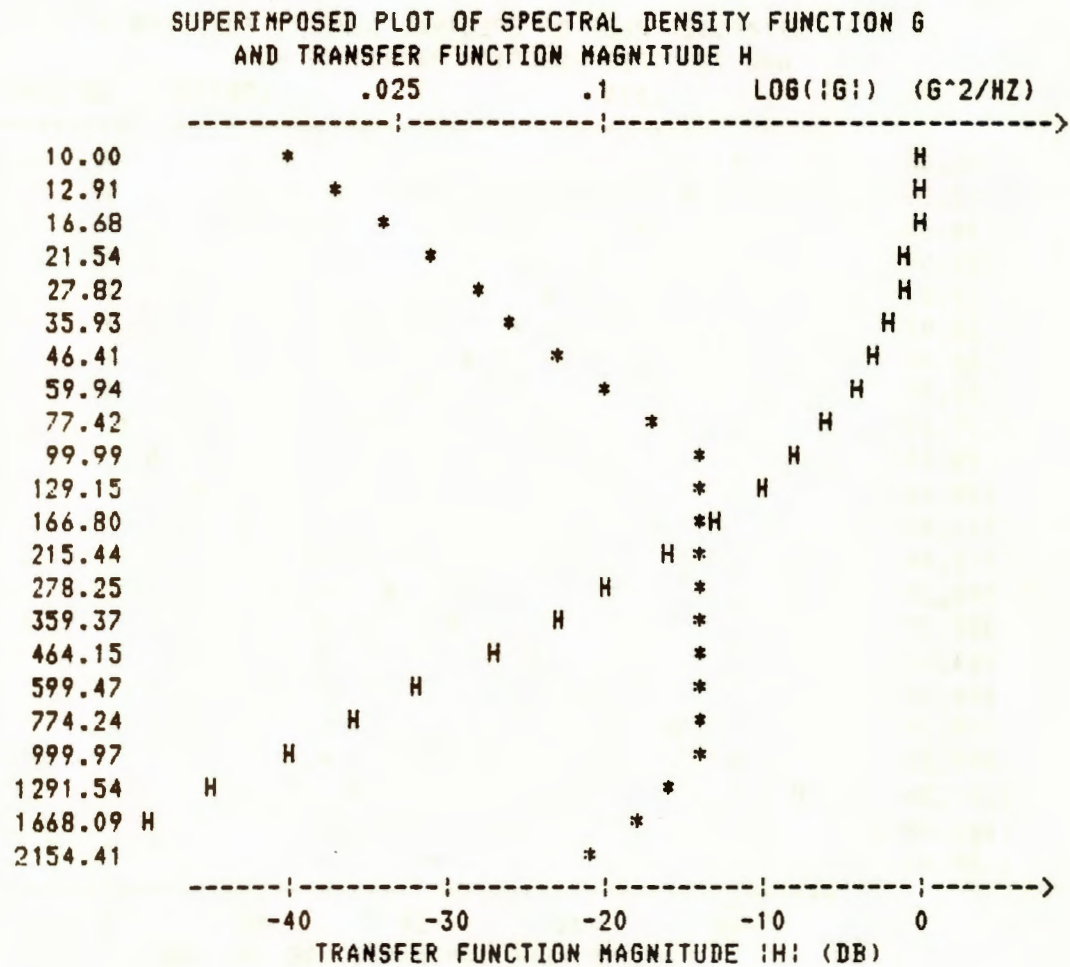
INPUT POINTS P(1),Q(1) AND R(1),S(1)
 ? 10,.01,100,.2

INPUT POINTS P(2),Q(2) AND R(2),S(2)
 ? 100,.2,1000,.2

INPUT POINTS P(3),Q(3) AND R(3),S(3)
 ? 1000,.2,2000,.1

NATURAL RESONANCE FREQUENCY (HZ) OF ACCELEROMETER =?100

NORMALIZED DAMPING COEFFICIENT =?1.2



RMS OUTPUT VALUE IN G UNITS = 2.29

RUN
 HOW MANY PARTITIONS ARE IN THE SPECTRAL DENSITY ENVELOPE ?3

FROM THE ABOVE DISPLAY, EACH PARTITION HAS AN INITIAL
 POINT P(I),Q(I) AND A FINAL POINT R(I),S(I)

INPUT POINTS P(1),Q(1) AND R(1),S(1)
 ? 10,.01,100,.2

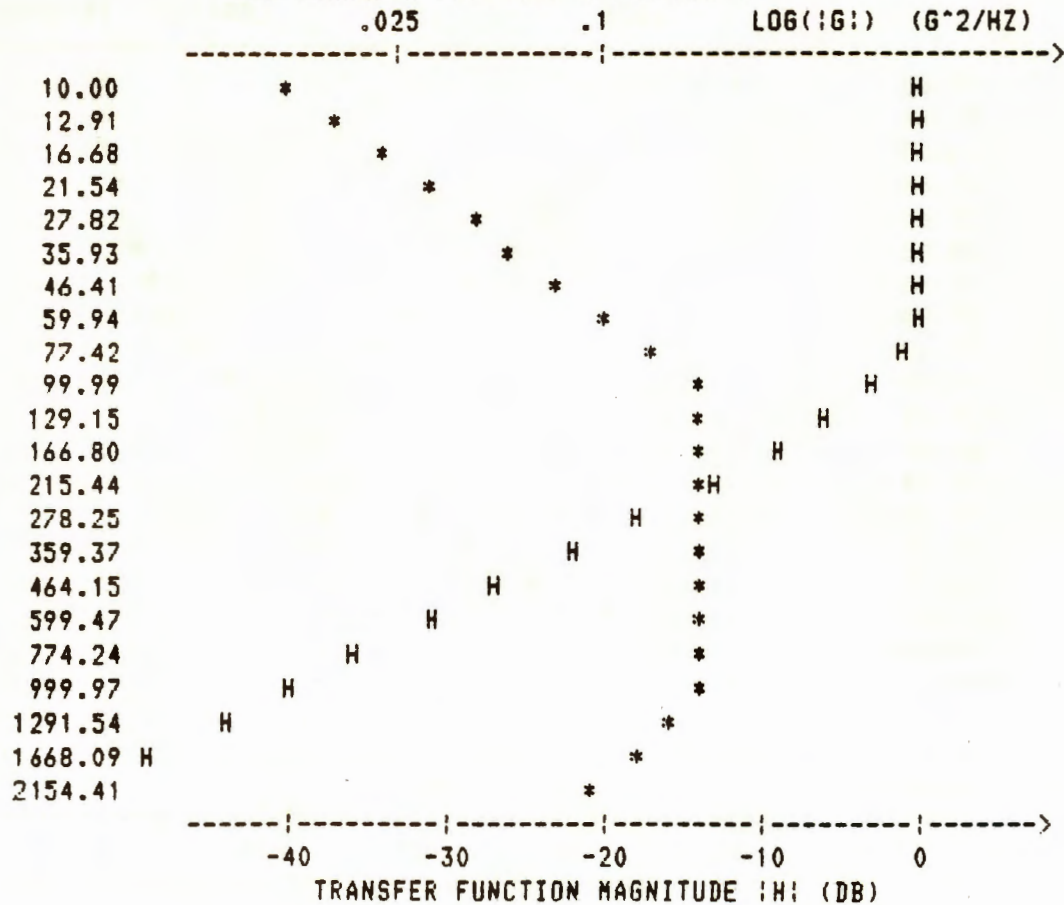
INPUT POINTS P(2),Q(2) AND R(2),S(2)
 ? 100,.2,1000,.2

INPUT POINTS P(3),Q(3) AND R(3),S(3)
 ? 1000,.2,2000,.1

NATURAL RESONANCE FREQUENCY (HZ) OF ACCELEROMETER =?100

NORMALIZED DAMPING COEFFICIENT =?.7

SUPERIMPOSED PLOT OF SPECTRAL DENSITY FUNCTION G
 AND TRANSFER FUNCTION MAGNITUDE H



RMS OUTPUT VALUE IN G UNITS = 3.41

RUN
 HOW MANY PARTITIONS ARE IN THE SPECTRAL DENSITY ENVELOPE ?3

FROM THE ABOVE DISPLAY, EACH PARTITION HAS AN INITIAL
 POINT P(I),Q(I) AND A FINAL POINT R(I),S(I)

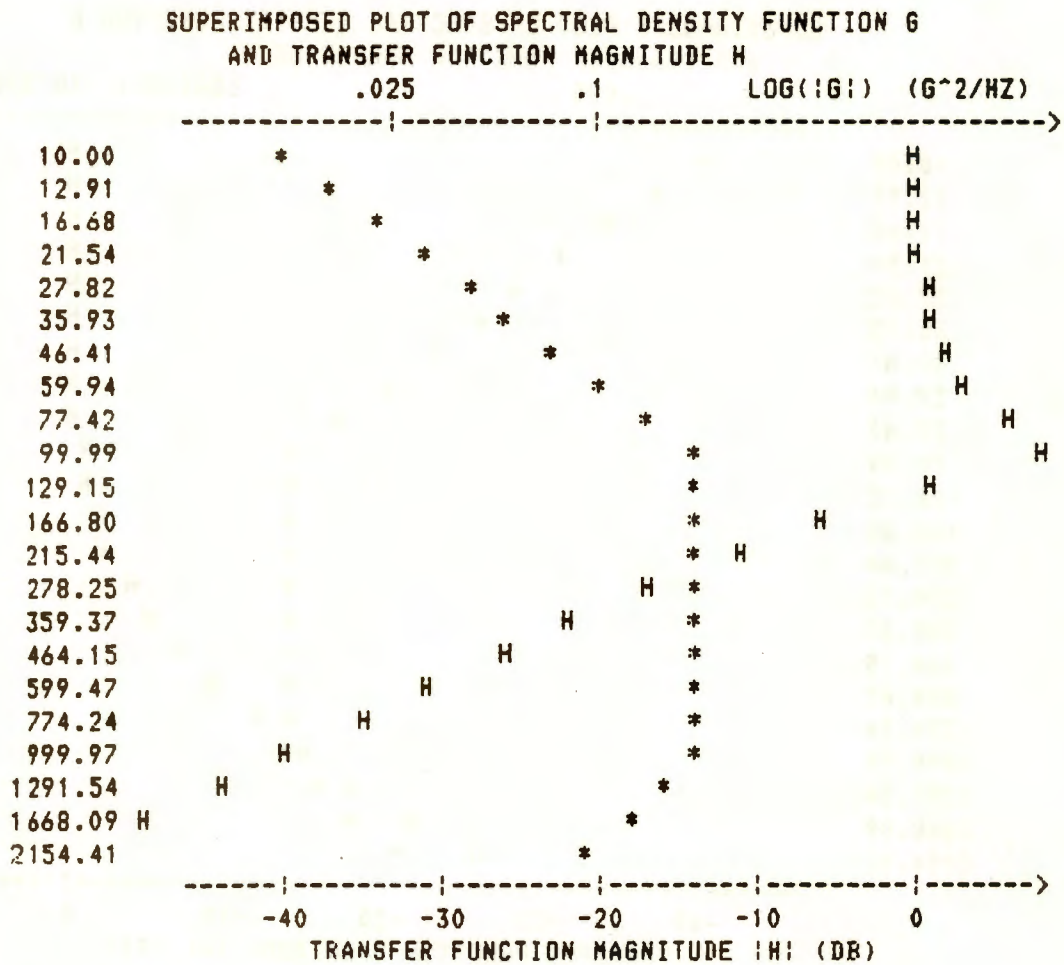
INPUT POINTS P(1),Q(1) AND R(1),S(1)
 ? 10,.01,100,.2

INPUT POINTS P(2),Q(2) AND R(2),S(2)
 ? 100,.2,1000,.2

INPUT POINTS P(3),Q(3) AND R(3),S(3)
 ? 1000,.2,2000,-.1

NATURAL RESONANCE FREQUENCY (HZ) OF ACCELEROMETER =?100

NORMALIZED DAMPING COEFFICIENT =?.2



RMS OUTPUT VALUE IN G UNITS = 7.72

RUN
 HOW MANY PARTITIONS ARE IN THE SPECTRAL DENSITY ENVELOPE ?3

FROM THE ABOVE DISPLAY, EACH PARTITION HAS AN INITIAL
 POINT P(I),Q(I) AND A FINAL POINT R(I),S(I)

INPUT POINTS P(1),Q(1) AND R(1),S(1)
 ? 10,.01,100,.2

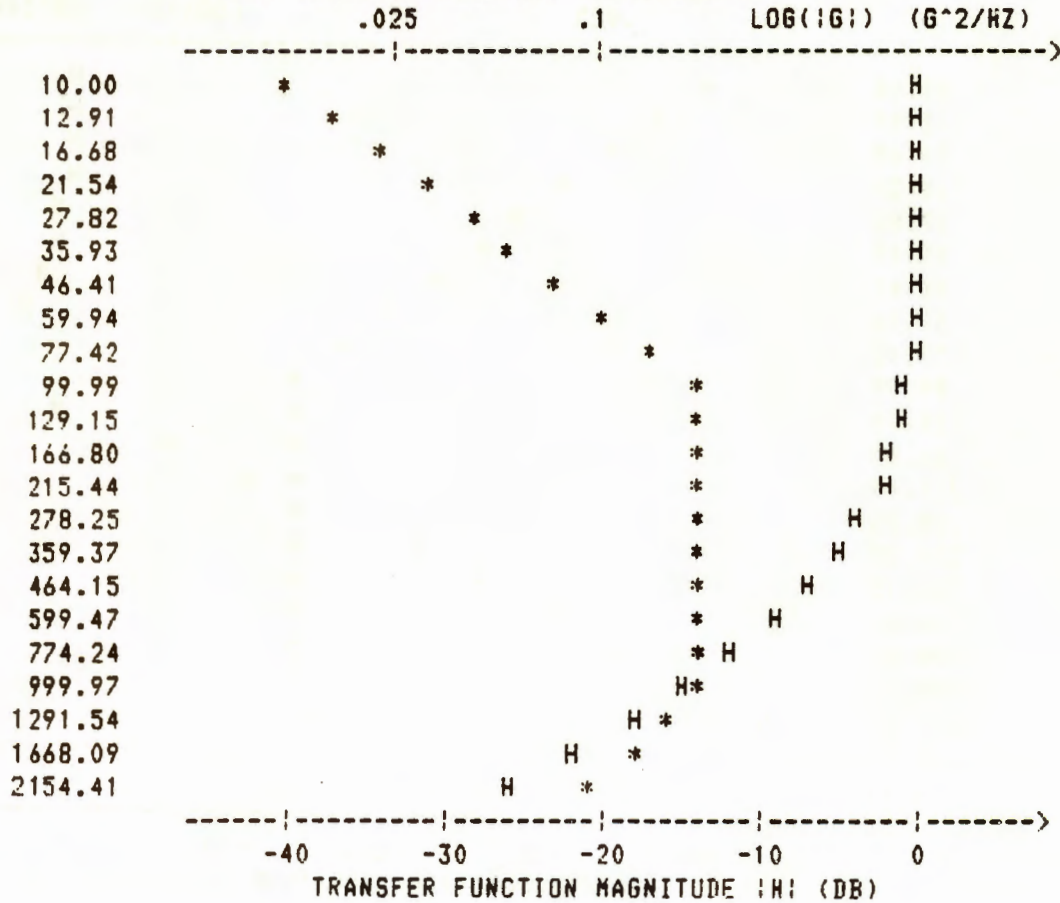
INPUT POINTS P(2),Q(2) AND R(2),S(2)
 ? 100,.2,1000,.2

INPUT POINTS P(3),Q(3) AND R(3),S(3)
 ? 1000,.2,2000,.1

NATURAL RESONANCE FREQUENCY (HZ) OF ACCELEROMETER =?500

NORMALIZED DAMPING COEFFICIENT =?1.2

SUPERIMPOSED PLOT OF SPECTRAL DENSITY FUNCTION G
 AND TRANSFER FUNCTION MAGNITUDE H



RMS OUTPUT VALUE IN G UNITS = 7.30

RUN
 HOW MANY PARTITIONS ARE IN THE SPECTRAL DENSITY ENVELOPE ?3

FROM THE ABOVE DISPLAY, EACH PARTITION HAS AN INITIAL
 POINT P(I),Q(I) AND A FINAL POINT R(I),S(I)

INPUT POINTS P(1),Q(1) AND R(1),S(1)
 ? 10,.01,100,.2

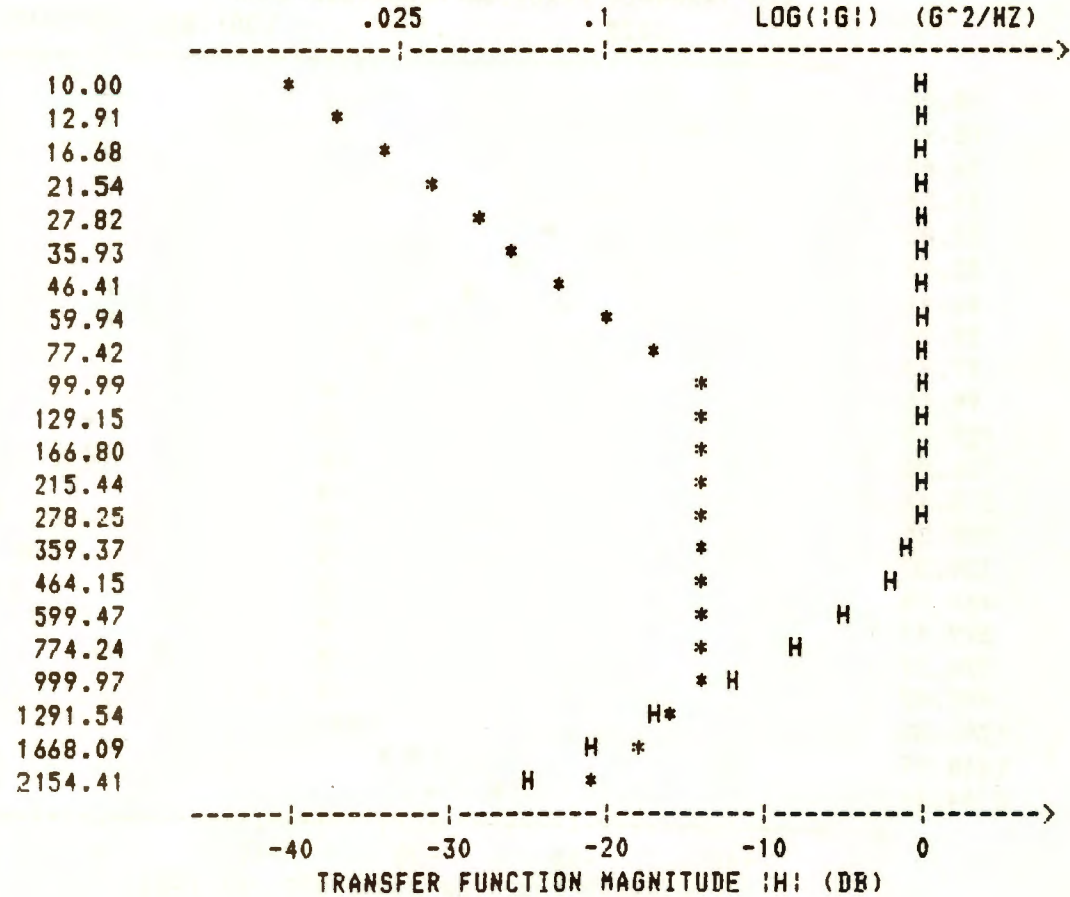
INPUT POINTS P(2),Q(2) AND R(2),S(2)
 ? 100,.2,1000,.2

INPUT POINTS P(3),Q(3) AND R(3),S(3)
 ? 1000,.2,2000,.1

NATURAL RESONANCE FREQUENCY (HZ) OF ACCELEROMETER =?500

NORMALIZED DAMPING COEFFICIENT =?.7

SUPERIMPOSED PLOT OF SPECTRAL DENSITY FUNCTION G
 AND TRANSFER FUNCTION MAGNITUDE H



RMS OUTPUT VALUE IN G UNITS = 9.97

RUN
 HOW MANY PARTITIONS ARE IN THE SPECTRAL DENSITY ENVELOPE ? 3

FROM THE ABOVE DISPLAY, EACH PARTITION HAS AN INITIAL
 POINT P(I),Q(I) AND A FINAL POINT R(I),S(I)

INPUT POINTS P(1),Q(1) AND R(1),S(1)
 ? 10,-.01,100,.2

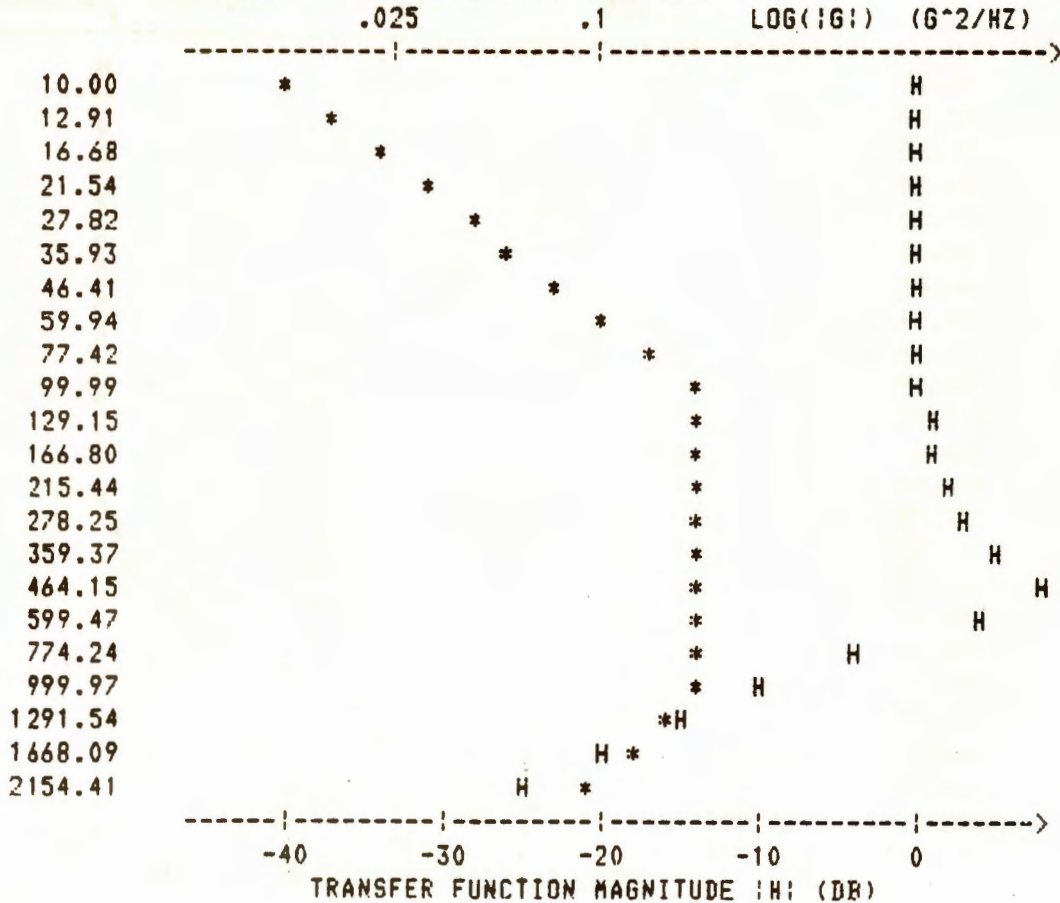
INPUT POINTS P(2),Q(2) AND R(2),S(2)
 ? 100,-.2,1000,.2

INPUT POINTS P(3),Q(3) AND R(3),S(3)
 ? 1000,-.2,2000,-.1

NATURAL RESONANCE FREQUENCY (HZ) OF ACCELEROMETER =?500

NORMALIZED DAMPING COEFFICIENT =?.2

SUPERIMPOSED PLOT OF SPECTRAL DENSITY FUNCTION G
 AND TRANSFER FUNCTION MAGNITUDE H



RMS OUTPUT VALUE IN G UNITS = 19.43

AN INTELLIGENT AMPLIFIER

Richard D. Talmadge
Flight Dynamics Laboratory
Air Force Wright Aeronautical Laboratories
Aeronautical Systems Division
Wright-Patterson AFB

ABSTRACT

In 1967 Structural Vibration and Acoustics Branch (FIBG) of the Air Force Wright Aeronautical Laboratories (AFWAL) sponsored its first development of an Automatic Gain Controlled amplifier (AGC) to solve the problem of recording transducer outputs which have large dynamic ranges. This amplifier has been used very successfully for the past 16 plus years in flight testing as well as ground applications. In February 1982 FIBG initiated an R&D effort with Aydin Vector to ake upgrade this technology to the state-of-the-art in so far as circuit design, accuracy and packaging concepts. The result of this program was an Automatic Gain Ranging Amplifier (AGRA) that has excellent performance. The amplifier is in the form of a hybrid and contains not only the AGRA but a 6 pole pre-sample filter that has four programmable ranges. With the use of a second hybrid FIBG has under development, a universal signal conditioner is available to handle almost any type of transducer whether it is self generating or non-self generating.

HISTORY

The first attempt by FIBG to build an airborne version of an automatic gain controlled amplifier (AGC) occurred in 1967. This organization contracted with Intech to build a true differential amplifier on a 4" x 5" card that could be used in airborne as well as laboratory applications.

The prototype design had several problems. The drift rate of the amplifier was higher than expected at 7.5 microvolts/^oC. Under certain conditions of output load and input signal, a gain change would drive the amplifier into oscillation; which then would force the amplifier to down range the gain. The prototype had an analog gain status output which was unstable and very difficult to digitize and then through the use of an algorithm determine the actual gain. Also, the amplifier required three power supply voltages because of the TTL logic in the control circuits. After several redesign efforts most of these problem areas were minimized.

The amplifier that resulted from the final redesign uses CMOS logic so only two power supplies are required, has digital gain codes and has the input/output reconfigured so that the output load does not affect the performance. The drift problem was solved by an elaborate bench trim process which took at least ten hours per amplifier to perform. This procedure was used for many years but, was recently dropped because

of cost factors.

The AGC amplifier uses average detection for the gain control circuit which is not very satisfactory for the typical vibration and acoustics data. This method weights the peak values to lightly and in most cases would cause some degree of clipping of the data do to the high peak to RMS (or average) ratio for random processes. The only way to overcome this is to be conservative in setting the upper gain change threshold and then if the signal becomes more sinusoidal in nature the signal-to-noise ratio decreases thus reducing the data quality.

This amplifier is in use today; however, the cost of repair is now approximately two to three times the original cost of the device and the lead times for parts is excessive since the modules are now custom built.

The state-of-the-art in amplifier design/performance has changed greatly in the last decade and we felt that it was time to look at a new design for the amplifier to provide better performance, reduced size and put more capability in the device. With the current requirement that the amplifier provide the front end signal conditioning for analog data acquisition systems as well as digital devices, a pre-sample filter is required to prevent aliasing of the data.

In February 1982 FIBG initiated a program with Aydin Vector to develop a hybrid amplifier with state-of-the-art performance and as much size reduction as possible. This amplifier would contain the gain block, a pre-sample filter of at least six poles and Butterworth characteristics, a quasi-peak detector for gain control and a line driver output that with the use of an external current (booster) amplifier could drive virtually any load without degradation of the system performance (see Figure 1). Peak detection was chosen over true RMS since most recording devices today are full scale limited. Because the crest factor varies between random and sine wave data the RMS detector would not correctly set the gain for all cases.

In September 1983, the Aydin Vector program was expanded to include the development of a second hybrid device to implement a technique recently developed by FIBG. This is a new approach to signal conditioning for resistance type transducers which provides improved accuracy under the adverse conditions encountered in airborne and field testing and greatly simplifies the acquisition system calibration.

The technique involves (1) using a dual tracking constant current circuit to supply the "bridge" power and then (2) measuring the differential voltage across the elements. The "bridge", in this case, is really a "Y" circuit composed of two series branches with a common node. In this configuration the two current sources are connected to the tips of the "Y" and the differential voltage between the supplies and the supply common is measured. The common node is connected to the power supply common. The change in voltage (ΔR) is a linear representation of the physical phenomenon at the transducer plus the lead wire effects. Since the circuit is symmetrical in every respect it requires only three wires to implement any conventional "bridge" circuit

with complete lead wire effect cancellation (see Figure 2).

PERFORMANCE

The first prototype Automatic Gain Ranging Amplifier (AGRA) was delivered in May of 1984. Some of the outstanding performance features are as follows;

1. Frequency response - 4 bands digitally selectable
(0-500Hz, 0-2kHz, 0-5kHz, 0-20kHz)
2. Gain - 0.25, 1, 4, 16, 64, 256, 1024
3. Amplitude error - < 0.1%, < 0.1dB with filter ripple
4. Temperature Drift(RTI) - less than 0.5 microvolts/°C
5. Input impedance - 10 megohms differential
5 megohms single ended
6. Input configuration -AC/DC internal coupling
7. Output noise - less than 2 millivolts RMS
@ gain = 1024 (dc -20kHz)
8. Operating Temperature - -55 to 85 °C
9. Control input - CMOS compatible(3 to 18 volts)
10. Size - 0.23 x 2.0 x 2.375 inches

The AGRA is designed to be digitally controlled either by the use of switches (or jumpers) or by the use of a microprocessor in the system. The following functions are under program control;

1. The mode of operation i.e. full automatic operation, manual gain control, or "down range only" (in this mode the AGRA will down range on overload but will not increase gain when the voltage falls below the up range threshold). The gain change can be inhibited at any time by raising a logic level on the control input. This function can be used to prevent gain changes during recording.
2. The input configuration (AC/DC coupling). In the past it has been a problem to maintain the temperature drift specification when an instrumentation amplifier is AC coupled. This was solved in the AGRA by using a DC stabilization loop in the front end when the amplifier is in the AC coupling mode. This allows the maintenance of high input impedance and essentially the same drift specification as when the AGRA is in DC mode.
3. The filter bandwidth and the peak detector response time may be programmed independently so that one can control the sensitivity of the detector to "out of band" signals. This prevents amplifier overloads due to data that are beyond the filter cutoff.

4. If DC data are being taken there is a control pin to momentarily disconnect the source and short the amplifier input to facilitate the measurement of the offset in the amplifier.

The amplifier also contains a pin to input a voltage to compensate the output of the amplifier for input offsets or to change the input range from bi-polar to uni-polar. This function requires additional support hardware since the offset control is injected at the output of the input stage (this stage is part of the gain circuit).

All of the programming signals with the exception of the mode control are momentary and are latched internally in the AGRA. Programming is performed by asserting the required control information and then providing a strobe signal to the AGRA.

Once the AGRA is set up to perform a specific function the amplifier will accomplish all of the required tasks by itself thus relieving the system of any overhead associated with controlling the front end of the acquisition system (thus the term "Intellegent Amplifier").

The Automatic Gain Ranging Amplifier (AGRA) will maintain its output (in the auto gain mode) within the predefined limits. These limits may be set to one of four values by strapping either +15 or +5 volts (internally generated) to one of two pins. This will give the full scale ranges of approximately 10, 5, 1.4 and 1.0 volts peak. If one wishes other ranges an external voltage may be applied to provide any range between 200 millivolts and 10.0 volts peak.

The output of the AGRA is an analog signal with digital status information which includes the gain code and the "Built In Test" (B.I.T.) bit. The B.I.T. provides information about the operation of the AGRA. This bit among other things is a flag for gain changes and will indicate overloads when the AGRA is in fixed gain mode. If this bit is put in as the LSB of the digital word it becomes a simple matter to check for gain changes during data processing. The AGRA will directly drive any reactive load from approximately 1000 ohms up. For the analog recording case; the gain and status bits must be encoded by some technique such as PCM or PAM so they can be recorded with the data. For the digital recording case; a sample/hold and an A/D are required. The A/D should be a 12 bit converter and the gain and status bits may be merged with the data to form a 16 bit word. An alternate method of including the gain status would be to block encode the data such that a number of samples is coded as a block with a header that includes the gain information.

In the 20kHz bandwidth mode the sampling rate must be approximately 65,000 samples per second to insure that the aliased data are below the LSB of the converter. The converter must operate at a minimum of 3.2768 times F_{max} .

The constant current hybrids were delivered in January of 1985. These modules have undergone extensive testing at Wright-Patterson AFB and have met all expectations. The units have an accuracy of approximately 0.01% of nominal programmed value at room temperature and

0.03% over a temperature range of -25 to 85 °C.

APPLICATIONS

Some of the possible uses of the AGRA are outlined in the following paragraphs.

One of the prime drivers to reduce flight test time is the high cost of the actual hours the aircraft is in use or unavailable for use by others. To minimize this cost one can reduce the number of test hours by increasing the amount of data acquired during any one mission. This requires the data system to be capable of handling more channels and the test conditions to be increasingly varied. All of which leads to the requirement for an increased dynamic range capability for the data channels. It is difficult to program the gains of the data acquisition system to cover the expanded scope of the measurements in an efficient manner (even if the data acquisition system has a multiple format capability). To solve this problem the AGRA was developed to adaptively change its gain based on the input signal level and is ideally suited to minimize flight test time.

Many transducers have in excess of 100 dB dynamic range. This is typical of accelerometers and strain gages among others whose dynamic range is limited primarily by the resolution of the measurement system. This range requirement is generated by the fact that a typical mission may entail everything from low level, high speed flight - to acceleration runs - to low speed, straight and level flight or in the case of Modal Testing numerous test conditions. To ease the burden on the pilot, flight engineer or data acquisition engineer of having to manage the data acquisition system as well as other things such as the aircraft one would use the AGRA. The AGRA in the fully automatic mode of operation will keep the output data signal within the bounds of the recording system, thus maximizing the amount of high quality data derived from each test. When the engineer is satisfied that the test condition has been attained the AGRA may be inhibited or locked so that no more gain changes will occur.

If one were to try to second guess the output levels of each transducer for all the possible test conditions one would have to be conservative or use split range techniques to guarantee the data integrity thus running the risk of having poor signal-to-noise ratio in the recorded data.

To handle the transient data case the AGRA has a mode called "down only". This mode allows the gain of the amplifier to decrease only after being reset to a given value. To use this function one would select an arbitrarily high value for the gain prior to the event of interest and then subject the vehicle or test article to the forcing function. The AGRA would down range to the gain required for the maximum signal encountered during the test cycle. From that point on, every time the test is repeated there would be no gain changes. For instance if the test cycle were a burst of gunfire, the first burst would set the gain and then, for each successive burst the gain would be set correctly.

For laboratory tests such as Modal Analysis this is a very important attribute. When the input is transient, as in impact testing, the first several impacts will set the gain and then the data are acquired for any number of successive impacts and averaged to compute the transfer functions without further gain changes.

For steady state Modal testing, such as random excitation, the automatic gain mode will speed the setup time from condition to condition since there is no operator intervention required for gain setting.

When the test calls for swept sine the test engineer can select the down only mode of operation for the AGRA. In this mode one sweep would be generated (and this could be a faster than normal sweep depending on the Q of the system under test) to set the gains of the amplifiers and then data taken on the next pass. The automatic mode could be used if one were willing to accept and correct for the gain changes that would occur during the test.

With the use of the Constant Current supply that was developed under the Aydin Vector program many resistance type transducers can be interfaced to the AGRA. These transducers include strain gages, potentiometers, RTDs, and transducers that contain built-in electronics requiring a current source to power them.

Commercial bridge type transducers would require a modification to take advantage of the attributes of this supply. This is because of the requirement to have one of the bridge nodes open to isolate the power inputs. The module provides either two single or one dual tracking current sources. Refer to Figure 3 for a typical configuration. The wiper of the potentiometer is connected to ground and each end is connected to a current source in the module. This configuration will provide lead wire error cancellation and produce a linear output with wiper position. It should be noted that this circuit will produce an output that is twice that of the conventional circuit configuration.

Figure 4 shows a configuration for a single element transducer that will provide lead wire correction. In this configuration one current source is connected to each end of the element and then one end is grounded. The current flowing through each of the wires will produce a voltage proportional to the wire characteristics (both dynamic and static) and will be subtracted at the amplifier input.

One application for this power supply is in multiplexed systems. The power supply may be switched so that the transducer is only powered just prior to and during the measurement. This significantly reduces the total power requirements in large systems. The power must be turned on early enough to allow for settling of the transducer but not so early as to produce significant amount of self-heating.

CONCLUSIONS

The Automatic Gain Ranging Amplifier (AGRA) is a precision instrumentation amplifier designed to provide the gain element in a data

collection system without any calibration required since it has no vernier gain adjustments. For this reason it is essentially transparent to the measurement system. It is an intelligent system element that has the capability of maintaining its output within the range of the recording system with no intervention from the control system. For these reasons it is an excellent choice for most transducer interface requirements.

REFERENCES

1. Talmadge, RD, "Non-self Generating Transducer Conditioning Technique", 12th Transducer Workshop Proceedings 1983 pg 99-113.
2. Talmadge, RD, Liron, E, "Automatic Gain Ranging Amplifier", International Telemetry Conference. Proceedings Vol XIX, 1983 pg 451-457.
3. Talmadge, RD, "An Intelligent Amplifier and its Application to Modal Analysis", International Modal Analysis Conference, 1985 pg 507-510.

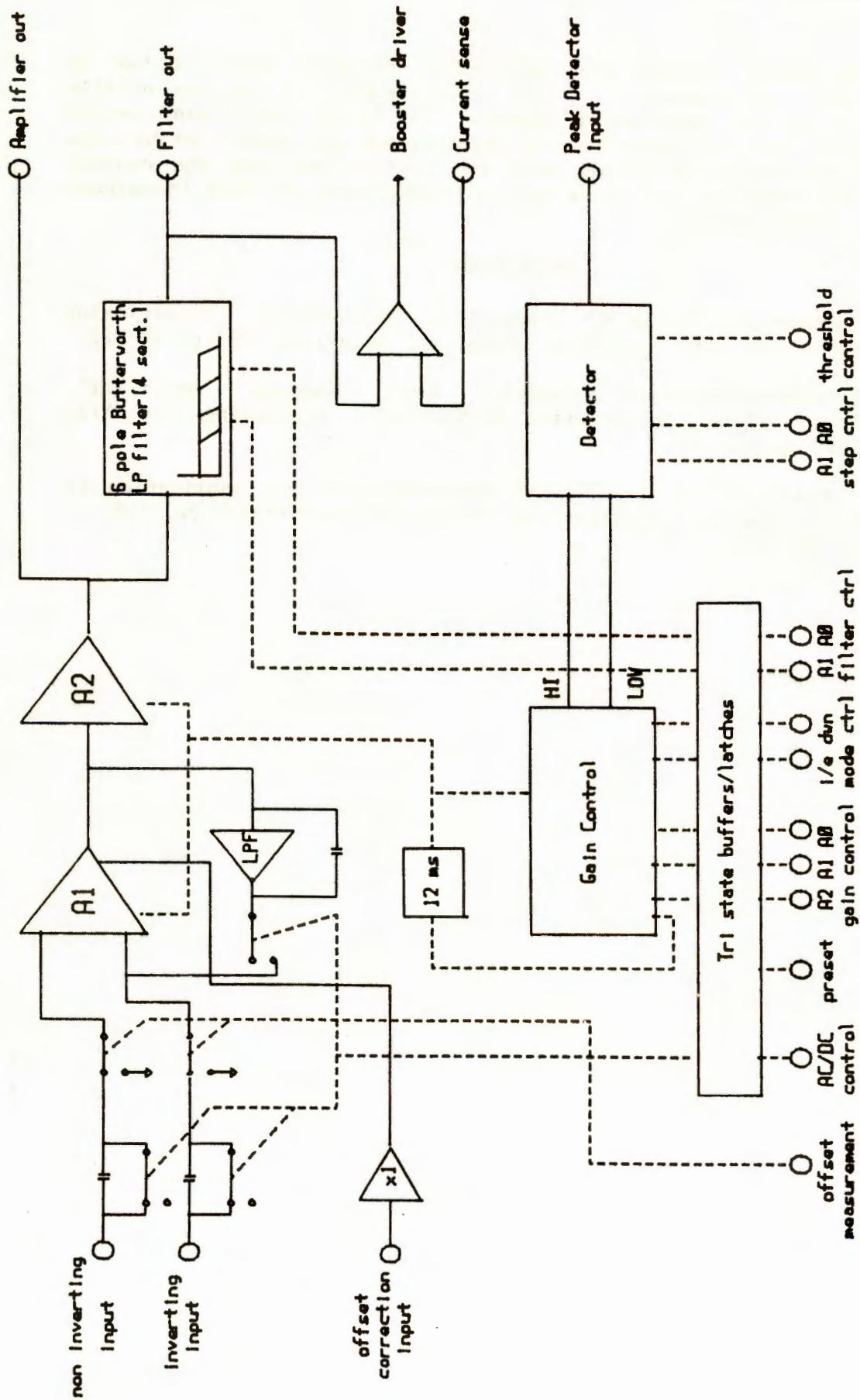


FIGURE 1 AGRA BLOCK DIAGRAM

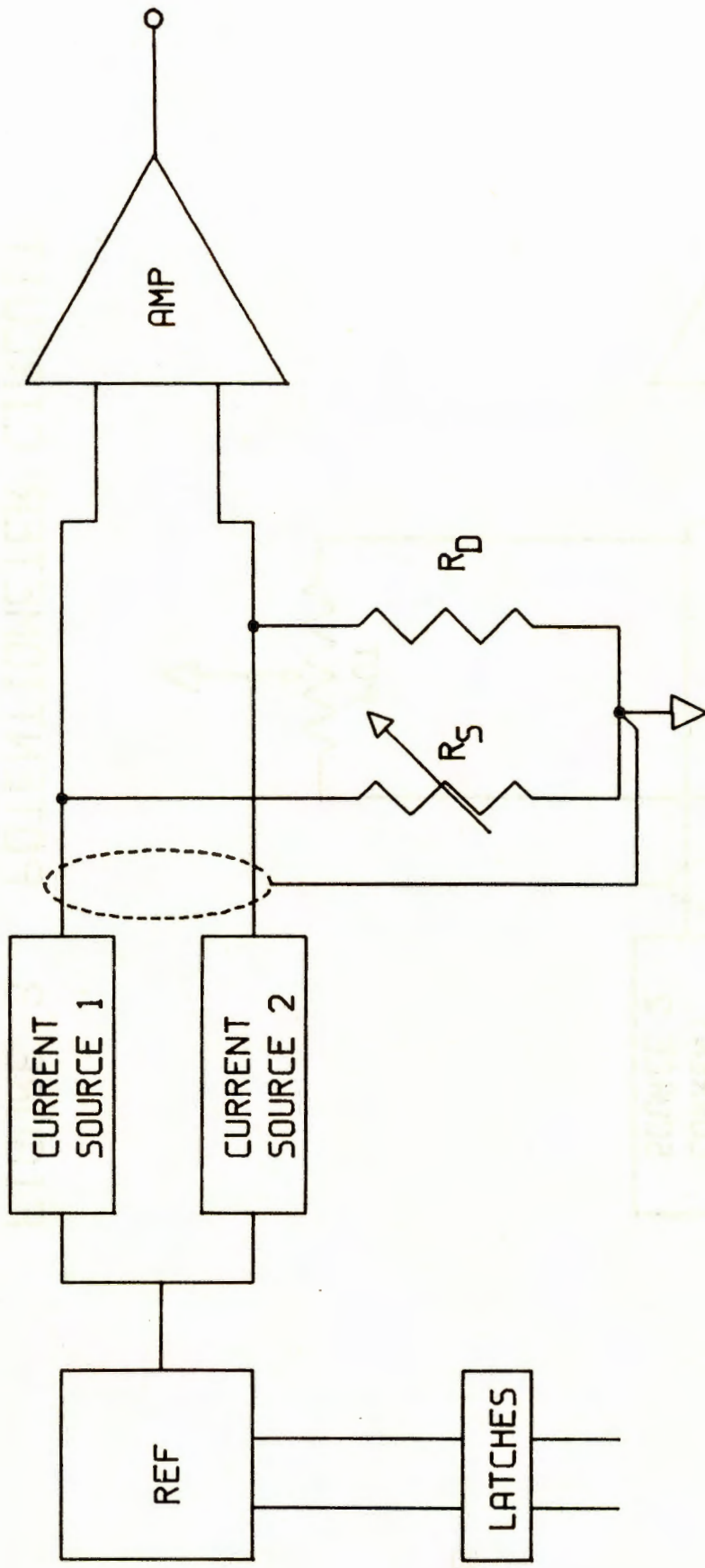


FIGURE 2 DUAL CONSTANT CURRENT SOURCE

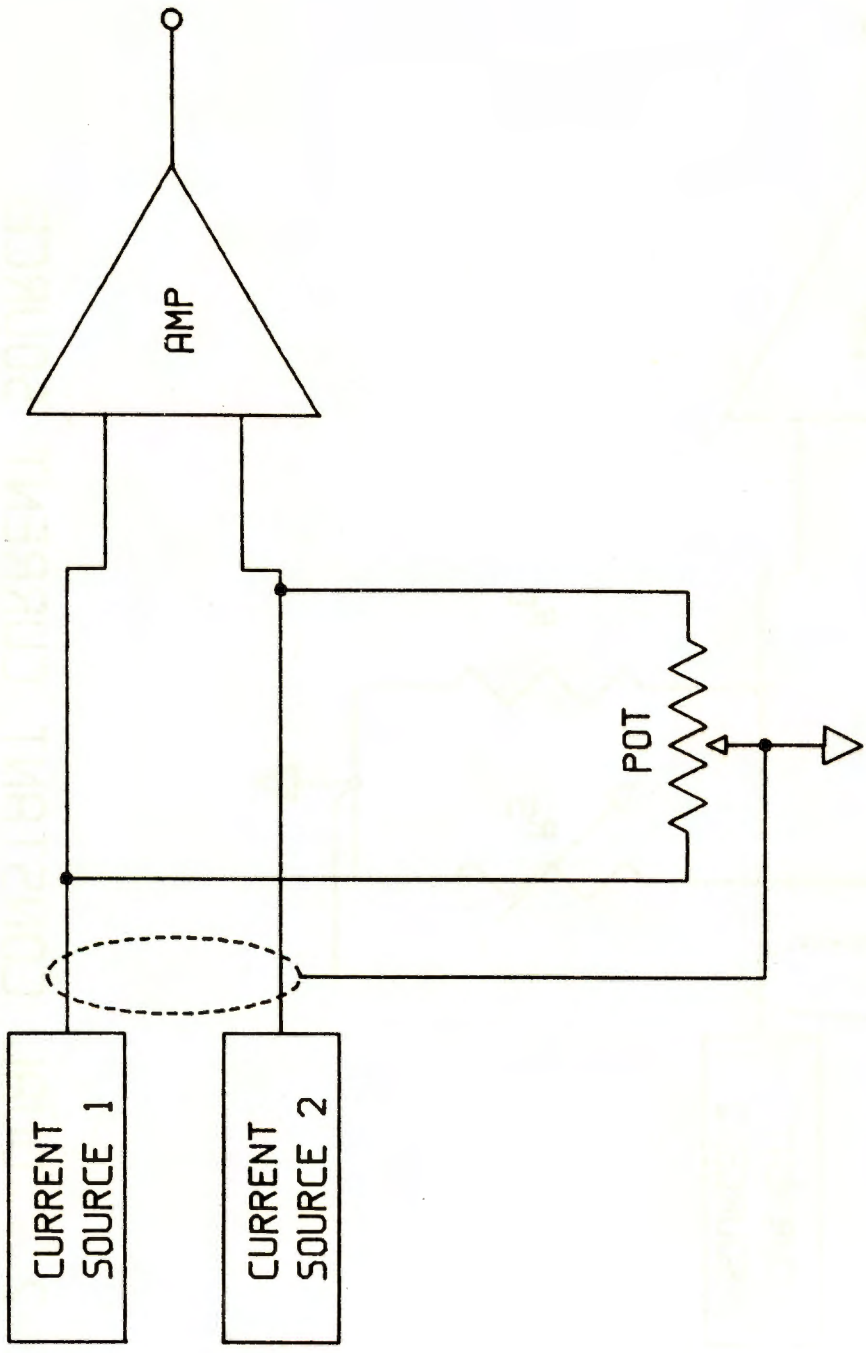


FIGURE 3 POTENTIOMETER CIRCUIT

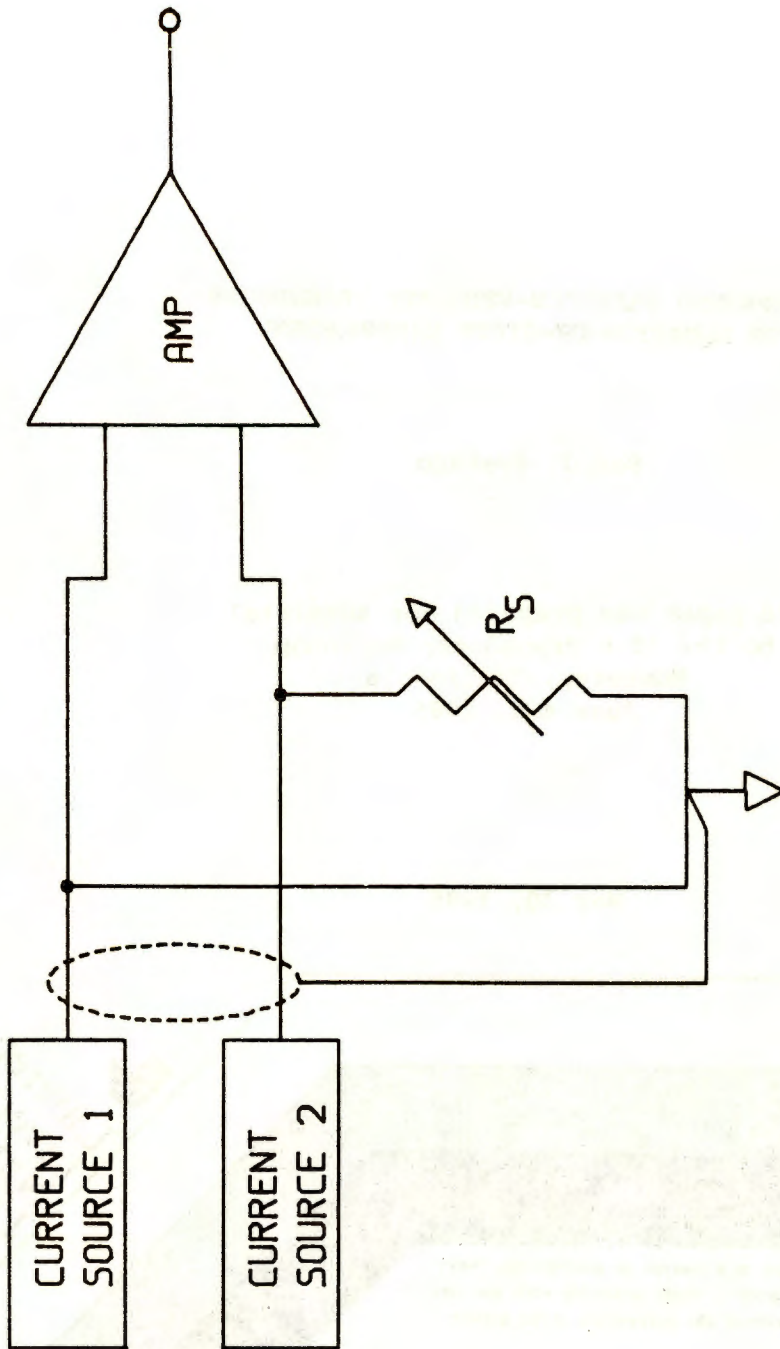


FIGURE 4 SINGLE ELEMENT CONFIGURATION

AN IMPROVED PARTICLE-VELOCITY TRANSDUCER
FOR EQUATION-OF-STATE EXPERIMENTS

Sam J. Spataro

This paper was prepared for submittal
to the 13th Transducer Workshop
Monterey, California
June 4-6, 1985

May 30, 1985



This is a preprint of a paper intended for publication in a journal or proceedings. Since changes may be made before publication, this preprint is made available with the understanding that it will not be cited or reproduced without the permission of the author.

DISCLAIMER

This document was prepared as an account of work sponsored by an agency of the United States Government. Neither the United States Government nor the University of California nor any of their employees, makes any warranty, express or implied, or assumes any legal liability or responsibility for the accuracy, completeness, or usefulness of any information, apparatus, product, or process disclosed, or represents that its use would not infringe privately owned rights. Reference herein to any specific commercial products, process, or service by trade name, trademark, manufacturer, or otherwise, does not necessarily constitute or imply its endorsement, recommendation, or favoring by the United States Government or the University of California. The views and opinions of authors expressed herein do not necessarily state or reflect those of the United States Government or the University of California, and shall not be used for advertising or product endorsement purposes.

AN IMPROVED PARTICLE-VELOCITY TRANSDUCER
FOR EQUATION-OF-STATE EXPERIMENTS *

Sam J. Spataro

University of California
Lawrence Livermore National Laboratory
Livermore, California

ABSTRACT

An improved particle-velocity transducer has been developed for use in equation-of-state experiments in the low (sub-kilobar) shock region. In low amplitude shock experiments, our standard one-turn transducer generated voltages so low that signal-to-noise problems were limiting our resolution. By using multiple turns in the new transducer, we get an increase in signal, proportional to the number of turns, with no apparent increase in noise.

The complete experiment system consists of passive, multiple-turn current-loop transducers, a Helmholtz pair of electromagnets, a firing and timing system, a data recording system, the material under study, and a small explosive charge.

Each current "loop" is actually a narrow linear strip (or element) of very thin copper foil, which is embedded in the test material. The shock wave from the emplaced explosive charge moves the element across an orthogonal magnetic field causing, for a brief period, a voltage output proportional to the velocity of the element.

In this paper I present the theory and design of a new three-turn transducer, its advantages, its error sources, and some typical test results. Also, I will briefly describe the magnetic field generator, the data recording system, and data processing.

*Work performed under the auspices of the U.S. Department of Energy by the Lawrence Livermore National Laboratory under contract No. W-7405-ENG-48.

INTRODUCTION

The objective of the equation-of-state (EOS) work at the Lawrence Livermore National Laboratory (LLNL) (Ref. 1) is to provide a data base for material response modeling and computer code development, and to test dimensional similarity for small-size to field-size experiments. This work has direct application in the LLNL Containment Program, Seismic Monitoring Program, Ice Penetration Program, and similar areas of research.

We have, for a number of years, conducted the EOS experiments using a single-turn passive transducer to measure particle velocity. We have recently developed an improved particle-velocity transducer for use in EOS experiments in the low (sub-kilobar) shock region.

The complete EOS instrumentation system (Fig. 1) consists of (1) ten or more passive multiple-turn current-loop transducers embedded in the material under study, (2) a Helmholtz coil pair of electromagnets to establish a magnetic field perpendicular to the transducer element and its motion, (3) a firing and timing system, (4) a data recording system, (5) a block of the material under study, and (6) a small explosive charge with a mild detonating fuse.

Each single-turn current loop, or element, is a narrow, linear strip of copper foil. The multiple-turn transducer provides an electrical signal that is proportional to the velocity at which a single-turn loop, embedded in the material under study, moves through the DC magnetic field. The transducer is moved through the field by a shock wave created by detonating the charge of chemical explosive emplaced in the material. By exciting the material with a shock from an explosive source, we obtain the time history representation of in-situ particle velocity that the embedded gage sees as it moves with the material. This method has been successfully used to measure dynamic loading and unloading of material to describe their EOS.

Standard time delays, synchronizing pulses, and fiducial markers, all accurately timed, are included in the overall measuring system to ensure synchronization of sweep time and signal arrival. The firing and timing system, as well as the data recording system, is illustrated in Fig. 2.

The data recording system consists of precision oscilloscopes and high-speed cameras to record the voltage output waveform as a function of time. The recorded trace is digitized, transferred to magnetic tape, and then

input to a computer for standard processing. The reduced data includes displacement, acceleration, and spectral information.

The reason for developing the improved transducer was that in recent investigations of very low (sub-kilobar) shocks, our standard one-turn transducer generated voltages so low that signal-to-noise problems were limiting signal resolution. Our new three-turn transducer overcomes this problem efficiently and economically. By using multiple turns, we obtain an increase in signal proportional to the number of turns with no apparent increase in noise.

THEORY OF OPERATION

The principle of operation for the transducer is governed by Faraday's Law (and is represented for our purposes in Figs. 3 and 4): i.e., the motion of a conductor in a magnetic field produces a voltage that is proportional to the velocity of the conductor. Mathematically,

$$\vec{V} = (\vec{B} \times \vec{u}) \cdot \vec{l},$$

where,

- V = output voltage (volts)
- B = magnetic field (webers/m²)
- u = velocity (m/sec)
- l = length of element (meters).

When \vec{B} , \vec{u} , and \vec{l} are mutually orthogonal, as they are in our experiments, the output voltage, V, is the scalar product of the three parameters. With B and l known, V is then proportional to the velocity, u.

The distance traveled, Δx , of the element, l, is very small, typically in the 100-microinch range. This very small travel assures us of a straight-line motion through the field, B, precluding any curved-path corrections.

The Lorentz force from the magnetic field acts on free charges within the metallic conductor (loop) to establish a voltage that is a function of the net charge motion. The relationship of voltage and velocity is derived from Faraday's induction law:

$$\phi = \oint \vec{B} \cdot dA , \quad (1)$$

which reduces to

$$\phi = B \cdot A .$$

It states that when there is a change in magnetic flux, ϕ , an electromotive force is established either by a change of the magnetic field, B , or by a change in the area, A , swept by the element, l . This induced voltage, V , is proportional to the rate of change in net flux. That is,

$$V = -n \frac{d\phi}{dt} , \quad (2)$$

where n = number of turns in the loop. The negative sign refers to the sense of V due to a collapsing field.

Combining Equations (1) and (2) we have

$$\begin{aligned} V &= -n \frac{d}{dt} (B \cdot A) \\ &= -n \frac{d}{dt} (B \cdot l dx) . \end{aligned}$$

Finally,

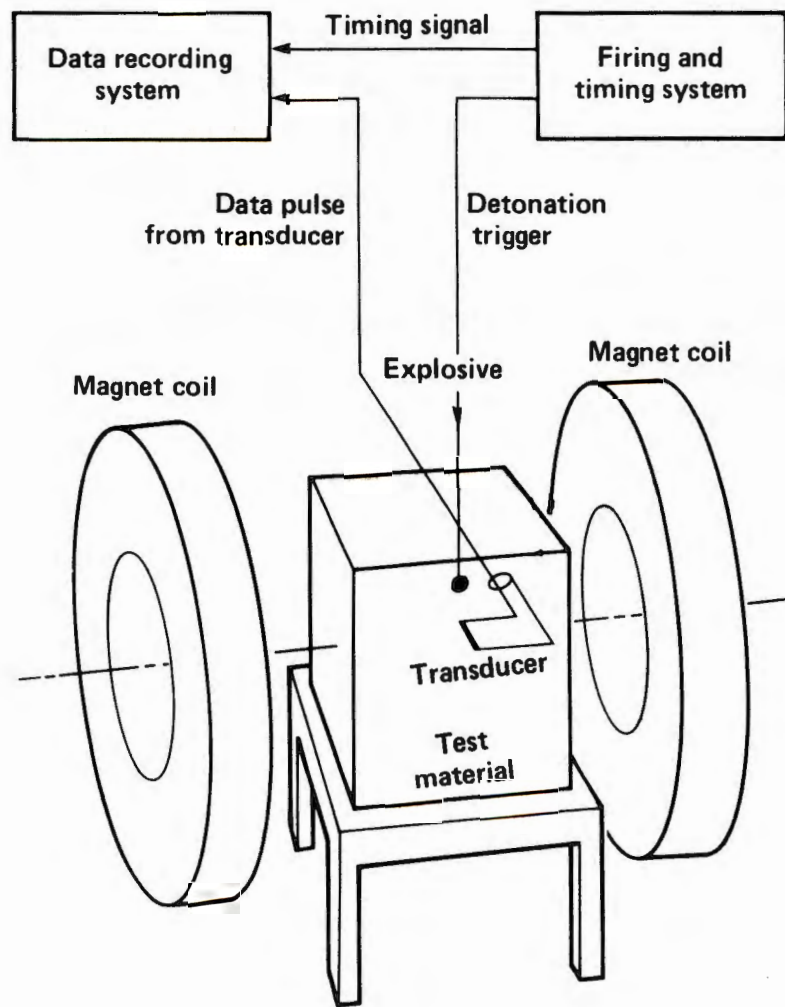
$$V = -n \cdot B \cdot u \cdot l ,$$

$$\text{where } u = \frac{dx}{dt} \quad (3)$$

We see, then, that we can achieve an increase in transducer sensitivity by merely increasing the number of turns, n .

THE TRANSDUCER

The previously used single-turn transducer and the new three-turn unit are shown pictorially and schematically in Fig. 5. Both transducers are fabricated from copper foil (≈ 1 mil thick) sandwiched between layers of 2 mil



Spataro – Fig. 1

Kapton, a transparent Mylar-type material. The Kapton acts as an insulator and also adds strength to the unit. The copper and Kapton are bonded with an epoxy resin approximately 0.1 mil thick.

The individual elements of the three-element unit are jumpered at their far ends so that the three loops are electrically in series. Care is taken to ensure that the jumpered end is sufficiently removed in distance from the active end so that there is no motion during the time the transducer is returning useful data.

The transducer leads are soldered to the center conductor and shield of RG-174/U, 50 ohm coaxial cable. The cable is then patched to RG-8/U coaxial cable, which completes the run to the oscilloscope/camera system.

In the original single-turn transducer, the element length was chosen to optimize signal output (V is proportional to l), and the "geometric resolution" of the transducer. The geometric resolution is the transit time, t , of a circular shock front sweeping across the active element, l . This time is a function of (1) the distance between the shock origin and transducer, (2) the shock velocity, v , and (3) the separation between lead wires, l . The time for the shock wave to totally engulf the element tends to "smear" the particle-velocity measurement across the element.

From the geometry in Fig. 6,

$$r^2 = (r - h)^2 + \left(\frac{l}{2}\right)^2,$$

where $h = v \cdot t$, from which

$$t = \frac{r - 0.5 (4r^2 - l^2)^{1/2}}{v}. \quad (4)$$

If we assume a transducer-to-explosive separation of $r = 200$ mm, $l = 9$ mm, $v = 3 \times 10^3$ m/sec, then the foil is engulfed in ≈ 17 ns. This time is some 2 orders of magnitude faster than the rise time of the particle-velocity pulse. Hence, there is little smearing of the velocity signal.

For the shock radii and velocities used in our experiments, $l = 9$ mm is an optimum transducer element length.

ERROR SOURCES

It is not the intent of this paper to engage in a formal, quantitative error analysis. Rather, I point out here some of the errors we are aware of that reside in both the old and new three-turn transducer system. Overall, we have a system accuracy of $\approx 2\%$.

There are several sources of possible measurement error common to both the single-turn and three-turn transducer:

- (1) The geometric resolution, mentioned above, results in an integrated measurement of u across the gage element and not at a point. This error, measured by the transit time, t , is of the order of 10 to 50 ns.
- (2) If the leads between the element, l , and the signal cable are not parallel to the magnetic field, we can get contributions due to the leads moving through the field. This is minimized by offsetting the transducer so it does not straddle the geometric center of the field (Ref. 2). Figure 7 is a pictorial representation of this problem.
- (3) The three individual loops must be connected beyond the point of any movement so that we maintain the X3 gain.
- (4) A "thick" transducer (the overall dimension, including copper and kapton) yields unwanted signals due to reflections off the transducer/material interface. The three-turn transducer is overall less than 12 mils in thickness, and the error contribution from this source is small.
- (5) There are errors of a lesser magnitude due to: nonhomogeneous magnetic field, transducer element stretching after shock impact, signal cable noise, and the Johnson noise of the transducer itself.

THE HELMHOLTZ MAGNETS

The DC magnetic field, which supplies the Lorentz force for the transducer, is generated by a Helmholtz coil pair. We have two such magnets--a small and a large--and a brief description of each is given in Table 1. (The small magnet is described in greater detail in Ref. 3.)

The small magnet is water cooled, and can handle about 1500 amperes (maximum) for an extended length of time. (This current yields about 2.5 kgauss.) Power consumption at this level is 200 kW.

The large magnet has been operated at 800 amperes, with field level at about 2 kgauss. Power consumption is 270 kW. A dual ranged, constant-current power supply, rated at 600 kW, supplies the current to both of these magnets.

THE DATA RECORDING SYSTEM AND DATA REDUCTION

Data from the transducer is recorded on Tektronix 7000 series oscilloscopes with 200 MHz band widths (see Fig. 2). Both the horizontal and vertical amplifiers are calibrated with frequency and voltage standards after every experiment.

Standard high-speed Polaroid film is used with the camera. The film is then photo enlarged to approximately 8x10 inches, and the trace is manually digitized and recorded on magnetic tape.

The tape is then interfaced to a Prime 750 computer where standard processing is done. Some of the data processing includes integration and differentiation of the velocity data to yield displacement and acceleration, and fast Fourier transforms for spectral information.

A hardcopy of the processed data is the final output. Figures 8 and 9 are typical data from our three-turn transducer.

FURTHER WORK

We are presently procuring and will soon evaluate a high speed (CAMAC) transient digitizing system that will be interfaced to either an LSI-11 computer or a personal computer. This will ultimately replace the oscilloscope/camera systems and will allow us near-real-time data processing capability. With 10-bit dynamic range and 10-MHz bandwidths, we can record very fast data with about an order-of-magnitude improvement in resolution over our existing oscilloscope/camera system.

We are planning some future development on n-turn units to get even more sensitivity and less unwanted signals:

- (1) We are looking at thinner insulating material and vapor depositions so we can approach 3 to 4 mil total thickness.
- (2) We have built and have done some limited testing on a five-turn transducer that has five times the sensitivity over our previous transducer, with no increase in noise.
- (3) We are considering a design that would have an increase in sensitivity of X12

CONCLUSIONS

We have designed and used in approximately twenty-five measurements an improved particle velocity transducer for EOS work. The advantages of this three-turn transducer over our previous single-turn transducer are:

- Three times the output with no discernible noise increase.
- No change is required in our data system.

ACKNOWLEDGEMENT

The author wishes to acknowledge Don Larson, LLNL physicist, who enthusiastically accepted the idea of the new transducer design and coordinated efforts to get it fabricated, tested, and used in his experiments. His timely comments, suggestions, and critique of this paper were very helpful.

REFERENCES

1. Don Larson, private communication, Lawrence Livermore National Laboratory, Livermore, California.
2. H. C. Rodean, D. B. Larson, J. R. Hearst, and S. R. Brown, ARPA-AEC Seismic/Evasion Research Program: Progress on Small-Scale HE Experiments and Computer Code Verification, Lawrence Livermore National Laboratory, Livermore, California, July 27, 1970.
3. Sam Spataro, Design of a Helmholtz-type Magnet for Equation-of-State Experiments, Lawrence Livermore National Laboratory, Livermore, California, Internal Report LER 70-105201, December 1970.

Table 1. Important features of the two Helmholtz coil pair of electromagnets available for EOS experiments.

Parameter	Small magnet	Large magnet
Mean diameter of coils	56 cm	230 cm
Gap spacing	Variable to 45 cm	100 to 150 cm
Field strength, kgauss	Variable to 2.5 kgauss (to 0.25 weber/m ²)	2.5 kgauss (nominal)
Homogeneity of field at geometric center of magnet	<1% over 150 cm ³ ; <0.5% over 100 cm ³	0.5% over a large volume
Ripple in field	<1% variation, long term	<1% variation
Portability	Easily moved with forklift	Permanently mounted

FIGURE CAPTIONS

Figure 1. A typical "shot" setup, with the material under study placed within the polegap of a magnet. The transducer is set up to measure in-situ particle velocity. The explosive is detonated at "zero-time," with all timing for the measurement system referenced to that time. In reality, we may have ten or more transducers at various radii from the charge, along with associated timing equipment and oscilloscope/camera systems.

Figure 2. Diagram of the firing and timing system and the data recording system. The test sequence is initiated manually with the firing switch. A pulse from the detonator pulser is sent to both the explosive charge and the timing circuits to ensure accurate synchronization of oscilloscope sweep time, signal arrival, and camera-shutter activation. The waveforms on the oscilloscopes are recorded on high-speed film.

Figure 3. Pictorial representation of the transducer element, l , moving through a distance, dx , in a magnetic field, B . The rate of motion of the element, dx/dt , is the in-situ particle velocity, u , of the transducer and material. The three-turn transducer is three of these loops connected in series to give a gain of X3.

Figure 4. Vector diagram for the three main parameters of the EOS experiments. Great care is taken to ensure that the three vectors, \vec{u} , \vec{B} , and \vec{l} , are orthogonal. When this is true, the output voltage developed across element, l , is simply the scalar product of the parameters; that is $V = -B \cdot l \cdot u$.

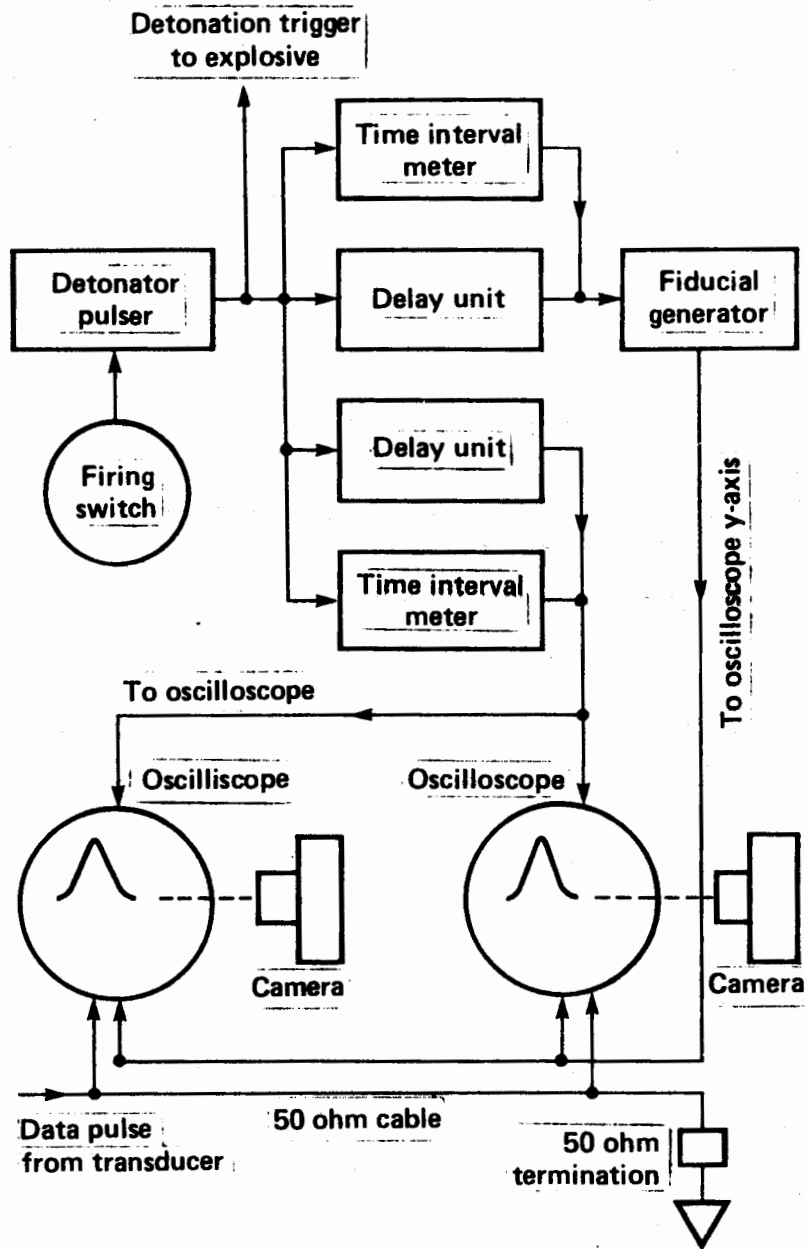
Figure 5. The previous standard transducer and the new three-turn unit, shown both pictorially and schematically. Both are constructed of the same materials. The three-turn unit is simply three single-turn units laid one on the other and electrically connected in series. The impedance of the transducer is in the milliohm range.

Figure 6. Diagram illustrating the parameters that describe the geometric resolution, which is the travel time, t , of a circular shock wave front with velocity v sweeping across the transducer active element, l . The radius of curvature of the shock front is r . The parameter h is the distance the shock front travels from first contact to total engulfment of the transducer element.

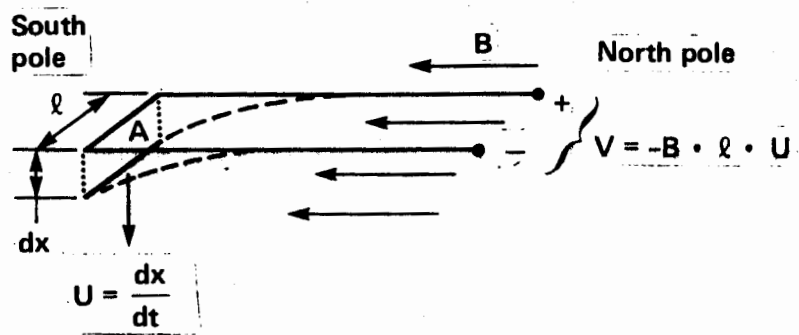
Figure 7. Explanation of method of compensating for nonparallel magnetic field by offsetting transducer from center of field. The B_y components of the nonuniform field through which these transducers move induce unwanted voltages in each of the leads. In transducer 1, both unwanted lead voltages add to the desired signal voltage, but in Transducer 2, one adds and the other subtracts. In the magnetic system now being used, the contributions from the leads in the Transducer 1 configuration represent about 5% of the signal. For the Transducer 2 configuration, however, the field orientation is such that no contribution is detected.

Figure 8. A typical particle-velocity time history. These signals were obtained from two transducers positioned side by side in compacted dirt, 70 mm from the center of a small explosive charge. The data scatter is typical of any transducer pair in pressed dirt.

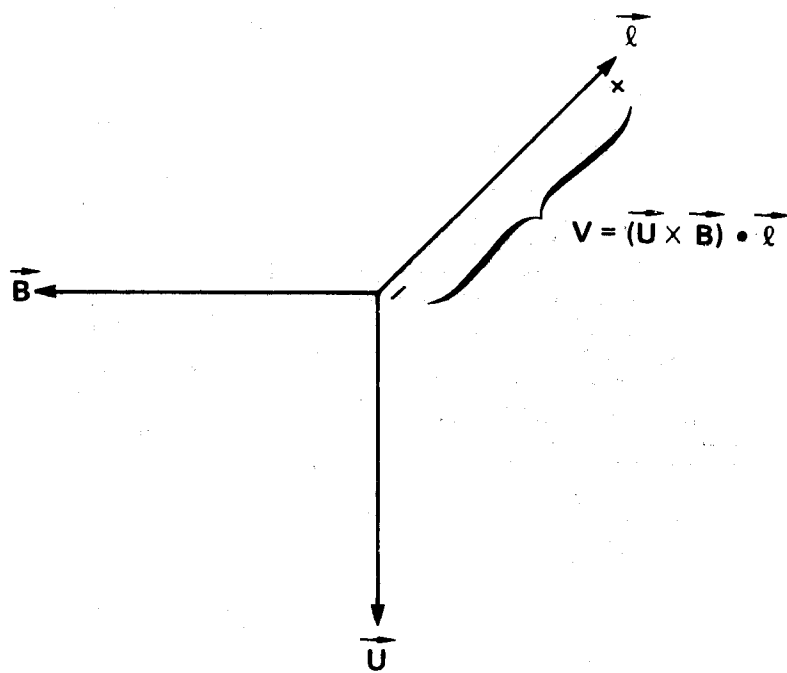
Figure 9. Typical suite of particle-velocity time histories. This ensemble of particle-velocity measurements is one form of data presentation. Displayed in this manner, one can easily see the delay in shock arrival times, the decay in amplitudes, and the slower rise times--all with increasing distances between the transducers and the chemical explosive charge.



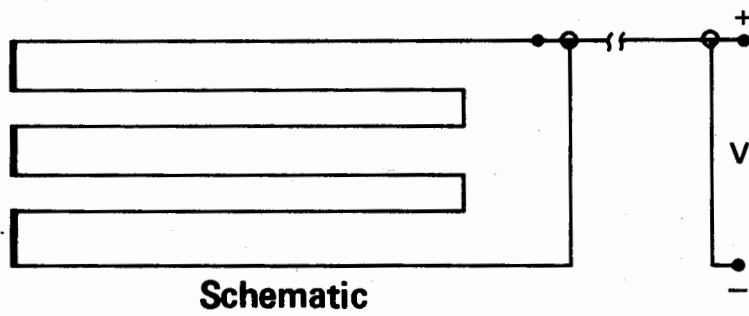
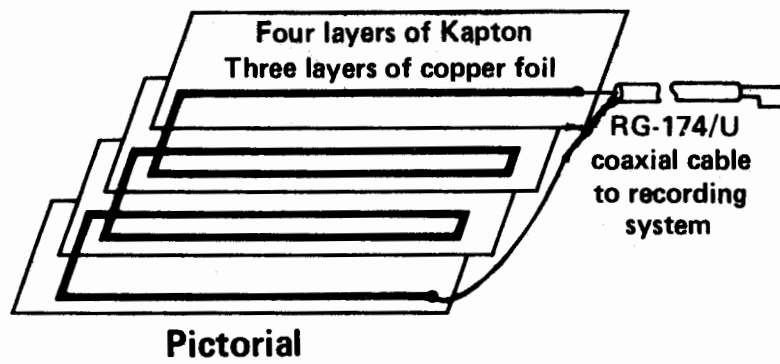
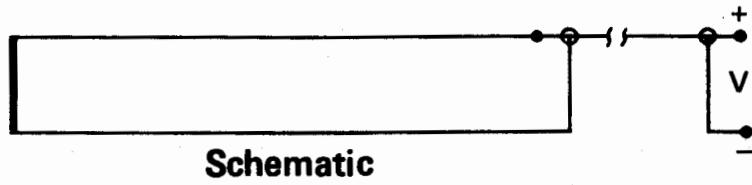
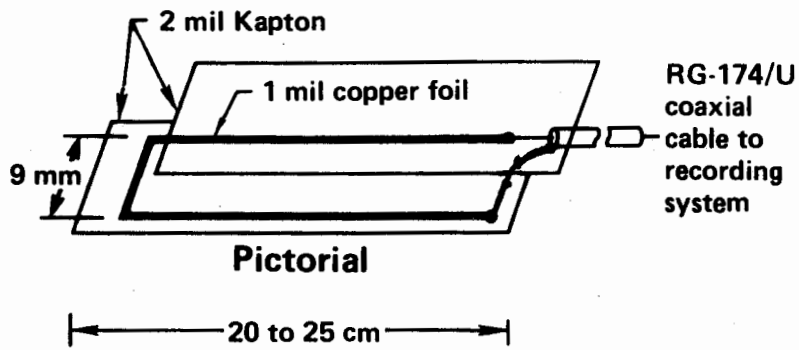
Spataro - Fig. 2



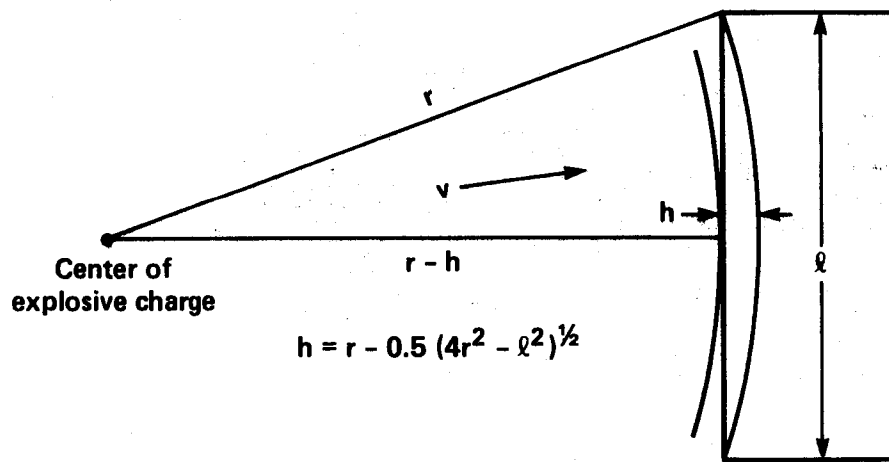
Spataro – Fig. 3



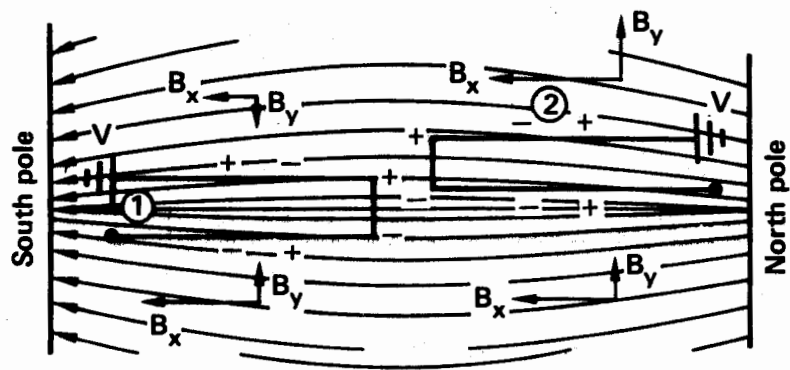
Spataro — Fig. 4



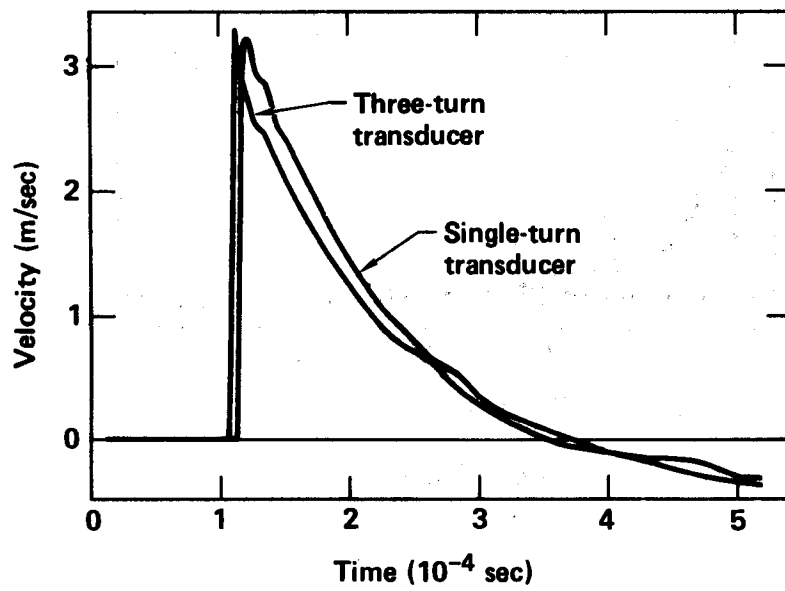
Spataro — Fig. 5



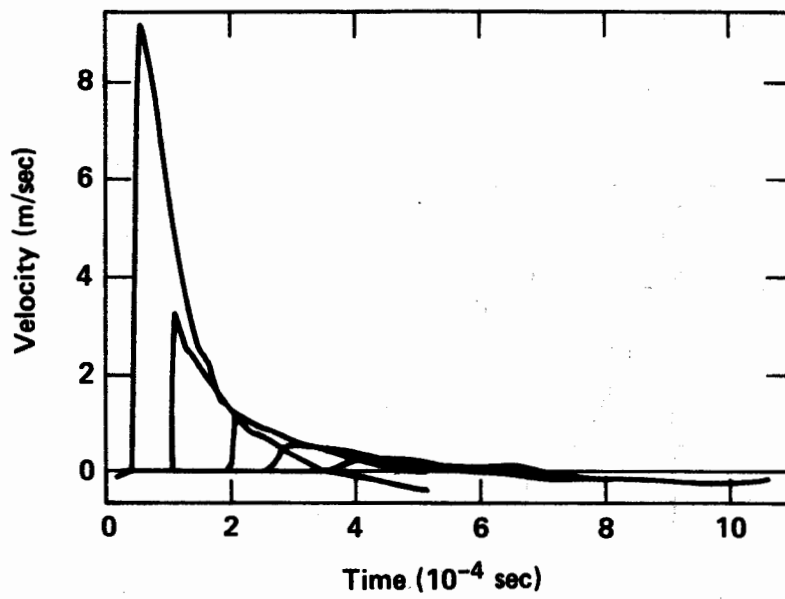
Spataro — Fig. 6



Spataro — Fig. 7



Spataro — Fig. 8



Spataro — Fig. 9

**Instrumenting and Interpreting the Time-Varying
Response of Structural Systems**

Instrumentation of the dynamic response of structural systems should be guided by the analysis to be performed on the system with transducer type and mounting location dictated by the structure's modal properties.

P. L. Walter

**Sandia National Laboratories
Albuquerque, New Mexico 87185**

Abstract

The dynamic testing performed on structural systems sometimes lacks specific objectives. In addition, the design of the measurement system intended to record the resultant data often does not receive adequate attention.⁷ This article presents the rationale for performing dynamic testing and provides insight for selecting transducers and determining their mounting locations to measure the resultant structural motion. Response measurements from transducers mounted on a freely-suspended bar structure are illustrated and explained. These results are generalized to more complex structures comprised of rod, plate, bar, and shell elements of varying geometries, boundary conditions, and materials.

List of Symbols

- A = bar cross sectional area
- $c = (E/\rho)^{\frac{1}{2}}$
- E = bar modulus of elasticity
- I = bar area moment of inertia about neutral axis
- l = bar length
- t = time
- u = bar axial displacement component
- U_n = n th axial mode shape
- v = bar transverse displacement component
- V_n = n th bending mode shape
- ϵ_{na} = bar axial strain distribution

ϵ_{nb} = bar bending strain distribution

$\lambda_n^4 = (\omega_n^2 A \rho) / (EI)$

ρ = mass density

ω_n = n th natural frequency

Introduction

Structural systems are fabricated from a collection of rod, plate, bar, and shell elements of either the same or differing materials. When designing these systems, their response to any time-varying loads they encounter in service must be considered. The origin of these loads can be as diverse as transportation and handling environments, acoustic waves, machine dynamics, earthquakes, and explosives. To evaluate the effects of dynamic loads on structural systems, instrumented tests are often performed under either simulated or actual loading conditions. It has been the author's experience that these tests are often poorly planned in terms of defined objectives and instrumentation selection. This article establishes the rationale for performing testing and provides guidance for interpreting the resultant data. Some background on the dynamic response of structural systems and its measurement follows.

Any time-invariant structural system possessing a linear input-output relationship has its dynamics completely defined by its natural frequencies, damping, and normalized vibratory mode shapes. These modal parameters are global properties of

a structure. They can be identified from responses attributable to a single point vibratory stimulus occurring at any location on a structure providing that location is not on a nodal line for a particular mode. Modal parameters differ from parameters associated with anti-resonant frequencies, which vary from one location on a structure to another.¹ The dashed line of Fig. 1 describes the shape associated with the first lateral vibratory mode of a 25-foot tall support tower for a TV camera. This mode occurs at a resonant frequency of 9.4 Hz.

To assist in design analysis, dynamic models of structural systems are developed using finite element techniques. With current technology, these analytical models can be refined using experimental modal analysis data obtained by multiple-channel spectrum analyzers.² The response of the model to analytically applied loads is predicted in terms of localized displacements. In dynamic testing, it is often difficult to acquire displacement measurements to compare to modeling results. Electromechanical motion-measuring transducers, such as potentiometers and linear variable differential transformers, afford poor frequency response and often modify a structure's response at the attachment point. Optical and eddy current based measuring devices overcome some of these difficulties but still require a fixed reference location to provide an absolute measurement.

In the dynamic testing of structural systems, displacement is typically measured in its derivative form as either strain or acceleration. Strain gages and accelerometers are available in small, rugged configurations. Accelerometers can provide constant amplitude frequency response to greater than 10 kHz, while strain gages can maintain their signal integrity to multiple 10s of kHz. In addition, both strain gages and accelerometers offer the advantage of providing absolute measurements while attached to a moving structure.

The following section provides criteria for determining whether strain or acceleration is the measurement parameter of interest. In discussing the measurement of the time-varying response of structural systems, we assume that the integrity of the signal from the strain gage or accelerometer is maintained as it passes through the measurement system.^{3,4}

Measurand Selection

The measurand is the object of any experiment. It is the physical or chemical process to be observed. The measurand associated with the time-varying response of structural systems is either strain or acceleration.

Figure 2a defines structural dynamics.² Depending on whether the forces acting on and/or the motion of a structure are accounted for, mechanical design can be divided into four categories. When neither the forces acting on

nor the motion of a structure is considered, the design problem is one of style. If the forces acting on a structure are considered but the structure is constrained from moving, the problem is one of statics. Similarly, the study of the motion of a structure with no applied forces is defined as kinematics. The remaining category is structural dynamics, which concerns itself with analyzing the effects of applied forces on a structure and the resultant motion of the structure.

Figure 2b is designated by the author as the Structural Dynamics Measurement Space. Structures typically are categorized as either rigid or elastic bodies. A perfectly rigid body would have no flexibility associated with it. While no perfectly rigid body exists, many structures approximate rigid bodies at frequencies well below their first resonant frequency. The controlled burning of its engine(s) determines the trajectory flown by a missile; when analyzing this trajectory, the missile is treated as a rigid body. However, in analyzing the response of the missile's control surfaces to air turbulence and acoustic disturbances, the elasticity of these surfaces is considered and the concept of a rigid body no longer exists. Figure 2b considers a structure as both a rigid and an elastic body and treats the measurand as either strain or acceleration.

The measurement of strain on a perfectly rigid body is meaningless since the response of a strain gage would be zero. The measurement of acceleration on a rigid body is not meaningless since, when multiplied by the mass of the body, information as to the inertial or D'Alembert force acting on the body is acquired. If incipient failure of an elastic engineering structure is of principal interest, strain is the preferred measurand. The strain limit of interest is the maximum strain which can exist within the structure without destroying its usefulness. The strain may or may not depend on a unique strength property of the structural material (e.g., proportional limit, elastic limit, yield point). Acceleration measurements on elastic engineering structures are used primarily to derive test specifications for components attached to the structure at the measurement location. An acquired acceleration-time history can be used to compute a shock spectrum⁴ for the component of interest. A shock spectrum is the envelope of peak responses of an infinite number of single-degree-of-freedom linear oscillators to an input transient. The principal application of the shock spectrum in structural testing is to permit component shock test specifications to be generated independently of specific time histories. In summary, instrumentation of the dynamic response of a structural system depends on whether one is interested in determining inertial forces acting on the structure, predicting

incipient failure of the structure, or deriving test specifications for components attached to the structure.

Data Interpretation

Figure 3a shows the initial portion of the response of a strain gage to a longitudinal force impact at one end of a 72-inch long, 3-inch diameter, freely suspended bar. The gage is located at the center of the bar. The amplitude of the Fourier transform of the entirety of this response was taken and normalized by the amplitude of the Fourier transform of the impacting force; this resulted in the frequency response function of Fig. 3b. From Fig. 3b, one might infer that the first axial resonant frequency of the bar is at 1,410 Hz and the second at 4,230 Hz. This inference would be in error. Furthermore, an axial accelerometer mounted at the same point as the strain gage would not have responded to either of these frequencies but would have identified an additional resonant frequency at 2,820 Hz. This simple example illustrates the potential for confusion in interpreting structural dynamic responses of systems.

To explain the results of the preceding example, it is necessary to review the classical solution of the axial and lateral modes of vibration of a bar. Based on this analysis, generalized conclusions will result which will be applicable to all structural dynamics measurements.

Figure 4 defines coordinate axes and displacement components for the bar analyzed. Both the axial and lateral bar motions are described by continuous mathematical models that are subject to both initial and boundary conditions. The resulting linear partial differential equations can be expressed in terms of two displacement components (u and v) which are functions of the spatial variable x within the boundaries of the bar. If the differential equations of motion and their associated boundary conditions are homogeneous, the boundary value problems are transformed to eigenvalue problems through solution techniques in the form of separation of variables. Separation of variables involves the assumption of solution forms $u(x,t) = U(x)T(t)$ and $v(x,t) = V(x)T(t)$. The task of determining the bar's axial natural frequencies for which the axial equation of motion has nontrivial solutions $U(x)$ and the bar's bending natural frequencies for which the bending equation of motion has nontrivial solutions $V(x)$ comprises the two eigenvalue problems. Each frequency (eigenvalue) has associated with it a corresponding function $U(x)$ or $V(x)$ (eigenfunction) of arbitrary amplitude and unique mode shape. The mode shapes and frequencies are uniquely determined by the bar's material properties, geometric factors, and boundary conditions.

An equation resulting from an elementary theory describing the free axial vibration of a homogeneous isotropic bar is:⁵

$$\frac{\partial^2 u}{\partial x^2} - \frac{1}{c^2} \frac{\partial^2 u}{\partial t^2} = 0. \quad (1)$$

The derivation of this equation assumes that the lateral motion of the bar is negligible, allowing the stress state to remain plane. The natural boundary conditions associated with a freely suspended bar require that the strain at both ends disappear. The solution $u_n(x,t) = U_n(x)T_n(t)$ corresponding to each axial natural frequency equal to $(n\pi c)/\ell$ is:

$$u_n(x,t) = \left[\cos(n\pi x)/\ell \right] T_n(t) \quad (2)$$

where $\cos(n\pi x)/\ell$ is the mode shape corresponding to the $n=1,2,3,\dots$ mode. Figures 5a to 5c plot mode shapes 1, 2, and 3, respectively. Note that there are one ($\ell/2$), two ($\ell/4, 3\ell/4$), and three ($\ell/6, \ell/2, 5\ell/6$) locations (nodes) where the axial displacement of the bar is zero. At these nodal points, eq (2) indicates that the time derivatives of the bar axial displacement (i.e., velocity and acceleration) also are zero. The bar axial strain distribution associated with each mode, however, is:

$$\epsilon_{na} = \partial U_n(x)/\partial x. \quad (3)$$

The strain distribution for the first three axial modes is shown respectively in Figs. 6a to 6c. Note that there are none, one ($\ell/2$), and two ($\ell/3, 2\ell/3$) interior points on the bar where the axial strain is zero. Figure 5 indicates that an accelerometer mounted at $\ell/2$ would respond to only the even axial bar modes; Fig. 6 indicates that a strain gage mounted at $\ell/2$ would respond to only the odd axial bar modes. Thus, axial strain and axial acceleration measurements from the same locations do not have to agree in frequency content; this explains the results and comments associated with Fig. 3.

The equation based on an elementary theory which describes the free transverse vibration of a homogeneous isotropic bar is:⁶

$$\frac{EI}{A\rho} \frac{\partial^4 v}{\partial x^4} + \frac{\partial^2 v}{\partial t^2} = 0. \quad (4)$$

The derivation of this equation assumes a long thin bar for which it is valid to ignore shear deformation and rotary inertia. The natural boundary conditions associated with a freely suspended bar require the bending moments and shear forces to disappear at both ends. The solution $v_n(x,t) = V_n(x)T_n(t)$ corresponding to each natural frequency is:

$$v_n(x,t) = \left[(\cos\lambda_n \ell - \cosh\lambda_n \ell)(\sin\lambda_n x + \sinh\lambda_n x) - (\sin\lambda_n \ell - \sinh\lambda_n \ell)(\cos\lambda_n x + \cosh\lambda_n x) \right] T_n(t) \quad (5)$$

where the bracketed term is the mode shape corresponding to the $n=1,2,3,\dots$ mode. Figures 7a through 7c plot the first three mode shapes, respectively. Note that there are two (.224 l , .776 l), three (.132 l , .500 l , .868 l), and four (.094 l , .356 l , .644 l , .906 l) nodes where the transverse displacement and, by eq (5), its time derivatives (velocity and acceleration) are zero. The bar bending strain associated with each mode is proportional to (α denotes proportional):

$$\epsilon_{nb} \propto \partial^2 v_n(x) / \partial x^2. \quad (6)$$

The strain distribution for the first three bending modes is shown respectively in Figs. 8a through 8c. In comparing Figs. 7a and 8a, 7b and 8b, and 7c and 8c, it is apparent that bending strain and transverse acceleration data from the same location on a free-free bar should agree in frequency content at all points except at the internal node shown in Fig. 7 nearest each end of the bar. Thus, disagreement will exist at the two outer nodes on the bar as to the frequency content of the responses from an accelerometer and strain gage to dynamic lateral loads; disagreement as to the intensity of these frequencies will generally exist at all other bar locations.

The lack of agreement between accelerometers and strain gages on bars can be generalized to other structural elements such as shells, plates, and rods of varying boundary conditions. In general, at any station on a structure, the intensity of response at a given frequency will differ

between an accelerometer and strain gage and at some stations will be mutually exclusive. This concept is simple to understand if one remembers that strain is a spatial derivative of first order or higher while acceleration is a second order time derivative.

Summary and Conclusions

Structural dynamics is the mechanical design problem associated with analyzing the effects of applied forces on a structure and the resultant motion of the structure. The measurement of the response of structural systems should be guided by whether one is interested in determining the inertial forces acting on the structure, predicting incipient failure of the structure, or deriving test specifications for components attached to the structure. The selection of a transducer's mounting location can be appropriately accomplished only after a modal analysis (either analytical, experimental, or a combination of the two) has been performed to define the dynamics of the structure. Interpretation of the transducer's signal depends on both its mounting location and whether it is responding to the time (acceleration) or spatial (strain) derivative of structural motion.

References

1. Lang, G. F., "Anti-Resonant Analysis," *Test*, April/May, 14-21, June/July, 12-17 (1982).
2. Richardson, M. H., Ramsey, K. A., "Introduction of Dynamic Testing into the Product Design Cycle," *Sound and Vibration*, 14-27 (Nov. 1981).
3. Walter, P. L., Nelson, H. D., "Limitations and Corrections in Measuring Structural Dynamics," *Experimental Mechanics*, 19 (9), 309-316 (Sept. 1979).
4. Walter, P. L., "Effect of Measurement System Phase Response on Shock Spectrum Computation," *Shock and Vibration Bul.*, 53(1), 133-142 (1983).
5. Thomson, W. T., *Vibration Theory and Applications*, Prentice-Hall, Inc., Englewood Cliffs, NJ, ch. 8, 267-269 (1965).
6. Meirovitch, L., *Analytical Methods in Vibrations*, The Macmillan Co., Collier-Macmillan Limited, London, ch. 10, 161-166 (1967).
7. Stein, P. K., "The Response of Transducers to their Environment-The Problem of Signal and Noise," *Shock and Vibration Bul.*, 40(7), 1-15 (1970).

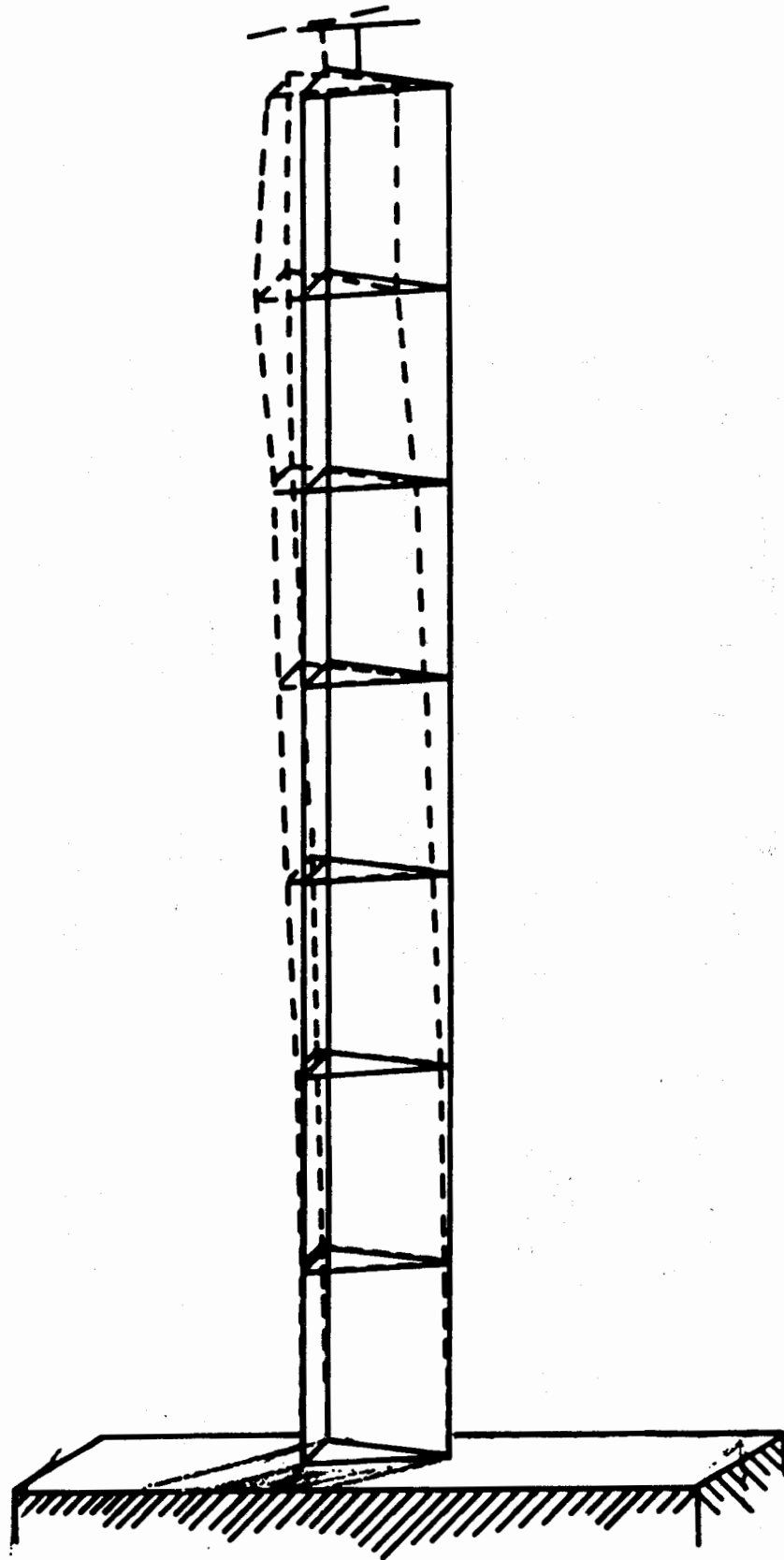


Figure 1. First lateral vibratory mode shape of a support tower.

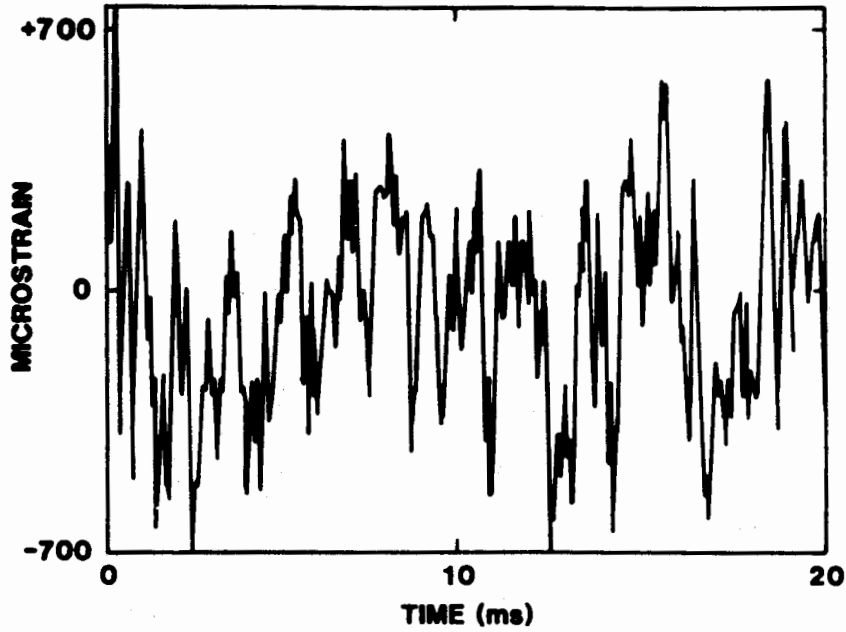
	FORCE ABSENT	FORCE PRESENT
MOTION ABSENT	STYLE	STATICS
MOTION PRESENT	KINEMATICS	STRUCTURAL DYNAMICS

(A) VARIOUS MECHANICAL DESIGN PROBLEMS

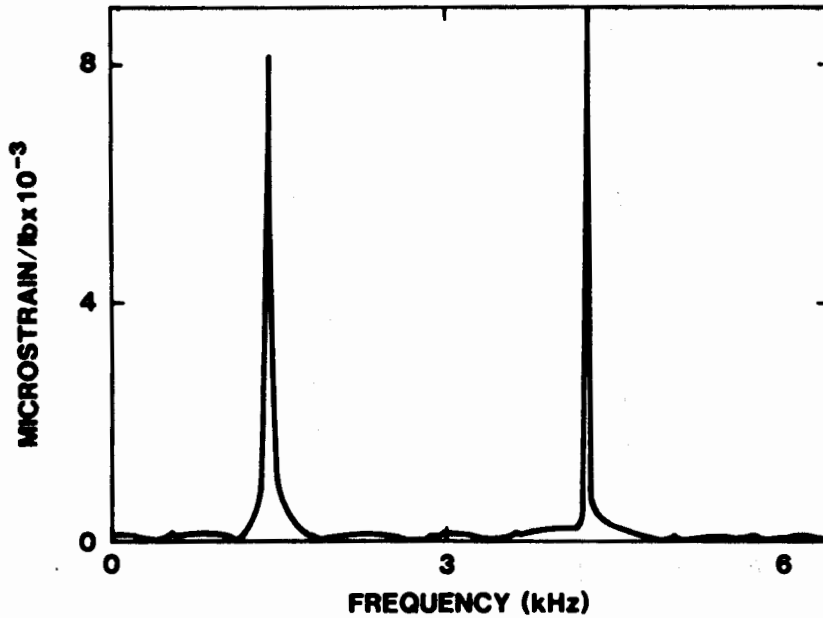
	MEASURAND STRAIN	MEASURAND ACCELERATION
STRUCTURE: RIGID BODY	NO RESPONSE	D'ALEMBERT'S FORCE
STRUCTURE: ELASTIC BODY	INCIPIENT FAILURE	COMPONENT TEST SPECIFICATIONS

(B) STRUCTURAL DYNAMICS MEASUREMENTS SPACE

Figure 2. Definition of and rationale for measuring structural dynamics.



(A) STRAIN GAGE TIME RESPONSE TO AXIAL INPUT



(B) MAGNITUDE OF FREQUENCY RESPONSE FUNCTION ASSOCIATED WITH STRAIN GAGE

Figure 3. Time response and frequency response function for strain gage at center of 72 inch long freely-suspended bar to axial impact at one end.

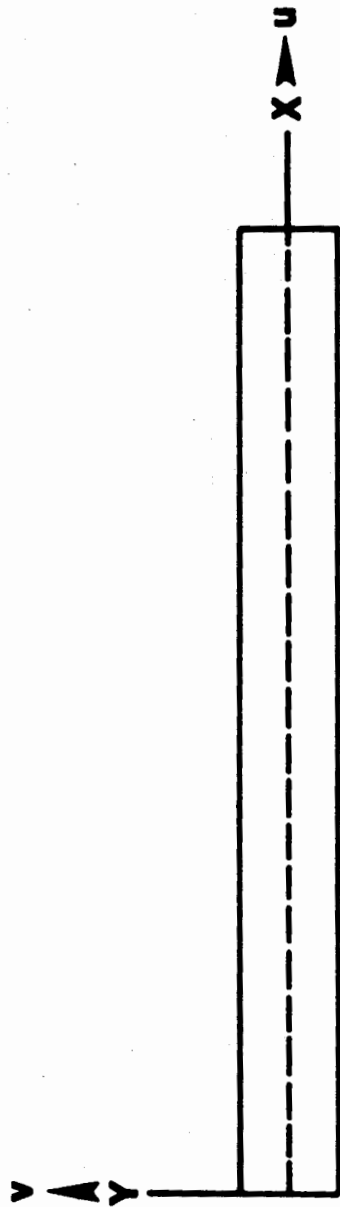
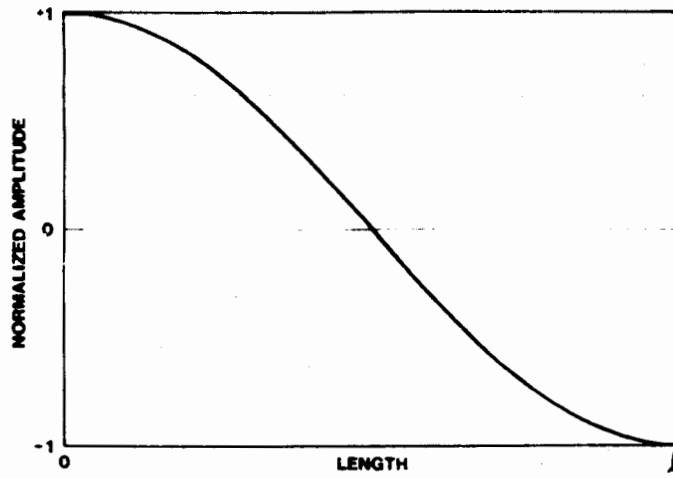
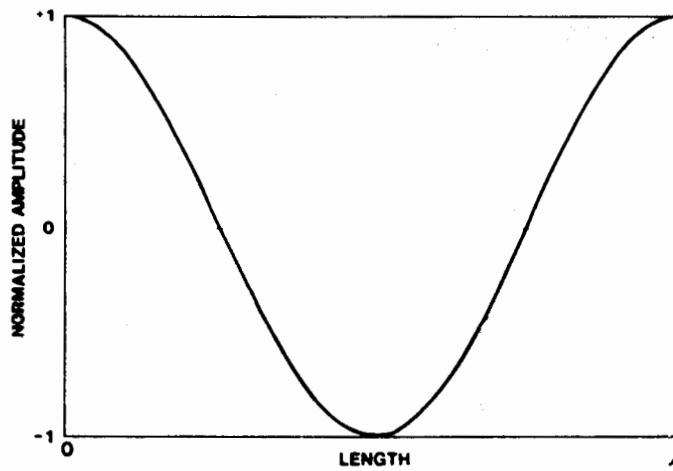


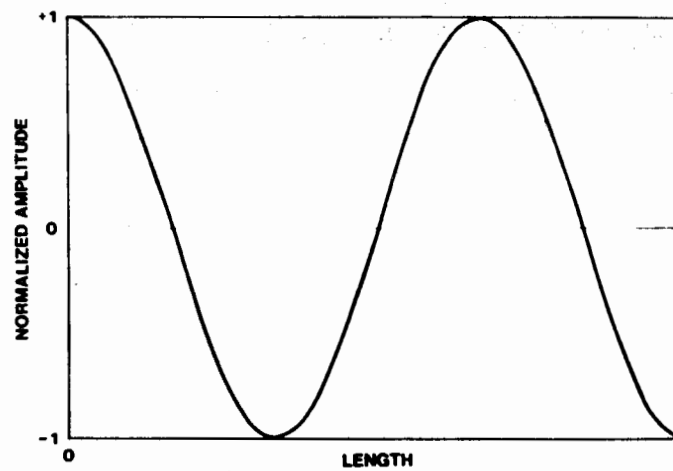
Figure 4. Coordinate axes and displacement components definition for a free-free bar.



(A) FIRST MODE SHAPE

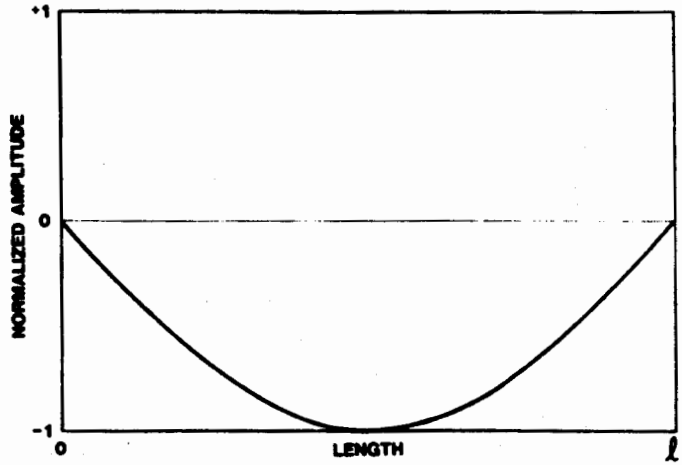


(B) SECOND MODE SHAPE

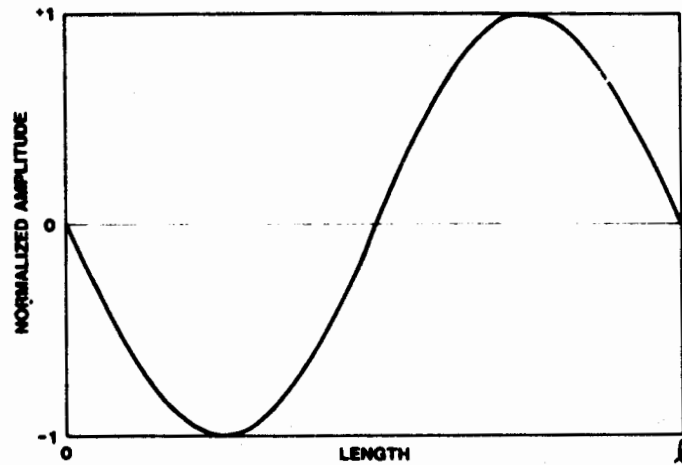


(C) THIRD MODE SHAPE

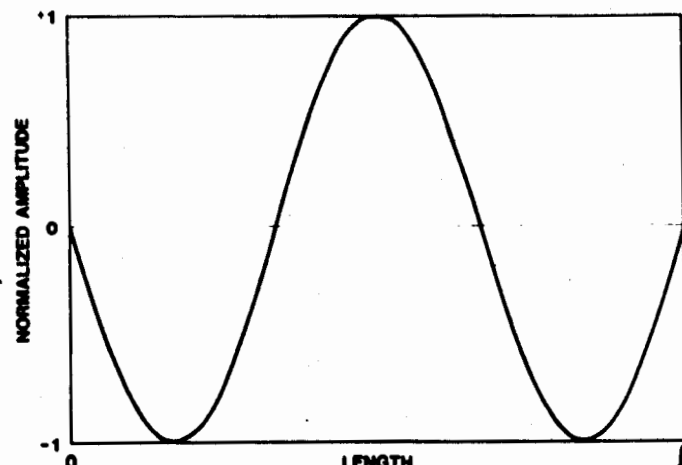
Figure 5. Closed form solution for the axial displacement distribution associated with the various modes of a solid free-free bar.



(A) FIRST MODE SHAPE

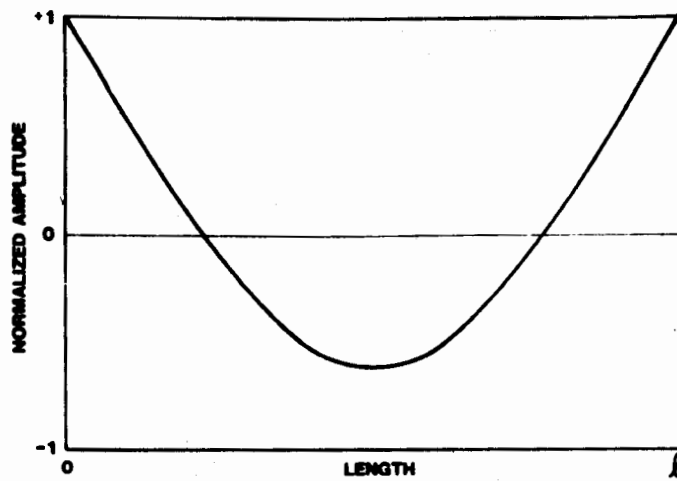


(B) SECOND MODE SHAPE

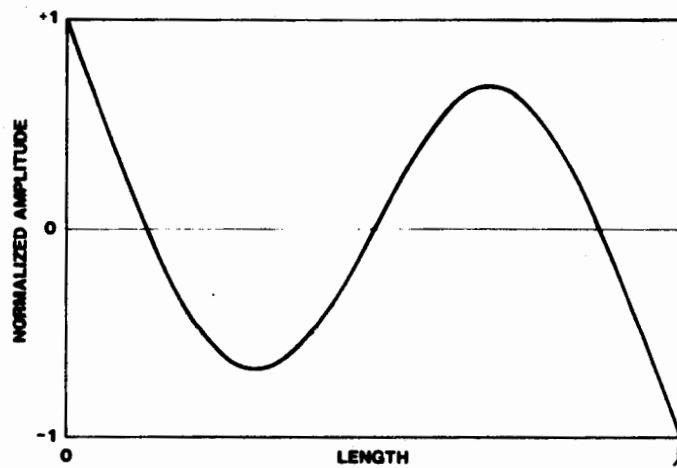


(C) THIRD MODE SHAPE

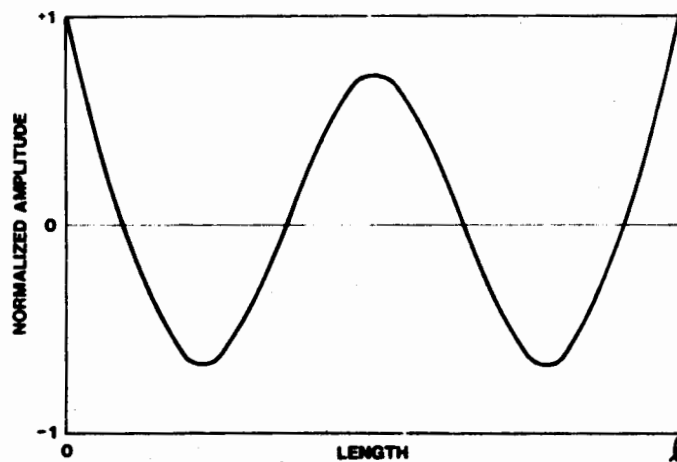
Figure 6. Closed form solution for the axial strain distribution associated with the various modes of a solid free-free bar.



(A) FIRST MODE SHAPE

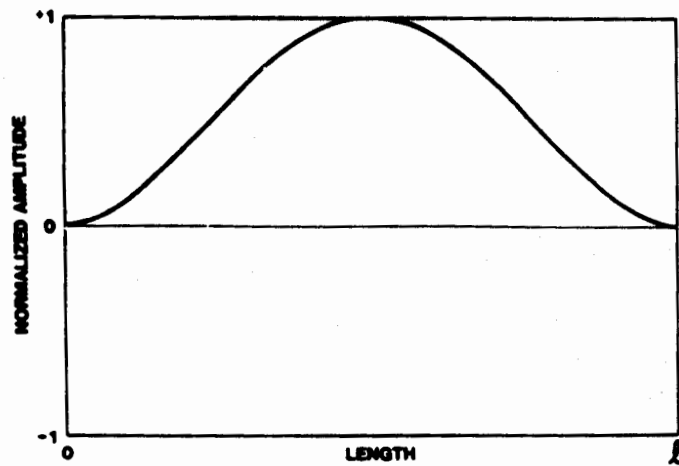


(B) SECOND MODE SHAPE

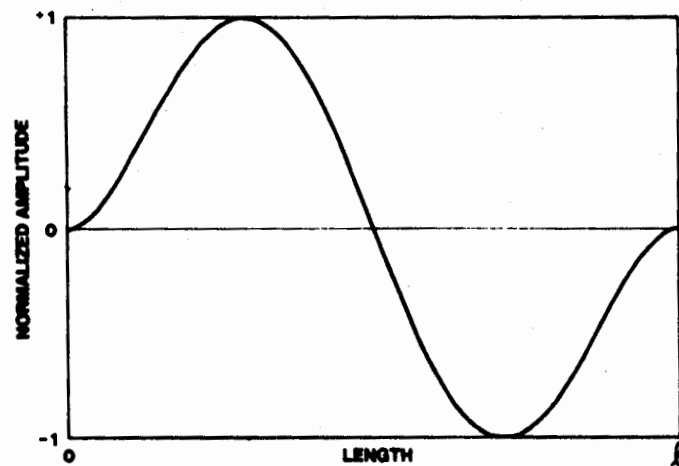


(C) THIRD MODE SHAPE

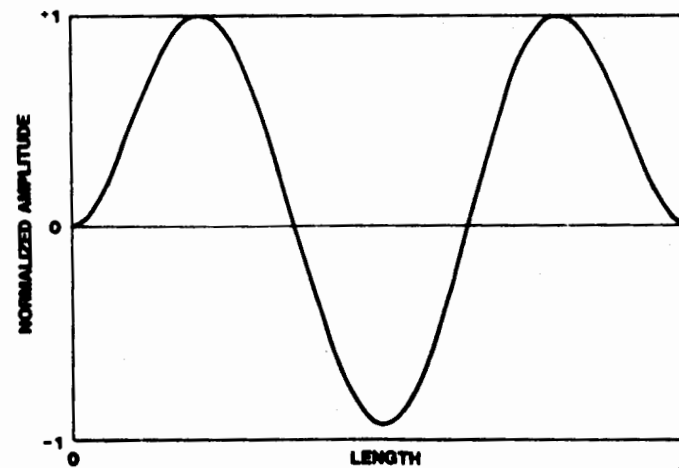
Figure 7. Closed form solution for the transverse displacement distribution associated with the various modes of a solid free-free bar.



(A) FIRST MODE SHAPE



(B) SECOND MODE SHAPE



(C) THIRD MODE SHAPE

Figure 8. Closed form solution for the transverse strain distribution associated with the various modes of a solid free-free bar.

SESSION 2

Q: BILL ANDERSON, NATC, PATUXENT RIVER, MD

I would like to start off with one question for Mr. Ach. Why don't more people use the AGRA amplifier than has currently been proposed?

A: JOHN ACH, AIR FORCE WRIGHT AERONAUTICAL LABS., OH

I think one reason is that most people shy away from the requirement that you keep track of the gain. You have to report that gain output and you have to apply that gain in the data reduction. In the past, people seem to have shied away from that. The amplifier, as it comes sold by the suppliers, is not ready to use. You have to house it and you have to provide all of the control voltages. It takes some effort to get that amplifier to where it's usable. People just seem like, they are reluctant to change. I think this is a case where they'd just as soon keep on using the old fixed gain amplifier rather than to make the big change.

Q: ROGER NOYES, EG&G, ENERGY MEASUREMENTS, LAS VEGAS, NV

I have a question for Sam. On your transducers, what do you do about characterizing or calibrating since, apparently, you probably do not reuse them?

A: SAM SPATARO, LAWRENCE LIVERMORE NATIONAL LABS., LIVERMORE, CA

Yes, in fact, we do indeed reuse them sometimes because in the low kilobar range that we're involved in, there's usually no damage to the transducer when it's out more than a few inches away from the temple charge. However, the way we calibrate them is we use just one material, polymethyl methacrylate, or PMMA, or just acrylic which is a common word that is very, very well known by all rock-mechanic type people. The Hugoniot for that is well known. The Hugoniot is the particle velocity, excuse me, the shock velocity versus particle velocity curve for that material. So what we do is we measure very accurately the shock velocity; we know the Hugoniot, therefore we derive the particle velocity from that and then we measure with the transducer. That's one way we calibrate them. The second way we calibrate them is by simply going through the calculation, the theoretical calculations I showed in the viewgraph, to see that the external results concur with that. Thirdly, on a three-turn transducer, the new one, we put them side by side with a standard one in exactly the same location or very near, and we simply do a comparison type calibration. So they're all calibrated in all cases. It's dynamic calibration, shock calibration.

Q: MIKE ENGLUND, GARRETT TURBINE ENGINE COMPANY, PHOENIX, AZ

On the AGRA 100 amplifier, when you're in the automatic mode, how quickly can the frequency autochange?

A: JOHN ACH

That depends on whether you're going just one step. One step, typically, I believe is 650 microseconds, very quick. Now if you're going from maximum gain down to minimum gain, it takes longer to do that. But just to step one step, it's down around 600 microseconds, I believe.

Q: PAT WALTER, SANDIA NATIONAL LAB., ALBUQUERQUE, NM

I have several questions to ask. While we're talking about the auto gain amplifier, I wanted to ask Mr. Ach a question on the logic. John, when you have to change gain on the random vibration, you were saying that you could either look at it wide band or look at it at the back end of the filter. I can understand why you'd want to at least consider some decisions like that. If you're interested in like 5 kilohertz data or 2 kilohertz data, why don't you prefilter it first before it goes into the front end of your autogain and then you don't have to worry about making a decision like that? And then I have another question.

A: JOHN ACH

Originally, we had planned to filter before the amplification but that created some problems in that we had a mutual agreement. The contractor, with our approval, switched that arrangement because it created problems. I don't know all the background on the problems that we had, but it was just not feasible to filter prior to amplifying. Now, you could use two of these in a series and do that. We've done that before where we go through one filter and then amplify the second time. That's essentially what you're suggesting. And that's the way we had planned to have it fabricated, but there were just some problems. Electrically, it wasn't feasible to do it that way.

Q: PAT WALTER

The other question I wanted to ask is about the logic that goes into changing gain on a random signal intuitively with seeing that with one threshold crossing. You wouldn't want to change gain but if you get a transient signal when you go by a certain threshold level, you would want to change gain right away. So if you're recording transient data versus random data, how do you handle those two situations or does it take different logic in the amplifier?

A: JOHN ACH

That's one of the control inputs. It's the response time for gain change. You could make that very small and in any crossing above the threshold, the amplifier could switch. Or you can, there's an integration time that you can link them at, have a number of crossings at the threshold at a certain given time before you'll get a gain change. So that's a variable that's programmable. You can make it change instantaneous at one crossing, or you can make up the average, enter

it with the integration time, and delay those changes. I believe there are four ranges you can select.

Q: LARRY SMITH, PACIFIC MISSILE TEST CENTER, CA

John, I'd like to know how you determine what your gain is every time you want to reduce your data? How do you do that? The automatic gain ... how do you know which gain you're in ... by setting a 4, 50, 100, or whatever?

A: JOHN ACH

Okay, there's an output out of the amplifier; there's a digital output. It's a three-bit code and since there are seven levels, you have these three bits that represent the seven levels. So, you record that along with the data in some form. You can record it in any form you want. The way we handle it is we reserve one track on a tape recorder, and we sample all the amplifier gains that we're using. Typically we may use 12 amplifiers. So we just sequentially sample those 12 amplifiers and put it through a PCM code or encoder and record that on a track by itself. Then on a playback, you go back and match up the gain with the amplifier.

Q: TORBIN LICHT, BRUEL & KJAER INSTRUMENTS, INC., DENMARK

Yes, it is commercially available. The company Aydin Vector sells it. I have a few preliminary data sheets that they have supplied, and I believe it sells for around \$1200 if you buy less than 50. It's not cheap. No precision instrumentation amplifier is cheap as you well know. And, yes it is available. We bought 25 on the development contract and we've ordered 50 additional units. You can contact Aydin Vector if you're interested, or I have some advanced data sheets if anyone's interested.

Q: TORBIN LICHT

A question for Mr. Articolo. You came to a conclusion about the rms values you were after, but you jumped very fast to the conclusion that we should have some more space saying that you needed three times the spread or something to be sure. But, I think you need to do some more work on amateur distributions and things like that to find out what we really need because you've only come one step of the ladder to tell people where to stop. You don't have any, you have a probability, maybe. You know something about your random signal but you have to be more sure about the peak values because that's what the accelerometer sees. Understand?

A: GEORGE ARTICOLA, SCHAEVITZ ENGINEERING, CAMDEN, NJ

If I do understand your question, you're correct. We do make the assumption that the noise is, say, what you might call random normally type distributed noise. Where we take for granted that if it is normally distributed that statistically three times the rms value would put you in a range where you probably would experience a minimal number of peaks.

Q: TORBIN LICHT

Yes, but that could depend very much on the kind of amplitude distribution you're actually having, which if you do not know it, you do not know very much about your random signals.

A: GEORGE ARTICOLO

I agree.

Q: TORBIN LICHT

Mr. Spataro don't you have any problems with the dynamic properties of your foreign transducer? There must be a time constant...

Q: SAM SPATARO

Like ringing? Is that what you're asking? Ringing of the transducer?

Q: TORBIN LICHT

Ringing and time constant.

A: SAM SPATARO

The transducer movement, first of all, is typically a few tenths of microinches at most. It travels a very, very timely distance. I don't know if we've ever measured the natural frequency of that system but I would imagine it's very, very high because of the very, very tiny, low; it's just a small system. Once in a while, when it's shocked very, very hard, again though, we're working in the very low shock regime, but when we were doing high frequency shock, we would see ringing in leading end at times depending on where we were with respect to the explosive charge. But in the work we're doing now where we're way down low in shock levels, that's not a problem at all.

Q: RAY REED, SANDIA NATIONAL LABORATORIES, ALBUQUERQUE, NM

Again to John Ach, with regard to the switching time. That's one of the critical things on your amplifier, you indicate that the switching time is nominally 650 microseconds, half a millisecond or so, is that a figure that includes setting time on the amplifier? Have they pressed their levels of technology pretty heavily for that? Is it possible to push that to a shorter switching time. And, third, presumably the gain is reproducible from step to step. Do you have any information on that particular thing, whether the gain can reliably be counted on from one step to another?

A: JOHN ACH

Answering the second question, yes. They had a figure of something like a half a percent. Within a half of a percent, the gain is repeatable. In the first question, I'm not sure, but I think that's the best setting, that does include setting time. I believe that is

pushing the state-of-the-art 650 microseconds minimum time above threshold voltage for step down. Well, I'd like to get with you after the meeting, I have a spec sheet. I guess it was last week we studied that and resolved that. I can't tell you just by looking at it here.

Q: RAY REED

There was one final question or confirmation. Because you carry the gain setting with each individual data sample, presumably you are not limited to one, two, three, or four. It's simply limited by the fact that you have a certain number of data samples available. Is that correct?

A: JOHN ACH

Right, there would be no limit. Theoretically you could get to a spot where you could just sit there and switch back and forth if the amplitude was just going above and below the threshold. If you didn't have your integration time set properly, you could sit there and just switch back and forth.

Q: RAY REED

So that's merely an inconvenience. It's not a technical limitation?

A: JOHN ACH

That would be an inconvenience, yes.

Q: RAY REED

If you have automatic data analysis that's not a problem?

A: JOHN ACH

That's not a problem, right. If you're going to read the gain and apply it, and the computer can handle it, that's no problem.

Q: ANDREW COLEE, EGLIN AIR FORCE BASE, AIRBORNE INSTRUMENTATION, FL

On the AGRA 100, two questions. I'm not quite sure I would know how any offset that you might have at the initial gain setting would be reflected in subsequent gain changes? The second question: is this unit going to be incorporated as part of the AFFTIS system? Is any consideration given to that?

A: JOHN ACH

Offset, if you have it, would be generated by your transducer, by some device that you're inputting into the amplifier. If you have an offset, it certainly would be amplified. The amplifier has the provision for externally generating a voltage to lower that offset. If you know you have an offset and if you'd like to eliminate the offset, then there's a way for putting it in. If you know you have half a volt offset, then you can externally generate a voltage that

will bring that to zero. There's a provision for doing that, handling offsets. You can also short the input to the amplifier and measure what offset you do have coming in. But any offset, of course, would be amplified, right? Now provisions were included in the Air Force Flight Test Instrumentation System or AFFTIS that they're developing at Edwards along with the other test centers. The wide-band signal conditioning for the AFFTIS system is going to be, if they do in fact develop the wide-band system, the AGRA, that's true.

Q: LOWELL WENDELL, LAWRENCE LIVERMORE LAB.

I have a couple questions. The amplifier you're using, you said, was a differential input, but you didn't give a number for common mode rejection capability. How well isolated is it from the input plus and minus 15 volts? Secondly, is there any optical isolation or any kind of isolation for the digital signals to prevent any back talk, cross talk from the digital lines back to the input of the amplifier?

A: JOHN ACH

You may be getting in over my head since I didn't write this paper. I have some spec sheets, and I think it would be better if we just sit down and look at them rather than me trying to pour through this thing and answer those questions. So, if you'll just see me after this meeting, we can sit down and talk about it.

Q: PAT WALTER

I had a couple of questions that I wanted to ask Dr. Articulo. I understand that the nature of the problem, George, is where a transfer function is causing the random vibration signal to be modified and either gives you a value that's too low or too high depending on the characteristics of the transfer function and the shape of the spectrum. If you're talking about control applications, although your algorithms give you a way to predict what it should be, the situation is still that the transducer is lying to you, that it's not giving you what the true input is. So, I was just wondering from the control stand point, what the predicted capability gains for you? And then I had a subsequent question I'll ask after that.

A: GEORGE ARTICULO

Unfortunately, the problem just requires we know what the input noise spectral density is, and that we know very clearly what the transfer function characteristics of the device are. With this information and, let's say, measuring the rms output, there is no way to go back to predict what the true characteristics of the input noise spectral density were. The noise that's going into the device may or may not be exactly what one defines it to be. There's no way to go back to predict whether or not it's true.

Q: PAT WALTER

I had a subsequent question that follows along that line, if you're familiar with it. I'm not sure what your responsibility is at

Schaevitz, but the limited experience I've had with servo accelerometers is built around the fact that sometimes if you're working with magnetic damping there's some. You don't have a second order system and there's some other filtering thrown into the back end of the servo so it gets to be a higher order system. If you get with fluid damping and pendulous devices, you start out with a given second order system but if you have an airborne environment you have temperature changes; therefore damping changes during flight make omegas and constant. I just wondered, does the Schaevitz model that you're familiar with, really follow an analytical model that's very close to second order and does it follow it over temperature or do you have those problems also?

A: GEORGE ARTICOLO

You can tell it's a question that comes from a man who's very well experienced in the field. This was just a very simplified beginning approach to try to get a better idea of what the rms response of the system is. We know its second order and we've modeled it by a very simplified second order transfer function. In real life, obviously from the way you put the questions you're very familiar with the nonlinearities that do exist in the system. We are aware of these things and I'm sure that in the future we'll begin taking into consideration the nonlinearities of these devices. Once we do have a very good idea of what the true transfer function is and if this transfer function does take into account the nonlinearities of the system, we will be able to get a much better idea of what the rms responses of these systems are. Let me just add that in addition to using this type of program with accelerometers we also had an opportunity to use it for an LVDT project. We were asked to determine what the rms displacement of an LVDT core rod would be under a given known noise spectrum density environment. And in this particular case, the LVDT was spring loaded so if we knew what the mass of the core rod was, and we know roughly what the spring constant of the spring loading on the rod was, then we were also able to use this program to evaluate what the displacement of the core rod would be from equilibrium.

Q: MIKE ENGLUND

Your paper was almost like a testing philosophy that, somehow for me, doesn't ring real true in the industrial environment. Probably I'm partially at fault, but do you profess that before you instrument an expensive test program like you were discussing, you must define the structure as a living, breathing entity? Do you really give your engineers the time to analyze the structure properly to define it as such? If so, that hasn't been my experience.

A: PAT WALTER

If that hasn't been your experience then that hasn't been what you've seen me do. No, I have an answer for that and I think the answer is yes, that we really do do that. The one thing gets down to basics and does get to be philosophy and we're all familiar with that. No one cares about the test state as long as it works. So you just slap on

some gauges, run the test, and if it stays together forget about the data. Maybe camera coverage of something like that's adequate, but when there's a failure the data becomes important and the bottom line is it's not philosophy. If you don't understand the dynamics of the structure, you can't understand the data; it doesn't mean anything. So if you look at the particular business that I'm in, which is the nuclear ordnance business, the first thing that happens on any of our programs, and right now the ones that we're working on are like the Trident 2 and the ASW programs, some of the cruise missiles, the warheads, is we assign a dynamicist and that dynamicist lives with that program the whole way through. They make a spring mass model and it's quite complex. Then we work through joint tests and they build up mass block ups. We do model analysis in the laboratories. The models are iterated and they go out and they do run tests on the blast tubes and then flight test. An instrumentation location is selected based on the understanding that the structure is a living breathing thing. So, I can look at you in good faith and say yes, we really do do that.

Q: RAY REED

I would like to make a comment about that last interchange. Somewhere in this world there has cropped up a notion that philosophy and practicality are mutually exclusive. I think your paper had no facts in it that anyone in this room didn't already know. I think you probably would agree with that. It is merely the philosophy, in other words, the comprehension of the significance of the facts that we're talking about. Occasionally facts do come as a surprise even though you know them, their significance comes as a surprise. I thought this was a particularly elegant example of how one can go ahead and do the practical thing, namely make an arbitrary measurement in an arbitrary way in an arbitrary place with no goals and be practical and completely miss the point. It's cheaper to get an answer that way and you can get into trouble very inexpensively. So, I appreciate your paper and I think, while the facts are elementary, I consider them to be elegant. That's a prime portrayal of problems, the way problems crop up in the physical world. In the measurement world, people just do things without thinking about what they're trying to accomplish and what the pitfalls are.

I did have a question for Professor Articulo about his paper. You mentioned that you have this basic code. Is the source code presented in the paper?

A: GEORGE ARTICOLA

No, it's not.

Q: RAY REED

If it is available, in which of the hundreds of basic dialects is it written?

A: GEORGE ARTICOLA

That I don't know, but I'm sure almost any basic dialect could be reoriented. I'll take orders on it later. Thanks for the question.

Q: PETER STEIN

If I can add my two cents worth to Dr. Reed's comment, I would add only that you also have to understand that the measuring system is a living, breathing thing before you use it. So, there are really two jobs you have to do in structural dynamics. But I also have a question for Sam Spataro. Are you working in the time frame where impedance matching between the cable and the transducer is important? Is this of any consideration to you at all?

A: SAM SPATARO

No, it isn't. I'm not sure I understand exactly what you mean by your question. Our typical data length is on the order of maybe 5 to 50 or 5 to 30 microseconds total duration time of our information. The transducer's impedance is just a few milliohms. So the answer to that question is no. We're not that fast.

Q: DAVE BANASZAK

I'd just like to follow up on the last question to Dr. Articola. Do you have any basic idea how long this program is? Is it just a page or is it 50 pages or 100 pages?

A: GEORGE ARTICOLA

It's only about two pages, very short.

Q: JOHN ACH

I'd like to ask Mr. Spataro a question. He said he used an acoustic digitizer to digitize those photos. I'm not familiar with that. Could you tell me what that is?

A: SAM SPATARO

Probably not very well because I don't do the digitizing, the experimenter does. But it's a system that allows you to move a couple of cursors, which yield X and Y coordinates. It's a manual process and maybe there are other people in this room that could tell you more about it. I really can't. It's a semi-automatic system where you have to actually tell it when to digitize. I can't go beyond that.

PAT WALTER

I just had one comment. I wanted to follow up on this morning's session. I think it's really appropriate to interject it here and it might be helpful to you. We were talking some about system calibration this morning, and the gentleman from AFWAL was talking about the

different tumble tests. I had an occasion recently to go back and look through some of the 118 documents that are available. I'd like to give some kudos to those of you in the audience that participated in that writing about 15 years ago and also encourage some of you to use it. In the early 1970's, within the RCC Telemetry Group, there was a section on system calibration and it started with the receiving antenna. It turned out to really be a ground base calibration. There was a loud voice of outrage from the transducer committee and it was pointed out that that wasn't a system calibration, that was just a receiving station calibration. And so within the 118 documents you'll find some information that's truly unique. It's not replicated in any textbook and there is not a collection any place else. It's not technically so deep, but what's unique is that it's collected. It does deal with system calibration of measuring systems. It goes through either the measure and substitution or it goes through an electrical substitution. It has all the equations in it for bridge calibration, series assertion, servo instruments, and for using piezo electrics and for breaking into the ground line with isolated power supplies. And that's all pulled together in one nice area in the 118 documents. Then over and above that, there are some test methods for instrumentation amplifiers. Alan Diercks was, I think, largely responsible for the charge amplifier part of that ten years ago. A fellow, Jacques Quei, I believe, from Ectron is not here. Fritz Shelby was responsible for the DC amplifier portion. I had occasion to dig into those things recently and they're very well written. Boy, there it is and you can't find it any place else. I'd like to encourage those of you that aren't familiar with the 118 documents to read them. When you need some test methods for the instrumentation amplifiers or some system calibration techniques, take a look at those documents.

STEVE KUEHN, SANDIA NATIONAL LABS., ALBUQUERQUE, NM

Any other questions? All right. Well, I want to thank you and I think these gentlemen deserve a hand for their efforts. (Applause)

RICHARD KRIZAN, ESMC

May I add also the 118 documents are being rewritten. At least there's a sheet out for looking at it to be rewritten, to update it, to make sure that some of the procedures that were used are still up to date. So probably about the next year or two, we'll probably be sent a revision to the 118 documents.

I'd like to thank everyone of their participation today in the workshop.

SESSION 3

A 150,000 POUNDS PER SQUARE INCH
DYNAMIC PRESSURE CALIBRATOR

A. A. JUHASZ
D. H. NEWHALL¹
C. D. BULLOCK
J. O. PILCHER, II
M. B. KRUMMERICH

U.S. Army Ballistic Research Laboratory
Aberdeen Proving Ground, MD
1. Harwood Engineering Company
Walpole, MA

ABSTRACT

A positive step pressure generator suitable for the dynamic calibration of ballistic pressure transducers is described. The device uses a hydraulic system to generate pressures up to 150,000 pounds per square inch and is capable of delivering pressure steps in one millisecond or less. Final pressure step values can be traced to conventional deadweight calibration figures with an accuracy of 0.2% by using a transfer standard between 25,000 and 125,000 pounds per square inch. Among the uses for the device are examining transducer response characteristics (such as ringing frequencies) to rapid positive pressure steps and comparing the relative response behavior of several transducers to a common pressure step.

INTRODUCTION

Although ballistic pressure transducers are used to measure dynamic events which occur in milliseconds, the response characteristics are routinely calibrated statically against deadweight pressure systems. The strength of this method is its link with a primary standard; its weakness is the assumption that the static and dynamic responses of the transducer are equivalent. Differences in gage response between static and dynamic events can lead to serious measurement errors. There has been general agreement in the measurement community that dynamic techniques are needed to supplement current static calibration methods. Several techniques have been developed to address this problem. [1,2]

A. Ballistic Pulse Method

In this technique, the gage is mounted at the end of a tube in contact with a hydraulic fluid confined by a movable piston. The tube guides a projectile which impacts the piston to create a pressure pulse in the fluid. Different pressures may be achieved by varying the compressibility of the fluid, the mass of the piston, and the mass and velocity of the projectile. The pulses rise within milliseconds and mimic the characteristic rising and falling of a ballistic pressure pulse. One such

device, capable of operating to a pressure of 100,000 pounds per square inch, is operational at the Combat Systems Testing Activity (CSTA), Aberdeen Proving Ground, Maryland. [3]

This method is quite useful for dynamic comparison of several different pressure gages; however, variations in projectile velocity, frictional effects on the moving piston, and other energy losses make it difficult to accurately compute the actual delivered pressures. Because a projectile is fired during the calibration process, this method requires more extensive safety provisions than are readily available in most laboratories.

B. Shock Tube Method

Two general approaches of shock tube calibration are followed. In the first, the test gage is mounted in the end wall of a tube and subjected to a reflecting shock wave. The gage output is monitored as the shock front arrives at and reflects from the end wall. In the second approach, the gage is mounted in the side wall of the tube and its output is monitored as the shock front passes. Both methods generate rapidly rising pressure pulses that are readily calculated by thermodynamic principles using velocity measurements and gas properties.

Shock tube methods are useful in establishing the dynamic response characteristics of pressure gages. However, calibration is generally limited to pressures below 1000 pounds per square inch, whereas ballistic applications require far higher pressures.

C. Negative-Going Pressure Step Method

In this technique, the gage is exposed to a given pressure under static conditions using a hydraulic fluid. The gage is then sealed off from the hydraulic system and its output is zeroed. The pressure on the gage is then relieved using a fast acting dump valve, bringing the system to atmospheric pressure. The gage output obtained during the depressurization is assumed to be the inverse of the corresponding positive pressure step.

This method's strengths include its relative simplicity and suitability for use in calibration facilities. The response of the negative step calibrator can be very quick, 100 microseconds or less. However, the major assumption, that the positive response of the gage is equal and opposite to the negative response of the gage, is not completely accurate; pressure preloading of the gage-to-mount interface and hysteresis can cause significant differences between the pressurization and depressurization pulses.

D. Positive-Going Pressure Step Method

In this technique, the gage, initially at atmospheric pressure, is subjected to a pressure increase by the opening of a fast-acting valve. Because the final pressure value is held, the method is suitable for obtaining calibration response data. Although this technique holds a great deal of promise, the engineering details of creating a working device can be formidable. Johnson and Cross of the National Bureau of Standards had designed a 50,000 pounds per square inch step calibrator in

the 1950's. Smith [4] and Dykstra [5] described low pressure versions of this device. These calibrators were successfully used to generate positive pressure steps up to 5000 pounds per square inch in less than one millisecond.

Building on these ideas, we have developed a device capable of generating precisely known positive pressure steps up to 150,000 pounds per square inch in less than one millisecond. The step calibrator may be safely operated in a laboratory environment and can compare the response of several transducers to a common pressure step. Additionally, it is economical to use as a routine laboratory tool for gage calibration and screening.

The discussion that follows describes the pressure step calibrator and presents several examples of its operation.

DISCUSSION

A. DESIGN CONCEPT

Figure 1 illustrates the basic configuration of the device. A large pressure reservoir is connected to a much smaller test chamber by a fast acting ball valve. The test chamber is equipped with several gage ports and a vacuum port which aids in filling the reservoir and setting the baseline chamber pressure. The large ratio of reservoir to test chamber free volume reduces overall system pressure drop while generating the pressure step. Reservoir pressure is provided by a conventional hydraulic high pressure panel and monitored by a high quality static reference gage. The maximum operating design pressure is 150,000 pounds per square inch and the specified action time (10% - 90% of peak pressure) is under one millisecond.

Outputs of both the reservoir reference gage and the ballistic test gages are monitored during the course of the test. The final steady state output of the reference gage is taken as the true value of the pressure step maximum. Both short- and long-term monitoring of the test gage outputs establish the relationship between dynamic and steady state response behavior.

B. DEVICE DESCRIPTION

The device, illustrated in Figure 2, consists of a large pressure reservoir (1) opening into a short wide channel (2) which terminates in a very small cylindrical test chamber (3). Located in the test chamber (3) is a ball valve (4) which provides a high pressure seal at either of the valve seats (5) located at each end of the test chamber (3). Located in the side wall of the test chamber (3) are four gage ports (6) and one vacuum line port (7). The channel (2), test chamber (3), gage ports (6) and vacuum line port (7) are contained in the test head (8), a monolithic assembly shown in lateral cross section in Figure 3. The test head (8) is readily removed from the assembly, allowing changing of the gage ports (6) and the test chamber (3). The ratio of the reservoir (1) volume to the test chamber (3) free volume is 197:1. The channel (2) is kept short and wide to minimize retardation of fluid flow during the

operation cycle. The end closure of the test chamber (3) is formed by the ball valve actuator piston (9) and the piston guide bushing (10). The piston is actuated by a quick release top-dead-center mechanism which consists of three pin joints (11), an air controlled trigger mechanism (12), a hydraulic jack (13) and a limit stop/buffer (14). The system shown in Figure 2 is in the cocked position with the ball (4) pressed against the seat (5) that isolates the test chamber (3) from the reservoir (1). The jack (13) is pressurized to provide sufficient force to seal the reservoir (1) from the test chamber (3). The ratio of reservoir (1) pressure to jack (13) pressure is approximately 100:1.

A hollow stem valve (15) connected to a vacuum/drain line is located at port (7).

A high pressure line (17) is connected to port (16) at the upper end of the reservoir (1). This line connects the pressure generation system to the measurement system.

Figure 4 shows the device after the trigger mechanism (12) is released. The trigger (12) forces the middle pin joint of the top-dead-center mechanism against the limit stop/buffer (14), relaxes the force generated by the jack (13) and withdraws the ball valve actuator piston (9) into the piston guide bushing (10). Differential pressure between the reservoir (1) and the test chamber (3) forces the valve ball (4) against the seat (5) on the piston guide bushing (9). This action forms a new seal at the piston end of the test chamber (3) and allows fluid to flow from the reservoir (1) to the test chamber (3) causing the pressure in the chamber to rise to approximately 98% of the original reservoir pressure. Figure 5 shows a typical pressure versus time history of the test chamber pressure for a 75,000 pounds per square inch pulse.

C. DEVICE OPERATION

Starting with a drained system, the top-dead-center mechanism is placed in the release position as shown in Figure 4. The high pressure line (17) is closed off and the vacuum valve (15) is opened. Gages are mounted in the gage ports (6), the system is evacuated to a pressure of 2 Torr and the vacuum valve (15) is closed. A 50% solution of water and glycol with a rust inhibitor enters the system through the high pressure line (17). Liquid is used rather than gas to minimize the level of stored energy. When the system is filled and stabilized at atmospheric pressure, the top-dead-center mechanism is cocked as shown in Figure 2. The hydraulic jack (13) is pressurized to approximately 1% of the desired reservoir pressure. Monitored by a primary or secondary standard gage, the pressure generation system pressurizes the reservoir (1). Once the desired reservoir pressure has been established, the high pressure line (17) is closed off from the standard gage and the pressure generation system by a constant volume valve. The device is now ready to be triggered.

Activation of the top-dead-center mechanism shown in Figure 4 initiates the event and the recording system. Pre-trigger delay features permit the recording of initial baseline pressures, the rising portion and final steady state values of the pressure-time

curve. One gage with exceptionally good response characteristics and known history is used as an informal laboratory standard. The output from this gage is monitored for at least 10 seconds after the trigger event to observe system behavior, particularly possible pressure losses from leakage. Soon after the system is triggered, the constant volume valve to the static reference gage is reopened and the reservoir pressure measured by the primary or secondary standard. Thus, the speed of the step can be measured using the timebase of the recording system and the magnitude of the dynamic response can be checked against the response of a reliable steady state gage.

At the completion of the test, the top-dead-center mechanism is recoiled, the test chamber (3) is drained through the vacuum valve (15), and the pressure is relaxed in the reservoir (1). The gages can now be replaced for further testing.

D. PROTOTYPE PERFORMANCE.

Examples of both short- and long-term responses of a commercial piezoelectric pressure gage to a positive-going pressure step are presented in Figures 5 thru 8. Figure 5 shows a typical pressure versus time history for a 75,000 pounds per square inch pulse acquired over 10 seconds. Monitoring the test gage response for 10 seconds allows correlation to the steady state response of the reference gage. Figure 6 shows a 20 millisecond window of the same 75,000 pounds per square inch pulse; Figures 7 and 8 present progressively shorter windows. Overlaying the traces indicates that the steady state value of the pressure step is rapidly achieved and held after initial oscillations have died out. Similar oscillations have been reported in lower pressure devices by both Smith and Dykstra; one may conclude that these oscillations are caused by actions within the pressure generation system and the mount, not by the gage itself.

One important application of the step calibrator is comparing the responses of different types of pressure gages to the same input. Figures 9 and 10 show the pressure versus time histories of both a piezoelectric gage and a strain-type gage measuring a positive-going 100,000 pounds per square inch pressure step. The traces are virtually identical, exhibiting initial system oscillations which quickly decay.

The calibrator may also be used to analyze the behavior of experimental gages by comparing their output with a known standard. Figure 11 shows the pressure versus time history of a developmental pressure gage subjected to a 125,000 pounds per square inch pressure pulse. This curve exhibits, as expected, a smooth pressure rise and stable output after the peak pressure has been attained.

The availability of the step calibration device in conjunction with conventional deadweight calibration methods can be very useful in isolating dynamic gage response problems. Figure 12 exhibits the pressure history of another developmental pressure gage exposed to a 130,000 pounds per square inch pressure step. The trace indicates a clear upward drift after the step is complete. Since any system leakage would be expected

to result in a decrease of pressure, the drift is probably due to faulty gage response. In fact, we found that the bond between the strain patch and the gage body was faulty.

The step calibrator prototype has been successfully exercised from 25,000 pounds per square inch to 150,000 pounds per square inch. For any given trial, the repeatability between gage ports is within 0.1%. For any series of shots, the experimental mean can be predicted within 0.2%. Series-to-series variations are 0.8%.

CONCLUSIONS

The positive-going step calibration device described allows the accurate, safe and simple dynamic calibration of ballistic pressure gages. The gage response obtained can be related to its static deadweight behavior. Several gages may be evaluated simultaneously to a common dynamic event. The calibrator may also be used as a diagnostic tool in analyzing and developing experimental pressure gages.

ACKNOWLEDGEMENTS

The authors gratefully acknowledge the contributions of the staff at Harwood Engineering Corporation for engineering design and construction of the step calibrator. Thanks are also extended to Mr. W. J. Donovan, Ballistic Research Laboratory, APG, MD and Mr. J. D. Dykstra, CSTA, APG, MD, for technical discussions relating to the project.

REFERENCES

1. National Bureau of Standards Report 4440, Measurement of High Pressure: Bibliography, Index and Preliminary Survey, W.G. Brombacher, U.S. Department of Commerce, National Bureau of Standards, October, 1955.
2. NBS Technical Note 914, A New Dynamic Pressure Source for the Calibration of Pressure Transducers, Carol F. Vezzetti, John S. Hilton, J. Franklin Mayo-Wells and Paul S. Lederer, U.S. Department of Commerce, National Bureau of Standards, June 1976. (and references therein)
3. Personal communication with J. D. Dykstra of the Combat Systems Testing Activity, Aberdeen Proving Ground, MD.
4. R. O. Smith, A Liquid Medium Step Function Pressure Calibrator, ASME Paper Number 63-WA-263. The American Society of Mechanical Engineers, 345 East 47th St. New York, NY.
5. J.D. Dykstra, "Evaluation of Pressure Transducer Response with a Pressure Step Generator", Bulletin of the Eleventh Meeting of the Joint Army-Navy-Air Force Solid Propellant Rocket Static Test Panel, SPIA Publication SPSTP/11, September, 1962.

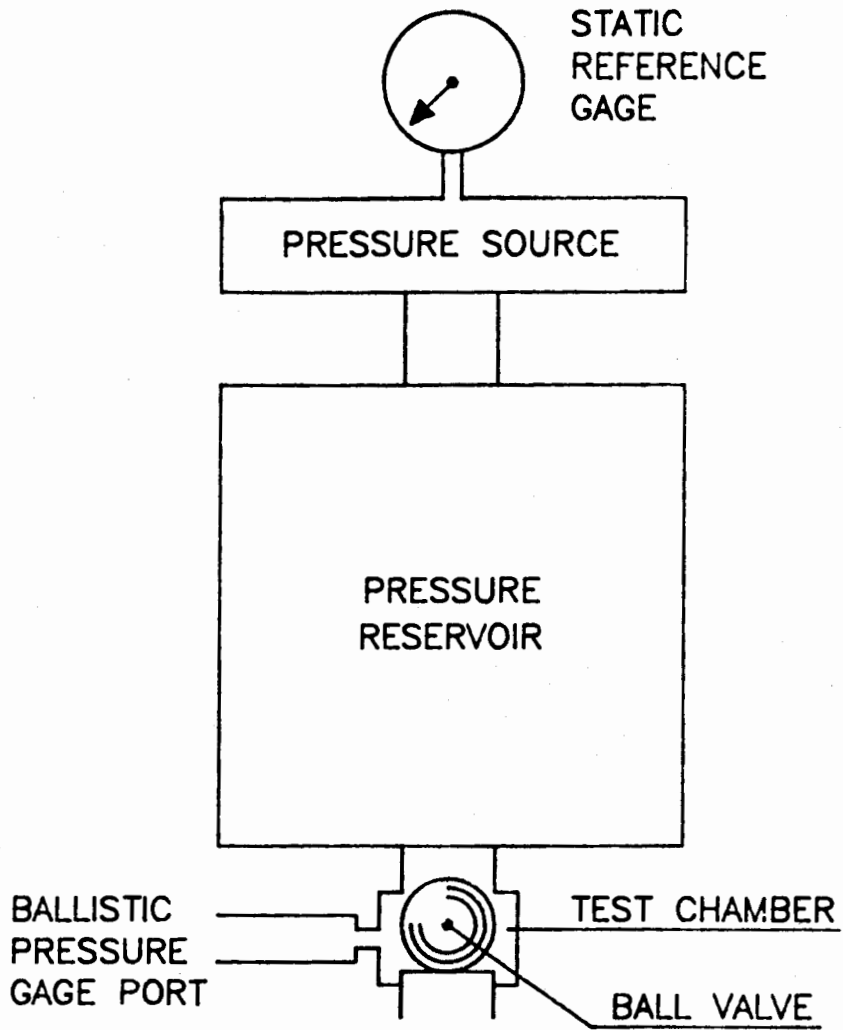


Figure 1. Design Concept for the Positive Step Pressure Calibrator

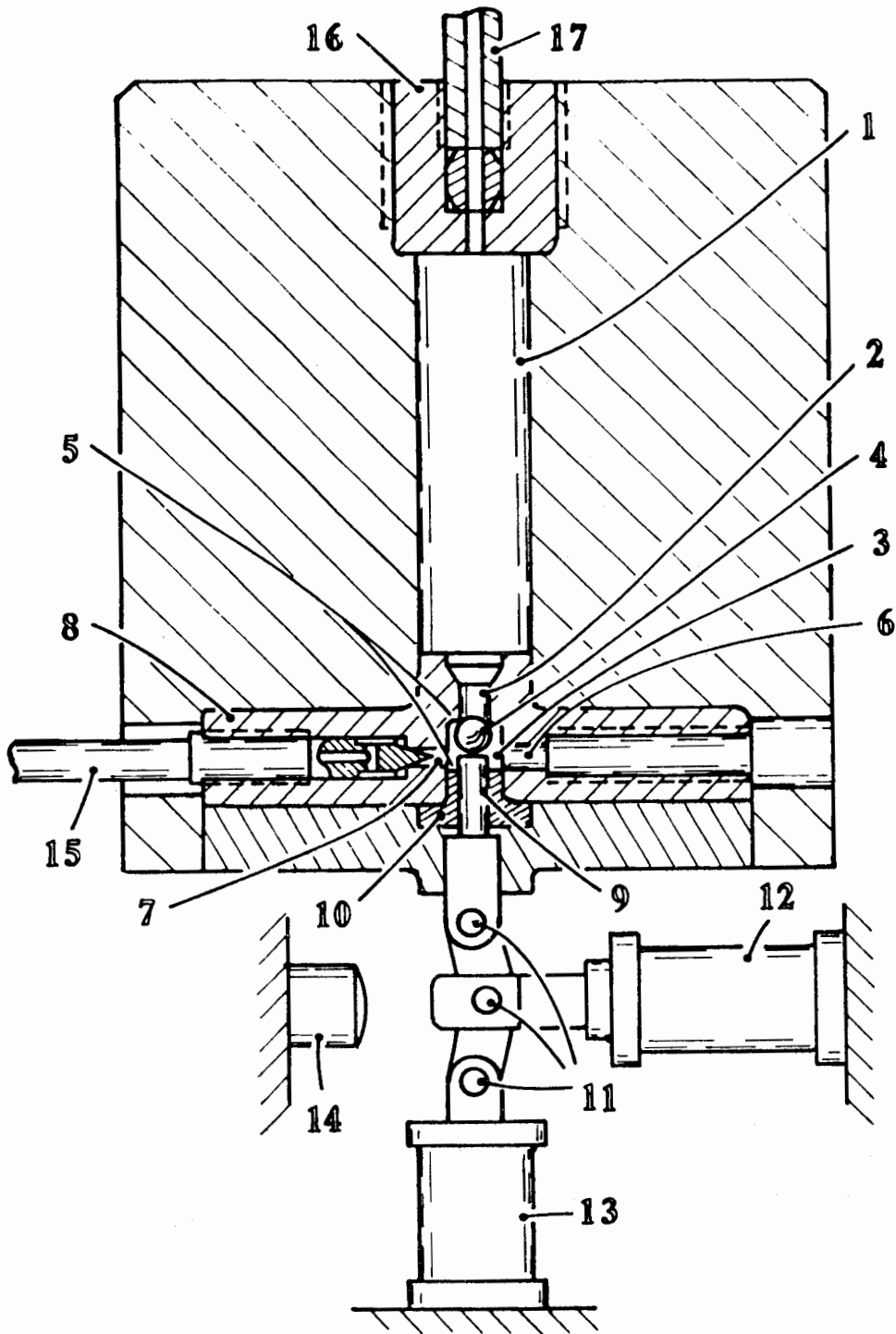


Figure 2. Engineering Schematic of 150,000 psi Positive Step Pressure Calibrator

- | | |
|------------------------|---------------------------|
| (1) Pressure reservoir | (10) Piston guide bushing |
| (2) Connecting channel | (11) Pin joints |
| (3) Test chamber | (12) Trigger mechanism |
| (4) Ball valve | (13) Hydraulic jack |
| (5) Valve seat | (14) Limit/stop buffer |
| (6) Gage port | (15) Vacuum stem valve |
| (7) Vacuum line port | (16) Port |
| (8) Test head | (17) High pressure source |
| (9) Valve actuator | |

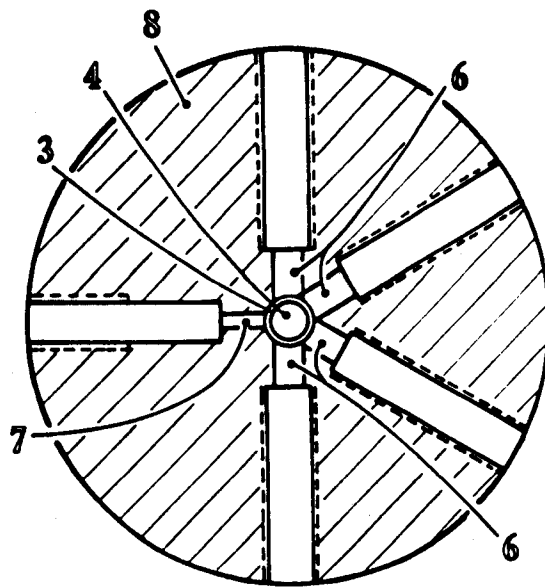


Figure 3. Lateral Cross-Sectional View of Test Head

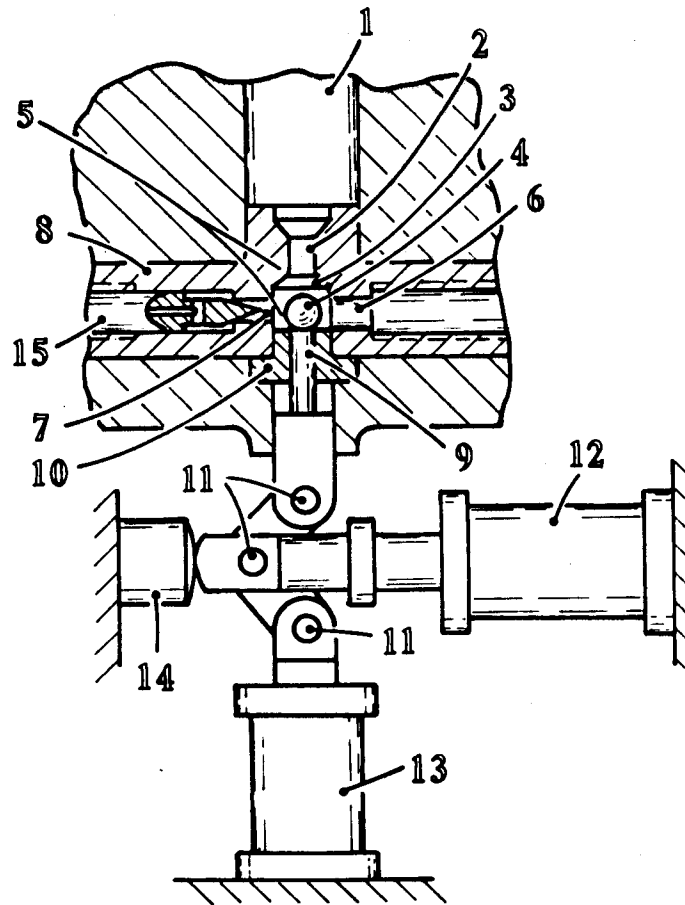


Figure 4. Closeup View of Test Chamber After Trigger Actuation

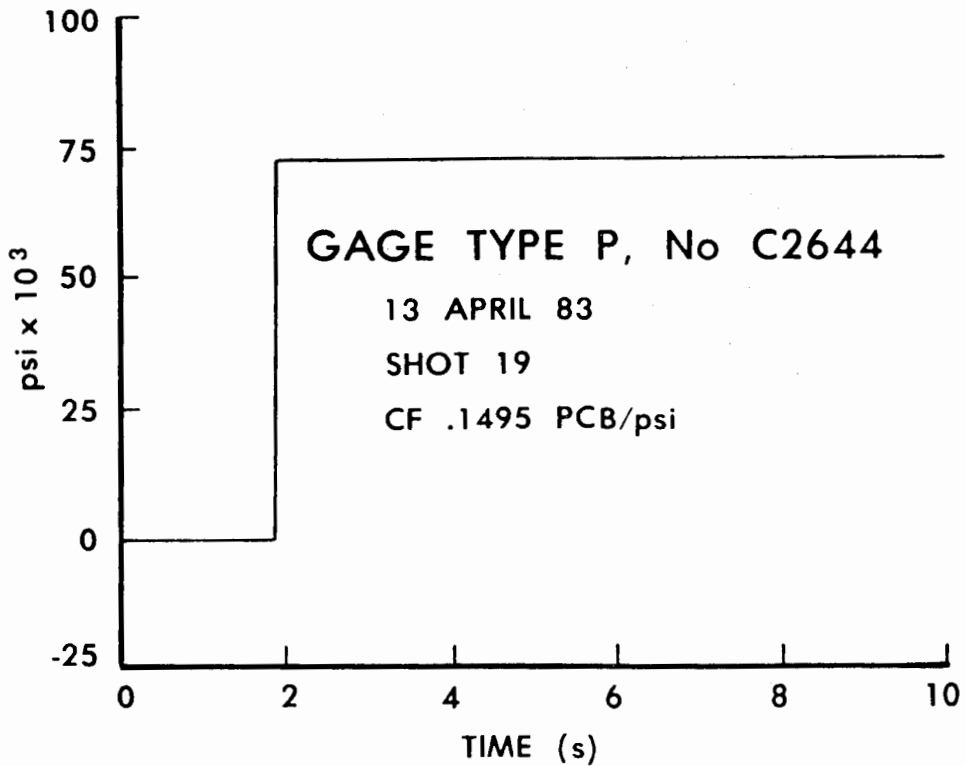


Figure 5. Pressure-Time History of a 75,000 psi Dynamic pressure Step; 10 second Window

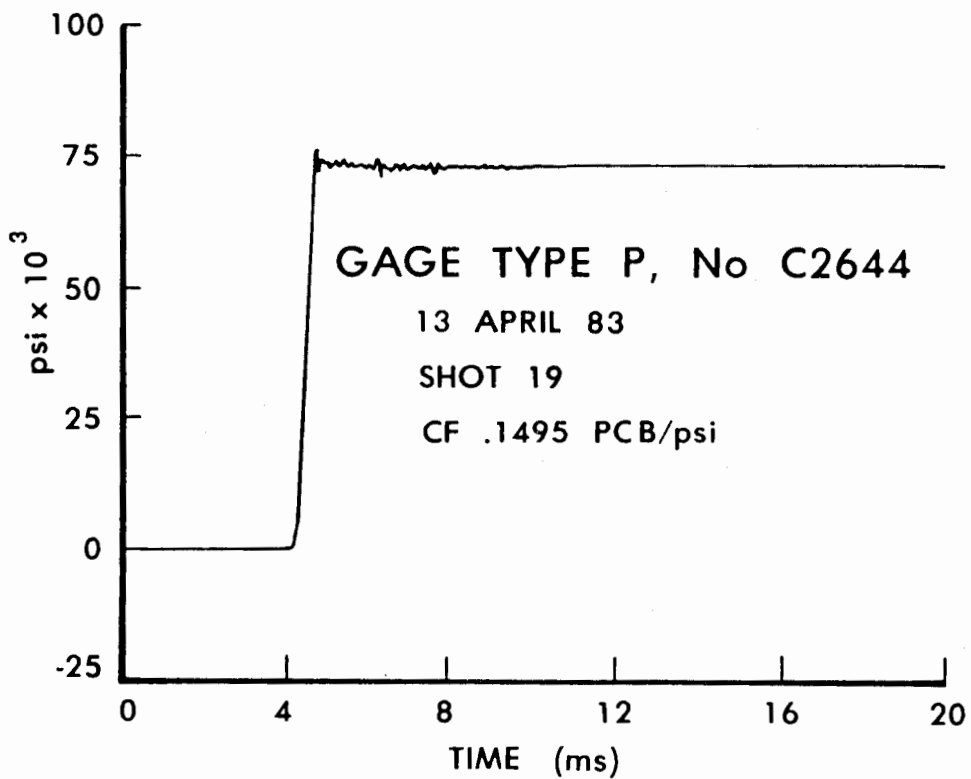


Figure 6. Pressure-Time History of a 75,000 psi Dynamic Pressure Step; 20 Millisecond Window.

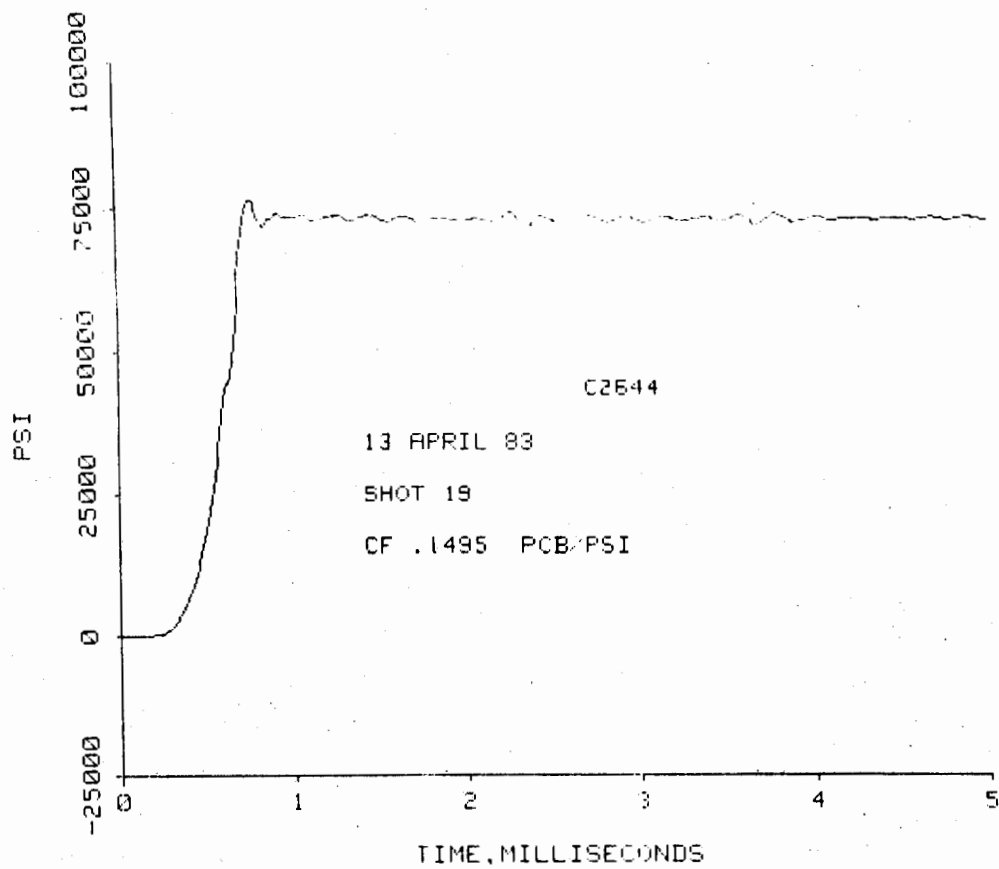


Figure 7. Pressure-Time History of a 75,000 psi Dynamic Pressure Step; 5 Millisecond Window

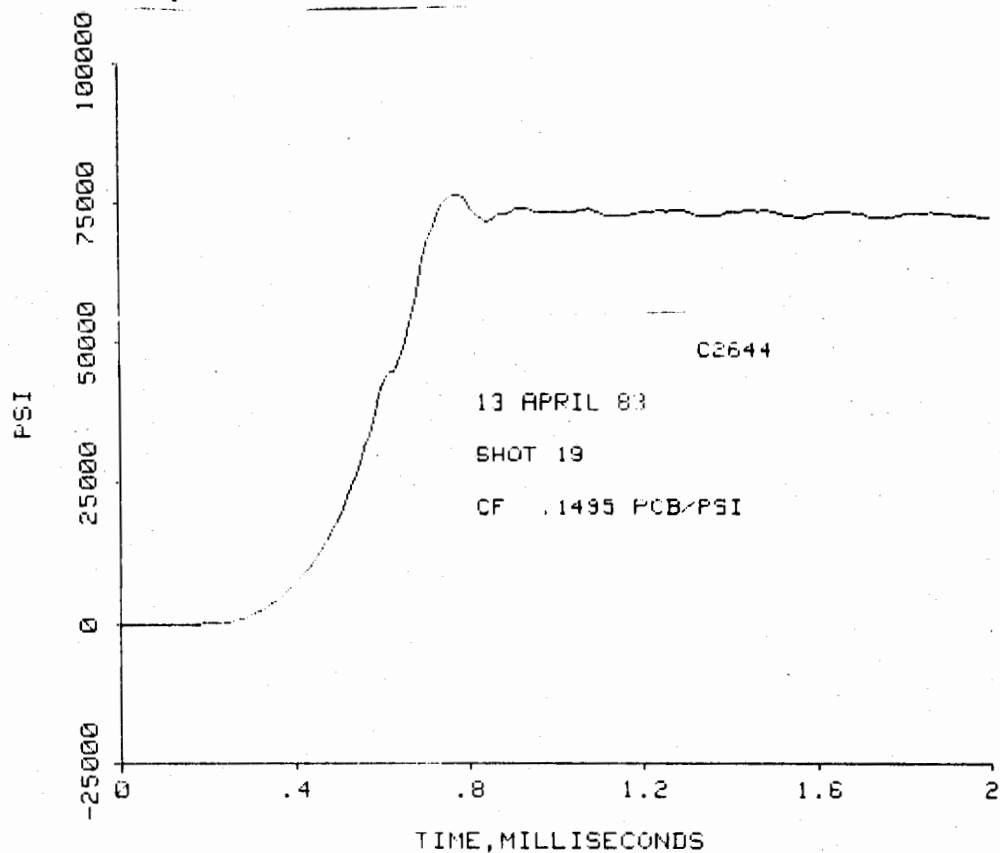


Figure 8. Pressure-Time History of a 75,000 psi Dynamic Pressure Step; 2 Millisecond Window

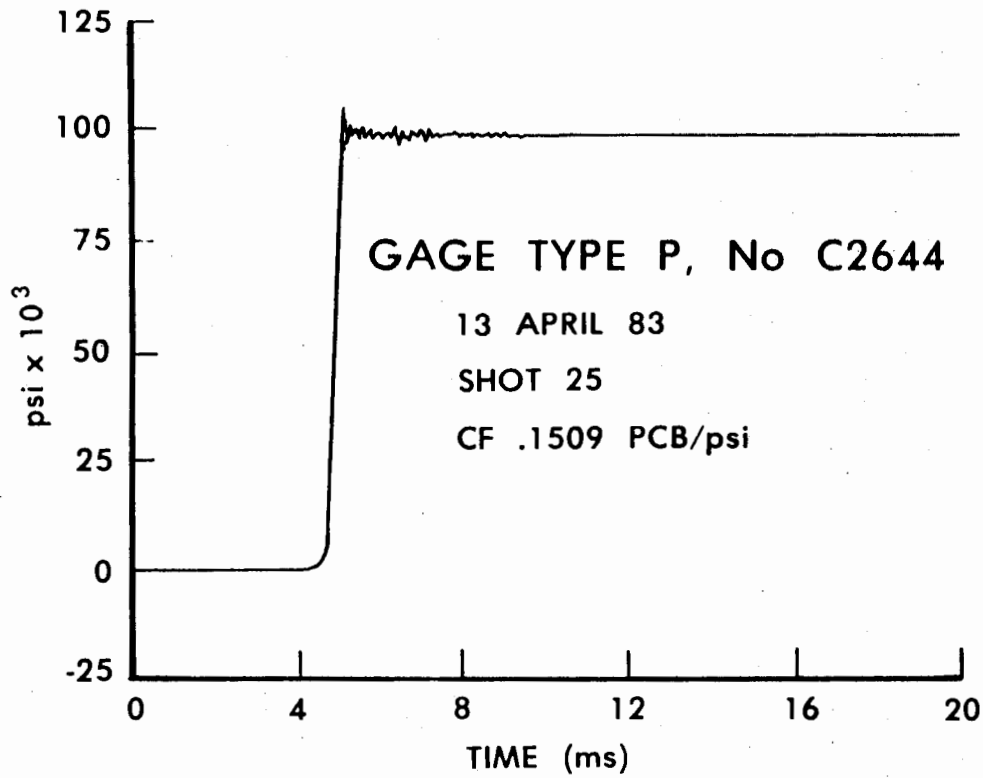


Figure 9. Response of a Piezoelectric Ballistic Pressure Gage to a 100,000 psi Positive Pressure Step

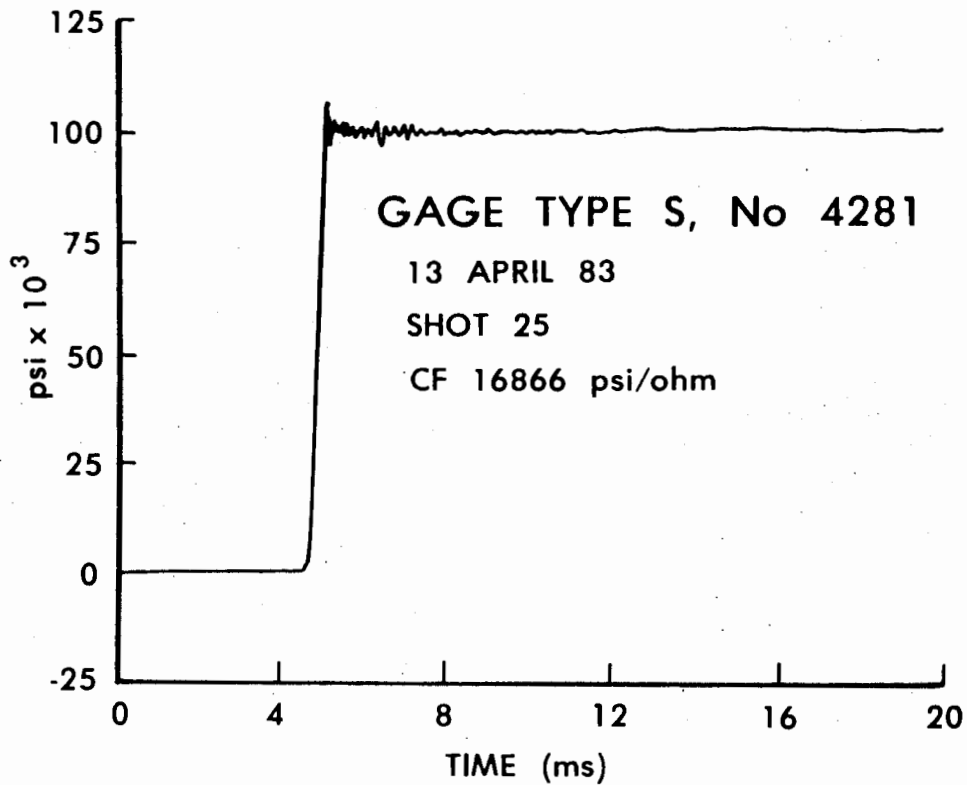


Figure 10. Response of a Strain Type Ballistic Pressure Gage to a 100,000 psi Positive Pressure Step

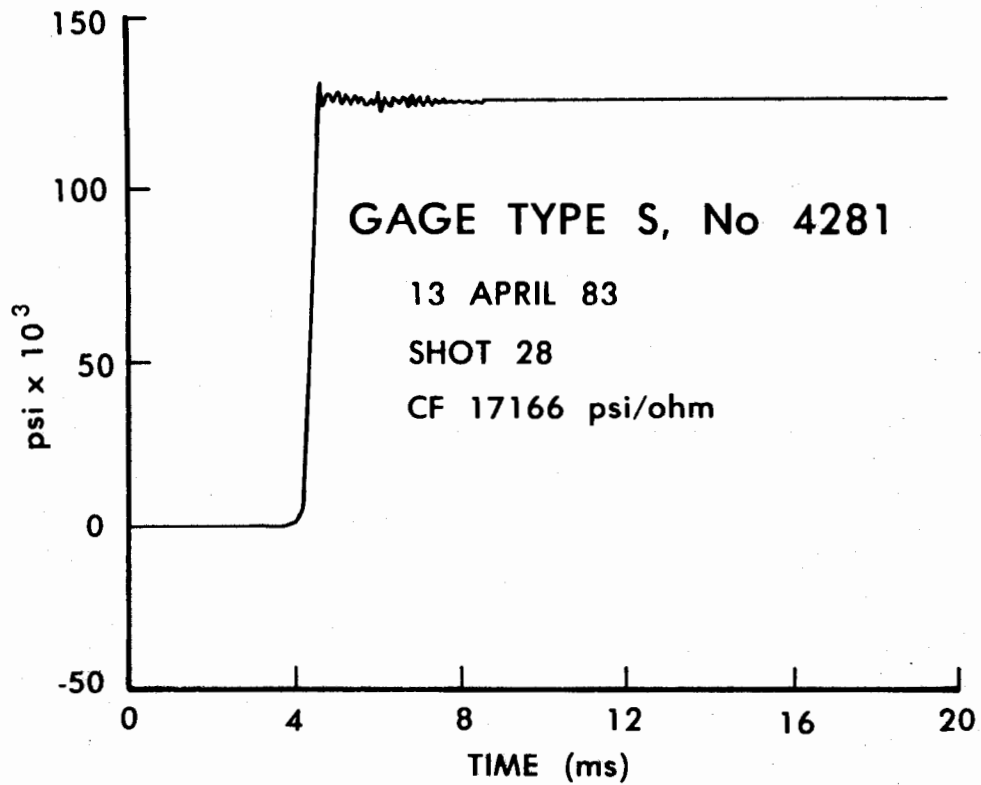


Figure 11. Response of a Developmental Pressure Gage to a 125,000 psi Positive Pressure Step]

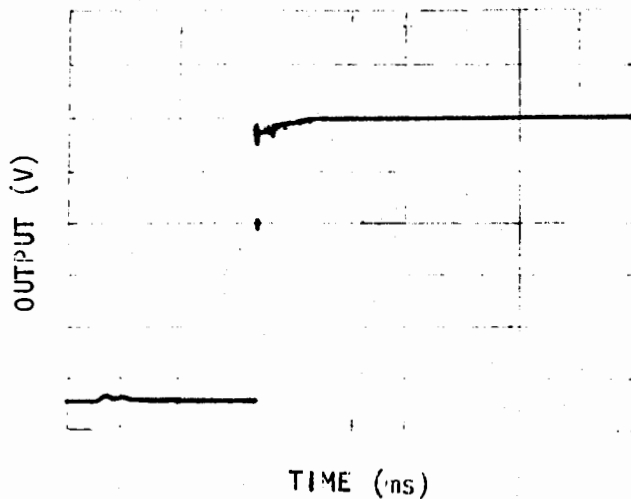


Figure 12. Response of a Faulty Developmental Pressure Gage to a 130,000 psi Positive Pressure Step



US ARMY TMDE SUPPORT GROUP

USATSG-S-85-8
MAY 1985

EVALUATION OF A NEW HIGH
PRESSURE TRANSDUCER

PRESENTED AT THE 13TH TRANSDUCER
WORKSHOP
SPONSORED BY RANGE COMMANDERS
COUNCIL,
TELEMETRY GROUP

JUNE 4-6, 1985

MONTEREY, CALIFORNIA

PHYSICAL STANDARDS AND DEVELOPMENT
LABORATORY
METROLOGY DIRECTORATE

REDSTONE ARSENAL, ALABAMA 35898-5400

J. R. MILLER III
LORI EDMONDSON
GREG RIGNEY
D. E. WOODLIFF

"combat readiness thru tmde readiness"

I. INTRODUCTION

We have a project to replace several outdated deadweight testers that are used to calibrate various pressure gages up to 10,000 psi. We have set the following goals for the new hydraulic pressure gage (Table 1). At the start of the project we reviewed the standards quality transducers available and tested several, including several strain gage types.¹

A new design transducer, bourdon tube/quartz oscillator, was included in these tests. Although a number of transducers passed many of the tests, the hysteresis of this transducer was so low, the rest of this paper relates characteristics of this particular item, see figure 1.

II. TEST RESULTS

A. EXPERIMENTAL APPARATUS

The equipment used in these tests is shown in figure 2. Note that the deadweight tester is only used as a pressure generator.

B. HYSTERESIS

The ability to produce consistent readings independent of increasing or decreasing pressure is an important characteristic of a transducer. The failure to do so, even if this failure follows a predictable path, is difficult to remedy even with a resident microprocessor.

We considered several transducers that had predictable hysteresis curves. The primary difficulty is the inability to control future users; hence, one cannot predict what portion of the curve will be developed.

The old advice of exercising the instrument a few times to reduce this hysteresis defeats a fast response, high accuracy, digital instrument.

The Digiquartz* pressure transducer exhibited such a small amount of hysteresis as to render this problem insignificant over most of its range. Figures 3-8 give typical results. Oftentimes the hysteresis the transducer may have was less than our ability to repeat the tests. We have established a limit on it of 0.02 percent reading from 20 percent fs to fs.

What makes this transducer have such low hysteresis? We speculate that in addition to the quartz oscillator, essentially hysteresis free, the metal bourdon tube is so stiff that hysteresis is much less than expected.

C. OPERATING EQUATION AND CURVE FIT

As the absolute pressure is increased the force on the quartz oscillator causes its frequency to change from approximately 38 to 42 kHz for a full scale pressure change.

Since the pressure transducer used in the Hydraulic Pressure Standard (HPS) will be used with a microprocessor the operating equation relating its output to the input must be known. Furthermore, the equation must accurately fit this data. This curve fit error limit (or "conformance" as one manufacturer calls it) should be within ± 0.01 percent to 0.02 percent over most (10 percent fs to fs) of the range.

*Trademark of Paroscientific Inc., Redmond, Washington.

After a great deal of work to obtain this accuracy of curve fit it has successfully been accomplished. Of major help in doing this is the Multiple Linear Regression (MLR) math software provided with the HP 9826 desktop calculator. One can simultaneously fit three (or more) variables. In our case, with the transducer being considered,* we fit pressure (P), frequency (f), and temperature (T). Table 2 gives the results for transducer SN 18858. This equation

$$P = p_0 + a_0f + a_1f^2 + a_2f^3 + a_3f^4 + a_4t + a_5t^2 + a_6P_nT \quad (1)$$

is quite a bit simpler than the manufacturers' or our earlier attempts.** In this relation P_0 , a_0 a_6 are constants and P_n is the nominal pressure. Note that in table 2 the temperature variation was purposely kept as small as possible; hence, the T-value, regression coefficient/standard error, of that coefficient, is small.

* Paroscientific DigiQuartz Pressure Transducer.

** Our earlier efforts and the manufacturer currently use

$$P = A(1 - (f/f_0)^2) + B(1 - (f/f_0)^2)^2$$

where f_0 is the frequency at zero pressure, f is the frequency at any pressure P and A and B are constants.

D. TEMPERATURE AND PRESSURE SENSITIVITY

If one reverses the role of P and f then the solution

$$f = f_0 + b_0p + b_1p^2 + b_2p^3 + b_3T + b_4T^2 + b_5pT \quad (2)$$

gives a good fit to the data, although not quite as good as Eq (1). Differentiating this equation with respect to P or T gives information relating to some important transducer characteristics

$$df/dp = b_0 + 2b_1p + 3b_2p^2 \quad (3)$$

$$df^2/dp^2 = 2b_1 + 6b_2p \quad (4)$$

$$df/dT = b_3 + 2b_4T + b_5p \quad (5)$$

$$d^2f/dT^2 = 2b_4. \quad (6)$$

The first term (3) is the linear pressure sensitivity while the third term (5) is the linear temperature sensitivity. Note that both these values are not constants, i.e., they depend on the pressure or temperature being measured.

Using the more familiar terminology of temperature coefficients

$$\alpha = df/dt \text{ (units of Hertz/}^\circ\text{C)}$$

$$\beta = d^2f/dt^2 \text{ (units of Hertz}^2\text{/}^\circ\text{C}^2)$$

then

$$f_R = f_t + \alpha (R-T) + \beta (R-T)^2 \quad (7)$$

where f_t is the frequency at some temperature t and R is the reference temperature.

Table 3 summarizes the known characteristics for three of these transducers.

In the actual microprocessor-based pressure standard the anticipated sequence of operations would be

1. Measure the transducers temperature, T,
2. Measure the transducers frequency at that temperature,

3. Using an appropriate number of terms in Eq 1 (2, 3, 4, or 5) obtain an approximate value for P_n , the nominal pressure,
4. Using P_n and Eq 5 and 6 calculate α and β ,
5. From Eq 7 find f_R , and
6. Using first five terms of Eq (1) calculate an accurate value of P and display it.

An error analysis has been completed that gives the expected error in P for errors in P_n , and temperature measurement errors.

E. REPEATABILITY

Because of the small pressure sensitivity of the Digiquartz transducer an exceedingly sensitive and fast frequency counter was needed, and a prime question to be answered was: If a frequency counter with a sensitivity of 0.0035 Hz (see appendix for derivation of this value) could be designed, would the transducer's repeatability be small enough to make it worthwhile? A corollary question was: Could one expect a high pressure transducer ($f_s = 10$ K psia) to offer good repeatability at its extreme low pressure (100 psia)?

Extensive tests were run to answer these questions.

The apparatus in figure 2 was used. The Ruska DDRS-6000's were calibrated against the US Army Primary Standards (Ruska 0-12,140 DWT) and the pressure-voltage relation was

$$P = -0.341788 \text{ psi} + 999.999 \frac{\text{psi}}{\text{volt}} [V - V_0] \quad (8)$$

where V is the voltage at the pressure of interest, P , and V_0 is the zero pressure volts.

A series of pressure runs were made over a 3-day period, each by loading the RQ-100 with a particular set of weights. By varying a nominal 5 pounds for another the small mass difference would provide a real pressure change,

bigger than the desired repeatability, and the experiment was designed this way. One would have A and B runs differing by this one weight.

It quickly became apparent that this was not necessary since the normal day to day atmospheric pressure variations provided a measurable pressure change. The Ruska DDRS-6000 barometer measured the atmospheric pressure.

The desired frequency resolution was provided by the HP 5316 counter reading eight significant figures. This made the readings quite slow (1 to 5 seconds); however, for these tests this was not too slow. It was necessary to measure and control the angular velocity and vertical position of the DWT. The desktop computer program took three frequencies and computed the average frequency.

E1. SHORT TERM REPEATABILITY

The repeatability of readings taken when the pressure is steady is within the frequency counter resolution, ≈ 1 in $3.3 * 10^7$, or a pressure value of ≈ 0.0027 psia at 100 psia this is ≈ 0.0027 percent, well within our goal.

E2. LONG TERM REPEATABILITY

Since a normal reading would take only a few fractions of a second and a normal pressure calibration takes upwards of an hour, repeatability over a day or 3 days could be considered long term. As given in reference 1 data was taken over a 3-day period. At the low pressures the transducer produces approximately ± 0.03 percent repeatability.

By applying temperature corrections,* zero shift, and referencing all data to the initial pressure an improvement to that data has been obtained. Table 4 presents these results.

* The temperature corrections may not be quite correct since that subject is still being worked on. See discussion on page 166.

The transducer, at the very lowest pressures, will have a repeatability error range of ± 0.02 to ± 0.03 percent (three SE values). It will, therefore, be useful to have a frequency resolution better than this; hence, the answer to both questions is yes.

F. ZERO SHIFT

Earlier work indicated the output frequency from the transducer changed more than strictly due to pressures. To determine the amount of zero shift a fiducial point is selected such as the initial pressures, P_i , and frequency, f_i . Since atmospheric pressure is a readily available pressure it has been the usual practice to measure it.

The frequency at any later time can be predicted if one knows the atmospheric pressure then, P_n , by

$$f_n = f_i + \frac{\Delta F}{\Delta P} (P_n - P_i) \quad (9)$$

where $\Delta f/\Delta p$ is the sensitivity of the transducer in the region of atmospheric pressure.* Then the frequencies on later days were predicted for the given atmospheric pressures. These predictions were then compared to the actual frequencies and a difference (= zero shift) found.

In general the zero shift is defined by

$$f_n(\text{actual}) - f_n(\text{predicted}) = \text{zero shift} \quad (10)$$

Typical zero shifts are given in Table 5 .

III. REMAINING PROBLEMS

A. TEMPERATURE COEFFICIENTS AND COMPENSATION

The biggest problem remaining with the transducer concerns temperature variations. Since a change of 20 °F from the calibration temperature of 73 °F is very likely and the error budget, Table 6 , allows only 0.02%.

* It may be necessary to include a quadratic term.

One must either measure the temperature, use the temperature coefficient and apply a correction, or surround the transducers with an oven to hold its temperature steady.

Since prior experience with ovens indicated the difficulty in obtaining good results the correction method is preferred.

To date the temperature coefficient characterization of these transducers has been difficult. Figures 9 and 10 show two transducers, one with a negative coefficient and one with a positive coefficient. Table 7 gives some data. This is undoubtedly caused by the quartz crystal TC changing sign from one crystal to another. It has been difficult to gather repeatable data on the transducer. Work on the subject is continuing.

B. ELECTRONICS

To take advantage of this transducer a new set of electronics is necessary. The main ingredient is a high speed, high resolution frequency counter. It will use a 100 MHz oscillator and be capable of 0.003 Hz resolution. It will have an update time no longer than 100 milliseconds. There will be a microprocessor in the instrument to do the calculations using a math chip, AM 9511 or 9512.

A prototype set of electronics has already been assembled and is working.

APPENDIX
ERROR ANALYSIS

A question related to temperature compensation by mathematical correction is this: What is the pressure error, $\Delta P/P$, of the DigiQuartz transducer, for a range of temperatures, 13 °C to 33 °C, if one attempts to correct out the temperature effect, using our present knowledge?

Eq 7 gives

$$f = f_0 + \alpha (T-R) + \beta (T-R)^2$$

or

$$\Delta f = f - f_0 = \alpha (T-R) + \beta (T-R)^2$$

then

$$\Delta(\Delta f) = \frac{\partial f}{\partial \alpha} \Delta \alpha + \frac{\partial f}{\partial (T-R)} \Delta (T-R) + \frac{\partial f}{\partial \beta} \Delta \beta + \frac{\partial f}{\partial (T-R)^2} \Delta [(T-R)^2] \quad (A1)$$

$$= |(T-R) \Delta \alpha| + |\alpha \Delta (T-R)| + |(T-R)^2 \Delta \beta| + 2\beta (T-R) \Delta (T-R)^2| \quad (A2)$$

where for SN 18858

$$\alpha = 0.27978 - 0.00928T + 0.00006 P$$

error is maximized if α is maximum so using maximum pressure and minimum temperature will give maximum α . If $P = 10$ K psia, $T = 13$ °C, then $\alpha = 0.75914$ Hz/°C.

$\Delta \alpha = \pm 0.00066$ Hz²/°C² from 90 percent confidence interval on MLR, sum of all terms involved in $\Delta \alpha$.

$$\beta = 2 (-0.00464) = -0.00928 \text{ Hz}^2/\text{°C}^2$$

$\Delta \beta = \pm 0.003$ Hz²/°C² from 90 percent confidence of MLR.

Table A1 summarizes the results of equation A2. The values are for SN 18858.

TABLE A1

PRESSURE ERROR AFTER TEMPERATURE CORRECTIONS OF DIGIQUARTZ TRANSDUCERS

$\Delta(\Delta f/\Delta T)$	$T-R$	$\Delta(T-R)$	T	$\Delta\alpha$	α	$\Delta\beta$	β	$\frac{\Delta P}{(\Delta T)} 1/P$	P	$\Delta P/P$
0.0084 Hz/°C	10 °C	0.05 °C	13 °C	0.00066 Hz/°C	0.75914 Hz/°C	0.0003 Hz ² /C ²	0.00928 Hz ² /C ²	0.0024%/°C	10K psia	0.024%
0.0058 Hz/°C	10 °C	0.05 °C	13 °C	0.00066 Hz/°C	0.239 Hz/°C	0.0003 Hz ² /C ²	0.00928 Hz ² /C ²	0.0017%/°C	1 K psia	0.017%
0.0054 Hz/°C	10	0.05 °C	13	0.00066 Hz/°C	0.16514	0.0003	0.00928 Hz ² /C ²	0.017%/°C	0.1K psi	0.17%

REFERENCES

1. Progress Report on Hydraulic Pressure Transfer Standard Repeatability Tests on Paroscientific DigiQuartz Pressure Transducer, USATSG-S-84-9, May 1984, J. R. Miller III and D. E. Woodliff.

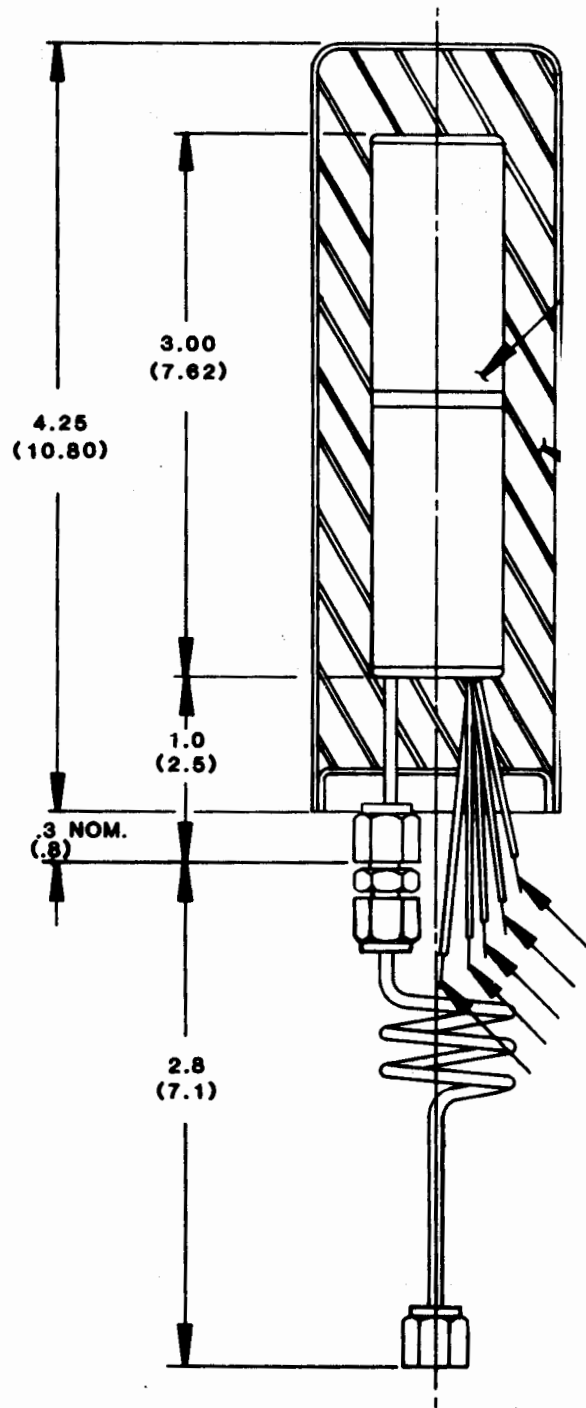


FIGURE 1.

DIGIQUARTZ PRESSURE TRANSDUCER

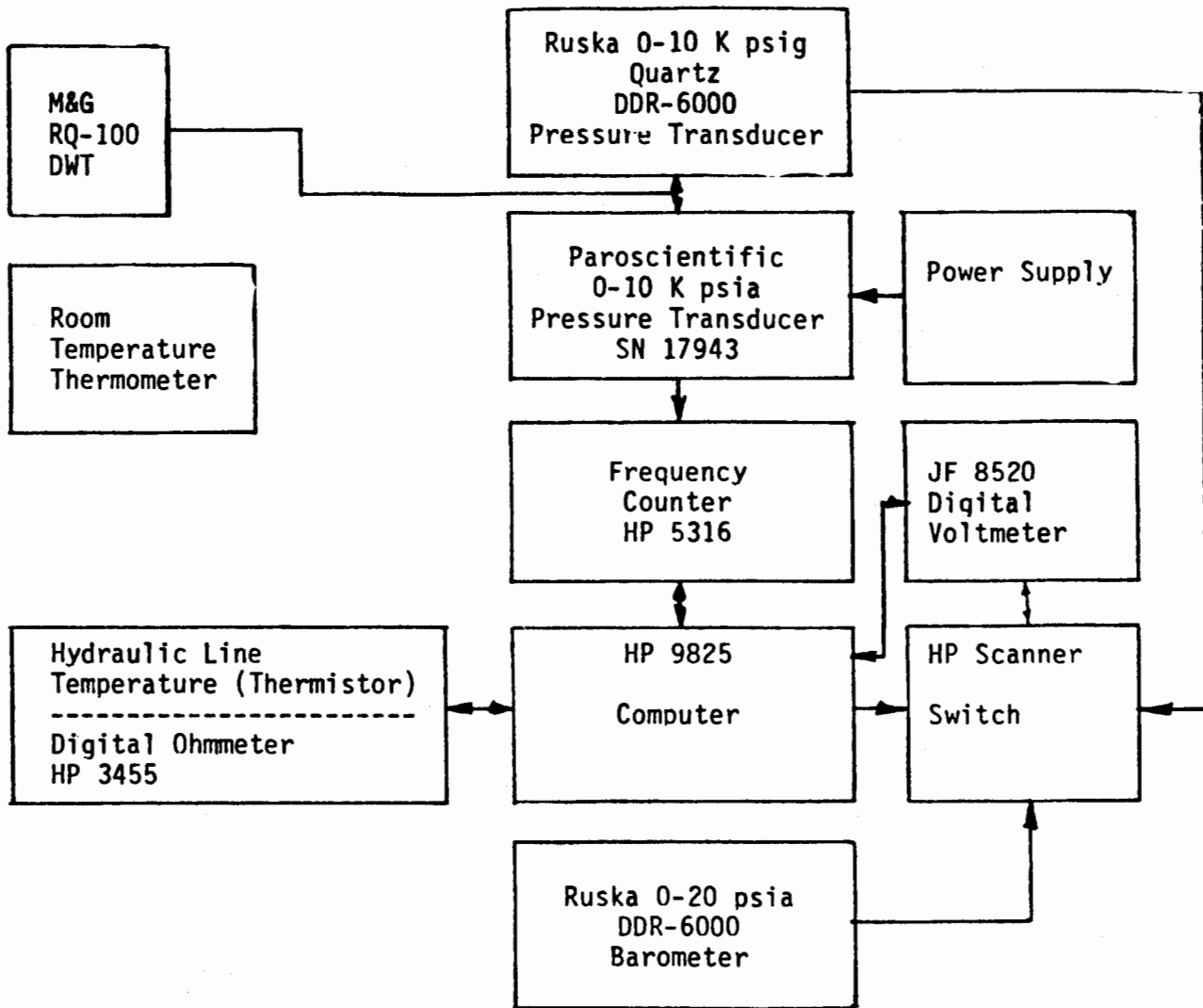
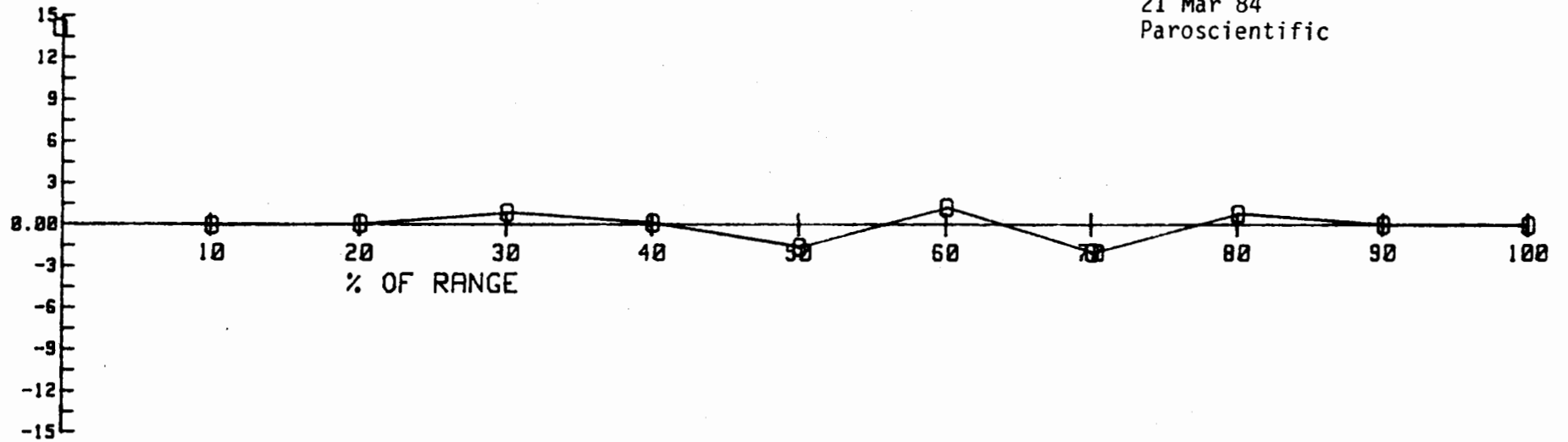


FIGURE 2.
TEST APPARATUS

FIG 3 PRESSURE TRANSDUCER HYSTERESIS CURVE

$P_{down} - P_{up}$, psi

21 Mar 84
Paroscientific



176

$(P_{down} - P_{up}) / P_{up} * 100\%$

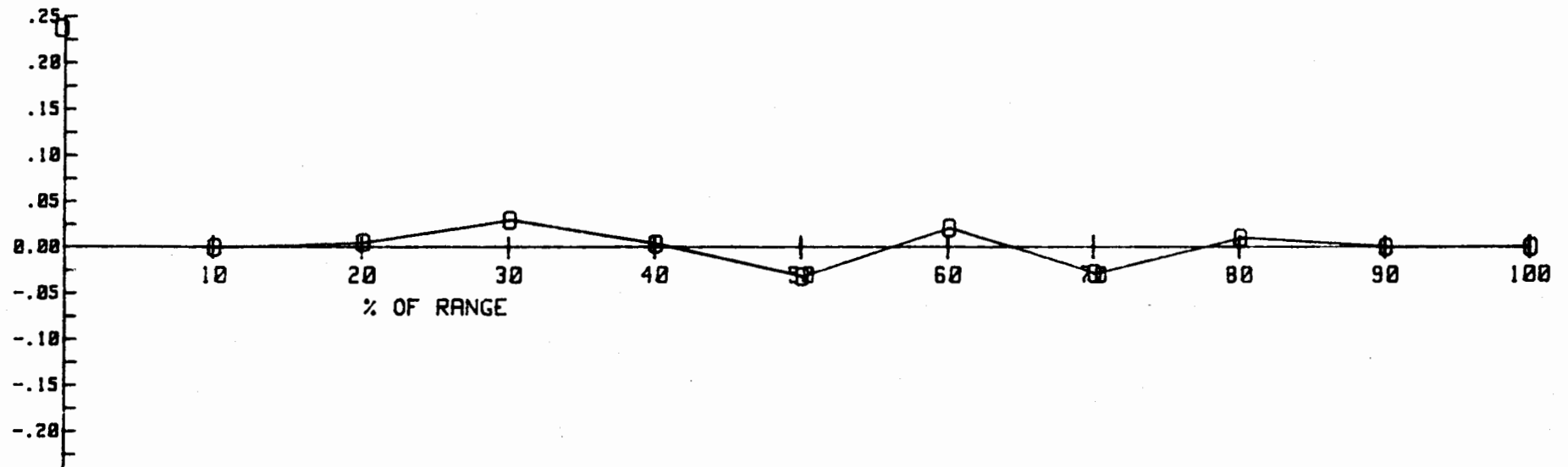
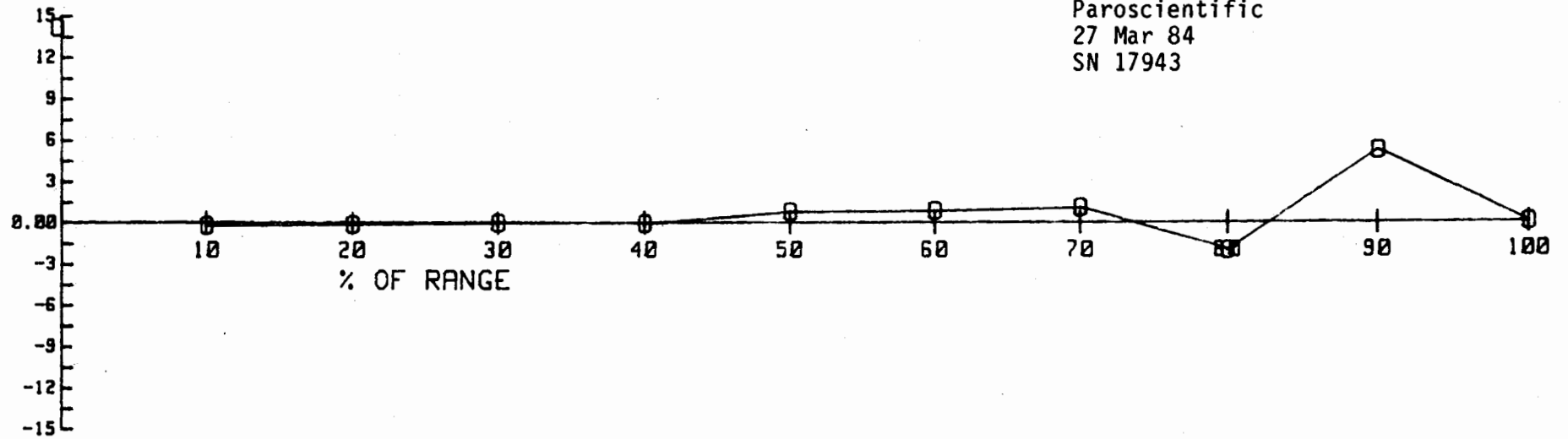


FIG 4 PRESSURE TRANSDUCER HYSTERSIS CURVE

Pdown-Pup, psi

Paroscientific
27 Mar 84
SN 17943



177

$(P_{down} - P_{up}) / P_{up} * 100\%$

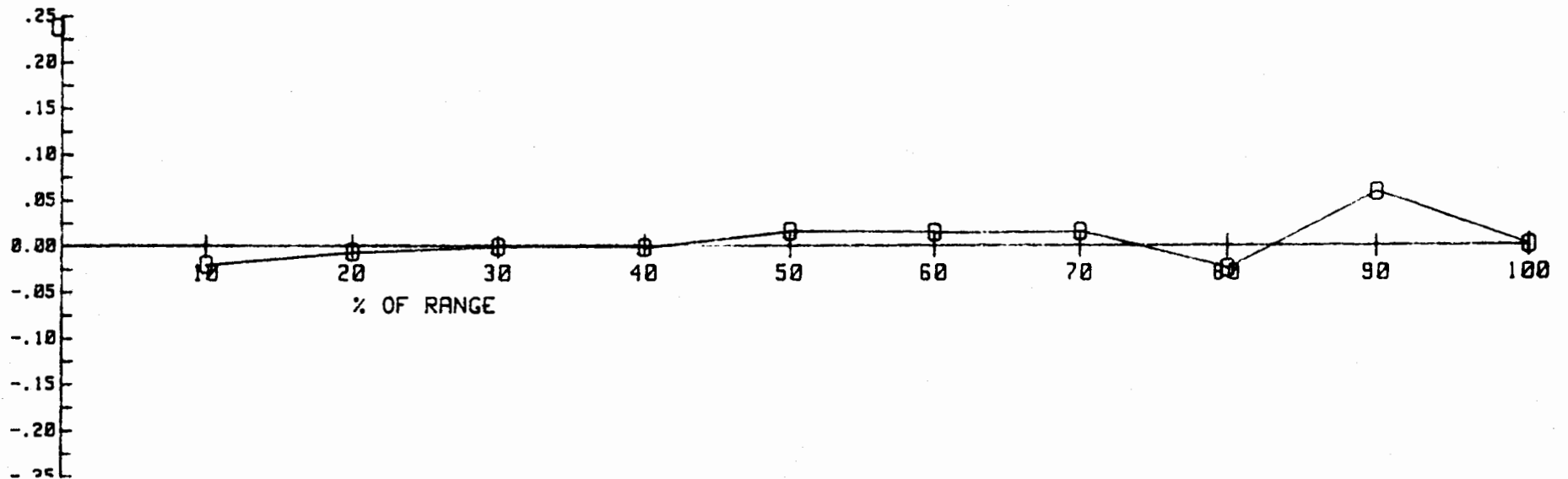
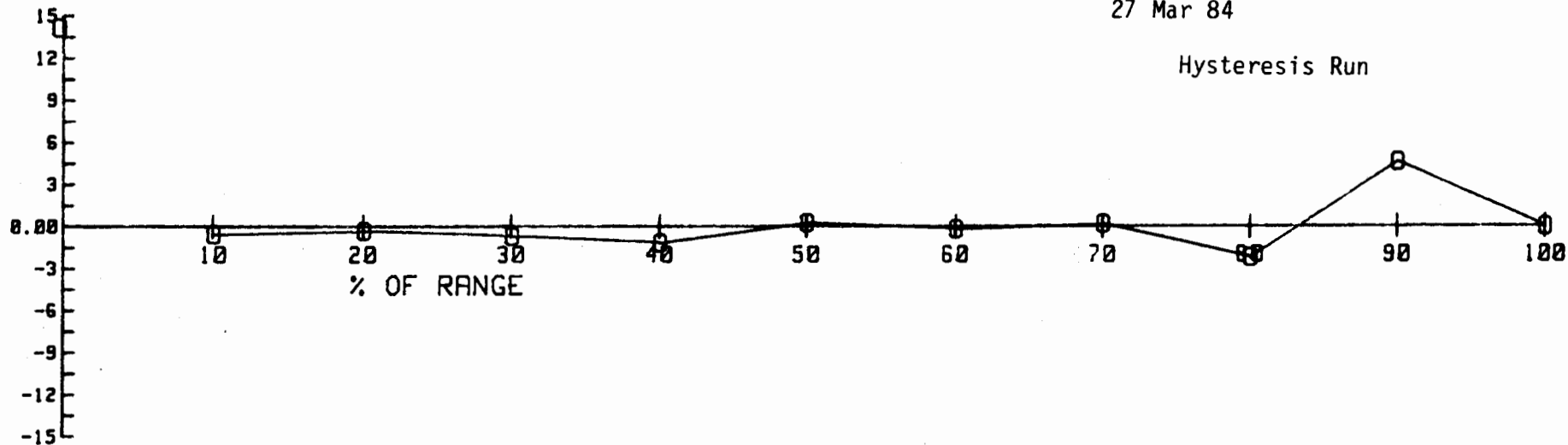


FIG 5 PRESSURE TRANSDUCER HYSTERESIS CURVE

Pdown-Pup, psi

Ruska Transducer
27 Mar 84

Hysteresis Run



178

$(P_{down} - P_{up}) / P_{up} * 100\%$

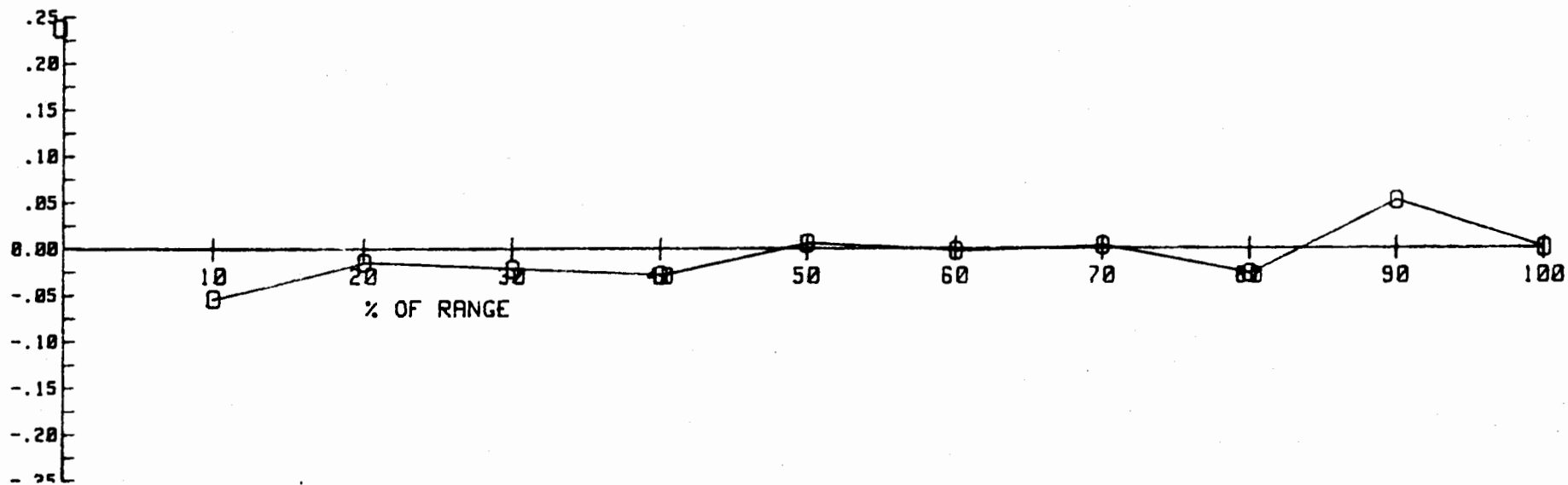


FIG 6 PRESSURE TRANSDUCER HYSTERSIS CURVE

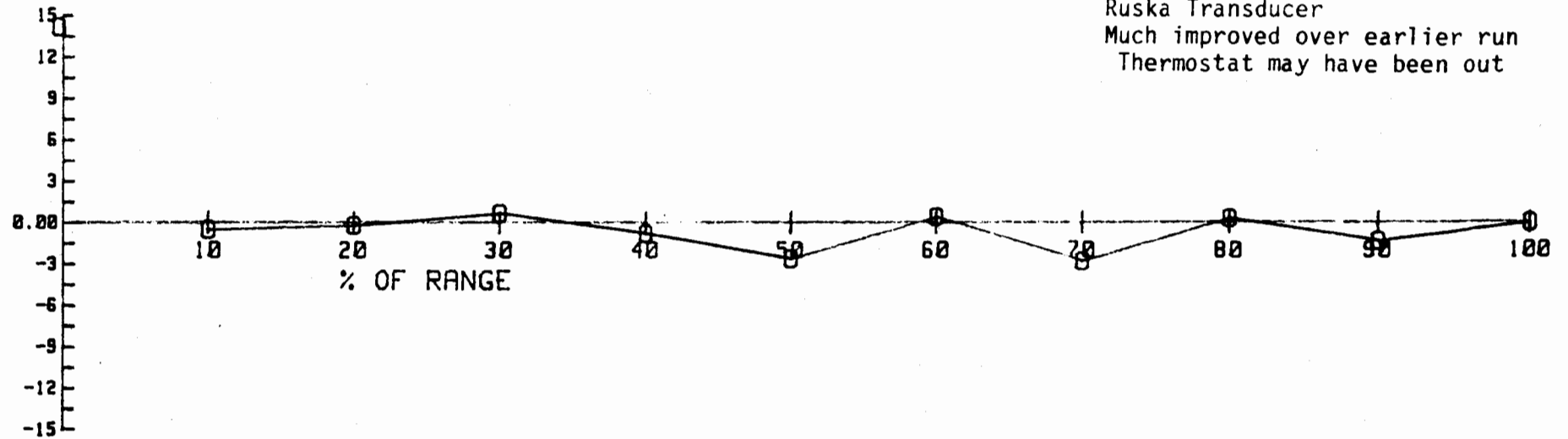
Pdown-Pup, psi

21 Mar 84

Ruska Transducer

Much improved over earlier run

Thermostat may have been out



179

$(P_{down} - P_{up}) / P_{up} * 100\%$

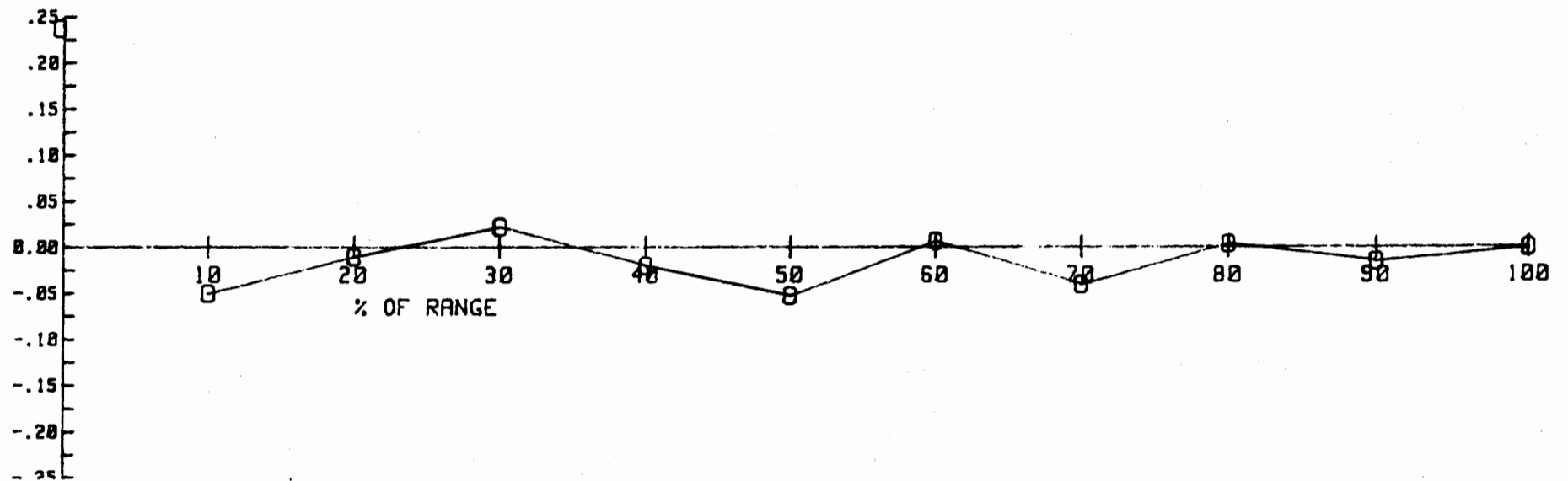
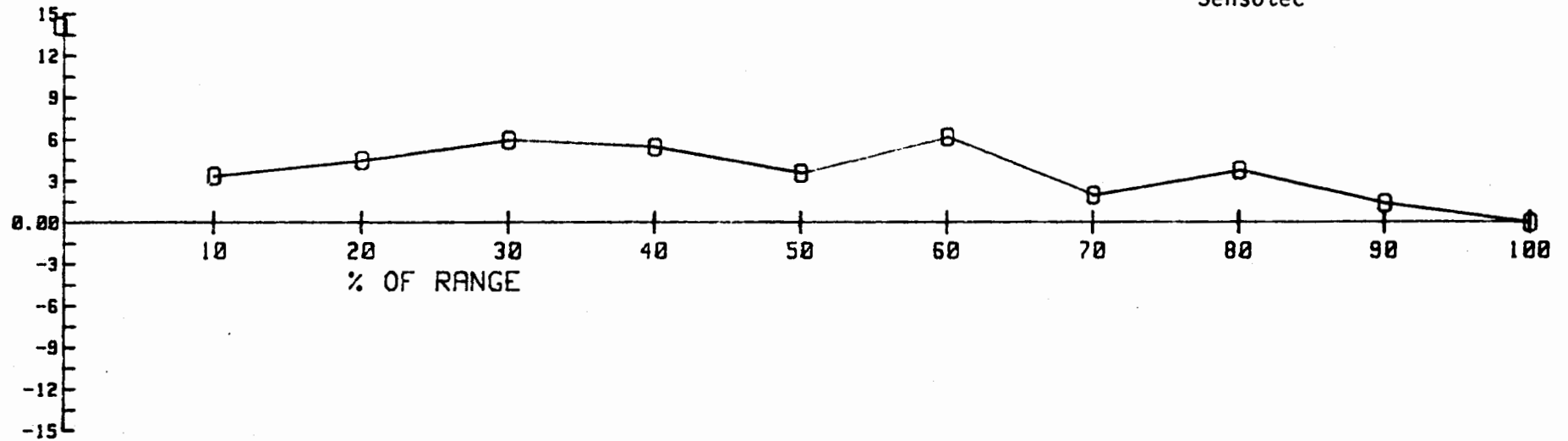


FIG 7 PRESSURE TRANSDUCER HYSTERSIS CURVE

Pdown-Pup, psi

21 Mar 84
Sensotec



180

$(P_{down} - P_{up}) / P_{up} * 100\%$

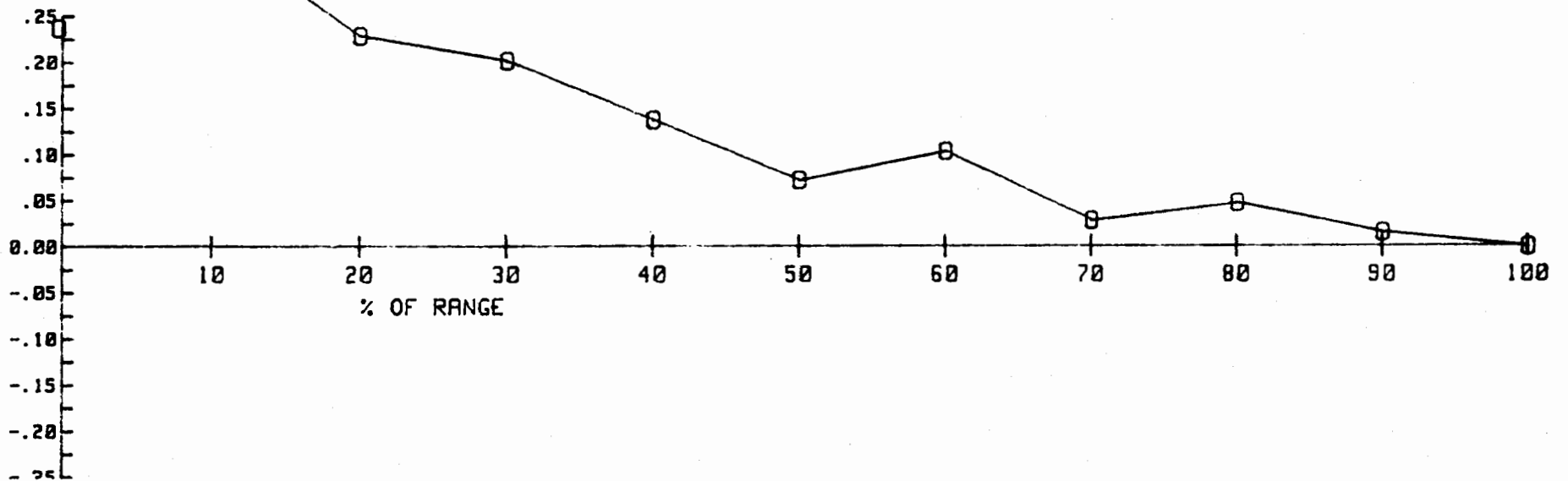
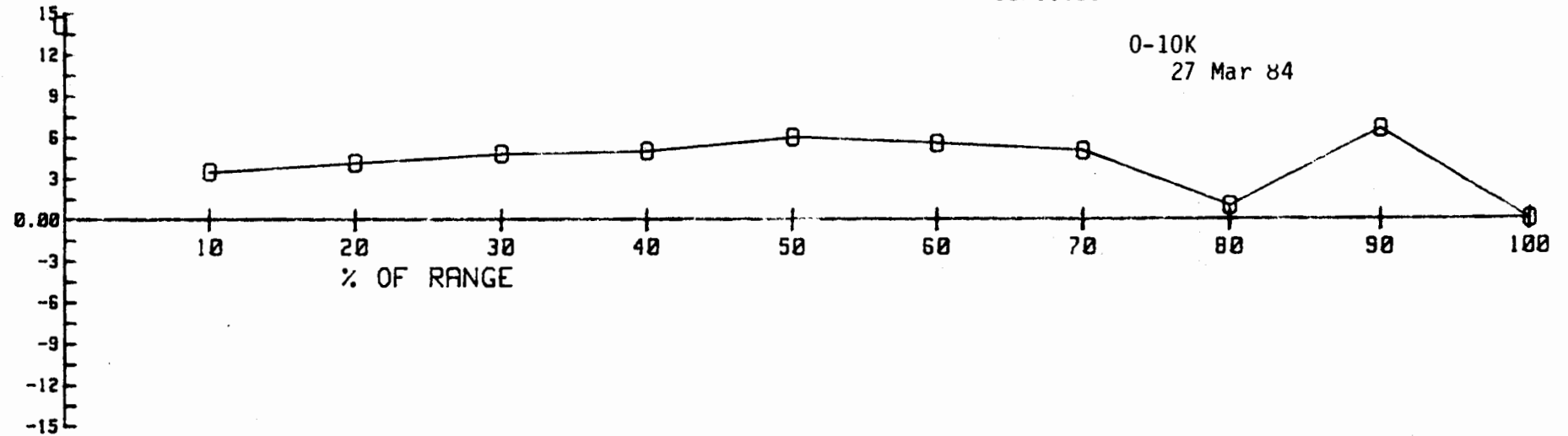


FIG 8 PRESSURE TRANSDUCER HYSTERSIS CURVE

Pdown-Pup, psi

Sensotec

0-10K
27 Mar 84



181

$(P_{down} - P_{up}) / P_{up} * 100\%$

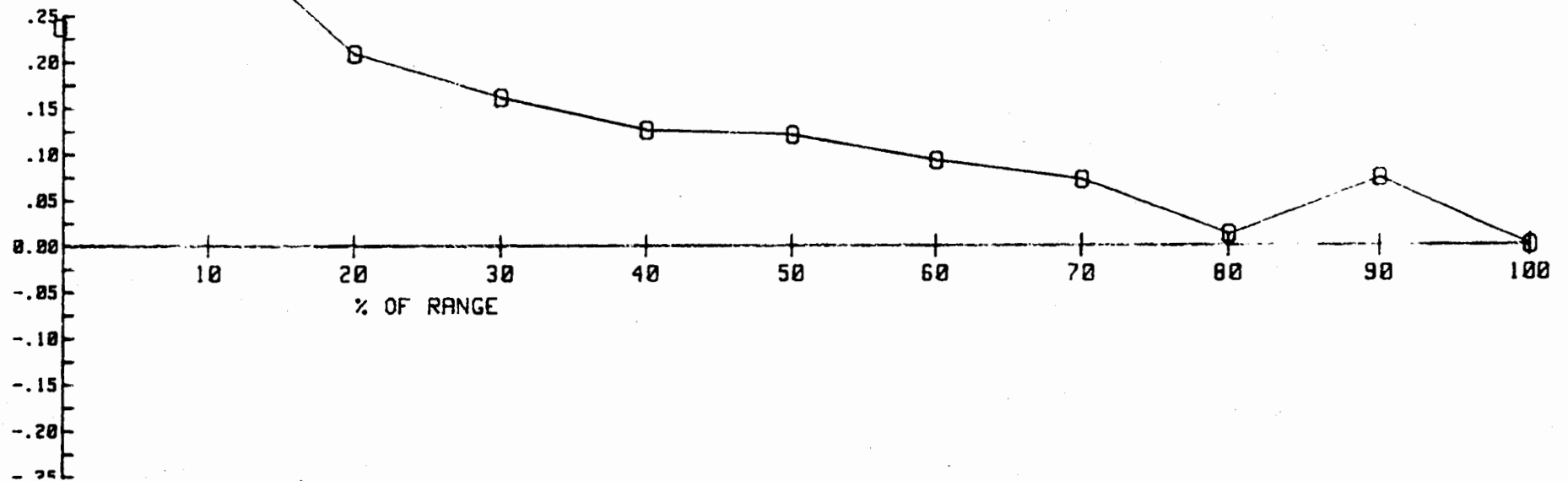


TABLE 1

NEW HYDRAULIC PRESSURE TRANSFER STANDARD GOALS

- (1) Insensitive to gravity.
- (2) Used with common hydraulic fluids.
- (3) Error limits of $\pm 0.05\%$ of reading, from 10% full scale to full scale.
- (4) Range to $\approx 70\text{Mpa}$ (10 Kpsi).
- (5) Digital readout-maximum resolution of 0.005% of reading.
- (6) Be lightweight and portable.

27 (340.00000
28 612.50000

MULTIPLE LINEAR REGRESSION ON DATA SET:

COMPLETE

TABLE 2

SN 18858

---where: Dependent variable = (1)OLD PRESS
Independent variable(s) = (2)FREQUENCY
(3)TEMP
(4)FREQ^2
(5)TEMP^2
(6)FREQ*TEMP

VARIABLE	N	MEAN	VARIANCE	STANDARD DEVIATION	COEFF. OF VARIATION
FREQUENCY	28	34747.60500	1057168.20033	1028.18685	2.95902
TEMP	28	24.56429	.14683	.38318	1.55990
FREQ^2	28		1208415465.42920		
.33213					72605313
FREQ^2	28		1208415465.42920		
213		6.00831			72605313.33
TEMP^2	28	603.54571	351.05163	18.73637	3.10438
FREQ*TEMP	28			853856.07739	
.64398					36955
FREQ*TEMP	28			853856.07739	
398		4.32809			36955.64
OLD PRESS	28	2683.26984	8612474.29204	2934.70174	109.37035

CORRELATION MATRIX

	TEMP	FREQ^2	TEMP^2	FREQ*TEMP	OLD PRESS
FREQUENCY	.8054064	.9999156	.8088850	.9785305	.9998879
TEMP		.7993601	.9999734	.9102744	.7984239
FREQ^2			.8028579	.9763701	.9999980
TEMP^2				.9126952	.8019246
FREQ*TEMP					.9760255

ANALYSIS OF VARIANCE TABLE

SOURCE	DF	SUM OF SQUARES	MEAN SQUARE	F-VALUE
TOTAL	27	232536805.88502		
REGRESSION	5	232536804.43650	46507360.88730	706354092.77
FREQUENCY	1	232484682.40130	232484682.40130	

TEMP^2 1
 FREQ*TEMP 1
 RESIDUAL 22

.09574
 .39141
 1.44851

.09574
 .39141
 .06584

1.45
 5.94

R-SQUARED = 1.00000
 STANDARD ERROR OF ESTIMATE = .25659584218

TABLE 2 - continued

VARIABLE	REGRESSION COEFFICIENTS		STANDARD ERROR	T-VALUE
	STD. FORMAT	E-FORMAT	REG. COEFFICIENT	
\CONSTANT\	-37432.93908	-.374329390834E+05	1138.49210	-32.88
FREQUENCY	-.49121	-.491210952569E+00	.03056	-16.08
TEMP	-7.01589	-.701588634530E+01	57.95765	-.12
FREQ^2	.00005	.462828021652E-04	0.00000	310.38
TEMP^2	-2.01993	-.201993429870E+01	1.09863	-1.84
FREQ*TEMP	.00310	.310031415177E-02	.00127	2.44

VARIABLE	COEFFICIENT	99 % CONFIDENCE INTERVAL	
		LOWER LIMIT	UPPER LIMIT
\CONSTANT\	-37432.93908	-40507.04476	-34358.83340
FREQUENCY	-.49121	-.57372	-.40871
TEMP	-7.01589	-163.51055	149.47878

FREQ^2	.00005	.00005	.00005
TEMP^2	-2.01993	-4.98642	.94655
FREQ*TEMP	.00310	-.00033	.00653

TABLE OF RESIDUALS

$P = \text{function}(f, T, f^2, T^2, f * T)$

OBS#	OBSERVED Y	PREDICTED Y	RESIDUAL	STANDARDIZED RESIDUAL	SIGNIF.
1	14.51920	14.57619	-.05699	-.22211	
2	92.61930	92.61768	.00162	.00632	
3	143.21800	143.22982	-.01182	-.04607	
4	192.91900	192.86713	.05187	.20215	
5	242.62000	242.59484	.02516	.09806	
6	292.52000	292.54207	-.02207	-.08602	
7	342.45000	342.44691	.00309	.01204	
8	392.42000	392.35129	.06871	.26777	
9	442.36000	442.28493	.07507	.29254	
10	642.03000	641.85098	.17902	.69768	
11	841.70000	841.49767	.20233	.78850	
12	1041.23000	1041.17215	.05785	.22546	
13	1240.83000	1240.86051	-.03051	-.11891	
14	1390.40000	1390.45679	-.05679	-.22131	
15	1589.93000	1590.16704	-.23704	-.92378	
16	1789.53000	1789.90821	-.37821	-1.47394	
17	1989.16000	1989.60572	-.44572	-1.73703	
18	2388.83000	2389.11309	-.28309	-1.10324	
19	2988.53000	2988.77899	-.24899	-.98101	

22	4587.33000	4587.08317	.24483	.73417
23	4986.99000	4986.71985	.27015	1.05282
24	5986.19000	5986.22733	-.03733	-.14549
25	6985.29000	6985.56418	-.27418	-1.06853
26	7984.52000	7984.83427	-.31427	-1.22477
27	8984.05000	8984.32632	-.27632	-1.07687
28	9983.45000	9983.05310	.39690	1.54677

Durbin-Watson Statistic: .837697302309

TABLE 2 - Continued

The following transformation was performed: $a \cdot (X^b) + c$

where $a = 1$
 $b = 3$

$c = 0$

X is Variable # 2

Transformed data is stored in Variable # 7 (FREQ^3).

COMPLETE

Data type is: Raw data

OBS#	Variable # 1 (OLD PRESS)	Variable # 2 (FREQUENCY)	Variable # 3 (TEMP)	Variable # 4 (FREQ^2)	Variable # 5 (TEMP^2)
1	14.51920	33797.21000	23.70000	1.142251E+09	561.69000
2	92.61930	33825.86000	23.90000	1.144189E+09	571.21000
3	143.21800	33844.46000	24.00000	1.145447E+09	576.00000
4	192.91900	33862.73000	24.00000	1.146684E+09	576.00000
5	242.62000	33880.99000	24.10000	1.147921E+09	580.81000
6	292.52000	33899.33000	24.20000	1.149165E+09	585.64000
7	342.45000	33917.66000	24.20000	1.150408E+09	585.64000
8	392.42000	33935.97000	24.30000	1.151650E+09	590.49000
9	442.36000	33954.29000	24.40000	1.152894E+09	595.36000
10	442.03000	34027.38000	24.50000	1.157863E+09	600.25000
11	841.70000	34100.30000	24.50000	1.162830E+09	600.25000
12	1041.23000	34173.06000	24.60000	1.167798E+09	605.16000
13	1240.83000	34245.63000	24.60000	1.172763E+09	605.16000
14	1390.40000	34299.88000	24.60000	1.176482E+09	605.16000
15	1589.93000	34372.15000	24.60000	1.181445E+09	605.16000
16	1789.53000	34444.25000	24.70000	1.186406E+09	610.09000
17	1989.16000	34516.16000	24.70000	1.191365E+09	610.09000
18	2388.83000	34659.49000	24.80000	1.201280E+09	615.04000
19	2988.53000	34873.22000	24.80000	1.216141E+09	615.04000
20	3588.09000	35085.38000	24.90000	1.230984E+09	620.01000
21	3987.83000	35296.25000	24.90000	1.230984E+09	620.01000

24	5986.19000	35920.35000	25.00000	1.290272E+09	625.00000
25	6985.29000	36261.76000	25.00000	1.314915E+09	625.00000
26	7984.52000	36599.52000	25.00000	1.339525E+09	625.00000
27	8984.05000	36933.84000	25.00000	1.364109E+09	625.00000
28	9983.45000	37264.50000	25.00000	1.388643E+09	625.00000

Variable # 6 (FREQ*TEMP)
Variable # 7 (FREQ^3)

TABLE 2- Continued

ORS#	Variable # 6 (FREQ*TEMP)	Variable # 7 (FREQ^3)
1	800993.87700	3.860491E+13
2	808438.05400	3.870317E+13
3	812267.04000	3.876705E+13
4	812705.52000	3.882987E+13
5	816531.85900	3.889272E+13
6	820363.78600	3.895591E+13
7	820807.37200	3.901914E+13
8	824644.07100	3.908236E+13
9	828484.67600	3.914569E+13
10	833670.81000	3.939903E+13
11	835457.35000	3.965287E+13
12	840657.27600	3.990723E+13
13	842442.49800	4.016201E+13
14	843777.04800	4.035318E+13
15	845554.89000	4.060879E+13
16	850772.97500	4.086488E+13
17	852549.15200	4.112136E+13

186

18	859555.35200	4.163576E+13
19	864855.85600	4.241077E+13
20	873625.96200	4.318954E+13
21	877133.62500	4.371186E+13
22	882358.89000	4.449772E+13
23	885822.97800	4.502387E+13
24	898008.75000	4.634701E+13
25	906544.00000	4.768114E+13
26	914988.00000	4.902597E+13
27	923346.00000	5.038177E+13
28	931612.50000	5.174709E+13

MULTIPLE LINEAR REGRESSION ON DATA SET:

COMPLETE

--where: Dependent variable = (1) QLD PRESS
Independent variable(s) = (2) FREQUENCY
(3) TEMP
(4) FREQ^2
(5) TEMP^2
(6) FREQ*TEMP
(7) FREQ^3

FREQUENCY	28	34747.60500	1057168.20033	1028.18685	2.95902	
TEMP	28	24.56429	.14683	.38318	1.55990	
FREQ^2	28		1208415465.42920			72605313
.33213						
FREQ^2	28		1208415465.42920			72605313.33
213		6.00831				
TEMP^2	28	603.54571	351.05163	18.73637	3.10438	
FREQ*TEMP	28		853856.07739			36955
.64398						
FREQ*TEMP	28		853856.07739			36955.64
398		4.32809				
FREQ^3	28		42061522882977.80000			3848151270819
.04000						
FREQ^3	28		42061522882977.80000			3848151270819.04
000		9.14886				
OLD PRESS	28	2683.26984	8612474.29204	2934.70174	109.37035	

CORRELATION MATRIX

TABLE 2 Continued

	TEMP	FREQ^2	TEMP^2	FREQ*TEMP	FREQ^3	OLD PRESS
FREQUENCY	.8054064	.9999156	.8088850	.9785305	.9996609	.9998879
TEMP		.7993601	.9999734	.9102744	.7932068	.7984239
FREQ^2			.8028579	.9763701	.9999148	.9999980
TEMP^2				.9126952	.7967226	.8019246
FREQ*TEMP					.9740535	.9760255

FREQ^3 .9999387

ANALYSIS OF VARIANCE TABLE

SOURCE	DF	SUM OF SQUARES	MEAN SQUARE	F-VALUE
TOTAL	27	232536805.88502		
REGRESSION	6	232536804.59340		38756134.09890
FREQUENCY	1	232484682.40130		3779904323.23
TEMP	1	31442.13717		511209.04
FREQ^2	1	20679.41088		336220.84
TEMP^2	1	.09574		1.56
FREQ*TEMP	1	.39141		6.36
FREQ^3	1	.15690		2.55
RESIDUAL	21	1.29161		.06151

R-SQUARED = 1.00000

STANDARD ERROR OF ESTIMATE = .248002905259

VARIABLE REGRESSION COEFFICIENTS STANDARD ERROR

STD. FORMAT

E-FORMAT

REG. COEFFICIENT

F-VALUE

'CONSTANT'	-48411.92114	-.484119211430E+05	6961.54300	-6.95
FREQUENCY	.51292	.512924078831E+00	.62939	.81
TEMP	-47.97155	-.479715519875E+02	61.60701	-.78
FREQ^2	.00002	.156206670823E-04	.00002	.81
TEMP^2	-3.89784	-.389783860404E+01	1.58428	-2.46
FREQ*TEMP	.00698	.698161760564E-02	.00272	2.56
FREQ^3	0.00000	.284480096401E-09	0.00000	1.60

	COEFFICIENT	99 % CONFIDENCE INTERVAL	
		LOWER LIMIT	UPPER LIMIT
'CONSTANT'	-48411.92114	-67287.66911	-29536.17317
FREQUENCY	.51292	-1.19362	2.21947
TEMP	-47.97155	-215.01473	119.07163
FREQ^2	.00002	-.00004	.00007
TEMP^2	-3.89784	-8.19351	.39783
FREQ*TEMP	.00698	-.00040	.01437
FREQ^3	0.00000	-0.00000	0.00000

TABLE OF RESIDUALS

$P = \text{function}(f, T, f^2, T^2, f*T, f^3)$

OBS#	OBSERVED Y	PREDICTED Y	RESIDUAL	STANDARDIZED RESIDUAL	SIGNIF.
1	14.51920	14.46945	.04975	.20060	
2	92.61930	92.65183	-.03253	-.13117	
3	143.21800	143.29100	-.07300	-.29433	

TABLE 2- Continued

4	192.91900	192.91621	.00279	.01125
5	242.62000	242.65261	-.03261	-.13150
6	292.52000	292.58399	-.06399	-.25802
7	342.45000	342.48741	-.03741	-.15083
8	392.42000	392.35740	.06260	.25242
9	442.36000	442.23217	.12783	.51543
10	642.03000	641.75754	.27246	1.09861
11	841.70000	841.44599	.25401	1.02422
12	1041.23000	1041.09312	.13688	.55194
13	1240.83000	1240.81891	.01109	.04470
14	1390.40000	1390.43326	-.03326	-.13413
15	1589.93000	1590.15493	-.22493	-.90698
16	1789.53000	1789.90890	-.37890	-1.52781
17	1989.16000	1989.61879	-.45879	-1.84993
18	2388.83000	2389.17550	-.34550	-1.39315
19	2988.53000	2988.42560	.10440	.42096
20	3588.09000	3587.70024	.38976	1.57158
21	3987.83000	3987.75356	.07644	.30820
22	4587.33000	4587.06526	.26474	1.06748
23	4986.99000	4986.60441	.38559	1.55477
24	5986.19000	5986.30988	-.11988	-.48339
25	6985.29000	6985.50303	-.21303	-.85899
26	7984.52000	7984.69613	-.17613	-.71019
27	8984.05000	8984.24058	-.19058	-.76846
28	9983.45000	9983.20777	.24223	.97671

The following transformation was performed: $a*(X^b)+c$

where $a = 1$
 $b = 4$

$c = 0$
X is Variable # 2
Transformed data is stored in Variable # 8 (FREQ^4).

COMPLETE

Data type is: Raw data

TABLE 2 - Continued

Variable # 8
(FREQ^4)

OBS#
1 1.304738E+18
2 1.309168E+18
3 1.312050E+18
4 1.314885E+18
5 1.317724E+18

6 1.320579E+18
7 1.323438E+18
8 1.326298E+18
9 1.329164E+18
10 1.340646E+18
11 1.352175E+18
12 1.363752E+18
13 1.375373E+18
14 1.384109E+18
15 1.395812E+18
16 1.407560E+18
17 1.419351E+18
18 1.443074E+18
19 1.479000E+18
20 1.515321E+18
21 1.539805E+18
22 1.576826E+18
23 1.601734E+18
24 1.664801E+18
25 1.729002E+18
26 1.794327E+18
27 1.860792E+18
28 1.928329E+18

189

MULTIPLE LINEAR REGRESSION ON DATA SET:

--where: Dependent variable = (1)OLD PRESS
 Independent variable(s) = (2)FREQUENCY
 (3)TEMP
 (4)FREQ^2
 (5)TEMP^2
 (6)FREQ*TEMP
 (7)FREQ^3
 (8)FREQ^4

VARIABLE	N	MEAN	VARIANCE	STANDARD DEVIATION	COEFF. OF VARIATION
FREQUENCY	28	34747.60500	1057168.20033	1028.18685	2.95902
TEMP	28	24.56429	.14683	.38318	1.55990
FREQ^2	28	28	1208415465.42920		
.33213					72605313
FREQ^2	28	6.00831	1208415465.42920		72605313.33
213					
TEMP^2	28	603.54571	351.05163	18.73637	3.10438
FREQ*TEMP	28	28	853856.07739		36955
.64398					
FREQ*TEMP	28	4.32809	853856.07739		36955.64
398					
FREQ^3	28	28	42061522882977.80000		3848151270819
.04000					
FREQ^3	28	9.14886	42061522882977.80000		3848151270819.04
000					

Table 2 - Continued 1

190

FREQ^4	28	1465351199629520000.00000			181431061574866000
.00000					
FREQ^4	28	12.38140	1465351199629520000.00000		181431061574866000.00
000					
OLD PRESS	28	2683.26984	8612474.29204	2934.70174	109.37035

CORRELATION MATRIX

	TEMP	FREQ^2	TEMP^2	FREQ*TEMP	FREQ^3	FREQ^4
FREQUENCY	.8054064	.9999156	.8088850	.9785305	.9996609	.9992340
TEMP		.7993601	.9999734	.9102744	.7932068	.7869512
FREQ^2			.8028579	.9763701	.9999148	.9996581
TEMP^2				.9126952	.7967226	.7904837
FREQ*TEMP					.9740535	.9715810
FREQ^3						.9999142

	OLD PRESS
FREQUENCY	.9998879
TEMP	.7984239
FREQ^2	.9999980
TEMP^2	.8019246
FREQ*TEMP	.9760255
FREQ^3	.9999387
FREQ^4	.9997078

ANALYSIS OF VARIANCE TABLE

SOURCE	DF	SUM OF SQUARES	MEAN SQUARE	F-VALUE
TOTAL	27	232536805.88502		
REGRESSION	7	232536805.17468	33219543.59638	935323633.75
FREQUENCY	1	232484682.40130	232484682.40130	6545797876.58
TEMP	1	31442.13717	31442.13717	885279.29
FREQ^2	1	20679.41088	20679.41088	582245.86
TEMP^2	1	.09574	.09574	2.70
FREQ*TEMP	1	.39141	.39141	11.02
FREQ^3	1	.15690	.15690	4.42
FREQ^4	1	.58128	.58128	16.37
RESIDUAL	20	.71033	.03552	

R-SQUARED = 1.00000
 STANDARD ERROR OF ESTIMATE = .188458563557

VARIABLE	REGRESSION COEFFICIENTS		STANDARD ERROR	T-VALUE
	STD. FORMAT	E-FORMAT	REG. COEFFICIENT	

TABLE 2 - Continued

'CONSTANT'	β_0 365880.67293	.365880672926E+06	102543.56831	3.57
FREQUENCY	a_1 -45.92312	-.459231184092E+02	11.48827	-4.00
TEMP	a_2 .70052	.700516867297E+00	48.33665	.01
FREQ^2	a_3 .00196	.196442942156E-02	.00048	4.08
TEMP^2	a_4 -1.70039	-.170039310824E+01	1.32077	-1.29
FREQ*TEMP	a_5 .00244	.244421477546E-02	.00235	1.04
FREQ^3	a_6 -0.00000	-.359700938656E-07	0.00000	-4.01
FREQ^4	a_7 0.00000	.252876619589E-12	0.00000	4.05

COEFFICIENT	99 % CONFIDENCE INTERVAL	
	LOWER LIMIT	UPPER LIMIT
'CONSTANT'	365880.67293	86558.82475 645202.52110
FREQUENCY	-45.92312	-77.21639 -14.62985
TEMP	.70052	-130.96530 132.36633
FREQ^2	.00196	.00065 .00328
TEMP^2	-1.70039	-5.29807 1.89729
FREQ*TEMP	.00244	-.00397 .00886
FREQ^3	-0.00000	-0.00000 -0.00000
FREQ^4	0.00000	0.00000 0.00000

looks good TABLE OF RESIDUALS

$$P = f(T, T^2, f*T, f, f^2, f^3, f^4)$$

OBS#	OBSERVED Y	PREDICTED Y	RESIDUAL	STANDARDIZED RESIDUAL	SIGNIF.
1	14.51920	14.51640	.00280	0.1497	

191

4	192.71900	192.85040	.06860	.36402
5	242.62000	242.61623	.00377	.02000
6	292.52000	292.60787	-.08787	-.46626
7	342.45000	342.46749	-.01749	-.09281
8	392.42000	392.42397	-.00397	-.02104
9	442.36000	442.41599	-.05599	-.29708
10	642.03000	641.93449	.09551	.50678
11	841.70000	841.45973	.24027	1.27491
12	1041.23000	1041.14003	.08997	.47738
13	1240.83000	1240.75628	.07372	.39120
14	1390.40000	1390.31311	.08689	.46108
15	1589.93000	1589.98766	-.05766	-.30596
16	1789.53000	1789.79695	-.26695	-1.41648
17	1989.16000	1989.48475	-.32475	-1.72320
18	2388.83000	2389.08414	-.25414	-1.34851
19	2988.53000	2988.40298	.12702	.67401
20	3588.09000	3587.71258	.37742	2.00268
21	3987.83000	3987.84101	-.01101	-.05840
22	4587.33000	4587.27834	.05166	.27413
23	4986.99000	4986.89755	.09245	.49058
24	5986.19000	5986.28893	-.09893	-.52495
25	6985.29000	6985.40351	-.11351	-.60231
26	7984.52000	7984.50518	.01482	.07862
27	8984.05000	8984.08087	-.03087	-.16382
28	9983.45000	9983.40389	.04611	.24469

3.77 * 10⁻¹
3.6 * 10³

**

Durbin-Watson Statistic: 1.09986418829

3.77 * 10⁻¹ = 10 * 10⁻¹
3.6 * 10³ = .017

192

TABLE 2 - Continued

The following transformation was performed: $a \cdot (X^b) + c$

where $a = 1$
 $b = 5$

$c = 0$

X is Variable # 2

Transformed data is stored in Variable # 9 (FREQ^5).

COMPLETE

Data type is: Raw data

Variable # 9
(FREQ^5)

OBS#
1 109651E+22
2 28373E+22
3 4.440562E+22

TABLE 3
SUMMARY OF PAROSCIENTIFIC DIGI-QUARTZ
PRESSURE TRANSDUCER CHARACTERISTICS
HIGH PRESSURE, 0 TO 10,000 PSIA, MODEL _____

<u>SN</u>	<u>fo, Hertz</u>
18858	33792.449 ^a
18858	33792.529 ^a
18858	33792.429 ^b
17943	33464.268 ^a
17943	33513.895 ^b
16767	35355.653 ^a
16767	35355.953 ^b

TABLE 3 (CONT)

TEMPERATURE SENSITIVITIES

<u>SN</u>	$\alpha, \frac{df}{dT}, H_3/^\circ C$
18858	$0.2798 - 0.928 \cdot 10^{-2}T + 0.595 \cdot 10^{-5}P$
17493	$0.1723 - 1.10 \cdot 10^{-2}T + 0.11 \cdot 10^{-4}P$
16767	$0.1043 - 0.38 \cdot 10^{-2}T + 0.73 \cdot 10^{-5}P$

$\beta, \frac{d^2f}{dT^2}, H_3/(^\circ C)^2$

18858	$-0.92 \cdot 10^{-2}$
17493	$-1.10 \cdot 10^{-2}$
16767	$-0.378 \cdot 10^{-2}$

PRESSURE SENSITIVITIES

$\frac{df}{dP}, H_3/psia$

18858	$0.3682 - 2 \cdot 0.2269 \cdot 10^{-5}P + 3 \cdot 0.216 \cdot 10^{-10}P^2$
17493	$0.3689 - 2 \cdot 2.34 \cdot 10^{-6}P + 3 \cdot 2.29 \cdot 10^{-11}P^2$
16767	$0.3043 - 2 \cdot 1.28 \cdot 10^{-6}P + 3 \cdot 4.76 \cdot 10^{-6}P^2$

$\frac{df}{dP^2}$

18858	$-0.432 \cdot 10^{-10} + 1.296 \cdot 10^{-10}P$
17493	$-0.436 \cdot 10^{-5} - 2.26 \cdot 10^{-11}P$
16767	$-0.256 \cdot 10^{-5} + 2.86 \cdot 10^{-5}P$

Table 4

Long Term Repeatability at Normalized Pressure*

Nominal Pressure, psia	Initial** Pressure, psia	Mean Frequency, Hz	Std Error, Hz	Std Error, ^a psia	3 Std Error % Normalized Pressure	3 Std Error, ^b % Normalized Pressure
atm	14.	33518.2398	$3.1 * 10^{-4}$	$8.4 * 10^{-4}$	0.018	0.010
119	118.7923	33556.756	$3.74 * 10^{-3}$	$1.1 * 10^{-2}$	0.027	0.015
169	168.7266	33575.157	$9.07 * 10^{-3}$	$2.4 * 10^{-2}$	0.043	0.025
319	318.763	33630.281	$2.4 * 10^{-2}$	$5.2 * 10^{-2}$	0.057 ^c	0.03
419	418.750	33667.0125	$2.28 * 10^{-2}$	$6.0 * 10^{-2}$	0.043	0.024
719	718.593	33776.826	$2.4 * 10^{-2}$	$6.4 * 10^{-2}$	0.027	0.015
918	918.429	33849.809	$3.4 * 10^{-2}$	$9.4 * 10^{-2}$	0.031	0.018

* After temperature correction, zero shift and referenced to initial pressures.

a. Based on a maximum of six readings, some pressures have less than six readings.

b. Extrapolated to 10 readings, i.e., $\text{Std Error}_{10} = \text{Std Error}_6 \sqrt{1/3}$.

c. Based on four measurements.

** Subsequent data referenced to this value using equation.

TABLE 5
ZERO SHIFT (SN 17943)

Date	Atm Press, psia	Room Temp, °C	Actual Freq, Hz	Freq at * 14.3236 psia and 23 °C, H	Zero Shift $f_n - f_{16Apr-A}$ Hz
16 April-A	14.3236	23.5	33518.258	33518.261	0
-B	14.3188	23.5	33518.236	33518.240	-0.021
17 April-A	14.3686	22.3	33518.322	33518.312	0.051
-B	14.3724	22.8	33518.296	33518.288	0.027
18 April-A	14.4410	21.4	33518.378	33518.372	0.111
-B	14.4360	22.7	33518.280	33518.248	0.013

*Using temperature coefficient and

$$f_n = f_i + \frac{df}{dp} (P_n - P_i) + \frac{d^2f}{dp^2} (P_n - P_i)^2$$

TABLE 6

ERROR BUDGET GOALS

<u>ERROR SOURCE</u>	<u>AT 0.7Mpa(100 psi)</u>	<u>100% full scale</u>
TRANSDUCER RELATED		
Curve Fit	0.02%	0.02%
Hysteresis	0.02%	0
Zero Drift (8 hours)	0.02%	0
Full Scale Drift (120 days)	0	0.03%
Temperature Effects ($\pm 20^{\circ}\text{F}$)	0.02%	0.02%
Repeatability	0.005%	0.005%
CALIBRATION STANDARDS	0.008%	0.008%
Electronics & Math Software		
Resolution	0.005%	0.005%
Round Off & Conversion		
Conversion to Pressure		
Units	<0.001%	<0.001%
Correction of Non-		
Linearity	0.005%	0.005%
Temperature Correction	<u>0.01%</u>	<u>0.01%</u>
ROOT SUM SQUARE (RSS)	0.043%	0.045%

TABLE 7
DATA
TEMPERATURE COEFFICIENT OF PAROSCIENTIFIC TRANSDUCER

SN 18838

<u>Dates</u>	<u>Pressure (old Ruska)</u>	<u>Frequency</u>	<u>Temperature, °C</u>	<u>Notes</u>
16 Aug 84	14.5664	33794.173	4.3	
	991.4996	34151.605	4.4	40 °F
	1989.962	34512.808	4.4	Run #1
	3988.691	35222.546	4.4	
	5987.153	35916.574	4.4	
	7884.683	36595.52	4.5	
	9984.280	37260.43	4.5	
17 Aug 84	14.543	33794.42	5.3	40 °F
	991.776	34151.883	5.3	Run #2
	1990.076	34513.087	5.2	
	3988.540	35222.777	5.1	
	5987.072	35916.793	5.0	
	7985.537	36595.673	4.9	
	9983.234	37260.693	4.8	
24 Aug 84	14.5556	33795.567	10.9	50 °F
	991.451	34153.127	11	Run #1
	1989.882	34514.397	11.2	
	3988.480	35224.243	11.5	
	5987.377	35918.253	11.6	
	7985.540	36597.33	11.7	
	9984.636	37262.413	11.7	
27 Aug 84	14.5864	33795.65	10.5	50 °F

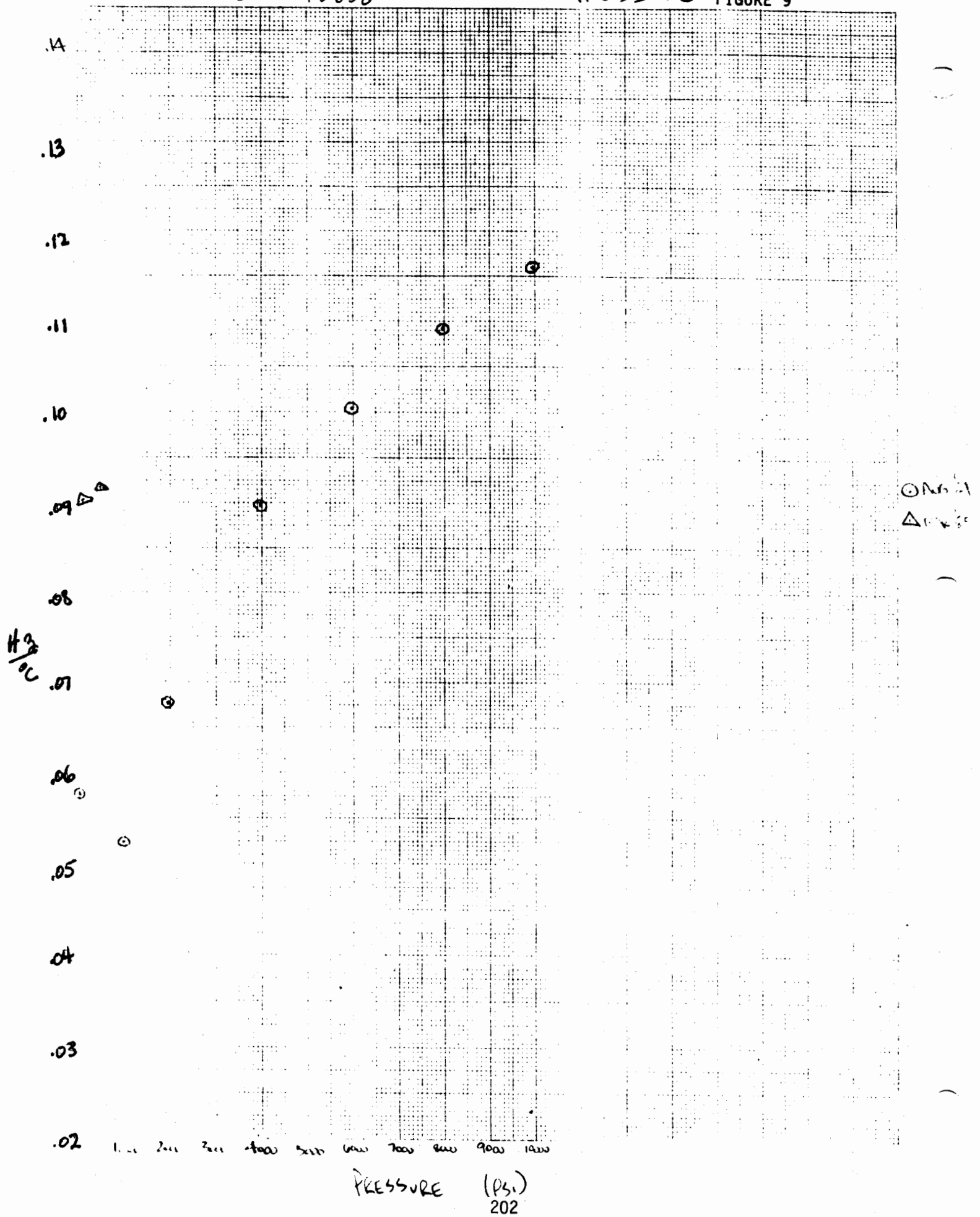
<u>Dates</u>	<u>Pressure (old Ruska)</u>	<u>Frequency</u>	<u>Temperature, °C</u>	<u>Notes</u>
	991.550	34153.143	10.5	Run #2
	1989.714	34514.39	10.5	
	3988.643	35224.18	10.5	
	5986.905	35918.31	10.4	
	7984.665	36597.27	10.6	
	9983.961	37262.23	10.5	
29 Aug 84	14.5818	33796.337	15.5	60 °F
	990.909	34153.85	15.5	Run #1
	1989.674	34515.113	15.6	
	3988.606	35225.033	15.5	
	5987.204	35919.133	15.6	
	7985.067	36598.123	15.6	
	9983.497	37263.123	15.6	
29 Aug 84	14.5586	33796.397	15.6	60 °F
	991.288	34153.91	15.6	Run #2
	1989.540	34515.133	15.7	
	3988.838	35225.083	15.7	
	5986.934	35919.14	15.7	
	7985.327	36598.113	15.7	
	9984.123	37263.143	15.7	
30 Aug 84	14.5506	33796.9	21.0	70 °F
	991.417	34154.447	21.0	Run #1
	1990.014	34515.740	21.0	
	3988.876	35225.767	21.0	
	5986.937	35919.87	21.1	
	7985.130	36598.87	21.0	
	9983.724	37263.943	21.0	

<u>Dates</u>	<u>Pressure (old Ruska)</u>	<u>Frequency</u>	<u>Temperature, °C</u>	<u>Notes</u>
31 Aug 84	14.5384	33796.9	20.9	70 °F
	991.236	34154.403	20.9	Run #2
	1989.534	34515.74	20.9	
	3987.894	35225.747	21.0	
	5986.357	35919.82	21.0	
	7985.552	36598.893	21.0	
	9983.818	37263.96	21.0	
5 Sep 84	14.5914	33797.233	26.5	
	991.522	34154.84	26.5	80 °F
	1989.952	34516.143	26.6	Run #1
	3988.514	35226.323	26.6	
	5986.611	35920.587	26.7	
	7985.172	36599.827	26.7	
	9983.936	37264.657	26.8	
6 Sep 84	14.6216	33797.22	25.7	80 °F
	991.754	34154.843	25.8	Run #2
	1990.019	34516.173	25.8	
	3988.949	35226.28	25.9	
	5987.212	35920.43	26.0	
	7986.176	36599.61	26.0	
	9984.669	37264.657	26	
7 Sep 84	14.6302	33797.24	31.7	90 °F
	992.194	34154.98	31.8	Run #1
	1989.959	34516.35	31.8	
	3988.922	35226.53	31.9	
	5987.884	35920.78	31.9	
	7986.113	36600.053	32	
	9984.692	37265.18	32.1	

<u>Dates</u>	<u>Pressure (ole Ruska)</u>	<u>Frequency</u>	<u>Temperature, °C</u>	<u>Notes</u>
18 Sep 84	14.6016	33797.263	32.3	90 °F
	991.567	34154.9	32.3	Run #2
	1989.498	34516.287	32.3	
	3988.896	35226.487	32.4	
	5987.627	35920.763	32.4	
	7986.356	36600.07	32.4	
	9984.354	37265.217	32.4	
20 Sep 84	14.4802	33797.16	34.9	100 °F
	991.577	34154.81	34.8	Run #1
	1989.706	34516.227	34.9	
	3988.535	35226.487	34.9	
	5986.632	35920.79	35.0	
	7985.730	36600.14	35.0	
	9984.828	37265.247	35.0	
21 Sep 84	14.4976	33797.16	34.8	100 °F
	991.263	34154.803	34.7	Run #2
	1990.527	34516.22	34.6	
	3988.858	35226.573	34.8	
	5987.087	35920.833	34.9	
	7984.517	36600.167	34.8	
	9983.612	37265.287	34.9	

SN 18858

TC² vs PRESSURE FIGURE 9



APPENDIX

FREQUENCY COUNTER SENSITIVITY

Assume a measurement of 200 psia and one wants a resolution of ± 0.005 percent (1/10 of the desired error limit of ± 0.05 percent).

The Digiquartz transducer has

$$\frac{df}{dp} \approx 0.35 \text{ Hz/psia}$$

and

$$\frac{\Delta p}{p} \approx 5 * 10^{-5}$$

hence,

$$\Delta p = 5 * 10^{-5} p = 0.01 \text{ psia}$$

$$\frac{df}{dp} * \Delta p = 0.35 \frac{\text{Hz}}{\text{psia}} * 10^{-2} \text{ psia}$$

$$df = 0.0035 \text{ Hz.}$$

" ARONSON "

SHOCKLESS PRESSURE-STEP GENERATOR

BY: J.F. LALLY, Pres.
PCB Piezotronics, Inc.

PRESENTED AT: THIRTEENTH TRANSDUCER WORKSHOP
June 4 to 6th 1985
Monterey, Ca.

Sponsored by: Vehicular Instrumentation/Transducer
Committee of Range Commanders Council.
Telemetry Group



PCB PIEZOTRONICS INC. 3425 Walden Ave. Depew, N.Y. 14043

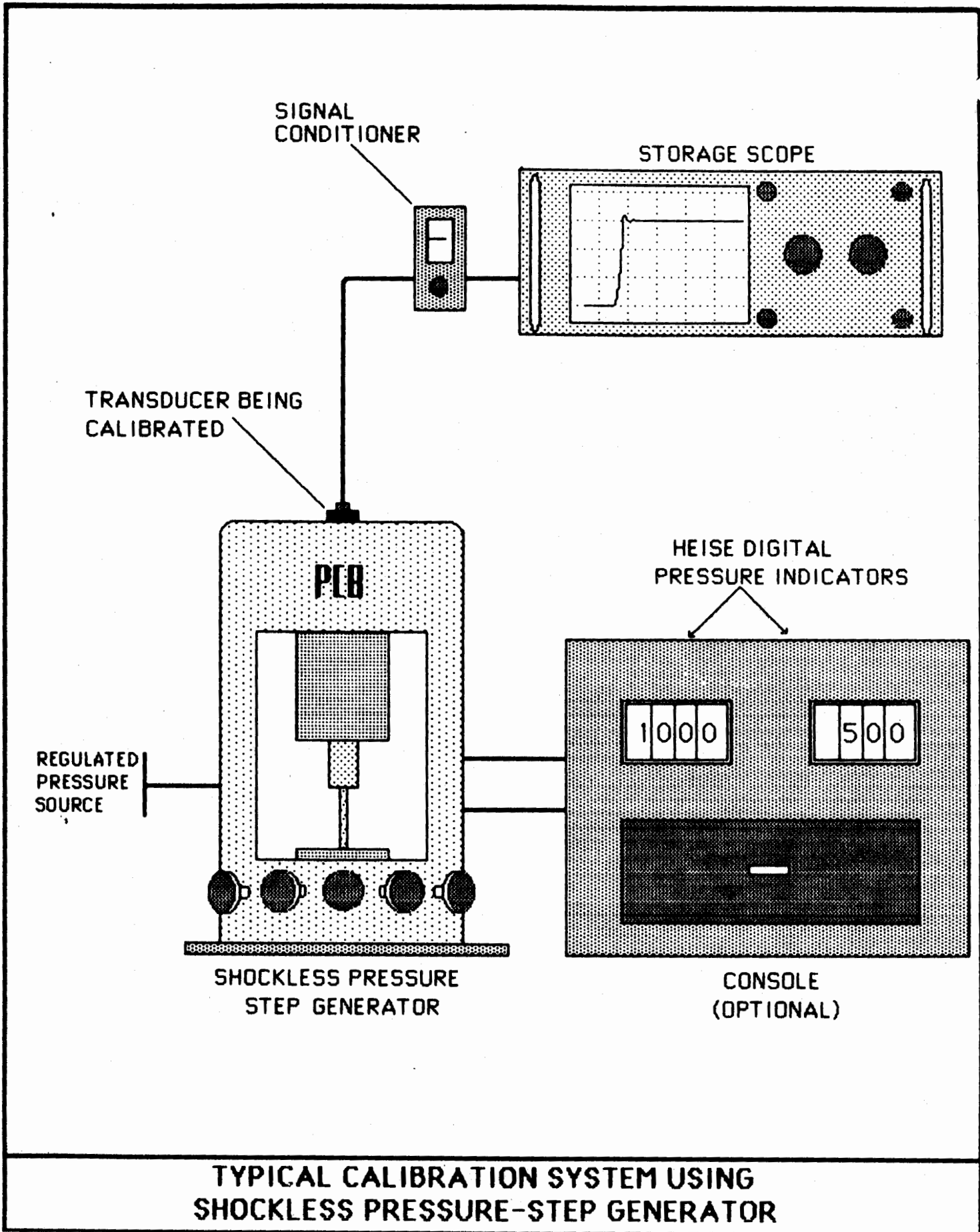
SHOCKLESS PRESSURE STEP GENERATOR

The "Shockless" pressure step generator is a device used to calibrate pressure transducers. It simply applies a known static pressure quickly. The term "shockless" describes the capability to generate a step change in pressure by a means other than a "shock tube." A quick opening poppet valve is used to produce a known step pressure with a rise time less than 50 microseconds. A typical system consists of the step pressure generator, a regulated pressure supply, accurate static pressure gages (Ref. D) and a readout instrument.

(See Figure 1)

The pressure step generator was invented by Philip Aronson and Robert Waser at the U.S. Naval Ordnance Laboratory where the first unit was constructed. Later it was produced under license from the U.S. Navy by a company called Application Technologies. When Phil Aronson, one of the founders of Application Technologies, passed away several years ago, the officers of the company decided the device could best serve the industry through a company deeply involved with dynamic measurements. PCB signed a sub-license agreement with Applications Technologies and the U.S. Navy for manufacturing rights to the Shockless Pressure Step Generator. In recognition of the years of devotion and effort Phil gave to the field of dynamic measurements, PCB renamed the device the "Aronson Dynamic Pressure Step Generator" in his honor.

Devices employed in the dynamic calibration of pressure transducers are described in ANSI Standard B88.1 "Guide for Dynamic Calibration of Pressure Transducers" (Ref. A), and "Specification and Tests for Piezoelectric Pressure and Sound Pressure Transducers" (Ref. B). These standards describe



TYPICAL CALIBRATION SYSTEM USING SHOCKLESS PRESSURE-STEP GENERATOR

several types of pressure generators including the shock tube, sinusoidal pressure generator, pressure step generators and others. Refer to the ANSI standard for a more detailed description of all these devices.

The SINUSODIAL PRESSURE GENERATOR creates a pulsating pressure which is usually limited in both amplitude and frequency. The absolute amplitude level is generally not known and must be measured by another "reference" transducer (Ref. A). This involves the use of a "pressure transfer standard" and leads back to the question of how it is calibrated.

The SHOCK TUBE is capable of generating pressure steps with rise times in the nanosecond range when operated in the reflected mode. The duration of the pressure step may be only a few milliseconds. The amplitude is computed from theoretical equations based on measurement of initial driver pressure as well as incident shock wave velocity, and sound speed of the gas in the low pressure chamber. Accuracy of the amplitude of the step change can only be determined to a few percent. The very fast rise time and short step duration of the shock wave can create problems when trying to calibrate pressure transducers with over or under damped natural frequencies. Such transducers either do not respond quickly enough or ring too long for a reasonable calibration by this method. The shock tube, measurement instrumentation and set-up time involved, make this one of the more costly methods of dynamic calibration.

The ARONSON PRESSURE STEP GENERATOR is capable of performing dynamic calibration with greater accuracy, speed and ease of operation than is possible with most other methods. The concept and operation of the step pressure

ARONSON SHOCKLESS PRESSURE-STEP GENERATOR

- A. PRESSURE RESERVOIR
- B. GAGE ADAPTOR PLUG
- C. PRESSURE TRANSDUCER
- D. POPPET-VALVE HEAD
- E. POPPET VOLUME
- F. COMPRESSION SPRING
- G. STEM
- H. POPPET LIFTER
- J. POPPET LOCKDOWN TAB
- K. IMPACT WEIGHT
- L. GUIDE TUBE
- M. IMPACT PLATE
- N. TRIGGER CONNECTOR
- P. HOUSING SUPPORT

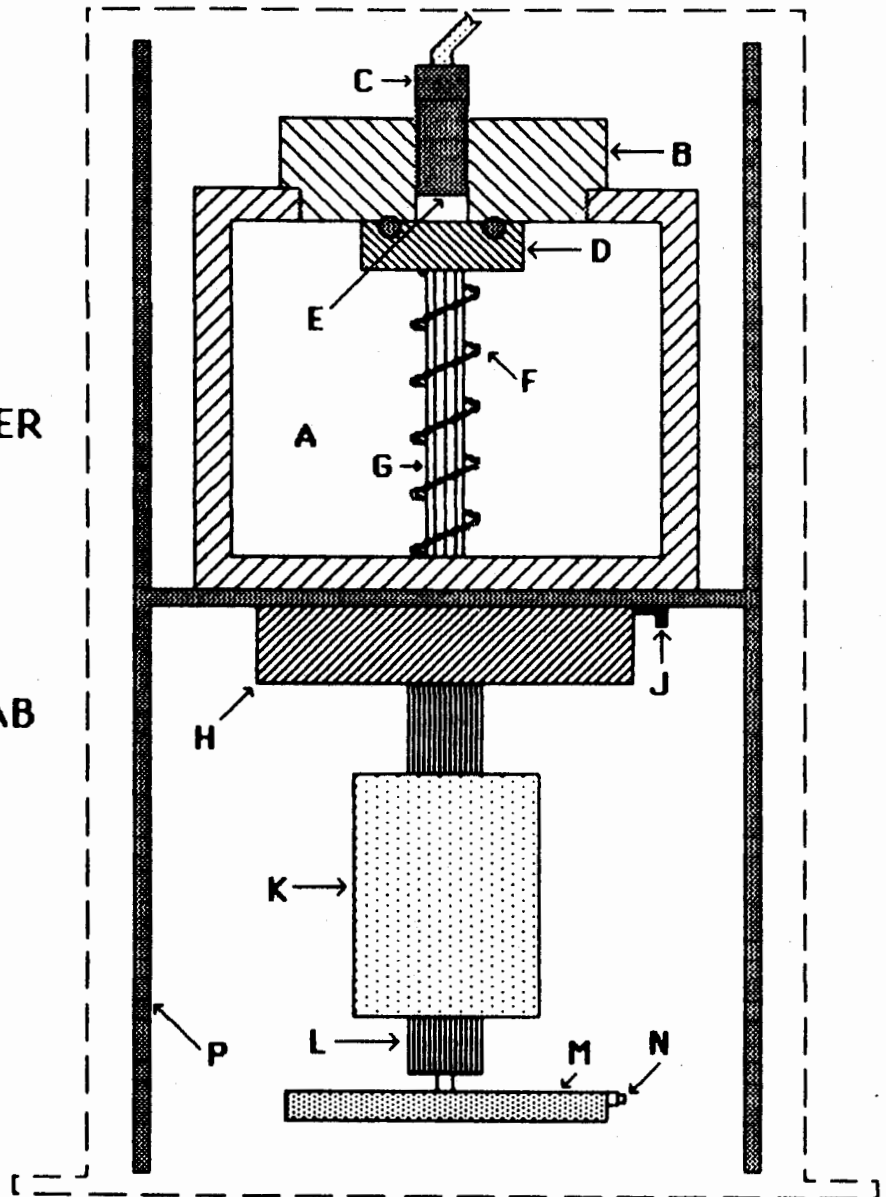


FIGURE 2
MECHANICAL SYSTEM DIAGRAM

generator is quite fundamental. It simply involves applying to the transducer a known static pressure very quickly. This is accomplished by setting a known static pressure in a reservoir, as measured by a highly accurate static pressure gage, and exposing the transducer to the pressure by means of a quick opening poppet valve. (See Figure 2). Dropping weight "K" causes the poppet to open quickly exposing the transducer to the known static pressure in reservoir "A." At the same time, a trigger signal is generated from a sensor in the impact plate "M."

The step pulse generator is easily adjusted to provide an initial pressure on the diaphragm end of the pressure transducer (poppet volume "E") of any desired value from 0 psia to 1000 psig. At the same time, it is capable of producing a known step pressure change of any desired amplitude up to 1000 psi on top of the initial pressure on the transducer. The capability to set different static pressures in chambers "A" and "E" and then switch rapidly between them offers several different calibration or test modes.

The Aronson Pressure Step Generator has a number of unique features which make it a useful device for applications requiring the generation of fast rising, long-duration, known pressure steps. A few of these applications are:

- * Dynamic calibration of pressure transducers. (See Figure 3)
- * Static vs. dynamic comparison calibration of a pressure transducer with the same pressure amplitude without removing it. (See Figure 3a)
- * Calibration of incremental pressure steps above or below preset static levels. It is possible to simulate the static pressure environment on the sensor diaphragm, while applying pressure steps of known amplitude.

- * Calibration of either positive or negative-going pressure steps.
(Figure 3a & b)
- * Calibration to determine damping characteristics of sensors.
- * The measurement of response times of ducts and cavities involved with recessed diaphragms. (Figure 3d) (Ref. C)
- * Measurement of discharge time constant of a transducer or complete measuring system. (Figure 3c)
- * Quick checkout of blast and shock wave transducers. Malfunctions are readily detectable when observing response to step pressure change on a storage oscilloscope.

The Aronson pressure pulse generator is supplied with a variety of adaptors for installing different sensors. Special adaptors are available for installing pencil and "pancake or lollipop" style blast probes. Several poppet valve heads are supplied to minimize volume at the sensor diaphragm. The smaller the volume, the faster the pressure rise time.

The reference gage console may be ordered with the step pressure generator or provided by the customer. The regulated pressure source is supplied by the customer. Helium will provide the fastest rise time.

Fig. 3a

Response of 113A24 500K Hz Pressure Transducer to 500 psi step change.

Rise Time 27 μ S
Helium

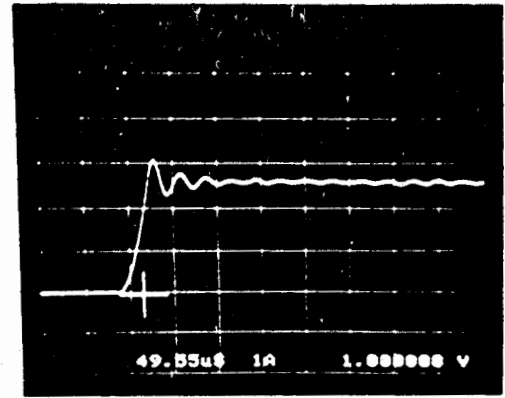


Fig. 3b

Response to 10 psi vacuum

Rise Time 65 μ S

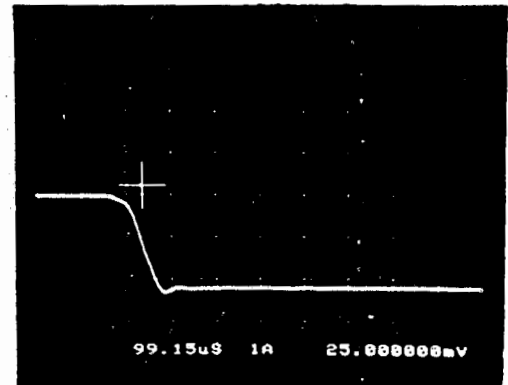


Fig. 3c

Time Constant 1.54 Sec.

Step change 100 psi

Helium Gas

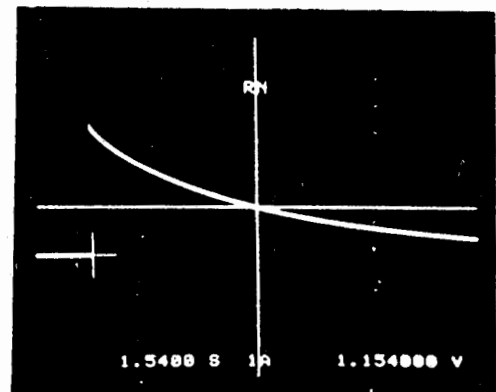


Fig. 3d

Cavity Resonance

Mod. 113A21 Sensor
Diaphragm recessed .320 in.
Cavity Diameter .220 in.
Resonance \approx 12K Hz

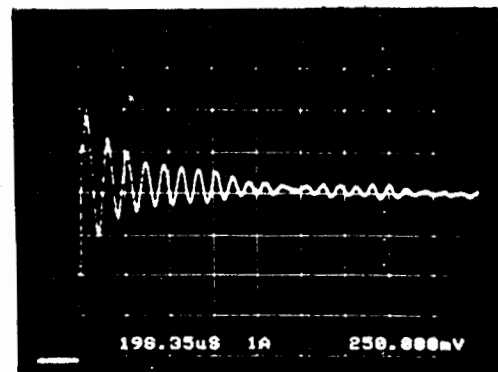


FIGURE 3.

References

- (A) "A Guide for the Dynamic Calibration of Pressure Transducers"
(B88.1 - 1972) American National Standards Institute.
- (B) "Specifications and Tests for Piezoelectric Pressure and Sound Pressure Transducers" (ISA-S-37-10 1982) Instrument Society of America.
- (C) "Response Tests of a Sputtered Gage Pressure Transducer"
(UCID-19466 1982) Lawrence Livermore Laboratory.
- (D) "Bulletin DP-1 Heise Series 7 Digital Pressure Indicators" Model 710A
0.1% span accuracy, Dresser Instrument Division, Newtown, CT.

ARONSON
DYNAMIC PRESSURE PULSE
CALIBRATOR
Model 907A



Developed by P. Aronson for US Navy Ord Lab

- generates rapid step pressure change
- adjusts pressure step amplitude over wide range
- produces positive or negative step changes
- compares static versus dynamic response
- operates in simple manual mode

The Model 907A Pressure Step Generator is a versatile, precision device used for dynamic calibration of pressure transducers. It may be used to calibrate transducers with a positive or negative-going step change in pressure, a small incremental change under high static conditions, vacuum, or for dynamic vs. static response comparison measurements. Because of its fast rise time, wide range, quick setup and ease of operation, the 907A meets the need for a practical dynamic calibrator long sought by instrumentation specialists.

As shown in the simplified schematic, the 907A consists of a pressure reservoir (A), gage adaptor plug (B) for mounting the transducer (C) being calibrated, a poppet valve (D) for sealing off the small volume (E) immediately in front of the transducer, a housing and support system (F), and precision high pressure valves for adjusting and controlling the gas pressure at the transducer and reservoir.

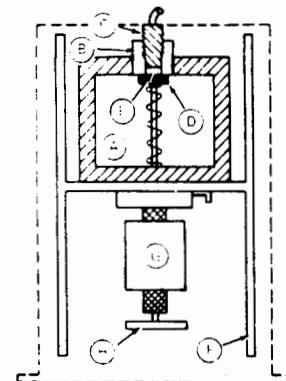
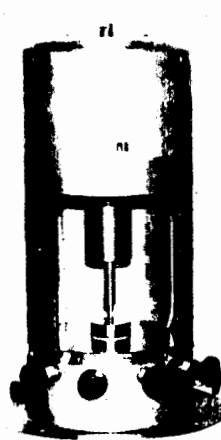
The generator relies on state-of-art techniques to achieve rapid opening of the poppet allowing the gas to flow from the reservoir to the transducer or vice versa. The poppet valve is opened rapidly by dropping weight (G) against impact plate (H). A piezo sensor on the impact plate generates an electrical output for triggering an oscilloscope.

The 907A can produce positive or negative pressure steps depending on the pressures set in the reservoir and in poppet volume. If initial pressure in the reservoir is higher than the poppet volume, a positive step results when the poppet is opened. If pressure is higher in the poppet volume, a negative pulse results.

The rise time of the pressure pulse generated depends on (1) type of gas used, (2) diameter of the poppet valve, (3) initial pressure difference across the poppet valve, (4) design of the transducer undergoing calibration and degree of flush mounting, and (5) design of the poppet valve and its opening system. Helium gas produces the fastest rise time. The 907A produces rise times of $\cdot 35$ microseconds at 1000 psi with helium gas, and $3/8$ -inch poppet valve. Nonflush diaphragm transducers have longer rise times.

The amplitude of a pressure step equals the difference between the final and initial pressure on the sensor. For most small flush diaphragm sensors, the poppet volume may be as small as $2/1000$ of reservoir pressure which means negligible reservoir pressure drop when the poppet valve is opened. Repeat calibrations can be run quickly with minimum adjustment of the reservoir gas pressure.

Since the initial pressure on the transducer diaphragm in the poppet volume can be set to any level, step changes above or below atmospheric can be made. Within the pressure limits of the device, it may be possible to simulate the pressure environment in which the transducer is to operate.



A - pressure reservoir B - gage adaptor plug C - pressure transducer D - poppet valve E - poppet volume F - housing and support system G - impact weight H - impact plate

A special lifting and locking mechanism facilitates seating the poppet valve for high pressure and locks the valve open or closed when static and dynamic comparison calibrations are done on the same transducer without removing it.

The 907A is not a stand alone calibrator. It requires a gas supply, a vacuum source if subatmospheric pressure is required, and two accurate external dial type static reference pressure gages for measuring the initial and final pressure on the transducers being calibrated. Model 907A05 is supplied complete with two 1000 psi reference gages and plumbing ready to connect to your pressure source. Lower pressure gages reading in both psi and bars can be supplied, if specified.

The gas pressure reservoir is hydrostatically tested to 4000 psi (272 bars) thus gas pressures to 2000 psi (136 bars) can be used safely.

Accessories furnished

Three Poppet valves - one blank for sensors to 1 inch, one for sensors under .5 inch and one for under .25 inch

Three transducer mounting adaptors - one with $3/8-24$ thread, one for PCB standard $5/16-24$ 'C' configuration mount, and one blank plug to accommodate up to 1 inch diameter sensor.

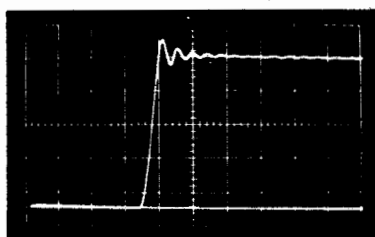
SPECIFICATION: Model No. 907A

Pressure Step Amplitude	0 to 1000 psi
Step Rise Time (10-90%)	35 microseconds (obtainable with a positive going pressure step of 1000 psi, a $3/8$ -inch diameter poppet valve, and helium gas)
Max Reservoir Pressure	2000 psi
Pressure Step Direction	Positive or negative going
Working Medium	Any noncorrosive gas
Max Transducer Size	1.00 inch diameter
Operating Mode	Manual
Calibration Modes	Dynamic and static (in place)
Locking Mechanism	Keeps poppet valve open or closed during static calibration
Trigger Signal Generator	Self-contained piezoelectric impact sensor for triggering external recording devices
Construction Materials	Stainless steel and aluminum
Gas Pressure Controls	6 precision stainless steel (316L) high pressure manually operated valves
Gas Access Ports	4 Swagelok type AN connectors 2 for gas pressure/vacuum sources; 2 for external static reference gages
Physical Size	12 inches max diameter, 21 inches max height
Weight	75 pounds

NOTE: Not furnished with the generator but required with its use - gas pressure and vacuum sources, 2 static-type pressure gages and/or manometers.

Optional Model with reference dial gages: 907A05

Response of PSG to a 1000 psi step.



Gas: helium
Initial Pressure (baseline): 14.7 psia
Sweep speed: 50 μ s major division

CERAMIC DIAPHRAGM THICK FILM STRAIN GAGE PRESSURE TRANSDUCER

Presented to the Range Commanders Council

June 1985

By Jean-Pierre Pugnare, DJ Instruments, Inc.

Appendix: An Introduction to DJ Transbar
Pressure Transducers
A New Technology

The latest entry into the field of piezo resistive technology is the "thick film" strain gage deposited upon a ceramic substrate. (U.S. Patent #4311980 of January 1982)

The high temperature (850°C), direct fusing of the strain gage to the ceramic creates an intimate bond without use of an intermediate system. This, coupled with the excellent elastic properties of ceramic, result into a stable, repeatable and hysteresis free system.

MANUFACTURING PROCESS:

The lead wires are first screen printed upon a polished 96% ceramic diaphragm and fired in a multizone high temperature oven using a specific temperature profile. The strain gages (strain sensitive conductive ink) are then printed, dried and fired at high temperature again following a very specific profile. A glass frit is printed around the periphery of the diaphragm and the corresponding area of a thick ceramic back plate. After fusing of the glass areas, the diaphragm and back plate are clamped together with a specified force and fired to the glass melting temperature resulting in a sealed joint.

On the outer face of the back plate, thick film resistors for bridge balance and span calibration together with associated leads have been deposited by the previously described process. Electrical connections between the back plate and diaphragm circuits are made via a conductive material injected into holes provided on the back plate.

For absolute pressure sensors, the pressure reference hole on the back plate is solder sealed in a vacuum chamber.

After hermeticity check, the sensors are zero balanced and span trimmed by computer controlled sand blasting machines. The result is a pressure capsule ready for installation into a housing or directly into a cavity provided in the customer's system.

Since the entire manufacturing process is automatic, the result is a uniform, high quality and low cost product.

INHERENT FEATURES:

This technology, commercially known as Transbar, offers the following advantages:

- Excellent media compatibility
- Excellent long term stability of span and zero
- Freedom from thermal hysteresis
- Excellent elastic properties
- Excellent resistance to shock and vibrations
- Ideal for sanitary applications
- Excellent diaphragm abrasion resistance
- Low apparent strain (35 PPM/°F)
- High temperature potentials (1000°F)
- Non magnetic
- Excellent thermal conductivity
- High resistance of circuit to case
- Low current drain
- Low cost

GAGE FACTOR:

In a uniaxial strain field, the gage factor is in the range from 6 to 10. It varies somewhat with the ink resistivity and grain size, the gage geometry and the direction of the current with respect to the strain. In a biaxial strain field however, the gage factor experimentally determined differs greatly from the theoretical.

The classical definition of gage factor does not apply to the thick film strain gage and work is being done to elucidate its piezo resistive properties.

For example, the strain gage at the center of a uniform thickness, clamped pressure diaphragm has a $\left| \frac{\Delta R}{R} \right|$ which is approximately twice that measured from the gage located at the diaphragm's edge.

There is no doubt that the non classical behavior of the thick film strain gage offers new challenge as well as opportunities to the transducer designer.

Two basic ink resistivities are used; the 10k ohm per square and the 1k ohm per square. For practical reasons, the strain gage active area is approx. .050" x .050"; therefore two basic bridge impedances are available: 10k ohm and 1000 ohm.

THE PRESSURE CAPSULE AND ITS BEHAVIOR:

The result of the manufacturing process previously described, is a solid state pressure sensor available in pressure ranges from 1.5 psia or g to 5000 psia or g and in various models. Model CS is the basic sensor, not zero balance. The zero load output of the CS series can be several times the full scale output. Model CA is a CS sensor which has been zero balanced within .2mv/v or approx. 3% of full scale based on the max. recommended pressure range. Model CP is a CA sensor span calibrated. For general specifications, refer to the Appendix.

ZERO TEMPERATURE EFFECT:

The zero TC value given in the specifications ($\leq .003\text{mv/v}/^{\circ}\text{F}$) is for uncompensated sensors. Capsule can be selected for better zero TC.

THERMAL EFFECT ON SPAN:

The capsule exhibits an uncompensated span drop of nearly 3% of reading per 100°F temperature rise. This characteristics being inherent to the gage/ceramic system is linear and quite repeatable from unit to unit and lot to lot.

This slope can easily be corrected by using a thermistor-resistor network or silicon diodes. Refer to the Appendix for details.

STABILITY:

Tests performed on Transbar indicate excellent zero and span stability. Sensors were subjected to 2×10^6 full scale pressure cycles without noticeable span change. Thermal cycling from -25°C to $+125^{\circ}\text{C}$ and 2000 hours exposure at 125°C did not result in any apparent zero nor span changes. Long term zero stability as expressed in percent of full scale (based on the max. recommended range) is typically .10% per year.

SENSOR SELECTION:

Since the Transbar technology offers unique characteristics, selection of a model to fit a specific application is somewhat different from that normally used.

The ceramic structure being an excellent elastic material, it behaves like a single crystal and is therefore limited in its overload capability. (The elastic limit and yield points being very close to each other). On the other hand, it is free from hysteresis or creep and exhibits very low thermal hysteresis. The total error band indicated on the bulletins in the Appendix is mostly due to non-linearity. The hysteresis and repeatability combined are less than .05% of full scale.

Selection of a model is first predicated on the max pressure requirement of the system. Since the natural frequency of the Transbar is high (6500 Hz to 50kc depending on range) the max dynamic pressure must be considered. To maximize accuracy (non linearity excluded) the output signal of the sensor expressed in mv/v should be as high as possible (signal to noise ratio). Refer to chart in the Appendix for sensor selection.

TEMPERATURE LIMITATIONS:

The transbar sensor is limited to 260°F due to the conductive material used for connections to the back plate. The glass seal is the next thermal limitation.

An interesting potential of the technology is for high temperature applications. A special sensor design is required, in which the outer ring is an integral part of the diaphragm, thus avoiding the glass joint thermal limitation. Connections to the sensor circuitry can be made by welded leads or possibly brazed terminal pins. Due to the high temperature manufacturing process and the excellent elastic behavior of ceramic at elevated temperature, it is possible to design a transducer capable of operating in the 1000/1200°F range.

INSTALLATION:

The Transbar pressure capsule is inserted into a cavity with an "O" ring seal and a clamping ring is used to preload the O ring and take up the reaction force. Details drawings of suggested installation schemes with recommended O ring sizes for each model are in the Appendix.

Special designs can be conceived for low pressure applications (below 200 psi) in which the pressure can be applied to the sensor thru a small dia tube soldered to a metalized hole on a front ceramic plate mounted on the capsule in the same manner as the back plate.

MEDIA COMPATIBILITY:

Just as ceramic contrasts greatly with common metals in physical properties; it does also in regards to chemical properties. Corrosion resistance of alumina is outstanding upon exposure to nearly all chemicals except HF, some fluorene solutions and strong aqueous alkaline solutions such as sodium hydroxide.

HIGH ACCURACY PRESSURE TRANSDUCERS:

Due to its outstanding stability, elastic properties, minimal thermal hysteresis and therefore good repeatability, the Transbar capsule is an ideal basic component of a microprocessor base high accuracy pressure transducer. The Transbar excellent thermal conductivity allows a temperature sensor mounted on the sensor base plate to faithfully transmit to the computer the thermally dependent parameters.

TRANSBAR WITH HYBRID ELECTRONICS:

The Model CC sensor is a 1 to 5 volt output device temperature compensated for mounting into a customer's housing. Model CC is available in a rugged housing for industrial use (Model TB) refer to the Appendix for specifications.

Available soon is a 4 to 20 ma transmitter in the TB or CC package.

BENDING BEAMS AND SENSING ELEMENTS:

The thick film technology lends itself naturally to the low cost manufacture of bending beams, deflection sensors or sensing elements for accelerometers, inclinometers or torsional sensors.

Since such devices must meet very specific requirements of range, deflection, etc., sensors must be designed specifically to meet these requirements.

Due to the elastic properties of ceramic, the anchoring of the device requires special embedment to avoid stress concentration. Bending beams up to 100 lbs. range are practical and force sensors in the 5 lbs. range have been produced in large quantity for a European customer. Due to the initial investment in design and tooling, these devices are economical only when quantity are large enough and therefore of interest to the OEM market.

SENSORS FOR SHOCK
PRESSURE MEASUREMENTS IN CONFINED EXPLOSIVES*

JAMES G. FALLER
J. DAVID DYKSTRA
US Army Combat Systems Test Activity
Aberdeen Proving Ground, MD 21005

ABSTRACT

The feasibility of making shock pressure measurements in munitions was investigated using manganin and carbon piezoresistive element gages. The gages were evaluated in two separate test setups; a preliminary experiment and an explosive test of a structural model in which carbon gages were applied to inert munitions stored on a magazine floor. It was found that the strain sensitivity of the gages coupled with the geometric complexity of the test setups made the results difficult to interpret. It was, however, possible to show through theoretical analysis that these results were in general believable if not well understood.

INTRODUCTION

The likelihood that an explosion can be transmitted from one round to the next makes stored munitions vulnerable to large-scale detonations. A massive explosion in a munitions storage area represents a particular hazard which has been the subject of a variety of studies. Although the velocity of the impacting surface can be correlated with the go/no-go detonation behavior of the stored munitions, it cannot be determined from velocity measurement how closely the munitions may have come to reacting. To obtain information on this point, it was thought desirable to measure the shock pressures induced in the munitions themselves. Pressure data could then be compared to the well-known p^2t criterion (p = pressure, t = time), which appears to apply to shock-induced chemical reactions in TNT-based explosives.

USACSTA undertook to evaluate the feasibility of making shock pressure measurements in the munitions. Any suitable methodology had to be developed quickly to apply it in time to scheduled model tests. With this goal in mind, a small scale field experiment was designed and conducted. The experiment resulted in gaining a working knowledge with two types of piezoresistive element gages, the manganin gage and the carbon gage. Three trials were carried out in this preliminary experiment. These were followed by three trials with inert rounds placed on structural models being tested for other effects. The results of these tests are presented and analyzed in this paper.

First presented at the 31st International Instrumentation Symposium sponsored by the ISA at San Diego, CA, May 6-9, 1985.

PROCEDURES

In 1979 US Army Ballistic Research Laboratory (BRL) published results of experiments on impacted explosives in which manganin foil gages were used. The high and variable strain sensitivity of the manganin gage introduced sizeable errors in the pressure records. This problem was overcome with some success by the use of constantan strain gages adjacent to the manganin gages to provide an independent strain record. This was then used to correct the pressure record. Since the BRL study a new gage element, the so-called carbon gage, has become available [1]. This gage has much higher pressure sensitivity and relatively less strain response and appears to offer some advantages for pressure measurement below 50 kbars.

Both manganin and carbon gages were selected for testing. The manganin gages are in the form of an etched foil grid on a flexible plastic backing, similar to a small foil strain gage. The carbon gage consists of a linear deposited film element between metal leads on a similar backing. Both respond to pressure with a change in their electrical resistance, increasing for the manganin and decreasing for the carbon element. The resistance change of the carbon gage is nonlinear but a calibration curve supplied by the manufacturer (Fig. 1) permits reduction of resistance versus time records to pressure-time history. The response time of the sensors is claimed to be 50 ns or better [1]. Useable measuring ranges are from 0.1 to 200 kbars for manganin sensors and 0.1 to 50 kbars for carbon.

Both types of sensor are sensitive to strain as well as pressure. Data provided by the manufacturer (Fig. 2) indicates that the strain coefficient for manganin is a function of strain level, varying from 1 to 2 over a strain range of 0.1 to 4% and remaining nearly constant at 2 above that range. The coefficient for carbon appears to be a constant 2 over the range from 0 to 1% and no data are presented above that level. Limited local testing at low strain seems to indicate a higher value, perhaps as much as 3.2. Considered in relation to the pressure response, however, the carbon gage has a significant advantage since its pressure coefficient of resistance is nearly 20 times greater than that of manganin in the range of interest.

During the preliminary experiment constantan foil strain gages were mounted adjacent to each pressure sensor to allow estimation of the strain levels and possible correction of the pressure data. Constantan has very little response to pressure so the resulting records were expected to be nearly pure strain. Strain measurement was necessarily omitted from the model test due to shortage of recording channels.

Due to the low sensitivity of manganin and the need to keep circuit resistance low in order to respond to very rapid events, most users of manganin gages for shock measurement have used a high powered pulse to excite a bridge circuit containing the gage. Because of the difficulty expected in obtaining reliable triggering of the pulser in the field environment, and the expectation of needing an expendable power source for later model tests, a different approach was used here. The circuit is shown in Figure 3. The resistor in series with the gage provides a quasi-constant current excitation for maximum signal at a given power level and the capacitor coupling eliminates the DC level on the gage without use of a bridge circuit. Use of a 4-wire connection with the series resistor near the gage minimizes cable capacitance effects.

Measurement of excitation voltage and series resistance and recording of the effect of a known calibration resistor shunted across the signal voltage lines permits calibration of the recording system in terms of resistance change in the gage. The same circuit configuration was used with the carbon and strain gages with necessary changes in the resistance values. For the model tests, the excitation supply was replaced by a 12 V mercury battery near the gage so that only a shielded 2-wire line was required from the model to the recording site.

The amplified gage output signals were recorded on analog magnetic tape and, for the preliminary experiment, a digital oscilloscope. The digital recorder was a 4-channel Nicolet (model 4094) operated at a sampling rate of 2 MHz. The analog tape (Honeywell model 101) was run at 120 ips in Wideband I FM mode providing a bandwidth of 80 KHz. Both systems appear to have an effective rise-time of about 3 μ s.

Three preliminary trials were carried out using the experimental arrangement sketched in Figure 4. A 2.3-kg (5-lb) charge of TNT was detonated 0.4 m (1.3 ft) below a 61-cm by 91-cm by 3.8-cm (24-in. by 36-in. by 1.5-in.) steel plate on which rested an instrumented steel cradle holding an instrumented section of steel pipe filled with paraffin. The cradle had a strain gage and either a manganin or carbon gage mounted at the center of the underside against the plate (Fig. 5). The underside was slightly recessed at the center and chamfered along the edges to protect the gages and wiring. A gage pair similar to that on the cradle was installed on the bottom of the inner surface of the pipe. Of the three preliminary trials, the first was used to test the manganin gage and the remaining two, the carbon gage. In trial No. 3 two additional gages were installed, a strain gage attached to the plate and a free floating carbon gage sandwiched between the cradle and plate. The plate-to-cradle and the pipe-to-cradle interfaces were greased to assure good coupling.

The model test setup is essentially as shown in Figure 6. Two trials were done on quarter-scale models and one trial, on a half-scale model. In the smaller models, two wax-filled (1.70 g/cm³) pipe bombs were stacked one above the other supported 3.2 cm (1.25 in.) above the model surface. The lower pipe bomb was instrumented with a carbon gage on the ID surface. Although it was intended that the pipe bombs be arranged with the gage down, the actual tests as revealed by photographs were done with the gage in the 10 o'clock (1st trial) and 3 o'clock (2nd trial) positions. On the half-scale model, three inert-loaded munitions were instrumented. They were placed with the gages toward the floor on the bottom of a short stack of two rows and on the top and bottom of a stack of six rows of munitions. Two velocity meters, two sets of contact pins, and a flag against a ruled grating were used on the models to measure the model surface velocity by electronic and visual means.

The projected schedule for testing and the lack of prior experience among USACSTA personnel in the area of high shock measurement led to an initial test design based more on intuition and rough analogy with earlier experience than through analysis. The first test results were obtained before the theoretical considerations were fully understood, and the difficulty of interpreting the data added impetus to the efforts already underway. In order to interpret the experimental findings, it was necessary to make an estimate of the pressures obtained at the various interfaces where gages were located and to rationalize the influence of gages and bond lines on the transfer of the pressure waves

[2,3]. It was determined that the experimental arrangement used in the preliminary experiment should result in pressures of 0.70 kbar at the plate-to-cradle interface and 0.10 kbar at the pipe-to-paraffin interface. On the models the pressures generated by the impact between the floor and pipe bombs were computed as being 7.4 kbars and 6.2 kbars at opposite vertical pipe-to-wax interfaces. Cruder computations were also done to arrive at estimates of the duration of the pressure waves.

RESULTS

The preliminary experiment trials resulted in little noticeable damage to the physical components, although the plate was propelled some 23 m (75 ft) in the air. Post-trial measurements, however, indicated that the cradle was bent around the longitudinal axis with an offset of 0.08 cm (1/32 in.) at the center. The models incurred extensive damage reflected in gross deformation of the structure and the impacted pipe bombs (Fig. 7).

Two of 14 gages mounted in the preliminary trials failed prior to detonation. The failed gages included the strain gage applied to the pipe section in trial No. 1 and the carbon gage applied to the pipe section in trial No. 3. One of the two carbon gages on the quarter-scale (2nd trial) and two of three carbon gages on the half-scale produced no detectable record. The gage installed in the bottom of the short stack of the half-scale was found to be electrically open when first connected after installation on the model. The two gages in the tall stack appeared to be good at that point, but after several hours operation, the one at the bottom was found to have changed resistance from its original 50 ohms to 86 ohms. It remained fairly stable at that point up to the time of the test. The gage in the top of the tall stack showed no abnormality before the test, but produced no detectable record prior to failing open during the test.

Representative plots of pressure records from two preliminary trials, the first quarter-scale model, and the half-scale model tests appear in Figures 8-14. Velocity records obtained with one of the velocity meters mounted on the floor plate of the models are included in Figures 15 and 16. On some records an arrow points to the part of the trace which was read and interpreted.

The preliminary trials resulted in small nonrepeatable pressures and large nonrepeatable strains. At the plate-to-cradle interface, where pressures of 0.70 kbar were predicted, pressures of 1.9 kbars, 0.3 kbar, and 0 kbar were obtained in successive trials (see Fig. 9, for example). The corresponding strain for these trials were 1500 microinch/in., -6000 microinch/in., and 4200 microinch/in. (see Fig. 8, for example). The pressure records obtained can, to a large degree be accounted for as the result of the large strains, with the possible exception of the 1.9 kbar record obtained with the manganin gage. If the strain equivalent output is subtracted from this reading, there remains about 0.9 kbar. Durations for the strains and pressures cited were about 10 us. In view of the test-to-test variability and lack of prior comparison data, these interpretations of the records are somewhat subjective.

In contrast to the preliminary experiment, substantial pressures were generated by the impacts between the floor plate and pipe bombs in the model tests (Figs. 12-14). In the quarter-scale test the overall pressure persisted about 500 us at an approximate level of 10 kbars. Closer examination of the initial portion of the trace reveals two successive spikes of 10 kbars and 11 kbars each with about 12 us duration. The appearance of the pipe bomb in Figure 7 suggests that a significant part of the long duration and a portion of the amplitude shown in Figure 12 is the result of deformation.

The bottom gage record for the half-scale test is shown in Figures 13 and 14 for two different calibration assumptions. The resistance shift by this gage prior to the test presents a difficult problem in interpretation. If one assumes that this is just a new gage resistance with the original calibration curve, the values are as shown on the record marked "Ref 86 ohms" (Fig. 13). It is difficult to imagine what mechanism would produce a change with that characteristic, however. It seems more likely that the 36 ohm change is a result of a break in the element, or a connection failure. In that case two extreme cases are easily conceived; either the original element responds as if it were still at 50 ohms with the change outside the active element and unaffected by pressure, or the pressure wave might reclose the bad connection responsible for the change resulting in a large step change uncorrelated with the magnitude of the pressure. Some combination of these extremes is also possible. One expanded time scale plot (Fig. 14) is calculated on the assumption that the effective resistance change with pressure all occurs in the original 50 ohms. The plot is marked "50 ohms", and results in considerably higher indicated pressure.

ANALYSIS

The failure to obtain significant pressures in the preliminary experiment was explained by computations based on shock theory and by the observed strains at the locations of the piezoresistive carbon gages. The results, nevertheless, revealed a severe limitation in attempting to generate shock directly by an air blast as opposed to an impact. They further indicated that even a setup which appeared simple was too complex to permit a clear understanding of the interactions between incident and rarefaction waves at the measurement sites. Ultimately, however, the preliminary experiment did achieve the purpose intended, which was to gain some experience with the piezoresistive gages.

The model tests represented a realistic environment for evaluating the carbon gage, and the results obtained with this gage are supported by theoretical computations. A graphical method can be used to estimate the shock pressures at various interfaces. This is done by using the initial impact velocity between the floor plate and pipe bomb and the Hugoniot curves for steel and wax (Fig. 17). Upon collision at a velocity of 520 ft/sec, a shock of 29.4 kbars is imparted to the pipe bomb. The shock propagates through the steel wall at 0.474 cm/us, preceded by an elastic precursor having a velocity of 0.580 cm/us and a pressure of 13.0 kbars (the Hugoniot elastic limit of steel). Both waves arrive almost simultaneously at the steel-to-wax interface where material mismatch results in only 7.4 kbars of pressure being transferred into the wax. This is what should be measured by a gage mounted on the steel or embedded in the wax. The pressure is further lowered to 6.2 kbars when the wave encounters the next interface in passing from the wax back into steel. Ideally, these

estimated pressures apply when the shock is being transmitted across flat materials with large dimensions. Under those conditions, elastic unloading waves or rarefactions are long delayed and do not interact with the incident wave. Clearly, in the model setup this situation does not exist. Moreover, given that the shape of the pipe bomb is changing during the course of the impact (Fig. 7), it becomes impossible to follow in detail what is happening to modify the incident shock wave. It is, nevertheless, heartening that what was measured (10 to 11 kbars in the quarter-scale and 6 to 16 in the half-scale) was not far off from what expected (6.2 kbars in the quarter-scale and 7.4 in the half-scale).

After the model tests were completed the results of a hydrocode computer analysis became available. The results are graphed in Figure 18 and show the pressure time history in the confined explosive charge of a pipe bomb subjected to different impact velocities. In the vicinity of 500 fps the peak shock pressures are about 7 kbars, which compares favorably with the experimental findings. As indicated in the plot the pressure reaches a peak in about 3 us and the entire event lasts no longer than about 13 us. Comparison with Figure 13 shows that both the rise time and duration obtained in the test were three to four times that predicted by the computer analysis.

The problem of measuring shock in confined explosives is clearly more formidable than was first thought. The strong dependence of shock pressure on target geometry, together with the possibility that factors other than pressure may be important in impact initiation of munitions, may place a practical limit on the utility of such measurements for the intended purpose.

CONCLUSIONS

Because of a comparatively higher pressure to strain sensitivity, the carbon gage appears superior to the manganin gage for shock pressure measurements in confined explosives. Little experience exists to support estimates of the integrity and reliability of the carbon gage.

The strain sensitivity of piezoresistive gages will always present a problem in clearly interpreting their results. In the case of munitions, it will be necessary to know how much strain the body undergoes in the vicinity of the gage.

The complexity of the physical situation requires modeling of the specific configuration to ensure proper interpretations of data. The optimum tool for this is the computer.

REFERENCES

- [1] Catalogue on Shock Pressure Sensors, Dynasen, Inc., Goleta, CA.
- [2] Zukas, J. A., Nicholas, T., Swift, H. F., Greszczuk, L. B., and Curran, D. R., Impact Dynamics, John Wiley and Sons, New York, NY (1982).
- [3] Rinehart, J., Stress Transients in Solids, Hyperdynamics, Santa Fe, NM (1975).

PIEZO RESISTANCE CHANGE
CARBON, MANGANIN AND CONSTANTAN GAGES

MANGANIN CARBON CONSTANTAN
—○— —+— ———

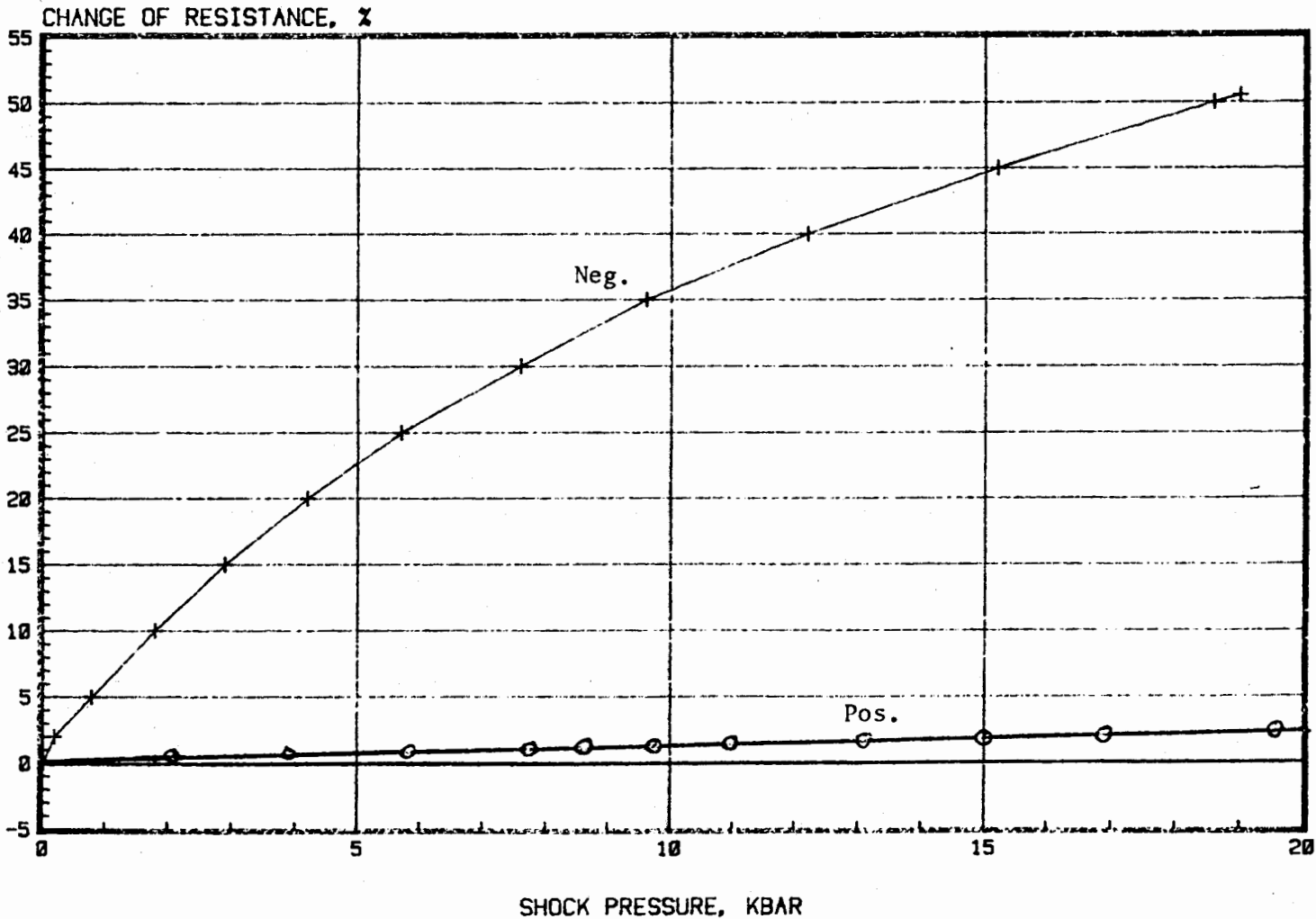


FIGURE 1 - CHANGE OF RESISTANCE WITH SHOCK PRESSURE OF CARBON, MANGANIN, AND CONSTANTAN GAGES (1). THE CONSTANTAN GAGE IS USED ONLY FOR STRAIN MEASUREMENTS.

STRAIN FACTORS FOR
CONSTANTAN CARBON AND MANGANIN GAGES

CONSTANTAN MANGANIN CARBON
— —+— —□—

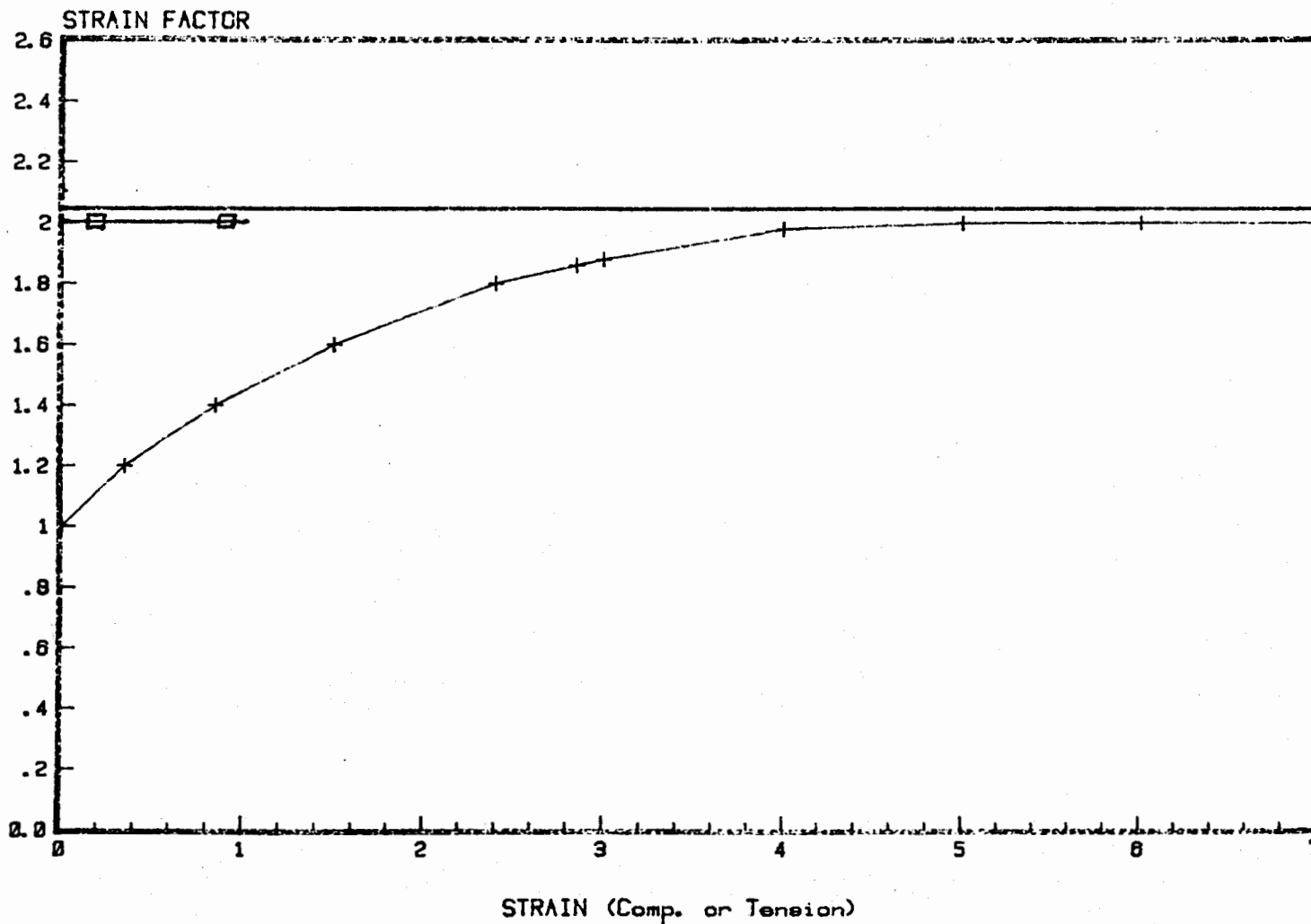
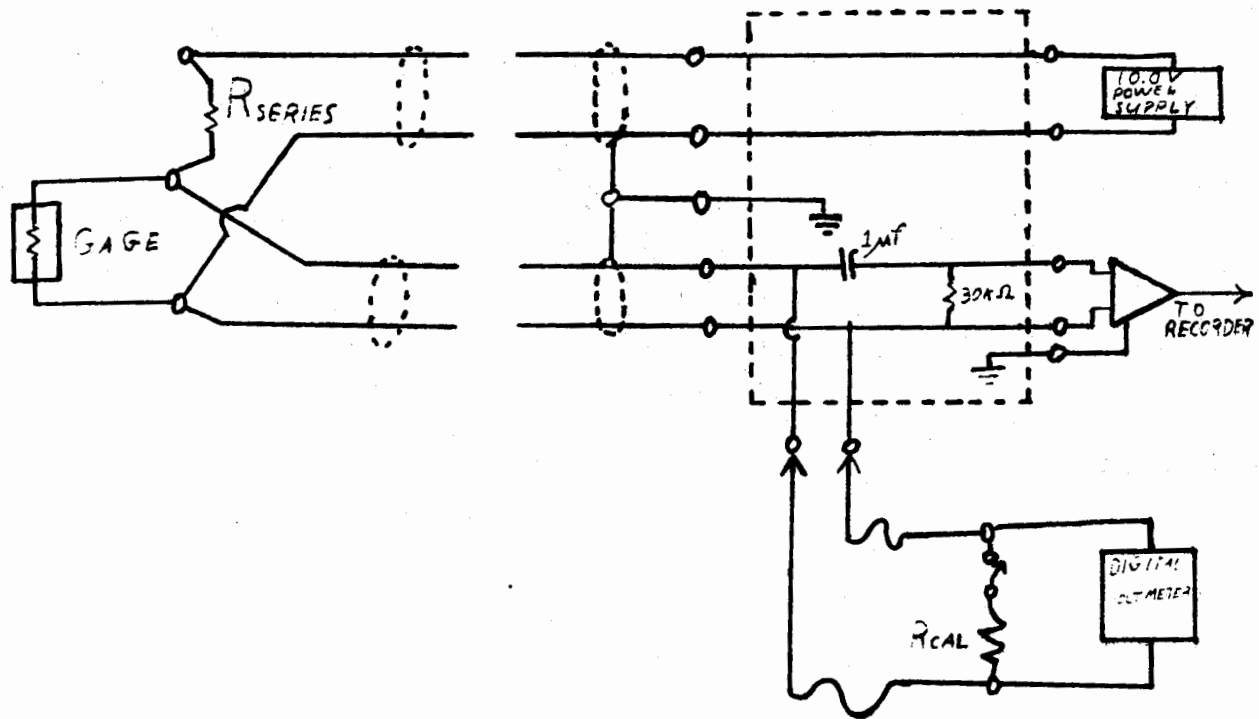


FIGURE 2 - STRAIN SENSITIVITY OF CARBON, MANGANIN, AND CONSTANTAN GAGES (1).



<u>Gage</u>	<u>R Gage</u>	<u>R Series (Nominal)</u>	<u>R Cal (Nominal)</u>	<u>Equivalent Calibration Step (approx)</u>
Manganin	50	510	5000	4.5 kbar
Carbon	50	510	270	3.8 kbar
Strain	120	1200	12000	4700 μ strain

FIGURE 3 - ELECTRICAL HOOKUP FOR GASES

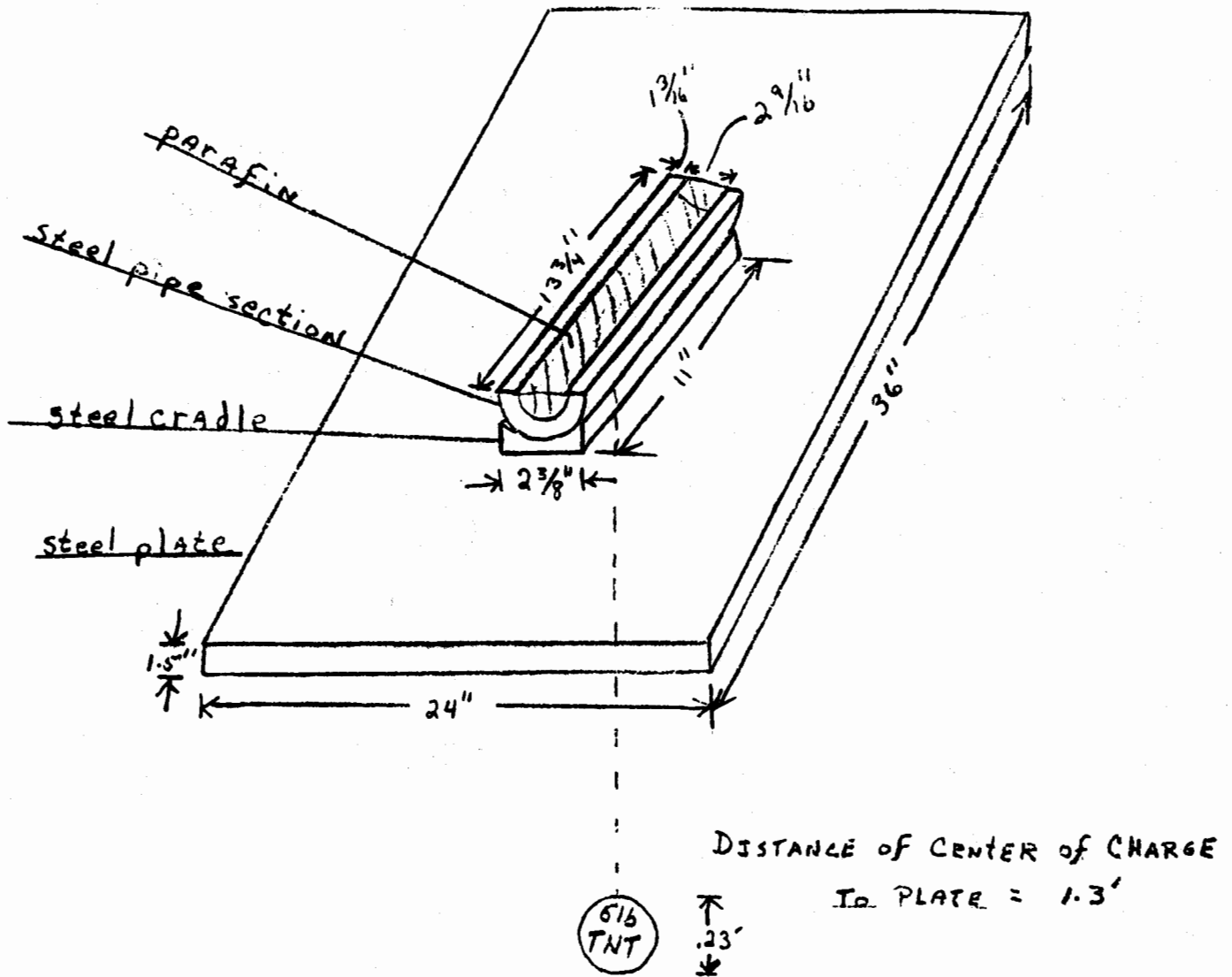


FIGURE 4 - SETUP FOR PRELIMINARY EXPERIMENT

Carbon gage

C 300-50-EKTRE, Dynasen, Inc.

Manganin gage

LM-55-210-FD-050, Micromasurements, Inc.

Strain gage

C6-122, Budd Co.

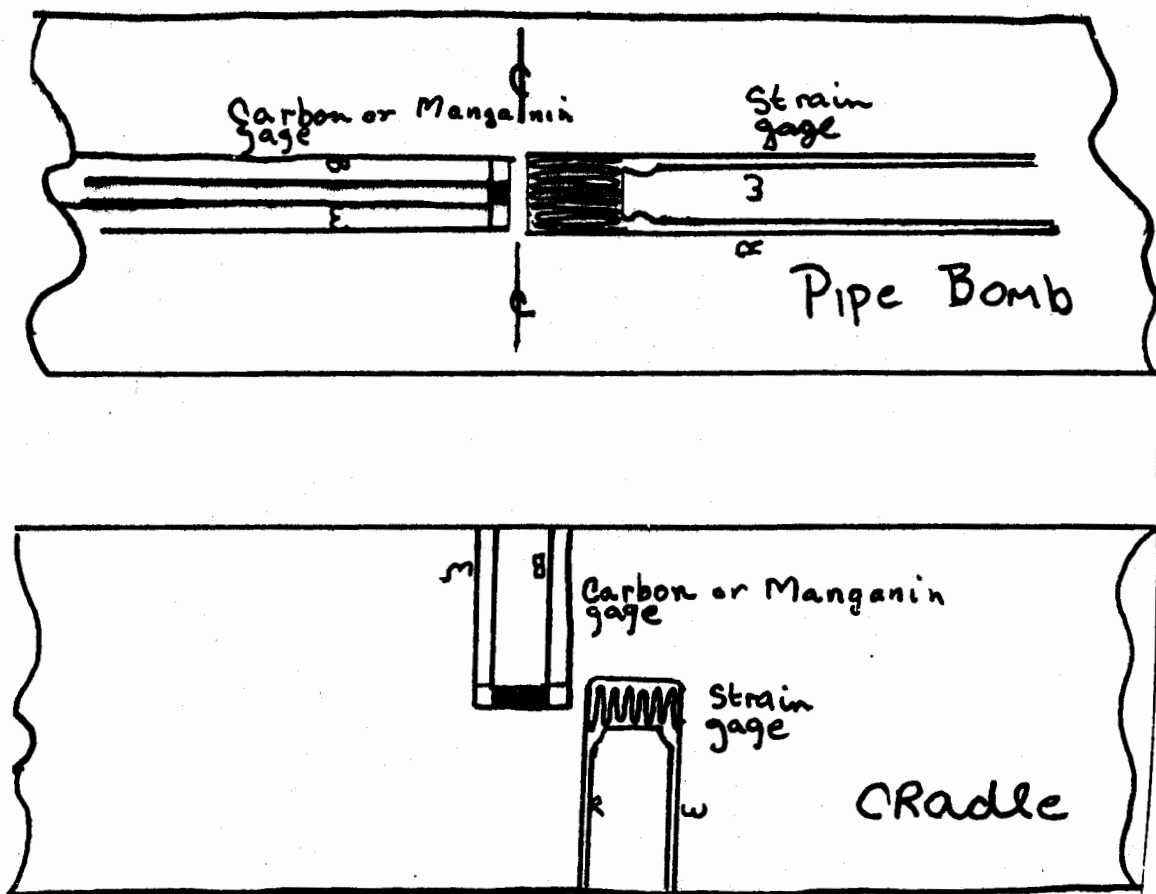


FIGURE 5 - GAGE ORIENTATION.

Munition Impact Test Setup

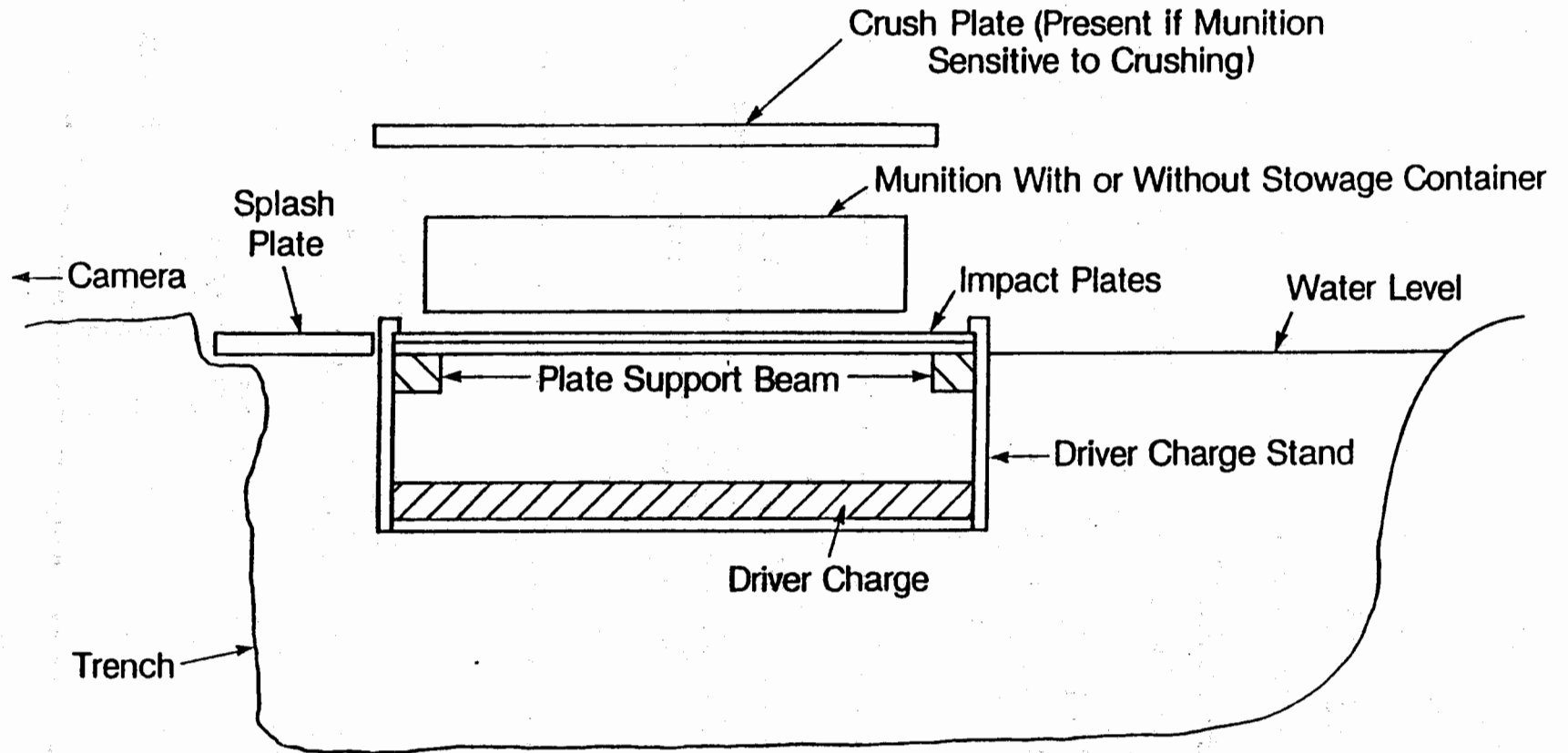


FIGURE 6 - MUNITION IMPACT TEST SETUP.

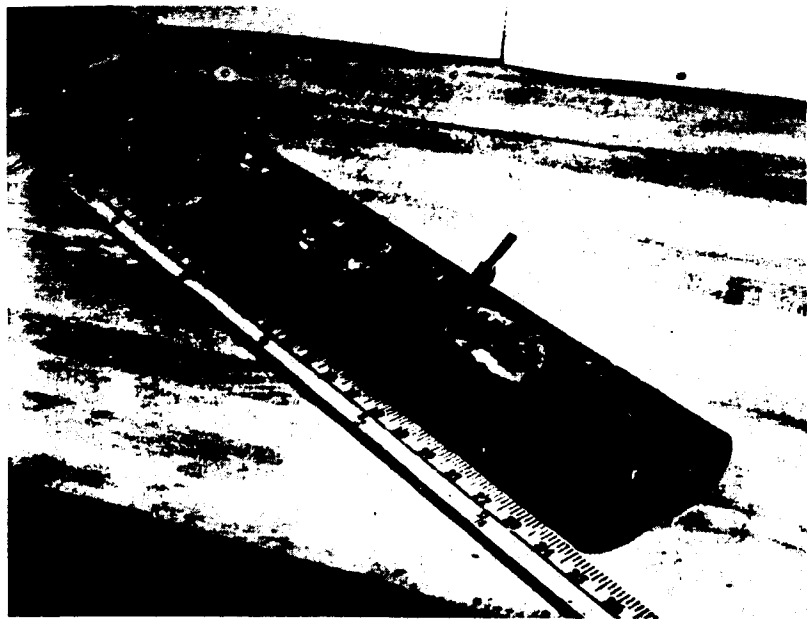


FIGURE 7 - INERT PIPE BOMB RECOVERED FROM QUARTER-SCALE MODEL TEST. THE CARBON GAGE BONDED TO THE ID SURFACE AT THE PLACE MARKED BY ARROW FAILED TO OPERATE DURING TEST. NOTE THE EXTENSIVE DEFORMATION OF THE PIPE BOMB FROM IMPACT WITH THE FLOOR.

234

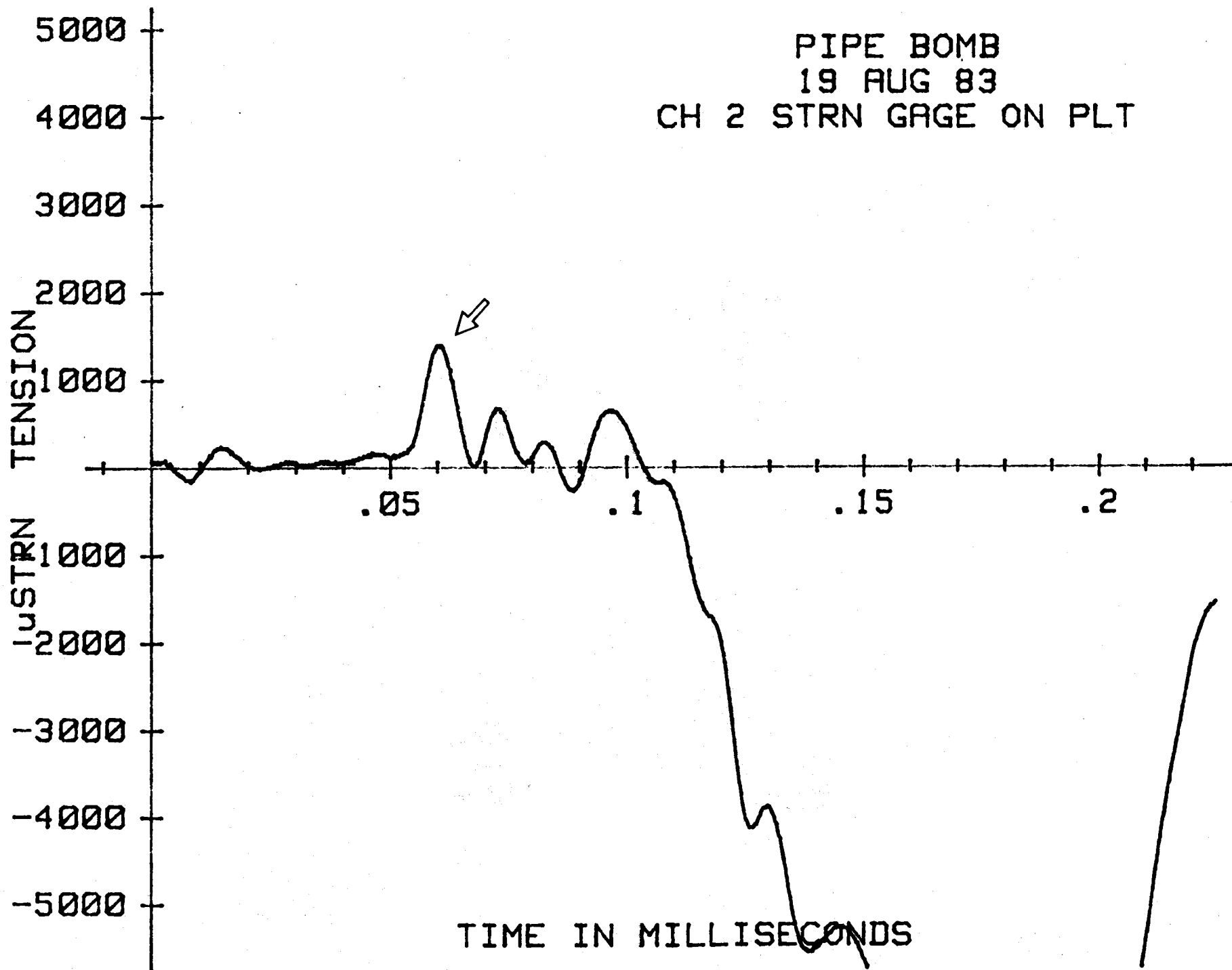


FIGURE 8

PIPE BOMB
19 AUG 83
CH 1 MANG GAGE ON PLT

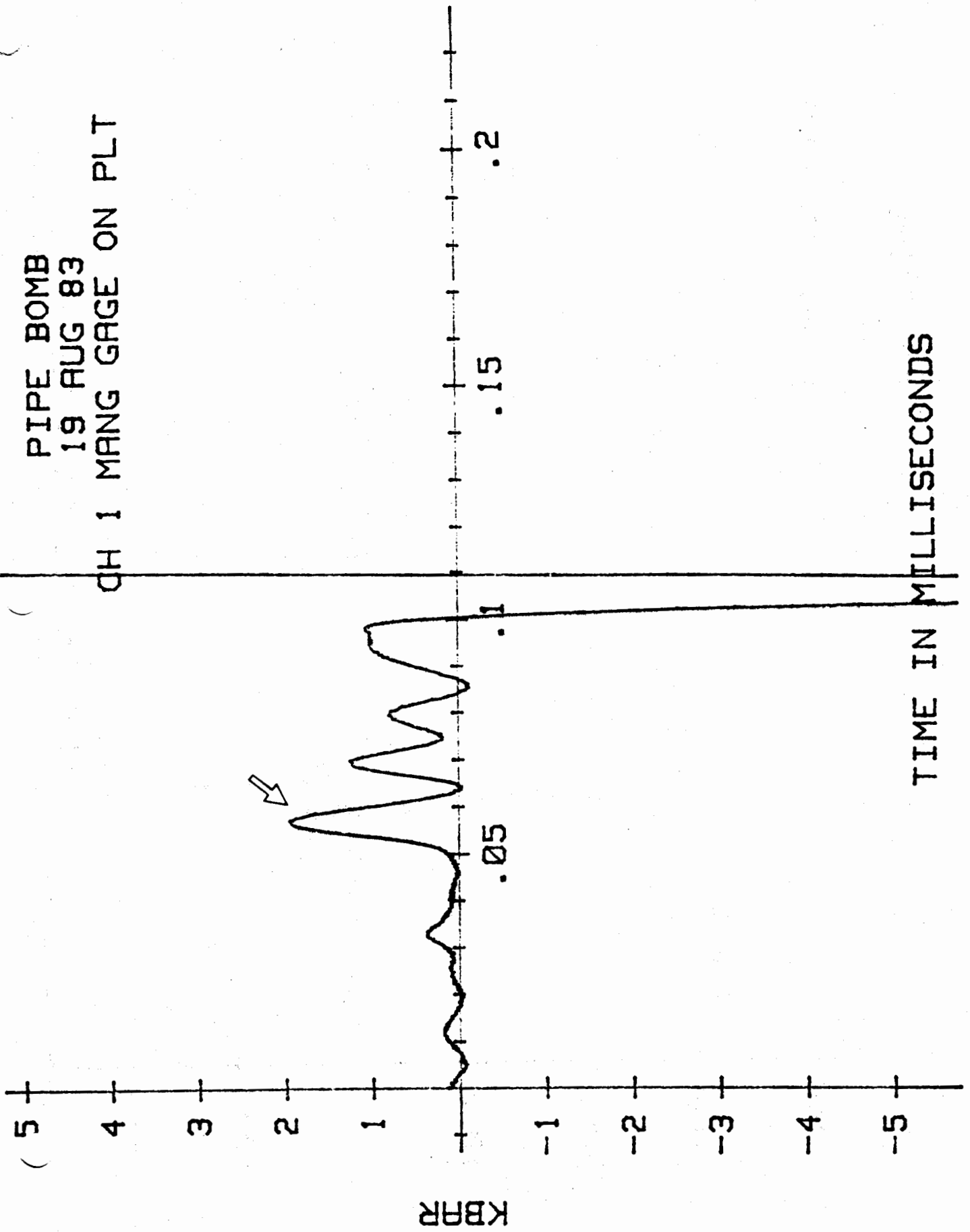
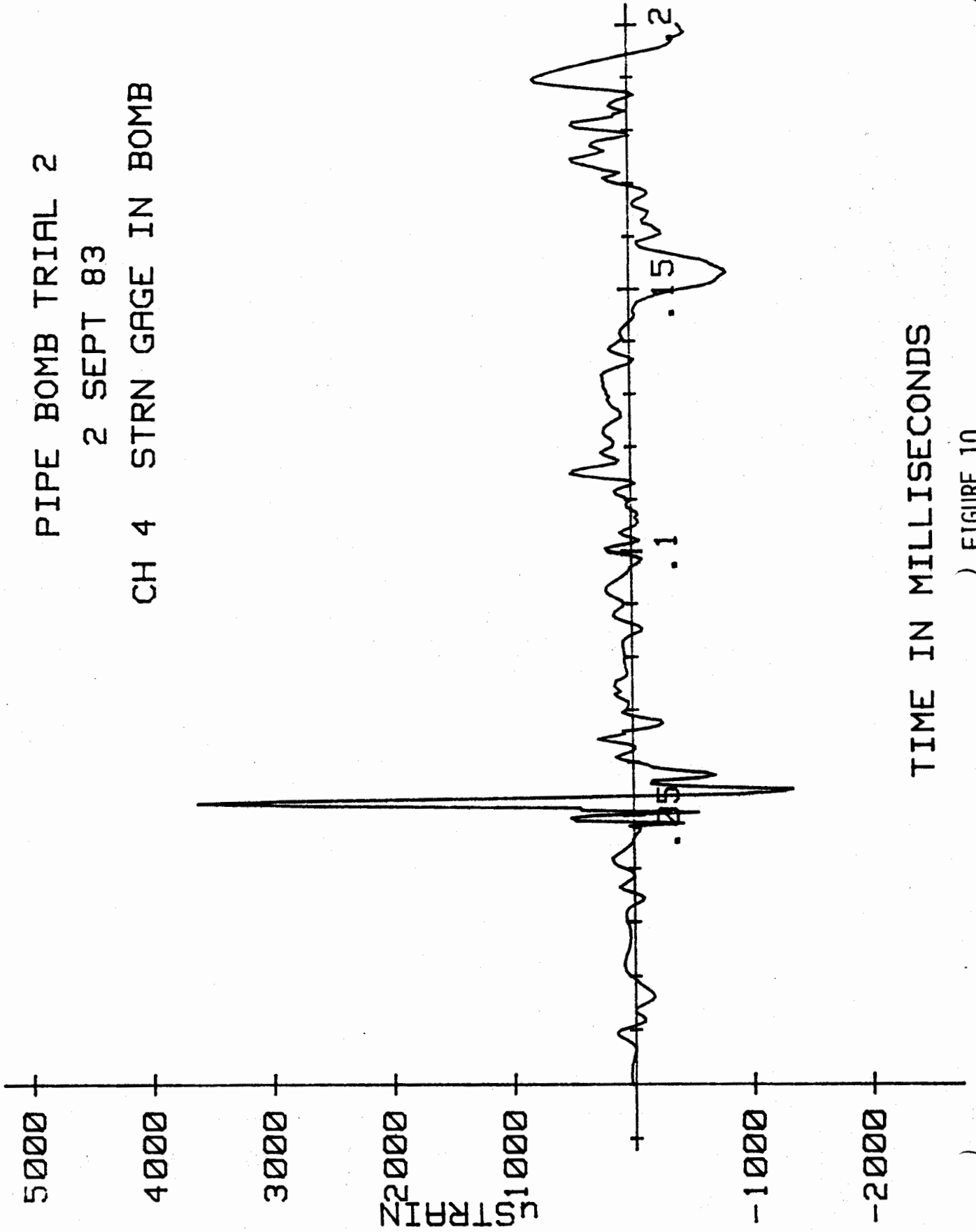


FIGURE 9

PIPE BOMB TRIAL 2

2 SEPT 83

CH 4 STRN GAGE IN BOMB

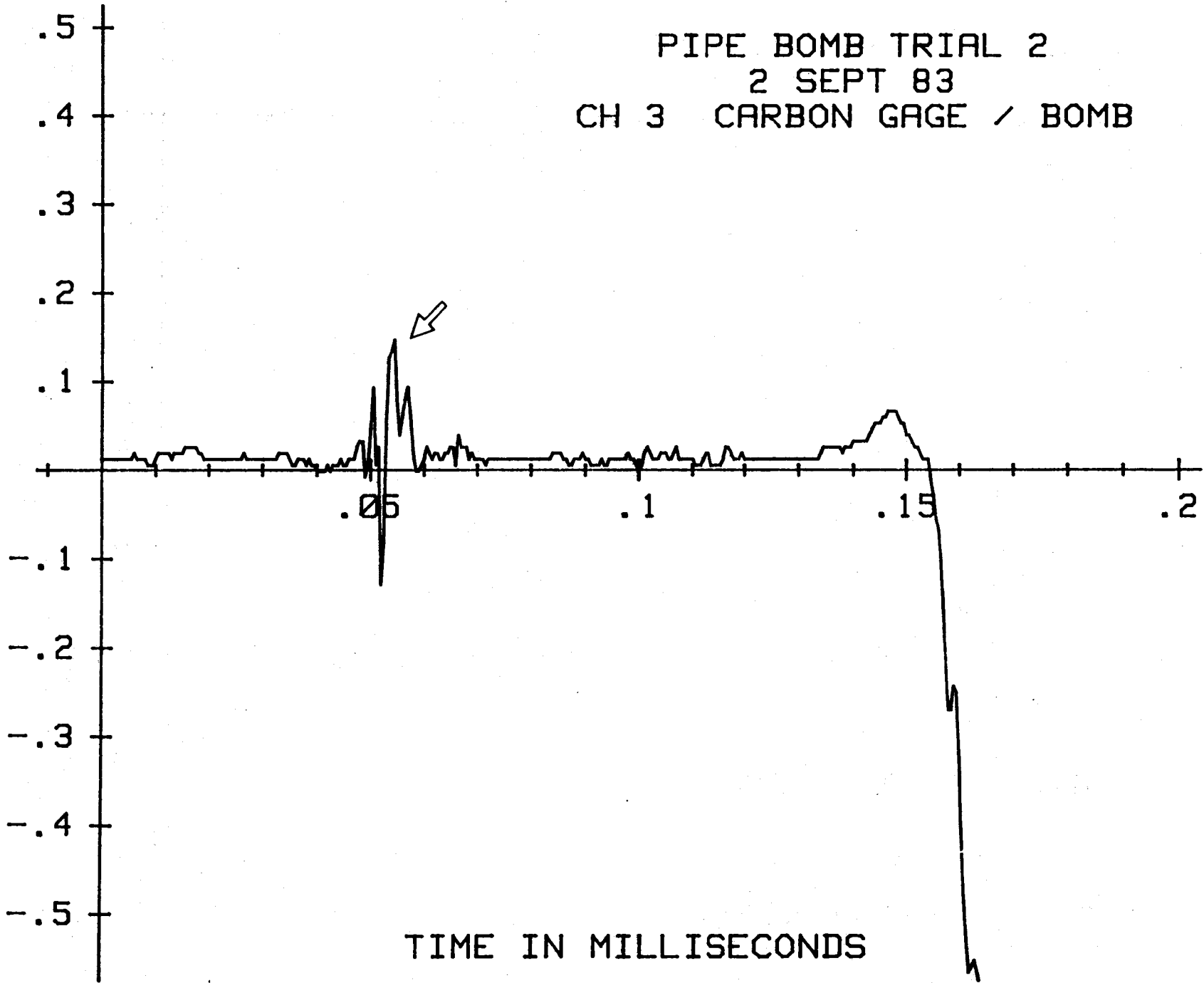


TIME IN MILLISECONDS

FIGURE 10

PIPE BOMB TRIAL 2
2 SEPT 83
CH 3 CARBON GAGE / BOMB

237
KBAR



TIME IN MILLISECONDS

FIGURE 11

238

KBAR

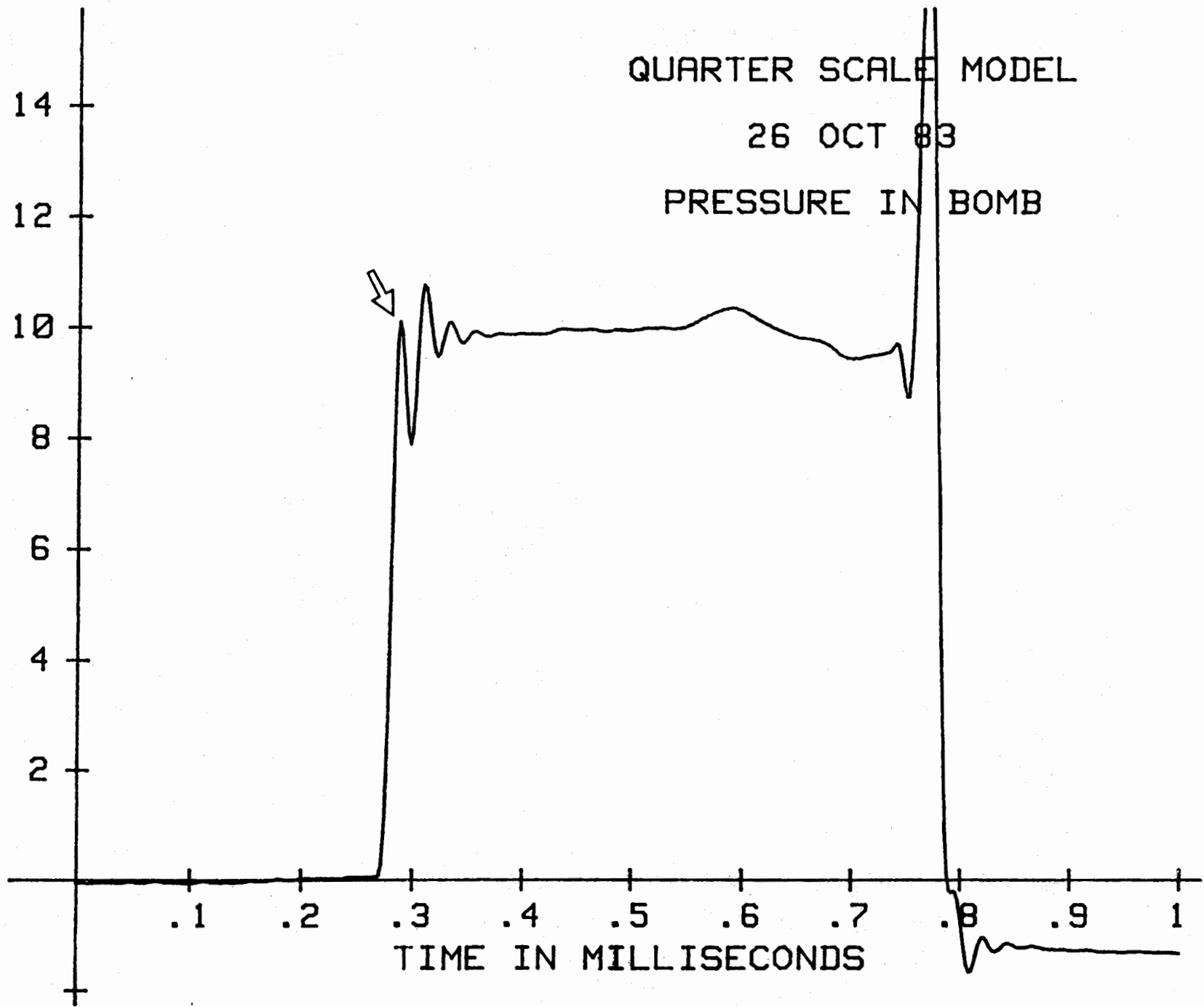


FIGURE 12

HALF SCALE MODEL

16 DEC 83

CHAN 7

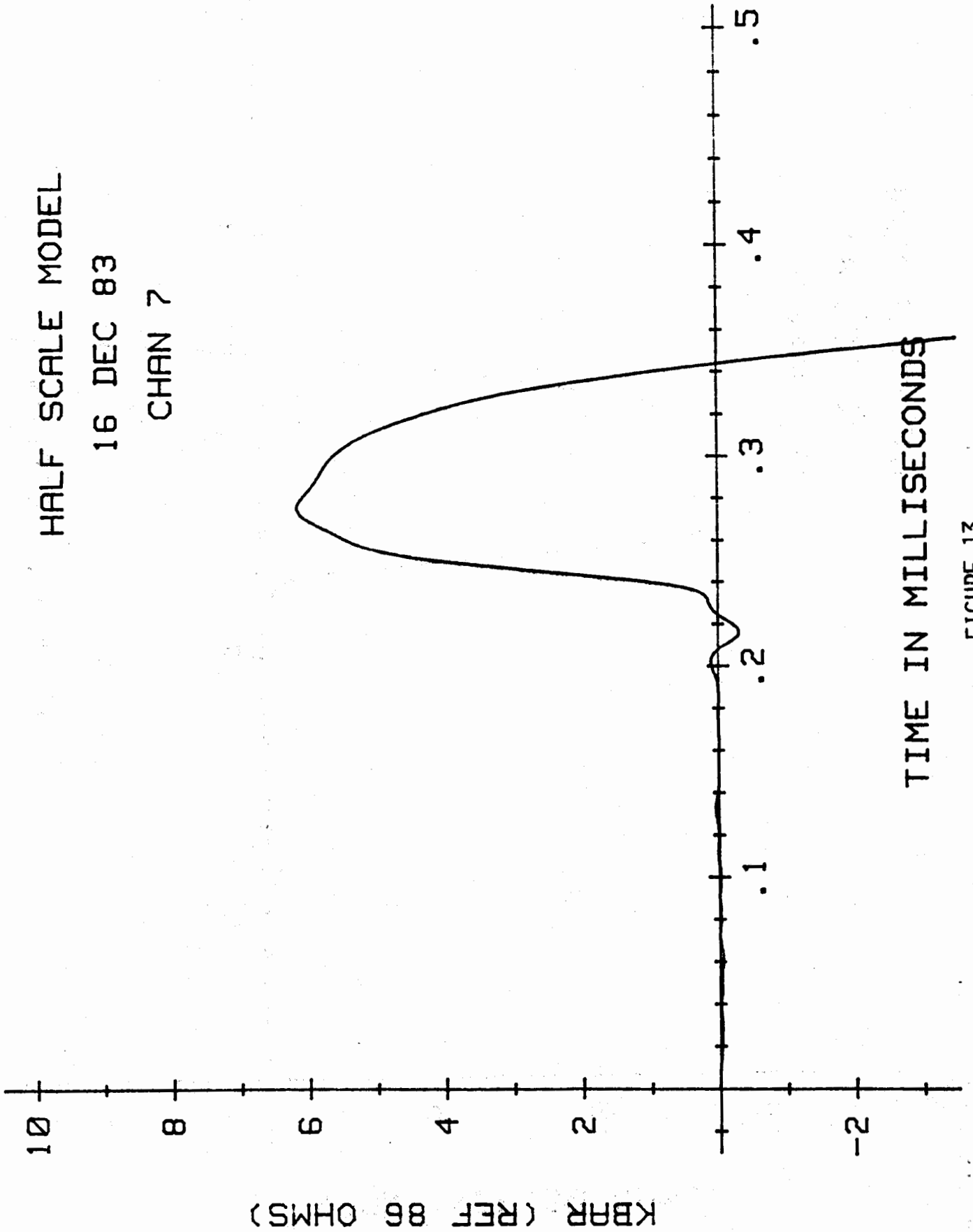


FIGURE 13

HALF SCALE MODEL

16 DEC 83

CHAN 7

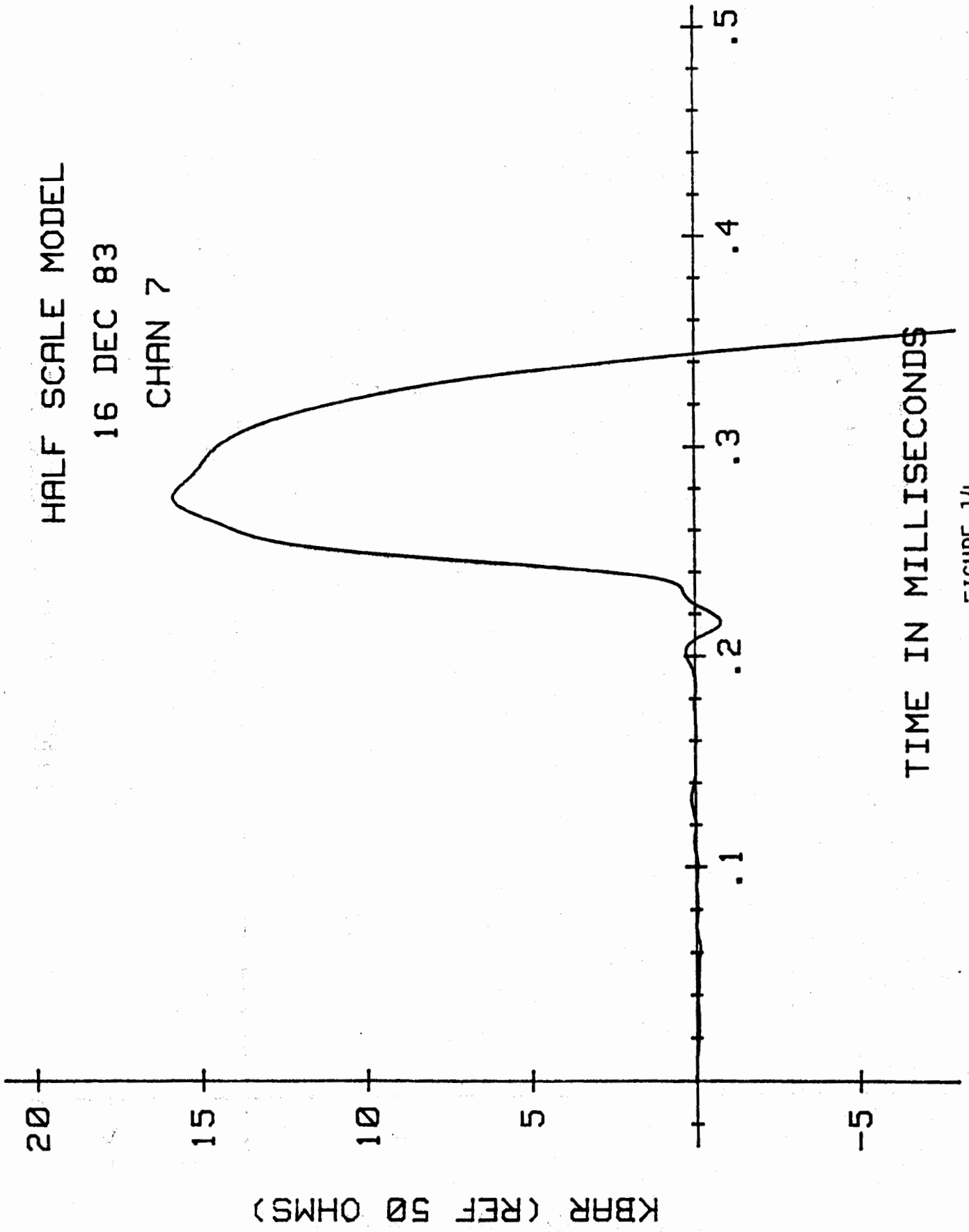


FIGURE 14

QUARTER SCALE

26 OCT 83

CH 3

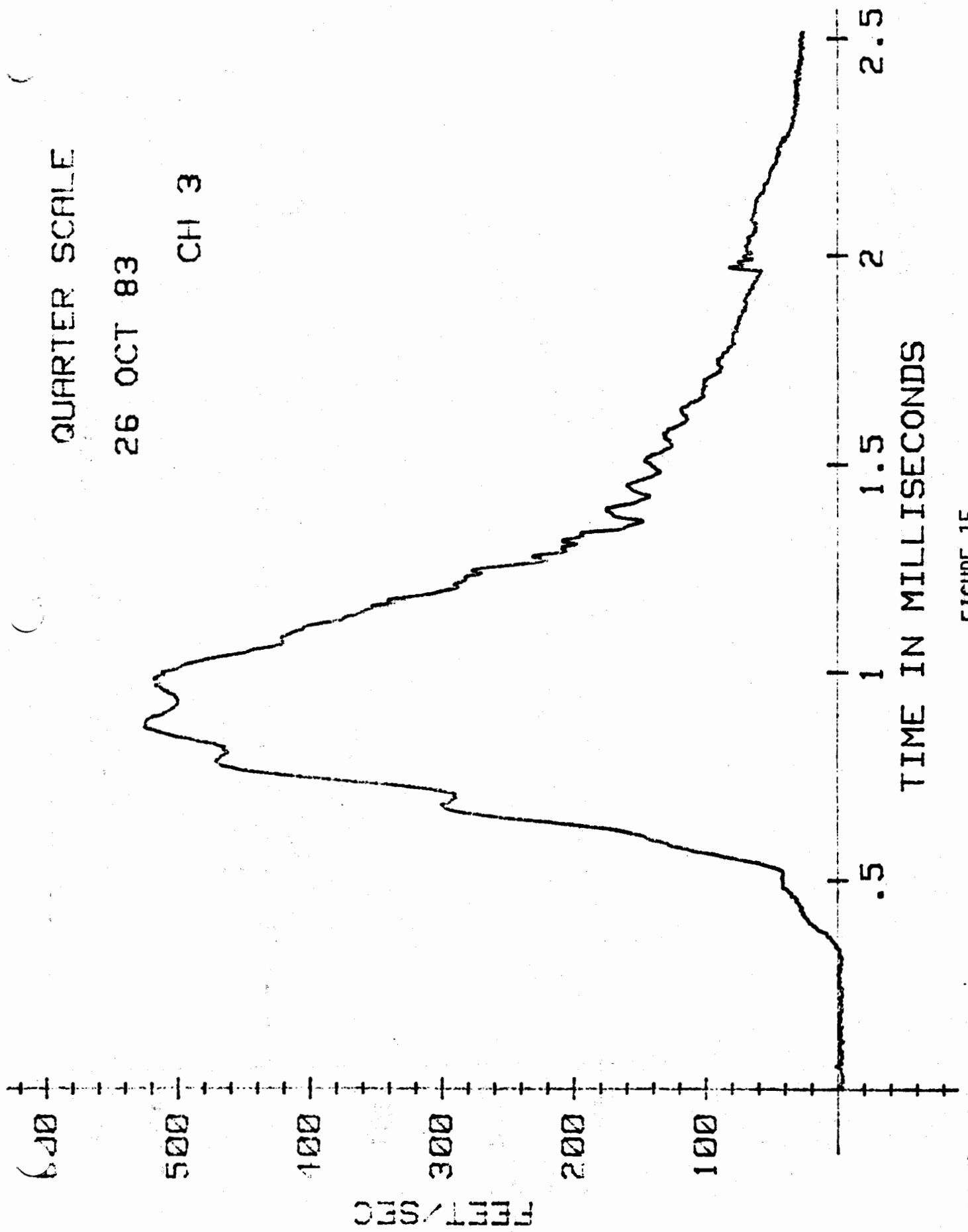
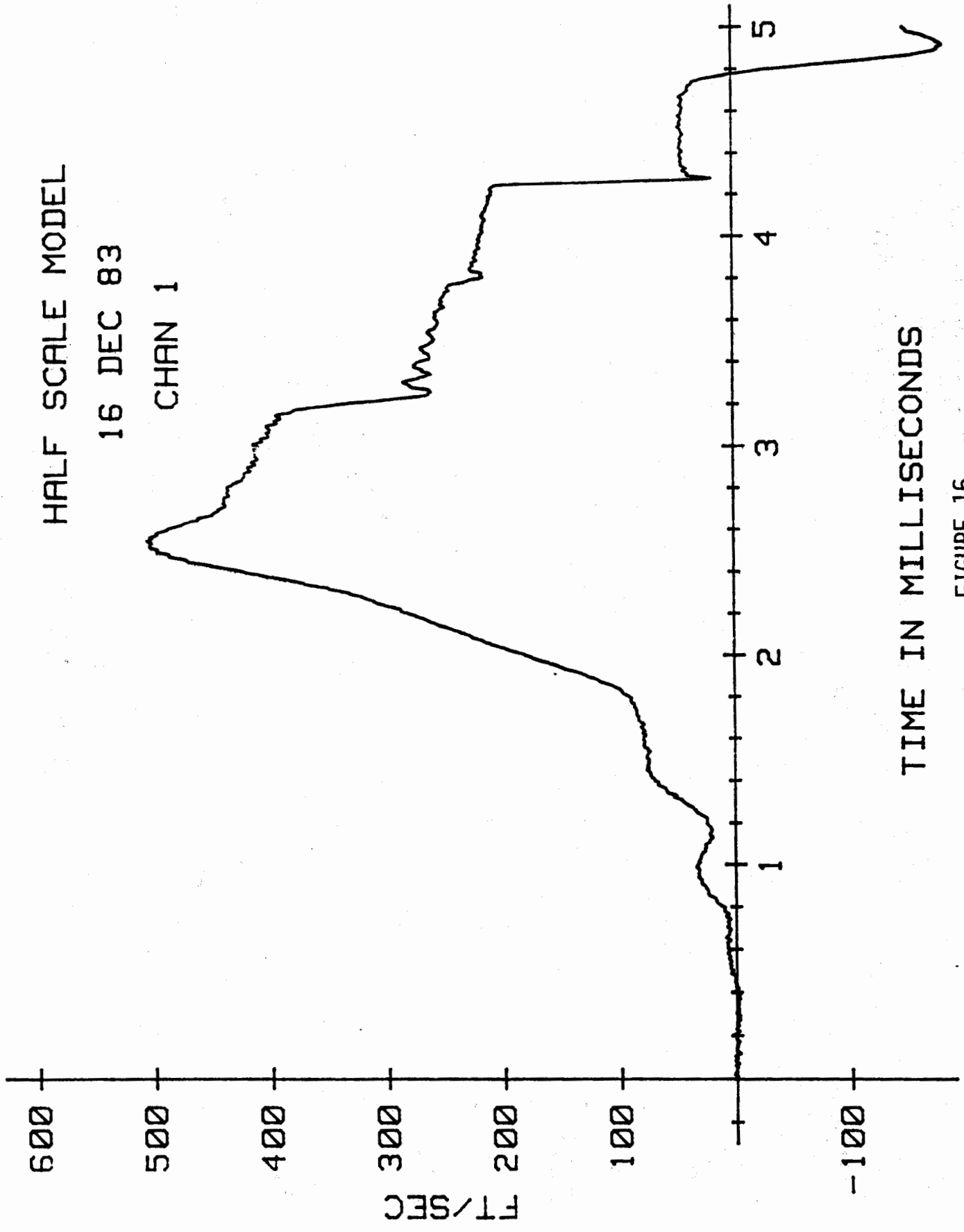


FIGURE 15

HALF SCALE MODEL

16 DEC 83

CHAN 1



TIME IN MILLISECONDS

FIGURE 16

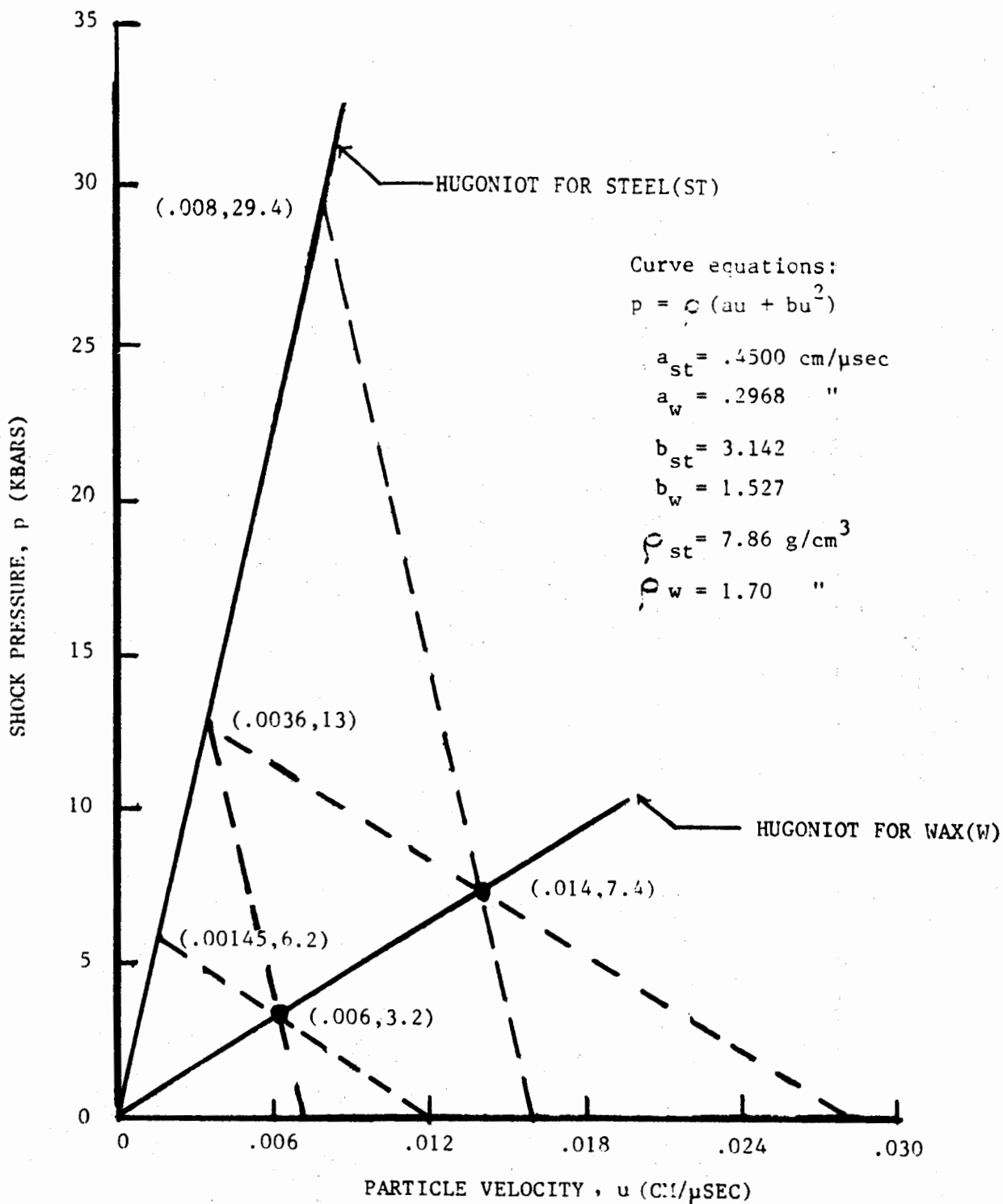


FIGURE 17 - PLOT METHOD FOR DETERMINING THE SHOCK PRESSURE INDUCED IN A PIPE BOMB BY AN IMPACT WITH THE FLOOR PLATE AT A VELOCITY OF $V=520 \text{ FPS}$ ($.016 \text{ CM}/\mu\text{SEC}$). THE INITIAL PARTICLE VELOCITY IS $V/2$.

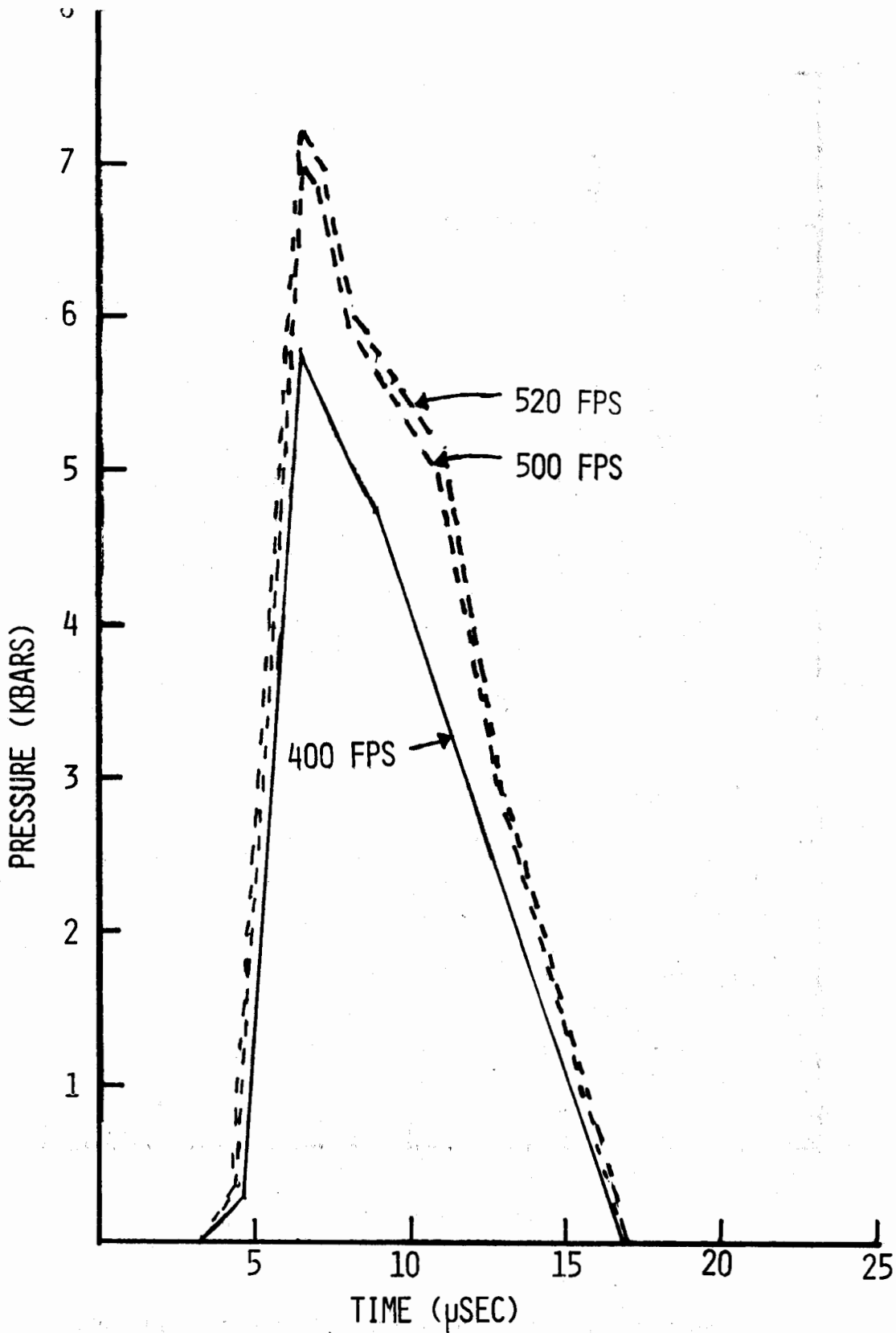


FIGURE 18 - PRESSURE INDUCED IN PIPE BOMB BY FLOOR PLATE IMPACT AT DIFFERENT VELOCITIES. COMPUTATIONS WERE DONE WITH THE PICES HYDROCODE FOR THE HALF-SCALE MODEL.

UNDERWATER BLAST MEASUREMENTS

Presented by:

**Larry L. Brown
Denver Research Institute
Laboratories for Applied Mechanics
University of Denver
P.O. Box 10127
Denver, Colorado 80210**

Presented to:

Thirteenth Transducer Workshop

Sponsored by:

**Vehicular Instrumentation
Transducer Committee of
Range Commanders Council**

Monterey, California

4-6 June 1985

UNDERWATER BLAST PRESSURE MEASUREMENTS

INTRODUCTION

Underwater shockwave pressures (to 25,000 psi) and time of arrival information were successfully obtained employing a unique piezoelectric transducer and installation technique. These transducers were arranged in a 12 gauge array to measure pressure-time phenomenon generated from explosive devices initiated underwater. A key feature in successfully profiling underwater types of pressure time events lies in the ability to effectively deploy transducer arrays in a reuseable fashion without destroying the transducer and/or its micro-electronic amplifier within their pressure design range up to 50 kpsi.

TRANSDUCER SYSTEM

The transducer element and housing for the above mentioned underwater pressure measurements that ranged up to 50 kpsi was originally developed by Mr. Ben Granath of Susquehanna Instruments. These gauge assemblies were used in conjunction with hardened micro-electronic circuitry developed by PCB Piezotronics Inc.. Since 1982 Susquehanna's product line, manufacturing and test equipment and it's technology have been transferred to PCB , and a continuing relationship exists between these two entities. These transducer systems shown in Figure 1 were developmentally tested initially by the Denver Research Institute (DRI) and subsequently, used on several major programs for the Naval Weapons Center (NWC).

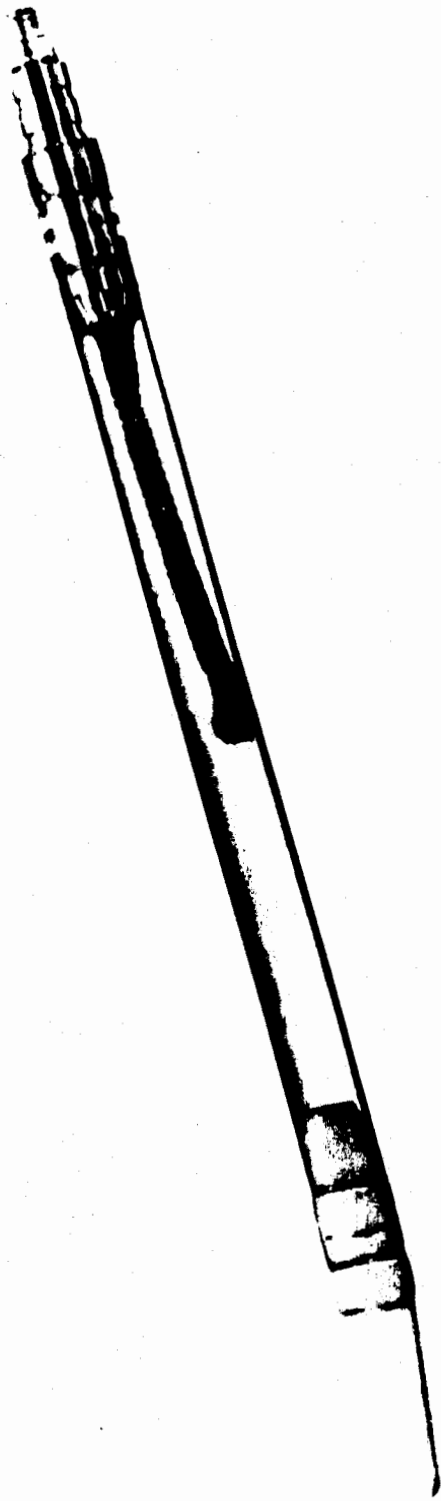


Figure 1. Complete Gauge Assembly.

Key parameters of the transducer are operating ranges up to 50 kpsi, resonant frequency of 1.0 MHz and rise times of 1.5 microseconds. This transducer system, utilizing the hardened micro-electronic circuitry (source follower) has an important feature in that it converts the high tourmaline crystal impedance from greater than 10,000 megaohm into a 100 ohm source impedance for low noise signal conditioning and data recording purposes. This low impedance source is less susceptible to induced EMI/RFI type of interference from sources such as high voltage firing systems and from normal operational conditions, such as wet connectors, etc.. Further EMI/RFI protection may be provided by an electrostatic shield surrounding the piezoelectric crystal and interface wires to the source follower.

Figure 2 depicts the underwater blast transducer. The gauge consists of a short piece of plastic tubing (3/8 inch diameter) containing a small 1/16 inch diameter, volumetric sensitive tourmaline crystal coupled to a source follower which conditions the signal generated by the crystal. The plastic tube, housing the crystal, is filled with silicon oil and capped at each end. The oil provides a fluidic coupling which closely matches the acoustic impedance of the surrounding water. The end, away from the signal cable, has a solid plastic nose with a hole drilled through it for attachment of a low yield strength thread for hanging a lead weight that holds the transducer assembly straight for positioning purposes. The gauge assembly is calibrated as a unit by the manufacturer in compliance with and according to the ANSI 1388.1-1972, "A Guide for the Dynamic Calibration of Pressure Transducers" and ISA 5-37-10, 1982 "Specifications and Tests

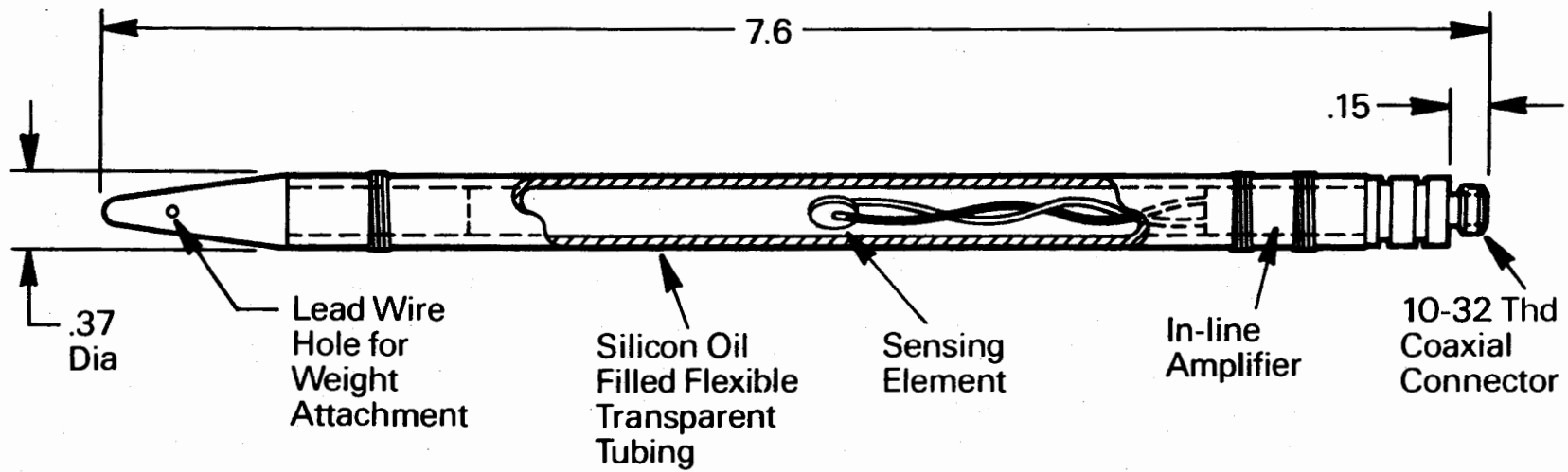


Figure 2. Schematic of Gauge Assembly.

for Piezoelectric Pressure and Sound Pressure Transducers". The pressure calibration transfer standard is a linear volumetric tourmaline pressure sensor designed to measure rapidly changing hydraulic pressures to 20,000 psi. Since there is no diaphragm or housing, this sensor makes an excellent calibration transfer standard for hydraulic impulse calibrators. Figures 3 and 4 depict the transducer outline and a record of a pressure pulse respectively. Figure 5 illustrates the total calibration system.

TEST FIXTURE

Measurements of underwater pressure distributions were from explosive devices were accomplished using a water-filled steel tank 10 feet in diameter by 10 feet in depth. The tank was buried in the earth to a depth of 9 feet and has a 12 inch thickness of concrete backing the steel around the entire perimeter. For experiments in the NWC program, the tank was filled to a depth of 9 feet to provide a 5 foot water head above the explosive device, leaving 4 foot of water below it.

Figure 6 is a schematic drawing of the water tank depicting gauge locations, mounting fixtures, and position of the explosive test device. The device to be tested was suspended from a steel beam welded across the top of the tank. The pressure gauges were supported from three wooden and steel beams cantilevered out from the wall and positioned 37 inches below the surface of the water. All gauges were in the same horizontal plane located 5 feet below the surface. The center of explosive device and detonator were also in this same plane.

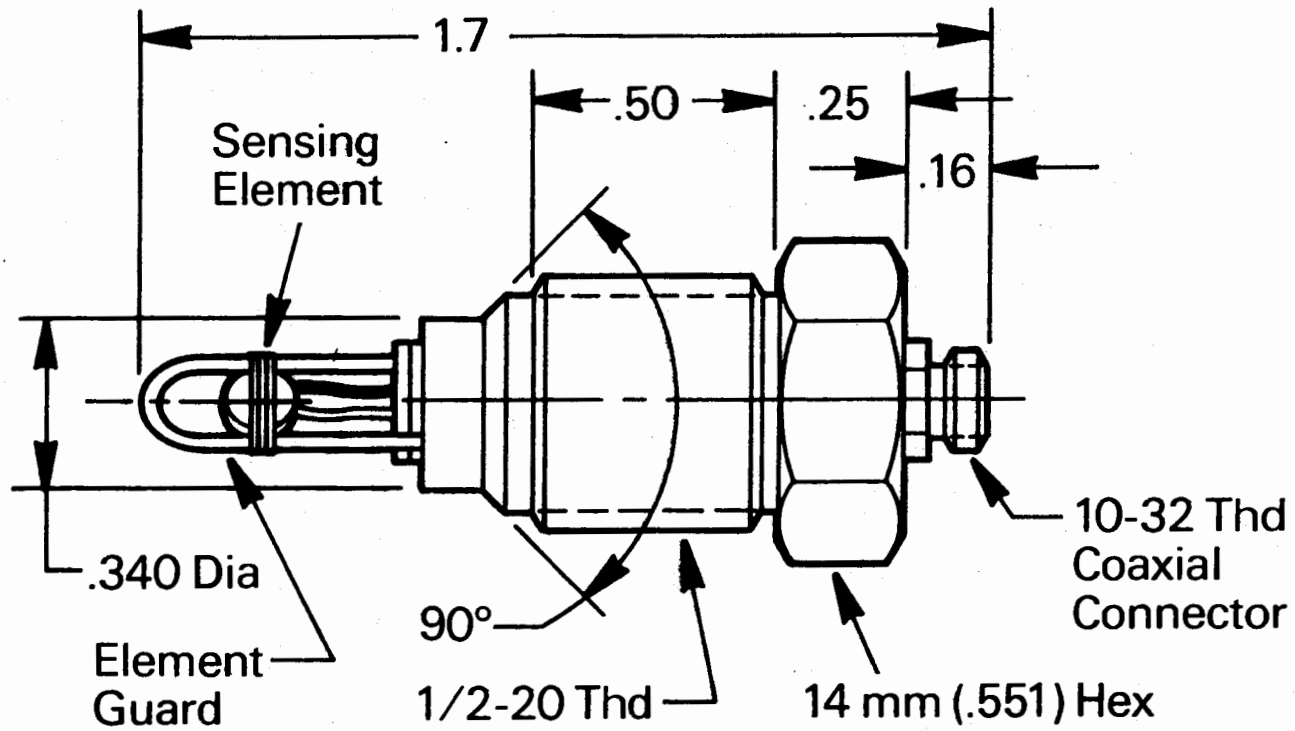


Figure 3. Pressure Calibration Transfer Standard.

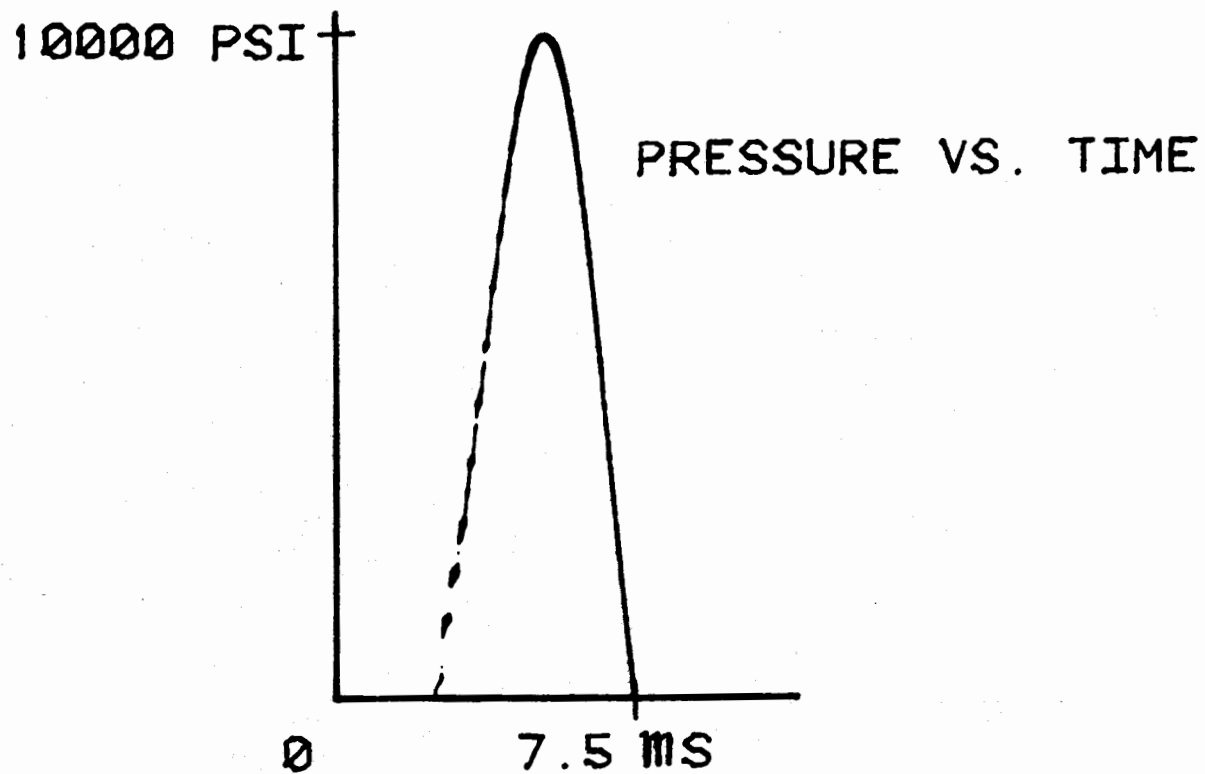


Figure 4. Record of a Typical Pressure Pulse from Transfer Standard Installed in a Hydraulic Impulse Calibrator.

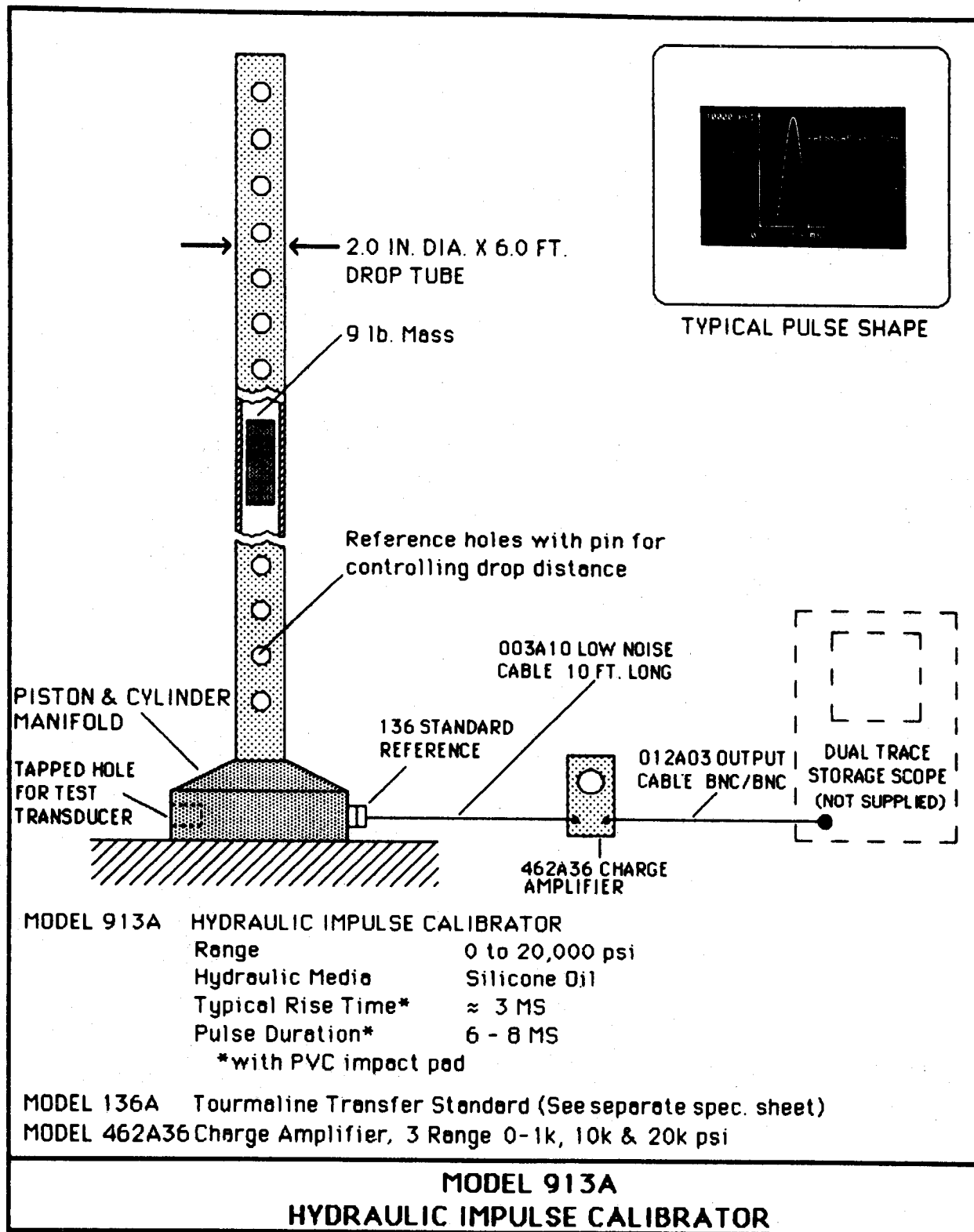


Figure 5. Total Transducer Calibration System.

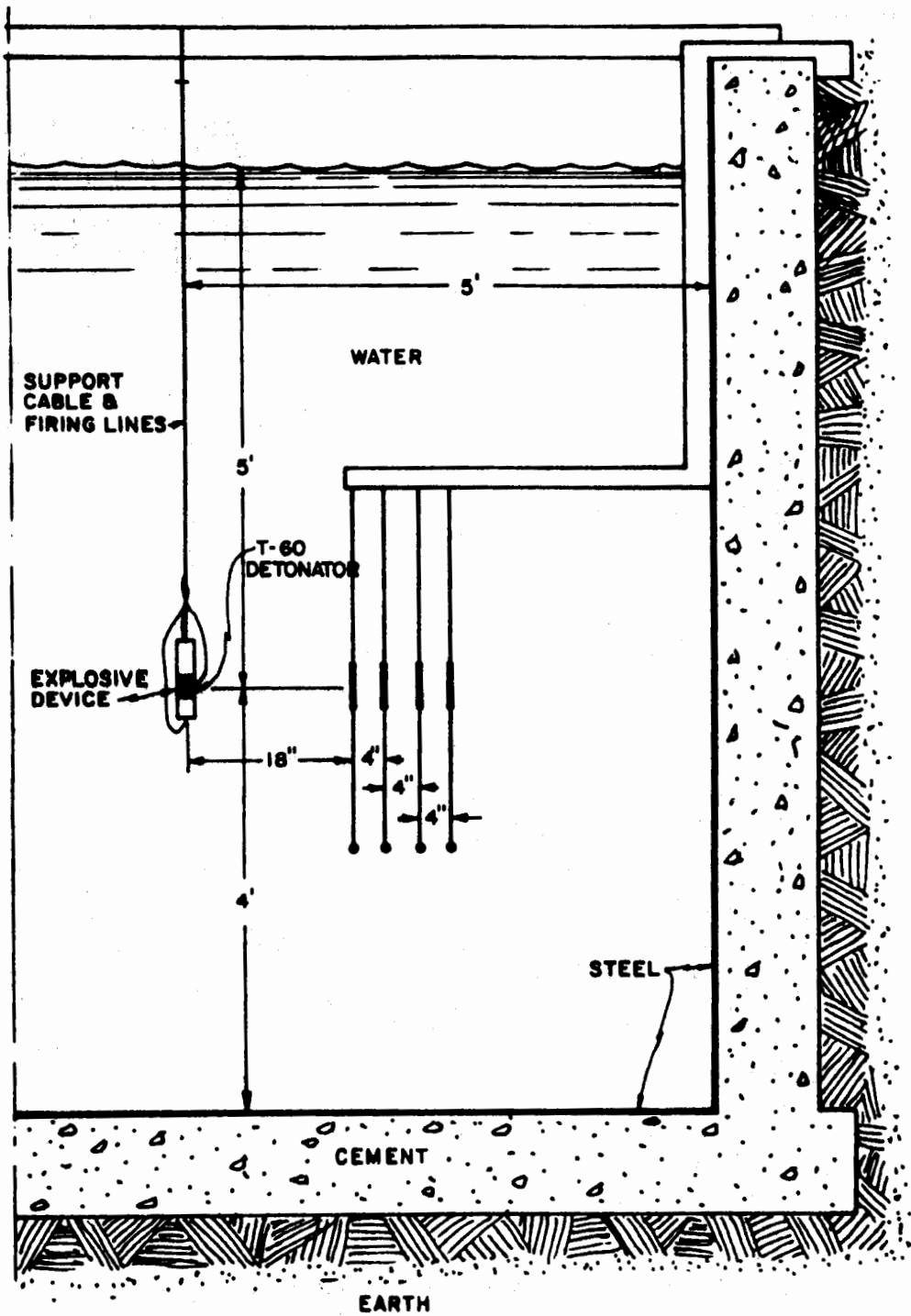


Figure 6. Schematic of Water Tank Depicting Gauge Locations, Mounting Fixtures and Locations of Explosive Device.

A top view of the pressure gauge array employed in these experiments is shown in Figure 7. Three gauge arrays containing four gauges each were positioned at orientations of 0, 45 and 90 degrees, with the zero degree direction being defined as the direction of a line passing through the center of the explosive and the detonation. Corresponding gauges in each array were located along radii equidistance from the charge center. Figure 8 shows the gauge array and their position in the tank.

The key to rapid, accurate and economical measurements of pressure time parameters is the ability to accurately and rapidly position the gauge lines and gauge array radials pre-shot, and to insure that minimum preparation is required between test events. DRI's approach to the gauge array positioning was accomplished during the pre-test build, which allowed the transducer signal lines to be pre-positioned leaving the only intershot setup required to re-attach the lead weight and verify positioning.

The interface from the actual tygon housed transducer and signal cable is critical to reduce transducer assembly damage during the explosively generated late time phenomenon. At the source follower end of the transducer, another length of tygon tubing was packed with silicon grease (to prevent water intrusion) and was banded with "TYRAPS" to form the mechanical bond between the transducer and the signal interface cable. The tygon tubing, which was banded to the transducer, was back filled with water (above the silicone grease) to prevent air cavities, extended underneath the cantilevered transducer support arm, and

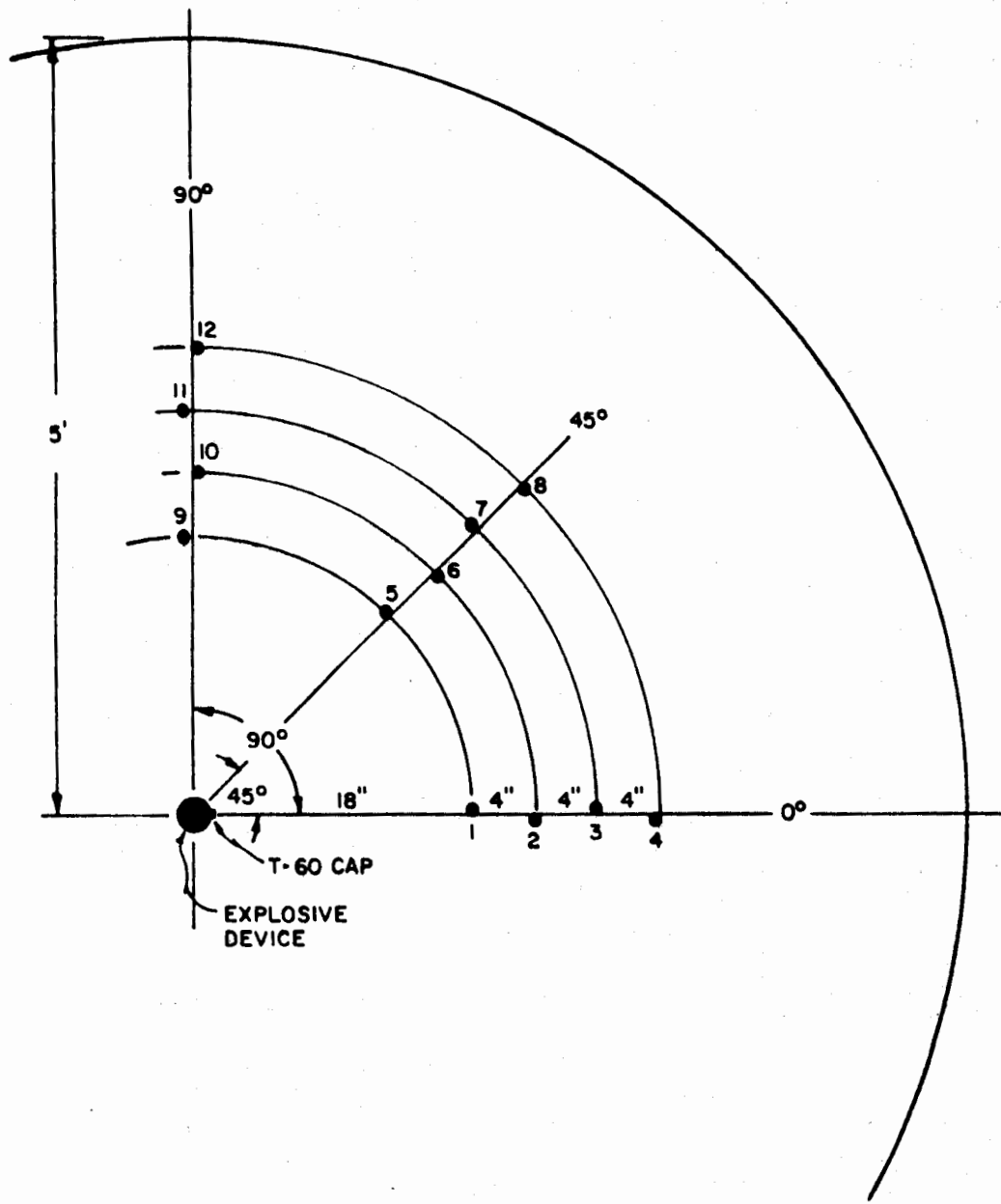


Figure 7. Top View of Pressure Gauge Array.

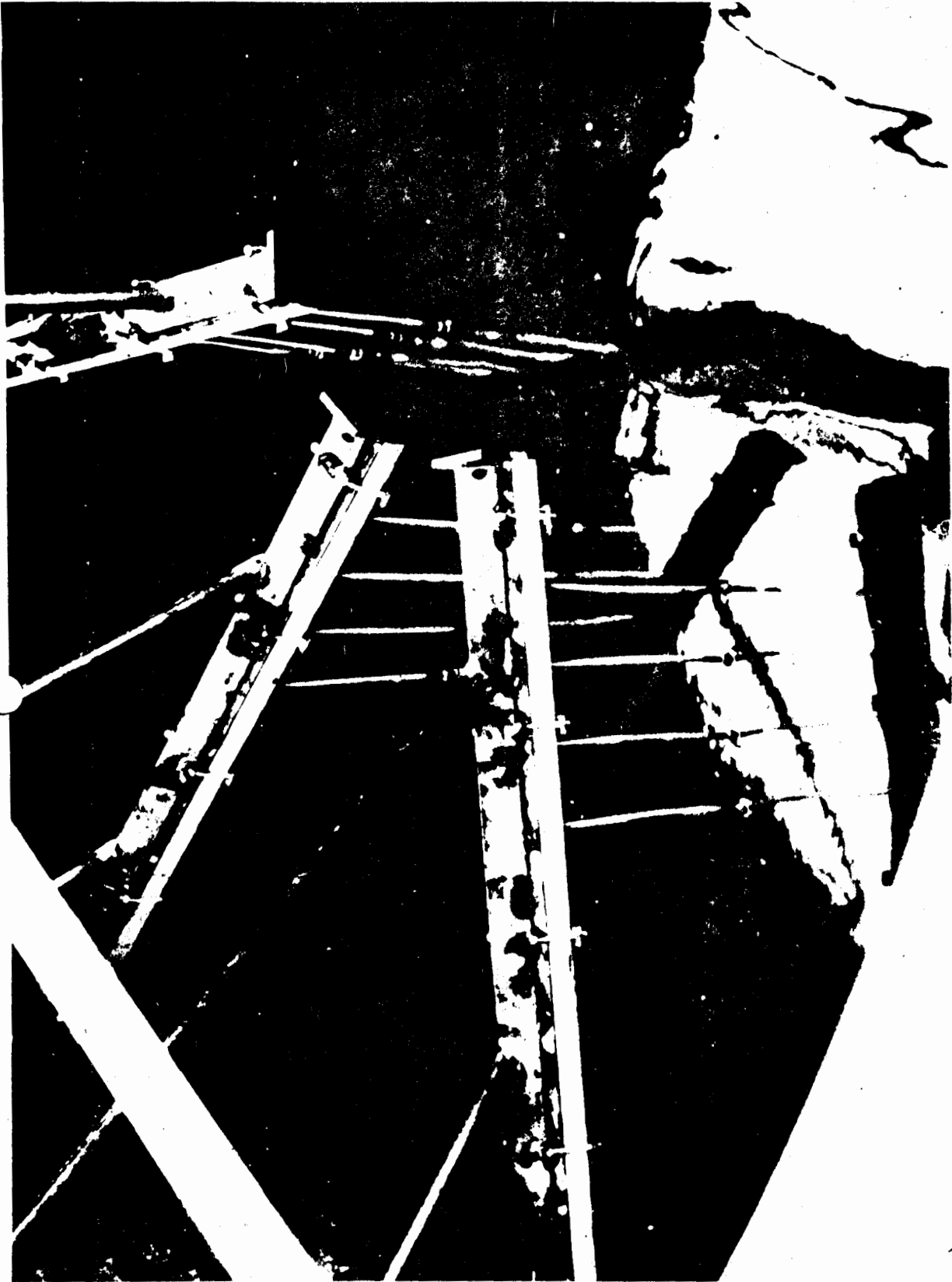


Figure 8. Gauge Arrays and Their Position in the Tank.

subsequently, out of the tank where normal instrumentation practices were employed.

The following is a chronological sequence that the transducer system is subjected to following explosive detonation: After the shockwave passes the transducer sensing crystal the explosively generated water cavity then creates a major displacement of the transducer assembly, after which the low yield strength thread breaks, dropping the lead weight from the transducer nose. This weight reduction allows the transducer and tygon interface cable to be thrown into the air along with expelled water with a minimum of mass. In addition, the tygon tubing interface, being elastic, creates a gentle deceleration of the transducer assembly when it reaches its maximum apogee to minimize structural catastrophic damage to the sensor assembly. With this gauge mounting procedure only minimum preparation is necessary before the next explosive event.

TEST RESULTS

Gauge records have shown excellent pressure-time histories. Figure 9 presents a Poloroid picture from an oscilloscope of a typical pressure-time trace with a peak pressure of approximately 15,000 psi. Good correlation was achieved from gauge to gauge, and to the theoretical calculations based on explosive weight versus distance in water.

From an operational viewpoint, the test setup performed as expected with minimal transducer damage during expulsion from the tank due to the explosively generated water cavity. These con-



Figure 9. Poloroid Picture of Typical 15,000 psi Pressure Pulse.

cepts can certainly be used on other larger scaled test site scenarios, such as, ocean-based tests where a minimum of test-site preparation is required and where damage mechanisms must be held to a minimum.

SESSION 3

Q: MONTY ORTIZ, EG&G, ENERGY MEASUREMENTS (EG&G), LAS VEGAS, NV

I'd like to know how your pressure steps are generated and controlled and secondly, how do you collect the data when you calibrate up to seven sensors at a time?

A: MARTHA WILLIS, ROCKWELL INTERNATIONAL, CANOGA PARK, CA

The pressure manifold isn't an automated manifold so to speak. The program at this point tells the operator what pressure values to set for the manifold. We plan to eventually automate the system but, you know budgetary requirements, we have to do one thing at a time at this point. First we want to get ourselves so that we're not relying on any offset processing for any of our sensors that we calibrate. Then we're going to go back and automate the pressure system, so that's not a controlled function. The setting of pressure is a manual function. The acquiring of the data is through a multiplexer. I'm not real familiar with the exact hardware but I can get that information for you. We can also actually take 20 transducers' data. The only problem is that physically we're constrained with a manifold. As it is, we only have room for seven sensors. Eventually we plan to expand that when we modify the system.

Q: MIKE ENGLUND, GARRETT TURBINE ENGINE COMPANY, PHOENIX, AZ

You mentioned that you use the Eranson pressure step calibrator with helium, primarily. Two questions: 1) is it at all compatible to use the Eranson calibrator with a hydraulic fluid and 2) what's the approximate cost of the step generator?

A: JIM LALLY, PCB PIEZOTRONIC, INC., DEPEW, NY

Well, it's primarily made to use with a gas environment. The helium was selected because it will provide the fastest rise time. You could use nitrogen or compressed air but it's going to sacrifice the rise time. Phil Eranson gave a report probably in 1977 or so. There's a reference in the back of the catalog involving a strain gauge type sensor with fluid coupling in front of it. They actually just couple the passage with fluid and then use the gas environment for the step change in pressure. So, the recommended procedure if you are using it with any type of fluid is to allow that to come in front of the diaphragm of the transducer.

Q: ARPAD JUHASZ, BALLISTIC RESEARCH LABORATORY

Without changing the design of the machine drastically but perhaps beefing up ratios and that sort of thing, how much further do you think you can push the pressure limits of the gadget?

A: JIM LALLY

Without beefing it up?

Q: ARPAD JUHASZ

No, I mean you can beef up the wall ratio and so forth, keeping with the basic design as it now is.

A: JIM LALLY

Well, I suspect if you calculated all your stresses and everything, you could probably go as high as you wanted with it. I understand from a couple of people around, that there are certain limits in some companies on use of pressure vessels, and there are limits set on those. This particular main reservoir we pressurize to about 3500 psi, and it's generally recommended up to about 2000 psi. It's not only a question of designing it for a certain level, but then you also have the problem of the safety factor on top of that. If you did something for 20,000 psi, you'd really have to design it for more like 50 to 100,000 psi. I don't really know. We haven't gone higher with it. I think there have been enough problems really in getting it perfected down to the level that it does operate. They just haven't reached the stage where they've started looking at higher levels.

ARPAD JUHASZ

Now, that would seem a nice growth area once you feel comfortable. Just with the different capabilities you talked about, I think just pushing the pressure up higher would be a good thing.

JIM LALLY

Someone had asked a question on the price of those. They run around \$16,000 for the basic unit and then with the reference standards, they run around something like \$18,000. That's with the Hiess Digital Reference Standards.

Q: NOT IDENTIFIED

Could I elaborate just a little bit on that upgrading thing. I can't speak from experience, just conceptually. As far as raising the pressure and that design is concerned, there would be a severe safety problem, I think, staying with gas up to the 20, 30, 40,000 psi pressure level. And I don't really believe that valve design is going to perform well in liquid. The flat, disc-type valve, I think, is going to cause considerable disturbance in the transient disturbance in the cavity if you try to move it through fluid. It's just not streamlined for that sort of thing. Now there's no requirement to stay exactly with that format, but the other thing is that you're going to have a problem with steel leakage where that stem comes out of the pressure vessel. That thing uses an external hammer essentially to move the valve stem. It's a lot easier to seal a gas pressure at 1,000 psi than it is to seal anything at 20. You still get it to move through there rapidly. So, I'm not sure that upscaling would give you exactly the same performance without further redesign.

LARRY SIRES, NAVAL WEAPONS CENTER, CA

I did build a similar device about eight years ago for the same purpose and ours was designed to go up to 20,000 psi. But, it was a somewhat different valve design, and the hammer mechanism was totally internal to the pressure volume rather than being external. So there are ways of designing that for higher pressures.

Q: RONALD TUSSING, NSWC, DAHLGREEN, VA

We do a lot of underwater explosions, so I'm very interested in that particular gauge. I have several questions. One, and I'm going to just give a little background. I did give a paper on internal gauges at the Eleventh Transducer Workshop and showed where the accuracy and calibration, and the oil filled boot did not affect the rise or the geometric response of the gauge. We have used a PCB amplifier in front of our gauge that we make and so I'm interested in the overall there. But one of the questions that I have is on the coding. You mentioned that it was over the crystal itself with an EMI or RFI shielding. Could you tell me a little bit more about that?

A: LARRY BROWN, DENVER RESEARCH INSTITUTE, DENVER, CO

Probably this question is best referred to Jim. The transducers that we used did not have the EMI or RFI shield on them. I might point out that ours were not sheath for that protection because of the requirements of this program. We had 5000 volts, one microfarad type of high voltage firing system. In fact, we had several high voltage lines into the tank which was about a 1.25 jewel system, and we had no debilitating effects from it. As to the actual operation of the shielded transducer, I think Jim would be better qualified to address that.

A: JIM DEXTER

Well, I don't really feel that I have anything to add to that, Larry. There is just a shield over it. The crystal is electro-static. We have gotten into some environments where there is electro-static pick up, and they have extended just a normal shield over the crystal and the wire going back to the source follower.

Q: RON TUSSING

I was particularly interested because we found that we had difficulty. Anything we put next to the crystal tended to generate a charge or would give us a stability in results.

JIM DEXTER

It is a fairly loose shield if you look at it. It's not a real tight shield like you find on a coaxial cable. It's more of a loose or open type of shield.

Q: RON TUSSING

I have a couple of other questions on the size charge. Could you tell me what size charge you use in the tank?

A: LARRY BROWN

No, I couldn't tell you the size of charge or its geometry because of the program requirements. I kind of gave you a generic picture of typical traces generated from that charge, and it wasn't truly spherical in nature. I might point out that we did do a lot of qualifications to the transducer by putting a spherical charge, like a one-pound charge, in the tank precisely located and by using Cook's data on underwater pressure time histories versus charge weight.

Q: RON TUSSING

Yes, I was curious. I noticed that there were some perturbations on the decay and a little ringing on the front. I wondered whether that was charge related or was gauge response?

A: LARRY BROWN

That is charge related and that's a good question. I didn't go into that for obvious reasons, but if you put a truly spherical charge in it, the classical, no ringing type of response...

Q: RON TUSSING

Okay, I was concerned about that. Another thing I might just mention for further experimentation is you do want to be careful about putting wood in. It looks like a large air mass and you'll get negative reflections. You don't want that close to the charge or within whatever duration. It looks like your reflection from the side of the walls is out past several ten theta, so that you'd have been all right anyway. But I just wanted to mention about the wood mass.

LARRY BROWN

Yes, I appreciate it. It was easy to work with and it stayed together. That's a very severe environment to operate in and the wood made it easy for us to let it take some of the impact because it was out of the regime where we could get reflections from the primary shock wave. It is affecting the data in the primary shock wave region.

Q: ARPAD JUHASZ, BRL TO MR. PUGNAIRE

What do you think are the limits, the pressure limits that these diaphragms can accept?

A: MR. PUGNAIRE

Well, right now, we go up to 5000 psi. Most of that limitation is because of the glass seal around the back plate. We're going to a smaller diameter and we hope to be in the 8000 psi range very soon. I

believe if we make an integral cast body, excluding the glass seal, we should be able to go to a higher pressure. Of course, we'll have to work on it.

Q: ARPAD JUHASZ, BRL

Okay, second question. The material is capable of going to high temperatures yet, and that might be very attractive in a ballistic application where you want to measure, let's say, machine gun fire or something like that. How about the drift problems that might happen because of the temperature change of the sensing element?

A: MR. PUGNARIE

Well, number one, we can select, as you know, the zero drift. The thermal zero drift of a transducer is statistical in nature. Nominally, we got about five percent of full scale. This is what we state as an average figure. Most units are much below that. We can also either select them for much better zero TC or compensate them for zero TC. So far, the curve is very linear. We haven't done over 150 C. What the curve looks like beyond this, I don't know. It would seem to me, however, that it should be still fairly linear, therefore, fairly easily compensatable.

Q: ALEXANDER YORGIADIS, STRAINSERT CO., WEST COAST OFFICE, ANAHEIM, CA

What is the elastic modulus or the allowable strains on the ceramic which carries, of course, the stress? That would be a very critical parameter for such a use of the device.

A: MR. PUGNAIRE

The modulus is about 40 to 42 million psi. In the maximum we commanded pressure range. The maximum stress is about 66 thousand psi. Much of the limitation of that overload is not only because of the elastic properties of the ceramic itself but of the embedment with the glass. How far you can go, I don't know. I'm sure theoretically you can go much higher than that provided you have no stress riser and no stress concentration.

Q: HARVEY WEISS, GRUMMAN AEROSPACE CORP., CALVERTON, NY

Am I to understand, sir, that the device you are showing us is the basic sensor with the housings, more or less, to be either provided by the user or to be discussed with your firm in an effort to try to develop something specific? The aerospace industry in which I'm involved, would more or less be interested in a piece of stainless steel that we can put in there with all of this interesting transduction taking place, fully compensated internally and hands-off type of thing.

A: MR. PUGNAIRE

Well, we have done those. Because the cell by itself is ideal only for large quantity users who can provide, in their pressure system, a recess for direct mounting of the sensor, thereby saving the cost of housing. Now, we have quoted for P1/P2 sensors, intelligent sensors mounted into a housing, two of them stainless with aluminum for weight, with a zicore memory and a temperature sensor to pick up all the parameters to correct for linearity, zero TCs, etc., to feed the information into a microprocessor. So we do both.

Q: DAVE BANASZAK, AIR FORCE WRIGHT AERONAUTICAL LABS., OH

I have several questions. I was just wondering what type of CPU system you use? Do you have an idea of the approximate cost of this system and whether you're dedicated to transducer calibration or do you perform other things too?

A: MARTHA WILLIS

We're dedicated strictly to doing the transducer at this point. Do you want the manufacturer of this system?

Q: DAVE BANASZAK

Yes, is it like a VAX system or a DEC system?

A: MARTHA WILLIS

It's Data General. It's an Eclipse MV4000 that we're using.

Q: DAVE BANASZAK

Do you know about what it costs?

A: MARTHA WILLIS

No, I don't, but I can get you that cost.

Q: TORBIN LICHT, B & K INSTRUMENTS, DENMARK

On the automated calibration system, do you have any plans of how to implement frequency responses of transducers for instance?

A: MARTHA WILLIS

For high frequency pressure sensors?

Q: TORBIN LICHT, B & K

It could be a frequency for pressure sensors or vibration sensors or such.

A: MARTHA WILLIS

I see. We haven't gotten to the point of implementing the system for those types of sensors yet. I would expect in the next year that we'll start examining those problems, and all I can do is suggest that you either give me your card or you take the paper. As we develop, we'll be more than willing to share with you what problems we find and what we end up doing.

Q: TORBIN LICHT, B & K

A question for Mr. Miller about the cost of laser transducers. You had some very nice formulas describing how the transducer behaves. Have you made any statistical attempt to see whether all the transducers have the same coefficients or have you only tried to do that for one or two transducers from the same batch for instance?

A: MR. MILLER

We've only looked at three transducers so far, and we did notice that the first one was considerably different in a number of aspects from the other two. These transducers, as developed by this company, are very new and we suspect that some of the things we saw in that first transducer were learning problems, for example, lower pressure sensitivity in that one transducer than the others. Now the other two, we have characterized both the same way and find reasonably good pressure sensitivity. The only thing that's a little bit disturbing is one of them had a positive temperature coefficient and the other one had a negative. But, it would fit in the same form of the equation and the processor could take care of that.

Q: TORBIN LICHT, B & K

Do you plan to include all these coefficients in your processor system every time? It would be a rather expensive transducer and computer.

A: JIM MILLER

There's one part we really haven't decided how to solve and that has to do with the temperature sensitivity. There are two ways to work on that problem: put an oven around the thing and control it at a certain temperature, or measure it's temperature and correct those problems analytically. It has a thermometer built in it. I didn't show that but there's a thermometer up in the device. In order to do this analytically, we have to either characterize each transducer ourselves or have the manufacturer's device. You have to hold the temperature to within .05 degree Fahrenheit at some high temperature and that's difficult. So you see, there are tradeoffs both ways. We really haven't decided which way to go, although at this stage it looks like the analytical treatment has the advantage on what we do.

Q: PETER STEIN, STEIN ENGINEERING

I have questions for a couple of the speakers. Mrs. Willis, in your output data, is there enough information to provide a nonlinearity

curve for whatever transducer you're testing, and do you provide your users with coefficients like for second or third order nonlinearity?

A: MARTHA WILLIS

Yes, we do provide coefficients in that data, and there are nonlinearity values for each print that's printed out.

Q: PETER STEIN

The printouts that you showed?

A: MARTHA WILLIS

Yes, I know that it looks so compact; there's so much data in there, but that is provided.

Q: PETER STEIN

I think a general comment or question for the explosion-oriented speakers on the panel. Every time there is a chemical explosion, there is also a transient magnetic field which is probably one of the reasons why you have that EMI shield around there. Also, there are self-generating voltages in manganese and carbon transducers. Once an explosion hits a cable, there'd be triboelectric effects. One of the ways to test for these is just simply to run a dummy channel without a bridge supply or a battery for the half bridge. I just wondered if that had been done, and if any results had been achieved from that kind of test?

Q: JIM DEXTER

I'll dive in where angels fear to tread. We ran the preliminary experiments, we did get about half way there, we did put up a dummy channel with just an inert resistor rather than carbon or the manganese gauge in the immediate proximity to the area so that cabling effects and so forth should have been identical. We saw no significant signals on that channel. Unfortunately, we ran out of channels when we got to the actual models. As I mentioned, we weren't even able to put strain gauges next to them to examine the possibility of strain compensation. So, that certainly ruled out the luxury, well, depending on where you come from, whether it is a luxury or not, I agree with its importance but I don't always get to plan the test.

A: JIM LALLY

The primary point on the underwater gauge is converting to low impedance at the transducer which eliminates much of following the long cable back up to the power unit or signal conditioner.

Q: PETER STEIN

Dynason makes a strain-compensated transducer, or is that more recent than your tests were?

A: JIM DEXTER

We found out about that well into the test and were interested in using it if we went further, but we didn't.

Q: LARRY REMPert, ALLISON GAS TURBINE, DIV OF GM, INDIANAPOLIS, IN

I have a question for the man from DJ Instruments. In one of your slides you showed some hybrid electronic circuitry behind the transducer. Has any thought or consideration been given to making that transducer into a smart transducer? In other words, putting an AD converter and a communication capability into that?

A: MR. PUGNAIRE

All we have done so far is the first phase of it which is to pick the temperature from two tests, pick out all of the thermal dependent parameters, and give that information to the user. We have coded that for a P1 over P2 type device. You have to understand this is new and there is a lot of work to be done on it. We're also working on a 4220 miniamp hybrid electronic circuit and a frequency output circuit as well. So, we have much to do yet.

Q: ROGER NOYES, EG&E, ENERGY MEASUREMENTS, INC., LAS VEGAS, NV

We've recently been looking at a group of para-scientific transducers. I wonder if you have any experience with their frequency response or dynamic sensor? People basically look at these as a number of periods being averaged. I wondered if you had any information on that.

A: MR. MILLER

We've evaluated a number of para-scientific digi-quartz devices over the years. The earlier ones that we looked at used a force technique, a bellows to force the crystal. That probably has a considerably different frequency response than the high pressure one I talked about today. We haven't really evaluated a frequency response because we're mainly interested in static measurements. So I can't say too much about this one as compared to the other, other than there's a very stiff Burdon tube in this one and there's a bellows force apparatus in the lower range ones. Even though we're interested in static measurements, that's only a matter of degrees. There's really nothing perfectly stable. Frequency counting techniques integrate and so to get high resolution, you take a long time but you don't want to take too long. It's a sort of tradeoff there. As far as actually checking the frequency response of either one, we haven't.

Q: LEROY ERICKSON, LAWRENCE LIVERMORE LABORATORY, CA

Just a comment with regard to the measurement of blast waves. It seems to me worthwhile for the record to comment that there's another distinct possibility for making those sorts of measurements as opposed to manganese gauges or carbon gauges and that's the PBF2 sort of gauge. Polybenelodinefloride is pressure sensitive and when activated behaves like a crystal. It's very thin; it's passive so you don't

have to energize it. The difficulty, of course, is that you do have to, in order to get a pressure profile, integrate the output of it. But, that's certainly not impossible. We're working on that now. The difficulty is these things are not generally available. The ones we're working with now we're getting from Francois Balli in France, although Dynason is making some for us. The source of the material is Penwalt, I think. They provide activated material. I'd like to make just one more quick comment. In measuring underwater blast waves, you must be careful of the frequency response. These are basically triangular-shaped waves and so rolling off the high frequency response can give you quite a difference in the pressure that you observe.

A: MR. PUGNAIRE

We haven't done enough to try to understand the gauge factor of the thick film. We found out that gauge factor is sensitive in three directions; therefore, you could have a pressure sensitive device. I don't know what the output is exactly, but it appears to be quite significant. The gauge can be very small, 50x50 mils, and so you could have a high frequency type response and high pressure. But again, if anybody's interested, I would be glad to supply some samples for you to play with.

Q: RON TUSSING, NSWC

Just a comment on Jim Lally and Peter Stein's interchange on cables. Of course, we do a lot of underwater explosions in the ocean and in the rivers and maybe on a larger scale than the tank tests. We've found when a gauge is used without a preamp certainly the tribo electric effect needs to be considered, and there you do your best to run your cables radially away from them when you can, that is, away from the charge. We also ran into the problem where we thought that if we put a preamp there we'd get rid of this cable noise. What we actually found was that you don't get rid of the cable noise, that you do have tribo electric effect, that you have an added thing that if you run or put a voltage on a preamp or current through the wire the compression changes the capacity in $Q=CV$. So you have a voltage generated because of the voltage that's on the cable. It's best, to still run it radially away, to keep your voltages down on the cable and to use low noise cable at that.

Q: GARY PATTERSON, PRECISE SENSORS, MONROVIA, CA

Typically, are your new pressure modules in any kind of a way that could be repaired or recalibrated or if they fail, is that's it? I'm speaking of ones that have been packaged into a finished transducer configuration, stainless steel, aluminum or whatever. Are they repairable?

A: MR. PUGNAIRE

Well, it depends on what's wrong with it. Usually they are not repairable. Number one, the sensor itself is low cost; therefore, the best thing to do is replace the sensor. Now, where the cost comes in is in the recalibration, and they'll have to be calibrated certainly.

The cost of the sensor for the capsule is very low and if you have trouble with it, the best thing to do is to replace it rather than trying to repair it. You will have, however, to recalibrate it unless you buy a CP which is already calibrated or within one percent of full scale, then you will have difficulty repeating within one percent full scale.

Q: LARRY SIRES, NAVAL WEAPONS CENTER

What is the cost? You say it's very low.

A: MR. PUGNAIRE

Well, it depends what type you get and what quantity you get, but we're talking in large quantity about \$10 for the sensor. By the way, bending beams can be made even cheaper than that.

Q: LARRY SIRES

If one wanted to grab hold of some of your source code, would you be willing to share that with us?

A: MARTHA WILLIS

I can't answer that. I can find out for you whether or not we can let people have it.

Q: LARRY SIRES, NWC

It's almost a standard question whenever anyone presents something with software. It's also becoming the stock answer, by the way.

I'd like to thank everybody and the panel members. I think it's been a very enjoyable session, at least for me, and I thank everybody for their attention.



SESSION 4

MANUFACTURERS' PANEL - 13th TRANSDUCER WORKSHOP

4-6 JUNE 1985
MONTEREY, CALIFORNIA
(Holiday Inn)

CHAIRMAN - TRANSDUCER GROUP/RCC

LeRoy Bates
NSWSES - Code 4250
Port Hueneme, CA 93043

GENERAL CHAIRMAN - TRANSDUCER WORKSHOP

Richard W. Krizan
ESMC/RSL
Patrick AFB, FL 32925-5532

MANUFACTURES' PANEL SESSION ORGANIZER

Stephen Kuehn
Engineer
Sandia National Labs
Division 7546
P.O. Box 5800
M/S 828-2
Albuquerque, NM 87185

MANUFACTURES' PANEL SESSION MODERATOR

Peter K. Stein
President
Stein Engineering Services, Inc.
5602 East Monte Rosa
Phoenix, AZ 85018

PANEL MEMBERS

Lawrence R. Dotl
President
Precise Sensors
235 West Chestnut
Monrovia, CA 91016

Fred Rehkop
Applications Manager
Hottinger Baldwin
Measurements, Inc.
P.O. Box 1500
Farmingham, MA 01701

Richard C. Phillips
Manager, Development Engineer
Easton Corporation/Physical
Measurements Products
P.O. Box 1089
Troy, MI 48090

Wilson A. Clayton
Director of Engineering
HY-CAL Engineering
9650 Telstar Avenue
El Monte, CA 91731

Henry F. Stry
Marketing Manager
Teledyne Tabor
455 Bryant Street
North Tonawanda, NY 14120

Elmer Hazelton
Senior Project Engineer
Piezoelectric Products
Gulton Industries, Inc.
1644 Whittier Avenue
Costa Mesa, CA 92627

SESSION 5

RECENT STRESS GAGE DEVELOPMENTS*

J. Kalinowski, T. Stubbs, L. Davies
EG&G Energy Measurements, Inc.
2801 Old Crow Canyon Road, San Ramon, California 94583

B. Hudson
Lawrence Livermore National Laboratory
P. O. Box 808, Livermore, California 94550

ABSTRACT

EG&G Energy Measurements, Inc. (EG&G) has been participating with the Lawrence Livermore National Laboratory (LLNL) in an effort to develop a stress gage which will measure stresses up to about 1 kilobar generated by an underground nuclear explosion. The design of the present fluid-filled cavity stress gage is discussed, as well as the instrumentation used to field the gage. Data gathered by this gage on a recent nuclear event are also presented.

INTRODUCTION

During the past few years, LLNL and EG&G have been involved with the development of a stress gage to measure stresses (up to about 1 kilobar) produced by the detonation of a nuclear device. This paper describes the design of the present fluid-filled cavity stress gage and its implementation in the field at the Nevada Test Site. In addition, data collected with this stress gage on a recent nuclear event are presented.

DESIGN

The stress gage contains two thin fluid-filled cavities, each having stress and strain measuring elements. One cavity is oriented perpendicular to the radial shock wave and the other cavity is oriented transverse to the shock wave. Figure 1 illustrates the stress gage design. Fluid-filled cavities are used to reduce gage element strain that may be induced by gage package deformation. The cavities are made thin in order to maintain a quasi-uniaxial gage; their walls are constructed of laminated fiberglass sheets that have been hollowed out to accept the gage elements. The cavities are filled, under vacuum, with a DC-704 fluid.

*This work was supported by the U.S. Department of Energy under Contract No. DE-AC08-NV10282. NOTE: By acceptance of this article, the publisher and/or recipient acknowledges the U.S. Government's right to retain a nonexclusive, royalty-free license to any copyright covering this paper.

The stress and strain elements are configured so that strain in the stress element can be accounted for. The stress and strain elements have the same dimensions (1 inch x 1 inch grid) and are overlaid on a Kapton sheet (DuPont polyimide film), with only thin strands of Kapton attached to the cavity sidewall. The Kapton sheet is reinforced with a steel shim to nullify any Kapton deformation. Independent measurement of the strain allows for a strain correction to the stress element data. Figure 2 illustrates the gage element packaging.

Ytterbium was chosen as the piezoresistive element because of its larger resistance change per given stress, about 4% $\Delta R_0/R_0$ at 1 kilobar. However, the strain gage factor of ytterbium is significant. To allow for strain correction, constantan--a material with nil stress sensitivity (1),(2)--was chosen to measure the strain on the ytterbium element carrier. The data from the constantan element are used to correct the strain component in the ytterbium stress data. Laboratory measurements are currently being conducted to verify the validity of the strain correction techniques and to provide better strain correction factors. This is important because of the different moduli of the element materials--constantan moduli are nearly a factor of 10 greater than that of ytterbium.

INSTRUMENTATION

Fielding stress gages on an underground nuclear test involve some difficult problems such as gage-to-medium coupling, cable survival during ground motion, cable lengths exceeding 2,000 feet, temperature variations, electromagnetic pulse (EMP), and instrumentation of the gage. The gage-to-medium coupling problem is being addressed by precasting the gage fiberglass cavities in a material similar to that in which the measurement is to be made, usually a gypsum-concrete mixture (3).

Cable survival has been attacked by using stretch cable and by making the cable an integral part of the stress gage. The elongation capability, greater than 20%, and flexibility of the stretch cable should allow gypsum-concrete and stemming motions without cable breakage by either stretching or kinking. The stretch cable may either extend to the surface or to a downhole multiplexing instrumentation package which is located in a more benevolent environment.

The problems of cable length, temperature, EMP, and instrumentation are being addressed by using a downhole multiplexing instrumentation package. The use of this package greatly reduces the length of cable that can influence the measurement. The stretch cable, from the stress gage to the downhole multiplexing instrumentation package, is usually only 100 feet long, and, because it is buried, is in a temperature-stable environment. A single coaxial cable provides communication from the downhole multiplexing instrumentation package to the recording trailer on the ground surface.

The downhole instrumentation package provides signal conditioning, bridge completion circuit, and multiplexing of the gage data. This signal conditioning is accomplished with constant current excitation, a half-bridge configuration, with signal inputs into a differential amplifier. The half bridge is completed with a resistance element constructed of the same material and with the same dimensions as the active element. Substitution calibration is also provided along with channel identification.

The multiplexing is accomplished by taking the signal from the differential amplifier and putting it into a voltage-controlled oscillator (VCO). The outputs of the VCOs are then coupled to the uphole cable for transmission back to the recording trailer on the surface. Data are recorded on tape machines, usually running at 120 inches per second. Figure 3 is a schematic of the stress gage, signal conditioning amplifier, and multiplexing package.

The reduction of EMP effects is being accomplished by careful grounding and shielding. The shell of the stress gage is covered with a thin copper sheath which is attached to the outer shield of each of the cable-shielded wire pairs. This forms a Faraday shield with both the instrumentation package casing and the outer conductor of the uphole coaxial cable. The outer conductor of the coaxial cable is then grounded to the outer shell of the recording trailer which is, in turn, grounded to the system ground (wire and/or pipe). An additional ground wire is also run the entire length--from the stress gage to the emplacement pipe. This wire is multi-point attached to the system to further reduce EMP-induced surface currents. Figure 4 schematically shows the grounding scheme. EMP is further reduced by using a differential amplifier with high common mode rejection in the signal input to the downhole multiplexing instrumentation package.

Figures 4 and 5 show data taken from stress gages that were fielded on a nuclear event. These gages were located in a gypsum-concrete plug, approximately 125 and 145 feet above the explosion point, and appear to have given reasonable data. Figure 4 presents the data taken from a radially oriented gage. Curves from the stress and strain elements are shown, along with the strain corrected curve. Stress data have been corrected for strain and the results are considered to be indicative of the stress only. The peak measured value (0.62 kbar) is within the prediction band. Figure 5 presents the strain, stress, and corrected stress curve data taken from a tangentially oriented gage. The residual stress (0.14 kbar) measured is within the expected range.

CONCLUSION

While reasonable data have been obtained with the present gage design, considerable work still remains in the development of the stress gage. Materials other than ytterbium and constantan are under review. Gage packaging is also under review and the design has already evolved. Better EMP protection is required. Stress gage and cable survival still remain a problem at higher stress levels.

REFERENCES

- (1) Chen, D. Y., et al., "Quasistatic Experiments to Determine Material Constants for the Piezoresistive Foils Used in Shock Wave Experiments," Journal of Applied Physics. Vol. 55, Number 11, June 1, 1984, pp. 3984-3993.
- (2) Charest, J. A., "Development of a Strain-Compensated Shock Pressure Gage," Report TR005. Dynasen, Inc., Goleta, California, February 1979.
- (3) Florence, A. L., et al., "Calculational Evaluation of the Inclusion Effects on Stress Gage Measurements in Rock and Soil." Symp. Proc. Interaction of Non-nuclear Munitions with Structures, U.S.A.F. Academy, Colorado Springs, Colorado, May 10-13, 1983.

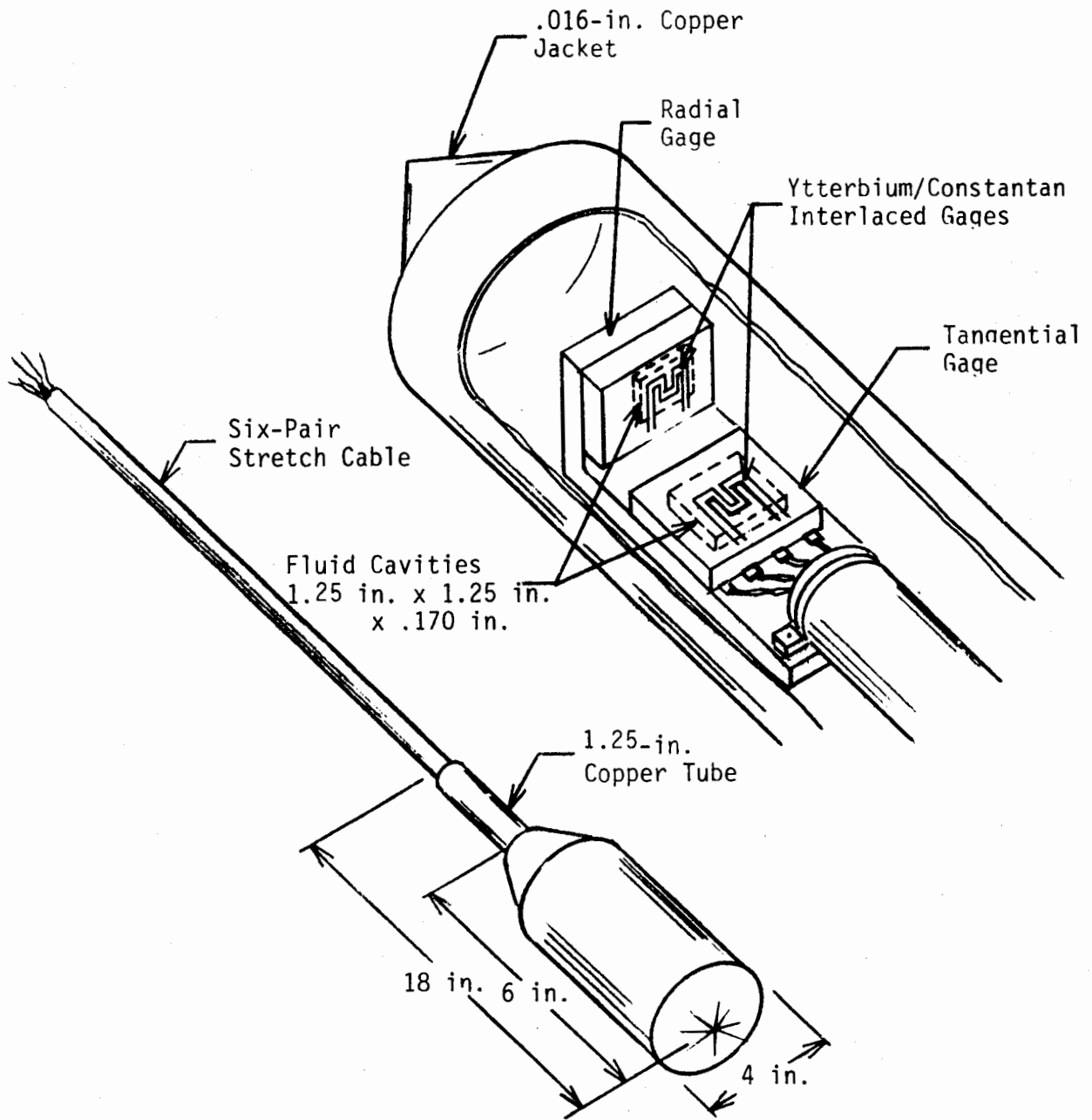


Figure 1. Stress gage design.

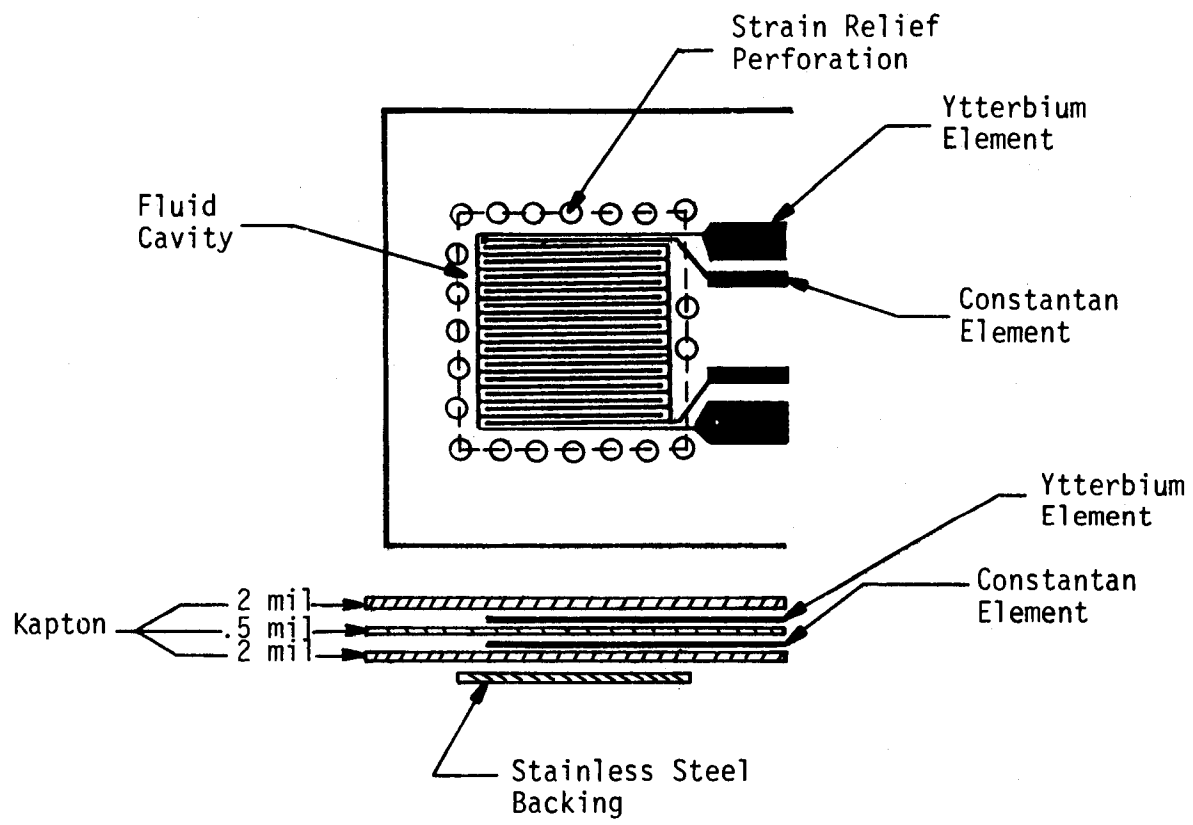


Figure 2. Gage element packaging.

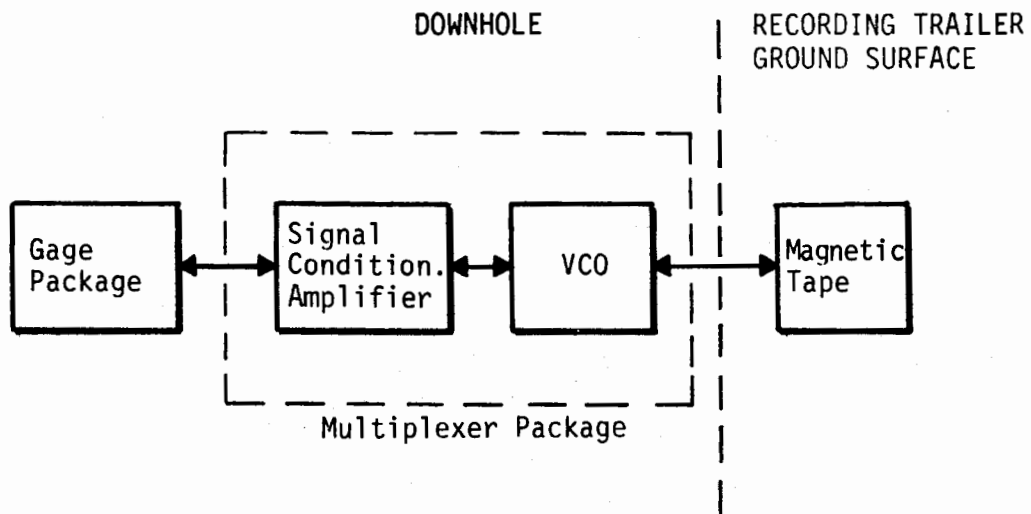


Figure 3a. Signal conditioning amplifier and multiplexing system diagram.

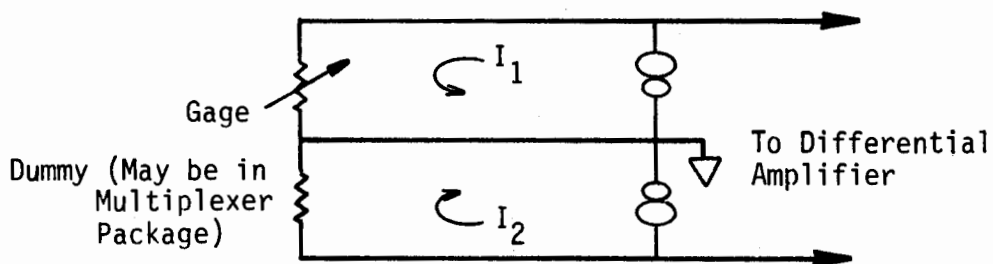


Figure 3b. Gage package.

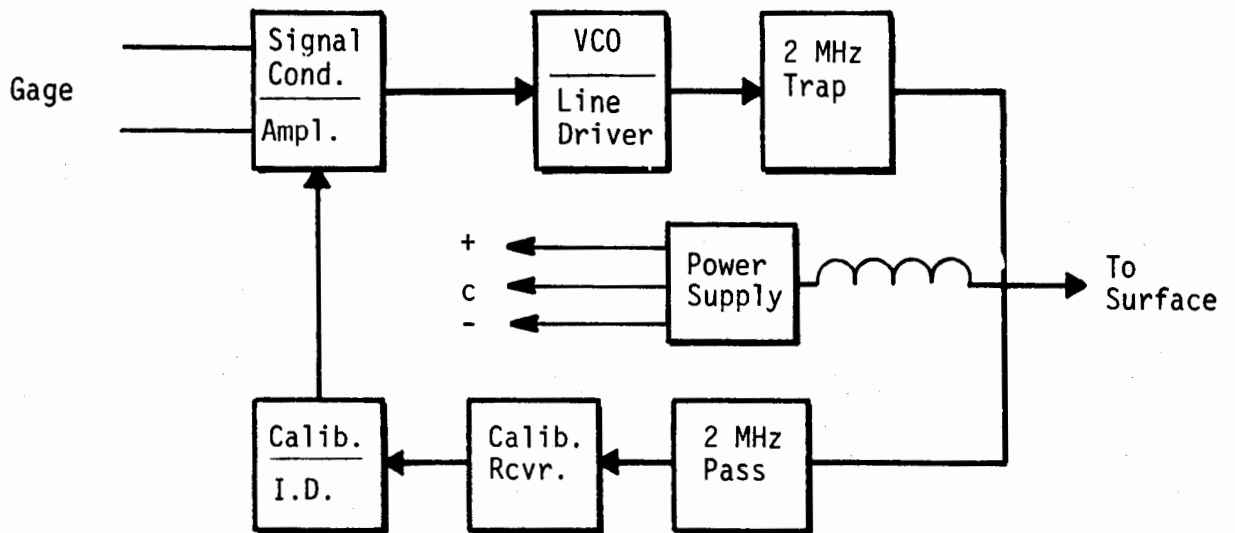


Figure 3c. Multiplexer package.

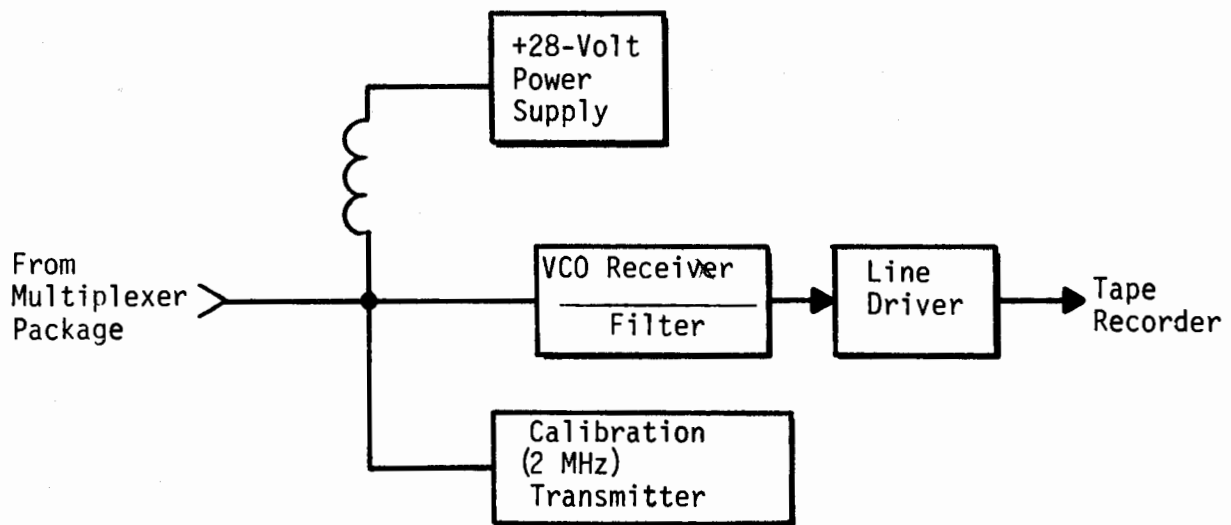


Figure 3d. Surface unit.

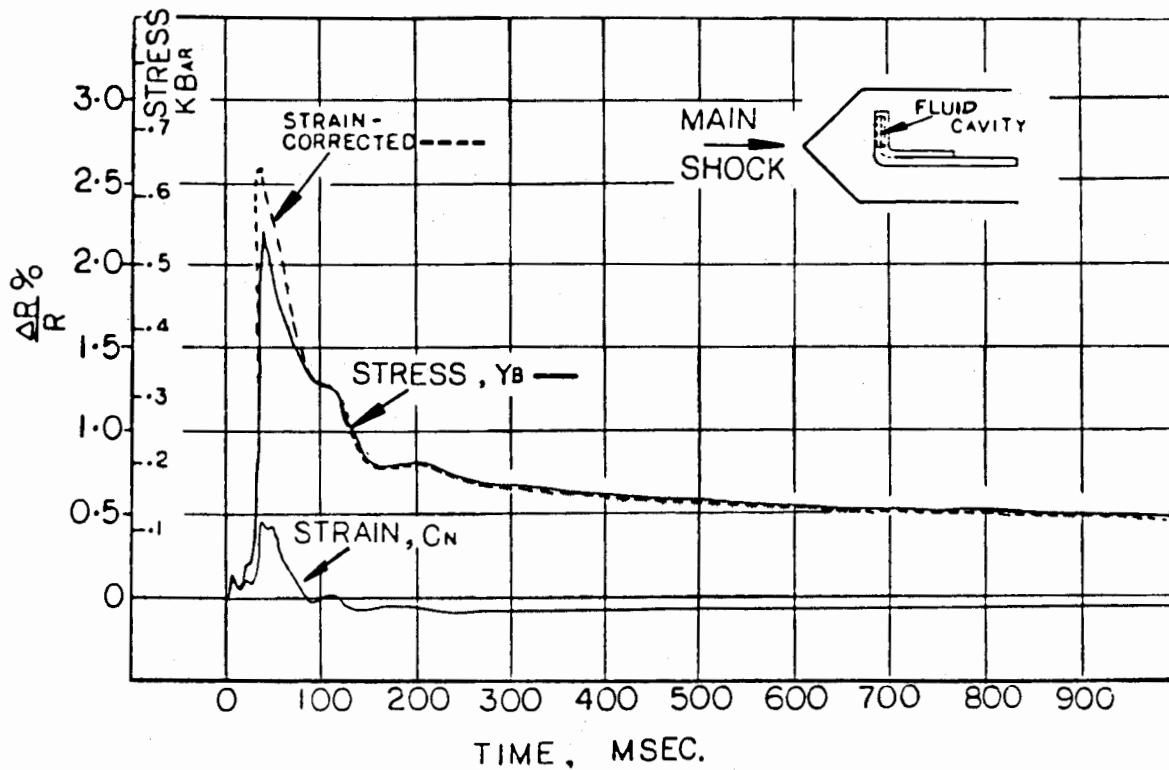


Figure 4. Data from radially oriented gage.

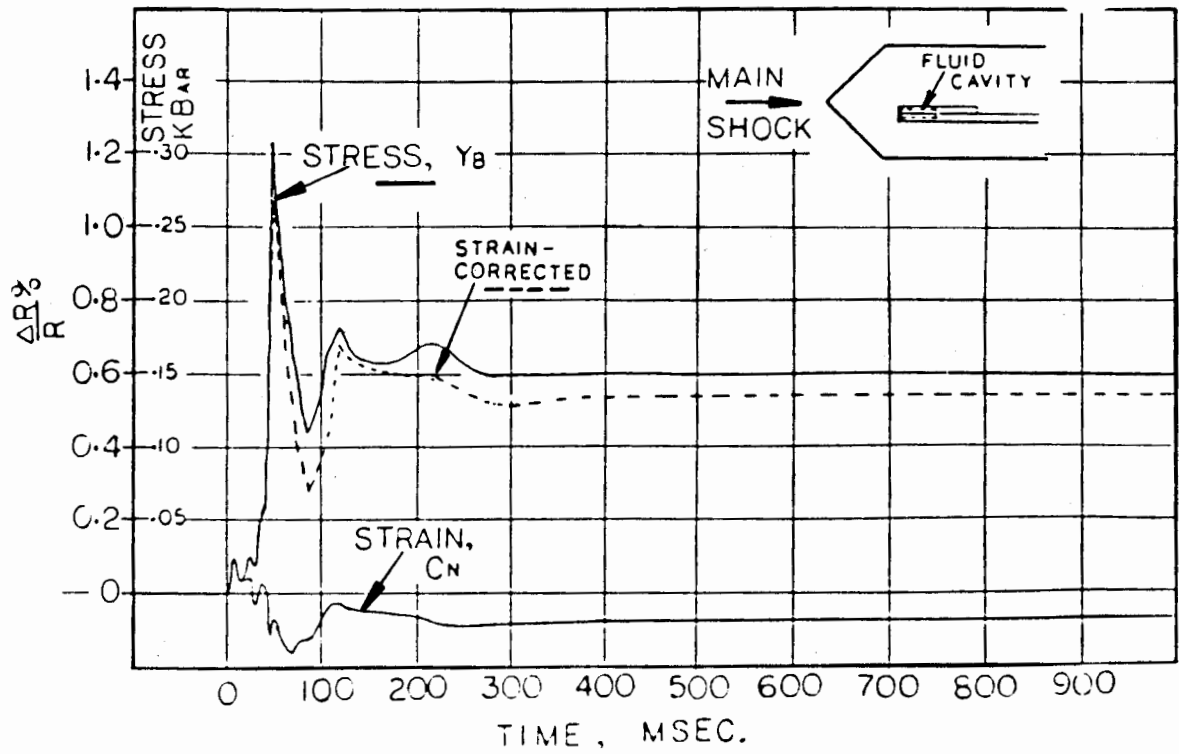


Figure 5. Data from tangentially oriented gage.

INTENT TO PRESENT

Range Commanders Council/Telemetry Group
Vehicular Instrumentation/Transducer Committee

13th Transducer Workshop, Monterey, CA

Author's Name J. A. Kalinowski
Co-Author's Name T. F. Stubbs
Co-Author's Name L. Davies

Organization EG&G Energy Measurements, Inc.
2801 Old Crow Canyon Road
San Ramon, CA 94583

Telephone (415) 838-3200

Co-Author's Name B. C. Hudson

Organization Lawrence Livermore National Laboratory
P. O. Box 808
Livermore, CA 94550

Telephone (415) 422-1100

Proposed Paper Title: Recent Stress Gage Developments

**PRACTICAL APPLICATION OF MAGNETOSTRICTION
TO A HIGH SPEED TORQUEMETER**

**FRANCIS E. SCOPPE AND KENNETH S. COLLINGE
AVCO LYCOMING DIVISION, STRATFORD, CONNECTICUT**

**THIRTEENTH TRANSDUCER WORKSHOP
SPONSORED BY
VEHICULAR INSTRUMENTATION/TRANSDUCER COMMITTEE
TELEMETRY GROUP
RANGE COMMANDERS COUNCIL
JUNE 4-6, 1985, MONTEREY, CALIFORNIA**

PRACTICAL APPLICATION OF MAGNETOSTRICTION

TO A HIGH SPEED TORQUEMETER

FRANCIS E. SCOPPE AND KENNETH S. COLLINGE
AVCO LYCOMING DIVISION
STRATFORD, CONNECTICUT 06497

Abstract

The principle of magnetostriction has been used to develop a highly accurate torque meter for gas turbine engines. This torque meter utilizes the effect of changing magnetic permeability in a ferromagnetic material subjected to mechanically induced torsional shear stress in a rotating shaft. The relationship of torque to shear stress is transduced through magnetic reluctance to produce an electrical information signal which is proportional to the engine shaft torque.

To extend this torque meters growth from its present operational capabilities of $\pm 2.5\%$ accuracy at speeds to 20,000 RPM to $\pm 1\%$ accuracy at 30,000 RPM, a test program (1)* was used to evaluate a new ferromagnetic material for use as the torque transducer. This program also evaluated a modified torque sensor design and, through extrapolation, the test data was used to prepare a specification for fabrication of a development system for a high speed application.

This paper summarizes the test program and results and describes a system which is presently undergoing evaluation tests.

Introduction

A sensor providing high accuracy, noncontact measurement of torque from rotating shafts has been developed and is in production use for all civilian and military versions of the Avco Lycoming T55 turboshaft engines and in all turboprop versions of the T53 gas turbine engines. This sensor applies the magnetostrictive principle of ferromagnetic materials as its basis for the design of a unique measurement transformer. This transformer produces an electrical signal as a function of the magnitude and direction of torque transmitted by the engine output shaft.

*Numbers in parenthesis designate references at the end of this paper.

One version of this system provides an accuracy of measurement to within $\pm 2.5\%$ of the actual value at speeds of 8000 to 16,000 RPM in a torque range from 800 to 1600 foot pounds in a 300°F temperature environment. An improved system is now under development with an output signal accuracy to within $\pm 1\%$ of the full scale value at speeds of 25,000 to 30,000 RPM in the same temperature environment.

General System Description

To adapt the magnetostrictive principle to a torque sensor, the known shear stress distribution of a torsionally loaded shaft is applied to the design of a variable reluctance transformer.

The following standard definitions are supplied for clarification:

Transducer - The magnetostrictive shaft material stressed by the transmitted engine torque.

Transformer - The laminated core and windings surrounding the transducer.

Torque Sensor - The magnetically coupled transformer and transducer assembly.

Torque meter - The torque sensor, power supply and signal conditioning circuitry supplying a torque related output signal.

The transformer is designed to use the stress related reluctance of the engine shaft material as a portion of its core path. This reluctance varies as a result of magnetostriction, decreasing in the plane of shaft tensile stress and increasing in the plane of shaft compressive stress.

The engine shaft, therefore, not only transmits the engine output power, but is also the torque transducer converting mechanical force to an electrical measurement variable. The relationship of a ferromagnetic material's magnetic property change with applied force is described in References (2) and (3).

The transformer functions as torque sensor using the following magnetic characteristic:

- A primary coil is used for producing a controlled level of magnetic flux.
- Four secondary coils, two at -45° to the shaft (transducer) axis sensing compressive load effects and two at $+45^\circ$ sensing tensile load effects are magnetically coupled to each primary.
- The torsionally loaded shaft (transducer) acts as a variable reluctance component of the transformer core.
- An air gap between the stationary and rotating components adds as a series element to the total core reluctance.

Multiple primary and secondary sections are used in the transformer to increase the stress sensitivity. The primary coils are connected in parallel to the power supply while the secondary coils are connected in series aiding voltage configuration.

Figures 1, 2 and 3 show the mechanical arrangement and electrical schematic for a three-section transformer. This transformer configuration is presently operational in production systems and has accumulated over four million of hours of successful operation.

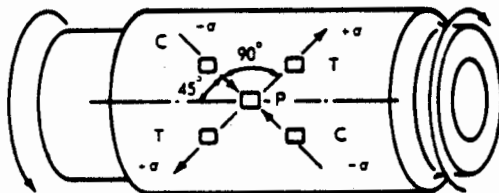


FIGURE 1. TRANSFORMER POLE LOCATIONS WITH RESPECT TO SHAFT PRINCIPAL STRESSES

Figure 4 shows the transfer curve for a Relay 5 silicon steel transducer material. Relay 5 material was selected for its high sensitivity, but special manufacturing techniques required to accommodate both its nonlinearity and its low mechanical strength limit its application. To overcome its strength limitation, a thin sleeve of the Relay 5 steel is bonded to a high strength steel selected for its mechanical properties. This assembly is then loaded to induce

residual shear stresses in an opposite sense to that of its normal loading. Normal engine loads thus operate on the more linear segment of the transfer curve--line segment O'A' rather than OA. However, this material is still limited due to the loss of signal resolution with increasing torque loads.

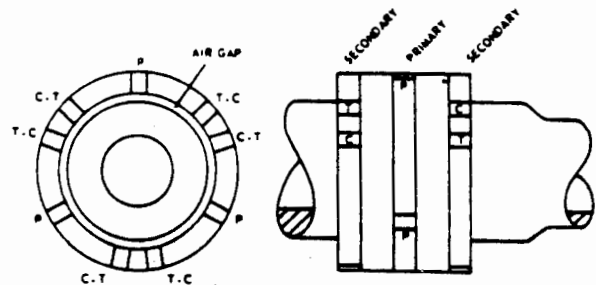


FIGURE 2. TRANSFORMER POLE LOCATIONS WITH RESPECT TO SHAFT

Significant improvements have been made in the torque meter system over the years. Reference (4) describes an improved electronic system utilizing a ratio detection system which, firstly, eliminates errors due to fluctuations in the primary coil power supply and, secondly, uses digital microprocessor technology to linearize the nonlinear material transfer curve shown in Figure 4. Other minor improvements were shown to be needed as a result of this effort, leading to the current program.

Current Development Program Scope

As accuracy requirements increased to require measured values to within $\pm 1\%$ of actual torque, transformer and signaling conditioning accuracy was unable to compensate for the transducer transfer curve variations. Using Relay 5 transducer material, nonlinearity and saturation was a major problem. This material is very sensitive to processing variables, not only from one heat lot to another, but from different bars within the same heat lot and even to different sections of the same bar. Clearly a material was required with consistent controllable properties.

It was also felt that bonding a sleeve to the power shaft, usually by electron beam welding, was a more expensive procedure than using the shaft material itself as the transducer.

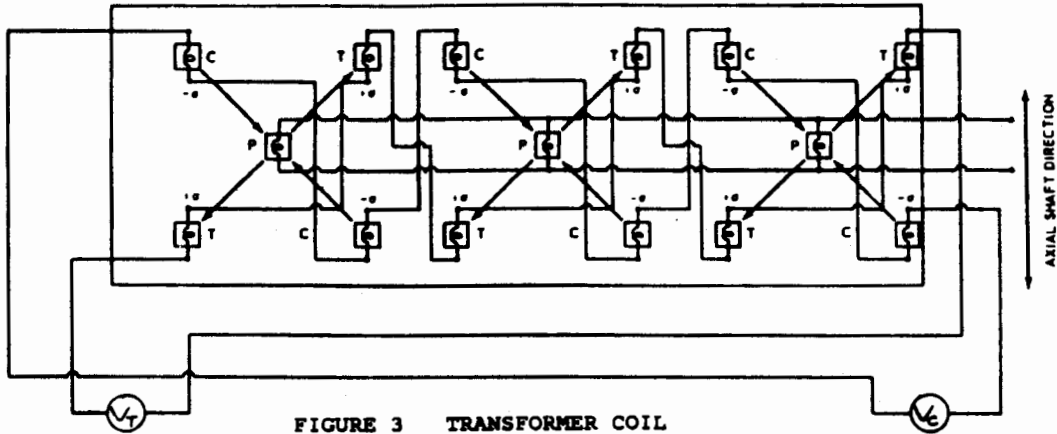


FIGURE 3 TRANSFORMER COIL CONNECTIONS WITH RESPECT TO SHAFT PRINCIPAL STRESSES

The transformer configuration was considered to be less than optimal because the circular configuration requires the load carrying shaft transducer section be the largest diameter on one end in order to assemble the transformer to the shaft. A split configuration transformer could be installed around an installed shaft (transducer) even if both shaft ends had larger diameters.

Development Torque Sensor Design

A 2-inch outside diameter shaft was selected based upon previous aircraft gas turbine engine experience. The inside diameter was defined to produce 8 psi shear stress per foot pound torque. Two

shafts were fabricated for the evaluation. One was made entirely of AMS 6265 carburizing steel. The other was composed of an AMS 6265 sleeve electron beam welded to a Nitralloy 135 shaft. The sleeve approach was retained since its obvious advantage of allowing transducer replacement without destroying an expensive shaft is considered a desirable manufacturing capability.

In prior tests, AMS 6265 steel had shown a suitable transfer curve for a torque transducer. Figure 5 shows cross sections of the two shaft specimens fabricated for the test program. The two specimens are dimensioned to produce equal surface shear stress to torque ratios. The transformer (lamination assembly) was designed as a five-ring structure fabricated from stamped 0.006 inch thick iron-nickel electrical sheet steel. The assembly was split along an axial line to provide symmetrical halves for ease of installation. Because of the symmetrical split line, an even number of primary poles was selected. Six primary coils with four secondary coils each was considered but due to limited space for coil windings, a 4 primary pole configuration was selected.

The outer rings contain pole structures for attachment of the secondary coils. Four secondary coils, two tensile plane and two compressive plane are spaced at $\pm 45^\circ$ from each primary. Figure 6 shows the pole surface dimension projections for one primary coil. The completed assembly, showing the pole face surfaces with respect to the shaft shear stress distribution is shown on Figure 7.

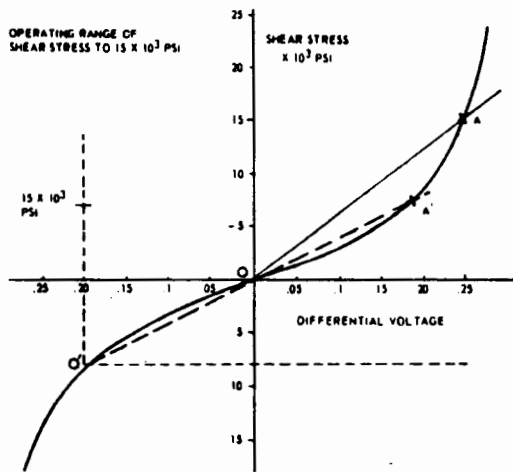


FIGURE 4 "RELAY 5" TRANSducer MATERIAL TRANSFER CURVE

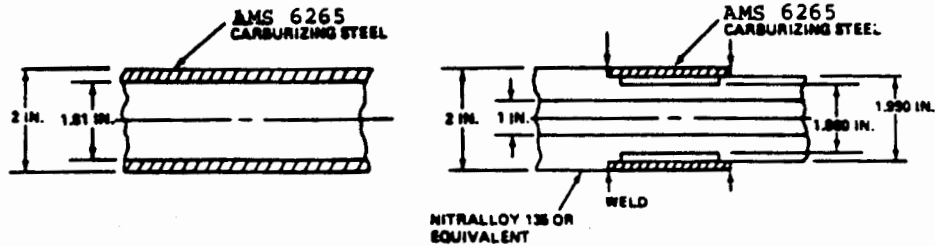


FIGURE 5 TORQUE TRANSDUCER (SHAFT) TEST SECTIONS

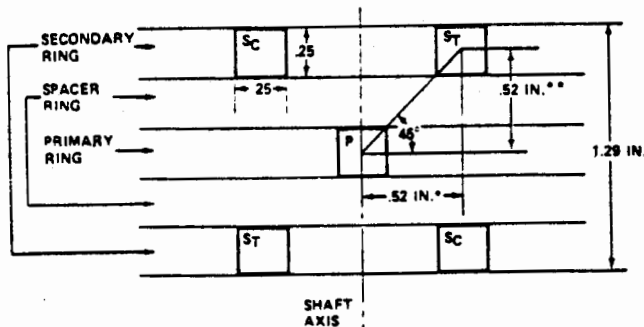
Both the primary and secondary coils were wound with the same number of turns as used with the operational three-pole sensor. The primary coils were wound with 420 turns of 30 AWG magnet wire and the secondaries coils with 900 turns of 40 AWG magnet wire.

To establish an optimal core flux, a variable current variable frequency power supply was used for primary coil excitation. Prior experience using a three-pole sensor configuration and a 2 1/2% silicon steel as the transducer material had shown a magnetomotive force of 75 ampere turns per primary coil, developing a core flux density of approximately 0.2 Telsas, as producing an acceptable level of stress sensitivity. The first phase of this test program concentrated upon establishing an optimal value of magnetomotive force for the AMS 6265 transducer material.

To increase the stress sensitivity and to minimize effects of the misalignment between the transformer assembly and the rotating shaft, all related secondary coils are connected in a series aiding voltage configuration, i.e., 8 tensile plane coils in series and 8 compressive plane coils in series. Figures 8 and 9 show the torque sensor in a static torsional loading fixture. Figure 10 shows the coil internal wiring.

Test Program

The test program was designed to achieve two objectives. The first was to establish the magnetic excitation level requirements for the torque sensor. This specifically included the practical considerations to minimize the supplied power for heat generation and to define the power supply requirements for current and frequency regulation.



* CALCULATED FROM THE SHAFT OUTSIDE DIAMETER AND SECONDARY ORIENTATION OF 30° WITH RESPECT TO THE PRIMARY.
 ** MADE EQUAL TO DIMENSION *

FIGURE 6 PRIMARY AND SECONDARY POLE DEVELOPMENT

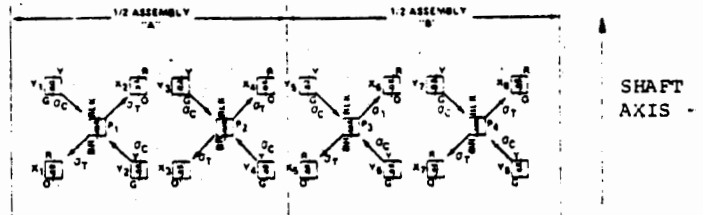


FIGURE 7 POLE FACE SURFACES WITH RESPECT TO SHEAR STRESS

The second objective was to evaluate the torque sensor performance in the operational environment at rotational speed and at engine temperature.

The program included both static (nonrotating) laboratory testing and dynamic (rotating) engine testing. The static test fixture employs a hydraulic loading system to apply torque thru a load cell with an NBS traceable accuracy of $\pm 0.5\%$ of full scale.

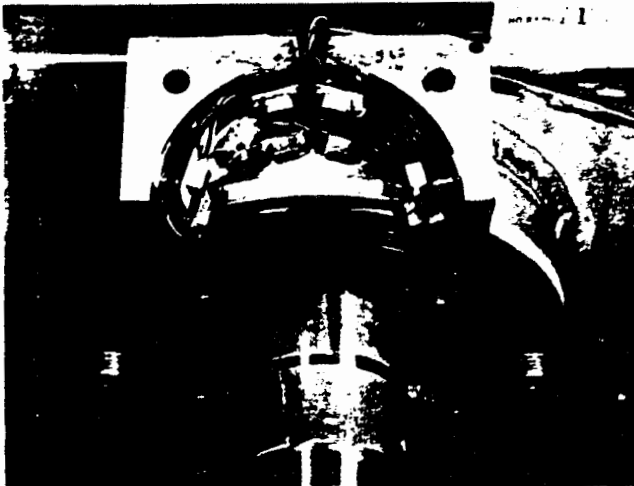


FIGURE 8 TORQUE SENSOR (DISASSEMBLED) IN STATIC LOADING FIXTURE

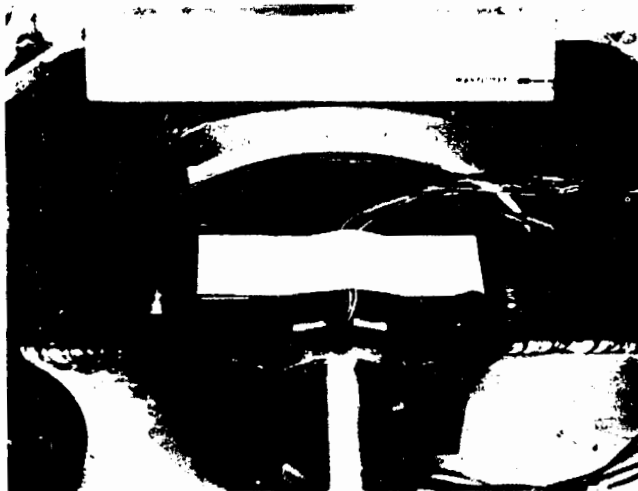


FIGURE 9 TORQUE SENSOR (ASSEMBLED) IN STATIC LOADING FIXTURE

For dynamic testing, a Lycoming T55-L-11 engine of 3750 SHP at 15,500 RPM was used as the loading device. A strain gaged torque element, with NBS traceable accuracy to within $\pm 1.5\%$ of reading, installed between the test specimen and a water brake as power absorber was used to provide the reference torque for comparison of the sensor data.

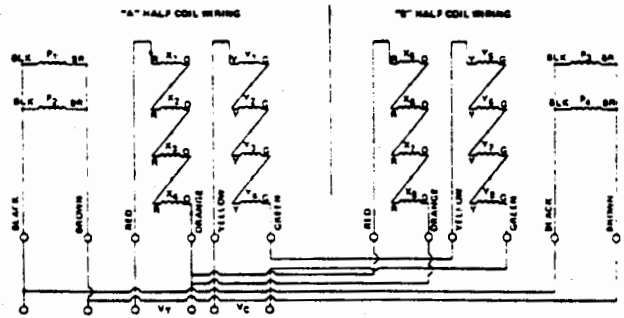


FIGURE 10 TRANSFORMER COIL INTERNAL WIRING

The torque sensor was powered by a variable frequency, variable current power supply. For signal detection both a differential detector measuring a rectified and filtered V_t minus V_c and a null balancing servo amplifier developing a voltage ratio were used. The differential voltages were used during the 1st phase of test when data was needed to determine the system operating levels. The null balance detector was used when signal accuracy was needed to determine effects of the operational environment.

Initial testing was performed to establish the required operating levels for the magnetic circuits. Test results, see Figure 11, show that there is no significant difference in signal sensitivity between the sleeved and the non-sleeved shafts. This initial transfer curve for the AMS 6265 steel did, however, show an unexpected nonlinearity suspected to be a result of a heat treat process which left the material in an annealed condition. To verify this, the non-sleeved shaft was heat treated to 1500°F, quenched in oil and then tempered at 300°F followed by air cooling. The resulting improvement in linearity is obvious as shown on Figure 12.

Figures 13 and 14 show the effects of input current and frequency on output voltage for the solid shaft. For this testing, a constant (nonrotating) load of 800 foot pounds (6400 PSI) was applied while varying primary current and frequency. A .015 inch radial air gap was maintained during this testing. This gap is a minimum for engine level requirement to avoid rub.

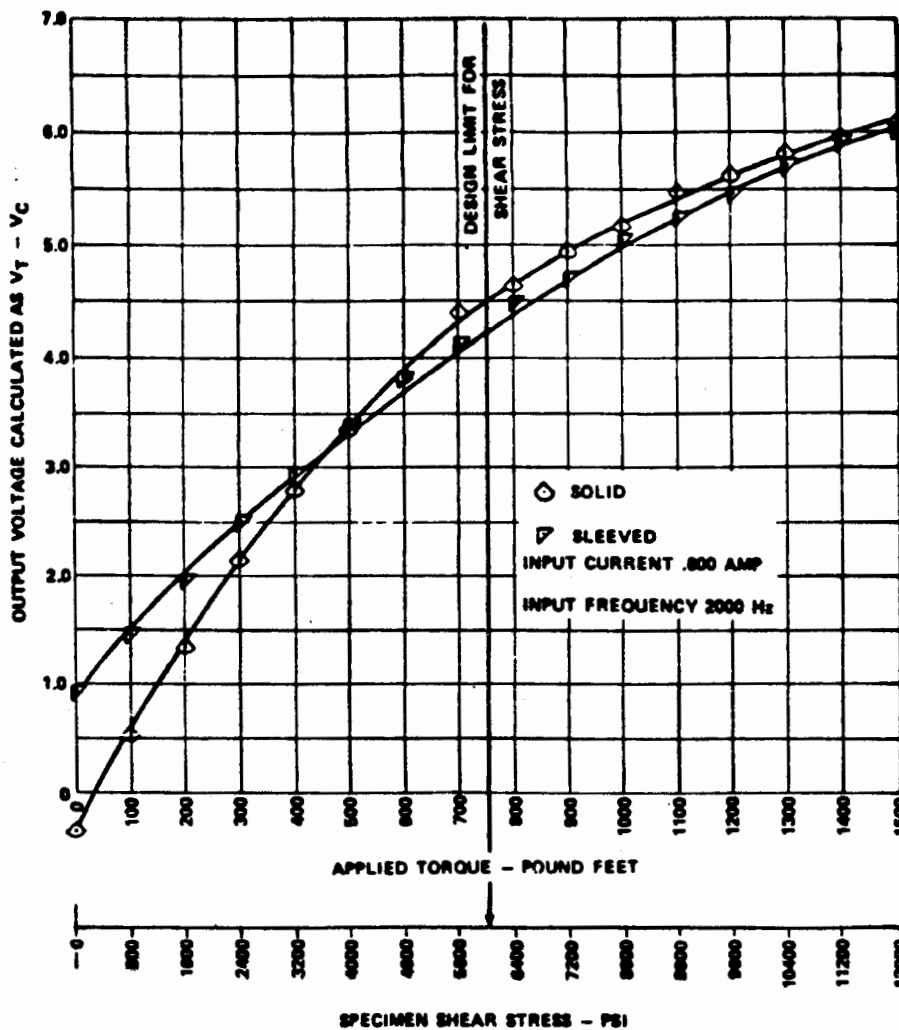


FIGURE 11 INITIAL TRANSFER CURVE FOR AMS 6265

The differential voltage, plotted on Figure 13, showed a current of .67 amps was optimal for sensitivity while maintaining minimal power supply requirements for current and frequency regulation. The .67 amp produces an 70. ampere turn magnetomotive force per primary coil which is consistent with the value used for the silicon steel transducer. As no significant differences were noted between the sleeved and nonsleeved specimens, a signal sensitivity as a function of air gap clearance was evaluated using the nonsleeved shaft and the static load fixture. This data plotted on Figure 15 shows the reduction of sensitivity as a function of increasing air gap. From this testing, a nominal gap of 0.035 inch was selected based upon signal sensitivity of approximately 90% of 0.015 inch clearance. Based upon this testing, a nominal excitation current of .670 amps at 3000 hz with an air gap of .035 inches was selected for the torque sensors design parameters.

Performance Evaluation Testing

For performance evaluation, data was obtained to analyze the following conditions:

1. Effects of temperature in the transducer material.
2. Effects of temperature on the torque sensor.
3. Static to Dynamic Calibration Coincidence.
4. Rotational effects with the shaft at speeds from 7500 to 15,000 RPM.

Metal Temperature Tests. To evaluate temperature effects on the AMS 6265 steel, a silicon fluid, temperature controlled from -35 to +240°F, was flowed through the bore of the non-sleeved specimen. This testing showed no change to the zero torque signal; however, the overall signal sensitivity was reduced by approximately 2.5% for

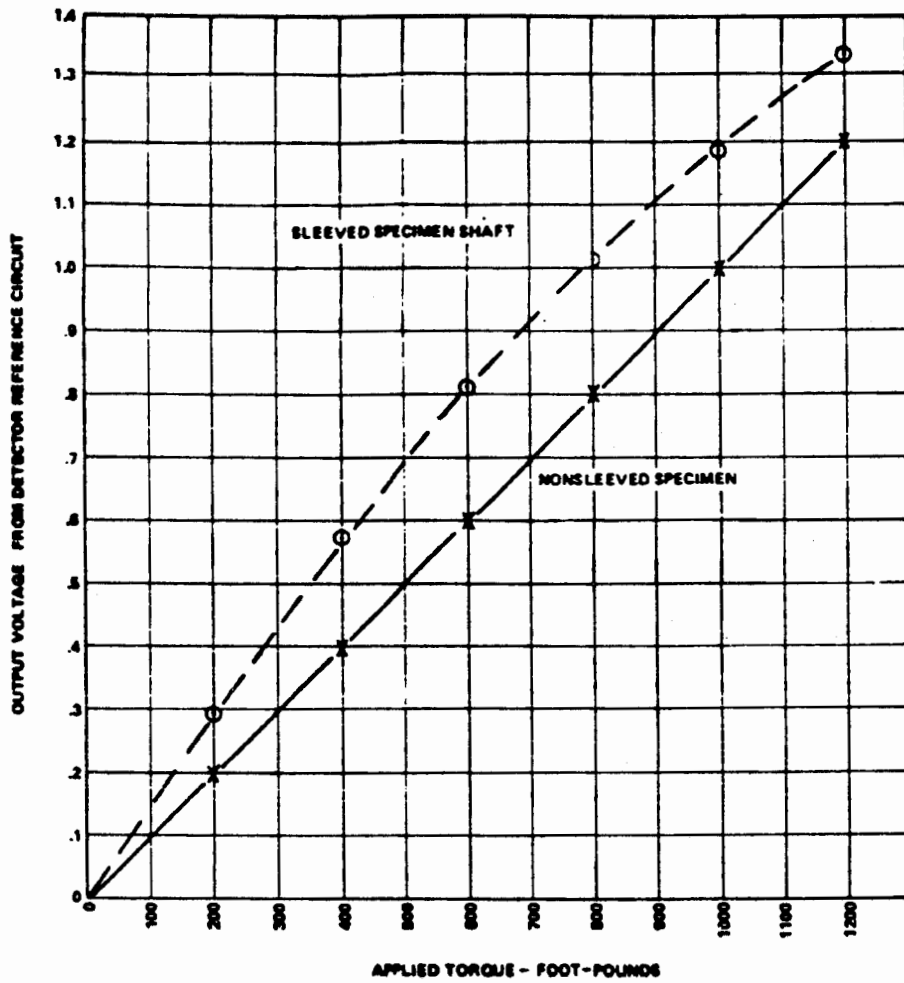


FIGURE 12 TRANSFER CURVE FOR AMS 6265 AFTER HEAT TREATMENT

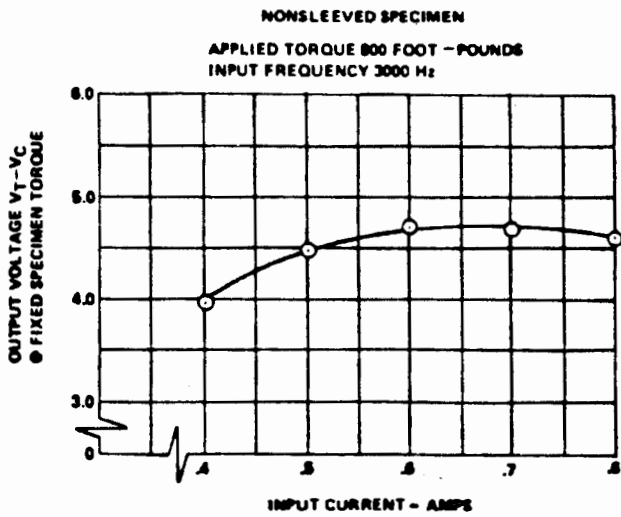


FIGURE 13 TRANSFORMER OUTPUT VOLTAGE VERSUS INPUT CURRENT

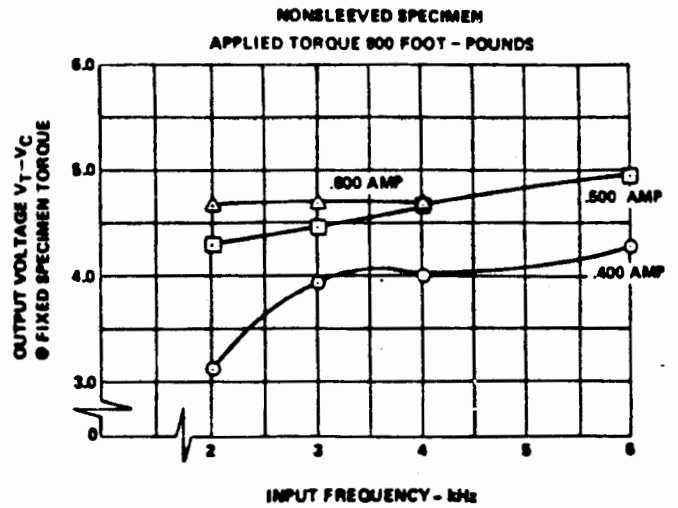
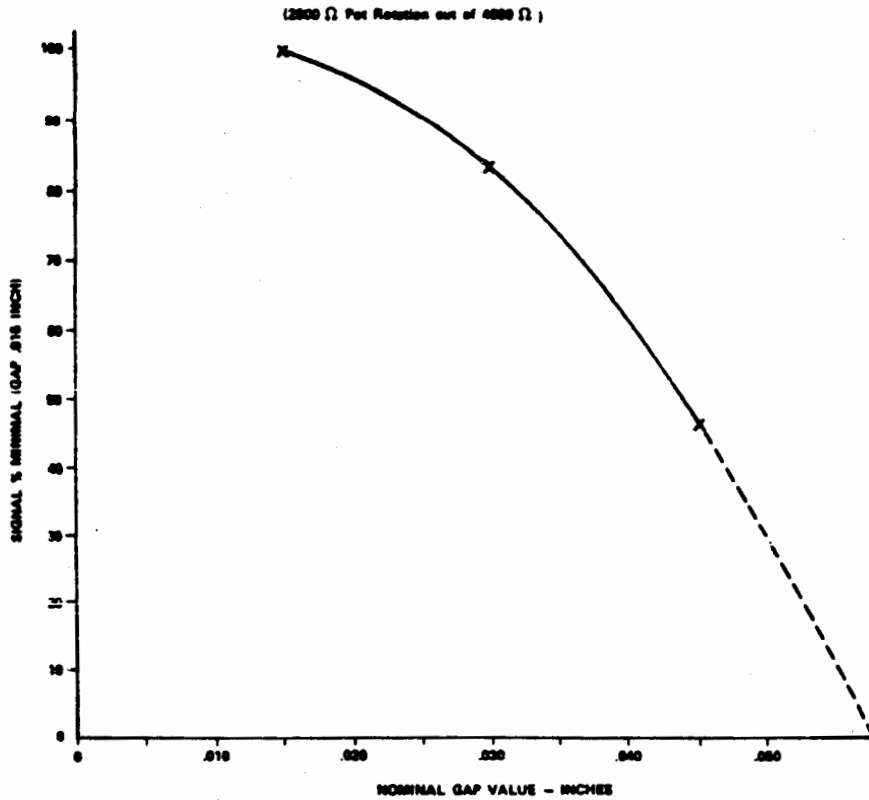


FIGURE 14 TRANSFORMER OUTPUT VOLTAGE VERSUS INPUT FREQUENCY



**FIGURE 15 SIGNAL SENSITIVITY
CHANGE DUE TO INCREASED
VALUES OF NOMINAL AIR
GAP**

the range from -80 to +240°F. This data is shown on Figure 16 with torque constant at 1200 foot pounds (9600 psi) and a fixed excitation current of .67 amps at 3000 Hz. To explain the reducing signal sensitivity with increasing metal temperature, reference is made to Figure 13 which shows signal sensitivity versus input current. For that condition, an increase of the exciting force from a .67 amps to .8 amps had shown an approximate 3.3% reduction of signal sensitivity. This is a probable effect from approaching magnetic saturation by operating along the knee of the normalized magnetization curve for the AMS 6265 steel. Since core flux would be proportionally increasing for either an increase of the magnetomotive force or by increasing material permeability, the loss of sensitivity with a constant excitation current was assumed as an effect of permeability change with temperature. Through independent testing, this was found to increase by approximately 11% for a temperature difference from 80° to 240°F.

A calculated percentage increase in permeability for the observed signal loss of -2.5% from 80 to 240°F, using the known percentage signal loss for excitation current, would equal 12%. This value is in good agreement with the permeability change of 11% for this temperature range and supports the assumption of increasing permeability as cause for the observed error.

Torque Sensor Temperature Evaluation. This test was performed on the sleeved specimen. In this case, the torque sensor, i.e., shaft and lamination assembly were subject to the same temperature environment. High temperature was obtained by using induction heaters with power off during the data recording and with immersion in dry ice for the low temperature.

Data from this test, showing the change in sensitivity at the same fixed torque as the metal temperature test, is shown on Figure 17. This data shows an increase of sensitivity whereas a decrease was

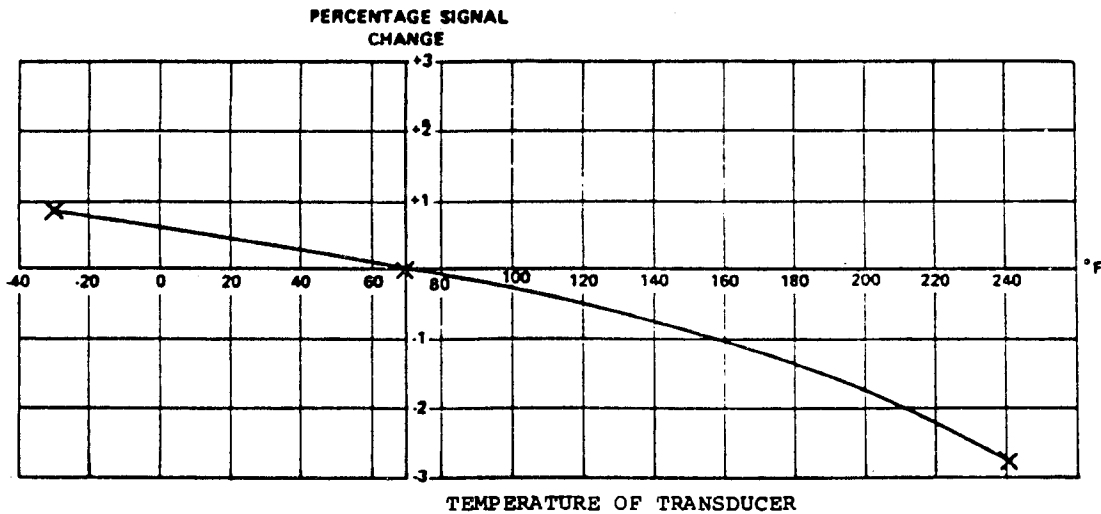


FIGURE 16 MATERIAL TEMPERATURE SENSITIVITY

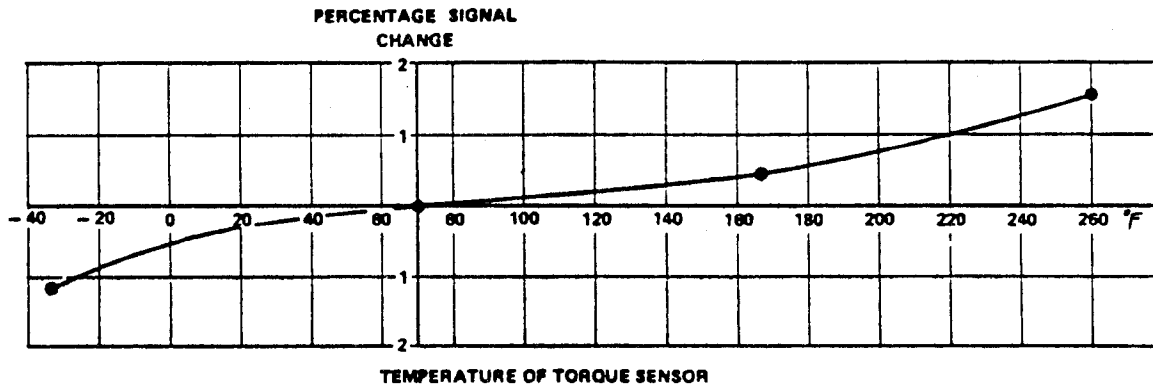


FIGURE 17 TORQUE SENSOR TEMPERATURE SENSITIVITY

seen on the metal temperature test. An explanation for this difference is through reduction of the air gap by growth of both the shaft and lamination assembly in combination with an increase to the depth of magnetic penetration with the temperature related increase of resistivity. By analysis, the depth of penetration for the AMS 6265 steel was calculated at 0.035 inches at room temperature. Using a resistivity change of 27% for steel(5), this would effectively increase the flux penetration to approximately .045 inches. This increase in the stress averaging is a probable explanation for a portion of the sensitivity increase. As further shown by Figure 15, the air gap reduction increases signal sensitivity. For this sensor with a nominal air gap of 0.035 inches, the gap signal sensitivity can be approximated as 1.5% per 0.001 inch of change. For a 170°F change (from 70° to 240°F), the total observed sensitivity

change would equal +3.75% (-2.5% for the metal only and +1.25% for the system) as shown in Figure 18. This would require approximately 0.0025 inches of gap change. The calculated change for the sensor gap is +0.0025, which is in agreement with the measured result.

Static To Dynamic Calibration Coincidence. For this testing, the hardened nonsleeved specimen and transformer assembly were used with a 0.045 inch air gap. For accuracy, the differential detector was used to minimize torque sensor sensitivity variations due to input current and frequency changes. Prior to the rotational test, the sensor was calibrated on the static test fixture. After this, the detector was moved to the rotational (engine) test site. No changes were made to the detector electronics which would affect the established electronic sensitivity or balance.

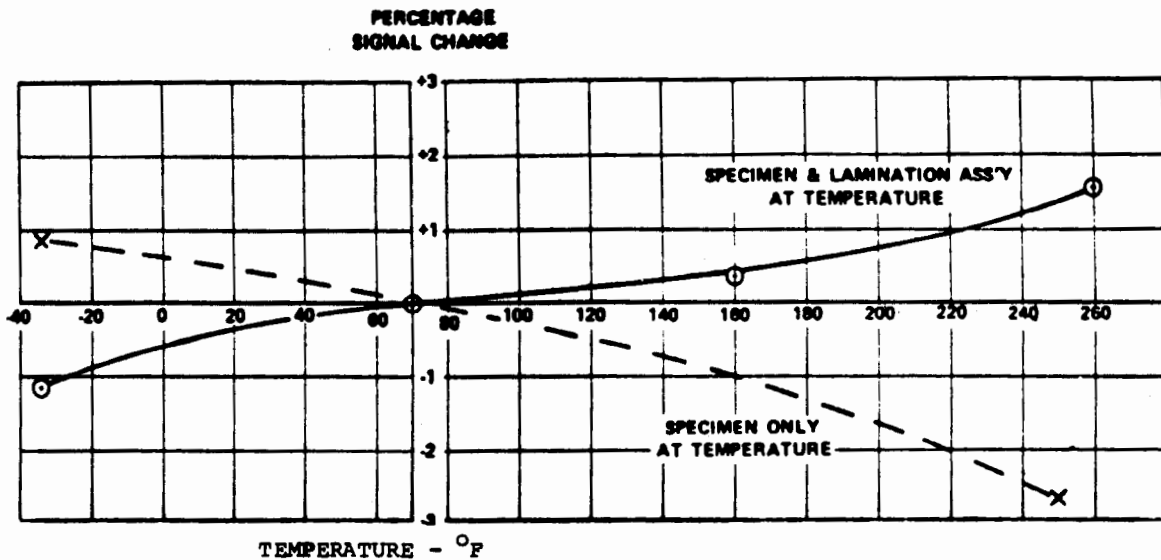


FIGURE 18 COMPARISON OF
TEMPERATURE EFFECTS DATA

Data from this test obtained at speeds from 4000 to 16,000 RPM and plotted on Figure 19, showed a marked difference in zero offset with little if any change to the torque sensors sensitivity. This difference appears to be an effect of rotation plus a tendency for the AMS 6265 steel to retain a small residual magnetic field.

As explained by Angeid (6), the effect of a proportional zero shift with rotation can be explained by nonsymmetrical alignment of the secondary pole structures or by other factors which effect the field symmetry. In this case, the effect was found to be caused by a magnetic remanance determined to be a characteristic of the AMS 6265 material. To correct this condition, an erasure cycle was incorporated into the design of the power supply.

Rotational Speed Sensitivity

To evaluate the effect on signal sensitivity as a function of the shaft speed, the torque sensor data was obtained at a fixed torque (800 ft. lbs) with shaft speed changing from >9000 to 16,300 RPM. This data showed a less than .2% change of sensitivity within this range which was considered as acceptable for design of a 1% transducer system.

This test demonstrated the need to select an excitation frequency whose calculated synchronous speed would exceed the maximum shaft rotational speed(6). Using 3000 Hz and the 8 pole sensor of this test, the calculated shaft synchronous speed of 45,000 RPM is approximately 3 times greater than the shaft

maximum. To extend this for design with a shaft rotating at 30,000 RPM, the excitation frequency would require an increase to 6,000 Hz.

Summary & Conclusion

The magnetostrictive torque transducer has demonstrated its capability to provide accurate and repeatable measurements of gas turbine engine shaft torque. This type of transducer, however, requires empirical analysis to support its design specifications. Using this method, testing was completed to specify an advanced concept transducer for use at rotational speeds approaching 30,000 RPM and in a temperature environment not exceeding 300°F. Testing was also used to evaluate concepts of producibility and maintainability for production units. In addition to the test data obtained for a transducer specification, an advanced method for signal detection by use of a ratio detector was investigated.

Following analysis of test data, a torque sensor was specified for design and fabrication with the following characteristics.

1. The SAE 9310 carburizing steel is to be used for the transducer material. A non-sleeved version of the shaft is to be used during the system development testing but until sufficient heat lots of this material are evaluated for determination of confidence in signal repeatability, a sleeved version of shaft to allow for sleeve replacement is being considered for production design.

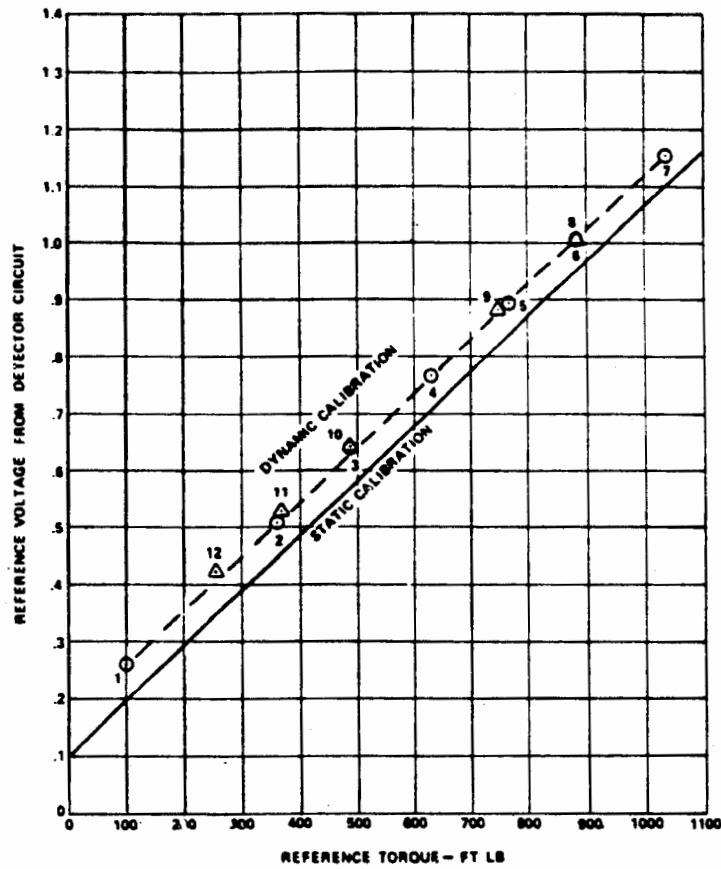


FIGURE 19 COMPARISON OF DYNAMIC AND STATIC CALIBRATION

2. The torque sensors air gap has been optimized at .020 of an inch as measured radially. This dimension was selected based upon providing an optimal inherent temperature compensation at 240°F.
3. A three primary pole transformer configuration was selected for the final design. The four pole symmetrically split sensor used for this testing was not selected for design based upon a trade-off between increased signal sensitivity and reduced operational reliability with the added coils and internal wiring connections.
4. Excitation current was reduced from the .670 amps of test to .600 amps. This was based upon the relatively flat curve of excitation current versus sensitivity at that level and the reduced requirement for power supply design.
5. The excitation frequency was increased from the 3000 Hz of test to that of 6000 Hz based upon extrapolation of stress sensitivity versus the synchronous frequency at 30,000 RPM.
6. An erasure cycle was built into design of the power supply to minimize the remance effect noted with the SAE 9310. This cycle is initiated at each turn on of the excitation current.
7. A ratio detector providing an output computed from the sum and difference of the two secondary coils, i.e.,

$$E_o = \frac{VT - VC}{VT + VC}$$
 is used for generation of an information signal. This method of detection minimizes the effects of current variations which improves signal accuracy and reduces power supply costs by minimizing the requirement for current regulation.

References

1. Frank E. Scoppe, "Advanced Torque Measurement System Technique for Aircraft Turbohaft Engines", USAAMRDL Technical Report, 73-37, June 1973.
2. R. Beth and W. Meeks, "Magnetic Measurement of Torque in a Rotating Shaft," Review of Scientific Instruments, Vol. 25, June 1954, pp. 603-607.
3. R. Bozorth, "Stress and Magnetostriction", Chapter 13, Ferromagnetism, D. Van Nostrand Co., Inc., New York, 1951, pp. 595-712
4. Francis E. Scoppe and Kenneth S. Collinge, "Improved Accuracy Magnetostrictive Torquemeter", Presented at AIAA/SAE/ASME 20th Joint Propulsion Conference, Cincinnati, Ohio, June 1984.
5. T.H. Barton and R.J. Ionides, "A Quantitative Theory of Magnetic Anisotropy Torque Transducers", IEEE Transactions on Instrumentation Systems, Vol. IM-14, No. 4, December 1965, pp. 247-254.
6. E. Angeid, "Non Contacting Torquemeters Utilizing Magneto-Elastic Properties of Steel Shafts", ASME Paper 60-GT-64, March 9, 1969.

MULTIPLEXING INSTRUMENTATION CABLES DOWNHOLE*

D. B. LONGINOTTI
EG&G Energy Measurements, Inc.
2801 Old Crow Canyon Road
San Ramon, California 94583

ABSTRACT

Measurements of underground nuclear explosion-driven dynamic motions are conducted by the Lawrence Livermore National Laboratory (LLNL) as part of its Underground Nuclear Test Containment Program. Previously, these measurements were performed using multiple-shielded-pair cables between individual canisters and the ground-level recording trailers. Each canister contains various transducers located downhole, with recording trailers placed up to several thousand (cable run) feet away on the ground surface. The cost of cable procurement and sealing the cables to prevent transmission of radioactive gases to the surface represents a major budget consideration. These costs, of course, are proportional to the number of measurements fielded. The LLNL Containment Program requested EG&G Special Measurements to design and build a multiplex cabling system to be placed downhole, thereby reducing cabling costs and enabling more measurements to be made within the budget constraints of the program.

EG&G designed a system that would consist of several instrumentation canisters, connected by multiple-shielded-pair cables to a multiplex canister, which would combine the signals of up to four instrumentation channels onto a single coaxial cable for uphole transmission. The downhole multiplex canister system receives d-c signals or carrier system signals from below, frequency modulates each channel, mixes the four FM channels into a single composite signal, and superimposes the composite signal onto the d-c power in a single coaxial cable. This system can survive in a severe dynamic and external stress environment with transient accelerations of up to 250 g's, velocities up to 25 m/s, and external pressures up to 300 bar (30 Mpa).

Although a reduction in cabling costs was the primary motivation for the development of this system, it has proven to be even more valuable to the LLNL Containment Program in its work with stress transducers. The signal conditioning amplifier can now be located in the multiplex canister downhole instead of in the recording trailer uphole. This shortens lead wire lengths from the stress element to the signal conditioning amplifier, and results in more accurate and reliable measurements.

*This work was supported by the U.S. Department of Energy under Contract No. DE-AC08-83NV10282. NOTE: By acceptance of this article, the publisher and/or recipient acknowledges the U.S. Government's right to retain a nonexclusive, royalty-free license to any copyright covering this paper.

INTRODUCTION

The LLNL conducts measurements of various underground phenomena as part of its Underground Nuclear Test Containment Program. Several thousand feet of multiple-shielded-pair cables were required between each canister and the recording trailer located on the ground surface (Figure 1a). Each cable had to be individually fitted with several gas-blocks in the field to prevent transmission of radioactive gases to the surface. The LLNL Containment Program requested that EG&G Special Measurements design and build a multiplex cabling system which could be emplaced downhole to reduce the amount of cable required for each measurement and the amount of gas-blocking which must be done in the field (Figure 1b).

In addition to reducing cabling costs, the multiplex system was beneficial to LLNL in its development of stress transducers. Previous to the development of this system, the signal conditioning amplifier containing the bridge completion resistors was located uphole in the recording trailer. Temperature changes which took place over the several thousand feet of lead wire from the stress element to the signal conditioning amplifier caused resistance changes sufficient to drift the zero signal off scale. The typical resistance of the piezoresistive stress sensing elements is approximately 350 ohms. Full scale $\Delta R/R$ is on the order of 0.04 for a 1 kbar input. The temperature coefficient of resistance/degree Celcius of a typical conductor-grade copper is 0.004.⁽¹⁾ For American Wire Gage number 16 conductors, this is approximately 9×10^{-6} ohms/ft-°F. Clearly, a change of 50° over a 4,000-ft two-way cable run could cause ΔR of about 2 ohm which is a significant distortion of an expected 14-ohm maximum ΔR . In terms of the maximum full scale reading, 2/14 equals 0.14 error. By placing the signal conditioning amplifier downhole, the lead wire lengths were shortened to a maximum of about 100 ft (0.003 error) and the result has been an increase in the success rate of these stress measurements.

ENVIRONMENT

The signal conditioning amplifier and multiplex electronics had to be packaged in a canister capable of surviving inside the dynamic environment which was being measured. However, these environmental conditions were difficult to determine. Shock response spectra of these acceleration histories were not available at the beginning of the design period. A combination of schedule milestones for completing the design and manpower shortages precluded the development of software to generate shock response spectra at that time.

Shock response spectra did become available during the project through the programming efforts of an EG&G data analyst who had access to digitized ground motion data from past events. These spectra, which covered frequencies up to 1,000 Hz, indicated that response amplification above the zero period acceleration was still occurring. The upper boundary of the frequency content of the ground motion is not accurately known. However, the hardware was already ordered by that time. Subsequent stress analysis performed using this data provided acceptable results.

To conduct an orderly analysis of the canister design, an environmental design specification was mandatory. When stresses from different influences acting on a canister must be combined, some basis for establishing the driving forces must be set. Consequently, an environmental design specification was written, reviewed, and revised until it was acceptable to the interested parties. The environmental design specification does not, however, constitute a governing criterion for siting the multiplex canisters downhole.

The environmental design specification described in Table 1 formed the basis for the design and subsequent dynamic analysis of the multiplex canister components. On any given installation, however, a canister may experience values more or less than those specified below.

Table 1. Environmental design specification.

I. Ground Motion

- Acceleration (approximately .010 sec pulse duration) 250 g
- Particle velocity (approximately .3 sec pulse duration) 25 m/sec
- Displacement 3 m (approximately)
- External soil pressure .3 Kbar (approximately 4,400 psi)
- Frequency content (see response spectrum, Figure 2)

II. Moisture

The canister exterior can be wet without significant hydrostatic head.

III. Radiation

The canister electronics are expected to survive a nominal external gamma dose rate of 1,000 rem per hour. This measurement is based on a rough estimate of the capability of unhardened components.

DESIGN

The design of the mechanical housing for the new multiplex cabling system proved to be an interesting challenge. The multiplex system itself consists of solid state components mounted on printed circuit (PC) boards (approximately 3 x 4 in.) which plug into a 3.50 x 18 x .125 in. motherboard. The signal conditioning amplifier and multiplex electronics assembly had to be a self-contained entity that would slide inside the main housing, would remain stiff during underground dynamic motion, and be strong enough to survive the compressive stresses accompanying dynamic ground motion.

Traditionally, electronics in similar applications have been potted, using solid plastic, foam, or rubber-like compounds. This procedure results in a self-contained electronic unit which does not flex during dynamic motions and is able to maintain its integrity during and after compressive

stresses. The electronics design engineers, however, would not allow the electronics to be potted for several reasons, including thermal considerations. The canister would be exposed to ambient temperatures of over 100°, the circuitry heat output of the multiplex electronics was unknown, and the maximum thermal temperatures the electronic assembly itself could withstand were unknown. Potting would only insulate the heat sources in the circuit electronics (creating a lack of heat conduction) and further increase the ambient temperatures.

Another reason potting was prohibited was because the signal conditioning amplifier requires numerous adjustments, up to and including the time of downhole emplacement. Also, a malfunction can sometimes occur in a canister assembly while being emplaced downhole, requiring that it be returned uphole for corrective action. In either event, if the circuitry were encased in plastic (potted), access to the circuitry would be prevented and a total loss of electronics would result.

It was concluded that potting may be done in later developmental design stages and then only in local areas. At this time, however, it has not been determined that potting is either necessary or desirable.

The signal conditioning amplifier and multiplex electronics assembly was ultimately made into a self-supporting structural element through the use of two semi-circular plastic (Delrin) bulkheads. These bulkheads are attached to opposing sides of the assembly every 4 in. to prevent low frequency flexural vibrations transverse to the housing axis (Figure 3). Machine screws penetrate through both bulkheads and the motherboard assembly to basically pinch the motherboard between the two bulkhead halves. The overall cross-section of the multiplex housing is cylindrical in shape, creating lateral support between the motherboard and the inside diameter of the housing. The multiplex canister is then vertically emplaced downhole so that maximum dynamic motion occurs along the long axis of the housing and motherboard. Figure 4 depicts the motherboard assembly sliding into the canister housing and Figure 5 illustrates the canister housing, adaptor sections, end plugs, and motherboard assembly.

Another design problem addressed was how to diminish the diameter of the canister so that it would be closer in size to the coaxial cable even though the electronics required a substantial motherboard. By keeping the diameters of the canister and cable similar in size, the possibility of the electrical cables breaking away from the canister during violent ground motions is minimized. A compromise was reached whereby the inside diameter was set at 4 in. and the outside diameter at 4.75 in.

Bridge resistors, located in the signal conditioning amplifier, are vulnerable to moisture on lead wires. Moisture contamination leads to the introduction of undesired shunts across the bridge. As was previously stated, the signal conditioning amplifier requires considerable adjustment prior to downhole installation. Thus, the challenge was to design a system which would provide access to the signal conditioning amplifier and maintain the integrity of the bridge resistors under high humidity conditions.

The multiplex cabling system that was designed provides electrical access to the front and back ends of the multiplex electronics, as well as to the bridge resistors, while maintaining the environmental seals on both. Adaptor sections on both ends of the canister were added to meet this requirement (Figure 5). Bolted joints were used to provide access to the circuit boards, without disconnecting the multiplex unit from either its uphole power supply or the downhole instrument canisters.

Coaxial cable was used for the cabling from the canister uphole because it can be factory gas-blocked, eliminating the need to gas-block individual cables in the field. Field gas-blocking individual cables is a time-consuming and expensive sealing method.

Natural frequency analyses were performed on parts of the multiplex canister housing. The housing was modeled using a collection of beams of several annular cross-sections. The results of this analysis were used to analyze a 4 in. by 4 in. representative section of PC board stock. This analysis was made on the PC board with and without both component masses. Table 2 illustrates the results of the natural frequency analysis.

Table 2. Natural frequencies below 10,000 Hz (or lowest if greater than 10,000 Hz).

LOCATION	TYPE	FREQUENCY (Hz)	
		FINITE ELEMENT	HAND CALCULATION
Canister	Longitudinal	1,482	1,300
	Transverse	338, 928, and 1,768	
	Shell expansion/contraction	14,623	13,300
PC board	Plate flexural modes	832 (no lumped masses) 603	758
PC board	Longitudinal modes	4,206	4,015

The external dynamic soil stresses acting around the outside of the canister are the most significant source of stresses in the structural elements. The results of the stress analysis for the design basis environment, including the combined effects of acceleration loads and external dynamic soil stresses, are summarized in Table 3.

Table 3. Summary of stress analysis.

ITEM	TYPE	STRESS (lb/sq in.)
Multiplex canister housing	Bending	+17,891
	Axial (acceleration forces)	+3,725
	Axial (external dynamic pressure)	-36,306
	Tangential (hoop)	-28,977
	Combined (Von Mises criteria)	33,253
Material yield strength	(6061 T6 aluminum)	35,000 minimum
PC board (1/8-in.-thick fiberglass-epoxy substrate)	Bending	+3,655
	Axial	+171
	Combined	+3,826
Material strength (ultimate)		7,000 (estimate)

PERFORMANCE

The multiplex canister system which has been designed does consistently survive dynamic ground motion, but only at ground motion levels below those specified in the design environment specification. However, the first field experience resulted in significant data loss, suggesting that the canister was more vulnerable to ground shock than had been anticipated. LLNL requested that a two-part test program (expedient and formal) be initiated to determine the cause of the data loss.

The expedient test was improvised using mechanical and data acquisition equipment on hand before the next anticipated field usage. Although a significant portion of the design environment was not covered by the expedient test, very high accelerations at short pulse widths were produced. The multiplex electronics were operational during this test and no loss of function was observed. Expedient testing was completed and a plot of the acceleration/velocity levels is presented in Figure 6.

Electronic tests, independent of the expedient test, were also performed on the multiplex system. It was discovered that the data loss was related to grounding rather than dynamic motion.

The formal test is still scheduled to be conducted at a shock and vibration facility most suited to simulate the environment described in the design environmental specification. This test is pending because a facility in which to conduct the test has been unavailable. This test will cover more, but not all of, the design environment specification.

Future plans include designing ports or doors which will provide quick access to the top of PC board modules so that adjustments can be made after the canister has been assembled. The canister also needs to be waterproofed so that it can be emplaced in grout (pressurized water-bearing material) without allowing the liquid to leak onto exposed conductors inside the canister. These goals are not necessarily compatible because the large size of the ports or doors required to make these PC board adjustments will also make waterproofing difficult.

The ability of the canister to withstand external stresses will be degraded by the addition of ports or doors, unless a substantial weight penalty is incurred to reinforce these openings. It is likely that these design goals will result in the development of two different versions of the canister. One canister will be waterproof, will be able to withstand greater external stresses, but will not have quick-access ports or doors. The other canister will not be waterproof, will have access ports or doors, but will only be able to withstand lesser external stresses. There are, however, a significant number of applications for the multiplex cabling system which can take place in environments mild enough to make access ports or doors practical.

REFERENCE

1. Bolz, R. E. and Tuve, G. L., Handbook of Tables for Applied Engineering Science, Second Edition, CRC Press, 1976. Tables 2-23 and 11-16.

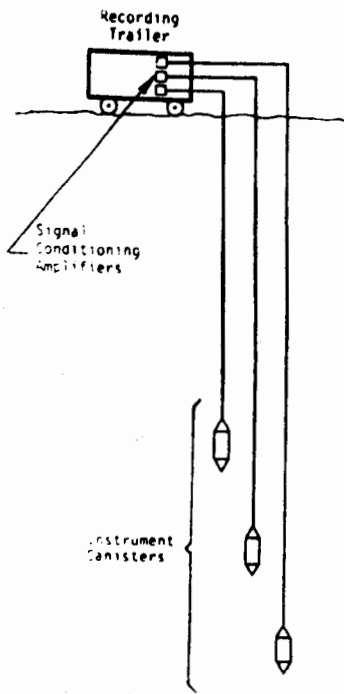


Figure 1a. Number of cables required (to surface) is between one and two times the number of stations.

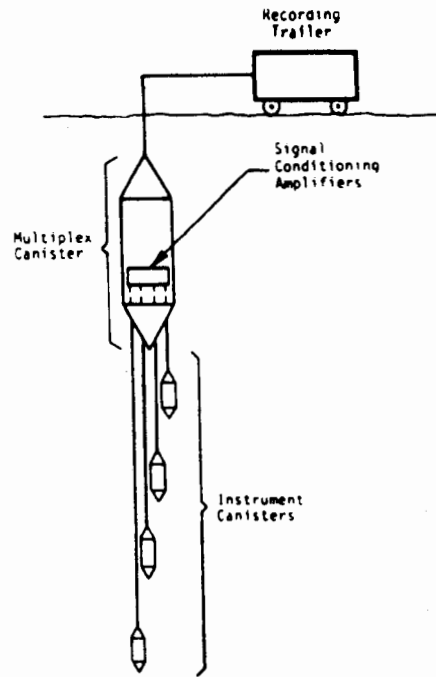


Figure 1b. Number of cables required (to surface) is only one-fourth times the number of stations.

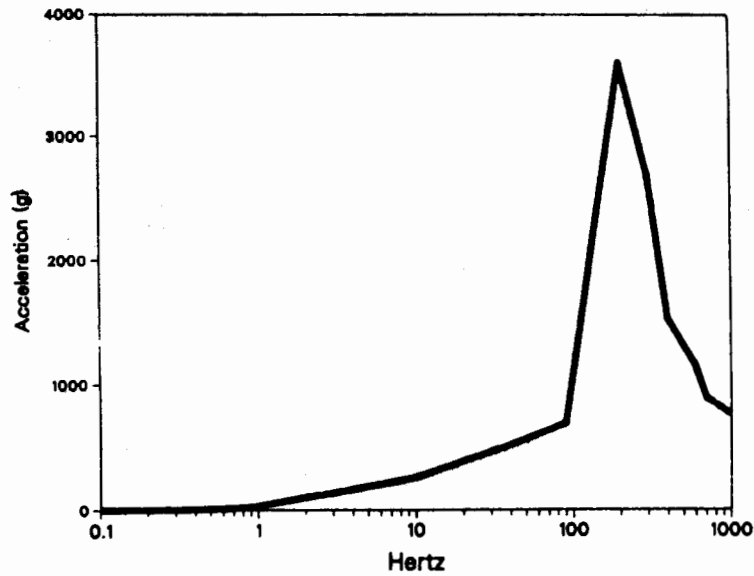


Figure 2. Multiplex canister acceleration response spectrum.

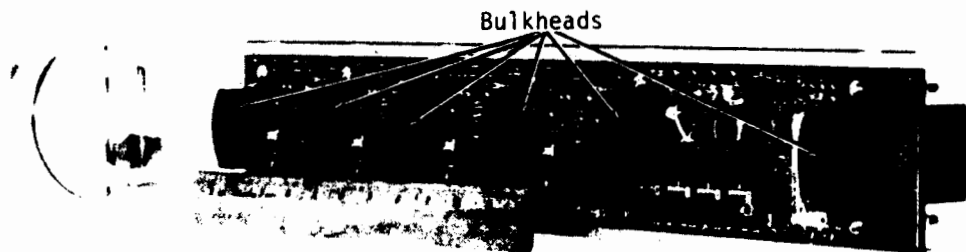


Figure 3. Bulkheads used to support motherboard assembly.

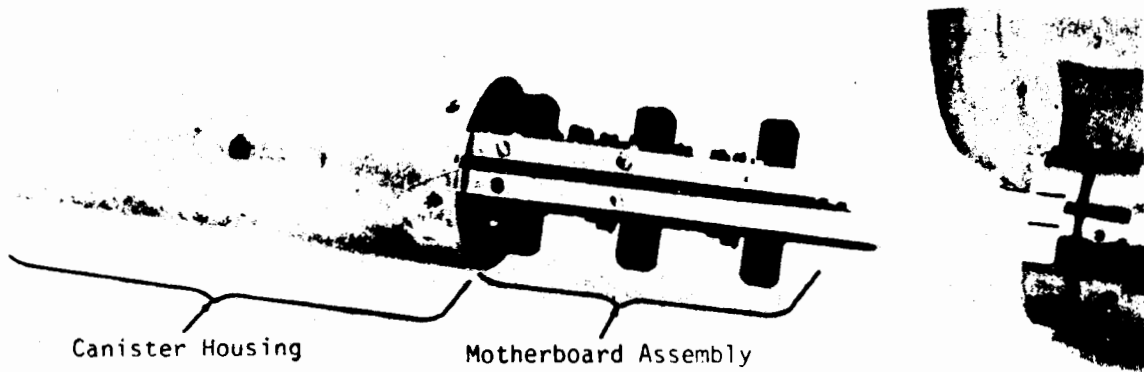


Figure 4. Self-supporting motherboard assembly being placed in the canister housing.

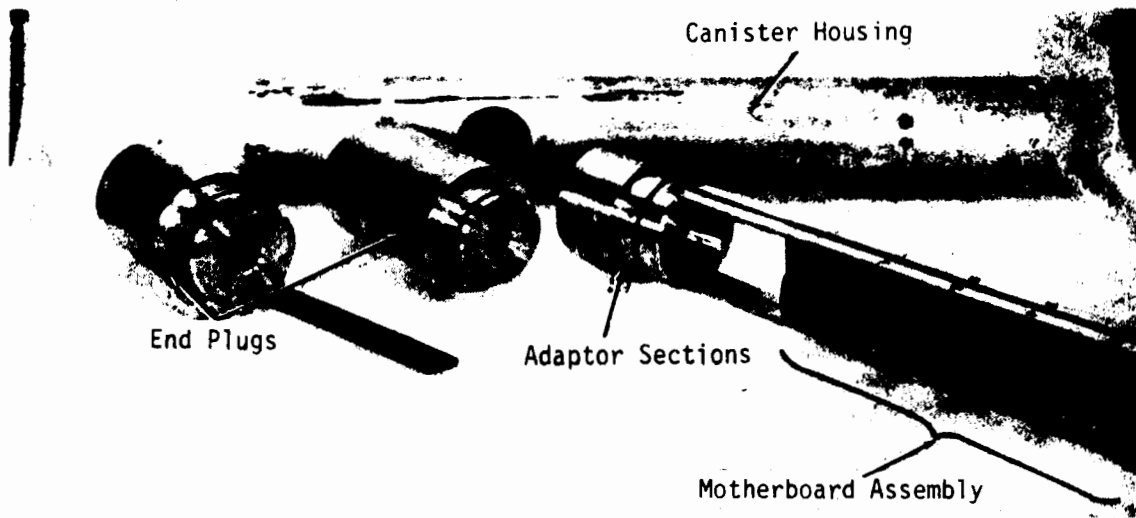


Figure 5. Multiplex canister components.

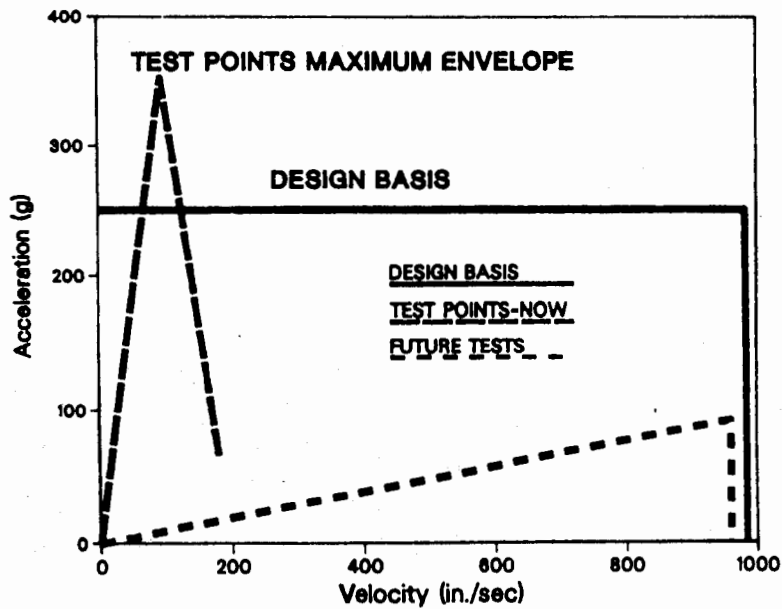


Figure 6. Multiplex canister acceleration/velocity envelope.

**High Accuracy Rotary and Linear INDUCTOSYN®
Position Transducers**

George Quinn

Farrand Controls

Division of Farrand Industries, Inc.

Valhalla, NY 10595

1. ABSTRACT

Current military/aerospace control systems are demanding higher positioning accuracies for gyros, gimbal platforms, optical sighting devices, and antennas. For more than 32 years, Farrand Controls has served the military/aerospace community with a broad selection of high accuracy Rotary and Linear INDUCTOSYN® position transducers. Accuracies in the order of ± 1 arc second (± 0.5 arc secs, selected) for the Rotary and ± 100 microinches (± 40 microinches, selected) for the Linear are typically achieved. This paper will review the basic concepts of INDUCTOSYN® position transducers and stress:

1. Theory of operation
2. Variety of sizes and configurations
3. Typical applications

2. INTRODUCTION

Farrand Controls, division of Farrand Industries, Inc., manufactures linear and rotary INDUCTOSYN® position transducers. Obtainable in absolute and incremental types, they are one of the most accurate transducers available for the measurement and control of linear and angular displacement. See Figure 1.



**Linear and rotary INDUCTOSYN® position transducers
Figure 1**

Currently used in military, aerospace, satellite, radar, and navigational systems, and in machine tools, their electrical output signals drive numerical readout displays, generate computer input data, and provide servo feedback signals.

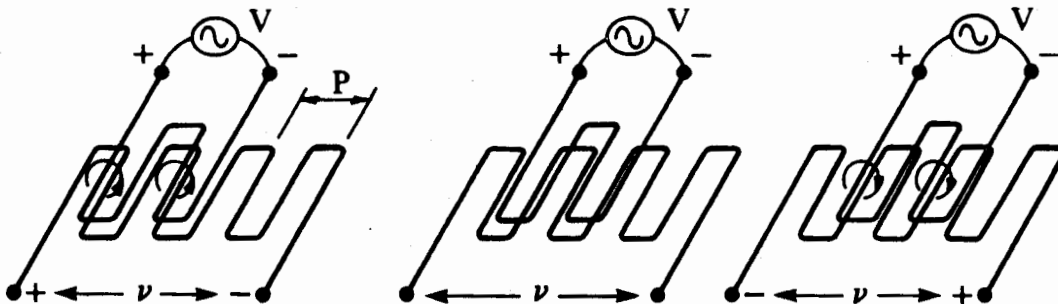
They can be designed to be unaffected by dust, oil films, vapors, sea water, light, radiation, extreme pressure, and temperature. INDUCTOSYN® transducers have operated at full accuracy for extended periods in space, immersed in liquid nitrogen, in strong magnetic fields, and immersed in 200 meters of sea water.

3. PRINCIPLES OF OPERATION

INDUCTOSYN® position transducers consist of printed circuit conductor patterns deposited or laminated on a pair of flat substrates of steel, other metals, or stable nonmetallic materials. This pair of transducer elements contains no moving parts, and is usually mounted directly on the user's fixed and moveable machine parts. Since the two transducer elements are not in contact, they are not subject to wear, and mechanical life is indefinite. The elements are simple and rugged, permitting the selection of alternate materials that can withstand nearly any environmental extreme. The operating principle used is the variation of inductive or capacitive coupling between the conductor patterns on the two elements as they move relative to one another.

3.1 Inductive INDUCTOSYN® Transducer Operation

Inductive coupling between the sets of printed circuit conductor patterns is used to measure displacement. The two INDUCTOSYN® elements, attached to fixed and moveable machine parts with the hairpin loops parallel, are separated by a small air gap. An alternating current flowing in one conductor will induce a voltage in the other that depends on the relative position of the conductors. The induced voltage is maximum when the loops are facing. Passing through zero midway, it rises to a negative maximum at the next facing location. See Figure 2.



Inductive coupling between precision windings
Figure 2

FARRAND CONTROLS

DIVISION OF FARRAND INDUSTRIES, INC.

Output as function of position

INDUCTOSYN® elements behave as transformer windings with a coupling constant k . Calling the pitch P and the input voltage V , the relation between induced voltage, v_a and displacement, x is:

$$v_a = kV \cos 2\pi \frac{x}{P}$$

A second output winding with the same pitch P , may be located adjacent to the first, and displaced $P/4$ from it. The voltage v_b induced in this conductor is:

$$v_b = kV \sin 2\pi \frac{x}{P}$$

Only the amplitudes of v_a and v_b change. Phase remains constant while amplitude is a function of relative displacement x/P . There is a unique pair of induced voltages v_a and v_b for every location within one cycle of the pitch P . Thus by measuring these voltages, we may subdivide the accurately known pitch interval with high precision.

Compared to resolvers

The INDUCTOSYN® windings in space quadrature act as a precision resolver. The fixed and moveable windings are called the stator and rotor, and one cycle length equals two poles of the comparable resolver.

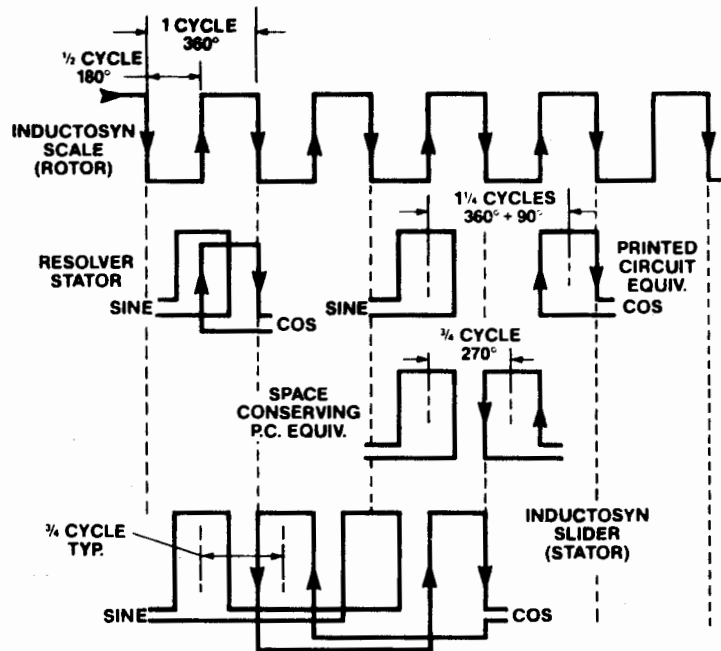
Linear INDUCTOSYN® "poles" are spaced at fixed linear intervals of $P/2$. The fixed and moveable elements are called the scale and slider, respectively.

Null output possible

Like resolvers, INDUCTOSYN® devices may be excited by in-phase carrier voltages proportional to the cosine and sine of $2\pi \frac{x}{P}$. The output voltage then equals zero, independently of input amplitude, when the rotor or slider is at the complementary angle, or linear position, of $\frac{1-x}{P}$. Null operation is very useful in feedback and servo applications.

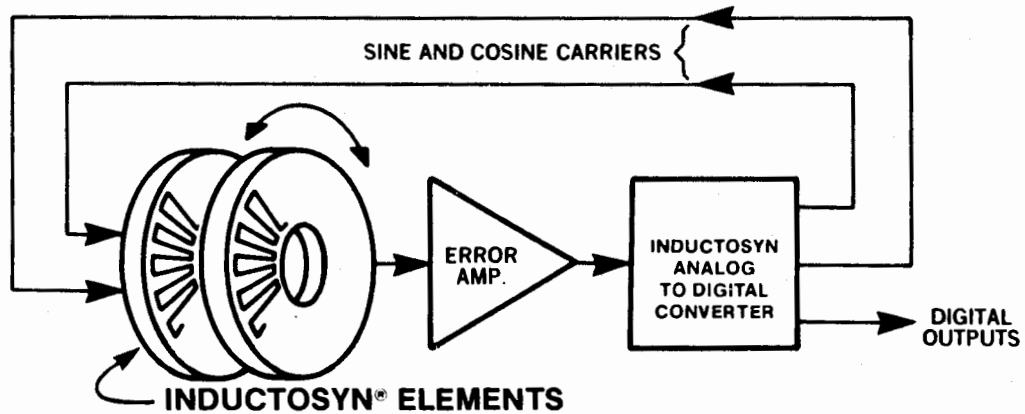
Using INDUCTOSYN® signals

As indicated, patterns for inductive coupling consist of precisely spaced and repeated hairpin turns that are connected externally as coils. As in the resolver example, one element contains a single conductor pattern, while the other element contains two patterns in space quadrature. Figure 3 illustrates the coupling between INDUCTOSYN® windings.



Magnetic field coupling
 Figure 3

INDUCTOSYN® winding outputs are amplitude modulated sine waves of 100 mV or less that may be used directly, as in servos. Farrand INDUCTOSYN® analog to digital converters, using null seeking techniques, provide excitation for the INDUCTOSYN® windings, subdivide each INDUCTOSYN® cycle, and provide digital outputs at standard TTL levels to interface to computers, N/C controllers, and position readouts. See Figure 4.



Digital output signals
 Figure 4

FARRAND CONTROLS

DIVISION OF FARRAND INDUSTRIES, INC.

Extremely high accuracy is achieved by averaging the measurement over many cycles of the scale pattern. Linear accuracies to .0002 inch or .005 mm T.I.R. (± 0.0001 inch, or ± 0.0025 mm), and angular accuracies to 2 arc seconds T.I.R. (± 1 arc second) are standard. With selected units, .000080 inch or .002 mm T.I.R. (± 0.000040 inch or ± 0.001 mm) and 1 arc second T.I.R. (± 0.5 arc second) can be achieved. Repeatability is 10 times better than rated accuracy in most models. Adjustable Linear INDUCTOSYN® Scales permit errors to be further reduced virtually to zero, referred to the user's standard.

Scale patterns can be provided for incremental and absolute measuring systems. Single and multispeed rotary patterns are available from one to 1080 speed (2 to 2160 pole count), in standard diameters from 3 to 12 inches. Standard linear cycle lengths are .1 inch, .2 inch, and 2 mm. Lengths over 92 feet (28 m) have been supplied (tape INDUCTOSYN® transducers).

3.1.1 Linear INDUCTOSYN® Position Transducers

The linear INDUCTOSYN® position transducer consists of two magnetically coupled parts. One part, the scale, is fixed to the axis along which measurement is to take place (e.g. the machine tool bed). The other part, the slider, is arranged so that it can move along the scale in association with the device to be positioned (e.g. the machine tool carrier). See Figure 5.



SCALE



SLIDER

**Linear INDUCTOSYN® transducer scale and slider
Figure 5**

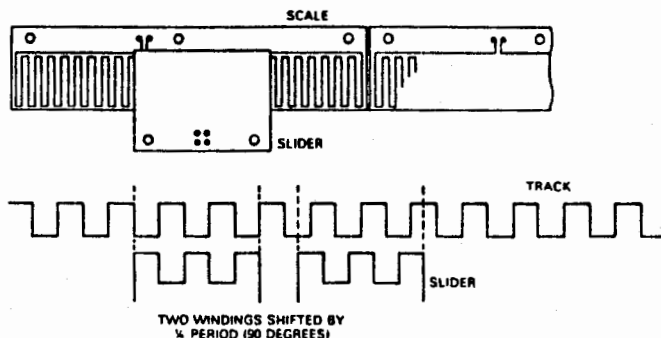
The scale consists of a base material such as steel, stainless steel, aluminum, etc. covered by an insulating layer. Bonded to this is a printed circuit track forming a continuous rectangular waveform. (In actual fact the scale is usually made up of 10 inch sections which have to be mounted end to end.) The cyclic pitch of the waveform is usually 0.1 inch, 0.2 inch, or 2 mm and is formed from two conductive poles.

The slider is normally about 4 inches in length and has two separate identical printed circuit tracks bonded to it on the surface which faces the scale. These two tracks are formed from a waveform of exactly the same cyclic pitch as on the scale but one track is shifted $\frac{1}{4}$ of a cyclic pitch from the other, i.e. 90° .

FARRAND CONTROLS

DIVISION OF FARRAND INDUSTRIES, INC.

The slider and the scale are separated by a gap of about 0.005 inches and an electrostatic screen is placed between them. A diagram of the relationship between slider and scale is shown in Figure 6.



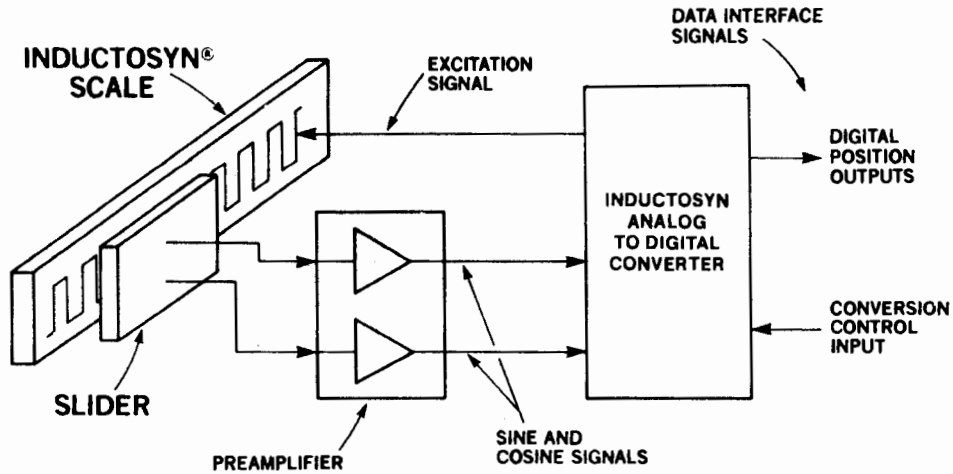
The relationship between the
Linear INDUCTOSYN® scale and slider
Figure 6

The principle of operation is similar to that of a resolver. If the scale is excited by an AC voltage, $V \sin \omega t$, (normally between 5 KHz and 10 KHz) then the outputs from the slider windings will be:

$$V \sin \omega t \cos \frac{2\pi x}{P}$$
$$V \sin \omega t \sin \frac{2\pi x}{P}$$

where x is the linear displacement of the slider and P is the cyclic length or pitch.

Therefore, the slider voltages are proportional to the sine and cosine of the distance moved through any one pitch of the scale. The INDUCTOSYN® transducer cycle length, P , is the displacement at which the output signal repeats itself. The output signals derived from the slider are the result of averaging a number of poles, and, therefore, the effect of any small residual errors in conductor spacing is averaged. This is one of the reasons why such a high accuracy can be achieved. The magnetic coupling between the slider and the scale is not nearly so high as the coupling between rotor and stator in a resolver, and for this reason the transformation ratio from input to output is very low giving rise to relatively small output signals. Digital output signals are obtained by using an INDUCTOSYN® analog to digital converter. See Figure 7.



INDUCTOSYN® analog to digital converter
 Figure 7

INDUCTOSYN® analog to digital converters, supplied by Farrand Controls and other manufacturers, are analog to digital converters that match the INDUCTOSYN® transducer output characteristics, and transform their accurate analog position signals to digital signals that meet user requirements. Virtually all such converters subdivide each INDUCTOSYN® cycle length into a number of equal intervals, such as 1000 or 1024. Thus, used with a 0.1 inch linear INDUCTOSYN® cycle length, the resolution per bit can be 0.0001 inch. By a proper selection of cycle length and cycle division ratio, the digital output can be direct reading in any units desired, and resolution can be commensurate with the inherent accuracy of the INDUCTOSYN® transducer itself.

In addition to the bar scales described above, Farrand also supplies linear INDUCTOSYN® tape scales and adjustable linear INDUCTOSYN® scales. Tape scales are manufactured in continuous lengths up to 200 feet (60 m), and then factory cut to length to form individual scales as needed.

Adjustable scales are one piece bars that can be adjusted after installation to virtually eliminate errors over their full length, limited only by the accuracy of the user's primary length standard and readout resolution. Lengths to 60 inches (1.5 m) have been supplied.

3.1.2 Rotary INDUCTOSYN® Position Transducers

Rotary INDUCTOSYN® scale elements consist of a pair of discs called the rotor and stator. They are mounted directly on the user's shaft and frame. The analogous linear INDUCTOSYN® scale elements are called the scale and slider, respectively. Rotary coupling transformers are built into the discs in some models, permitting continuous rotation without the use of slip rings and brushes. See Figure 8.



Rotary INDUCTOSYN® transducer rotor and stator
Figure 8

Rotary INDUCTOSYN® position transducers were developed to provide the highest possible accuracy in applications typically served by resolvers. Certain terminology has thus been carried over from resolver practice.

The simplest possible resolver has two poles, and its output signal repeats itself once for each full revolution. To increase resolution, step-up gears are introduced between the resolver and the shaft to be measured, and the resolver is said to operate at a "speed" numerical equal to the gear ratio. For example, a resolver that makes 18 turns for each turn of the measured shaft is called "18 speed." In practice, this would be combined with a "single speed" resolver that simultaneously provided absolute angle information at lower resolution.

Since the output of a rotary INDUCTOSYN® transducer repeats itself once each cycle length, it is equivalent to a simple, two pole resolver with a gear ratio numerically equal to the number of INDUCTOSYN® cycle lengths per revolution. Thus a rotary INDUCTOSYN® transducer with a 1° cycle length is called "720 pole" or "360 speed." One cycle length equals two poles. The length of one complete cycle of the pattern is called the pitch or cycle length. One complete INDUCTOSYN® cycle length corresponds to one complete revolution of our two pole resolver example, and the variations of inductive coupling as the patterns slide relatively past each other produces output signals identical to resolver signals.

The stator of a rotary INDUCTOSYN® has the two separate rectangular printed track waveforms arranged radially on a disc. The sine track is made up of a number of sections which alternate with the cosine track. In this way the whole of the stator disc is covered in track and any errors in spacing will be averaged out. This gives the rotary INDUCTOSYN® its exceptionally high accuracy.

FARRAND CONTROLS

DIVISION OF FARRAND INDUSTRIES, INC.

The rotor of the device is a disc with a complete track of near rectangular printed track waveform. The coupling from the rotor to the outside world can be either by sliprings and brushes or by a rotating transformer as in the case of an electromagnetic brushless resolver.

Rotary INDUCTOSYNS® come in diameters of 3, 4, 7, and 12 inches and have pole counts in the range of 2-2160.

The units can be supplied as separate stator and rotor discs or as a complete mounted and assembled unit.

When the rotor of the rotary INDUCTOSYN® is excited by the AC voltage, $V \sin \omega t$, (normally 5 KHz to 10 KHz), the stator voltages will be

$$V \sin \omega t \sin \frac{N\theta}{2}$$
$$V \sin \omega t \cos \frac{N\theta}{2}$$

where θ is the angle of rotation of the rotor with respect to the stator and N is the number of poles of the rotor.

Standard Cycle Lengths

Every INDUCTOSYN® transducer is characterized by the specific cyclic pitch (cycle length) of its scale pattern. For standard linear INDUCTOSYN® transducers standard cycle lengths are 0.1", 0.2", and 2 mm. For standard rotary INDUCTOSYN® transducers standard pole patterns are:

2, 36, 72
108, 128, 144, 256,
360, 512, 720,
800, 1000, 1024,
2000, 2048, 2160

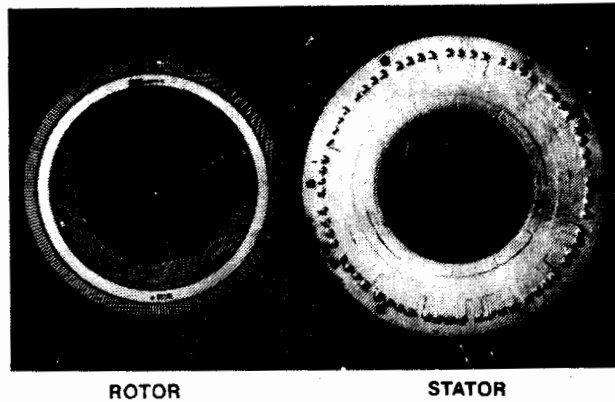
Other cycle lengths or pole patterns can be provided.

3.1.3 Absolute INDUCTOSYN® Position Transducers

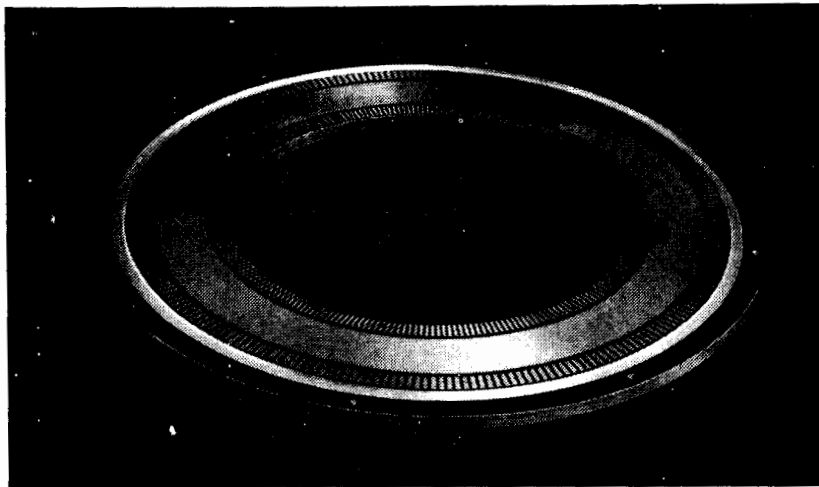
Absolute INDUCTOSYN® transducers are available in both linear and rotary forms. Two scale patterns are formed on a single substrate. They provide immediate, precise absolute position information without resetting or passing through home position after power outages and other disruptions. They are supplied in several forms, the two most common are one speed and multispeed, and N/N-1 speed. Figure 9-1 illustrates a 1 speed and a 128 speed absolute rotary INDUCTOSYN® transducer. The rotor shows the 128 speed outer pattern and the 1 speed inner pattern. The electrostatic shield can be seen covering the pattern face of the stator. Very accurate absolute rotor position information is obtained by combining the high accuracy 128 speed

FARRAND CONTROLS
DIVISION OF FARRAND INDUSTRIES, INC.

data with the absolute 1 speed data. Figure 9-2 illustrates the rotor of an N/N-1 absolute rotary INDUCTOSYN® transducer. Incremental transducers can also be supplied with an index or once per revolution marker output via a separate scale element or embedded Hall effect devices.



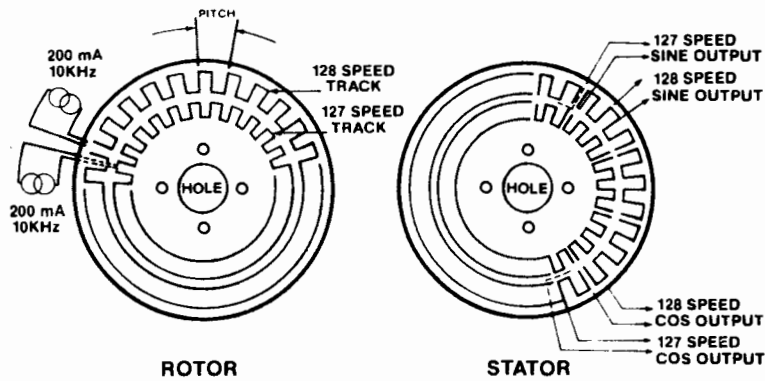
One speed and 128 speed absolute rotary INDUCTOSYN® transducer
Figure 9-1



N/N-1 Absolute rotary INDUCTOSYN® transducer rotor
Figure 9-2

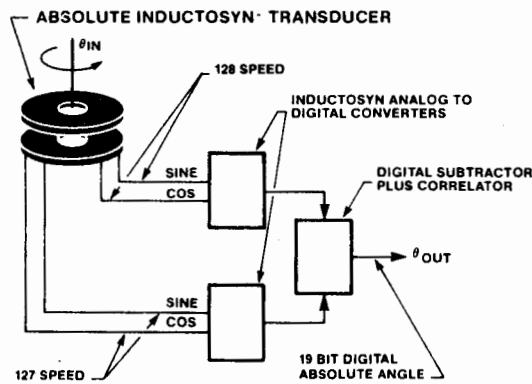
FARRAND CONTROLS
 DIVISION OF FARRAND INDUSTRIES, INC.

Figure 10 illustrates an absolute rotary INDUCTOSYN® transducer with patterns differing by one speed, i.e. 127 speed (254 pole) and 128 speed (256 pole). With the rotors energized at 200 mA at 10 KHz, the outputs of the stators are fed into matched preamplifiers to raise the output to the level required by an INDUCTOSYN® analog to digital converter.



Absolute rotary INDUCTOSYN® transducer
Figure 10

Using a digital subtraction technique, the absolute rotor angle can be determined by combining the signals as shown in Figure 11. This system provides 19 bit resolution with a total system accuracy of ± 6 arc seconds including the INDUCTOSYN® analog to digital converter and preamplifier error.



Absolute INDUCTOSYN® transducer output
Figure 11

INDUCTOSYN® Position Transducer Accuracy

Table 1 lists the accuracy achieved for several models.

Rotary Types	ACCURACY
3" (75 mm) dia., 360 pole (180x)	±3 arc sec
4" (100 mm) dia., 512 pole (256x)	±2 arc sec
7" (175 mm) dia., 720 pole (360x)	±1 arc sec
12" (300 mm) dia., 720 pole (360x)	±0.5 arc sec
12" (300 mm) dia., 1024 pole (512x)	±1 arc sec
Linear Types	
10" (250 mm) bar scale	±0.000040" (±0.001 mm)
Tape, to 100' (30 meters) or more	0.000100"/foot T.I.R. (0.008 mm/meter T.I.R.)
Adjustable Linear INDUCTOSYN® scale, maximum travel 115" (2920 mm)	Length errors associated with the scale can be virtually zero over full length. Adjustment is limited by accuracy of standard and resolution of readout or numerical control system.

Table #1

Accuracy involves the difference between separate readings at the start and end of the displacement interval (length or angle). Accuracy specifications state the maximum amount by which the indicated displacement may differ from its true value, in terms of comparisons to independent, external standards. Specification of accuracy inherently includes the effects of repeatability, since one must obtain the specified accuracy on every attempt.

Repeatability is the amount by which successive readings of the same displacement may differ from each other. The repeatability of INDUCTOSYN® transducers is typically about 10 times better than the rated accuracy. Systems with digital resolution equivalents comparable to the specified repeatability are entirely practical, and can fully exploit the accuracy specification.

Resolution is a function of INDUCTOSYN® analog to digital converters available from Farrand or other manufacturers.
 Example: A 1024 pole (512x) rotary INDUCTOSYN® transducer has 2^9 cycles. Interfaced to a 2^{12} bit INDUCTOSYN® analog to digital converter yields a system with 2^{21} bits of resolution equivalent to 0.62 arc sec.

FARRAND CONTROLS
 DIVISION OF FARRAND INDUSTRIES, INC.

Typical performance levels achieved with standard INDUCTOSYN[®] transducers and INDUCTOSYN[®] analog to digital converters are listed in Table 2 to illustrate practical levels of accuracy, repeatability, and resolution.

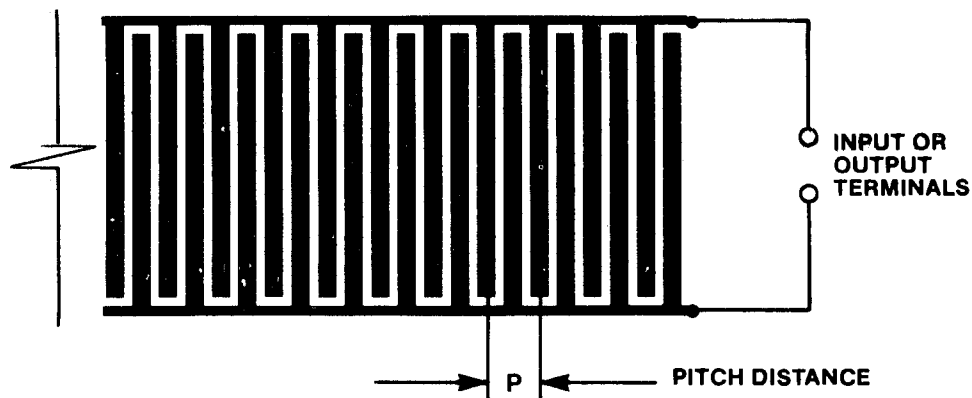
	LINEAR EXAMPLE	ROTARY	
		EXAMPLE 1	EXAMPLE 2
CYCLE LENGTH	0.1"	1° (720 pole)	0.36° (2000 pole)
TRANSDUCER ACCURACY	±0.0001"	±1 arc sec	±2 arc sec
TRANSDUCER REPEATABILITY	±0.00001"	±0.1 arc sec	±0.2 arc sec
DIGITAL CYCLE DIVISION	2000	1000	1000
DIGITAL RESOLUTION	0.00005"	0.001° (3.6 arc sec)	0.00036° (1.3 arc sec)

Table 2

3.2 Capacitive INDUCTOSYN[®] Transducer Operation

Capacitively coupled INDUCTOSYN[®] transducers can be constructed to perform analogously to inductively coupled counterparts. Capacitive coupling is advantageous for operation in strong magnetic fields, and capacitively coupled units are easily interfaced with MOS circuits. Operation is based on the capacitive coupling between two closely spaced elements that are directly attached to fixed and moving parts.

Linear units have interleaved comb-shaped precision conductor patterns applied to suitable mechanical supports. See Figure 12. Center-to-center spacing of the teeth of the comb is called the pitch.



Capacitive INDUCTOSYN[®] conductor pattern
 Figure 12

FARRAND CONTROLS
DIVISION OF FARRAND INDUSTRIES, INC.

Two such sets of patterns are mounted on fixed and moving parts, respectively, so that the teeth of the comb patterns pass over each other as the parts move. The capacity between the comb patterns thus varies cyclically, with one complete cycle for each pitch distance traveled.

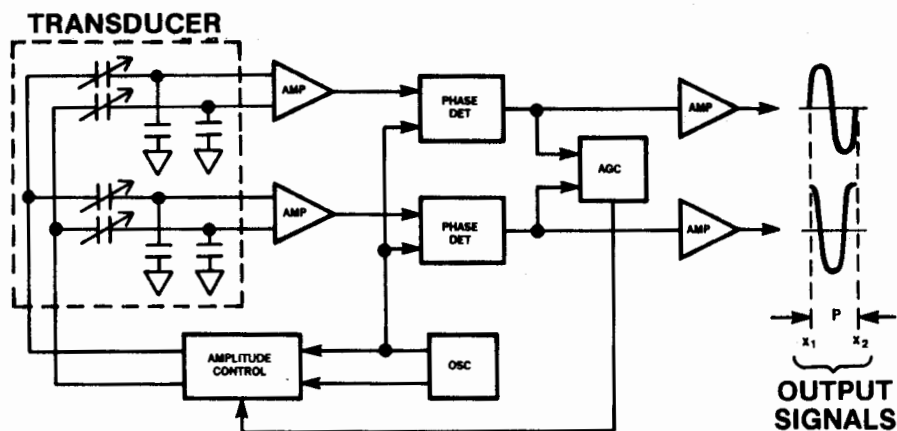
A second set of patterns may be added, in space quadrature with the first. This permits sensing the relative direction of motion, and subdividing the pitch interval with great accuracy.

Auxiliary patterns with only one or a few elements may also be placed on the substrate. These may serve as an absolute index of position, or may signal control circuitry that the moving part is passing through one or more special locations. Track location signals on digital disc recorders are a typical example.

The pitch of the comb pattern may be chosen to precisely match the desired dimensions or motions of the mechanism. Recorder track spacing is again a good example. The pitch may also be exactly 0.01 inch, 0.5 mm, or some other convenient interval for measuring instrument applications. Pitches of typical units now in production are 0.01", 0.0202125", 0.2", and 0.4 mm.

Rotary units are made in a comparable way, with the teeth of the pattern extending radially. The two elements are mounted concentrically, and the pitch distance is measured angularly. Auxiliary signals are still possible. The capacitive analog of a multispeed resolver can be supplied by concentric patterns with coarse and fine pitch.

Figure 13 is a block diagram showing typical capacitive INDUCTOSYN® transducer operation. Table 3 lists typical specifications for capacitive rotary and linear INDUCTOSYN® position transducers.



Typical capacitive INDUCTOSYN® transducer operation
Figure 13

**Typical Specifications for Capacitive
 Rotary and Linear INDUCTOSYN® Position Transducers**

Type of motion	Linear (straight line) Rotary - disc type Rotary - flexible tape wrap
Substrate material	Aluminum, steel, G-10 fiberglass, Flexible or rigid
Pattern material	Copper (other materials on special order)
Pattern pitch	0.01", 0.02", 0.10", 0.20", 1.0 mm, 2.0 mm
Accuracy	100 microinch T.I.R. for short travel, linear ± 15 arc seconds for 3.7 inch O.D., rotary
Excitation frequency	10 to 400 kHz
Voltage transfer ratio (VTR)	(V in/V out) 12-2000
Protective finish	Varnish, epoxy, polyurethane

Table 3

4. Rotary INDUCTOSYN® Position Transducer Applications

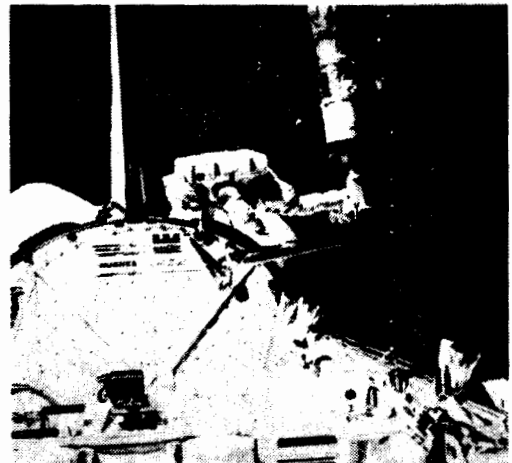
Example applications range from the Very Large Array radiotelescope to compact, field transportable radars. New designs, based on flat and compact INDUCTOSYN® transducers, have dramatically reduced envelope size and simplified mechanical design as well as improved accuracy. Their resistance to shock and vibration is vital in many applications.

Figures 14-17 illustrate current rotary applications.



The Very Large Array (VLA), largest radio astronomy and tracking array in the nation, uses two rotary INDUCTOSYN® transducers in each antenna mount to provide azimuth and elevation signals for servo control of array pointing. Standard 12 inch diameter stock units provided better than 1 arc second accuracy.

Figure 14



A total of six rotary INDUCTOSYN® transducers are used in the shoulder, elbow, and wrist joints of the Remote Manipulator System (RMS) arm installed in the cargo hold of the Space Shuttle. These specially designed rotary transformer coupled 2 inch diameter data elements provide 8 arc second accuracy for precise servo control.

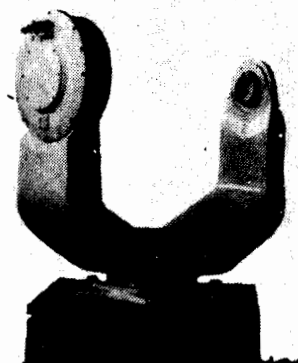
Figure 15



The Rapier Laserfire low level air defense system uses INDUCTOSYN® transducers to transmit target tracking and missile launch angles.

Built by British Aerospace Dynamics Group, Stevenage, Herfordshire, England

Figure 16



This yoke frame tracking mount contains two direct drive motors and INDUCTOSYN® rotary transducers for precision azimuth and elevation drive.

Type 459, built by Rademec Defense Systems, Ltd., Chertsey, Surrey, England

Figure 17

FARRAND CONTROLS
DIVISION OF FARRAND INDUSTRIES, INC.

REFERENCES

1. Grace W and Quinn G, Farrand Controls.
"Principles of INDUCTOSYNS®"
2. Horner G and Lacey R, Hightech Components Limited.
1984 Drives/Motors/Controls.
"A Review of Currently Available Rotary Velocity and Position Transducers."
3. Geoffrey S. Boyes, Analog Devices, Synchro & Resolver Conversion.

Acknowledgements

The author acknowledges the assistance of the engineering staff at Farrand Controls.

INDUCTOSYN® is a registered trademark of Farrand Industries, Inc.

SESSION 5

Q: JOHN ACH, AIR FORCE WRIGHT AERONAUTICAL LAB., OH

I'd like to open with a question for John Kalinowski. You mentioned that during the calibration of the gauges that they put on some type of identification signal. Could you just give me an idea of what you do in the way the strain gauge puts out a signal that identifies it? What gauge is it? Can you elaborate at all on that?

A: JOHN KALINOWSKI, EG&G ENERGY MEASUREMENTS, INC., SAN RAMON, CA

Yes, the board is set up, as I mentioned in the cal lab, so it uses that particular sensor and then we have the cal steps. Following the cal steps, we have a couple other steps where amplitude is comparable to the temperature. Then we have a very short code which will describe which sensor we're looking at. We know that we're looking at the turbine sensor in the radial direction. When the data comes out it better be that. Otherwise, there's a lot of times the line could get mixed up and when they get back in the trailer they can see and correct it before we go down hole.

Q: PATRICK WALTER, SANDIA NATIONAL LABORATORIES, ALBUQUERQUE, NM

I'm going to apologize in advance because I'm going to ask a question and then, when it culminates after an answer, I'm going to go run for an airplane. I hope it's not an offense to the rest of you that gave such nice papers. I wanted to ask the gentlemen from Farrand a question. On your inductive syntax, and I did perceive the advantages you said about the transformer typing and sensitive dirt and oil and things like that that I realize an optical tachometer would provide. Not having a great deal of depth in optical tachometers, I wonder if you could give me some comparison under idealized circumstances as to how the accuracy of your INDUCTOSYN® might compare to an optical tachometer, and also some comparison of costs between the two.

A: GEORGE QUINN, FARRAND CONTROLS, VALHALLA, NY

Okay. It's a position transducer that the velocity is derived from the output of the electronics. I did find the books, apparently the hotel delivered them here, so there are some up here with some data if anybody wants them. But the INDUCTOSYN® by itself is just a position transducer, and the velocity signal is derived from the output of the converter that converts the analog information with digital pulses. It's buried in the back of this. I'll give you one before you leave; it's the analog devices data sheet. It has a sixteen bit converter with a velocity output for tach information. As to the cost, INDUCTOSYN® can be as cheap as \$500 or as expensive as \$20,000.

Q: PATRICK WALTER

I was still seeking something a little more specific. You gave some figures I believe as to resolution in terms of arc seconds and could you compare that to what you could achieve with an optical tach?

A: GEORGE QUINN

Well, an optical encoder, is that what you mean? An INDUCTOSYN[®] is an analog device and we've discussed accuracy only. The resolution is a function of electronics. We could provide a one arc second accuracy transducer and you could resolve that to 25 bits if you want. But, it's still only accurate to one arc second. Like an optical encoder, they talk resolution only; they're not talking accuracy. We have only talked accuracy, not resolution.

Q: PATRICK WALTER

I think the culmination is that I just take your book and leave.

Q: FREDRICK RAKHOV

I have a question about the talk transducer. What kind of frequency do you use in you excitation voltage?

A: JOHN KALINOWSKI

The new design frequency, the one we're running today at the high speed system is around 6000 hertz.

Q: FREDRICK RAKHOV

Six thousand hertz? The second question is, did you try to make the shaft out of laminated material?

A: No, we've never tried that. I've read their papers but we've never tried that.

Q: RAY REED

John, the answer to the last question, I guess, leaves me unclear about what's being identified. The identification you speak of sounds like a digital identification. It sounds like it's a channel identification rather than a sensor identification is that correct?

A: JOHN KALINOWSKI

Correct.

Q: RAY REED

Do you still depend on getting the wires correctly connected to the input of the multiplexer and is the multiplex channel actually what's being identified?

A: JOHN KALINOWSKI

Yes.

ALBERT YUHOSH

A comment to Mr. Longinotti. A nice simple way of setting up a test for the acceleration problems with the unit you were talking about would be to use things like shotgun shells in a little man barrel type of situation, either using a billiard ball effect with the projectile against this device or putting the device up against it and so forth. It wouldn't be very expensive to set something like that up, and you could have a pretty good profiling of just what kind of loading conditions the thing can survive.

Q: TED STUBBS, EG&G

John, you mentioned that you had very little time to develop that thing and Dave also commented that it was down hole before he got all his computations completed. Now, how long did you have?

A: JOHN KALINOWSKI

We received a request from Livermore to develop a down-hole multiplex system which three months later had to go down hole. So, we had three months in which to develop an entire concept, electronic system, mechanical system, and have it going down hole. Three months.

Q: MIKE ENGLUND, GARRET TURBINE ENGINE COMPANY

On the magnetostriction torquemeter, you listed the advantage of that system as taking up a shorter length on the shaft relative to strain gauge type transducers. How short and how much volume does it occupy?

A: FRANCIS SCOPPE, AVCO LYCOMING DIV.

We're probably 1 1/2 to 2 inches in axial length and the diameter is dependent upon the shaft diameter, if you allow another 3/4 of an inch over and above the shaft diameter.

Q: MIKE ENGLUND, GARRETT

And is it designed to withstand internal turbine engine environments? Oil mist?

A: FRANCIS SCOPPE

Yes, there's a weakness in oil. I don't know how the problem affects the inductive position sensors, but we do find with contaminated oil - oil which has picked up metallic content or becomes acidic - there is a problem, not so much in the transducer, but in the spacing between the interconnecting wires where we have leakage paths. We have a very small signal. Leakage does effect this.

Q: PETER STEIN, STEIN ENGINEERING

I have a general question on nomenclature to a number of people on the panel and also I'm a little bit confused on some things. John, you

talked about a large electromagnetic pulse that is a problem in your test and that you had a copper shield around the instrumentation. Copper, in general, will shield you against electric fields, or are you in that frequency region where copper also is a good magnetic shield? Or, is it a question of nomenclature that we're confusing here?

A: JOHN KALINOWSKI

You're correct. The machine we work in is very high, like 700 volts per meter with that field. The closeness that we are to the implacement pipe helps us because the EM field being a vector cancels out at that time, pretty much. So if we were inside the implacement pipe, we would have zero EMP effects unless there was an aperture. But we do have currents. We have currents generated by the weapons affluent, constant currents and everything. And these are the things we have to watch out for, so this is where we come to copper the complete outside, to cover the cage, to keep the currents on the outside. In addition, we run down a copper wire all the way and we make a multi-point connection, in many cases, in order to get these currents off before they do find some aperture in which to spill their guts. Once they do that, we have EMP, in a sense, electromagnetic fields. You are right.

Q: PETER STEIN

I have a question on the magnetostrictive torquemeter. And there may be others in the group who are more adept at Greek nomenclature than I am, but to me, the magnetostrictive phenomenon applies a magnetic input and a change in displacement output. Magnetostriction is a valuable mechanism for measurement. I personally would feel very confused, unless I had heard your paper, understanding the basis of the transducing mechanism which was really a mechanical input and a change in magnetic reluctance. So, it ought to be called piezoreluctive. It depends on where you read the literature and what field; there doesn't seem to be a standard. But, I think Jim Dorsey mentioned ISA has standards, so I'd be very happy to be educated on this.

A: FRANCIS SCOPPE

I have no answer for that if what you're saying is true. The Volarey and the Wiedenmann effect is, I guess, very similar to a Peltier and Seebac. One is the change in the temperature as a function of a current through two metallic points, and the other is the change in voltage as a function of it. It's just a converse relationship. In general these are magnetostrictive effects.

Q: PETER STEIN

That implies, though, a magnetic input, mechanical output and a self-generating effect, where as yours is an impedance-based effect which is a totally different family member. And unless we get our nomenclature cleaned up in this crazy business, I think there's very little chance that somebody could read a paper and it be understood by others. If John Kalinowski had read his paper next week at the

Society for Experimental Mechanics Congress, he would find that his use of the word "stress" for what he really means, hydrostatic pressure, would be very confusing to the audience. But, he mentioned that he has referred to hydrostatic pressure psi as a stress psi, which leaves us experimental mechanics people way out on a limb unless we knew of this convention.

RAY REED, SANDIA NATIONAL LABORATORIES

I think it wasn't emphasized quite in John's presentation, but it was said on the slides that you're making a hydrostatic pressure measurement in the cell of the device. This is what we call a fluid couple deterbium gauge. In fact, what they really are trying to measure is a bona fide extensor stress, particularly in the stress regime that they're talking about. They really mean the same things the engineering mechanics people normally do except the terminology is not always expressed. Specifically, they hope in the business that John is engaged in that they relate the pressure that is actually imposed on that transducer to some sort of stress which they don't always define well. It's a classic problem. But the problem is not in the definition of the term but even the recognition that tensors exist in many cases.

Q: JOHN ACH, AIR FORCE WRIGHT AERONAUTICAL LABS.

Any more questions for any of our presenters? Any other discussion? If not, I'd like to thank the four presenters for doing a nice job, and I'd like to thank the audience for some very pertinent questions and discussions, and return control of our session back to our general chairman.

DISTRIBUTION LIST

COPIES

TG CHAIRMAN

Mr. D. K. Manoa (WSMC) 2

MEMBERS

Mr. G. E. Wooden (KMR) 1
Mr. A. E. Hooper (YPG) 1
Mr. K. O. Schoeck (WSMC) 1
Mr. R. W. Krizan (ESMC) 1
Mr. G. Nelms (ESMC) 1
Mr. A. Yamaguchi (AFFTC) 1
Mr. S. Morton (AFFTC) 1
Mr. H. Armstrong (AFFTC) 1
Mr. R. Pozmantiar (AFFTC) 1
Mr. C. M. Tucker (AD) 1
Mr. B. Weathers (AD) 1
Mr. C. Kern (AD) 1
Mr. J. H. Eggleston (AD) 1
Mr. B. Mixson (AD) 1
Mr. N. F. Lantz (AFSCF) 1
Mr. R. E. Rockwell (NWC) 1
Mr. H. Duffy (NWC) 1
Mr. J. Rieger (NWC) 1
Mr. L. Rollingson (NWC) 1
Mr. L. M. Sires (NWC) 1
Mr. C. G. Ashley (PMTC) 1
Mr. E. L. Law (PMTC) 1
Mr. D. Duval (PMTC) 1
Mr. A. Quinones (AFWTF) 1
Mr. J. W. Rymer (NATC) 1
Mr. R. J. Faulstich (NATC) 1

TG ASSOCIATE MEMBERS

Mr. G. P. Cunningham (USAMICOM) 1
Mr. J. Vesco (USAEPG) 1
Mr. L. H. Glass (ARDC) 1
Mr. D. G. Henry (PSL) 1
Mr. R. Wilton (AFGL) 1
Mr. M. A. Pierson (FLTAC) 1
Mr. B. F. Wagner (FLTAC) 1
Mr. L. Bates (NSWSES) 1
Mr. W. B. Poland, Jr. (NASA/GSFC) 1
Mr. R. S. Reynolds (SNL/ABQ) 1
Mr. H. O. Jeske (SNL/ABQ) 1
Mr. S. F. Kuehn (SNL/ABQ) 1
Mr. R. R. Beasley (SNL/TTR) 1
Mr. D. L. Gilbert (AFWAL) 1
Mr. J. T. Ach (AFWAL) 1

COPIES

Mr. R. T. Hasbrouck (LLNL)	1
Lt C. York, USAF (AEDC)	1
Mr. J. Temple (AEDC)	1
Mr. G. Feuer (NADC)	1

OTHER ATTENDEES

Mr. W. D. Anderson	1
Dr. G. Articulo	1
Mr. D. Banaszak	1
Mr. P. J. Barthelow	1
Ms. V. I. Bateman	1
Mr. C. R. Belensky	1
Mr. F. L. Benedict	1
Mr. R. J. Bohle	1
Mr. D. Boremann	1
Mr. N. E. Broderick	1
Mr. L. L. Brown	1
Ms. V. Brown	1
Mr. C. D. Bullock	1
Mr. P. Cayere	1
Mr. R. F. Clark	1
Mr. H. Clarke	1
Ms. H. M. Clarke	1
Mr. R. N. Clarke	1
Mr. W. A. Clayton	1
Mr. A. Colee	1
Mr. W. H. Connon, III	1
Mr. P. Curran	1
Mr. L. Davies	1
Mr. A. Diercks	1
Mr. J. Dorsey	1
Mr. J. M. Dubler	1
Mr. J. D. Dykstra	1
Mr. M. Englund	1
Mr. L. M. Erickson	1
Mr. T. Escue	1
Mr. J. Finney	1
Mr. C. Forbes	1
Mr. H. S. Freynik, Jr.	1
Mr. J. Gartner	1
Mr. H. Gilmore	1
Mr. C. Grabenstein	1
Mr. B. Granath	1
Mr. L. F. Green	1
Mr. L. Gregory	1
Mr. G. C. Hall	1
Mr. J. Hall	1
Mr. B. Ham	1
Mr. M. A. Hatch, Jr.	1
Mr. C. J. Hattaway	1
Mr. E. Hazelton	1

COPIES

Mr. C. E. Holstein	1
Mr. J. Horner	1
Mr. E. D. Jorgenson	1
Mr. A. A. Juhasz	1
Mr. J. A. Kalinowski	1
Mr. W. R. Kitchen	1
Ms. M. B. Krummerich	1
Mr. J. Lally	1
Mr. J. Lara	1
Mr. W. B. Leisher	1
Mr. T. Licht	1
Mr. D. B. Longinotti	1
Mr. T. Macaluso	1
Mr. J. Magdziak	1
Mr. L. Maier	1
Mr. J. McGee	1
Mr. D. McLeod	1
Mr. D. McMahon	1
Mr. J. R. Miller, III	1
Mr. T. B. Miller	1
Mr. J. P. Mulhall	1
Mr. R. P. Noyes	1
Mr. M. Ortiz	1
Mr. D. Page	1
Mr. G. R. Patterson	1
Mr. T. S. Pounds	1
Mr. J. Pugnaire	1
Mr. G. A. Quinn	1
Mr. J. T. Rambo	1
Mr. R. Reed	1
Mr. L. A. Rempert	1
Mr. G. M. Rendla	1
Mr. F. Schelby	1
Mr. E. Schonthal	1
Mr. F. E. Scoppe	1
Mr. W. M. Shay	1
Mr. S. A. Siegel	1
Mr. R. D. Sill	1
Mr. C. Sisemore	1
Mr. F. Smith	1
Mr. L. A. Smith, Jr.	1
Mr. S. J. Spataro	1
Mr. P. K. Stein	1
Mr. H. Stonelake	1
Mr. W. Stringham	1
Mr. H. Stry	1
Mr. T. Stubbs	1
Ms. G. Stuebner	1
Mr. R. D. Talmadge	1
Mr. J. A. Tavis	1
Mr. D. R. Taylor	1
Mr. K. Thorstensen-Woll	1
Mr. R. B. Tussing	1

COPIES

Mr. C. Ulrich	1
Mr. P. A. Urtiew	1
Mr. D. Vollmer	1
Mr. P. L. Walter	1
Mr. H. Weiss	1
Mr. L. Wendell	1
Mr. R. M. Whittier	1
Ms. M. Willis	1
Mr. M. Wilt	1
Mr. S. Wnuk	1
Mr. A. Yorgiadis	1